



COLECȚIA MANIFESTĂRI ȘTIINȚIFICE

TRANSPORTATION INFRASTRUCTURE SCIENTIFIC OPINIONS

Constantin Ionescu
Rodian Scînteie
Andrei Radu
Alina Mihaela Nicuță
Editors



Editura Societății Academice "Matei - Teiu Botez"

TRANSPORTATION INFRASTRUCTURE SCIENTIFIC OPINIONS

Constantin Ionescu, Rodian Scînteie,
Radu Andrei, Alina Mihaela Nicuță
editors

Editura Societății Academice “Matei - Teiu Botez”
Iași 2007

Proceedings of the Fifth International Symposium

"Highway and Bridge Engineering 2007"

Iași, România, December 7, 2007

Descrierea CIP a Bibliotecii Naționale a României

Transportation infrastructure : scientific opinions / editors:

Constantin Ionescu, Rodian Scînteie, Radu Andrei, Alina

Mihaela Nicuță. - Iași : Editura Societății Academice

"Matei - Teiu Botez", 2007

Bibliogr.

ISBN 978-973-8955-29-5

I. Ionescu, Constantin (ed.)

II. Scînteie, Rodian (ed.)

III. Andrei, Radu (ed.)

IV. Nicuță, Alina Mihaela (ed.)

625.7

Table of Contents

1. Radu Andrei, Constantin Ionescu, Neculai Tautu, Rodian Scinteie, Diana Vranceanu, Alina-Mihaela Nicuta Actual Trends in Highway Engineering (Synthesis of proceedings)	1
2. Rodian Scinteie, Constantin Ionescu, Cristian Claudiu Comisu Actual Trends and Developments in Bridge Engineering. (Synthesis of Proceedings)	8
3. Josef Stryk Road Diagnostics - Ground Penetrating Radar Possibilities	18
4. Rudolf Cholava, Michal Matysik, Petr Smekal Road design for sustainable transport promotion	28
5. Constantin Amariei, Ioan Buliga The analysis of the compatibility of rotations within plastic hinges from reinforced steel structures	38
6. R. Andrei, N. Taranu, H. Gh. Zarojanu, N. V. Vlad, V. Boboc, I. D. Vrancianu, M. Nerges, M. Muscalu, R. Cojocar Actual Trends on Long Lasting Rigid Pavements (LLRP)	49
7. Cornelia Victoria Anghel The optimization of transport problems using linear programming	71
8. Marinela Bărbuță, Daniel Lepădatu Polymer concrete optimization using mixture design of experiment and response surface methodology	75
9. Dorel Bolduș, Radu Băncilă, Edward Petzek Strengthening and reconstruction technology of an old steel highway bridge	84
10. Cristian Claudiu Comisu Integrated system for monitoring bridge structures	94
11. Cristian Claudiu Comisu Structural identification – decision factor in bridge rehabilitation	101
12. Mihai Dicu, Carmen Răcănel, Adrian Burlacu, Claudia Murgu, Iuliana Bălan The necessity to reduce the material structures from the road layers tested with the temperature control cracking device at a modeling scale	108
13. Ioan Florin Drăgan, Florina Crăciun, Delia Drăgan The Highways Noise Reduction Methods	118
14. Emil Doupal Traffic and loading data for the highway and bridge management	126
15. Elisabete Freitas, Paulo Pereira Analysis of the functional quality of pavements from texture measurements	140
16. Ramona Gabor, Anca Gido, Radu Bancila Friction Stir Welding – an innovative solution for civil engineering	158

17. Ovidiu Gavris Using the finite strip method in determining the static response of the deck bridges	170
18. Ștefan I. Guțiu, Petru Moga, Cătălin Moga Fatigue design considerations of the steel plate girders	177
19. Petr Kalvoda, Miroslava Suchá, Josef Podstavek and Jiří Vondrák Photogrammetric measurement of deformations during the load test of brick vault	186
20. Iulian Mata Considerations Regarding the Rebuilding of a Prestressed Concrete Bridge Damaged by High Floods	193
21. Pavla Matulova Repair of sub-base by large – sized grouting and potential use of recycled raw materials as substitution of binding components of grouting materials	201
22. Călin Mircea, M. Filip Research upon the Cracking Induced by Restrained Contraction of Mass Concrete Elements	209
23. Călin Mircea, M. Filip Service Tests on PC Beams	230
24. Jana Neumanová Geodetic Measurement of Line Constructions for Control and Security of Construction Reliability	242
25. Nicuță Alina Mihaela, Ionescu Constantin Consideration regarding the quality costs in the process of total creation bridge	252
26. Joel Oliveira, Hugo Silva, Paulo Pereira Pavement recycling: an environmentally sustainable rehabilitation alternative	261
27. Jorge C. Pais, Paulo A.A. Pereira The improvement of pavement performance using asphalt rubber hot mixes	277
28. Vít Petránek Surface application of polymer coating for concrete curing	295
29. Vít Petránek, Tomáš Melichar Slip-resistant Surface Treatments on Bridge Construction Walking Areas – the First Stage	305
30. Mario Paolo Petrangeli, Luigi Fieno, Ciprian Dan Loata Seismic isolation of the Italian bridge: a case study	316
31. Carmen Răcănel, Adrian Burlacu The Influence of Size of Asphalt Mixture Samples Compacted with Gyrotory Compactor on Volumetric Properties	333
32. Ionuț Radu Răcănel The evaluation of dynamic effect of vehicles on bridges using the finite element method	344
33. Claudiu Romanescu, Cristina Romanescu, Rodian Scînteie Applicability conditions of various methods for mitigation of the scour phenomena to road bridges infrastructures	360
34. Cristina Romanescu, Claudiu Romanescu, Rodian Scînteie Condition assessment of reinforced concrete bridges using nondestructive testing techniques	370

35. Liliana Stelea	
Present Trends in Improving Quality of Pavement Bitumen	384
36. Mircea Suci	
Comparison between the parabolic counter deflection and the one made up of the average deflections in the case of a high speed railway bridge	394
37. Mircea Suci, Gavril Kollo	
Advantages and disadvantages of the counter deflection based on the average of the deflections recorded in the sections of the superstructure of a railway bridge	404
38. Jan Valentin, Michal Grochal, Tomáš Prudký	
Experimental testing and assessment of stiffness modulus and fatigue of various cold recycling mixes	412
39. Irinel – Diana Vrancianu	
Preliminary results obtained with various structural design methods, considered for validation of Long Lasting Rigid Pavements (LLRP) concept using Accelerated Testing (ALT) Facility	425
40. Horia Gh. Zarojanu, Radu Andrei	
Calculation of the Equivalent Traffic Based on Structural Design Criteria of Flexible and Semirigid Pavements	434
41.	
“Highway and Bridge Engineering 2007” in images	440

Actual Trends in Highway Engineering (Synthesis of proceedings)

Radu Andrei¹, Constantin Ionescu², Neculai Tautu³, Rodian Scinteie⁴, Diana
Vranceanu⁵ Alina –Mihaela Nicuta⁶

^{1,2,4,5,6}) Technical University “Gh. Asachi”, Iasi., 700050, Romania

³) Romanian Professional Association for Road and Bridges- Moldavian Branch, Iasi, Romania

⁴)Romanian Centre for Road Engineering Studies and Informatics-CESTRIN, Bucharest, Romania

The papers presented in the frame of this new annual edition of the international symposium on Highway and Bridge Engineering are focusing on some of the most challenging issues of the actual road research, such as sustainable development of roads and of road transport, development of long lasting pavements and validation of the new concepts by using accelerated testing facilities, assessment of functional quality of pavements and road transport management, traffic investigations, new road materials, construction and testing technologies and modern solutions for earth and slope consolidation.

1. SUSTAINABLE DEVELOPMENT OF ROADS AND OF ROAD TRANSPORT

Sustainability is defined, according Brundtland definition [1], as “*development that meets the needs of the present without compromising the ability of the future generations to meet their own needs*”. As usually, in the particular case of roads, sustainability is defined by taking into consideration the economic, social, and ecological aspects, in the decision-making and evaluation process.

Road infrastructure can be divided into two main categories: technical and social. The papers presented in our symposium are addressing the first category, the main emphasis being on sustainable aspects of physical road pavement structures.

In their paper, entitled *Pavement Recycling: an Environmentally Sustainable Rehabilitation Alternative*, Joel Oliveira, Hugo Silva and Paulo Pereira, from the Department of Civil Engineering, University of Minho, Guimarães, Portugal, focus on preservation of environment, by reducing the use of material and natural resources together with important economic savings. In this context, their analysis of a heavily trafficked urban road rehabilitation project, has finally led to the conclusion that pavement recycling should be considered as a prime solution for pavement maintenance/rehabilitation. This solution allowed the maintenance of the

pavement level (without the need for footpath reconstruction) and minimized the use of new materials, contributing towards a sustainable development.

The Check researchers Rudolf Cholava, Michal Matysik and Petr Smekal, from the Brno Transport Research Centre (CDV), are addressing, with their paper, *Road Design for Sustainable Transport Promotion*, the sustainability issue from the point of view of road design, by presenting the results of specific projects, carried out by CDV, targeting at increasing energy efficiency and savings. The integration of construction and vehicle energy usage with relevant measures for reducing traffic noise (low-noise pavements) into road design are considered by the authors to substantially contribute to reducing environmental burden resulted from transport and thus to promote its sustainability.

2. DEVELOPMENT OF LONG LASTING RIGID PAVEMENTS AND VALIDATION OF THE NEW CONCEPTS BY USING ACCELERATED TESTING (ALT) FACILITIES

Although in the past, the majority of pavements were designed on the basis of a 20- to 25-year initial service life, more recently, there has been a movement toward a longer initial service life of 40 or more years. Recent advances in design, construction, and concrete materials give us the knowledge and technology needed to achieve long-life pavements. Worldwide, it has been aimed to develop infrastructure for surface transport using alternative concrete bases for reducing the maintenance (and though the life-cycle costs) of pavements and doing so at an initial cost lower than for traditional rigid pavements. This is attainable in the general context of developing the concept of Long Lasting Rigid Pavement (LLRP).

The following three papers drafted by the members of the Work Package 3 (WP3) involved in the development of the actual FP6–STREP (Strategic European Program) EcoLanes [2] are addressing specific issues related with development of the concept of long lasting pavements and its validation by using ALT facilities, in parallel with similar experiments envisaged to be conducted on the road network.

With the first paper, entitled *Actual Trends on Long Lasting Rigid Pavements (LLRP)*, the authors, from Technical University “Gh. Asachi”, Iasi, Romania, are introducing some projects that proved to have extended life, emphasizing the changes in overall pavement design and construction materials, that occurred over the years, with the purpose to define the concept of LLRP and to propose some options on LLRP, envisaged to be studied in the frame of EcoLanes Project. These proposed options, have been considered in planning of the experimental design on the ALT facility, now under construction.

The comparative study of various structural design methods envisaged to be used in the frame of the EcoLanes project, conducted on these selected pavement structures, makes the subject of the second paper, entitled : *Preliminary Results Obtained with Various Structural Design Methods, Considered for Validation of Long Lasting Rigid Pavements (LLRP) Concept Using Accelerated Testing (ALT) Facility*. In her paper, the author Irinel Diana Vrancianu, from Technical University “ Gh, Asachi” of Iasi, presents the early design results using the first two of the three selected methods, namely: the Romanian NP 081-2002 method, the U.K. Highway Agency Method and the Mechanistic – Empirical Pavement Design Guide (M-E PDG) developed in USA.

The design study has been conducted on slabs with the same thickness, but constructed from different materials (plain concrete/steel fiber reinforced concrete (SFRC), rolled compacted concrete). Both design methods used in the investigation produced thickness of SFRC slab lower than that obtained for unreinforced concrete slab, and significantly reduced in case of the Romanian method. The study is under way and it will be extended to the AASHTO Mechanistic – Empirical Pavement Design Guide (M-E PDG) and, if necessary , to the other methods.

In his paper, *Calculation of the Equivalent Traffic Based on Structural Design Criteria of Flexible and Semirigid Pavements*, professor Horia Gh. Zarojanu and his collaborators from Technical University “Gh. Asachi” Iasi. present a methodology for calculation of the equivalent traffic, intended to be applied in the frame of an analytical structural design method for flexible and semirigid pavements. This methodology eliminates conventional or empirical equivalence, by using the structural design criteria expressed in terms of allowable deformation/stresses. Finally, for a representative construction case for a European/National Road, a comparison between the proposed method and the actual one, used in the frame of structural design of pavements in Romania, is given.

3. MANAGEMENT OF ROAD TRANSPORT AND ASSESSMENT OF FUNCTIONAL QUALITY OF PAVEMENTS

Functional requirements, such as roadway safety, environmental quality, driving comfort and operating costs in the road network are assessed by indicators whose limits are continuously adjusted.

In their paper, *Analysis of the Functional Quality of Pavements from Texture Measurements*, the authors Elisabete Freitas and Paulo Pereira, from the Department of Civil Engineering, University of Minho, Guimarães, Portugal, after undertaking an overview of the concepts related to texture and the effects of texture including unevenness, on safety, driving comfort, ride quality and environmental

quality, are presenting a case study involving a highly trafficked road in the north of Portugal. Their results, obtained by using a high speed profilometer, proved to be adequate for the analysis of longitudinal profile, macrotexture and unevenness. Finally, specific indicators such as the mean profile depth, the IRI, the rutting depth and the corresponding effects are addressed.

Highway traffic noise problem is addressed in their paper, *The Highways Noise Reduction Methods*, by Ioan Florin Drăgan, Florina Crăciun and Delia Drăgan, from the Technical University of Cluj-Napoca, Romania. The authors describe acoustical techniques and methods for measuring and reducing the traffic noise. Some of the most common methods used by highway planners and designers, construction engineers, and private developers are different types of noise barriers.

In the context of implementation of mathematical methods in the field of transport management, the author Cornelia Victoria Anghel, from the Computer Science Department, Eftimie Murgu University of Resita, Romania, with her paper, *The Optimisation of Transport Problems Using Linear Programming*, recommends the „Linear Programming”, as an efficient method of solving the optimization problems of various phenomena resulting from different economic processes , including the transport.

4. TRAFFIC INVESTIGATIONS: NEW HORIZONS

The WIM system, based on the modern quartz sensor technology combined with new data logger and video systems, is providing data that are used for a wide variety of applications depending on the requirements of the road authorities or user groups (police, traffic engineers, road designers).

Dr. Emil Dupal’s paper, from the Transport Research Centre (CDV), Brno, Czech Republic, *Traffic and Loading Data for the Highway and Bridge Management*, provides information on multi-purpose applications of automatic WIM (weigh in motion) stations for overloading control, traffic data collection and the following evaluations, operated in various remote control modes. An example shows specific methods of pre-selection of overloaded vehicles, online traffic data collection and automatic statistic evaluations. Generally, any type of station which gathers real data and allows remote management can be implemented in the all traffic on-line product for dynamic weighing of vehicles (ATOL) system. The author concludes that this system ensures an easy access to data, according to customer wishes and his trade policy of data mediation.

In her paper, *Geodetic Measurement of Line Constructions for Control and Security of Construction Reliability*, the author Jana Neumanová, from the Czech Technical University in Prague, Czech Republic, addresses theoretic problems in

the area of geometric accuracy, affecting resulting quality in constructions and describes a graphic model of geometric parameters.

5. NEW ASPHALT ROAD MATERIALS, CONSTRUCTION AND TESTING TECHNOLOGIES

The research seeking the developing of new performant road materials and improving of the existing construction and testing technologies are still a major challenge for road researchers. In this context, the authors Jorge C. Pais and Paulo A. A. Pereira, from the University of Minho, Department of Civil Engineering, Guimarães, Portugal, present their results on *The Improvement of Pavement Performance Using Asphalt Rubber Hot Mixes*. The asphalt rubber, used by the authors to modify the bitumen, produced asphalt mixes with superior performance and with higher resistance to climatic effects, compared to the conventional ones. Based on these assumptions, the authors present the results of the evaluation of mechanical properties, the materials performance being evaluated through stiffness, fatigue and permanent deformation tests. Reflective cracking performance has been also predicted using a mechanistic-empirical method.

Carmen Răcănel and Adrian Burlacu, from the Department of Roads and Railways, T. U. C. E., Bucharest, Romania, present their results on *The Influence of Size of Asphalt Mixture Samples Compacted with Gyrotory Compactor on Volumetric Properties*, in terms of evaluation of air voids, voids in mineral aggregates and voids filled with asphalt, their study being conducted on a classical asphalt mixture, BA16 and on an asphalt mixture stabilised with cellulose fibres, type MASF16. With this study, the authors are bringing a significant contribution to the implementation of the volumetric mix design in our country, as recommended by the actual European and other international norms.

Cold recycling in pavement rehabilitation and new construction are considered as element of a sustainability strategy in road engineering. In their paper, *Experimental Testing and Assessment of Stiffness Modulus and Fatigue of Various Cold Recycling Mixes*, the authors, Jan Valentin, Michal Grochal and Tomáš Prudký, from the Czech Technical University, Prague, Czech Republic, focus on the testing methods of reclaimed asphalt pavement mixes, especially on measurement of stiffness modules at different temperatures (5°C, 15°C, 27°C) representing different pavement conditions during the year and fatigue tests for different stress conditions. These results and their comparison for different mixes are presented and discussed in the paper.

M. Dicu, C. Racanel, A. Burlacu, C. Murgu, I. Balan, from the Technical University for Constructions Bucharest, Romania are presenting, in their paper, *The Need of Scaling for Modelling the Materials Used in Road Layers Tested with*

a Crack Measurement Device, at Various Temperatures, an efficient accelerated testing methodology for evaluating the quality of road pavement materials, by performing specific laboratory tests on scaled pavement structures. The geometric scaling of pavement structures implies also the dimensional adaptation of other characteristics of the materials including the grading, this research being under way.

In the paper entitled, *The Use of Modified Bitumen in Romania, from Theory to Practice*, the author Eugen C. Florescu, PhD, from COLAS Romania, presents an interesting point of view concerning the use of polymer modified bitumen in our country, by taking into consideration the severe climatic conditions (severe winters and very hot summers) and significant growth of heavy traffic on our public road network.

The PhD student Liliana STELEA, with her paper : *Actual Trends for the Improving of Bituminous Binders* , presents a synthesis of the recent researches undertaken in this country , and concludes that the laboratory study for an asphalt mix has to integrate all the results obtained for each component, each component having a significant role on the performance of pavement.

6. MODERN SOLUTIONS FOR EARTH CONSOLIDATION AND SLOPES STABILITY

In their paper, the authors, professor Nicolae Botu, – from UT Iasi , Dan Carastoian and Daniel Purice, from SC Proexrom SRL, Iași are proposing *Modern Solutions for Rehabilitation of the Monumental Complex “Rapa Galbena”* in the Iasi City. Their solutions are involving lowering the water table level to 9.00 – 9.50m depth and the improvement of the retaining wall strength by applying cement mortar injections, in parallel with the rehabilitation of the drainage system and protection of the slopes.

The landslides as natural phenomena COULD be INCLUDED in the category of natural catastrophes, with high risks from the point of view of the danger. The authors Ana Nicuță and Vasile Grecu, from the Technical University “Gh. Asachi” Iasi , present, in their paper, *Romania Roads Performance on Difficult Foundation Soils - Case Study*, their analysis and recommendations for a construction site, characterized by the presence of a clay and silty clay package, with high sliding potential

In their paper, *The analysis of Cotumba Monastery Site Stability*, the authors Ana Nicuță and Mihaela Stoicescu, from the Faculty of Civil Engineering and Building Services, Iași, Romania, and SC LAFORSERVICE SRL, Bacău, Romania, respectively, present the analysis of a construction site stability. The authors

analyze the causes which lead to the partial loss of the stability but also the approaches for slowing the effects of stability loss phenomena.

7. CONCLUSIONS

Based on the analysis of the papers received for the Symposium, one may observe a growing interest and preoccupation of the road researchers for addressing road management issues in terms of sustainable development, extended and professional use of recycled materials, conception of long lasting, durable pavements and validation of this concept using accelerated testing facilities, scaling and/or modeling, in parallel with observing performance on experimental sectors constructed on the existing road network.

There is also a positive trend, expressed in some of the presented papers, towards the use of mathematical methods for solving the both highway engineering and transportation problems.

That's why, some of the most significant papers, addressing these actual challenges in highway engineering, will be selected to be published in the coming 2007 issue of the international journal INTERSECTIONS/ Transportation Infrastructure Engineering [3], (4-th Edition)

References

1. Lathi, P. et. al., *Towards Sustainable Urban Infrastructure*, Multiprint Oy, Helsinki, 2006
2. <http://ecolanes.shef.ac.uk>
3. Intersections 2006: http://www.ce.tuiasi.ro/intersections/No1/No1_eng.pdf
4. Intersections 2005: http://www.ce.tuiasi.ro-intersections-No9-No9_eng.pdf
5. Intersections2004: http://www.ce.tuiasi.ro-intersections-archive-2004-No6-No6_eng.pdf

Actual Trends and Developments in Bridge Engineering. (Synthesis of Proceedings)

Rodian Scinteie¹, Constantin Ionescu², Cristian Claudiu Comisu²

¹ *Romanian Centre for Road Engineering Studies and Informatics-CESTRIN, Bucharest, Romania*

² *Technical University “Gh. Asachi”, Iasi., 700050, Romania*

1. INTRODUCTION

The interest for bridge engineering section was very high. From the articles received 24 were selected. They may be classified in 6 main areas:

- Road structures management,
- Works for bridges,
- Materials for bridge,
- Methods of calculation and design ,
- Modeling in bridge engineering,
- Teste, încercări și măsurători pentru structuri.

The papers come from many institutions and many research areas proving that the problems of bridge are of strict actuality and there are far from being solved. More and more subjects arise while experts are going deeper into their research.

The papers are only a small contribution, one of the many steps to be followed in the years to come to construct a transportation infrastructure worth of its name, capable to offer comfortable traffic in safety and security.

2. ROAD STRUCTURES MANAGEMENT

In the article “BMS – A Romanian perspective” **Scînteie Rodian** presents the development of the Bridge Management Systems in use at the National Company of Motorways and National Roads. The system is the result of a 7 years program conducted and CESTRIN Bucharest. The system includes the data collection, condition assessment, needs evaluation, and strategic allocation of funds. While much is still to be done, the system fits the need of the administration and is appreciated by World Bank and experts from other countries.

Alina Mihaela Nicuță and **Constantin Ionescu** take in consideration the problems regarding the quality costs in the process of total realization of a bridge. Quality costs have the purpose to assure a good quality on a long period of time. The idea is to consider the principle of the work “well done from the first time”. The necessary costs for a high quality must be evaluated in order to be able to predict and control the total cost for quality.

In order for a construction to fulfill the principles of quality system is necessary to create equilibrium between quality and costs. The decrease in quality determines an increase of the overall costs. Quality costs are the costs due to the NON creation of a quality product or service. In general terms, the quality system has two types of costs: quality costs and non-quality costs. First of them include prevention costs and evaluation costs. The other ones include the costs of internal faults and costs of external faults. The paper presents some examples of detailed activities that determine these costs. Each and every cost is influenced by its own specific activities.

The paper intends to create a unified quality cost system for the area of bridge engineering. Therefore it is necessary to take into consideration all the phases of the bridge life meaning design, execution, exploitation and post-utilization with the included proper costs.

Raluca Popa in the paper “Considerations on the bridges and roads from Neamt historical area” analyzes the transportation network in Neamt County and its present condition. The article presents statistics on the development of the network, its present situation. The condition of the structures is also presented.

Mircea Suci and **Gavril Kollo** studies the “Advantages and disadvantages of the counter deflection based on the average of the deflections recorded in the sections of the superstructure of a railway bridge”.

Objectives of the article are to determine the vertical displacements of a railway bridge with a special shape of counter deflection, steel-concrete composition, 50m span, under the action of a high speed train. In order to determine the impact of the increased speed upon the vibrations and deflections of a mixed section railway bridge superstructure, this superstructure has been carried into the SAP2000 finite element software.

Two variants of superstructure have been analyzed, one without counter deflection and one with counter deflection, based on the average of the deflections obtained in the bridge that had a straight running track. Twelve non-linear dynamic analyses have been performed for each model, with the Thalys train that covers the analyzed

models with speeds: 1, 10, 20...110m/s (3.6...396km/h). The maximal value of the counter deflection is 10.323mm.

3. WORKS FOR BRIDGES

Boldus D., Bancila Radu, Petzek E. present the “Strengthening and reconstruction technology of an old steel highway bridge”. The article deals with historical bridge which are in the authors’ view "witnesses of the past". One such a bridge, which resisted to two World Wars, is the bridge in Săvârșin over the Mureș River on the local highway DJ 707 A.

Due to the fact that technical condition of the bridge was unsatisfactory, the elements are corroded and some verticals and diagonals are damaged by the impact with the vehicles, the structure is under a complete process of strengthening. The existent floor beams, stringers and cross girders are simple supported elements. The deck consists of Zorres elements filled with ballast, supporting an asphalt surface. In present the structure has a special importance being the only crossing of the river in a large area. Taking into account the importance of the structure, its historical value the decision of rehabilitation of the structure was taken. The paper presents some aspects of old structure’s strengthening and reconstruction works.

In the article “Considerations Regarding the Rebuilding of a Prestressed Concrete Bridge Damaged by High Floods” **Mata Iulian** presents the problems encountered in Buzău, to the bridge on the county road DJ102B crossing the Basca Chiojdului River.

After presenting the general hydrological conditions in 2005 over the country, the author focuses on the damages that the floods produces on the selected bridge and solutions that the experts found for getting this structure opened for traffic.

The importance of this example arise from the fact that the same situation is relevant to and coincides with many other of the cases met during the period of February-September 2005: the lack of bank protection, the insufficient draining section or the insufficient foundations of the infrastructures contributing decidedly to bridge damaging.

The author concludes that this effort has two main causes:

- The lack of involvement from the part of administrators in actions of maintenance and periodical or capital repairing of bridges and bank protection devices, their accentuated decay eventually leading to the construction’s lack of protection in front of high floods and finally ending in its collapse.

- Forest cutting and non-corresponding agricultural works that facilitate the process of corrosion which, in turn, leads to increasing the coefficient of water flowing down slopes carrying great amounts of alluvia and floating debris that affect the structure of the bridge and seriously erode the foundations or clog the span of the bridge.

Mario Paolo Petrangeli, Luigi Fieno, Ciprian Dan Loata present the paper “Seismic isolation of the Italian bridge: A case study”.

The seismic isolation of a structure represents a very efficient technique to guarantee security against collapses and damages to persons and/or other structures in case of a catastrophic seismic event, and it is therefore expressively suggested by normative, especially in sites of medium to high seismicity. In the case of bridges and viaducts such technique finds its natural implementation due to their “mono-dimensional” conformation and their structural response. The new Italian seismic legislation, adhering to international regulations and specifically to the Eurocodes approach, proposes two main methodological approaches for the dimensioning of bridges under seismic actions: “elastic” or “ductile”.

The article describes the 777m long Vomano viaduct and the 2504m long Sant’Antonio viaduct which, together with Carestia Gallery represent the main structures for the completion of the doubling of Teramo – L’Aquila motorway in the Appennini tract. The conditions, the calculations and the solutions are included.

The authors wish to synthesize the Italian experience in bridge seismic isolation by defining a relatively less expensive technique which, in association with a correct design approach, as well as a correct construction procedure, allows to effectively and elegantly solving the issue of conformation to seismic regulation even for large structures.

Romanescu Claudiu et. al. treat the subject of scouring at bridge. In their article, “Conditions to apply different methods of elimination of scouring of infrastructures of road structure”, they deal with the stability of the structures. It is widely known that most of the bridges failed because of the problems in the water channel. Therefore, the paper presents a method to select the optimal solution according to the type of scouring, configuration of the channel, to offer to the administrator a decision instrument based on scientific knowledge.

4. MATERIALS FOR BRIDGES

Marinela Bărbuța and Lepădatu Daniel in their paper “Polymer concrete optimization using mixture design of experiment and response surface methodology” present the use of statistical technique to analyze data from mixture experiment design and involve regression models to determine the response surface of polymer concrete. The experimental studies were realized on polymer concrete prepared of epoxy resin, silica fume and aggregates. The combinations were designed based on the mixture design concept of design of experiments. For each polymer concrete combination, the mechanical properties were studied. The results are reported for polymer concrete realized of epoxy resin and silica fume (SUF) as filler. Each response (mechanical property) was individually optimized and compared with experimental data.

The article “Friction Stir Welding – an innovative solution for civil engineering” of **Ramona Gabor, Anca Gido, Radu Bancila**, presents the method of Friction Stir Welding (FSW). This method conquered the interest of the industrial companies because the good quality of the weld and because it possible to weld components with high requirements as regard compression strength and tightness. The process is a solid – state one, being considered an ecological process. The applications to the industrial scale are known in aircraft industry, automotive industry and shipbuilding industry. Since the aluminum becomes more often used in civil engineering, FSW presents interest also in this domain. Two of the big number of aluminum alloys that can be welded with FSW seems to be most indicated for superstructure of the bridges: AA 5083 and AA 6082. These two alloys have a very good behavior to corrosion – one of the biggest problems of steel bridges. This paper presents the future welds that can be used for bridge constructions.

The paper of **Pavla Matulova** is “Repair of subbase by large – sized grouting and potential use of recycled raw materials as substitution of binding components of grouting materials”

The cracks and caverns of different types belong to the most frequent failures within concrete, reinforced concrete and masonry structures. These can appear also in the bottom surface, in rocks and grounds under the structure. Very efficient method of these failures rehabilitation is the grouting with a medium which has better physical properties than the original structure. The paper describes the possibilities of grouting strategy and especially the development of new progressive materials containing different by-product (fly ash, washing wastes, foundry sand, slag etc.) under respecting the increase of quality. Attention was paid especially to properties of the fresh mixture namely to the setting time of modified

materials and to the fulfillment of demanded physic-mechanical parameters of the hardened mixture. Particular formulae were designed following optimization calculations for the broad utilization in practice.

In the article „Slip-resistant Surface Treatments on Bridge Construction Walking Areas – the First Stage” Vít Petránek and Tomáš Melichar deal with the problem of the construction completing period of bridge structure, whereas research of suitable slip-resistant surface treatment for bridge sections, where it is demanded or appropriate.

Contribution of the research performed within the paper is secondary raw material (SR) utilization on the surface treatment preparation. Primarily optimal SR was selected, which was then applied in suitable specific proportion and grain size to prepared matrix (epoxy resin). In the next phase of the research, basic properties determination of the prepared mixtures was carried out, i. e. tensile strength by rip off test by another name standstill to bedding. During the last one stage some tests, which are characterising durability of investigated surface treatment, will be performed, concretely abrasive and frost resistance.

5. METHODS OF CALCULATION AND DESIGN

Ștefan I. Guțiu, Petru Moga and Cătălin Moga present the paper „Fatigue design considerations of the steel plate girders”.

This article presents the fatigue checking methodology of the steel bridge members according to Romanian norm SR 1911-98 and EC 3. A comparative analysis regarding the fatigue checking of the main girders of a 30 m span steel railway bridge is made. The concluding remarks and observations are useful in the design activity of this type of structures.

Călin Mircea and M. Filip, in their article “Research upon the Cracking Induced by Restrained Contraction of Mass Concrete Elements”, present aspects of an investigation made upon the cracking states induced by early age restrained shrinkage of concrete, at the piers and abutments of the bridges from the new Transylvania Motorway, Romania. The National Building Research Institute [INCERC] Cluj-Napoca Branch and Technical University of Cluj-Napoca performed the investigation at the request of the general contractor Bechtel International Inc.

At approximately one month age of concrete, crack widths range between 0.05-0.5 mm were observed. The paper emphasizes the analyses, interpretations and analytical predictions for the future progress of the cracking states, based on the

data acquired from the technical documentation supplied by general contractor, and monitoring of the crack widths.

The good match of theoretical results with the real registered data led to the conclusion that cracking states are caused mainly by restrained volume contraction within the first week. Thus, repair measures could be done in time and the normal progress of the works continued.

Mircea Suciu presents the paper “Comparison between the parabolic counter deflection and the one made up of the average deflections in the case of a high speed railway bridge”. The paper analyses two shapes of counter deflection from the point of view of the vertical deformations railway bridge. The bridge has a 50m span and is made of steel-concrete without ballast bed. The purpose is to make the decision over introduction of the high speed trains.

In the article “The analysis of the compatibility of rotations within plastic hinges from reinforced steel structures” **Constantin Amariei and Ioan Buliga** present the possibilities for the assessment of the actual rotations and rotation capacity for the verification of the fulfillment of the compatibility condition of these deformations, one of the stages from the analysis of the behavior of reinforced concrete and steel structures in the post-elastic field.

Relations of cause deformations are presented in the likeness of dot-matrix in the sight used the automatic calculus.

6. MODELLING IN BRIDGE ENGINEERING

Gavris Ovidiu is included in the symposium with the article “Using the finite strip method in determining the static response of the deck bridges”

The paper presents aspects related to using the Finite Strip Method in obtaining the static response (static displacement or static moments) of the road deck bridges, having various forms (rectangular, oblique or trapezoidal plates), a constant or variable thickness and various boundary conditions.

The method has a good apply to the deck bridges, modeled by orthotropic and isotropic plates and the results are very similar to the ones obtained through the analytical calculus.

Păuleț-Crăiniceanu Fideliu makes an “Analysis of active seismic response for controlled structures using stochastic models”.

This paper investigates the seismic response of active controlled structures using a stochastic approach. The study is at a starting point for the author and it is intended to focus on principles and methodologies for simple structures and simple active control strategies. Also, the study is envisioning validating stochastic domain strategies for active controlled structures that have been already validated in time and frequency domains.

The article is based on the wide experience of the author in structural active control. A stochastic approach for the seismic response of structures with active control is proposed. The seismic action is described as a system with a white noise input and a seismic-like time-history response. A non-negative envelope function is modeling the input stationary random process.

Application of the methodology on very simple structures is in the views in order to begin a longer term investigation in the field. The main results show the differences between the controlled and the non-controlled cases.

From the stochastic point of view, results show that the active controlled structures behave very well. It is confirmed that this type of analysis is very useful in judging a control methodology together with other analysis as time-history response and/or frequency response analysis.

Rodian Scînteie, Constantin Ionescu, Cristina Romanescu and Claudiu Romanescu in their article “Subjective and uncertainty in bridge assessment” deal with the problem of the difference in output of specialist when assessing the bridge stock. Due to the fact that most of the bridge evaluations are made through visual inspections, the process becomes a highly subjective one. The article makes a comparison between the evaluation using directions of the AND522 regulation and the specialist opinion. A way to calibrate the provision of the regulation was proposed.

One of the most important factors for final surface quality in concreting of large dimension slabs is to secure minimum vaporization of water and limit the undesirable tensile and compressive stresses in concrete structure which can be formed by quick drying of the concrete surface. Only purpose of ordinary type of treatment for fresh concrete is to secure sufficient amount of water during hydration. These materials have to be removed or left on place to be worn off. **Vít Petránek** in the article “Surface application of polymer coating for concrete curing” presents new material, based on polymer resin, which has been developed to keep necessary amount of water to secure proper hydration process in concrete. The intended use of the newly developed product is mainly for horizontal concrete slabs, floors. Polymer is applied onto fresh concrete before or during final surface treatment. Main aim of the research described in the proposed paper is to evaluate

effect of polymer on vaporization and with consequences on hydration process. Different amount of dosage of treated and not treated concrete were compared. Paper also describes three different testing methods of evaluation. Main advantage of this product is that this product can be also used as final treatment of concrete with good quality and appearance but also as bonding agent for following polymer layers.

7. TESTS AND MEASUREMENTS FOR STRUCTURES

Petr Kalvoda, Miroslava Suchá, Josef Podstavek, and Jiří Vondrák present “Photogrammetric measurement of deformations during the load test of brick vault”. The area of constructional element strengthening and subsequently strengthening of construction has been researched many times. These techniques lead so far to dimensional redesigning of the construction. Usage of the new technological procedures and especially utilization of new materials allows keeping existing dimensions of the construction. Their project is part of research project focused on additional strengthening of engineering construction particularly on monolithic concrete and brick construction. Few methods were used parallel together: tensiometric measurement, electronic tacheometry, very precise levelling and digital method of close range photogrammetry. The method of close range photogrammetry was used again as a complementary method just for data comparison and for photogrammetric technology improvement in application demanding high precision.

Mircea Călin and M. Filip M. in their article “Service Tests on PC Beams” present aspects from the testing of full scale PC prefabricated bridge girders, to be used at the new Transylvania Motorway. The tests were performed by INCERC Cluj-Napoca, at the order of Bechtel International Inc., general contractor and producer of the prefabricated units. The paper aims to offer to the specialists valuable experimental data, obtained through state of the art testing techniques.

General frame and testing conditions, the paper continues with a comprehensive presentation of the tested PC girders, based on the design documentation, a non-linear evaluation and records of the producer is presented. Results are emphasized in a synthetic manner, based on graphical figures resulted from digital processing, and commentaries. The paper ends with the final remarks and the acknowledgement bring to the supporting colleagues from the general contractor.

Jana Neumanová is involved in “Geodetic Measurement of Line Constructions for Control and Security of Construction Reliability”.

The report appropriates to theoretic problems (correct terminology) in the area of geometric accuracy that affecting resulting quality the constructions. Further it is aimed to the applications of empirically intended tolerant intervals, especially to the non - parametric methods that it is possible bring to bear into verification of geometric accuracy of the roads and highways. These methods have more general usage, the calculation is simpler and their characteristics are independent on the distribution of basic set.

In the next parts is described graphic model of geometric parameters like possibility to visualization results of geodetic control measuring of geometric accuracy. The graphic model is given from difference measured and project highs of line constructions by the help of izogram for individual constructional section.

Cristina Romanescu et al. in the paper “Condition assessment of reinforced concrete bridges using nondestructive testing techniques” treats the fact that a realistic and reliable assessment of a damaged bridge structure must comprise the evaluation of bridge condition, load bearing capacity, remaining service life and functionality. This paper present defects, the factors having strong impact on the deterioration and different nondestructive testing techniques used in the assessment of concrete bridge structure and promote the ability of these methods to detect defects with varying precision.

Defects evaluation should be done for individual structural materials with respect to the damage type, its intensity and extent and to the affected structural element.

Bridge engineers involved in the routine or extraordinary inspection of bridges have to take correct and reliable decision about the defect type, the associated deterioration process, the relevant cause and possible propagation of the damage in the future. This evaluation should be not based only on the expertise, engineering judgment and experience of the inspector.

Road Diagnostics - Ground Penetrating Radar Possibilities

Josef Stryk

*Josef Stryk, CDV - Transport Research Centre, v.v.i., Infrastructure and Environment Division,
Lisenska 33a, 636 00 Brno, Czech Republic, tel.: +420 549 429 330, e-mail: josef.stryk@cdv.cz,
skype: josef.stryk.cdv*

Abstract:

GPR (Ground Penetrating Radar) is non-destructive equipment coming to be accepted in diagnostics of road structures. The paper describes state-of-the-art of a GPR usage in several European countries in this field. Beside basic GPR applications in the field of road diagnostics like a determination of pavement layer depths and a location of joint dowel bars in concrete pavements the more complicated application possibilities are mentioned such as detection of voids under the concrete slabs of rigid pavements, detection of excessive amount of water in structural layers of pavements, determination of crack depth in the bituminous layers etc.

The situation in the Czech Republic is described in the paper and some projects concerning GPR testing, the author participated on, are mentioned.

KEYWORDS: NDT, Non-destructive testing, GPR, Ground Penetrating (Probing) Radar, Pavement diagnostics, PMS, Pavement Management System

1 GPR INTRODUCTION

Ground Penetrating Radar (GPR) is equipment, which uses high frequency electromagnetic waves. In combination with a suitable software it provides evaluation of electrical and magnetic features of studied environment. GPR has the highest resolution from all geophysical methods used in non-destructive diagnostics.

Boom in GPR usage started with commercial selling of this equipment by American company GSSI in 1972. GPR started to be used in a lot of different areas. One of these areas is diagnostics of roads and bridges.

A use of GPR in the field of road diagnostics is common today [1], while GPR usage in the field of bridge diagnostics is ordinarily limited to a pavement and a bridge deck control [2].

2 DIFFERENT INPUTS TO PMS

One of the main inputs to Pavement Management System are results of road condition measurements.

Road diagnostics is realized both on project level (mostly local) and network level (continuous). The diagnostics on project level is commonly realized on selected places where some problems occurred or on chosen sections with connection to planning of maintenance, repair or reconstruction. The diagnostics on network level is normally carried out at a primary road network (motorways, high speed roads, etc.).

Typical areas which are realized as a part of diagnostics on network level are:

- a) visual inspection (basic diagnostic method),
- b) unevenness and macrotexture (riding comfort and safety),
- c) skid resistance (safety).

In addition there are other diagnostics methods which are carried out locally:

- d) bearing capacity (durability; LCA: life cycle analyse),
- e) diagnostic of pavement structure (layer composition, localization of structural defects, etc.),
- f) noise - wheel/surface interaction (environmental friendliness),
- g) analyze of cores (real structure of the pavement), etc.

It is evident that a preference is given to nondestructive diagnostics methods, mostly to the methods that do not disturb the traffic on roads. For area a, b, and c the measurements are normally realized under the traffic speed. For area e and f there are already some systems allowing traffic speed measurements (up to 80 km/hour). We still cannot exclude some destructive methods from road survey, the basic one is taking of cores.

The common equipment used in the Czech Republic for individual areas mentioned above are as follows:

- area a, b: ARAN: Automatic Road Analyzer, ARGUS: Automatic Road Condition Graduating Unit System (traffic speed measuring cars),
- area c: TRT: Czech measuring car, SCRIM: Sideway-force coefficient routine investigation machine (traffic speed measuring cars),
- area d: FWD: Falling weight deflectometer or deflectograph (local and slow speed measuring equipment),
- area e: e.g. GPR system with dipole or horn antennas (local or traffic speed measuring equipment),

- area f: SPB: statical pass-by method (measuring system situated near a road) or CPX: close proximity method (traffic speed measuring trailer or car),
- area g: local analyse by drilling rig.

There are some innovations in this field currently realized abroad. Two basic ones are mentioned below.

In the field of bearing capacity measurements two prototypes of high speed deflectograph exist which allow a traffic speed measurement. The owners of them are DRI (Danish Road Institute) and TRL (Transport Research Laboratory - UK). This method is based on contactless measurement with the help of new lasers. This measuring car is currently in the stage of testing and calibrating.



Fig. 1 - GSSI integrated system: measurement of bearing capacity by FWD and diagnostics by GPR

In the field of GPR usage there are developed multichannel systems with an autocalibration function in TRL. In some cases there are produced combinations of more measurements within one measuring car. Figure 1 shows the combination of GPR and FWD - producer: American company GSSI: Geophysical Survey Systems, Inc.

3 ROAD DIAGNOSTICS BY GPR

In Europe and USA there is popular using of horn antennas, which are placed 300 - 500 mm above the pavement surface (for continual measurements). In United Kingdom there are much popular dipole antennas. Better results are obtained in case that a dipole antenna is placed directly on the pavement surface (for continual measurements it is placed approximately 30 mm above the pavement surface). Figure 2 and 3 shows examples of horn and dipole antennas which are used in German institute BAST: Bundesanstalt für Straßenwesen.



Fig. 2 - 2 GHz GSSI horn antenna: attachment to the measuring car



Fig. 3 - 1,5 GHz GSSI dipole antenna: measuring in test pit

It is possible to measure locally or continually. In case of continual survey the GPR system is fixed to an auxiliary equipment or to a measuring car. Survey is carried out in a slow speed (from walking to 25 km/h - mostly dipole antennas) or in a high speed (80 km/h and more - mostly horn antennas). The main advantage of the high speed survey is fact that you do not need to close a measured road.

One of the first application of GPR in the field of road diagnostics was location of joint dowel bars in rigid roads [3] and determination of pavement layer depths [4]. Currently a GPR application in those areas is used ordinarily. The interpretation of measured data is mostly sufficient (frequency range of antennas in GHz, a controller capable to operate more channels simultaneously, 3D software, etc.) [5].

Figure 4 and 5 shows radargram example with indication of layer depths and GPR data interpretation in MS Excel sheet.

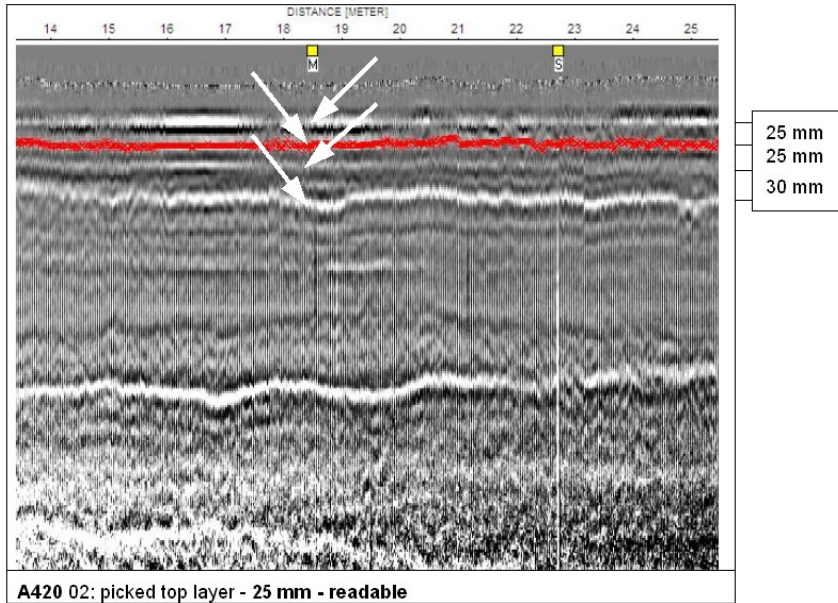


Fig. 4 - Radargram example: measurement of layer depths by 4 GHz antenna

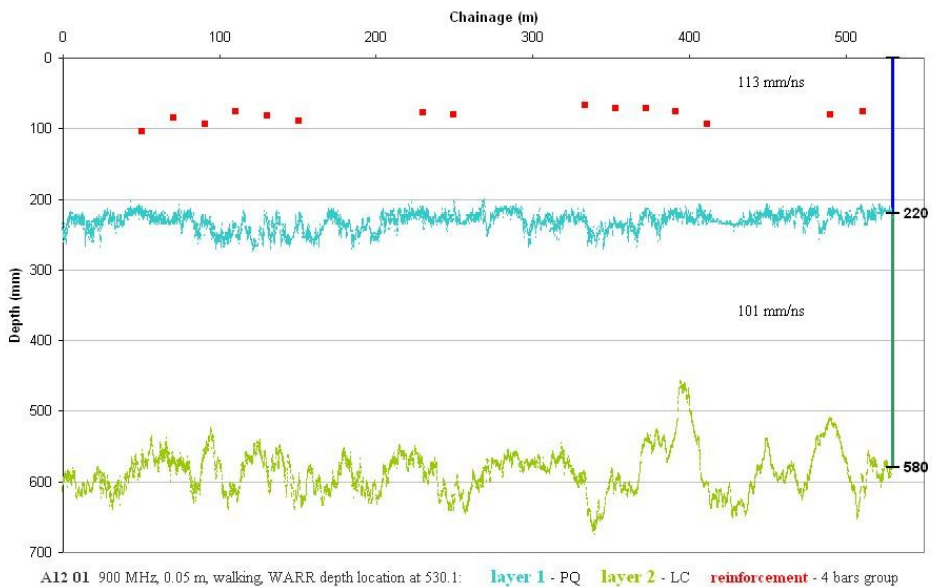


Fig. 5 - GPR data interpretation in MS Excel: location of rebar in rigid pavement, determination of pavement quality concrete depth and lean concrete depth, calibration by core

The other contribution to the development of GPR systems was usage of antennas' array, see figure 6. On the base of its usage it is possible to carry out autocalibration of layer depth measurements. The main advantage is minimization of needed cores along investigated area [6].

The current experience indicate that the accuracy of determination of roadbase depth is approximately 5 %, in case of slow speed measurements and up to 10 % in case of high speed measurements. For the lower layers the accuracy is between 10 and 30 % in dependence on used velocity of measurement [1].

During the high speed measurement it is possible to locate bigger defects. The smaller defects can be detected but you have to use smaller measurement speed. The main disadvantage of slow speed measurements is a limitation of traffic and a need of road closures.

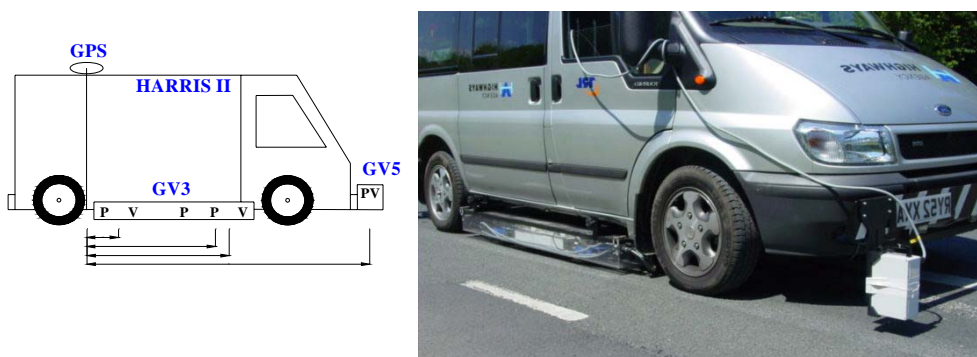


Fig. 6 - Four-channel system used in TRL: attachment to measuring car Harris (photo TRL)

Currently, researchers are dealing with application of GPR in further areas on several places all around the world. These areas are:

- detection of voids under roadbase of rigid pavements,
- detection of excessive amount of water in structural layers of pavements,
- determination of crack depth in the bituminous layers, etc.

3.1 Detection of voids under roadbase

The formation of voids under roadbase of jointed unreinforced concrete pavements is caused by movement of concrete slabs, high loading or poor subgrade/ subbase. The project dealing with detection of such voids was solved in TRL in 1993-1994. The applied system was capable to detect air voids of 30 mm thick. In case of voids filled with water it was possible to detect voids of 10 mm thick. With the use of current more sophisticated technique these numbers should be even lower.

3.2 Detection of excessive amount of water

Problem of detection of excessive amount of water in structural layers of pavements is directly connected with underdrain problems. In TRL in 1993 there was carried out project focused on detection of water table, which was based on evaluation of changes in EM wave velocity. A disadvantage of this research is a need for more comparative measurements (in the period with minimal rainfall and in period with maximal rainfall). A project dealing with determination of road subgrade moisture was realized in 2001 in TRL. The comparison of signals reflected from interface between the granular foundation layer and the overlaying layers were carried out. This method has the following limitations: there is need for more comparative measurements (dry and wet season), there are difference in absorption of the GPR signal by overlaying bituminous layers on different sites. Currently there is third project in progress. The change in the frequency content of the radar signal reflected from the foundation layer is investigated. The research is realized also at other places [7].

3.3 Determination of crack depth

For a long time a visual control was the only possibility for a road crack monitoring. Subsequently a software for a processing of video records during continuous survey was used. It was able to detect cracks but it was not able to determine their depth. Company Utsi Electronics Ltd. in cooperation with TRL researches started to develop GPR system for determination of crack depths in 1999. At present it is capable to detect cracks depth higher than 25 mm, better results are obtained with 50 mm and deeper cracks [8]. The research is still in progress. Picture of equipment is shown at figure 7. An example for comparison of results with a core taken from the measured place is shown at figure 8.

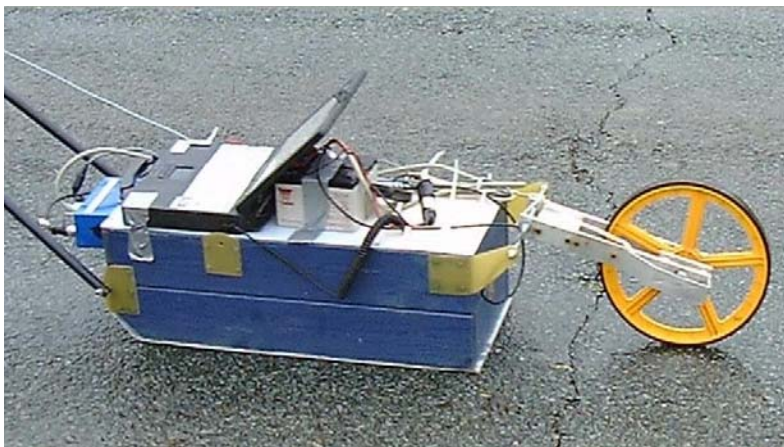


Fig. 7 - GPR crack depth detector (photo TRL, Utsi Electronics)

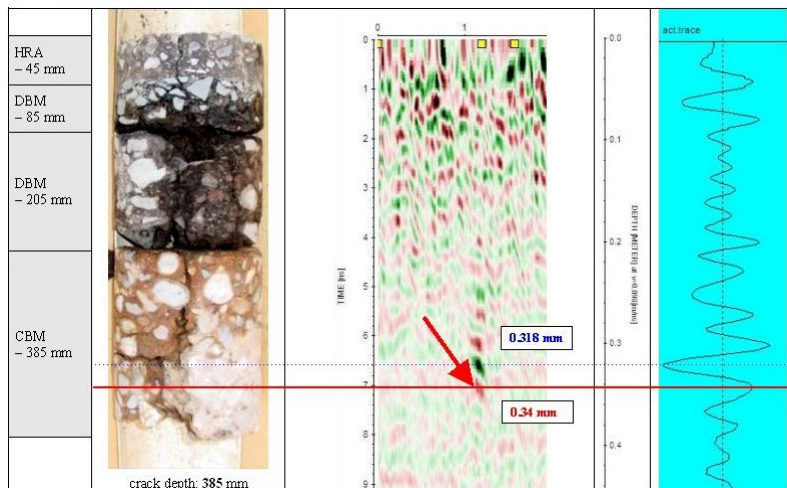


Fig. 8 - Result of crack depth survey: core, radargram, signal from one shot (location of the signal in the radargram is marked by the arrow)

4 OTHER GPR TOPICS

There are specific topics in the field of GPR road diagnostics which should be improved and further developed. The basic ones are mentioned below:

- influence of measurement speed on quality of GPR data (different sampling frequency),
- localization of measured data during high speed measurements (usage of measuring wheel, GPS and other systems),
- data interpretation and automation of this process (filtering, gain, etc.),
- autocalibration of layer and defect depths (using of multichannel systems, and different methods - WARR method: Wide Angled Reflection Refraction Analysis, CMP method: Common Mid-Point method, etc.),

Important area is also selection of correct antennas for specific measurements. This choice will affect the reach of measurement and its accuracy. The basic types of currently used dipole antennas with their basic parameters (wavelength, resolution, penetration) are mentioned in table 1. In the table there are mentioned also parameters of new 4 GHz horn antenna produced by company Utsi Electronics Ltd.

Tab. 1 - GPR antenna types with basic parameters

Frequency	900 MHz	1 GHz	1.5 GHz	4 GHz
Wavelength /mm	136	122	81	31
Resolution /mm	68	61	41	15
Penetration to /mm	1000	800	500	100

5 SITUATION IN THE CZECH REPUBLIC

In the Czech Republic there are some companies which offer GPR road diagnostics. They are commercial companies which are concentrated mainly on determination of pavement layer depths and location of major defects.

In the Czech Republic there are no standard for GPR usage in the field of roads, but there is one standard for diagnostics of railway formation [9]. Figure 9 shows a railway radargram and its interpretation.

In USA they have two standards in the field of road diagnostics [10, 11], in the United Kingdom there are two specifications in Design Manual for Roads and Bridges [12, 13] (parallel with Czech technical specifications of Ministry of transport).

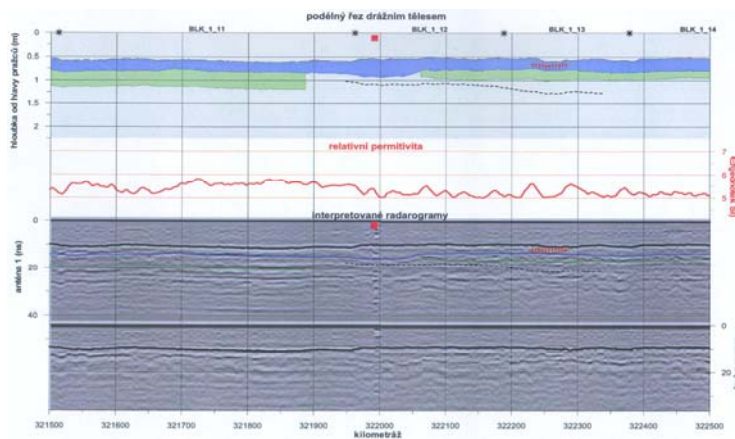


Fig. 9 - Czech Railways: GPR - longitudinal section of railway formation (radargram and its interpretation)

6 CONCLUSION

Usage of GPR in road diagnostics has a big advantage in obtaining of continual information about the structure and defects of measured road sections. Results of measurements are supplemented by information from control cores whose number is minimal. Traffic speed GPR measurements (more than 80 km/h) have positive impact on traffic flow.

Limitation of closures is important factor today. The traffic intensity is increasing every year and therefore the maintenance works and measurements which need a closure even of one lane have very negative impact on it.

Acknowledgement:

The preparation of the article has been supported by the Ministry of Transport of the Czech Republic, under the contract No. MD04499457501 and by European Commission within project TITaM: Transport Infrastructure Technologies and Management.

Foreign experience was obtained during author's secondments in TRL (Transport Research Laboratory, United Kingdom) and BASt (Bundesanstalt für Straßenwesen, Germany) as a part of TITaM project.

References

1. FOREST, R., PYNN, J., ALANI, A., FERNE, B. The Use of Ground Penetrating Radar for the Monitoring of Road Properties. In: *TRL annual research review 2003*. Crowthorne: TRL, 2004, pp. 25-37.
2. HUGENSCHMIDT, J. A One-to-one Comparison between Radar Results and Reality on a Concrete Bridge. In: *9th International Conference on Ground Penetrating Radar*, 29 April - 2 May, 2002, Santa Barbara, USA, CD-ROM.
3. UTSI, V., UTSI, E. Measurement of Reinforcement Bar Depths and Diameters in Concrete. In: *10th International Conference on Ground Penetrating Radar*, 21-24 June, 2004, Delft, pp. 659-662.
4. AL-QADI, I. L., LAHOUAR, S., JIANG, K., MEGHEE, K. K., MOKAREM D. Validation of Ground Penetration Radar Accuracy for Estimating Pavement Layer Thicknesses. In: *84th Annual Meeting of Transportation Research Board*, January 9-13, 2005, Washington, D.C., CD-ROM.
5. FAN-NIAN Kong. Choice of Antenna Type and Frequency Range for Testing of Concrete Structures. In: *8th International Conference on Ground Penetrating Radar*, 22-26 May, 2000, Gold Coast, Australia, CD-ROM.
6. GREEN, R., LUND, A., BIRKEN, R. Generation of Utility Mapping Data via Processing of Multi-Channel Signals Collected by Arrays of GPR and EM Antennae. In: *85th Annual Meeting of Transportation Research Board*, January 22-26, 2006, Washington, D.C., CD-ROM.
7. MASER, K., WEIGAND, R. Ground penetrating radar (GPR) investigation of a clogged underdrain on interstate I-71. In: *85th Annual Meeting of Transportation Research Board*, January 22-26, 2006, Washington, D.C., CD-ROM.
8. FOREST R., UTSI V. Non destructive crack depth measurements with Ground Penetrating Radar. In: *10th International Conference on Ground Penetrating Radar*, 21-24 June, 2004, Delft, pp. 799-801.
9. Directive of Czech Railways: Usage of non-destructive geophysical methods for diagnostics of railway formation, 2006
10. ASTM D 6432: Standard guide for using the surface ground penetrating radar method for subsurface investigation, 1999.
11. ASTM D 6087: Standard test method for evaluating asphalt-covered concrete bridge decks using ground penetrating radar, 2005.
12. Design Manual for Roads and Bridges: 7.3.2 Structural assessment methods - annex 5 HD 29/1994 - Ground Radar for non-destructive testing.
13. Design Manual for Roads and Bridges: 3.1.7. Advice notes on the non-destructive testing of highway structures - advice note 3.5 BA 86/2004 - Ground Penetrating Radar.

Road design for sustainable transport promotion

Rudolf Cholava, Michal Matysik and Petr Smekal

Transport Research Centre, Lisenska 33a, 636 00 Brno, Czech Republic, rudolf.cholava@cdv.cz

Summary

In the paper there are presented results of selected research projects being carried out by Transport Research Centre (CDV) together with other partners, which are focused on road design from the point of view of sustainable transport promotion. These projects, both at national and international level, are targeted at increasing energy efficiency and savings in road designs, the aim is to facilitate and promote integrating energy aspects into this field. Energy issues relating to route selection, construction energy usage and vehicle energy usage are respected. Noise from road traffic, included in other ongoing projects, is also a very important aspect which has to be reflected in road designs. There is a wide range of relevant measures for road traffic noise abatement e.g. low-noise pavements etc., which can achieve reduction of noise burden from road transport in the different extent. The integration of the mentioned aspects and findings from the presented projects into road design will contribute to reducing environmental burden resulted from transport and thus to promoting its sustainability.

KEYWORDS: road design, energy efficiency, traffic noise, noise mitigation, road surfaces.

1. INTRODUCTION

The development of transport brings together with positive effects also the amount of negative impacts, including high energy consumption in the transport sector and the excessive noise burden especially in the vicinity of roads.

Reduction of non-renewable energy sources consumption in transport significantly relates to increasing energy efficiency during construction and operation of roads. In the contribution there are presented results of selected projects being carried out by Centrum dopravního výzkumu (Transport Research Centre) together with other partners, which are focused on integrating energy aspects into road design. The most important of them are as follows: the international project „Integration of the Measurement of Energy Usage into Road Design“ (IERD) [1] in the frame of the SAVE programme – the programme of the European Union aimed at promotion of increasing energy efficiency and savings in particular sectors including transport,

and also the national project „Transport and Environment“ [2] launched by the Czech Ministry of Transport. These projects are focused on increasing energy efficiency and savings in road designs, the aim is to facilitate and promote integrating energy aspects into this field. Energy issues relating to route selection, construction energy usage and vehicle energy usage are respected. Reduction of construction and vehicle energy consumption represents the contribution to reducing environmental burden resulted from transport and thus to promoting its sustainability.

Creation of the methodical guidance, which will enable the elaboration of noise action plans for the vicinity of transport infrastructure according to Directive 2002/49/EC and the systematic approach to the management of traffic noise in accordance with the directive, is the main objective of the next presented ongoing research project „Methodology for elaborating action plans for the neighbourhood of major roads, major railways and major airports“ [6]. The project is supported by the Czech Ministry of Transport which is designated as the competent authority for the development of action plans for major roads, railways and airports specified by the directive and the project is being worked out by the team from Transport Research Centre (CDV) together with other partners. Significant reduction of road traffic noise is feasible in dependence on the suitable road surface type, this issue is being solved in the frame of another research project of CDV titled “Optimisation of technical traffic noise mitigation measures in the neighbourhood of roads”. The aim of the project is to determine and evaluate the relation between technical parameters of road surfaces and traffic noise and the optimisation of these parameters for minimizing noise burden caused by transport.

2. ENERGY ASPECTS

2.1 Particular route options and construction energy usage

In the field of construction energy usage there were identified actions which are essential for the assessment of energy consumption and for the serious explanation of different construction energy usages of particular options. Road construction is split into 6 sectors: drainage, services, earthworks, pavement, road markings and traffic signs and structures. The relevant equipments were specified as well, including specification of their output power and energy or fuel consumption.

In the frame of the project, 2 route options of the Motorway R43 (Figure 1) were assessed: Variant D (“Bystrcká) and Variant F („Holedná“). Road alignment and specification of assessed sections of the presented Variant D are given in Figure 2,

basic input data for calculation of construction energy usage of the mentioned variant are given in Table 1.

Table 1. Energy for Construction – Works (Variant D)

Sector	No.	Item & Description	Units	Total Energy (MJ/Item)	Total Energy per Sector (TJ/Sector)
Drainage	02	Culverts incl headwalls	m	22248	3,46
	03	Retraining watercourses	m ³	46272	
	04	Ditches incl outfall	m	383088	
	05	Piped Drains incl manholes	m	3018272	
Services	07	Install ducting for Utilities	m	740215	0,74
Earthworks	09	Strip Topsoil incl site clearance	m ²	1162562	224,48
	10	Tree Felling	nr	3263131	
	11	Break up any redundant pavement	m ³	6252439	
	12	Excavation Type C material	m ³	0	
	13	Excavation of Type B material	m ³	5965772	
	14	Excavation of Type A material	m ³	10635300	
	15	Disposal of contaminated material	m ³ km	4895748	
	16	Disposal of Unacceptable material	m ³ km	78331968	
	17	Deposition of acceptable material in embankments and other areas of Fill	m ³ km	102480449	
	18	Deposition of acceptable material in Landscape Areas	m ³ km	1436292	
	19	Import acceptable material in and under embankments and other areas of fill	m ³ km	123172	
	20	Compaction in layers of acceptable material under embankments and other areas of fill, in capping areas and landscape areas	m ³	4778881	
	21	Vertical Drains	m ³	0	
	22	Geosynthetics	m ²	527026	
23	Topsoiling	m ²	3499610		
24	Landscaping	m ²	1137373		
Pavement	25	Sub - base in carriageway, hardshoulder and hardstrip	m ³	11255520	38,31
	26	Soil Stabilisation	m ³	2877395	
	27	Put Down Road Base	m ³	12427215	
	28	Put down Base Course	m ³	6628251	

Sector	No.	Item & Description	Units	Total Energy (MJ/Item)	Total Energy per Sector (TJ/Sector)
	29	Put down Wearing Course	m ³	4192725	
	30	Put down concrete kerbs where required	m	733268	
	31	Put down concrete footpaths where required	m ²	200698	
Road Markings Traffic Signs	32	Road Lining	m	194141	2,01
	33	Road Signing (each junction)	nr	1809844	
Structures	34	Bridges up to 10m span	m ²	124586169	238,11
	35	Bridges 10 - 50 span	m ²	71955961	
	36	Bridges > 50 span	m ²	31753588	
	37	Concrete median barriers	m	995628	
	38	Retaining Walls	m ²	8821098	

In Table 1 there are outputs from calculations for particular works and sectors. It is obvious the different energy consumption in particular sectors and thus their potential for energy savings. Regarding to the high energy consumption in the earthworks sector, pavement and structures sector, it is important to put attention especially on these fields.

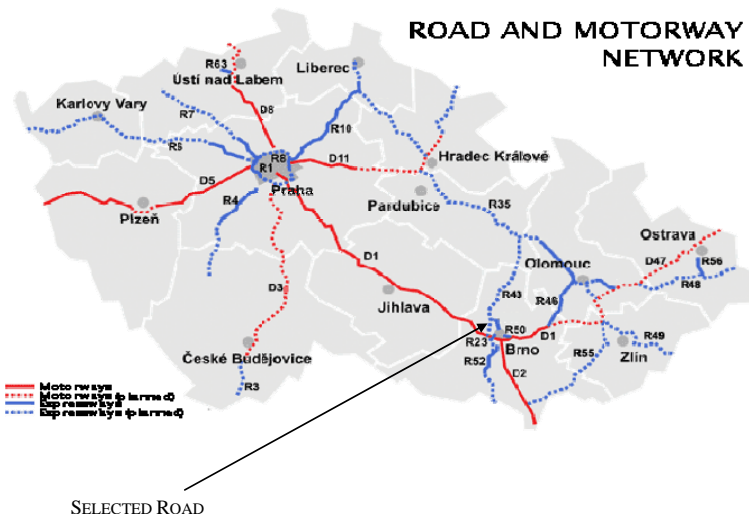


Figure 1. Location of the evaluated Motorway R43 in the road and motorway network in the Czech Republic

ROAD R43
variant D (.....)
year 2010

Traffic Volumes:
Total number of
vehicles/number
of heavy vehicles
[thousands/24h]

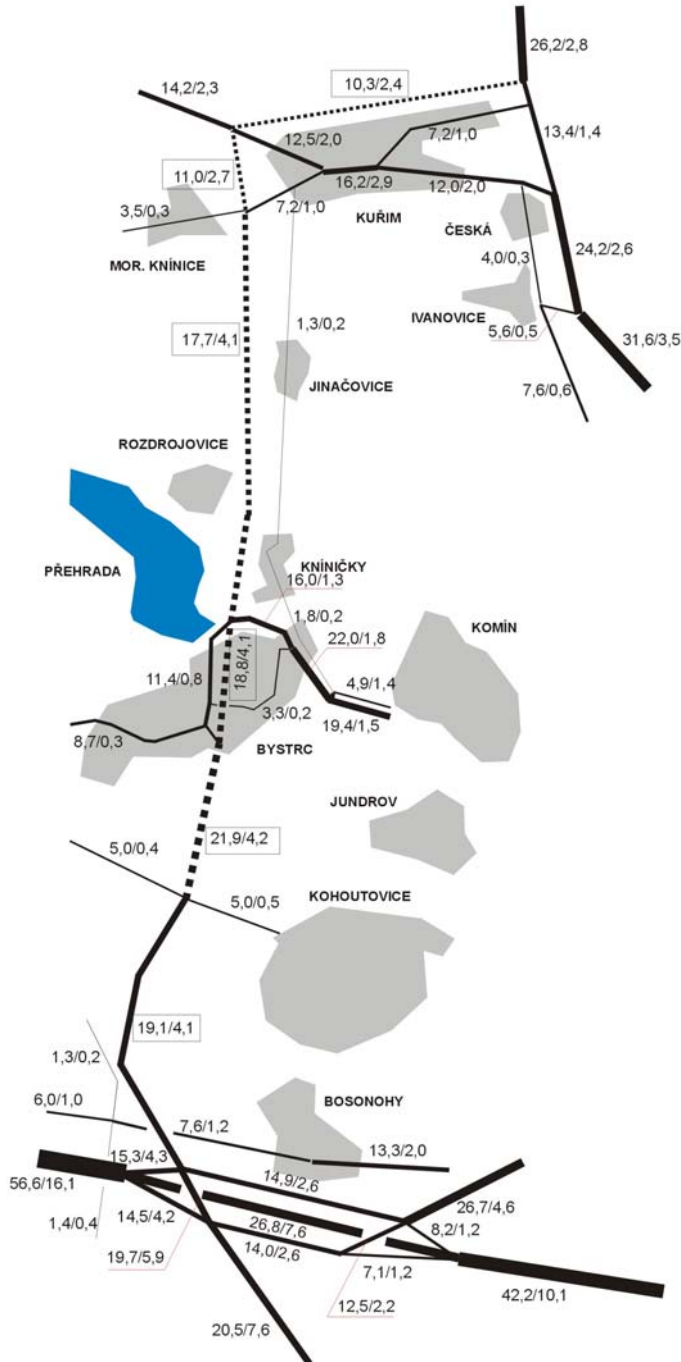


Figure 2. Road alignment and specification of assessed sections (Variant D)

2.2. Particular route options and vehicle energy usage

Special stress was laid on vehicle operation energy of particular route variants of designed roads for their assumed lifetime. The VETO programme was applied for modelling traffic operation [1]. The following three programmes were evaluated in detail from the point of view of their application in the project: the HDM programme (Highway Development and Management system [3]), the CMEM programme (Comprehensive Modal Emissions Model [4]) and the VETO programme.

In the evaluations the attention was paid especially on how these softwares meet the necessary requirements i.e. to model the energy used by vehicles considering all essential aspects, have open interface and be compatible with relevant software systems.

Based on the evaluations, it was decided to use the VETO programme to model traffic operation on a road. The programme calculates energy respective fuel consumption for optional routes on the basis of input data which include vehicle and road parameters, information on driver behaviour, meteorological conditions and parameters of traffic stream.

The calculations for the input data of designed options D and F of the Motorway R43 were followed by other calculations, which were focused on the exploration of the influence of selected road parameters on vehicle operation energy.

The impact of road gradient, vehicle speed etc. were analyzed in detail, these simulation calculations were carried out for the route option D of the mentioned Motorway R43 [5] and were realized in close cooperation with the Swedish authors of this software.

Table 2 summarizes energy use for all vehicles and presents the results of energy use on particular route sections and finally the total energy use for road traffic per year and road in 2010.

Table 2. Total energy use for all vehicles (Variant D, Year 2010, Speed limit 90 km/h)

Section		Energy use for all vehicles		
From-to [km]	Length [km]	Per section and day [MJ]	Per road and day [MJ]	Per road and year [MJ]
4,00 – 4,72	0,72	75211,27	731962,96	267166,48
4,72 – 6,41	1,69	115322,07		
6,41 – 7,91	1,50	82431,06		
7,91 – 15,13	7,22	301912,82		
15,13 – 16,91	1,78	54641,75		
16,91 – 20,73	3,82	102444,00		

2.3. Comparison

Comparison of construction energy and vehicle energy for the assessed route options is enabled by Table 3, which contains data recalculated per kilometre.

Table 3. Comparison of energy consumptions

Route Variant	Road Type	Placement Energy [TJ/km]	Material Energy [TJ/km]	Total Construction Energy [TJ/km]	Total Vehicle Energy 2010-2029 [TJ/km]
Variant D	motorway	30,32	3,09	33,41	386
Variant F	motorway	20,70	3,09	23,79	543

The comparison shows that total vehicle operation energy for the assumed lifetime is approximately 12 times respective 23 times higher than total construction energy and thus it is essential for selecting the optimal variant.

3. NOISE ASPECTS

A wide ranging review of the most important measures, which can achieve reduction of noise burden from transport in the different extent, was carried out in the first stage of the project [6].

This review covered relevant sources of information and also reflected findings and experience of the project team. The output from this initial phase is the database of information sources described later which should be helpful particularly for future developers of action plans.

In the wide field of measures for road traffic noise abatement, which includes measures at sources, on the way of noise propagation and at receivers, there exist different approaches to classifying those measures. In the project the hierarchic approach was respected and anti-noise measures were split into the following categories regarding the priorities:

- urban-architectural measures,
- urban-traffic measures,
- traffic-organizational measures,
- building-technical measures.

Table 4 contains selected measures at the source [6] and shows their potential.

Table 4. Noise reduction at the source (selection for road traffic)

Measure		Local effect [dB(A)]
Low-noise road surfaces		0-10
Traffic management	volume, redirection, by-passes	0-5
	restrictions in time and area	0-15
Speed reduction, traffic flow	speed limits	0-4
	traffic restraints	0-3
	optimal flow, accessibility, green wave	0-2
	road junction design	0-2
	road alignment	0-2
	driver behaviour	0-5

The database of information sources on anti-noise measures, which is based on the carried out review and analyses, is the outcome of this phase of the project. Acoustical situations and the effect of selected anti-noise measures have been modelled by using the software SoundPLAN [6]. Based on the described activities and in accordance with the Directive 2002/49/EC [8], and the Czech legislation, the proposal of the methodology for elaborating noise action plans was worked out. Activities realized in the frame of the following feasibility study of the proposed methodology were focused on the most important selected procedures and measures. The example of the calculation road traffic noise map of town Vysoke Myto, that was chosen for the feasibility study in the field of road traffic noise [7], is presented in Figure 3 for the situation with the proposed bypass.

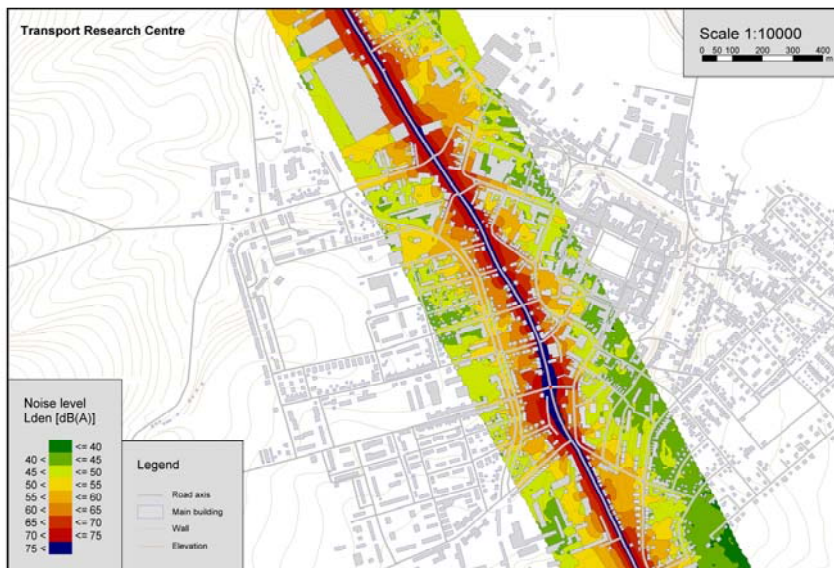


Figure 3. Noise map of town Vysoke Myto (option with the bypass)

The proposed methodology defines steps to develop action plans for the efficient management of noise issues in the specified areas. During the next period this proposal will be refined and modified according to findings from the feasibility study in a selected region and with reference to the development in the legislation.

Determination and evaluation of the relation between technical parameters of road surfaces and traffic noise and the optimisation of those parameters to minimize noise burden from transport represent the aims of the national project No. CG712-102-120 launched during 2007. Two main methods will be used for measuring the influence of road surfaces on traffic noise, i.e. the Statistical Pass-By (SPB) method and the Close-Proximity (CPX) method. At the end of the project, the recommendation for minimizing road traffic noise at the source (tyre/road noise) will be formulated.

4. CONCLUSIONS

The partial results of the mentioned projects, aimed at promotion of integration of energy and noise aspects into road design, are presented in the paper. The outputs enable to quantify energy consumption in all phases of road construction and also vehicle operation energy for the assumed lifetime and thus to assess the energy impacts of particular road designs. This integration and selection of the optimal variant will contribute to reducing energy consumption and thus to reducing environmental burden. Road traffic noise is also a very important aspect that has to be reflected in road designs, reduction of noise burden from road transport can be achieved through relevant measures for road traffic noise abatement. The integration of the given aspects and findings from the presented projects into road design will contribute to reducing environmental burden resulted from transport and thus to promoting its sustainability.

Acknowledgements

This research is supported by the European Commission as the project No. 4.1031/Z/02-091/2002 and by the Czech Ministry of Transport as the research projects No. 4499457501, No. 1F52B/103/520 and No. CG712-102-120.

References

1. Butler, R., Connor, B. P., Timoney, D. J., Jackson, P., Dumas, P., Bollinger, P., Sardinha, R., Hammarström, U., Cholava, R. *Integration of the Measurement of Energy Usage into Road Design*. Final Report. EU SAVE Programme, Project No. 4.1031/Z/02-091/2002. Tramore: THRDO, 2006, 579 p.

2. Adamec, V., Dufek, J., Huzlik, J., Cholava, R., Jedlicka, J., Kutacek, S., Licbinsky, R., Dostal, I., Dvorakova, P., Smekal, P., Pokorna, B. *Transport and Environment*, (In Czech), Technical report of the project No. 4499457501, Part 5. Brno: CDV, 2006, 41 p.
3. Bennett, CH. R., Greenwood, I. D. *Volume 7 – HDM-4 Modelling road user and environmental effects in HDM-4*. Paris: The World Road Association (PIARC), 2001. 374 p. ISBN: 2-84060-103-6.
4. Barth, M., An, F., Younglove, T., Scora, G., Levine, C., Ross, M., Wenzel, T. *Comprehensive modal emissions model (CMEM), version 2.02*. User’s Guide. Riverside: University of California (URC), 2001.
5. Cholava, R., Dvorakova, P., Kalab, M. *Simulation of the effect of selected road parameters on energy efficient driving by applying the VETO programme*. In Butler, R. et al. Integration of the Measurement of Energy Usage into Road Design. Final Report. EU SAVE Programme, Project No. 4.1031/Z/02-091/2002. Tramore: THRDO, 2006, p. 457-478.
6. Cholava R., et al. *Methodology for elaborating action plans for the neighbourhood of major roads, major railways and major airports*, (In Czech), Technical report of the project VaV No. 1F52B/103/520. Brno: CDV, 2006, 64 p
7. Cholava R., et al. *Methodology for elaborating action plans for the neighbourhood of major roads, major railways and major airports*, (In Czech), Technical report of the project VaV No. 1F52B/103/520. Brno: CDV, 2007, 84 p.
8. 2002/49/EC: *Directive of the European Parliament and of the Council of 25 June 2002*, Official Journal of the European Communities. Brussels: 2002.

THE ANALYSIS OF THE COMPATIBILITY OF ROTATIONS WITHIN PLASTIC HINGES FROM REINFORCED STEEL STRUCTURES

Constantin Amariei¹, Ioan Buliga²

¹ Structural Mechanics Department, T.U. " Gh. Asachi " Iasi , 700050 , Romania

² S.C. BULCON GRUP SRL, Constanța , 900132 , Romania

SUMMARY

In this document, are presented the possibilities for the establishment of the actual rotations and rotation capacity for the verification of the fulfillment of the compatibility condition of these deformations, one of the stages from the analysis of the behaviour of reinforced concrete and steel structures in the postelastic field.

Relations of cause deformations are presented in the likeness of dot-matrix in the sight used the automatic calculus.

KEY WORDS: postelastic design, plastic hinge, rotation capacity, compatibility of rotation.

1. INTRODUCTION

The sizing of reinforced steel structures following their calculation in the postelastic field does not provide, implicitly, the fulfillment of all the requirements on which depend the resistance, durability and operation of these structures. These requirements are grouped [5] into:

Requirements of compliance specific to the last stage, regarding:

- the compatibility of the plastic hinges rotations;
- resistance to the action of cross forces;
- the positions of plastic hinges;
- the size of the bolts in the last stage;
- the pillars flexibility in the last stage;

Exploitation requirements, specific to the exploitation stage, regarding:

- the size of the maximum tensions from the stretched reinforcement of critical sections;
- the size of the maximum specific deformation from the compressed concrete area in the critical sections;
- the size of the maximum aperture of the cracks;

- the size of the bolts occurred at nominal loads.

In the paper, is presented the execution of the practical verification of the compatibility requirements concerning the rotations within the plastic hinges. It is about the analysis of the proportion of the maximum rotations developed by the plastic hinges within the reinforced steel structure, in comparison with the rotations imposed on these hinges by the requirement that the structures subsidence be produced through their transformation into mechanisms. Essentially, it is necessary that the maximal rotations possible to be developed by the plastic hinges within the reinforced steel structure be greater or at least equal with the ones necessary for the respective structure to entirely or partially transform itself into a mechanism, meaning:

$$\theta_i \leq \theta_{pi} \quad (1)$$

where:

θ_i is the rotation of the plastic hinge from the critical section “i”;

θ_{pi} the rotation capacity of the plastic hinge from the critical section “i”

The inequality (1) expresses the compatibility of the plastic hinge rotation from the critical section “i”, until the formation of the subsidence mechanism for the respective structure.

Notice: If one of the structure plastic hinges exhausts its rotation capacity before the transformation of the structure into a mechanism, the structure subsides locally under the action of smaller loads than the loads from the mechanism, the local subsidence residing in the collapse of the concrete compressed area on the point where the plastic hinge has outworked its rotation capacity.

2. THE ESTABLISHMENT OF THE ACTUAL ROTATIONS FROM THE PLASTIC HINGES

In any stage of the postelastic behaviour, the structure may exhibit three categories of bars:

a) Bar with rigid joints at both ends

For such a bar (Photo 1a,b,c), the rotation of the bar ends φ_{ij} coincide with the sizes of the elastic rotation of the knots they are part of and the jointing relations between these rotations and the θ_{ij} , θ_{ji} rotations, measured in relation with the line that unites the displaced bar ends and the bar rotation ψ_{ij} are:

$$\theta_{ij} = \varphi_i - \psi_{ij} \quad (2)$$

$$\theta_{ji} = \varphi_j - \psi_{ij} \quad (3)$$

$$\varphi_i = \varphi_{ij} = \theta_{ij} + \psi_{ij} \quad (4)$$

$$\varphi_j = \varphi_{ji} = \theta_{ji} + \psi_{ij} \quad (5)$$

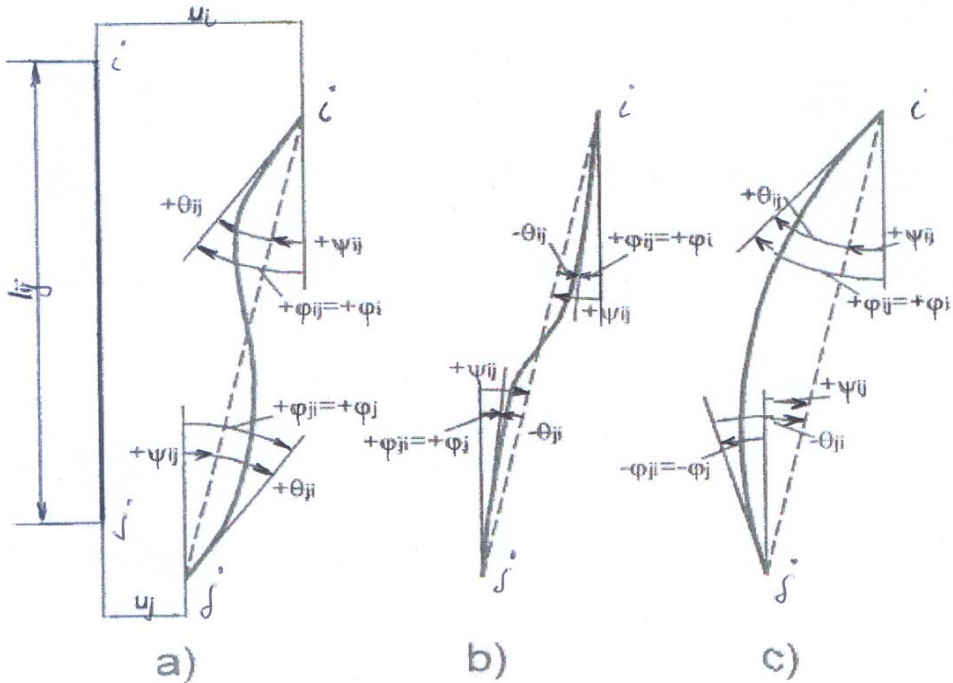


Photo 1.

The bar rotation ψ_{ij} is calculated as follows:

$$\psi_{ij} = \frac{u_i - u_j}{l_{ij}} \quad (6)$$

Note: In these relations, the rotations bear the signs corresponding to the adopted convention: “plus” for the clockwise rotations.

b) Bar with rigid joint in one end and with hinge in the other end

For the bar with rigid joint in “i” and the “j” hinges (photo 1.a), the φ_{ij} and φ_{ji} rotations of the bar ends have the expressions:

$$\begin{aligned} \varphi_i &= \varphi_{ij} = \theta_{ij} + \psi_{ij} \\ \varphi_j &= \varphi_{ji} = \theta_{ji} - \psi_{ij} \end{aligned} \quad (7)$$

By replacing $\theta_{ij} = \varphi_i - \psi_{ij}$ results:

$$\varphi_i = (1 - t_{ij})\psi_{ij} - t_{ij}\varphi_j \quad (8)$$

$$\varphi_j = (1 + t_{ij})\frac{u_i - u_j}{l_{ij}} - t_{ij}\varphi_i \quad (9)$$

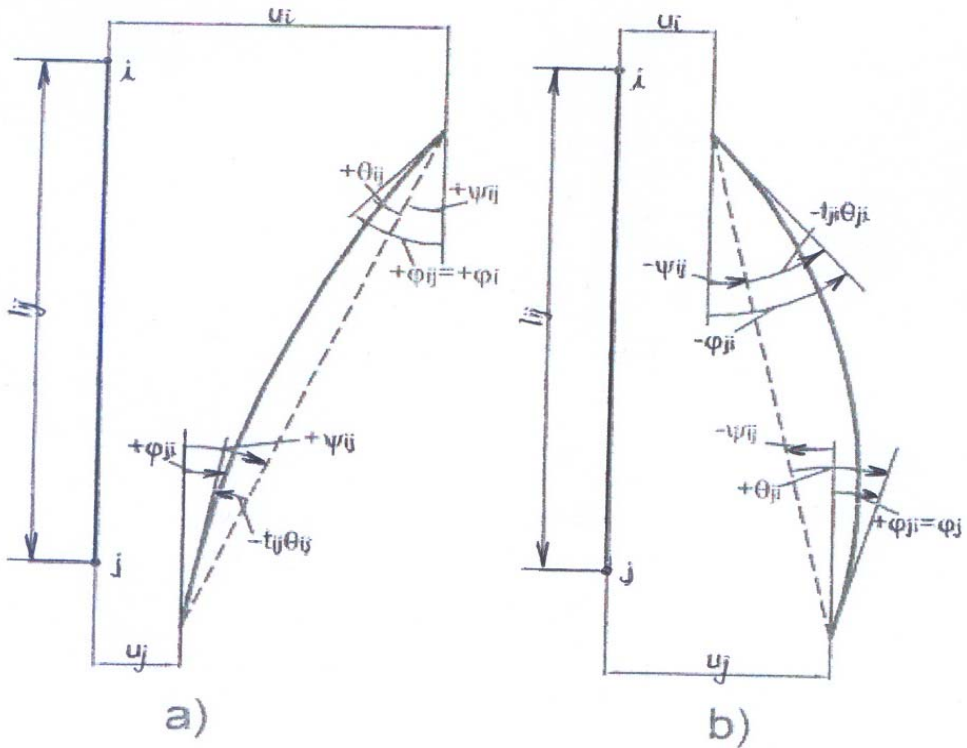


Photo 2.

For the bar jointed in “i” and with the rigid joint in “j” (photo 2.b) results:

$$\varphi_i = (1 - t_{ij})\frac{u_i - u_j}{l_{ij}} - t_{ij}\varphi_j \quad (10)$$

$$\varphi_j = \varphi_j \quad (11)$$

c) The bar jointed at both ends (photo 3)

For this bar, there results:

$$\varphi_j = \varphi_{ji} = \psi_{ij} = \frac{u_i - u_j}{l_{ij}} \quad (12)$$

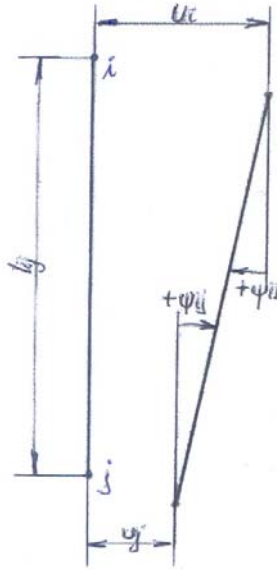


Photo 3

For the bar with constant moment of inertia, there results in the four cases:

b) Bar with rigid joints at both ends (photo 1):

$$\varphi_{ij} = \varphi_i \quad (13)$$

$$\varphi_{ji} = \varphi_j \quad (14)$$

b.1. Bar with rigid joint in "i" and articulation in "j" (photo 2.a):

$$\varphi_{ij} = \varphi_i \quad (15)$$

$$\varphi_{ji} = -0,5\varphi_i + 1,5\frac{u_i - u_j}{l_{ij}} \quad (16)$$

b.2. Bar with articulation in "i" and rigid joint in "j" (photo 2.b):

$$\varphi_{ji} = -0,5\varphi_j + 1,5\frac{u_i - u_j}{l_{ij}} \quad (17)$$

$$\varphi_{ji} = \varphi_j \quad (18)$$

Bar jointed at both ends (photo 3):

$$\varphi_{ij} = \varphi_i = \frac{u_i - u_j}{l_{ij}} \quad (19)$$

Matrix general form for the establishment of rotations from the bar ends in all the stages of the elasto-plastic analysis is the following:

$$\{\varphi\} = \{g\}\{\delta\} \quad (20)$$

or

$$\begin{Bmatrix} \varphi_j \\ \varphi_j \end{Bmatrix} = \begin{Bmatrix} g_{11} & g_{12} & g_{13} & g_{14} \\ g_{21} & g_{22} & g_{23} & g_{24} \end{Bmatrix} \cdot \begin{Bmatrix} \varphi_i \\ \varphi_j \\ u_i \\ u_j \end{Bmatrix} \quad (21)$$

If the alternation coefficients c_{ij} , c_{ji} are used, with the variants:

$$c_{ij}(c_{ji}) = 1 \text{ if } M_{ij} < M_{ij}(p)[M_{ji} < M_{ji}(p)] \quad (22)$$

$$c_{ij}(c_{ji}) = 0 \text{ if } M_{ij} = M_{ij}(p)[M_{ji} = M_{ji}(p)] \quad (23)$$

the expressions of the matrix elements $[g]$ are as follows:

$$g_{11} = c_{ij} \quad (24)$$

$$g_{12} = -t_{ji}(1 - c_{ij})c_{ij} \quad (25)$$

$$g_{13} = (1 - t_{ij}) \cdot \frac{(1 - c_{ij})c_{ij}}{l_{ij}} + \frac{(1 - c_{ij}) \cdot (1 - c_{ji})}{l_{ij}} \quad (26)$$

$$g_{14} = -(1 - t_{ji}) \cdot \frac{(1 - c_{ij})c_{ij}}{l_{ij}} - \frac{(1 - c_{ij}) \cdot (1 - c_{ji})}{l_{ij}} \quad (27)$$

$$g_{21} = -t_{ij}(1 - c_{ji})c_{ij} \quad (28)$$

$$g_{22} = c_{ji} \quad (29)$$

$$g_{23} = (1 + t_{ij}) \cdot \frac{(1 - c_{ji})c_{ij}}{l_{ij}} + \frac{(1 - c_{ij}) \cdot (1 - c_{ji})}{l_{ij}} \quad (30)$$

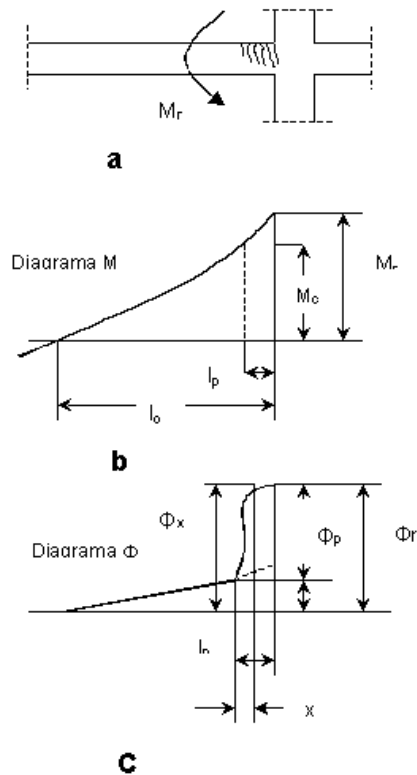
$$g_{24} = -(1 + t_{ji}) \cdot \frac{(1 - c_{ji})c_{ij}}{l_{ij}} - \frac{(1 - c_{ij}) \cdot (1 - c_{ji})}{l_{ij}} \quad (31)$$

This way, according to the values of the symbols c_{ij} and c_{ji} are determined the rotations in all the four possible cases of joints from the bars ends with constant moment of inertia – the relations (13)÷(19)- or with a variable moment of inertia - the relations (7)÷(12).

3. THE ESTABLISHMENT OF THE ROTATION CAPACITY OF PLASTIC JOINTS

3.1. The analytical solution

The moment-curve diagram presented in figure 4 shows that the formation of a plastic hinge on a concrete element takes place when the curve from the respective critical section becomes equal with Φ_c . Subsequently, the curve increases up to the Φ_r value, this corresponding to the beginning of the collapse of the concrete compressed area.



Picture 4

The rotation capacity of concrete steel plastic hinge is thus characterized by the increase of the curve from the respective critical section, from Φ_c value to Φ_r value, so with the plastic curve Φ_p .

The plastic hinge formed on a concrete steel element spreads over a l_p width area, within which the curves are larger than Φ_c , but smaller than Φ_r . Noting with Φ_x the curve from a section located at x distance from the section which Φ_c corresponds to, for the plastic hinge rotation capacity the following expression is obtained (photo 4):

$$\Theta_p = \int_0^{l_p} (\Phi_x - \Phi_c) dx \quad (32)$$

where, to the limit, $\Phi_x = \Phi_c$ for $x=0$ and respectively $\Phi_x = \Phi_r$ for $x=l_p$.

The expression (32) can be put under the form:

$$\theta_p = \eta l_p \theta_p \quad (33)$$

The plastic curve can be expressed as follows:

$$\Phi_p = \frac{1}{h_0} \left[\frac{\varepsilon_r}{\xi_r} - \frac{\varepsilon_c}{1 - \xi_c} \right] \quad (34)$$

The values of the product:

$$\Phi_p h_0 = \frac{\varepsilon_r}{\xi_r} - \frac{\varepsilon_c}{1 - \xi_c} \quad (35)$$

are given in the tables [5]. The product $\Phi_p h_0$ can be calculated using the approximate relation:

$$\Phi_p h_0 = \frac{0,8(\varepsilon_r - \varepsilon_0)}{\alpha - \alpha' + n_r} = \frac{0,0012}{\alpha - \alpha' + n_r} \quad (36)$$

where the coefficients α , α' and n_r are given in [5].

The plastic hinge formed on a concrete steel element is spread, in the outwork stage of its rotation capacity, over the length on which the curving moments are bigger than the flow moment, but smaller than the moment of fracture of the respective critical section (photo 4).

For the calculation of this length, the following expression is used:

$$l_p = \left(1 - \frac{M_c}{M_r} \right) \cdot l_0 \quad (37)$$

where:

M_c is the flow moment of the critical section;

M_r – the moment of fracture of the critical section;

l_0 - the distance comprised within the plastic hinge critical section and the cancellation point of the moment diagram.

Theoretically, the proportion $\frac{M_c}{M_r}$ has values comprised between 0.98 and 0.92 in case of bended sections simple and between 0.96 and 0.86 in case of eccentrically bended sections. Actually, the establishment of the plastic hinges rotation capacity in the area of stressed angle of the moment diagram, the ratio is taken to be equal with the average value of the effective limits of this ratio and namely with 0.875. The expression (33) is written as follows:

- for the plastic hinges formed at the ends of the concrete steel bars on whose length loads are applied, when these hinges are spread on a single side of the respective critical sections:

$$\theta_p = 0.0125\Phi pl \quad (38)$$

- for the plastic hinges formed at the ends of the concrete steel elements on whose length loads are applied, when these hinges are spread on both ends of the respective critical sections:

$$\theta_p = 0.0250\Phi pl \quad (39)$$

where the length l is taken to be equal with the average of the free apertures located on one side and the other of the plastic hinges;

for the plastic hinges formed at the ends of the concrete steel elements on whose length no loads are applied, when these joints are spread on a single side of the critical sections:

$$\theta_p = 0.0250\Phi pl \quad (40)$$

for the plastic hinges formed at the ends of the concrete steel elements on whose length no loads are applied, when these hinges are spread on both sides of the respective critical sections:

$$\theta_p = 0.0500\Phi pl \quad (41)$$

where the length l is taken to be equal with the average of free apertures located on one side and the other of the plastic hinges. With regards to the Wit regards to the plastic hinges formed at the critical sections in T shape from the concrete steel field elements on whose length loads are applied, these have such big rotation capacities

that it is no longer necessary to verify the compatibility of these rotations under the action of the calculation loads.

3.2. The semi-empirical relations for the calculation of the plastic hinge rotation capacity

The second modality for the establishment of the rotation capacity of plastic hinges formed at the end of the concrete steel elements resides in the replacement of the ηl_p product from the relation (33) with an equivalent length l_e , calculated using the semi-empirical relation:

$$l_e = \eta l_p = k_1 k_2 k_3 h_0 \sqrt{\frac{l_0}{h_0}} \quad (42)$$

where:

k_1 is a coefficient which takes account of the reinforcement type used;

k_2 coefficient which takes into consideration the effect of the force of compression from the respective critical section;

k_3 coefficient whose value depends on the concrete resistance to compression.

The k_1 coefficient is equal with 0.7 in case of the reinforcement formed of steel bars laminated at hot and with 0.9 in case of reinforcement of steel bars processed at cold.

The k_2 coefficient is given by the relation:

$$k_2 = 1 + 0,5 \frac{N_r}{N_0} \quad (43)$$

where:

N_r is the force of compression in the respective critical section, at the moment of its fracture;

N_0 the force of compression which produces the fracture of the respective critical section, in the hypothesis of its stress at centric compression.

The k_3 coefficient has the value 0.6 for $R_b = 420 \text{ daN/cm}^2$ and respectively the value 0.9 for $R_b = 140 \text{ daN/cm}^2$, R_b being the nominal resistance of the concrete to centric compression, determined on cubes whose side is of 20 cm. For values of the resistance R_b comprised between 140 daN/cm^2 and 420 daN/cm^2 , the size of the coefficient k_3 is established by linear interpolation.

Taking into account the relations (33) and (42), the semi-empirical formulas for the establishment of the rotation capacity of the plastic hinges formed at the ends of concrete steel elements are presented as follows:

for the plastic hinges which spread on a single side of the respective critical sections:

$$\Theta_p = k_1 k_2 k_3 h_0^4 \sqrt{\frac{l_0}{h_0}} \cdot \Phi_p h_0 \quad (44)$$

- for the plastic hinges which spread on both sides of the respective critical sections:

$$\Theta_p = 2k_1 k_2 k_3 h_0^4 \sqrt{\frac{l_0}{h_0}} \cdot \Phi_p h_0 \quad (45)$$

In the relation (45), the length l_0 is taken to be equal with the average of the distances between the respective critical section and the two points of null moment from its adjacent apertures.

Note: As in the case of the analytical solution, the rotation capacity of the hinges formed at the critical sections of rectangular shape from the fields of the concrete steel elements on whose length loads are applied, is established, overall, using the relation (45), where the length l_0 is taken to be equal with the biggest of the distances comprised between the critical sections on the supports of the respective elements and the null moment points of the diagram with moments adjacent to these sections.

References:

1. AMARIEI C. The calculation of the structures in the plastic field, I.P.IASI,1974.
2. AMARIEI C. DUMITRAS AI. Elements of structure matrix analysis, Ed.Soc.Acad. " Matei-Teiu Botez", Iasi, 2003.
3. BALAN ST.,PETCU V. A new concept of degree expression for the security in the calculation of elastic-plastic structures, Studies and research on applied mechanics. Bucuresti, 4,5, 1970.
4. COHN M.Z. – Analysing and design of Inelastic Structures ,vol.2,
5. University of Waterloo Press, 1972.
6. PETCU V. The calculation of concrete steel structures in the plastic field, Technical Publishing House, Bucuresti,1971.
7. xxx - CR 2-1-1.1/2005 , Design code of concrete steel structural walls constructions, M.T.T.C., 2006.

Actual Trends on Long Lasting Rigid Pavements (LLRP)

R. Andrei¹, N. Taranu², H. Gh. Zarojanu³, N. V. Vlad⁴, V. Boboc⁵, I. D. Vrancianu⁶, M. Nerges⁷, M. Muscalu⁸, R. Cojocaru⁹

^{1, 3, 4, 5, 6, 8, 9}Department of Roads and Foundations, Technical University "Gh. Asachi", Iasi., 700050, Romania, randreir@ce.tuiasi.ro, zarojan@ce.tuiasi.ro, vboboc1956@yahoo.com, vrancianu_diana@yahoo.com

^{2,7}Department of Civil and Industrial Engineering, Technical University "Gh. Asachi", Iasi, 700050, Romania, taranu@ce.tuiasi.ro, swingamos@yahoo.com

Summary

Although in the past, the majority of pavements were designed on the basis of a 20- to 25-year initial service life, more recently, there has been a movement toward a longer initial service life of 40 or more years. Recent advances in design, construction, and concrete materials give us the knowledge and technology needed to achieve long-life pavements.

Worldwide, it has been aimed to develop infrastructure for surface transport using alternative concrete bases for reducing the maintenance (and though the life-cycle costs) of pavements and doing so at an initial cost lower than for traditional rigid pavement systems. This is attainable in the general context of developing the concept of Long Lasting Rigid Pavement (LLRP).

Incorporation of steel fibres is due to reduce the thickness of the pavement layers. Also, the use of steel fibres recovered from used tyres would answer the need to develop new recycled products and applications.

The EcoLanes Project (<http://ecolanes.shef.ac.uk>), an international endeavour with participants from 7 European countries, at which the Technical University "Gh. Asachi" is partner, tries to answer these demands.

An initial stage of this endeavour is to assess the state of the art in design and construction of LLRP, using steel fibre reinforced concrete (SFRC), and evaluate the available options, from both construction and design point of view, to attain this objective.

The present paper introduces some projects that proved to have extended life, emphasizing the changes in overall pavement design, materials and construction materials that occurred over the years, with the purpose to define the concept of LLRP and also some options on LLRP, envisaged in the frame of EcoLanes Project.

KEYWORDS: concrete pavements, long lasting rigid pavements (LLRP), steel fibers reinforced concrete (SFRC), accelerated load testing (ALT)

1. INTRODUCTION

In the past, concrete pavements were routinely designed and constructed to provide low maintenance service lives. In fact, the majority of pavements were designed on the basis of a 20- to 25-year initial service life. More recently, there has been a movement toward a longer initial service life of 40 or more years, particularly in high-volume, urban corridors where traffic disruptions and user delays can be especially acute because of frequent or extended lane closures.

Long-life concrete pavements have been attainable for a long time (as evidenced by the fact that a number of very old pavements remain in service); however, recent advances in design, construction, and concrete materials technology give us the knowledge and technology needed to achieve consistently what we already know to be attainable. To achieve long life, pavements must not exhibit premature failures and must have a reduced potential for cracking, faulting, spalling, and materials-related distress.

According to international practice [1] some approaches to improving longer life are as follows:

- Increase the specified aggregate size from 19 mm to 32 mm to improve flexural strength without significant increases in cement content.
- Eliminate the use of thin asphalt overlays on CRCP and replace asphalt with cement-based products that offer similar low noise and durability.
- Construct these layers within the one-slipformed layer rather than a multilayer approach.
- Continue to provide incentives to contractors to encourage pavements to be constructed to lower tolerances or to better medium-term performance indicators.
- Manage heavy-vehicle usage to reduce or eliminate overloading from heavy trucks.
- Road authorities should support training of engineers and paving crews to promote the adoption of best practices.

A significant example of a motorway construction [2], with extended life road pavement is the project E5 Brussels–Liège. Traffic intensity on this motorway amounted to 112,000 vehicles per day in 2000, 14 percent of which was heavy traffic. The only maintenance during the first 30 years consisted of replacing the joint fillings. Because the road structure was still in good condition, no structural maintenance or renewal was planned and it was to be expected that this motorway would have a life span of 40–50 years.

The cross section of 40 m consists of two carriageways, separated by a central reserve, with three traffic lanes, each 3.75 m wide, with a hard shoulder that is 3 m wide. Outside the short zone in the Brussels metropolitan area, where in certain places there are eight traffic lanes with asphalt pavement to interchange the traffic

to different directions, the actual road is a continuously reinforced concrete pavement (CRCP). The reason why CRCP was chosen is the combination of the comfort provided by an asphalt road support and the advantages of the concrete pavement, namely greater sustainability, little maintenance, and greater reflection of light in the dark. The structure of the motorway is shown in Figure 1.

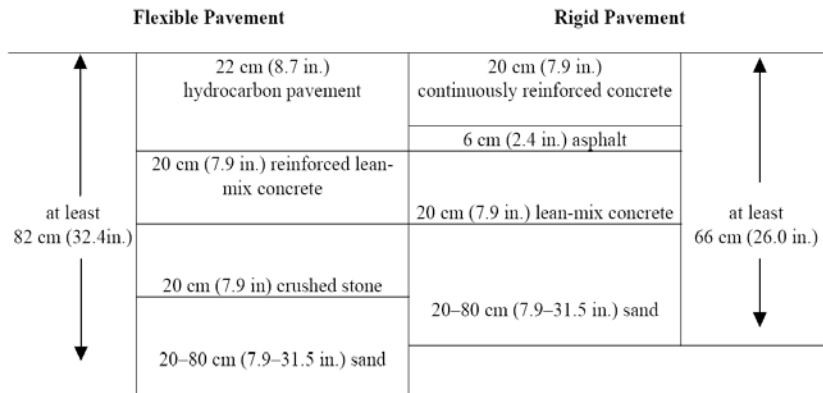


Figure 1. Structure of E5 motorway in continuously reinforced concrete and comparison to structure in asphalt [2]

2. DEFINITION OF THE CONCEPT OF LONG LASTING RIGID PAVEMENTS (LLRP)

The concept of Long Lasting Rigid Pavements can be defined only in conjunction with the world wide evolution in the last 20 years of modern paving in terms of design, materials, specification and construction, maintenance. The definition of the LLRP is also conditioned by the traffic envisaged (e.g. typical concrete local roads constructed over 60 years ago in Sydney remain open to traffic due to light loadings and aggregates that have not polished [1]). Also, it is related to the following issues: design, materials, specifications, construction (the quality of the concrete used in these pavements is a major factor in ensuring long-term performance) and maintenance, low-maintenance costs being also an indicative of long-life pavements. According the international road practice, with the introduction of the slipform paver in the late 1970s, concrete pavements were better able to compete against flexible pavement configurations in terms of initial and life cycle costs. As life cycle costing became increasingly important, concrete pavements became more cost effective.

Thus, a review was undertaken by the Roads and Traffic Authority in Australia, looking at maintenance costs of concrete pavements compared with asphalt pavements (AC) on a 97 km length of New South Wales's main highway, the Hume Highway. A cost analysis was performed of all routine and specific maintenance treatments, including agency costs, over a period of between 12 and 23 years. These costs were then converted to 2002 dollars so that life cycle maintenance costs of asphalt concrete, plain concrete pavement, and continuously reinforced concrete pavement (CRCP) could be compared. This section of highway was chosen for similar traffic and environmental conditions and has several repetitive sections of asphalt, PCP, and CRCP. Since 1979, traffic has increased from 10,000 AADT to 25,000 AADT, with almost one-quarter of all vehicles being heavy vehicles. The typical comparative maintenance costs are shown in Figure 2.

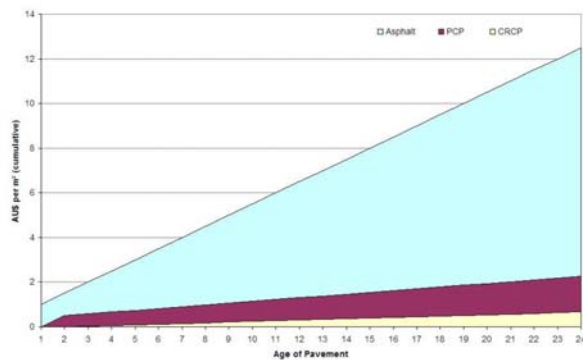


Figure 2. Comparative maintenance costs between each pavement type [1]

The study found a large variability in concrete pavement maintenance costs (PCP and CRCP), reflecting differences in construction and projected over 20 years, that was anywhere between AUS\$3/m² and \$28/m². In comparison, asphalt pavement maintenance costs ranged from \$35/m² to \$50/m².



Figure 3. Coefficient of variation data on paving projects from 1975 to 2005 in Australia[1]

2.1. Changes in materials and concrete technologies

The quality of the concrete is a major factor in seeking long-term performance. A study of the coefficient of variation on compressive strength and density on numerous projects, in Australia [1], has shown a decline over the last 20 years, leading to the conclusion that better uniform materials in the road are likely to lead to long-term performance. Figure 3 presents the evolution of the coefficient of variation data on paving projects from 1975 to 2005 in Australia.

2.2. Changes in overall pavement thickness design

Highway engineers may seek an increase in pavement thickness to achieve longevity, thickness of the concrete slab being one of the significant elements in achieving long-life concrete pavements. Thus, according to the Romanian practice, the minimum thickness recommended for rigid pavements has increased along the years as follows: 14 cm in the beginning, then 16 cm, and nowadays 18 cm.

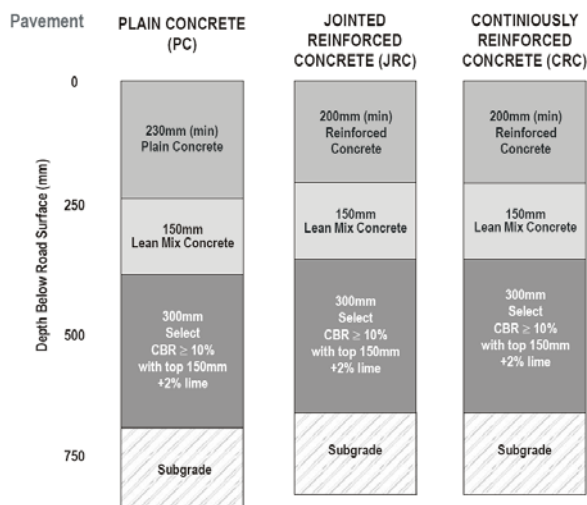


Figure 4. Typical plain concrete pavement, jointed reinforced concrete pavement, and continuously reinforced concrete pavement configurations for heavy-duty roads [3]

Besides the increase of the minimum recommended thickness, the following aspects have been also reconsidered in the design of long – life concrete pavements:

- A refined thickness design procedure gave more conservative outcomes.
- A change from using nomographs to computer programs and spreadsheet analysis reduced human error.
- Skew to transverse contraction joints changed from 1:6 to 1:10.

- Better collection of heavy traffic data provided better input into fatigue analysis.
- Minimum base layer thickness for different pavement types have been introduced in the last years.
- Development of various design catalogues for heavy-duty pavements (see Figure 4).

2.3. Changes in construction requirements

In many countries tolerances for thickness and strength were modified to ensure that more of the pavement was built above the minimum limit rather than an average around the design requirement [1]. Also, focused compliance on relative density to ensure optimum modulus and flexural strength was emphasised. The minimum recommended thickness has been increased to higher values. Better preparation of the selected material, including spray sealed surface treatment, reduced the risk of construction traffic damaging the surface during construction of the subbase and base layers.

In parallel with these positive changes, significant improvements have been undertaken to the slipform pavers [2]. The number of vibrating pokers was increased and a finishing beam that moves transversely was added so as to improve the finish of the concrete and to correct the possible faults in the tightness of the surface. Also, better training of staff at all levels, and toolbox sessions conducted prior to construction has proved to be beneficial.

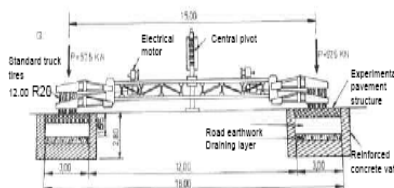
2.4. Accelerating loading test (ALT) for validation of various extended life concrete pavements

Accelerated loading facility (ALF) was typically used in Australia [1], to predict the performance of seals and flexible pavement configurations under dual wheel loading. Australia has conducted one accelerated loading trial on a plain concrete pavement using ALF 4. The trial had two objectives: to validate and refine the existing fatigue design criteria for PCP and to investigate the impact of various subbase types on the performance of PCP. Unfortunately, the dual-tire assembly with 8 t loading did not precipitate fatigue cracking and limited the findings from the ALF repetitive loading. In terms of subbase support, the study did confirm that a lean-mix concrete or heavily bound subbase would perform better than an unbound granular material as a subbase. The prediction of long-life, heavy-duty concrete pavements using the ALF device was inconclusive, but their two SHRP LTPP sites are showing low levels of deterioration, the concrete pavements at these sites appearing to have a long life.

Romania took the opportunity to be directly involved in the Strategic Highway Research Program (SHRP) in order to evaluate the performance of Romanian pavements and to enhance its pavement performance prediction models. There are currently over 30 LTTP test sections in the Romanian program, including asphalt and concrete pavements situated in specific rural and urban locations. Some of the RO-LTTP sites were specifically set up to compare the relative performance of full-scale, in-service pavement test sections under real traffic-loading conditions with those performance characteristics determined under ALT loading. One of such RO-LTTP sector is involving a specific road experiment equipped with continuously reinforced concrete pavement (CRCP) realised on a national road NR – 12A – Miercurea Ciuc – Onesti, km. 30 +000 – 30+150, 25 years ago [4]. This section could be considered as a typical Romanian rigid pavement with extended life, its technical condition still being satisfactory, and its envisaged design life being of 40 to 50 years. Therefore, it is expected that the use of the ALT facility existing at Iasi Technical University (see Figure 5) to simulate the performance of the LLRP envisaged to be constructed according to the new concept, derived from the EcoLanes project, with similar replica on the national road NR 17, will produce an increased level of confidence in this type of trials. Figure 6 presents the experimental sectors on ALT testing facility of the Technical University “Gh. Asachi” Iasi, in the frame of EcoLanes Project.

Type: Circular Test Track

Construction (commissioned): 1982



Dimensions

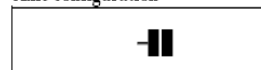
Mean diameter	15
No. of arms	2

Loading

Range of Load ⁽¹⁾	115 kN
Transverse distribution	± 300 mm

⁽¹⁾ Wheels loads (half axle) are converted to the corresponding axle loads.

Axle configuration



Speed

Vehicle Speed (max.)	40 km/h
Test frequency (max.) (passes/hour/section)	1700
Practical output (loadings/month/section)	50.000

Sections

No. of Sections	8
Thickness	2000 mm
Width	3000 mm

Figure 5. ALT –LIRA track test [7]

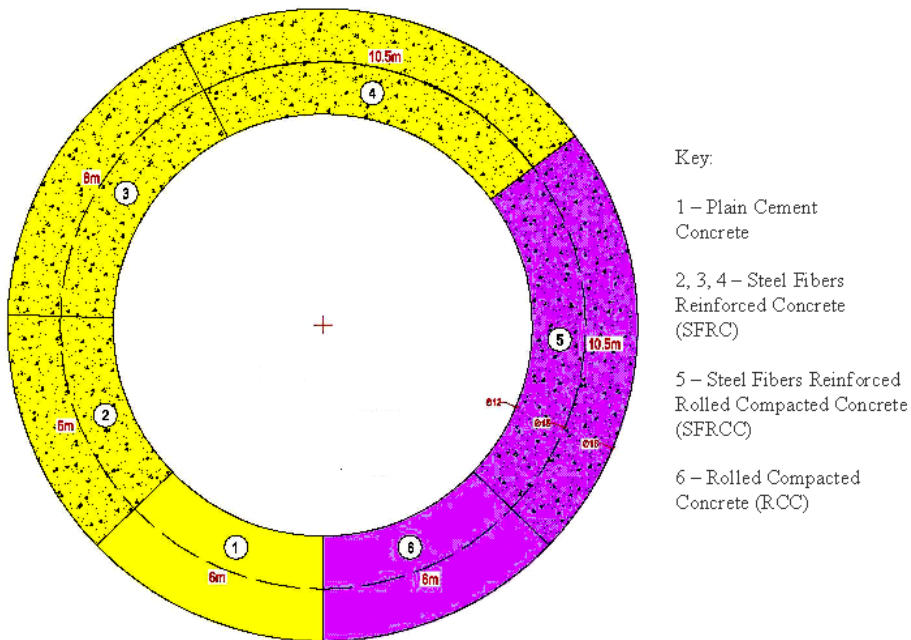


Figure 6. Experimental sectors on the ALT circular track facility

These circular sectors and their respective pavement structures have been proposed by the working group from our University, involved with ALT testing [5], [6] and they were approved, in principle, during the last EcoLanes meeting, held in Antalia.

3. MATERIALS, TECHNOLOGIES AND EXPERIENCES WITH DESIGN AND CONSTRUCTION OF LLRP, AROUND THE WORLD

Apart from the typical rigid pavement types (jointed plain concrete pavement, jointed reinforced concrete pavement, continuously reinforced concrete pavement), more performant concepts have been developed and used, with the aim of attaining long life rigid pavements.

3.1 High Performance Concrete Pavements

In general terms High Performance Concrete (HPC) may be defined as any concrete that provides enhanced performance characteristics for a given application [8]. For example, concretes that provide substantially improved durability under

severe service conditions, extraordinary properties at earlier ages, or substantially enhanced mechanical properties are potential HPCs. These concretes may contain materials such as fly ash, granulated slags, fibres, chemical admixtures, and other materials, individually or in various combinations. Highway engineers are making increasing use of HPC for a variety of highway applications, including new constructions, repairs, and rehabilitation. Higher durability of these concretes will significantly increase the service life of various engineering structures, including pavements, which may reduce life-cycle cost.

HPC is defined in terms of certain target strength and durability criteria as specified in Table 1.

Table 1: Criteria for HPC [8]

Category of HPC		Minimum Compressive Strength	Maximum Water/Cement ratio	Minimum Frost Durability Factor
Very early strength (VES)	Option A (with Type III cement)	14 MPa in 6 hours	0.40	80%
	Option B (with PBC-XT cement)	17.5 MPa in 4 hours	0.29	80%
High early strength (HES) (with Type III cement)		35 MPa in 24 hours	0.35	80%
Very high strength (VHS) (with Type I cement)		70 MPa in 28 hours	0.35	80%

Potential applications of VES concrete are for situations in which construction time is critical and the cost of materials is only marginally important in comparison with the costs of closing a bridge or a section of pavement to traffic [8]. The use of this concrete would be limited to full-depth pavement patches, short stretches of new pavement, bridge deck, and pavement overlays. VES concrete would probably be inappropriate for most structural applications.

HES concrete is probably the most universal material in terms of potential applications. With its enhanced performance characteristics, it would be useful for structural members, full-depth pavement patches, or new pavement construction and overlays -situations where the speed of construction is important but not critical, even though the cost of materials may be relatively more expensive. As with VES concrete, hand or machine finishing is possible with pavements, and conventional concrete placements practices would be used in structural applications.

Although machine placement is likely for overlays or larger pavement sections, a slump of 75 to 100 mm would more commonly be needed. Table 2 summarizes the potential applications of the three categories of HPC.

Table 2: Potential applications of HPC [8]

Potential Applications	Concrete Type			
	VES (A)	VES (B)	HES	VHS
New pavement	X		X	
Full-depth pavement patch	X	X	X	
Pavement overlay	X	X	X	X
New bridge deck			X	X
Full bridge deck replacement			X	
Bridge deck overlay	X	X	X	
Bridge girders			X	X
Precast elements		X	X	X
Prestressed piles		X	X	X
Columns and piers			X	X

VHS concrete would be useful primarily for structural members, for which the construction time is not a critical factor. Little, if any, direct application of its very high strength characteristics to pavement is anticipated for VHS concrete. However, if including a mineral admixture such as silica fume or fly ash would improve abrasion resistance or pavement deleterious alkali-silica reactivity, VHS concrete might be chosen for application in a pavement.

3.2. Fiber Reinforced Concrete Pavements

The use of fibre reinforcement in concrete pavements is continuing to see more attention, since these types of concrete pavement projects are increasingly being used and are exhibiting excellent performance [9]. Fiber-reinforced concrete (FRC) is made of hydraulic cements containing fine or fine and coarse aggregates, and discontinuous, discrete fibres [10]. Fibers used in concrete pavements are typically made from steel or plastic and are available in a variety of lengths, shapes, sizes, and thicknesses. They are added to fresh concrete during the batching and mixing process. There are several advantages, to reinforcing concrete with uniformly dispersed and randomly oriented fibres, including improvement in ductility, impact resistance, tensile and flexural strength, fatigue life, durability and abrasion resistance. Improvement in ductility is the most important property of FRC, the strain capacity of concrete being greatly increased [11]. In addition to steel fibres, which are the most dominant fibres, several other types of fibres have the potential to improve concrete and mortar properties, these types including glass, plastic, carbon, and wood fibres.

3.2.1 Polymer fiber reinforced concrete pavements

Synthetic fibres are manufactured from materials such as acrylic, aramid, carbon, nylon, polyester, polyethylene, or polypropylene. Their primary use in concrete

pavements to date has been in ultra-thin whitetopping, where 5 to 10 cm of concrete is bonded to an existing asphalt pavement to form a composite pavement [9].

The benefits of polypropylene fibres included reduced plastic shrinkage and subsidence cracking, as well as increased toughness or post-crack integrity. In fresh concrete, polypropylene fibres also reduce the settlement of aggregate particles from the pavement surface, resulting in a less permeable and more durable, skid resistant pavement [9]. However, according to relative recent SHRP research [10], it was found that mixtures containing 1 or 2% by volume of propylene fibres showed deterioration in compression stress-strain response when compared with the control mixture. The mixture with 2% by volume of propylene fibres was more difficult to mix and led to a large volume of entrapped air, thus resulted in poorer properties than mixtures with 1% propylene fibres. Therefore, the use of propylene fibres only to improve compressive strength and elastic modulus is not recommended. They can be used for improving the toughness index of the material.

3.2.2 Steel fiber reinforced concrete (SFRC) - SFRC with steel fibres industrial produced

The most significant effect of incorporating steel fibres in concrete is to delay and control the tensile cracking of concrete. This crack-controlling property of the fibre reinforcement delays, in turn, the appearance of flexural and shears cracking, imparts extensive post-cracking behaviour, and significantly enhances the ductility and energy absorption properties of concrete. These properties, besides the increased resistance to impact and repeated loading, make SFRC an adequate material for pavement construction [12].

Interest in using SFRC in highway structures started in the early 1960s, when bridge decks and pavements were the attractive areas for such applications in various countries. SFRC was used in bridge deck surfacings constructed in the United States [13], in the 70's. Most of these overlays, bonded to the existing deck, developed some cracks but remained tight and have not adversely affected the riding quality of the decks. SFRC was also used in pavement and overlays in residential, rural, urban, industrial, and airport areas [14].

Steel fibers used for pavements are generally 12.7 - 63.5 mm long, and 0.45 - 1.0 mm in diameter. The usual amount of steel fibres ranges from 0.25% to 2% by volume, or 20 - 157 kg/m³. Some steel fibres have hooked ends and are collected in bundles that break apart during mixing while others may be crimped in shape and unattached, as seen in Figure 7.

Extensive research on the use of the combined steel and polymer fibres reinforced concrete has been conducted in frame of Strategic Highway Research Program [15], [16], with the aim to develop technical recommendations for use of HESFRC.

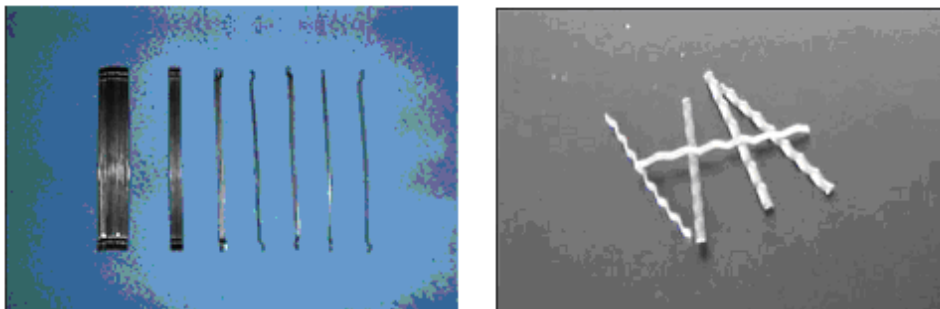


Fig. 7: Steel fibers: with hooks (left) and crimp-shaped (right)

SHRP studies on fiber reinforced concrete indicated that the greatest benefit of introducing fibres into the concrete consists in improvement of mechanical characteristics. Thus, it was found that two percent by volume of 30/50 hooked steel fibres was found to be the optimal amount.

The additional 2% by volume (2% of an equal combination of 30/50 and 50/50) steel fibres caused significant increases in the compressive strength, modulus of rupture, splitting tensile strength, toughness indices, ductility, and fatigue limit when compared with control mixture without fibres. In comparison with the control mixture, it was obtained an average increase of 30% in compressive strength, 270% in modulus in rupture, and 250% in splitting tensile strength.

Next in performance were the mixtures containing 1% by volume (of 50/50 or an equal combination of 30/50 and 50/50, hooked) by volume. In comparison with the control mixture, without fibres, these materials led to the little change in compressive strength, but an increasing in the modulus of rupture and splitting tensile strength by 200% and 173%, respectively.

Similar effects were obtained from research conducted in this country [17]. Table 3 presents the limits within which some mechanical characteristics vary, function of the reinforcement percentage per volume (μ_v) and per weight (μ_g), respectively, considering for the non-reinforced concrete the reference value of 100%.

Table 3: Variation of some mechanical characteristics of SFRC function of the reinforcement percentage per volume (μ_v) and per weight (μ_g) (adapted from [17])

μ_g	0	2%	4%	6%	8%	10%
μ_v	0	0.61%	1.22%	1.84%	2.45%	3.06%
Tensile strength from bending (%)	100	110...150	150...200	160...210	180...230	200...250
Toughness (%)	100	200...500	300...600	350...800	-	-
Bending ductility (%)	100	120...150	300...450	400...700	500...800	-

(The bending ductility is defined as the area enclosed by the characteristic curve for the bending test. It refers to the entire area enclosed by this curve, only to the maximum load value.)

According to the Romanian studies [17], it is recommended that the steel fibres have tensile strength of approx 1000MPa. The soft wires, with low stiffness, cannot be uniformly spread in the concrete mass, which leads to low strength and insufficient improvement of concrete characteristics. The ratio between the length of the fibre and the minimum length of the concrete element is recommended to be in the range of 0.4 to 0.6. The maximum recommended aggregate size is 10 mm, in order facilitate the workability of the fresh concrete.

3.2.3 *Steel fibre reinforced concrete (SFRC) - SFRC with steel fibres recovered from used tyres*

Used tires cause environmental stress in many ways, mainly through their use and what happens to them when they are worn out. Governments in various UE countries are concerned in particular about the waste management of used tyres, since the disposal of whole tyres to landfill is not environmentally friendly. As the current recycling rate of used tyres is relatively low and to comply with new EU directives, there is a great need to develop new recycled products and applications that will accommodate the used tyres. The EcoLanes project tries to answer all these needs.

Used tyres are recycled by either mechanical or chemical processes. Tyres can be mechanically reduced to rubber and steel by either using the shredding or cryogenic process. The pyrolysis process is applied to chemically decompose tyres down to oil, gases and steel. The commercial viability of these processes is largely affected by the quality of the recycled end – products and the availability of markets for this end – products [18]. In the frame of the EcoLanes project, both types of fibres, industrially produced and recovered from used tires are intended to be investigated.

3.3 Roller Compacted Concrete (RCC) for pavement bases

Roller compared concrete (RCC) has the constituents of conventional concrete, but they are mixed with different proportioning, resulting to a material with distinctive properties and behaviour. The placing operations are different from conventional concrete, utilising techniques borrowed mainly from road construction, and traditionally linked to operations involving earthworks and asphalt. It provides the strength and durability of concrete but with the economy and speed of construction of asphalt. An important distinction is necessary to be made at this point between RCC prepared for dam, pavement and cement treated base (CTB) applications, as the quality of the mix can be significantly different for each of those cases [19]. A

more illustrative definition of the material may be found in Figure 8, where it may be noticed a clear distinction between RCC and CTB based on the cement content as for the former is typically in the range of 3-5%, while for RCC ranges between 10-14%, by mass.

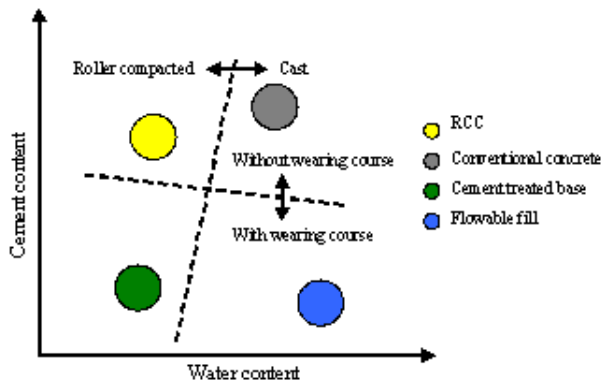


Figure 8. Distinction between the different types of concrete based on the cement content and water ratio [19]

RCC mixtures can attain high compressive strengths, even up to 80 MPa. Flexural strength of RCC is evaluated through bending tests of beam specimens, sawed from full-scale RCC pavements and, hence, there is limited information about the flexural strength of RCC. Data published in the literature suggests that flexural strengths of up to 7 MPa can be obtained for RCC pavements. Based on this data, it was also suggested that the relationship between the flexural and compressive strength of RCC is similar to that for conventional concrete. Cores from full-scale RCC pavements are used to evaluate the splitting tensile strength of RCC and, hence, the RCC tensile strength characteristics are evaluated easier and more reliably than the flexural strength characteristics. Depending on the RCC mix, the splitting tensile strength of RCC ranges from 2.8 to 4.8 MPa.

The elastic modulus is ranging from 19 to 30 GPa. In general, the RCC elastic modulus is similar or slightly higher than the elastic modulus of conventional concrete. There are very few studies on the fatigue behaviour of full-scale RCC pavements. Overall, it was evaluated that the fatigue behaviour of RCC is similar to that of conventional concrete.

In general, RCC pavements do not require reinforcement, but laboratory studies have shown that steel fibre reinforcement improves the mechanical properties of RCC mixtures and may also lead to a reduction of the pavement's thickness.

Up to now, there has been limited use of reinforcement (including fibers) in RCC mixtures mainly due to difficulties in incorporating the reinforcement in the mixture. Hence, research should be carried to develop practical fiber mixing and RCC placing techniques. The durability of RCC pavements, in context of LLRP,

requires further examination, especially frost resistance. Since air entrainment is not always possible due to the low water content of RCC, it is necessary to develop alternative methods and materials, which will improve the frost resistance of RCC pavements.

4. OPTIONS FOR THE LLRP STRUCTURAL CONCEPTS ENVISAGED FOR ECOLANES

Eight pavement structure solutions have been selected for the application in frame of Ecolanes project, grouped in three major option groups.

Option A refers to one lift construction and two variants of this option are described below. According Option A1 the rigid pavement structure is composed by a slab constructed from SFRC surface course, having a reinforcement percentage resulted from previous laboratory study conducted for SFRC mix design, laid on cement stabilized or low-strength concrete base course, as shown in Figure 9.

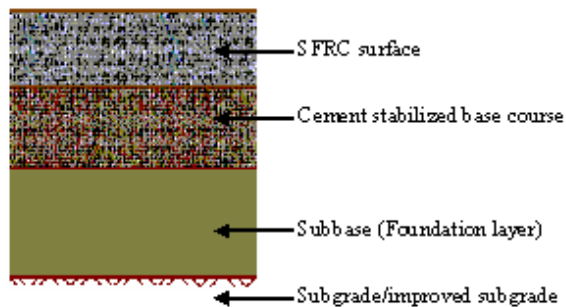


Figure 9. Option A1 - Steel fibres reinforced concrete (SFRC) surface course on cement stabilized or low-strength concrete base

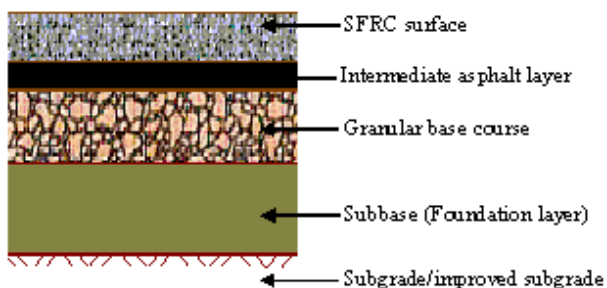


Figure 10. Option A2 - Steel fibres reinforced concrete (SFRC) surface course on asphalt intermediate layer and granular base course

According Option A2 the rigid pavement structure is composed by a slab constructed from steel fibers reinforced concrete (SFRC) surface course, having a reinforcement percentage resulted from previous laboratory study conducted for SFRC mix design, laid on a relative thin asphalt layer constructed over a base course granular supported by a classic foundation, as shown in Figure 10.

Option B, according to Figures 11 to 14, refers to a two-lift construction and the various alternatives of this option are presented below.

For option B1, a concrete slab realised by two lift construction from a SFRC surface course with a percentage by weight of reinforcing fibre resulted from laboratory studies, and having a minimum thickness of 6cm, and a Portland cement concrete (PCC) base course. This concrete slab is laid on a cement stabilised subbase supported by a classical foundation and subgrade or improved subgrade.

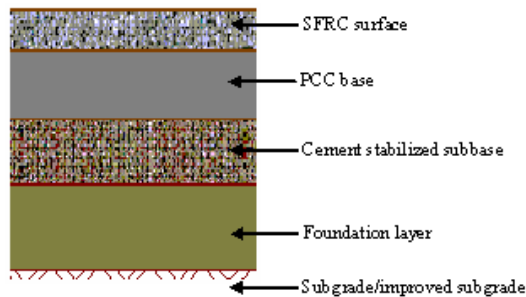


Figure 11. Option B1 - SFRC surface on PCC base and cement stabilized or low-strength concrete subbase

For the option B2, a concrete slab realised according two-lift construction from both SFRC layers, with different reinforcement percentages by weight (for example, minimum 2.0% for the upper layer, and minimum 1% for the bottom layer). This slab will be laid on cement stabilized or a low strength concrete subbase course, supported by a classical foundation and subgrade or improved subgrade.

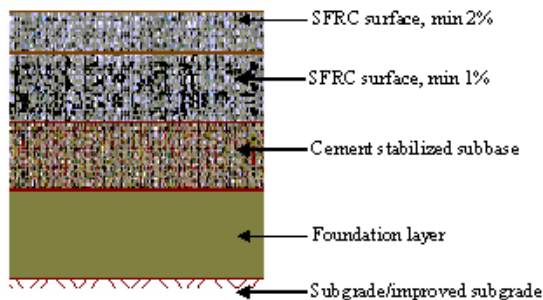


Figure 12. Option B2 - SFRC surface and base, with different reinforcement percentages on cement stabilized or low-strength concrete subbase

Option B.3 refers to a concrete slab realised from a SFRC surface layer, of a minimum 6 cm thickness and a RCC layer, laid on a granular base course, supported by a classical foundation and a subgrade or improved subgrade. Option B.4 refers to a concrete slab realized from a SFRC surface layer, of a minimum 6 cm thickness and a Fiber Reinforced Rolled Compacted Concrete (FRRCC) layer, laid on a granular base course, supported by a classical foundation and a subgrade or improved subgrade.

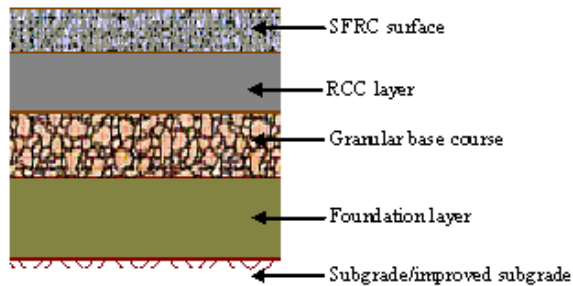


Figure 13. Option B3 - SFRC surface on a RCC layer and granular base

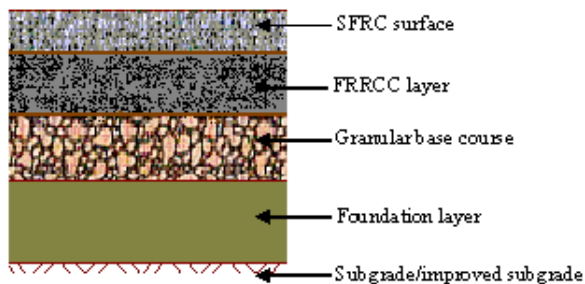


Figure 14. Option B4 - SFRC surface on a FRRCC layer and granular base

Option C refers to composite pavement structures, with an asphalt surface having with a thickness resulted from the design study, conducted by taking into consideration the specific of composite pavement structure.

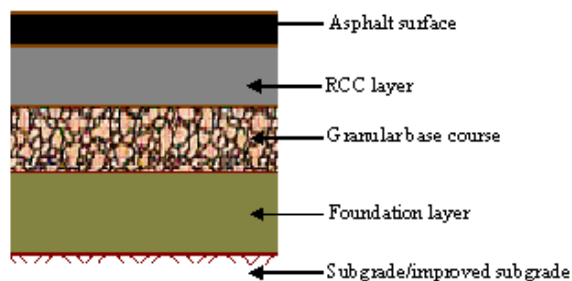


Figure 15. Option C1 - Asphalt surf ace course on RCC base and granular subbase

For option C1, presented in Figure 15, the bituminous surface course is laid on a Rolled Compacted Concrete (RCC) base, supported by a granular base course, a classical foundation, and a subgrade or improved subgrade.

For the option C.2, in Figure 16, the bituminous surface course is laid on a Steel Fiber Reinforced Rolled Compacted Concrete (SFRRCC) base, supported by a granular base course, a classical foundation, and a subgrade or improved subgrade.

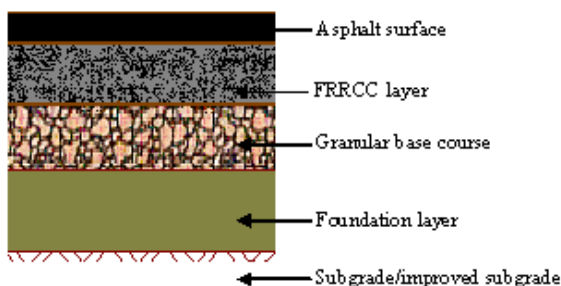


Figure 16. Option C2 - Asphalt surface course on SFRRCC base and granular subbase

General considerations concerning the envisaged options:

For options A and B, all pavement structures are recommended to be provided with a surface treatment realized according to the following alternatives:

- a) asphalt layer: a thin asphalt layer/ or slurry seal, double bituminous surface treatment (double chip seal) or a heavy bituminous surface treatment (heavy chip seal asphalt treatment);
- b) thin polymeric layer (certified material);
- c) surface mechanical processing plus alternatives a) or b).

All pavement structures will be provided with improved subgrade, function of the geotechnical characteristics of the subgrade (foundation) soil.

For options C, by adopting the assumptions that, between the asphalt surface and the concrete base there is no bonding, it is highly recommended that, for the thickness design of the whole structure, the design studies to be conducted separately for each layer, according the specific existing norms (Romanian and other), as follows:

- for concrete base: “Technical Norm for Structural Design of Concrete Base for Pavements”: NP 111-04, 2005,
- for RCC layers: recommendations from EcoLanes internal report [19].

Other specific norms to be used are the Romanian ones referring to the establishment of performance criteria and composition of SFRC (GP 075 – 2002), design of rigid pavements (NP 081 – 2002), execution of plain, reinforced and pre-stressed concrete pavement layers (NE - 012 – 1999), execution of rigid pavements with fixed and sliding forms (NE – 014 – 2002).

5. THICKNESS DESIGN METHODS ENVISAGED FOR ECOLANES PROJECT

The main objective of rigid pavement design is to determine the thickness of the concrete slab that will be adequate to carry the projected traffic load for the design period. Several design methods have been developed over the years, some of which are based on the results of full-scale road tests, others on theoretical developments on stresses on layered systems and others on the combination of the results of tests and theoretical developments. However, for the objective of the Ecolanes project, seeking the development of the LLRP concept, at least three methods are envisaged to be used for each option, except for option C, which is considered as a composite structure.

For each of the envisaged options, mentioned in Chapter 4, at least three alternative methods of thickness design, including the Romanian official method, are recommended to be used; finally the best one will be selected, taking into consideration various extensions of design life, based on technical and economical criteria, in order to be proposed for the various EcoLanes demo projects.

For A and B options, at least three alternative methods of thickness design, including the Romanian method, are intended to be used, as follows: The Highway Agency Design Method (UK-2006), Rigid Pavements Design (Romanian Standard NP 081 – 2002) and NCHRP Mechanistic –Empirical Design Method (USA-2004/2006). They are shortly presented in the following.

The British (UK Highway Agency) method for thickness design of concrete roads This method is based on the systematic observation of the performance of a considerable number of experimental roads , provided with unreinforced and reinforced concrete pavement, and on regression equations which have been developed for the structural design of both types of pavements. The design life is defined as the traffic carried to a well defined condition of pavement deterioration, and a simple method based on thickness elastic analysis it is used to evaluate pavement foundation support. According this method, stresses predicted by multi-layer elastic analysis for various pavement designs, developed from regression equations for unreinforced concrete are giving a unique relationship between the design life and the ratio of flexural concrete strength to combined traffic and thermal stresses within the slab, this suggesting as possible and reliable, a criterion of design based on this ratio. The regression equations developed for the unreinforced concrete pavements are giving similar results to those obtained from the AASHTO Design method. According the Highway Agency method the practical choice of foundation was restricted by the need to provide a sub-base/subgrade combination that is not erodable and is providing an all weather platform for road construction (cemented sub-base foundation yielding a minimum value of equivalent foundation modulus of 270 MPa and concrete with

28-day mean compressive strength of 50 MPa chosen for pavement slabs). The design curves are extrapolated in order to provide designs for roads with very heavy traffic, up to 300 million single axles (msa).

According to Romanian Standard [20], the thickness design of the rigid pavements is based on the allowable strength criterion, considering the tensile strength from bending in the cement concrete, σ_{tadm} . The computation model is a finite element one, using a multi-layer structure, made-up from the PCC layer and an equivalent layer of the under-lying real layers (base course, subbase course, foundation). The main stages of the rigid pavement design are establishing the design traffic, establishing the bearing capacity of the foundation soil, conceiving the rigid pavement structure, depending on the technical class of the designed road, establishing the bearing capacity at the level of the base course, determining the thickness of the surface course, using the design criterion, in various design hypothesis.

In one of the most recent developments, the American Association of State Highway and Transportation Officials' (AASHTO's) Joint Task Force on Pavements endorsed a new design guide. The National Cooperative Highway Research Program (NCHRP) has developed a new pavement design and analysis tool, The Mechanistic-Empirical Design Guide (M-E PDG) for New and Rehabilitated Pavement Structures, under NCHRP 1-37A. The Guide employs mechanistic-empirical approaches. These approaches provide a more realistic characterization of in-service pavements and provide uniform guidelines for designing the in-common features of flexible, rigid, and composite pavements. By using these approaches, engineers can create more reliable pavement designs.

During the last 5 years, M-E PDG has taken giant strides in moving from the conceptual stages to full implementation. It includes a number of input parameters related directly to placement conditions and mix design, conditions during paving which can have impact on the resulting roadway's performance. The new guide also includes defined modes of failure including cracking, faulting, and IRI (International Roughness Index) for concrete pavements and rutting, fatigue cracking, thermal cracking, IRI, and others for asphalt pavements.

In the frame of Ecolanes project, the three design methods are intended to be used. Finally the best fitted one will be selected, taking into consideration various extensions of design life, based on technical and economical criteria, in order to be proposed for the various EcoLanes demo projects.

For options C, by adopting the assumptions that, between the asphalt surface and the concrete base, there is no bonding, it is highly recommended that the layers thickness design to be conducted separately for each layer, according the specific existing norms, as follows: for concrete base: "Technical Norm for Structural Design of Concrete Base for Pavements": NP 111-04, 2005 and Ecolanes internal reports [19] and for asphalt layers, the Asphalt Institute Design Method and the

Romanian official method. Other Romanian norms to be used will be referring the execution of plain, reinforced and prestressed concrete pavement layers (NE - 012 – 1999), execution of PC pavement layers with fixed and sliding forms (NE – 014 – 2002) and practice code for establishing the performance criteria and composition of SFRC (GP 075 – 2002).

6. CONCLUSIONS

As a result of the wide experience accumulated all over the world, with a rigid pavements the extended life, it seems too early to predict the long-term performance of heavy-duty highways built to the current configuration of PCC pavements or with SRCP base layer with lean-mix concrete subbase. Those pavements built on very good formations are likely to have longevity; however, other pavements with variable or weak support from the foundations have shown signs of distress even during their design life.

Also, the prediction of long-life, heavy-duty concrete pavements using the ALT devices was not always conclusive, and the existing SHRP LTPP sites in Romania and abroad, are showing low levels of deterioration, these pavements appearing to have a long life.

An analysis of life cycle costing of concrete and asphalt pavements on various experimental sections indicates that concrete pavements designed according to extended-life criteria, will have a low-maintenance regime. If maintenance costs are an indication of long life, data are currently being gathered at international level may indicate that these are long-life pavements. From the existing experience, it was found that the following points could better describe the techniques that may lead to long – life rigid pavements:

- Concrete base with a minimum compressive and flexural strength of 35 MPa and 4.5 MPa, respectively, at 28 days age.
- The use of concrete tied shoulders with a width of 2 to 3 m in the curb lane and 0.6 m in the median lane.
- Appropriate joint layout to reduce corner stresses and to allow heavy vehicles to travel in the “middle” of the slab.
- A stabilized upper formation to provide long-term support.
- Thin layers of asphalt on CRCP to reduce the wheel footprint on the concrete and minimize the thermal effects on the base slab.
- Top of the formation prepared with a primer seal or with a thin asphalt layer both this layers besides ensuring an uniform support surface for the concrete slab have also a significant role in facilitating the drainage of the infiltration surface waters to the subgrade, that preventing the faulting of the slabs during the exploitation of road.

- More accurate traffic projections and more advanced design tools have led to thicker designs of concrete plus an additional 25 mm thickness expected to be removed during a future diamond grinding to restore smoothness.
- A relative thin asphalt layer over an aggregate base and a classic foundation, are used to limit slab deflection and pumping.
- The initial concrete pavements omitted dowel bars; however, they are now recommended to be used in order to minimize faulting potential.

References

1. Vorobieff G., Moss J., *Australia's Experience With Long-Life, Heavy-Duty Concrete Pavements*, Proceedings of the International Conference on Long-Life Concrete Pavements, Chicago , Illinois, October 2006
2. Caestecker, Chris, *The Motorway E40 (Formerly E5) From Brussels to Liège*, Proceedings of the International Conference on Long-Life Concrete Pavements, Chicago , Illinois, October 2006
3. Helmus V., *The Walloon Motorway, From One Millennium To Another*, Proceedings of the International Conference on Long-Life Concrete Pavements, Chicago , Illinois, October 2006
4. Boboc, V. et al, *Realizarea investigatiilor RO-LTPP de teren periodice in raza DRDP Brasov, A44/T4 Research Report*, Technical University "Gh. Asachi", Iasi,2002 (in Romanian)
5. *Incipient Deliverable 3.2 Report: Laboratory Accelerated Load Testing & Further Developments on Deliverable 3.1*, EcoLanes Internal Report, 2007
6. N. Taranu, *EcoLanes WP 3 Monthly Progress Report*, Antalia, 2007
7. COST 347 Final Report, *Improvements in Pavement Research with Accelerated Load testing*, 2005
8. SHRP-C-362, *Mechanical Behavior of High Performance Concretes*, Volume 2, Production of High Performance Concrete, Strategic Highway Research Program, National Research Council, Washington, DC, 1993
9. AASHTO Task Force 36 Report, *The Use and State-of-the-Practice of Fibre Reinforced Concrete*, August 2001
10. SHRP-C-345, *Synthesis of Current and Projected Concrete Highway Technology*, Chapter 2: Current and Projected materials Technology – Admixtures, p.73, Strategic Highway Research Program, NRC, Washington DC, 1993
11. Bayasi, Z., Soroushian, P, *Optimum use of Pozzolanic materials in Steel Fibre Reinforced Concretes*, Transportation Research Record, 1226:25-30, 1989
12. Ramakrishnan et al., *Performance characteristics of fibre reinforced concrete with low fibre contents*, ACI Journal 78 (5):388-94, 1981
13. FHWA_RD_77-110 Report, *Identification of candidate zero maintenance paving materials*, 2vols., 1977
14. Galloway, J., W., Gregory, J.M., *Trial of a wire-fibre-reinforced concrete overlay on a motorway*, TRRL Laboratory report 764, 1977
15. SHRP-C-361, *Mechanical Behaviour of High Performance Concretes*, Vol 1, Summary Report, Executive Summary, Strategic Highway Research Program, NRC, Washington DC, 1993
16. Ramakrishnan, Wu, Hosalli, G., *Flexural fatigue strength endurance limit and impact strength of fiber reinforced concrete*, Transportation Research Record 1226:17-24, 1989
17. Avram, C-tin, Filimon, I., Bob, C., Buchman, I., *Indrumar pentru folosirea betonului armat cu fibre metalice*, Buletinul constructiilor, no.3, 1977 (in Romanian)
18. Tlemat, Houssan, *Steel fibers from Waste Tyres to Concrete; testing, modelling and design*, doctoral thesis, Sheffield University, 2004
19. Angelakopoulos, Harris, *Rolled Compacted Concrete*, EcoLanes Internal Report, 2007
20. NP 081 – 2002, *Normativ pentru dimensionarea sistemelor rutiere rigide* (in Romanian)

THE OPTIMIZATION OF TRANSPORT PROBLEMS USING LINEAR PROGRAMMING

Cornelia Victoria ANGHEL

Computer Science Department, EFTIMIE MURGU University of Resita, 320085 Resita, Romania,
canghel@uem.ro

Summary

The article presents some notions about „Linear Programming”, as a mathematical method of solving the optimization problems of phenomena resulting from different economic processes. Thus, we seek to obtain some optimum results of production quantity at low costs. An eloquent numerical example is given in order to describe how to obtain the optimum solution of transportation problems.

KEYWORDS: optimization, linear programming, transport problem

1. GENERAL NOTIONS OF LINEAR PROGRAMMING

The linear programming or the linear optimization is a part of the disciplines having several practical applications. It allows the analysis of some economic or social activities and it proposes the optimization of the solutions for the problems of these domains.

The objective of the problem is the optimization of a certain process depending on the same variables which appear in the restrictions system. This process is described through a function, called *objective function*, efficiency function or economic function.

Mathematically the objective function is determined by the relation:

$$Z(x) = \sum_{i=1}^n c_i \cdot x_i \quad (1)$$

in which: $Z(x)$ – represents the objective function

c_i - represents the costs coefficients

x_i - represents the activities vector

By this notations the linear optimization problem aims at finding a solution in the multitude of solutions for which the maximum or minimum value of the objective function is obtained.

Thus the standard form of a programming problem or linear optimization is:

$$\text{opt } Z(x) = \text{opt} \left(\sum_{i=1}^n c_i \cdot x_i \right) \quad (2)$$

where the optimization terms the minimization or maximization of the objective function on the multitude of admissible solutions and the system of equations which has to be solved is written:

$$\begin{cases} \sum_{i=1}^n a_{\alpha i} \cdot x_i = b_{\alpha}, & \alpha = 1, 2, \dots, m \\ x_i \geq 0 & i = 1, 2, \dots, n \end{cases} \quad (3)$$

where $A = \parallel a_{\alpha i} \parallel$ represents the matrix (the vector) of technologic coefficients and $B = (b_1, b_2, \dots, b_m)$ the matrix (the vector) of resources.

To bring the linear optimization problem to the standard form is possible because an inequation can be transformed into an equation by introducing some variables called separation or compensation variables.

Likewise, because the objective function is a linear function, a maximum problem can be studied as a minimum problem because:

$$\max [Z(x)] = - \min [- Z(x)] \quad (4)$$

The linear optimization developed simultaneously with the practical applications. That is why some notions have names which disclose this side.

2. TRANSPORT PROBLEMS

It is considered that a certain product is stocked in m supply centres (warehouses or suppliers) which have to reach the consumers (shops, enterprises, etc). The considered product is available in quantity a_i ; $1 \leq i \leq m$ at supplier I and is demanded in quantity b_j by the consumer j ; $1 \leq j \leq m$.

We note with x_{ij} the quantity of the considered product which supplier i makes available for consumer j (known quantity) and the unitary transport expenses from supplier I to consumer j are c_{ij} .

We have to determine the product quantities x_{ij} which are to be allotted to the warehouse centers, to the consumption centers, so that the available elements to be finished in each warehouse, the demand to be satisfied in each consumption centre and the transport total cost to be minimum.

It is supposed that $\sum_{i=1}^m a_i = \sum_{j=1}^n b_j$ this is a *balanced* transport problem.

The mathematical model of the problem in this case, is expressed as follows:

Minimize the function:

$$[\min] Z(x) = \sum_{i=1}^m \sum_{j=1}^n c_{ij} \cdot x_{ij}$$

in the conditions:

$$\left\{ \begin{array}{l} \sum_{j=1}^n x_{ij} = a_i; 1 \leq i \leq m; \\ \sum_{i=1}^m x_{ij} = b_j; 1 \leq j \leq n; \\ x_{ij} \geq 0; 1 \leq i \leq m; 1 \leq j \leq n; \end{array} \right.$$

3. NUMERICAL APPLICATION

A society has the executed product deposited in 3 warehouses D₁, D₂, D₃. It must be distributed to 4 consumers (beneficiaries) C₁, C₂, C₃, C₄. The available and necessary conditions and the transport unitary price are given in the following table:

Table 1.

Consumers	C ₁	C ₂	C ₃	C ₄	Available (offer)
Warehouses					
D₁	2	3	1	4	140
D₂	3	1	4	3	160
D₃	4	2	3	2	200
Necessary (demand)	115	135	130	120	500

The problem is balanced (the demand is equal to the offer).

The north-west corner method does not take into account the unitary price and the following solution is found:

$$X_{11}=115; \quad X_{12}=25; \quad X_{13}=X_{14}=0;$$

$$X_{21}=0; \quad X_{22}=110; \quad X_{23}=50; \quad X_{24}=0;$$

$$X_{31}=0; \quad X_{32}=0; \quad X_{33}=80; \quad X_{34}=120;$$

$$Z_{\min}=2*115 + 3*25 + 1*110 + 4*50 - 13*80 + 2*120=1095 \text{ u.m.}$$

The line minimum cost method takes into account the fact that the transport is paid by the supplier.

4. CONCLUSIONS

The linear programming or the linear optimization is a mathematical method used in solving the problems met in different domains of economic or social activity. The advantages of its use consists in the calculation algorithmic effect and through the correct imposing of restrictions the objective function will reach the optimal (the minimum or the maximum).

References

1. Anghel C.V. ș.a. – „Cercetări operaționale. Aplicații”, Ed. Modus PH, Reșița, 2005;
2. Anghel C.V. ș.a. – „Programarea liniară – metodă matematică de rezolvare a problemelor multidisciplinare”, Simpozion Științific, Timișoara, 2002;
3. Anghel, I., Anghel C.V. – „Matematici pentru economiști”, Ed. UEM Reșița, 1994.

Polymer concrete optimization using mixture design of experiment and response surface methodology

Marinela Bărbuța¹ and Daniel Lepădatu²

¹Concrete, Material, Technology and Organization Department, Technical University "Gh. Asachi",
Iasi, Romania

²Civil Engineering Department, Technical University "Gh. Asachi", Iasi, Romania

Abstract

The aim of this paper is using statistical technique to analyze data from mixture experiment design and involve regression models to determine the response surface of polymer concrete. The experimental studies were realized on polymer concrete prepared of epoxy resin, silica fume and aggregates. The combinations were designed based on the mixture design concept of design of experiments. For each polymer concrete combination, the mechanical properties were studied. The results are reported for polymer concrete realized of epoxy resin and silica fume (SUF) as filler. Each response (mechanical property) was individually optimized and compared with experimental data.

KEYWORDS: resin, polymer concrete, optimization, mixture design of experiment

1. INTRODUCTION

The processes optimization is one of the most important problems that appear in the activity of the researchers and engineers. The polymeric concrete [1-3] occurred and developed in construction industry due to its advantages compared with the Portland cement concrete, such as: quick setting characteristics, high mechanical strength, chemical resistance and wear resistance. In the composition of polymeric concrete are used the same components: aggregates and the binder that for polymeric concrete is a resin that reacts with a hardener and bind together the aggregates. Different types, properties and applications of polymer concrete have been reported [4]. The performances and the use domain of polymer concrete depend on the polymer binder, type of filler and aggregates. The mechanical properties and the curing behavior depend on the selection and the content of the polymer, temperature and aggregate type and dosage. The presence of filler is also important and the use of silica fume in the mix improved the mechanical properties. The present paper deals with the influence of polymer concrete components on its characteristics. The optimizing of polymer concrete mix was

realized by experimental researches on the basis of mixture design of experiments and response surface methodology.

2. EXPERIMENTAL PROGRAM

The materials used were: epoxy resin, silica fume (SUF) and crushed aggregates of two grades 0-4 mm (Sort I) and 4-8 mm (Sort II).

The epoxy resin in combination with the hardener forms the binder of the polymer concrete.

The silica fume is a by-product that results from ferrosilicon production having the following characteristics:

- particle sizes of 0.01...0.5 μ ,
- shape of particles is spherical,
- specific surface is between 13000 and 23000 m^2/kg ,
- density between 2.1 and 2.25 g/cm^3 [2].

The aggregates were obtained from river stone by crushing.

Polymer concrete of different compositions as is given in Table 1 was prepared by mixing required quantities of epoxy resin firstly with aggregates, than with the filler (SUF) was added slowly in a mechanical mixer. Than the casting of specimens (cubes of 70.7 mm sides) were prepared for determining the densities and the mechanical characteristics (Compressive Strength - CS).

Table 1. Mixture design combinations for polymer concrete

Mixture	Epoxy resin (%)	SUF (%)	Aggregate Sort I (%)	Aggregate Sort II (%)
PC1	18.8	6.48	37.4	37.4
PC2	12.4	12.8	37.4	37.4
PC3	12.4	6.4	43.8	37.4
PC4	12.4	6.4	37.4	43.8
PC5	15.6	9.6	37.4	37.4
PC6	15.6	6.4	40.6	37.4
PC7	15.6	6.4	37.4	40.6
PC8	12.4	9.6	40.6	37.4
PC9	12.4	9.6	37.4	40.6
PC10	12.4	6.4	40.6	40.6
PC11	16.4	7.2	38.2	38.2
PC12	13.2	10.4	38.2	38.2
PC13	13.2	7.2	41.4	38.2
PC14	13.2	7.2	38.2	41.4
PC15	14.0	8.0	39	39,0

3. MIXTURE DESIGN OF EXPERIMENT AND RESPONSE SURFACE METHODOLOGY

3.1. Mixture design of experiment

Research in many disciplines frequently involves blending two or more ingredients together. The design factors in a mixture experiment [5-7] are the proportions of the components of a blend, and the response variables vary as a function of these proportions making the total and not actual quality of each component. The total amount of the mixture is normally fixed in a mixture experiment and the component settings are proportions of the total amount. The component proportions in a mixture experiment cannot vary independently as in factorial experiments since they are constrained to sum to a constant (1 or 100% for standard design). Imposing such constraint on the component proportions complicates the design and the analysis of mixture experiments. Although the best-known constraint in a mixture experiment is to set the sum of the components to one (100%) additional constraints such as imposing a maximum or minimum value on each mixture component may also apply.

3.2. Response surface methodology

The Response Surface Methodology (RSM) provides an approximate relationship between a true response y and p design variables, which is based on the observed data from the process or system [8-12]. The response is generally obtained from real experiments or computer simulations, and the true response y is the expected response. Thus, real experiments are performed in this paper. We suppose that the true response y can be written as:

$$y = F(x_1, x_2, \dots, x_p) \tag{1}$$

where:

the variables x_1, x_2, \dots, x_p are expressed in natural units of a measurement, so are called as the natural variables. The experimentally obtained response Y differs from the expected value y due to random error.

In many cases, the approximating function F of the true response y is normally chosen to be either a first-order or a second-order polynomial model, which is based on Taylor series expansion. In general the second-order model is:

$$Y = \beta_0 + \sum_{j=1}^p \beta_j x_j + \sum_{j=1}^p \beta_{jj} x_j^2 + \sum_{i < j}^p \beta_{ij} x_i x_j + \varepsilon \tag{2}$$

4. RESULTS AND DISCUSSIONS

Out of number of factors identified by their simplified notation (A, B, C and D), the following ones were considered to be most important and necessary to control:

- Epoxy resin (A),
- Silica fume (B),
- Aggregate sort I, 0-4 (C),
- Aggregate sort II, 4-8 (D).

The input variables, range chosen for the study, their coded value, and mixture design combination are given in Table 2 and 3.

Table 2. Range of variables and their coded form

Sample	Variable	Lower limit		Upper limit	
		%	Coded value	%	Coded value
1	A	0	0.108	1	0.236
2	B	0	0.064	1	0.192
3	C	0	0.06	1	0.728
4	D	0	0.1	1	0.228

Table 3. Mixture design combination for Polymer Concrete

Combination reference	A(%)	B(%)	C(%)	D(%)
1	0.236	0.064	0.6	0.1
2	0.108	0.192	0.6	0.1
3	0.108	0.064	0.728	0.1
4	0.108	0.064	0.6	0.228
5	0.172	0.128	0.6	0.1
6	0.172	0.064	0.664	0.1
7	0.172	0.064	0.6	0.164
8	0.108	0.128	0.664	0.1
9	0.108	0.128	0.6	0.164
10	0.108	0.064	0.664	0.164
11	0.188	0.08	0.616	0.116
12	0.124	0.144	0.616	0.116
13	0.124	0.08	0.68	0.116
14	0.124	0.08	0.616	0.18
15	0.14	0.096	0.632	0.132

Each polymer concrete mixture was prepared and tested under identical conditions. The density of hardened concrete and the compressive strength at 14 days were determined experimentally. Table 4 summarizes mixture design and their experimental responses, Compressive Strength (CS) for each polymer concrete combination based on the concept of design of experiments. Mixture designs (1-10 runs) are sometimes augmented by adding interior points (11-15 runs). A center points will be added to the design data (Table 4) with 5 runs making 15 runs total. This addition will change the design from simplex-lattice to simplex-centroid design. The experimentally studied response based on the results observed at the 14-days was analyzed statistically used Statistica software.

Table 4. Mixture design combination and their experimental responses

Combination Reference (runs)	A (%)	B (%)	C (%)	D (%)	Compressive Strength
1	0.236	0.064	0.6	0.1	59.2
2	0.108	0.192	0.6	0.1	58.79
3	0.108	0.064	0.728	0.1	59.59
4	0.108	0.064	0.6	0.228	57.61
5	0.172	0.128	0.6	0.1	64.08
6	0.172	0.064	0.664	0.1	58.62
7	0.172	0.064	0.6	0.164	43.47
8	0.108	0.128	0.664	0.1	45.95
9	0.108	0.128	0.6	0.164	55.21
10	0.108	0.064	0.664	0.164	55.62
11	0.188	0.08	0.616	0.116	58.8
12	0.124	0.144	0.616	0.116	63.2
13	0.124	0.08	0.68	0.116	65.32
14	0.124	0.08	0.616	0.18	57.61
15	0.14	0.096	0.632	0.132	57.75

Analyzing the experimental results we can observe the following:

- The values of compressive strengths varied between 65.32 N/mm² (for concrete type BP13) and 43.47 N/mm² (for concrete BP7) - that characterizes the polymer concrete as a high strength concrete.
- The epoxy resin dosage varied between 10.8% and 23.6% - the maximum compressive strength was obtained for 12.4%.

In the mixture design approach the total of amount of the input variables was fixed and constrained to sum 100. For each statistical combination, all proprieties of interest were measured and empirical models for each property as function of the input variables were determined from regression analysis. The advantage of the mixture approach is that the experimental region of interest is more naturally defined. To simplify calculation and analysis, the actual variables ranges were transformed to dimensionless coded variables with a range 0 and 1. Intermediate values were also translated similarly. The variables A, B, C, and D were codified using the following formula:

$$Pseudo = (R_i - L_i) / (1 - L) \quad (3)$$

where:

$R_i = A_i / \sum A_i$, L_i is the lower constraint in real value, L is the sum of lower constraint in real value, A is the actual value, and A_i is the total of actual values.

The second-order polynomial relation with special cubic interactions can approximate the mathematical relationship between four independent variables and the response:

$$Y = \beta_0 + \sum_{j=1}^p \beta_j x_j + \sum_{j=1}^p \beta_{jj} x_j^2 + \sum_{i < j} \beta_{ij} x_i x_j + \sum_{i < j} \sum_{k=1}^p \beta_{ijk} x_i x_j x_k + \varepsilon \quad (4)$$

where:

β_i are linear coefficients, β_{ii} are quadratic coefficients, β_{ij} are cross-product coefficients, β_{ijk} are the special cubic coefficients and ε is the random error witch includes measurement error on the response and is inherent in the process or system. These coefficients are unknown coefficients usually estimated to minimize the sum of the squares of the error term, which is a process known as regression.

A standard statistical technique to carry it out is the analysis of variance (ANOVA), it is routinely used to provide a measure of confidence. ANOVA results for 14-day strength are shown in Table 5. By this way we can observe the importance of interaction effect of the three leading factors (ABC), which is expressed by the coefficient R-sqr – 0.99987 (Table 5). This coefficient shows an adequate fit for the predictive response surface model of Compressive Strength.

Table 5. Summary of ANOVA

	SS Effect	df Effect	MS Effect	SS Error	df Error	MS Error	F	p	R-Sqr	R-Sqr Adjusted
Linear	10.4285	3	3.4761	228.504	11	20.77316	0.16734	0.916175	0.043646	0
Quadratic	155.595	6	25.932	72.9095	5	14.58191	1.778405	0.272058	0.694854	0.145591
Special										
Cubic	72.8799	4	18.219	0.02963	1	0.02963	614.9242	0.030235	0.999876	0.998264
Total										
Adjusted	238.933	14	17.066							

Pareto chart obtained from the statistical analysis is presented in Figure 1, and shows the importance order of the variables. This chart shows the variables effects on the compressive strength variation of the polymer concrete.

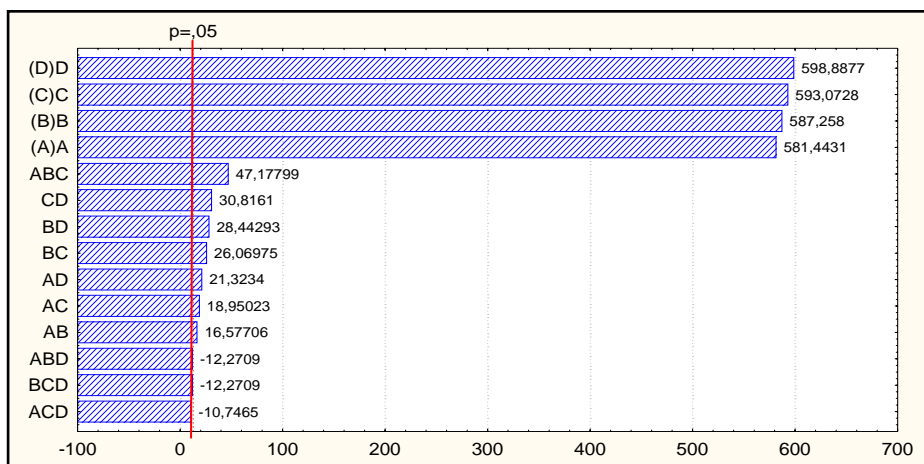


Figure 1. Pareto chart of standardized effect of CS

The Pareto diagram shows that the four leading factors, epoxy resin (A), silica fume (B) and crushed aggregates sort I, and II (C and D) in the inverse important order.

Analysis of variance gives the non-linear response surface with the significant interactions: ABC (epoxy resin (A), silica fume (B) and crushed aggregates sort I (C) - Figure 2).

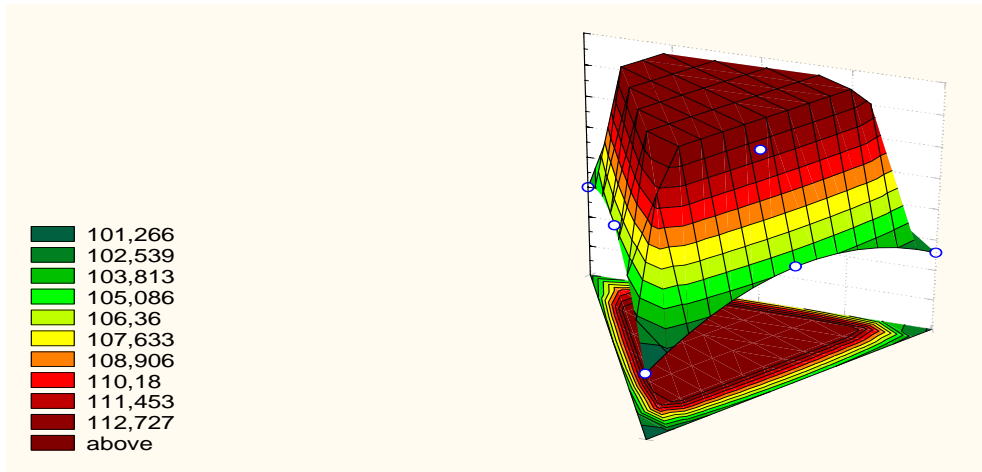


Figure 1. Response surface.

(a) Effect of Silica fume, Epoxy resin and Aggregate sort I on CS.

The results from the designed experiment indicate that the factors have very significant effects. The all second-order interactions have an important role. The special cubic interaction ABC has very significant effects and all others interactions have very weak effects whereas the other interactions are barely noticeable at all. As a consequence, those interaction effects can be neglected. If we neglect those interactions, the response surface of the Compressive Strength can be predicted by the following regression equation:

$$Y_{CS} = 99.993 \cdot A + 100.993 \cdot B + 101.993 \cdot C + 102.993 \cdot D + 13.970 \cdot AB + 15.970 \cdot AC + 17.970 \cdot AD + 21.970 \cdot BC + 23.970 \cdot BD + 25.970 \cdot CD + 990.4 \cdot ABC \quad (5)$$

If we choose following combination (in coded factor):

$$A(0.5), B(0), C(0) \text{ and } D(0.5)$$

It is possible to reduce the Compressive Strength to: $CS = 43.47$. This value corresponds to trial 7.

5. CONCLUSIONS

Polymer concretes were made with epoxy resin, silica fume and aggregates. Response surface method has been used for a better understanding of the influence of the deviation of the polymer concrete parameters on the Compressive Strength evolution. The properties of polymer concretes made with epoxy resin, silica fume

and aggregates was studied. For compressive strength were obtained high values, that show that there is a high strength concrete. The optimizing of compressive strength as maximum strength (CS = 65.32) was obtained corresponding to a resin dosage of (12.4%) which is the same with that obtained experimentally.

References

1. Blaga A., Beaudoin J.J., *Polymer Concrete - Canadian Building Digest*, CBD 242, Ottawa, 1985.
2. Bărbuță M., Nour D.S., C. Szalontay, *Aderenta mortarelor polimerice la zidarie*, Simpozionul national cu participare internationala „Probleme actuale privind conservarea si reabilitarea cladirilor cu valoare istorica” Iasi 18 mai 2007 Editura Societatii Academice „Matei-Teiu Botez” ISBN 978-9738955-10-3, pp.49-54, 2007.
3. Abdel-Fattah H., El-Hawary M. *Flexural behavior of polymer concrete*, Construction and Building Materials 13, pp:253-262, 1999.
4. Fowler D.W., *Polymers in concrete :a vision for 21st century*, Cement and Concrete Composite 21, pp: 449-452, 1999.
5. Muthukumar, M., and Mohan, D., *Optimization of Mechanical Proprieties of Polymer Concrete & Mix Design Recommendation Based on Design of Experiments*, Journal of applied Polymer Science, Vol. 94, pp: 1107-1116, 2004.
6. Muthukumar, M, Mohan, D., and Rajendran, D., *Optimization of mix proportion of mineral aggregates using Box Behneken design of experiments*, Cement and Concrete Composites, Vol. 25, pp: 751-758, 2003.
7. Marcia J Simon, Eria Slagergren, Kenneth A Snyder, *Concrete mixture optimization using statistical mixture design method*, Proceedings of International Symposium of Height Performance Concrete, New Orleans, Louisiana, October 20-20, 1997.
8. Cornell, J.A., *How to Apply Response Surface Methodology*, vol. 8, ASQC, Wisconsin, 1990.
9. Mayer RH and Montgomery DC, *Response Surface Methodology process and product optimization using design of experiments*, Wiley, New York, 1995.
10. Montgomery Douglas C., *Design and analysis of experiments*. – 5th edition by Wiley & Sons, Inc., New York., 2001.
11. Lepadatu D. et all, *Optimization of springback in bending process using FEM and Response Surface Methodology*, International Journal of Advanced Manufacturing Technology, 27, pp: 40-47, 2005.
12. Lepadatu D. et all, *Statistical investigation of die wear in metal extrusion process*, International Journal of Advanced Manufacturing Technology, 28, pp: 272-278, 2006.

Strengthening and reconstruction technology of an old steel highway bridge.

Dorel Bolduş¹, Radu Băncilă², Edward Petzek³

¹"Politehnica" University Timișoara, Faculty of Civil Engineering, e-mail: d_boldus@yahoo.co.uk,

²"Politehnica" University Timișoara, Faculty of Civil Engineering, e-mail: radu.bancila@ct.upt.ro

³"Politehnica" University Timișoara, Faculty of Civil Engineering, e-mail: edward.petzek@ct.upt.ro

Summary

*In the western part of Romania, on the highway network still are in operation, after two World Wars and other events, some old highway bridges erected on the beginning of the last century. These structures are "witnesses of the past" representing technical monuments with emblematic character. The duty of the administration is to maintain these structures in service. The bridge in **Săvârșin** over the Mureș River on the local highway DJ 707 A (km 1 + 271 m) is a remarkable structure with four spans erected in 1897. The technical condition of the bridge was unsatisfactory, the elements are corroded and some verticals and diagonals are damaged by the impact with the vehicles. The existent floor beams, stringers and cross girders are simple supported elements. The deck consists of Zorres elements filled with ballast, supporting an asphalt surface. In present the structure has a special importance being the only crossing of the river in a large area. Taking into account the importance of the structure, its historical value the decision of strengthening of the structure was taken. The structure is in present subdued to a complete strengthening activity, which is due to be finished probably at the end of 2007. The paper will present different aspects of old structure's strengthening and reconstruction works.*

KEYWORDS: old highway bridges, witnesses of the past, reinforcement, reconstructions, maintenance.

1. INTRODUCTION

In the western part of Romania – in Banat, the highway and railway network is dense. Consequently many bridges were built at the end of the XIX and the beginning of XX century. With a total surface of 28 000 km² the Banat county is located between the Mureş and Tisa River, the Danube in the south and the Carpathians mountains in the Est. There are many rivers in this region, all of them finally effluents of the Danube. The bridge in Săvârşin over the Mureş River on the local highway DJ 707 A (km 1 + 271 m) – Figure 1, is a remarkable structure with four spans erected in 1897. In present the structure has a special importance being the only crossing of the river in a large area. It can be also mentioned that in Săvârşin is the present summer residence of the former King of Romania Mihai I.

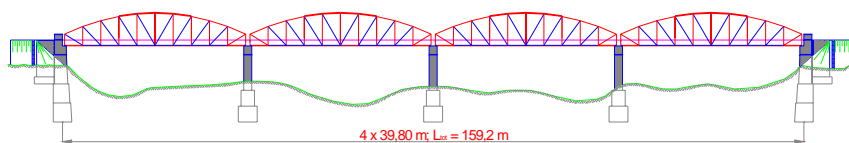


Figure 1. The bridge in Săvârşin, general view

2. REHABILITATION OF THE STRUCTURE

Taking into account the importance of the structure, its historical value and the aesthetic appearance (Figure 2) the decision of strengthening of the structure was taken:

- for the stringers the flanges were consolidated by supplementary plates (Figure 3);
- the cross girders were transformed in switch girders (Figure 5);
- for the lower chord of the main girder a supplementary tie member was chosen (Figure 4 and Figure 5);
- for the upper chord the direct strengthening with two angles, improving also the local stability was chosen (Figure 3);
- diagonals and vertical members have to be first of all straighten, and strengthen by additional plates;
- the old floor system was replaced by a composite deck (Figure 5).

All these operations are difficult and suppose a high technical level of all in situ works.



Figure 2. The bridge in Săvârșin; general view

2.1. Direct reinforcement

It is used for local deterioration or the increase of bearing capacity; reinforcement is carried on by additional elements. This method was used for the elements showed in figure 3 and figure 4.

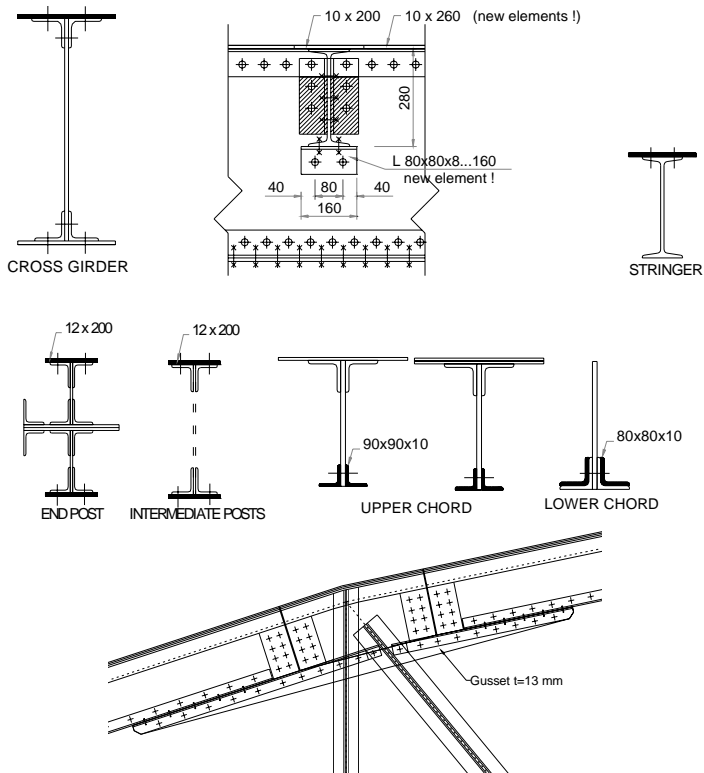


Figure 3. Direct reinforcement with additional elements

2.2. Indirect reinforcement

Additional elements were inserted as independent pieces (tie consolidation without pre-stressing) (Figure 4, Figure 5).

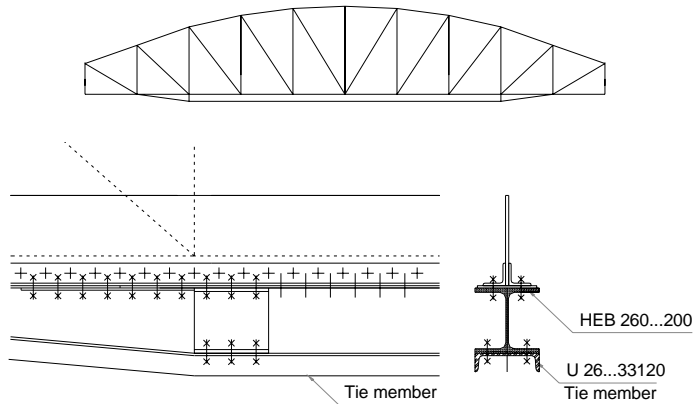


Figure 4. The reinforcement of the main girder with tie member

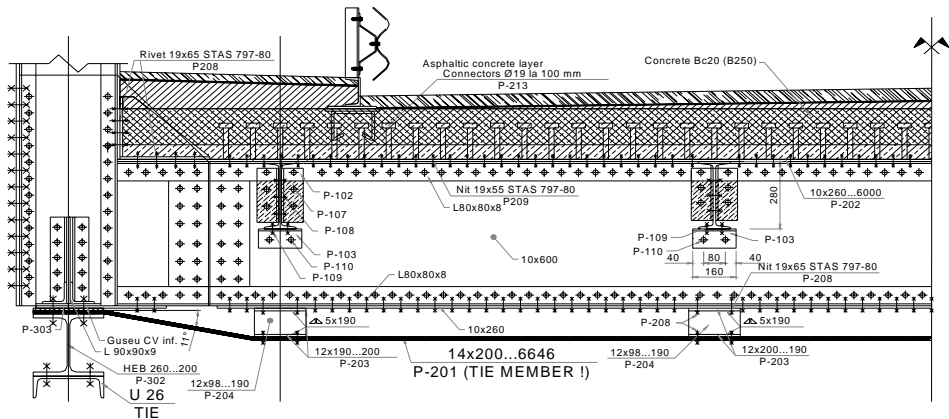


Figure 5. The reinforcement of the cross girder with tie member

2.3. The reinforcement of the deck by transforming it into a composite structure

The concrete slab can be placed over the upper flanges of the stringers and cross girders using steel sheets and stud shear connectors (see Figure 6).

Note: The connectors are welded only on the new reinforcement plate.

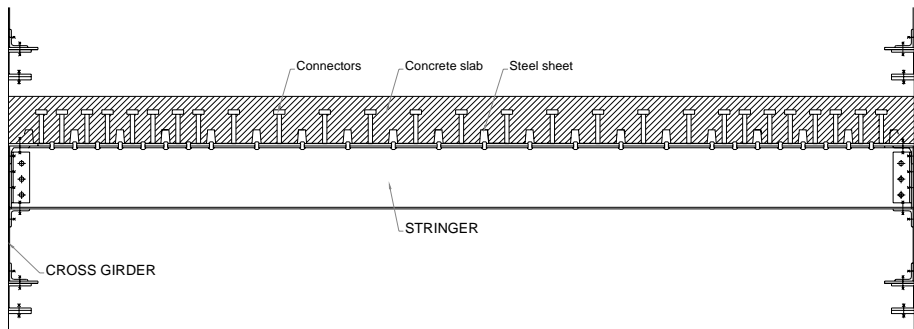


Figure 6. The new deck of the bridge

2.4. Other aspects of reinforcement

- the replacement of the superior wind bracing (see figure 7);

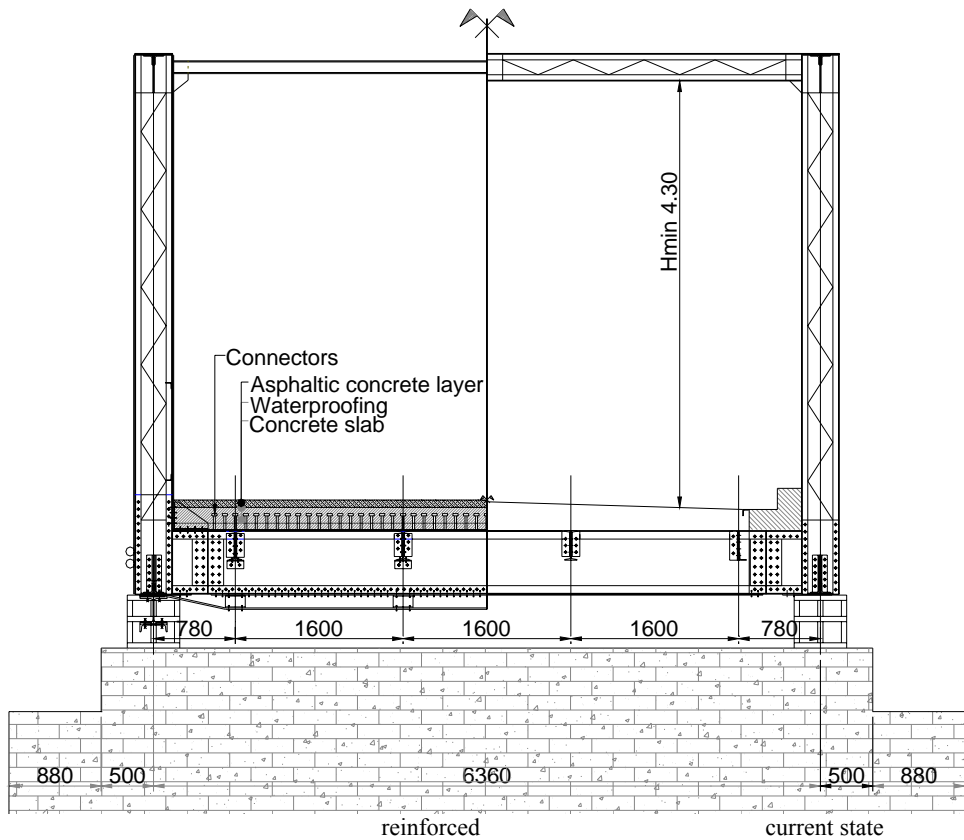


Figure 7. Cross section of the bridge

- the placing of a safety parapet (see figure 5) and the disposal of two final portal frames to limit the gauge.

3. IN SITU WORKS

Some phases from the rehabilitation works at the Săvârșin Bridge are shortly presented in the following.

The works began by removing the pavement (Figure 8) and then by straightening the deformed posts (Figure 9 and Figure 10).



Figure 8. Removing the pavement supported by Zorres profiles



Figure 9. Deformation defect



Figure 10. Warm straightening of the deformed posts

Sand blasting of the structure (Figure 11) and after that cutting the new consolidation elements and their positioning, was one of the next steps.



Figure 11. Sand blasting of the structure



Figure 12. New consolidation elements



Figure 13. Riveting of the new steel elements

New reinforcement of the corner post – cross girder was disposed (Figure 12).

One of the most difficult problems was the riveting of the new elements (Figure 13). In order to maintain the initial character of the structure rivets with diameter of 21 and 23 mm were chosen.

In figure 14 the reinforcement of a current upper chord joint is presented.



Figure 14. Reinforcement of upper chord joint

In figure 15 the tie member of the lower chord and the tie member of cross girder can be seen.

In figure 16 the local consolidation in a current joint of the upper chord is shown.



Figure 15. Lower chord indirect reinforcement



Figure 16 .Detail of local joint consolidation (upper chord)

For the deck, the solution of a composite structure was chosen. The thickness of the new concrete deck is 22 cm. Headed studs with $D=22$ mm welded through steel sheets (Figure 17) were used.



Figure 17. New deck of the bridge; steel sheets and connectors welding

4. CONCLUSIONS

The paper gives an overview of the in situ assessment methodology for old steel highway bridges. Every case must be separately considered. Nevertheless the rehabilitation of such representative structures is one of the main tasks of the bridge engineers.

Some general aspects can be pointed out:

➔ A better knowledge of the fatigue resistance of riveted details and of the repair and strengthening of riveted bridge members damaged by fatigue, could extend the service life of a large number of bridges. In many cases there is a need to retain particular bridges as historical monuments.

➔ For a reliable assessment of existing bridges a unified methodology is needed including damage accumulation method and fracture mechanics concepts.



Figure 21. Bridge in Săvârșin, general view at final reconstruction works

The conclusions can be extended to other countries from Middle and Southeast Europe, where the situation of the existing bridges is similar.

References

1. * * * Code UIC 778-2R; Recommandations pour la détermination de la capacité portante des structures métalliques existantes; Union Internationale des Chemins de fer, Paris, 1986.
2. * * *, ICPTT Bucharest, „Laboratory and in situ tests for old steel bridges - Regional Railway Administration Timisoara”, contract nr. 6077, vol. I & II, Bucharest, 1987.
3. * * * Code UIC 778-2R; Recommandations pour la détermination de la capacité portante des structures métalliques existantes; Union Internationale des Chemins de fer, Paris, 1986.
4. * * *, DS 805 „Bestehende Eisenbahnbrücken. Bewertung der Tragsicherheit und konstruktive Hinweise, 1999.
5. * * *, SR 1911-98, „Railway steel bridges. Design rules”, Institutul Român de Standardizare, Bucharest, 1998.
6. AND 522-2002. Bridge Verification Methodology, Romanian Highway Administration.
7. ESDEP, vol. 28, 1995. Lecture 16.5 Structural Systems - Refurbishment, London.
8. I-AM 08/2002. Richtlinie für die Beurteilung von genieteten Eisenbahnbrücken, SBB CFF FFS.
9. STAS 1844-75. Steel highway bridges. Design of the superstructure.

INTEGRATED SYSTEM FOR MONITORING BRIDGE STRUCTURES

Comisu Cristian Claudiu

Technical University "Gh. Asachi" of Iasi, Romania

Summary

Use of integrated monitoring system for composite bridges ensures an increased structural durability and leads to a reaction of costs for inspection, repairs and rehabilitation. Integrated monitoring system assists and improves investigation and planning activities and allows optimized allocation of financial resources.

The permanent bridge monitoring system presents the following advantages:

- reduces the interferences with traffic;*
- reduces the costs of access to the structure elements;*
- allows monitoring of structural elements with difficult access;*
- allows a precise real time assessment of bridges conditions;*
- allows a precise evaluation of the degradation mechanisms and of their appearance;*
- defines precise elements parameters of a bridge maintenance and repair strategy.*

Use of integrated monitoring system for composite bridges secures a reduction of 25% of maintenance costs and increases by 10% the operation life of concrete bridges.

1. INTRODUCTION

The major part of the European infrastructure has reached an age where capital costs have decreased. But inspection and maintenance costs have grown such extensively, that they constitute the major part of the current costs. An ageing and deteriorating bridge stock presents the bridge owners with the growing challenge of maintaining the structures at a satisfactory level of safety, performance and aesthetic appearance within the allocated budgets.

Selecting the optimal maintenance and rehabilitation strategy within the actual budget is a key point in bridge management for which an accurate assessment of performance and deterioration rate is necessary. For this assessment, the use of an integrated monitoring system has several advantages compared to the traditional approach of scattered visual inspections combined with occasional on-site testing

with portable equipment and laboratory testing of collected samples. For this reasons, attention is more and more focusing on the development of permanent integrated monitoring system for durability assessment of concrete bridges.

2. INTEGRATED MONITORING SYSTEM

The main scope of the research is to develop an integrated monitoring system for durability assessment of existing and new concrete bridges. The system must interface and integrate the actual practice mainly based on visual inspections and combines the response of a number of different reliable sensors, installed on the structure to monitor the progress of damage, with enhanced realistic deterioration models. The system and the sensors were developed to cover the parameters for the most important deterioration mechanisms: corrosion of reinforcement in bridges, carbonation of concrete, freeze-thaw cycles, alkali-silica reaction and mechanical damage, as well as the changes in the structures behavior and safety: static deformation, strains; crack widths and vibrations (frequencies, amplitudes, accelerations and vibration modes).

The progress of the various types of damage mechanisms can be predicted by monitoring the key physical and chemical parameters of the materials (such as temperature, humidity and pH for the concrete, measured on the surface of the structure and as a profile through the concrete thickness, and/rate of corrosion of reinforcement), and key mechanical parameters (such as strains, deflections, vibrations). As the sensors have to be permanently installed on the structure, they must present special characteristics of durability, easiness of installation and substitution, apart from being obviously low cost.

The next point concerns the acquisition of the data collected on site and their transmission to a remote PC. All data must fit into numerical models to represent and to predict the deterioration of concrete bridges. Finally, the last component of the integrated monitoring system is given by software able to help in assessing the strategies of intervention for the individual bridges.

The research is divided in 7 tasks (figure 1).

Task 1 describes the state of the art of current practice in the fields of inspections, monitoring and maintenance, both in European Community and in the USA, underlying advantages and possible disadvantages as well. It results in a number of requirements and system specifications for the integrated monitoring system from the end-user point of view.

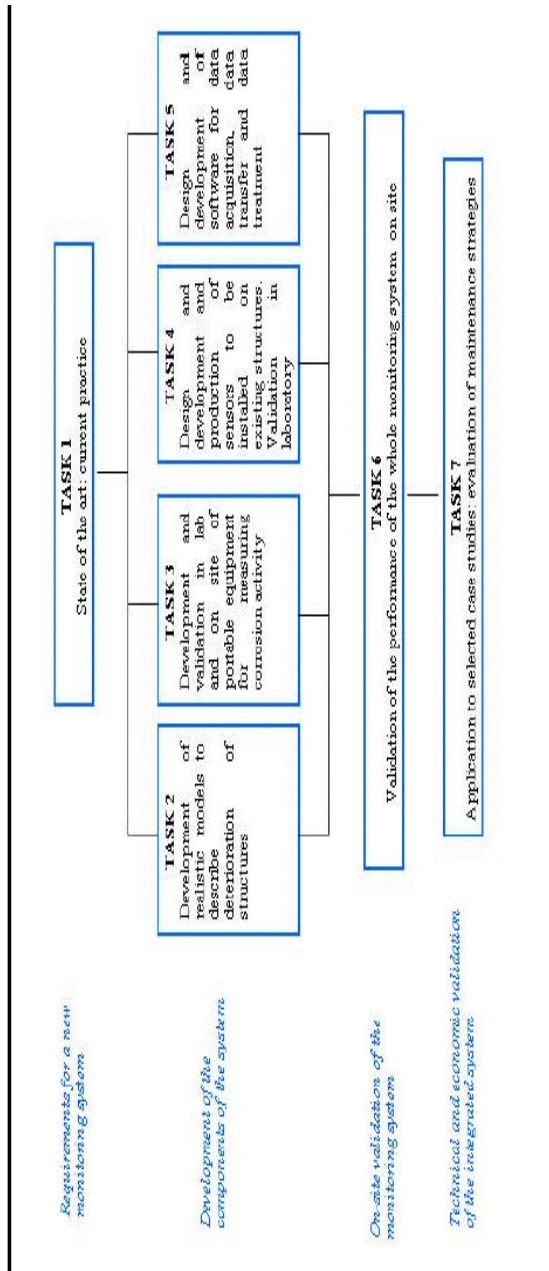


Fig. 1 The main tasks of the research

Task 2 concerns the description and correlation of the most relevant deterioration mechanisms for the structures with the parameters that may be measured on site. The focal point is the determination of the critical levels of both the parameters of the models and of the corresponding measurable parameters.

Task 3 is related to the implementation of portable equipment to measure corrosion activity. This equipment may be used to support the current activity of monitoring and inspection of bridges.

The objective of task 4 is the design, development and production of a number of sensors to be installed on the bridges to monitor their progressive deterioration. They have been firstly tested in laboratory where their performances have been compared to those of sensors and probes available on the market, to be next successfully installed and tested on an existing bridge.

Task 5 aims at designing and integrating the systems for data acquisition and transfer with the software for data treatment and analysis.

Task 6 represents the validation of the whole system that has been installed on an existing bridge in Romania. Data collected on site and transferred according to the results of task 5, are processed to evaluate the progress of deterioration, to define alarm thresholds and to establish maintenance strategies and compute the overall costs.

Finally, task 7 deals with the technical and economic validation of the entire integrated system, as it is necessary to evaluate the potential market for the developed system.

3. OPTIMAL MAINTENANCE STRATEGY

The bridge owners' main interest in permanent monitoring systems for durability and performance assessment of concrete bridges is to reduce the inspection, maintenance and rehabilitation costs as well as the traffic interference and yet still maintain a satisfactory level of safety, performance and aesthetic appearance.

The knowledge on the development of deterioration of structures, in both its aspects of initiation and quantification, is a key activity for the management of bridges, especially where it deals with the planning of maintenance and repair activities. It is particularly difficult to assess the conditions of bridges and to foresee the evolution of their damage as this process is affected by many factors, some of which interact and some of which have no measurable effects.

Permanent monitoring systems should therefore provide information that can be used as input for the decision making process (e.g. for estimating the extent and budgets for maintenance, rehabilitation and repair activities) such as probable deterioration mechanisms, estimates of the time for initiation and future development of deterioration, assessment of structural safety.

Permanent monitoring systems should be able to monitor the relevant deterioration mechanisms such as corrosion of reinforcement initiated by chloride ingress or

carbonation, freeze-thaw damage and alkali-silica reaction damage. Ideally, one or more measurable key parameters that can describe the progress towards initiation and subsequent growth of damage should be identified for each deterioration mechanism as well as simple deterioration models allowing for prediction of the initiation and growth of damage. Furthermore, the structural performance and the effects of e.g. mechanical damage due to deterioration, vehicle impact, overloading or loss of prestressing should be covered by the monitoring system (table 1).

Table 1.

Process to monitor	Relevant parameters	Location	Component of the system	Requirements
<ul style="list-style-type: none"> - corrosion - freeze-thaw - alkali-silica reaction - mechanical damage 	<ul style="list-style-type: none"> - humidity/moisture content - temperature - pH - chloride content - corrosion initiation/rate - permanent deflections - cracks - static and dynamic behavior (structural safety) 	areas critical: <ul style="list-style-type: none"> - safety - development of deterioration 	sensors /probes	<ul style="list-style-type: none"> - robust - accurate - durable - easy to install/operate
			empirical models	reliable trends of deterioration
			data acquisition	<ul style="list-style-type: none"> - automatic acquisition - adjustable frequency
			data transfer	remote communication site/office
			software for data treatment	-compatible with standard programs

To be effective, a permanent monitoring system must include a number of sensors installed on the structure, a data acquisition/transfer system and integrated software for analysis and treatment of information. They must have a long service life, be easy to install and to operate (traffic interference) and have a limited need for maintenance and calibration.

The data acquisition system should allow for adjustable measuring frequency (preferably on-line control), two-way communication between site and office, and send out warnings if parts of the system have stopped working. The software should be compatible with recognized standard programs. Results and data for daily operation or for research purposes should be easily accessible. The software should enable a simple and easy to understand presentation of the development of the monitored key parameters, i.e. the history, current situation and future development based on simple models for extrapolation to result in quick answers for the end users in the light of the management of bridges.

4. ADVANTAGES OF MONITORING SYSTEM

The integrated monitoring system should be able to help the end- user in his daily and long term management of the bridges.

The use of integrated monitoring systems has several advantages once the system is installed:

- Traffic interference is reduced
- The costs of access to the structure and resources for inspection and testing are reduced
- Structural elements with difficult access are easily monitored
- A more precise evaluation of the actual conditions of the structures with particular regard to the timely warning of the onset of durability and structural problems
- A more reliable prediction of the progress of damage as a function both of the measured parameters and of the application of realistic deterioration models, as well as a better understanding of individual deterioration mechanisms and their interaction
- An input for undertaking preventative actions for low levels of deterioration
- An input for defining maintenance and repair strategies (time and extent) as a function of the actual and foreseeable levels of deterioration
- A feedback on the effectiveness of repairs
- An evaluation of the need for further inspection and testing.

It is estimated that with the implementation of such integrated monitoring systems it should be possible:

- To reduce the operating costs of inspections and maintenance by 25%;
- To reduce the traffic-related costs by 30 % by reducing the number and extent of site inspections;
- To reduce the overall life costs of bridges by 10 % by applying the improved lifetime prediction models already from the design stage;
- The operator of the structures will be able to take protective actions before damaging processes start.

5. CONCLUSION

The integrated system for monitoring and assessment of concrete bridges will result in an improved knowledge of individual mechanisms and their interaction, and in early warnings of initiation and progress of durability and structural problems, thus finally reducing inspection, maintenance and rehabilitation costs as well as traffic delays.

This system may easily integrate and supplement the current practice in the field of inspection and testing and assist the end-user in the planning of maintenance programs. Additionally the operator of the structures will be able to take protective actions before damaging processes start. Their application will result in reduced costs of inspection and reduced interference to traffic.

The use of permanent monitoring systems has several advantages once the system is installed:

- Traffic interference is reduced
- The costs of access to the structure and resources for inspection and testing are reduced
- Structural elements with difficult access are easily monitored
- A more precise evaluation of the actual conditions of the structures with particular regard to the timely warning of the onset of durability and structural problems
- A more reliable prediction of the progress of damage as a function both of the measured parameters and of the application of realistic deterioration models, as well as a better understanding of individual deterioration mechanisms and their interaction
- An input for defining maintenance and repair strategies (time and extent) as a function of the actual and foreseeable levels of deterioration
- An evaluation of the need for further inspection and testing.

It is estimated that with the implementation of such integrated monitoring systems it should be possible:

- To reduce the operating costs of inspections and maintenance by 25%;
- To reduce the traffic-related costs by 30 % by reducing the number and extent of site inspections;
- To reduce the overall life costs of bridges by 10 % by applying the improved lifetime prediction models already from the design stage;
- The operator of the structures will be able to take protective actions before damaging processes start.

References

1. *Pardi L, Thøgersen F*-Smart Structures: An European research funded project”, Proc.IABMAS 02
2. *Bäßler R., Mietz J., Raupach M., Klinghoffer O.* - Corrosion Monitoring Sensors for Durability Assessment of Concrete Structures”, Proc. SPIEs 7th Internat. Symp. on Smart Structures and Materials, Newport Beach, article 3988 06 (2000).
3. *Bäßler R., Mietz J., Raupach M., Klinghoffer O.* - Corrosion Risk and Humidity Sensors for Durability Assessment of Reinforced Concrete Structures, Proc. EUROCORR 2000, London, article 100805 (2000).
4. *Goltermann P., Jensen F., Andersen M.E.* - Smart structures: Possibilities, experiences and benefits from permanent monitoring”, Proc. IABMAS 02.
5. *Bäßler R., Mietz J., Raupach M., Klinghoffer O.* - Corrosion Monitoring Sensors for Durability Assessment of Concrete Structures, Proceedings SPIEs 7th International Symposium on Smart Structures and Materials, Newport Beach, article 3988 06, 2000
6. *Schießl P.; Raupach M.* - A New Sensor System for Monitoring the Corrosion Risk in Existing Structures. In: Second International Conference on Concrete Under Severe Conditions - Environment and Loading (CONSEC 98), Tromsø, Norway, 565 – 573, 21.- 24.06.1998

STRUCTURAL IDENTIFICATION – DECISION FACTOR IN BRIDGE REHABILITATION

Cristian-Claudiu Comisu

*Department of Bridges, Faculty of Civil Engineerig,
Technical University "Gh. Asachi", Iasi, Romania*

Summary

The bridges from a motorway network are extremely vulnerable points. Interrupting their function may lead to severe economic, social and political consequences. In case to produce some catastrophic events (floods, earthquake, terrorist attack, etc.), the most serious consequences affect resistance of the bridge structure, affect serious the traffic and pedestrians comfort and. To re-establishment the traffic on the hi-way ,it is necessary to make an rapid intervention where the bridges are effected, to take in real time the decision to continue or to stop the circulation, to stabilize and identify the best reparation solution.

All this objectives can be touch thought construction a mobile laboratory with modal attestation and diagnostic in real time and who can ensure the possibility an quick intervention at distressed bridges, he is equipped with an electronic device capable to adopt and prioritize in real time the optimum reparation solution, who can give as the possibility to reestablish the vehicle traffic in the short time possible.

1. STRUCTURAL IDENTIFICATION OF BRIDGE STRUCTURES

National Roads Administration of countries throughout the world has the responsibility of maintaining the safe and efficient road networks that are important for a nation's economic development. A key element of any road network is the bridge infrastructure. Also, bridge maintenance is becoming an increasingly important issue in most developed countries. Limitations in the budgets available to Road Transport Authorities for bridge maintenance, rehabilitation, and reconstruction programs necessitate implementing comprehensive Bridge Management System that can accurately priorities this expenditure.

Damage or fault detection, as determined by changes in the dynamic properties or response of structures, is a subject that has received considerable attention in the literature. The basic idea is that modal parameters (notably frequencies, mode shapes, and modal damping) are functions of the physical properties of the

structure (mass, damping, and stiffness). Therefore, changes in the physical properties will cause changes in the modal properties.

A system of classification for damage-identification methods, as presented by Rytter (1993), defines four levels of damage identification, as follows:

Level 1. Determination that damage is present in the structure

Level 2. Determination of the geometric location of the damage

Level 3. Quantification of the severity of the damage

Level 4. Prediction of the remaining service life of the structure

For bridges damage may be material or structural defect formed during the construction stage or during its service life span resulting from natural disasters or man-made actions. Concrete bridges, for example, may experience tensile cracking, compression crushing and other forms of damage due to various types of loading such as earthquake, wind, thermal effect and accidental impact. If not detect and rectified early, such damage would increase maintenance cost, render the structures of bridges unserviceable and, in the extreme event, cause them to collapse catastrophically involving fatalities and injuries. It is therefore essential and necessary to carry out regular monitoring for early detection of structural damage.

While periodic visual inspections provide a generally economical means of condition assessment, they tend to be subjective so that reported results can vary from operator to operator.

Current damage-detection methods are either visual or localized experimental methods such as acoustic or ultrasonic methods, magnet field methods, radiographs, eddy-current methods or thermal field methods. All of these experimental techniques requests that vicinity of the damage is known a priori and that the portion of the structure being inspected is readily accessible. Subjected it these limitations, these experimental methods can detect damage on or near the surface of the structure.

Structural health monitoring systems, based upon some form of bridge response measurements, can be used to alleviate some of the shortcomings of traditional visual inspection techniques. Ideally, the SHM system should be inexpensive, non-invasive and automated, so that subjective operator differences are avoided. In particular, neither the implementation nor operation of the system should involve closure of the bridge.

Vibration data are ideally suited as the basis for a structural health monitoring system; they are cheap to collect, give a picture of the global response from relatively few sensors, and they can be used to identify changes in stiffness associated with damage from changes in the modal parameters. A reduction in

stiffness will lead to a reduction in natural frequency and a change in distribution of stiffness will lead to changes in mode shape.

2. STRUCTURAL IDENTIFICATION

Traditionally, vibration data for structural health monitoring or damage detection have been processed according to a system identification paradigm, the aim being to obtain the modal characteristics and track changes.

The use of system identification (SI) for structural health monitoring (SHM) has received considerable attention in recent years. System identification can be described as the process of deducing or updating structural parameters based on dynamic input and output (I/O) measurements, or in some cases solely based on output measurements. The structural parameters of concern could be stiffness, damping or modal parameters. Based on the change of structural parameters, the condition of structure of bridge can be monitored.

Many different methods of system identification have been developed. They can be broadly classified in various ways, such as frequency and time domain, parametric and nonparametric models, deterministic and stochastic approaches, on-line and off-line identifications, and classical and nonclassical methods (Koh and See, 1999). Thus far, the main categorization is by means of frequency and time domain methods.

Besides the disturbing action on the traffic, the methodology applied at this time in Romania and other countries of European Community has another series of major disadvantages, such as:

1. The low precision in indicating the moment of appearance, the evolution and the moment in which a critical point is reached during the process of deterioration that can be observed on the structure.
2. The observations are made exclusively visual without any possibility of receiving information about the gravity of the structural degradation process.
3. The great time interval between the moment in which the technical state is established and the decision of intervention, in case of major structural degradation which can seriously affect the safety and traffic, comfort on the highway.
4. In Romania there is no protocol meant to assure the results continuity and correlation between the stages of establishing the technical state.
5. There is no possibility to determine the exact time interval in which the bridge can still be exploited until the next stage of intervention.

6. There is no possibility for optimized administration of the financial resources by rational planning of repair and maintenance works.

Applying the of system identification (SI) for structural health monitoring (SHM) of composite bridges by creating a mobile laboratory, leads to elimination of any deficiency of the current methodology used at this time in Romania and allows it to become compatible with the technical requirements specified by the technical standards applied in the European Community.

The interest for applying system identification (SI) is an up-to-date matter and the numerous studies, research programs and scientifically manifestations of the last few years underline the increased attention given to this matter on the international level. Important research groups from the European Union (Switzerland, Germany, Great Britain, Italy, Denmark, France) but also from the USA, Canada and Japan, have begun since 1996 the implementation of important research programs whose results have already been communicated in conferences organized in this field of activity.

3. OBJECTIFS OF RESEACH PROGRAM

The research program has as goal the creation of a mobile laboratory with a complete set of equipment and calculation technique in order to accomplish the following objectives:

1. Dynamic testing of bridges with electrodynamic vibrators. The modal testing will be made every 5 years for the functional bridges or after special events – terrorist attack, earthquakes, and accidents by striking the structural elements of the bridge, exceptional transportation.
2. The determination of the dynamic characteristics (mode shapes, natural frequencies and damping ratios) with the help of electronic equipment and a calculation program dedicate to modal analysis.
3. The 3D modulation of the tested bridge structure with the help of a specially designed calculation program based on the method of finite elements.
4. The calibration process of the 3D calculation model is made in the auto laboratory in due time and consist in comparing the model's theoretical dynamic characteristics with those of the real structure obtained at the site. In successive stages the theoretical dynamic values of the 3D model are changed until these will be equal to the experimental ones, case in which the model is considered calibrated.

5. The permanent comparison process in due time of the characteristics calculated at the moment of the bridge testing with those calculated in the previous testing stage.
6. The diagnosis of the structure in due time. When receiving the warning signal, the direct consequence is the immediate redirecting of the attention on the 3-D calculation calibrated model.
7. The application of the bridge protection protocol.

4. EXPERIMENTAL MODAL ANALYSIS

Experimental modal analysis (EMA) testing techniques use in this research program, require identification of the frequency response functions (FRFs) for each response measurement location of the composite bridge, obtained from a controlled form of excitation (such as an impact device or some form of shaker).

Estimation of the FRFs, $\tilde{h}_{jk}(\omega)$, are obtained via:

$$\tilde{h}_{jk}(\omega) = \frac{X_j(\omega)}{F_k[\omega]} \quad (4.1)$$

where $X_j(\omega)$ and $F_k(\omega)$ are the Fourier Transforms of $x_j(t)$, the displacement response at point “j”, and $f_k(t)$, the excitation force at position “k”, respectively. The EMA algorithms seek to fit modal properties (mode shapes, natural frequencies and damping ratios) contained in the theoretical form of the FRF, $h_{jk}(\omega)$, given by:

$$h_{jk}(\omega) = \sum_{n=1}^N \left(\frac{\varphi_{jn} \cdot \varphi_{kn}}{(i\omega - \lambda_n)} + \frac{\varphi_{jn}^* \cdot \varphi_{kn}^*}{(i\omega - \lambda_n^*)} \right) \quad (4.2)$$

in which φ_{jn} and φ_{kn} represent the j th and k th elements of the complex eigenvector for the n th mode shape of vibration and λ_n is the complex eigenvalues for this mode, and the symbol “*” represents complex conjugation.

Commercially available EMA packages normally exercise a two-stage fitting procedure to obtain estimates of the modal properties from the experimentally obtained FRFs. The complex eigenvalues, λ_n , are first estimated followed by a linear least squares fitting procedure to establish the eigenvectors. The Direct Simultaneous Modal Analysis (DSMA) algorithm is an alternative approach which

has been found to exhibit superior performance over conventional methods. This uses a non-linear least squares fitting procedure described by:

$$\{\lambda_s^{\min}, \varphi_{jn}\}_{\omega} = \sum \left[\sum_k \left(\sum_{j=1}^N \left| \tilde{h}_{jk}(\omega) - \sum_{n=1}^M \left[\frac{\varphi_{jn} \cdot \varphi_{kn}}{(i\omega - \lambda)} + \frac{\varphi_{jn}^* \cdot \varphi_{kn}^*}{(i\omega - \lambda)} \right] \right|^2 \right) \right] \quad (4.3)$$

where ω_{\min} and ω_{\max} represent the minimum and maximum values of circular frequency pertinent to the test results. A ‘‘Simplified’’ form of Experimental Modal Analysis (SEMA) can still be performed on a structure in the event that measurement data for response alone is available. This situation normally arises in practice when it is not possible to measure the excitation force, such as when ambient excitation is used on bridges. Here, the assumption is made that response measurements are dominated by ‘‘resonant’’ modes at their corresponding natural frequencies. The method is based on the relative response function, (FRF), defined by:

$$\tilde{R}_{qo}(\omega) = \frac{X_q[\omega]}{X_o(\omega)} \quad (4.4)$$

in which $X_q(\omega)$ and $X_o(\omega)$ are the Fourier Transforms of the measured response records at locations ‘‘q’’ and ‘‘o’’ respectively, in which ‘‘o’’ is treated as the ‘‘reference’’ point.

Now,

$$X_q(\omega) = \sum_{k=1}^N h_{qk}(\omega) \cdot F_k(\omega) \quad (4.5)$$

where $F_k(\omega)$ would correspond to the Fourier transform of the force trace at point ‘‘k’’. Substituting Equation (4.5) into Equation (4.4), the RRF, $R_{qo}(\omega_i)$ can be approximated to:

$$R_{qo}(\omega_i) = \frac{X_q[\omega_i]}{X_o(\omega_i)} \approx \frac{\varphi_{qi}}{\varphi_{oi}} \quad (4.6)$$

provided that the ‘‘separated modal frequency’’ assumption holds good for mode ‘‘I’’. Under these circumstances, the RRF reduces to the ratio of the modal amplitudes of mode ‘‘I’’. Modal frequencies can be ascertained from inspection of $S_o(\omega)$, the autospectrum of response at the reference location. Locations in

frequency of well-defined peaks in this spectrum correspond closely to natural frequencies of participating modes in the response.

5. CONCLUSIONS

The use of system identification (SI) for structural health monitoring (SHM) of bridges involves:

1. The optimized administration of the financial resources dedicated to the bridges maintenance and repair. The significant drop of the resources used for this sector, allows them to be redirected to other sectors such as the investment one.
2. The optimization of the maintenance and repairing works leads to an increased duration of exploitation of the bridge in question, which allows the achievement of benefits that can be redirected towards the investment sector.
3. The maintenance for a long time in a good technical state of the bridges on a highway section, for which are necessary only current maintenance works, leads to the traffic fluidization on that highway sector.

References

1. *Aktan A.E., Chuntavan C., Toksoy, T., Lee, K.L.* - Modal Testing for Structural Identification and Condition Assessment of Constructed Facilities, Proc., 12th IMAC, 1994
2. *Comisu Cristian Claudiu* - Sistem integrat de monitorizare pentru îmbunătățirea durabilității structurilor de poduri inteligente. Program de cercetare Facultatea de Construcții și Instalații Iași, cod CNCISIS 438, 2006
3. *Comisu Cristian Claudiu* - Mobile Laboratory for dynamic Testing and Diagnosis of Highway Bridges, Propunere program de cercetare COST, 2006
4. *Hunt D.L., Weiss S.P., West W.M., Dunlap T.A., Freesmeyer, S.R.*, - Development and Implementation of a Shuttle Modal Inspection System, Sound and Vibration Magazine, August, 1999
5. *Tomoyuki I.* - Development of Takenaka Mobile Laboratory, Intelligent Structures - 2, Monitoring and Control, ed., Wen, Y.K., Elsevier Publ., 218-227, 2004

The necessity to reduce the material structures from the road layers tested with the temperature control cracking device at a modeling scale

Mihai Dicu¹, Carmen Răcănel², Adrian Burlacu³, Claudia Murgu⁴, Iuliana Bălan⁵

¹Department of Roads and Railways, T. U. C. E., Bucharest, Romania, mdicu@cfdp.utcb.ro

²Department of Roads and Railways, T. U. C. E., Bucharest, Romania, carmen@cfdp.utcb.ro

³Department of Roads and Railways, T. U. C. E., Bucharest, Romania, aburlacu@cfdp.utcb.ro

⁴Department of Roads and Railways, T. U. C. E., Bucharest, Romania, claudia@cfdp.utcb.ro

⁵Department of Roads and Railways, T. U. C. E., Bucharest, Romania, iuliana@cfdp.utcb.ro

Summary

The TEMPERATURE CONTROL CRACKING DEVICE is a complex equipment for the laboratory research in accelerated conditions of the road materials performances used in execution of the pavements. This method consists in testing on elements at a reduced scale, from the road layers stabilized with binder, at simulated traffic loads and temperature fluctuations.

By reducing at scale the loading of the external factors (traffic and temperature fluctuations), it is, practical, required a scale reduction of the structural elements of the road material, from which is made the testing specimen.

The scale reduction of the geometrical elements of the road layer presumes also the analysis of the possibility to adapt the dimensions and the grading curve, from which results the necessary binder.

This paper puts to the issue a procedure used to achieve this purpose, which, in future, will have to be associated with a program of research more ample, which will allow the determination of some coefficients of equivalence between the behaviour of the road layer in reality and the one tested in laboratory by phenomenologic simulation.

KEYWORDS: cracking device, rigid/composite pavement, fatigue life

1. INTRODUCTION

The identification of the performances of the road materials, as optimal solutions to apply in the roads execution, may be obtained by laboratory research with complex equipments. In this category, it is included the TEMPERATURE CONTROL CRACKING DEVICE, which is an equipment for the fatigue testing of the materials within the layers stabilized with road binder, in the shape of a specimen, slab style.

The TEMPERATURE CONTROL CRACKING DEVICE allows the laboratory research by phenomenologic modeling at a reduced scale, of the specific characteristics for the cracking effect by fatigue of the road material, in accelerated test conditions. It could be obtained information about the capacity of the road material to support the loads from a traffic equivalent with the real one and temperature fluctuations, assimilated into the temperature control room.

Under the accomplishment of the equalization by reducing at scale the traffic loads and temperature fluctuations loads, it is necessary to adapt the manufacturing recipe of the road material, at the reduced dimensions of the testing specimen, from a geometrical point of view.

This method represents a research version for the using of experimental sectors at scale 1:1, RO LTPP style (Long Term Pavement Performance), which suppose a long period to watch the propagation phenomenon of the roads damages during the exploitation. Thus, it could be estimated the behaviour during exploitation for the road materials used in execution, and also, it could be identified the service life of the rigid or composite pavement (asphalt on concrete), which is recommended for roads with intense and heavy traffic.

2. THE CHARACTERISTICS OF THE TEMPERATURE CONTROL CRACKING DEVICE

Starting from what has been related about the description of the damage phenomenon by fatigue during exploitation of a road and from the necessity to establish some methods of investigation in laboratory for the performances of the road layers as far back as the designing and elaboration phase of the optimal recipes for the road materials, it can be established the parameters of the phenomenologic simulation by assimilation of the real factors.

Thus, a first stage consists of the establishment of the geometrical elements of the slab at the level of a reduced scale of the simulation model, where through it can be established the interval of the loading force. Starting from the real dimensions of a cement concrete slab used in pavement, which has the dimensions 3.5m (4.0m) x

6.0m (4.0m), so the surface is between 24.0m² and 16.0m², and also, starting from the acceptance of the modeling slab dimensions at a reduced scale, deduced initially (at the beginning of the research), as being 0.5 x 0.15m² (slab dimensions), so the surface is about 0.075 m², it can be established the loading range. For 115 ESAL (equivalent single axle load), which at the wheels level distributes 57.5 kN, it can be estimated that the interval of the force that loads the model reduced at scale, could be between 18-27 daN. Whereas the calculus pressure for 115 ESAL is 6.25 daN/cm² (0.625 MPa), would result a contact diameter of 2.35 cm. To eliminate the eventual process of stamping due to the unique diameter, it is necessary to choose a diameter of 5 cm, which, with a pressure of 6.25 daN/cm² leads to a necessary force of 123 daN.

In these conditions it has been fixed the maximum level for the loading force of the cracking device at $P=200$ daN. Taking into account that the loading is in dynamic regime, the dynamic coefficient is $\psi=1.2$, it has been accepted that the maximum loading level is $P_{din}=150$ daN.

The constructive disposal of the stand has the formation from figure 1 as main scheme:

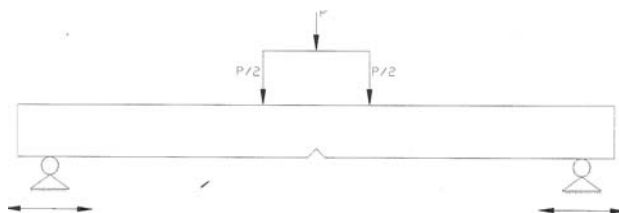


Figure 1. The main scheme of cracking stand

The tested slab is seated on two free bearings with the possibility to close the distance between them, in terms of the necessity of laboratory loading. For the simulation of the calculus axle, the loading with force P will be made through a cross beam with the road territory variable in terms of the necessities of loads.

The loading will be made at a controlled frequency, imposed by the values recommended by the speciality literature, respectively 20 Hz.

The mechanical system provides the positioning of the specimen on two sliding bases, the transmission of the force at the hydraulic cylinder, the correct and stable positioning of the other systems of the equipment (hydraulic system, junctions, sensors, video cameras, connectors, climatic camera). The main constructive elements are presented in figure 2:

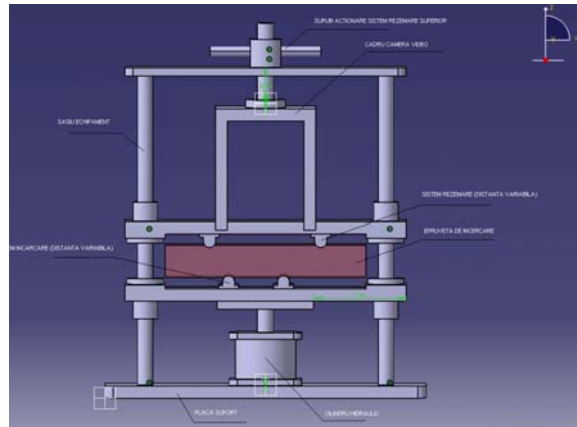


Figure 2. The main constructive elements of cracking device

Systems for acquisition of images

The acquisition of images is based on the same components as the data acquisition (National Instruments). The images are converted by the shooting camera in electrical signals, which are characterised by high speed of variation. The images contain a great quantity of information, that is why the modules of the acquisition of images have high sampling and transfer speeds of data to PC.

For the visualization of the cracking phenomenon and of correlation of this phenomenon with the number of cycles, at which the specimen is subdued to fatigue, it will be had in view the simultaneous acquisition with three cameras (figure 3).

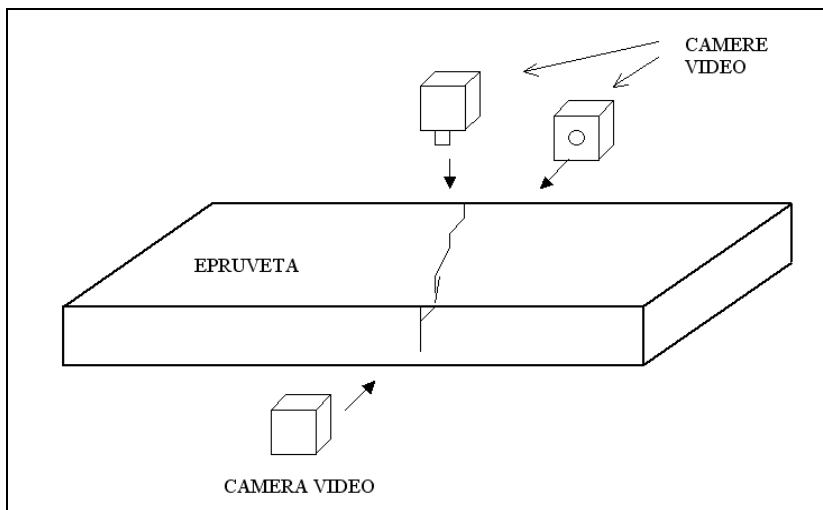


Figure 3. Visualization of the cracking phenomenon

3. THE EVALUATION PROCEDURE AT A REDUCED SCALE OF THE MATERIAL STRUCTURES IN THE ROAD LAYERS

In this stage are presented the hypothesis of scale reduction and the types of the behavioural similitude tests, according to the working standards in the infrastructure domain of the road transport.

Later, when the control temperature cracking device will be functional and gauged, the next step will be the approaching of specific research themes, that must improve the levels of performance at the road materials.

Considering as initial hypothesis that the scale reduction is five times, we can upgrade to the procedure of reducing at scale the road structure. More correctly, it has to be elaborated a method to reduce at scale the mineral skeleton from the material structure of the road layer and the necessary binder quantity.

For start, the reduction coefficient identifies through the ratio of the geometrical dimensions of the equivalent diameter, used at modelling device loading unto the equivalent diameter of the calculus vehicle. This correlation can be assimilated to the mineral skeleton from the road layer that takes up the load on the equivalent circle from the superior face and distributes it to the interior face (table 1).

Table 1. The correlation between the reality and the model

LOADING SCALE	REALITY	MODEL
LOADING IMPRINT	$D_1=34$ cm	$D_2=7$ cm
MINERAL AGGREGATE RECIPE	SAND 0/4	SAND 0/1
	CRUSHED STONE 4/8	GRIT 1/2
	CRUSHED STONE 8/16	GRIT 2/4
	CRUSHED STONE 16/25	GRIT 4/6

In terms of this grid for reduction at scale of the mineral skeleton, it will be calculated the binder percent, which depends on the specific surface of the resulted aggregate. The coefficient for the reduction at scale is $K=1/4.86$.

The coefficient for the reduction at scale corresponds to a diameter of the contact equivalent circle of 7 cm.

It is chosen this variant of loading to reduce the possibility of local crushing due to the stiffness on the contact track contour.

In the mentioned hypothesis, it will pass to the stage of laboratory testing for the identification of the behavioural similitude between the standard recipes for cement concrete and asphalt mixtures and recipes for the confection of specimens for the reduction scale model (table 2).

Table 2. The correlation between standard specimens and model specimens (cement concrete)

STANDARD SPECIMENS	MODEL SPECIMENS AT A REDUCED SCALE
CEMENT CONCRETE	
CUBE 14 x 14 x 14	CUBE (14 x 14 x 14)*K ³
VOLUME V ₁ =2744 cm ³	V ₂ =24 cm ³
SIDE L ₁ =14 cm	L ₂ =3 cm
BREAKING FORCE F ₁ =	F ₁ =F ₁ /4.86
BENDING TENSILE BEAM	
10 x 10 x 54	(14 x 14 x 14)*K ³ EQUIVALENT
F _{i(1)} =	F _{i(2)} = F _{i(1)} /4.86

In terms of the existent possibilities in the speciality laboratory, the scale reduction will be correlated with the endowment mouldes.

Analogous with the principle applied to the cement concrete, it will be proceeded with the specimens from the asphalt mixture (table 3).

Table 3. The correlation between standard specimens and model specimen (asphalt mixture)

STANDARD SPECIMENS	MODEL SPECIMENS AT A REDUCED SCALE (K=1/4.86)
MARSHALL SPECIMENS	SPECIMENS
Φ ₁ =10 cm, h ₁ =6 cm	Φ ₂ =10/4.86=2 cm, h ₂ =6/4.86=1.5 cm Hubart Field equivalent Φ' ₂ = h' ₂ =
MARSHALL STABILITY	
S ₁ = CREEP INDEX I ₁ =	S ₁ =S ₁ /4.86 I ₁ =I ₁ /4.86
THE BRAZILIAN TEST (INDIRECT TENSION BY COMPRESSION ON GENERATRIX)	
R _{tB1} =	R _{tB2} =
BENDING TENSILE PRISM	
10 x 10 x 55 R _{ti1} =	10 x 10 x 55*K R _{ti2} = R _{ti1} /4.86

From the analysis of the presented tables, by laboratory research, it will be established the similitude adopted by dimensional reduction with the coefficient $K=1/4.86$.

At the level of STUDY CASE, it has been made a research of the enunciated principle, which, for the cement concrete, could be framed in the category MICROCONCRETE.

In this study, it has been taken into account the theory known for the testing of the performances of a cement concrete at bending tension on prism $10 \times 10 \times 55$ and for mortar, on beams $4 \times 4 \times 16$.

The reduction at scale of the simple cement concrete structure has been made by reduction of the grading curve from the real one that has been used for the beam $10 \times 10 \times 55$ to the one with scale reduced used for the beam $4 \times 4 \times 16$.

For this study case it has been used a classic cement concrete after the A recipe (table 4, 5):

Table 4. Classic cement concrete recipe for aggregates

REALITY (A)	MODEL AT A REDUCED SCALE (B)
0/4 3.89 kg	0/1 1.19 kg
4/8 2.22 kg	1/2 0.685 kg
8/16 2.22 kg	2/4 0.685 kg
16/25 2.78 kg	4/6 0.856 kg

Table 5. Classic cement concrete recipe for water and cement dosage

REALITY	MODEL AT A REDUCED SCALE
WATER, $A'=1.31$ l	$A'=0.41$ l
CEMENT, $C'=2.6$ kg	$C'=0.81$ kg

The microconcrete with granulation reduced at scale has the maximum dimension of the granule of 6 mm and it is proposed the granulation zone (B). With this recipe it has been manufactured beams $4 \times 4 \times 16$ (figure 4).



figure 4a



figure 4b



figure 4c



figure 4d



figure 4e

Figure 4. Manufacturing of microconcrete specimens: 4a – Shape of specimen; 4b – Casting of beams 4x4x16; 4c – Finishing of beams 4x4x16; 4d – Manufacturing of beams 10x10x55; 4e – Finishing of beams 10x10x55

It has been tested the two types of beams after the method according to regulation of the beam 10 x 10 x 55 (figure 5).

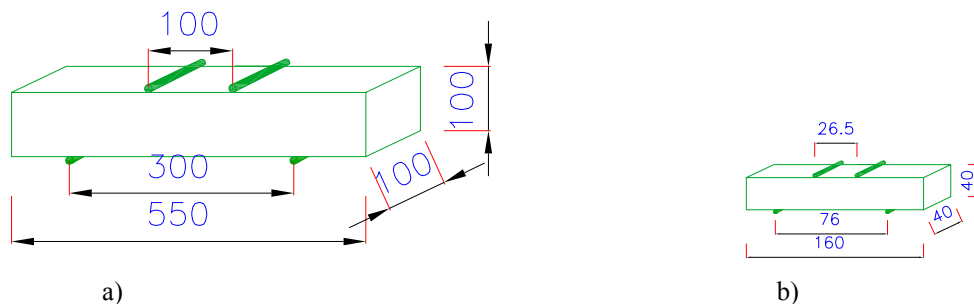


Figure 5. Testing of the concrete and microconcrete at bending tension: a) Beam – test of the cement concrete at tension bending; b) Beam – test of the cement microconcrete at tension bending

In the first iteration, the results from table 7 have been obtained:

Table 7. Results obtained in the first iteration

CHARACTERISTICS	CONCRETE	MICROCONCRETE
BEAM GEOMETRY	10 x 10 x 55 cm ³	4 x 4 x 16 cm ³
VOLUME	V=5500 cm ³	v=256 cm ³
	$K_v=v/V=1/22=0.05$	
LENGTH	L=55 cm	l=16 cm
	$K_l=l/L=1/3.44=0.29$	
BREAKING FORCE	F ₁ =1010 daN	F ₂ =492 daN
	$K_f=F_2/F_1=1/2.1=0.48$	
R _{ti}	R _{ti1} =40.4 daN/cm ²	R _{ti2} =123 daN/cm ²
	$K_{R_{ti}}=R_{t2}/R_{t1}=3.05$	

4. CONCLUSIONS

From the interpretation of the obtained data, results the necessity of reevaluation of the ratio water/cement for the reduction of the value R_{ti2} at MICROCONCRETE and for bringing this parameter at the limit $K=1/4.86=0.21$.

This necessity presupposes the extension of the laboratory tests, which will be the subject of a separated research.

Through this study case, it was intended to adjust a procedure for reduction at scale of the material structure for the model pattern, which will be used in fundamental research with the TEMPERATURE CONTROL CRACKING DEVICE.

References

1. Dicu M., *Fisurarea Structurilor Rutiere Mixte* – Teza de doctorat 1996
2. Laveissiere D., *Modelisation de la Remontee de Fissure en Fatigue dans le Structures Routieres par Endommagement et Macro-Fissuration* (these doctorat Ecole Doctorale STS)
3. Pouteau B., *Durabilite Mecanique du Collage Blanc sur Noir dans les Chaussees* (these de doctorat l’Ecole Centrale de Nantes et l’Universite de Nantes)
4. Dat Tran Q., *Modele Simplifie pour les Chaussees Fissurees Multicouches* (these de doctorat l’Ecole Nationale des Ponts et Chaussees)
5. Soares J. B., de Freitas F. A. C. , Allen D., ***Crack Modeling of Asphaltic Mixtures Considering Heterogeneity of the Material*** (TRB 2003 Annual Meeting)
6. Romanescu C., Răcănel C., *Reologia Lianților Bituminoși și a Mixturilor Asfaltice*, Editura Matrix ROM, București 1998
7. EN 12697-26 – *Bituminous Mixtures – Test Methods for Hot Mix Asphalt – Part 26:Stiffness*
8. LabView - *Manual*

The Highways Noise Reduction Methods

Ioan Florin Drăgan¹, Florina Crăciun², Delia Drăgan³

¹*Electric Measurement Department, Technical University of Cluj-Napoca, Romania,*

Florin.Dragan@mas.utcluj.ro

²*Descriptive Geometry and Engineering Graphics Department, Technical University of Cluj-Napoca, Romania ,*

florina.craciun@gdgi.utcluj.ro

³*Railways, Roads and Bridges Department, Technical University of Cluj-Napoca, Romania,*

Delia.Dragan@cfdp.utcluj.ro

Summary

In recent years, highway traffic noise has been increased. At the same time, modern acoustical technology has been providing better ways to lessen the adverse impacts of highway traffic noise. The purpose of this paper is to describe acoustical techniques and methods for measuring and reducing the traffic noise. Some of the most common methods used by highway planners and designers, construction engineers, and private developers are different types of noise barriers.

KEYWORDS: highway, traffic, noise, barrier, decibel, berm, vegetation

1. INTRODUCTION

As we all know, sound is created when an object moves: the rustling of leaves as the wind blows, the air passing through our vocal cords, and the almost invisible movement of the speakers on a stereo. This movement causes vibrations or waves in air molecules, like ripples on water. When the vibrations reach our ears, we hear sound. Sound is quantified by a meter which measures units called decibels (dB).

2. NOISE MEASURE

Murray Schafer, the Canadian musician updated the list first created by the British scientist Sir James Jeans, which reflects some noise values from our surroundings. Schafer named the discipline he was studying and teach based on sounds people could perceive, soundscape (Table 1).

For highway and railway traffic noise, an adjustment, or weighting, of the high-and low-pitched sounds is made to approximate the way that an average person hears sounds. The adjusted sounds are called "A-weighted levels" or dB(A).

Table1. Schafer’ soundscape list [3]

Threshold of hearing	0 dB
Leaves rustle	20 dB
Whisper	30 dB
Normal conversation	60 dB
Motorcar	70 dB
Underground	75 dB
Open truck	80 dB
Kitchen robot	100 dB
Mower	107 dB
Pneumatic drill	118 dB

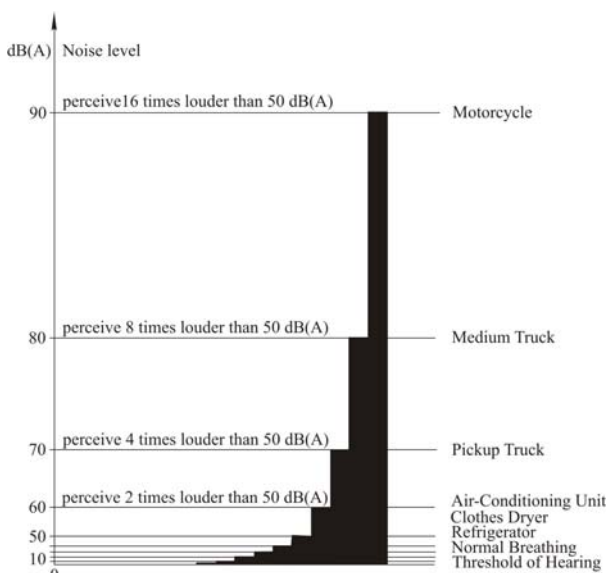


Figure 1. Noise level perception scale

The A-weighted decibel scale begins at zero. This represents the faintest sound that can be heard by humans with good hearing. The loudness of sounds (that is, how loud they seem to humans) varies from person to person, so there is no precise definition of loudness. However, based on many tests of large numbers of people, a sound level of 70 is twice as loud to the listener as a level of 60 (Fig.1) [1].

3. CAUSES OF TRAFFIC NOISE

The level of highway traffic noise depends on many factors. Three of the main important ones are considered to be: the volume of the traffic (Fig.2), the speed of the traffic (Fig.3), and the number of trucks in the flow of traffic (Fig. 4) [1].



Figure 2. 2000 vehicles per hour (b) sound twice as loud as 200 vehicles per hour (a).

The volume of traffic consists of the number of vehicles per hour.

So, 2000 vehicles per hour, as represented in figure 2, are perceived twice as loud as 200 vehicles per hour.

Vehicles speed makes them be perceived more noisily. So, traffic at 120 km /hour sounds twice as loud as traffic at 60 km/ hour (Fig.3):



Figure 3. Traffic at 120 km/hour sounds twice as loud as traffic at 60 km /hour.

Generally, the loudness of traffic noise is increased by heavier traffic volumes, higher speeds, and greater numbers of trucks. One truck at 100 km/hour sounds as loud as 10 cars at 100 km/hour (Fig.4)



Figure 4. Traffic noise level is higher if there are heavier traffic vehicles

On the other hand, vehicle noise is a combination of the noises produced by the engine, exhaust, and tires: The loudness of traffic noise can also be increased by defective mufflers or other faulty equipment on vehicles. Any condition (such as a steep incline) that causes heavy laboring of motor vehicle engines will also increase traffic noise levels.

4. CAUSES OF RAILWAY NOISE

The railway noise has been serious reduced since Diesel replaced steam engines and silent and economical power of electricity drives most of trains. We have to

take into consideration the noise level along railways too, depending on engine type and speed, as shown in table 2:

Table2. Railway noise level [2]

Engine	Speed (Km/h)	Noise level dB(A)
Diesel engine	30 - 50	67 - 70
Electric engine	30 - 90	66 - 72

There are other more complicated factors that affect the loudness of traffic or railway noise. For example, as a person moves away from a highway or a railway, traffic noise levels are reduced by distance, terrain, vegetation, and natural or manmade obstacles.

5. NOISE IMPACT

The noise level is always changing with the number, type, and speed of the vehicles which produce the noise. Traffic noise variations can be plotted on a graph as shown below. However, it is usually inconvenient and cumbersome to represent traffic noise in this manner. A more practical method is to convert the noise data to a single representative number. Statistical descriptors are almost always used as a single number to describe varying traffic noise levels. The two most common statistical descriptors used for traffic noise are L_{10} and L_{eq} . L_{10} is the sound level that is exceeded 10 percent of the time.

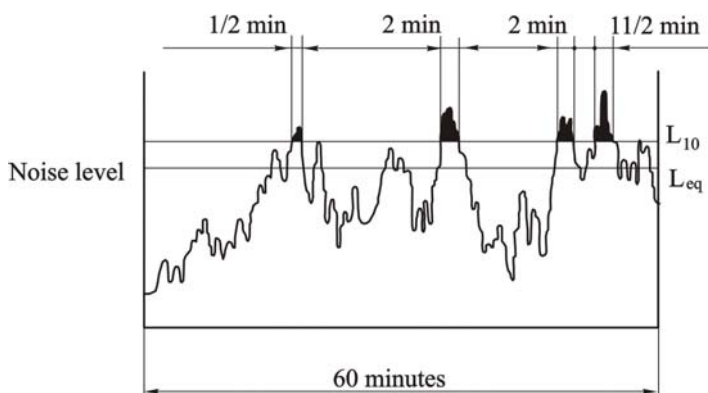


Figure 5. L_{10} and L_{eq} traffic measuring principle [1]

In the graph shown in figure 5, the shaded areas represent the amount of time that the L_{10} value is exceeded. Adding each interval during which this occurred shows that during the 60 minute measuring period the L_{10} was exceeded 6 minutes ($1/2 + 2 + 2 + 11/2 = 6$) or 10 percent of the time. L_{eq} is the constant, average sound

level, which over a period of time contains the same amount of sound energy as the varying levels of the traffic noise. L_{eq} for typical traffic conditions is usually about 3 dB(A) less than the L_{10} for the same conditions.

Table2. L_{eq} and L_{10} values for two types of areas [1]

Land Use	L_{10}	L_{eq}
Residential	70 dB(A)	67 dB(A)
Commercial	75 dB(A)	72 dB(A)

Generally, the railway noise does not affect residential sectors, as they are usually planned outside cities and subways used silent electric power. Although there are acceptable noise levels architects and civil engineers have to know when they are planning districts, homes and roads:

Table3. Acceptable railway noise levels [2]

Land Use	Noise level dB(A)			
	Secondary routes		Principal routes	
	Daytime 6 - 22	Night 22 - 6	Daytime 6 - 22	Night 22 - 6
Agreement areas, hospitals	55	45	60	50
Rural residential	60	50	65	55
Urban residential	65	55	65	55
Industrial sectors with institutes	65	55	65	55

6. NOISE REDUCTION METHODS

Highway noise is being attacked with a three-part strategy: motor vehicle control, land use control, and highway planning and design.

6.1 Motor Vehicle Control

The first part of the strategy goes right to the source of traffic noise: the vehicles. For example, vehicles can be designed with enclosures for the engine fans that turn off when not needed, and better mufflers. Quieter vehicles would bring about a substantial reduction in traffic noise along those roads and streets.

6.2 Land use control

There are several hundred thousand kilometres of existing highways in this country bordered by vacant land which may some day be developed. Prudent land use

control can help to prevent many future traffic noise problems in these areas. Such controls need not prohibit development, but rather can require reasonable distances between buildings and roads.

6.3 Highway or Railway Planning and Design

Buffer zones are undeveloped open spaces which border a highway (Fig.6). Buffer zones are created when a highway agency purchases land or development rights, in addition to the normal right of way, so that future dwellings cannot be constructed close to the highway (Fig.6,a). This precludes the possibility of constructing dwellings that would otherwise experience an excessive noise level from nearby highway traffic. Less noise-sensitive commercial buildings can be placed next to a highway, if necessary, with residences farther away. Open space can be left as a buffer zone between residences and a highway (Fig.6, c). A 65 m width of dense vegetation can reduce noise by 10 decibels, which cuts the loudness of traffic noise in half. [1]

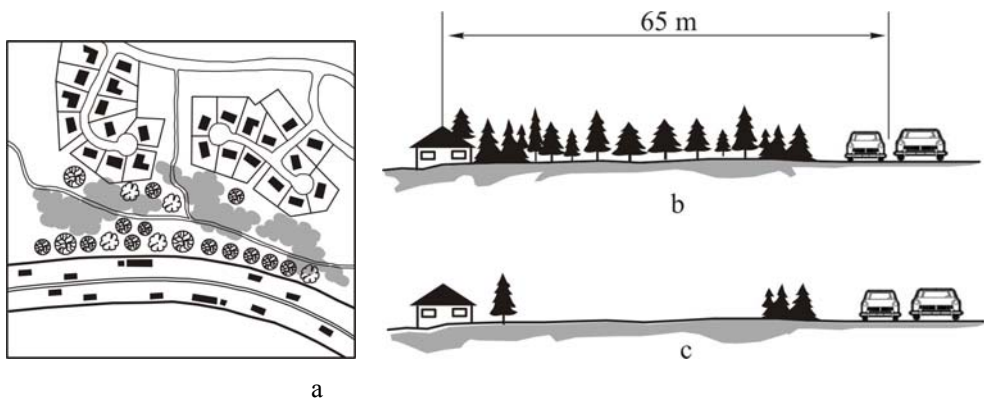


Figure 6. Buffer zones: plan view (a) and front views (b, c)

It is often impractical to plant enough vegetation along a road to achieve such reductions; however, if dense vegetation already exists, it could be saved. If it does not exist, roadside vegetation can be planted to create psychological relief, if not an actual lessening of traffic noise levels.

6.4 Noise Barriers

Noise barriers are solid obstructions built between the highway (Fig.7) or railway (Fig.8) and the homes along them. These barriers can reduce noise levels by 10 to 15 dB, cutting the loudness of noise in half. For a noise barrier to work, it must be long enough (Fig.6, b,c) and high enough (Fig.7) to block the view of a road.

As shown in figure 7, b each additional metre over the line of sight means 1,5 dB(A) additional attenuation of noise. For instance, 3 m barrier height entails 4,5 dB(A) noise attenuation. [1]

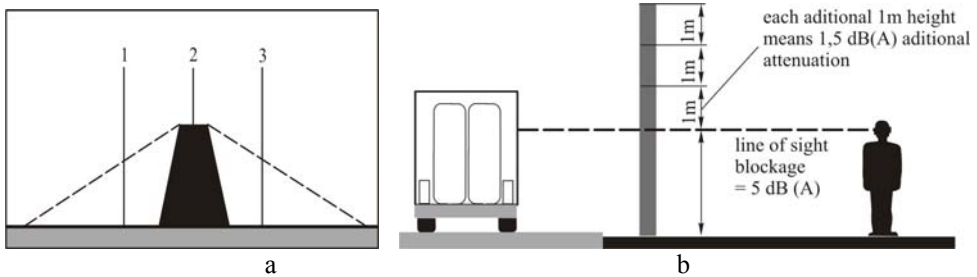


Figure 7 Noise barrier principle for traffic noise

Barriers can be formed from earth mounds along the road, usually called earth berms, (Fig.8,b,c) or from high, vertical walls (Fig.8,a). Earth berms have a natural appearance and are usually attractive. However, an earth berm can require quite a lot of land if it is very high and not based on natural land configuration (Fig. 8,b,c).

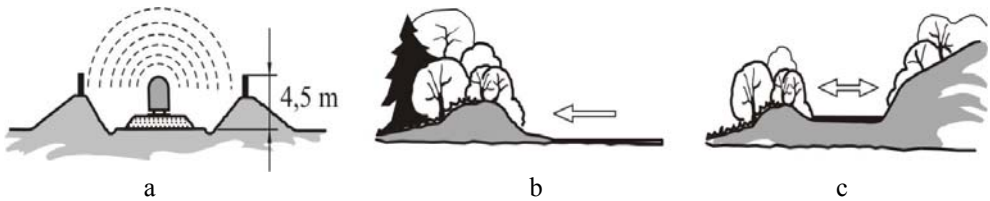


Figure 8 Railway noise barrier (a) and earth berms (b, c) [2]

Walls take less space (Fig.8,a). They are usually limited to 8 m in height for structural and aesthetic reasons. As shown in figure 9 there are unshielded floors in case of blocks of flats near the highways (Fig.9,a), or unshield houses if they are situated on a higher land level than the berm (Fig.9,b).

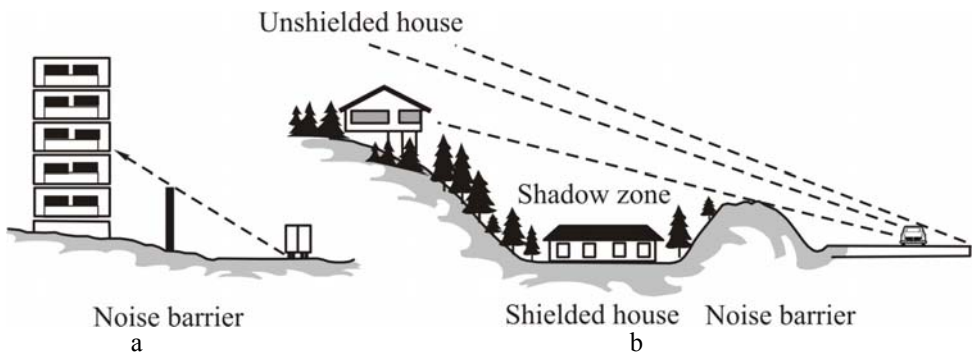


Figure 9 Unshielded floors (a) or house (b)

On the other hand, a certain distance between the highway or railway diminish the noise level anyhow. **Vegetation**, if high enough, wide enough, and dense enough (cannot be seen through), can decrease highway traffic noise. Railway noise reduction depend on distance e , barrier and house height (Fig. 10).

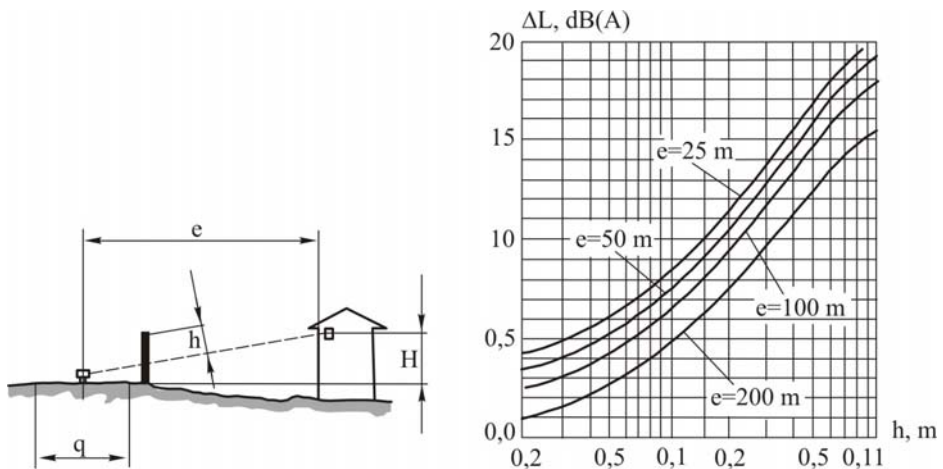


Figure 10 Noise barrier dimensions for railway noise [2]

7. CONCLUSION

Noise walls can be built of wood, stucco, concrete, masonry, metal, and other materials. Many attempts are being made to construct noise barriers that are visually pleasing in their surroundings. Noise barriers in dense, urban settings should be designed differently than barriers in more open suburban or rural areas. Their design has to take into consideration the material, the proper shape and dimensions and the aspect as well. Wherever possible, for both ecological and aesthetical reasons, vegetation may be successfully used in the design process.

References

1. http://www.avtinc.net/barrier_walls/highway_barriers.html
2. Köllö G., Căi ferate, viteză și protecția mediului, UTC-N, 2001
3. Menuhin, I., Davis, C.W., “Muzica omului”, Ed. muzicală, 1984.

TRAFFIC AND LOADING DATA FOR THE HIGHWAY AND BRIDGE MANAGEMENT

Emil Doupal

Transport Research Centre v.v.i, Brno, 639 00, Czech Republic, emil.doupal@cdv.cz
Road and Traffic Systems Consulting GmbH, Switzerland, rts.consult@gmail.com.ch

Summary

The paper provides information on multi-purpose applications of automatic WIM (weigh in motion) stations for overloading control, traffic data collection and the following evaluations, operated in various remote control modes. An example shows specific methods of pre-selection of overloaded vehicles, online traffic data collection and automatic statistic evaluations. The WIM system based on the modern quartz sensor technology combined with new data logger and video systems. The WIM data are used for a wide variety of applications depending on the requirements of the road authorities or user groups (police, traffic engineers, road designers). The system for the highway, road and bridge management in general is designed for management of any data, mostly in a sphere of telematic and traffic infrastructure. Basic criteria and a recognition sign for „DATA” are a type and specification of a „station“, where data are obtained. Currently a station type WIM is implemented in ATOL (all traffic on-line product for dynamic weighing of vehicles. In addition an implementation of a traffic counting, vehicle license plate reading and section speed measurement stations is prepared to measure speed for enforcement, register license plates and to categorize vehicles, which is also part of assortment. Generally, any type of station which gathers real data and allows remote management can be implemented in ATOL system. This ensures an access to data exactly according to customer wishes and in accordance with his trade policy of data mediation.

KEYWORDS: weigh in motion, pavement loading, remote control, traffic data

1. INTRODUCTION

WIM (Weigh-In-Motion) technology can play a vital role by monitoring bridge loading and restricting dangerous overloads. WIM has been an accepted instrument for truck weight measurement monitoring and weight enforcement screening for more than 20 years. As a first step, the system can collect data on the traffic which is travelling across the bridge. From this data, authorities can determine the loadings on the bridge and take the appropriate counter-measures to protect the bridge structure. A WIM system in advance of the bridge will detect overweight

vehicles and can warn the driver of restricted access or take other counter measures to automatically restrict access or inform the authorities with an alarm and/or a video image of the offending vehicle.

As vehicles approach the bridge, the WIM System automatically determines the size and weight classification of the vehicle and compares this information with the allowable loads for the upcoming bridge. If the vehicle exceeds the allowable weight limits, an advisory sign will be illuminated advising the driver that the vehicle should not travel across the bridge. The truck operator can then stop the vehicle and exit prior to crossing the bridge.

Additionally, the WIM can be integrated with a video tracking, monitoring and image grabbing system to ensure that vehicles obey the signals and warnings when advised to not cross the bridge. In the event a driver does not obey the message, an image of the vehicle, with the corresponding size and weight information is generated and stored for further action. The compliance and enforcement aspect of the system will deter drivers from purposely driving overloaded vehicles on a load sensitive bridge structure.

Weigh-in-Motion (WIM)

Advantages

- More vehicle weighed, better coverage, unbiased sample

Disadvantages

- Installation costs, equipment and maintenance costs, fixed locations

WIM Sensor Technology

- Load Cell – Hydraulic load cells
- Bending Plates – Strain gauge load cells
- Piezo-electric cables / film
- **Piezo quartz**
- Fibre Optics
- Capacitance mats / pads / strips
- Strain gauges on bridge beams

WIM systems are finding increasingly widespread use as a valuable extension to conventional traffic counters and classifiers. They provide a whole spectrum of information on the traffic flow, including dynamic weights of all axles, gross vehicle weights, axle spacing, distance between the vehicles, speed and so on. Axle load measurement provides a better vehicle classification rate than conventional traffic counters.

Traffic flow analyses including weight data are useful beyond statistics for traffic planning, maintenance prognostics and for automatically influencing the rolling traffic.

The evaluated results can also be used as a basis for determining dimensions in road and bridge constructions or for optimizing resurfacing work.

Both traffic volume and axle loading are continuously increasing world wide and with the repetitive pounding of roads, this results in often quite complex fatigue failure types. In the interest of minimizing the damage inflicted by overloaded vehicles passing over critical road sections, particularly older bridges, various highway authorities are pursuing a policy of spot checks on vehicles suspected of infringing the stipulated maximum load regulations.

The remote WIM site can be controlled and operated from a central location using web-based or independent communication systems.

The principle of a virtual WIM site is similar to that of a remote WIM site, as it makes use of an existing or new weigh-in-motion traffic data collection site. For each vehicle the traffic data are collected, including vehicle classification and weight data and then transmitted together with a video picture, to an enforcement operator (police). In case of an overloaded vehicle, the operator will see the relevant weight data highlighted and the picture of the vehicle on the same screen and can pull the vehicle over for further checking.

The pre-selection of vehicles allows enforcement persons (police) to concentrate on the potentially overloaded trucks, instead of detaining many unsuspecting vehicles from the traffic stream. A typical virtual WIM system complements fixedly installed automatic high speed WIM stations and remote data evaluation, traffic control and enforcement scale systems.

Depending on user requirements, different data formats and retrieving modes can be selected for the whole WIM station or for individual traffic lanes. The multi-user system is based on a password access control system defined separately for every WIM station.

2. QUARTZ SENSOR TECHNOLOGY

For every WIM site a careful selection of the installation location is absolutely essential as the accuracy of the system strongly depends on the quality of the pavement. Therefore refer to the requirements of COST 323 (<http://wim.zag.si>) standard specification draft and ASTM 1318-02 (<http://www.astm.org>) standard. Rutting, bumps and pavement cracks will impair the system performance. Straight highways with uniform vehicle speed distribution and good pavement flatness are best suited to achieve optimum results.

2.1. Sensors

The Lineas WIM sensor is based on quartz technology. Quartz is a unique material with very useful characteristics; it is the core element of most of our thousands sensors. It is appreciated by our customers for its stable behaviour and extraordinary performances.

The main advantages of piezoelectric quartz sensors are:

- extremely high rigidity (measuring deflections are typically in the μm range)
- high natural frequency (up to over 500 kHz)
- extremely wide measuring range (span-to-threshold ration up to over 108)
- very high stability (with transduction elements made of single crystals)
- high reproducibility
- high linearity of the dependence of the output on the measuring
- wide operating temperature range
- insensitivity to electric and magnetic fields ant to radiation

One traffic lane is instrumented with two sensor rows with a distance of about 4 m. Each row consists of 4 quartz crystal sensors. According to the lane width, the appropriate sensor length should be chosen. Thanks to the modular design of the sensor s(0.75 m and 1 m length), every lane width can be covered. The cable length (40m or 100m) will be chosen depending on the distance between sensors and electronic cabinet.

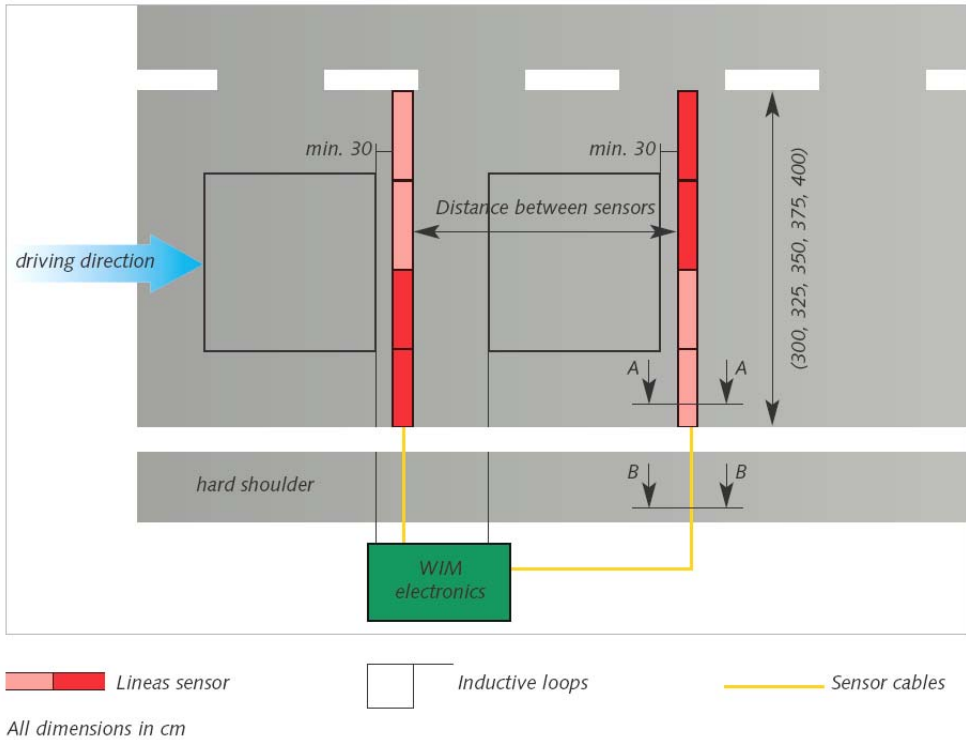


Figure 1. Standard WIM System – 2 rows of 4 sensors

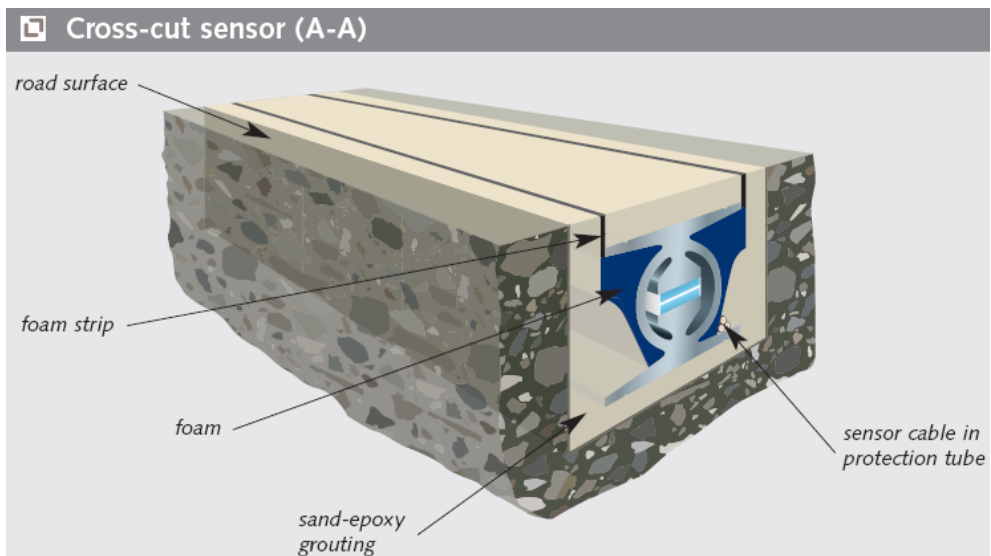


Figure 2. Cross cut of the quartz sensor road installation

Influence on data quality

Road

- Geometry of the road (radius, lateral and transverse slope), Type of pavement and foundation, Condition of the road respectively pavement (ruts, cracks, plane etc)

WIM Sensor

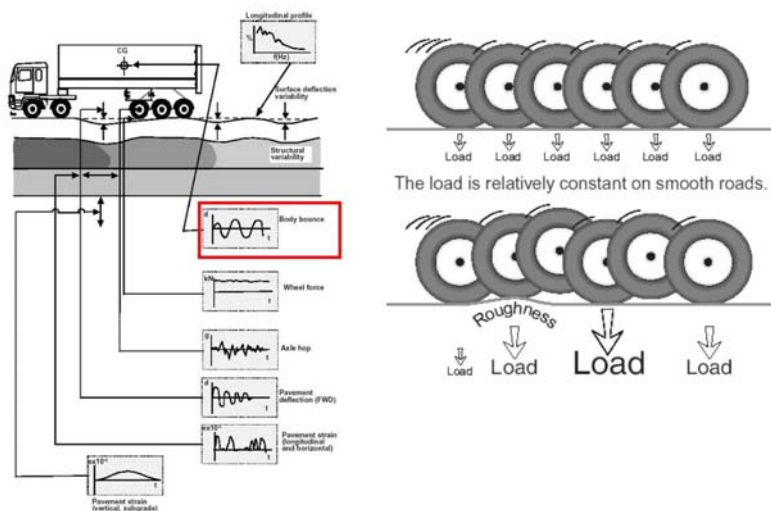
- Accuracy, stability, durability, installation, ...

Vehicle

- Suspension type (air, conventional), State of vehicle (suspension, vibration), Type of tires, tread, Loading (full, empty or partial loaded), place and type of load

Drive

- Acceleration, break, Change of lanes, Side-wind



2.2. Data logger

The data loggers contain typically from:

A central processor board (CPU), loop boards and connectors, communications card, primary battery, harness and connectors.

When fitted with two 8-loop boards, the data logger can monitor 16 lanes of traffic. A lane may be a running lane or hard shoulder according to the needs. The following sections describe each of the main assemblies within the loop-monitoring unit.

2.2.1. Processor Board

The card performs the following tasks: Receives vehicle detection “events” from the loop card, Processes these events and derives vehicle counts etc., using the straddle algorithm for increased accuracy, provides data memory for the accumulation of traffic data, maintains a real-time clock. (updated from the instation clock), interfaces to the Engineer’s terminal, conducts battery measurement and management.

In order to operate for extended periods on battery (in case the mains power fails for a short time), the processor board has to be designed for low power operation.

2.2.2. Loop Board

The loop card has been designed to give good accuracy with low power consumption. It uses a unique processing algorithm that examines the loop signal in real time. The traffic data could be available simultaneously in different channels:

- real-time vehicle-by-vehicle records directly immediately available to any application
- vehicle-by-vehicle records stored in the internal memory in a compact format making maximum use of memory
- Interval recorded data accumulated into bins for vehicle class, speed, length, axle weight, gross weight, axle separation and many other parameters.

The motherboards are fitted with a CPU card and sufficient WIM and loop cards for the individual station requirements.

Typically an RS232 port is provided, offering the following configuration options:

- Baud rates 1200, 2400, 4800, 9600, 19200, 38400, 57600 or 115200
- Data bits - 7 or 8
- Parity - Odd, Even or None
- Flow control - XON/XOFF and RTS/CTS

Using this port the data logger will be able to communicate with the remote station, or with other equipment as required.

2.3. Remote and communication system ATOL

ATOL (All Traffic On Line) is a product for data management and administration in a sphere of telematic and transportation. ATOL gathers all data in the above mentioned sphere regardless of a final product platform used /individual gauge places and telematic stations/ and provides its user with those data through WEB in a form known as User Friendly.

2.3.1. Data types

The system in general is designed for management of any data, mostly in a sphere of telematic and traffic infrastructure. Basic criteria and a recognition sign for „DATA“ are a type and specification of a „station“ where data are obtained. Their ratings and real representation /weight, speed, temperature, dampness etc./ are defined based on individual gauge places, in other words stations. Currently a station type WIM /Weight In Motion/ is implemented in ATOL product for dynamic weighing of vehicles.

Generally, any type of station which gathers real data and allows remote management can be implemented in ATOL system.

2.3.2. Users communication dividing line, SW user platform

According to customer requirements individual users with defined authority to access data in individual stations within each station are defined in ATOL. This ensures an access to data exactly according to customer wishes and in accordance with his trade policy of data mediation.

As mentioned above, the user environment has been created on a base of WEB dividing line. Each user with an internet access /intranet/ and with defined authority can enter the system and obtain data in it. It can be achieved regardless of user SW platform, there's no need to install additional SW equipment and it is possible to use even a different HW other than PC /MAC, Handheld, Mobile phone suitably equipped etc./

2.3.3. System description

Figure 4 shows general scheme of ATOL system operation. Its core is a part known as SERVER. Its task is to gather individual data from stations using system's DB uploaded and present those data to user through WEB dividing line. Each station mediates its data through an unit known as ATOL ADMS /Automatic Data Management System/, which downloads its own data from the station and sends it out to server in set time. This unit has its own defined protocol for a data exchange with the server on one side, on the other side it has its protocol defined

by the station manufacturer. This arrangement allows any registered station to be connected with the whole ATOL system.

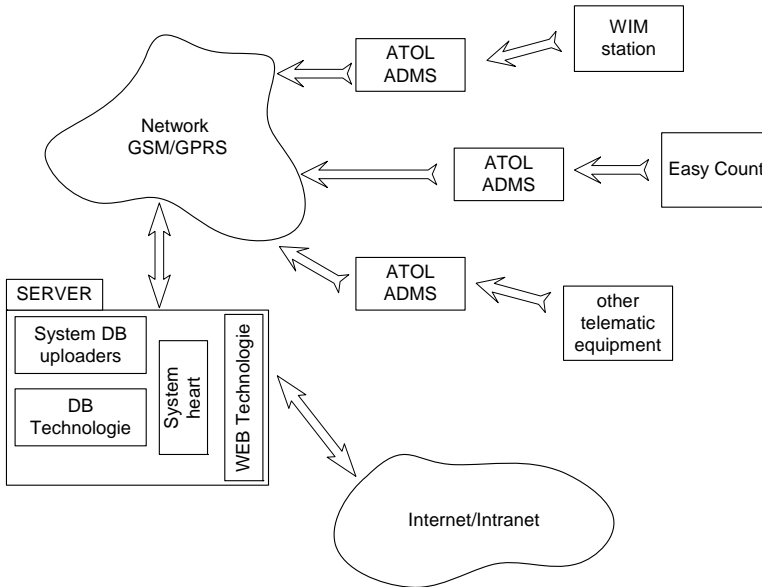


Figure 4. ATOL system parts

2.3.4. ATOL ADMS compound

ATOL ADMS is a completely autonomous /independent/ unit which provides connection with the server based on a principal Client/Server where ADMS represents the Client, which means connection with the server is established through ADMS unit side. This is very important where minimalization of requirements for GPRS internet connection is concerned. ADMS is able to communicate also through regular Ethernet, protocol TCP/IP speed 10MBit/s.

The ADMS has its own defined protocol of remote management through communicational protocol with the server or SMS. Majority of required ratings and parameters' necessary for ADMS operation can be set from a WEB dividing line by an authorized user.

2.4. WIM Applications for bridges

A scientifically very attractive application for WIM systems is the analysis of dynamic deformations of bridges under the influence of moving traffic. The influences on the load of location and time can be precisely correlated with the stress and strain parameters of the bridge elements by means of WIM sensors measuring in real time. This opens up new possibilities for comparing the

simulation calculations of the dynamic behaviour of model bridge structures with actual measured data. An even broader field of application relates to influencing the traffic in the interests of the safety of road and freeway bridges. The entire road network contains many bridges with restrictions on permissible vehicle weights. At these points, the use of WIM systems is desirable in order to prevent the danger of the potential overloading of bridges by heavy vehicles.

WIM systems also make a worthwhile contribution to an increase in the efficiency of traffic information systems. WIM data can be used to control display boards according to load so that, for example, only vehicles with 4 axles and over are informed of diversion routes, allowing traffic to flow unhindered and without damage to the bridge concerned. It is even possible to influence heavy traffic selectively according to the different signal characteristics of buses and trucks of the same weight.

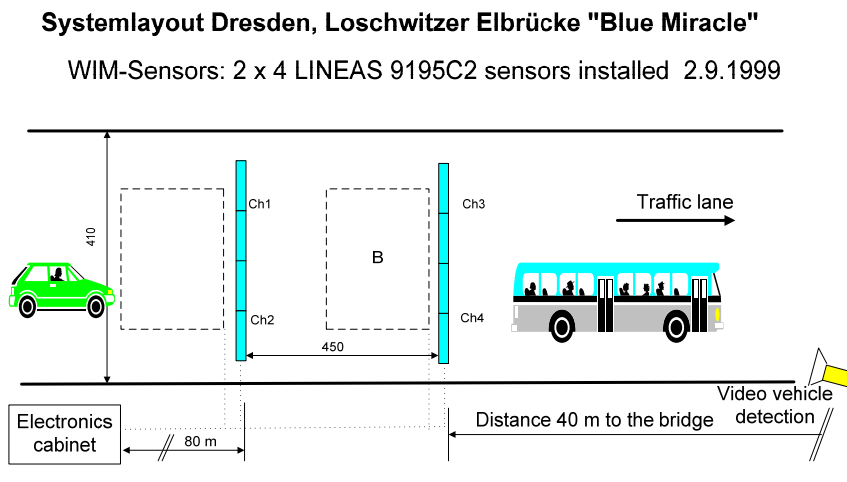


Figure 5. Bridge protection example

The Elbe bridge between the Dresden districts of Loschwitz and Blasewitz was opened to traffic in 1893. It is a protected historical monument and, as a masterwork of steel structure, is well known by the name “Blue Miracle”. There is a ban on trucks over 15 tons weight, but this is often ignored. It is for this reason that a WIM installation was demanded, which in the event of overweight vehicles triggers an alarm, but only when goods transport is involved, not for city transport vehicles or for sightseeing or tourist buses. The WIM installation was installed on 1999. A new type of software for vehicle classification to handle the critical differentiation between buses and trucks has been developed. A teach-in procedure uses the characteristic signatures of the induction loop signals together with axle loads and wheelbases to optimize the vehicle classification. The traffic data are processed in real time, both for statistical evaluation according to 8 vehicle

categories and to control the traffic distribution system. The classified data is also used to operate a video monitoring system with license plate acquisition software. This ensures the automatic and reliable recording of trucks which exceed the weight restrictions.



Figure 6. WIM system with camera for violator's enforcement

These types of WIM applications are therefore not intended for the punishment of overweight vehicles, but act mainly as a deterrent and to persuade the driver to keep to the regulations. Most drivers, even without an enforced diversion, will plan their next journey so that the total weight will be within the restrictions, in order to avoid the loss of time caused by a diversion.

2.5. Application for the Management Information System

The WIM systems data could be used for different purposes and different users. The example for effective using has been done on figures 5 – 7 below.

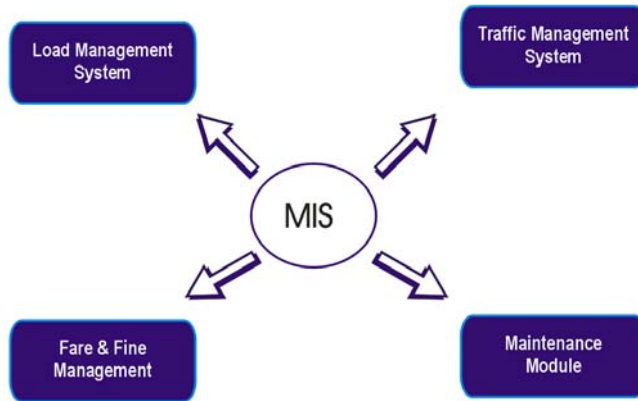


Figure 7. Subsystem for Load Management

- Centralized Data Analysis
- Customized Design for Axle Overload Control Management
- Axle Over Load Control Management Tool
- Designed for Remote Video Enforcement of Axle Overload Control Regime
- Modular Structure
- Centralized Configuration Control & Management
- Standardized Financial Control & Reporting
- Data Archiving & Storage for Multiple use

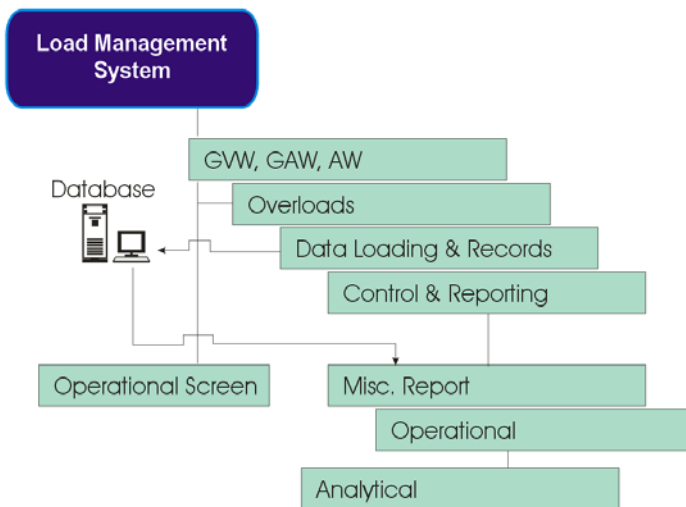


Figure 8. Subsystem for Load Management

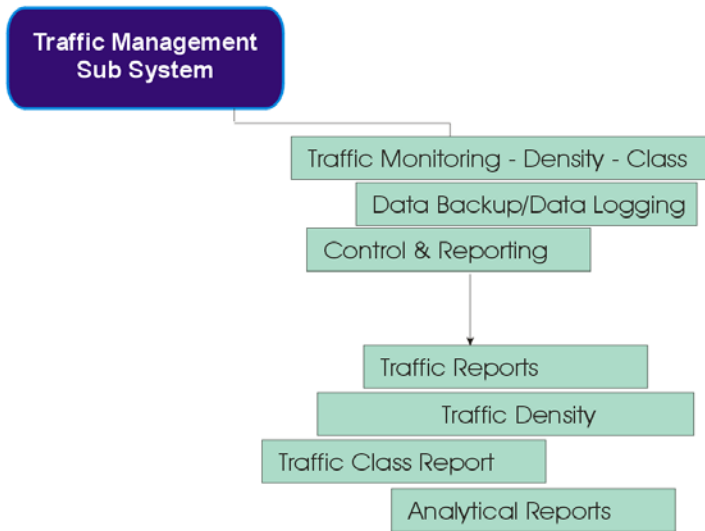


Figure 9. Subsystem for Traffic Management

3. CONCLUSIONS

The dynamic loads can be accurately quantified for the planning of bridge reconstructions and road repairs, and this facilitates planning of the most appropriate repair methods and bridge maintenance.

WIM systems provide specific national economic advantages for preventative measures for the protection of bridges against overload, since the design of many older structures is no longer equal to the more than proportionate growth in traffic volumes in recent years. It is often the case that dynamically fluctuating loads not only damage the supporting structure and road surfaces, but also the insulating layers, in which under certain conditions even a relatively small number of overloads can cause costly consequential damage.

It is well known that vehicles with a high overall weight are not necessarily the most decisive damage factors, because damage to supporting structures and road surfaces such as cracks and lane grooves increase with approximately the fourth power of the axle loads. It is therefore desirable not only to give the usual attention to overall weights, but increasingly also to give particular attention to excessive axle loads.

WIM systems are the most efficient method in this respect, both for traffic management and for monitoring purposes

With regard to the cost-benefit ratio, WIM systems with quartz sensors and their durability and accuracy can be regarded as an appropriate and effective investment.

Acknowledgements

The model in this file was first drafted by Dr. Emil Doupal, ass. prof. of civil engineering, and was subsequently modified and adapted for the purpose of this particular seminar.

References

1. Doupal E. (2000), Measuring of dynamic influence or wheel load distribution, tire width, type and pressure to pavement damage, 1st Pavement Research Conference, Sept.2000, Budapest, Hungary
2. Doupal E., Calderara R., Jagau R.(2002) “Measuring of Dynamic Wheel Loads”, 9th Internat. Conference on Asphalt Pavements, Copenhagen, Denmark, August 2002.
3. Cornu D., Anwar A., Ijaz A., Doupal E., (2006) ”Weight of intellect” Traffic Technology International, August/September 2006
4. COST323, B.Jacob, ed. (1999) “ European Specification on Weigh-in Motion of Road Vehicles, Draft 3.0”, EUCO-COST/323/5/97, LCPC, Paris, (56pp.)
5. ASTM E 1318-94 (1994) “Standard Specification for Highway Weigh-in-Motion (WIM) Systems with User Requirements and Test Method”, ASTM
6. Calderara R., Helg Ch., Doupal E. (2000) Plane sense, Toll Trans Aug/Sept 2000

Analysis of the functional quality of pavements from texture measurements

Elisabete Freitas and Paulo Pereira

Department of Civil Engineering, University of Minho, Guimarães, 4800-058, Portugal,

efreitas@civil.uminho.pt

Department of Civil Engineering, University of Minho, Guimarães, 4800-058, Portugal,

ppereira@civil.uminho.pt

Summary

The surface texture of a pavement, including unevenness, is largely determinant of drivers' safety and comfort. It is undoubtedly a major cause of road traffic accidents all over the world. Statistics show that one million killed and 50 million injured are reported every year by Competent Authorities.

The effect of traffic noise has also become a critical public issue. On the road networking the surface characteristics of pavements also contributed to nearly 80-90% of roadway traffic noise. Not only engines or exhaust systems generate noise. The impact of tire-surface at speeds above 50 km/h also needs to be added to prime offenders. Functional requirements such as roadway safety, environmental quality, driving comfort and operating costs in the road network are assessed by indicators whose limits are continuously adjusted. The roadway texture is again a main intervenient.

This paper aims at describing the texture indicators that can be used for the assessment of the texture of a pavement from a network point of view, based on profiles acquired at high speeds, including megatexture.

First an overview of the concepts related to texture and the effects of texture, including unevenness, on safety, driving comfort, ride quality and environmental quality is given. Then, a case study related to a highly trafficked road in the north of Portugal is presented. This study is the second phase of a broader study that started with the analysis of the structural capacity of that road. In this second phase, a high speed profilometer was used to measure the pavement profile with a sampling rate which is considered to be adequate for the analysis of longitudinal profile, macrotexture and unevenness. Indicators such as the mean profile depth, the IRI and the rutting depth and the corresponding effects were addressed.

KEYWORDS: pavement; profile, texture ranges, texture spectrum, texture level, indicator, mean profile depth, IRI.

1. INTRODUCTION

Road pavements have two main functions, structural and functional, the indicators and corresponding limits of which evolve with time. Relatively to the functional component, that evolution is a consequence of the road users' demands. These demands include safety and driving comfort. Moreover, environmental indicators such as noise are also included. At present, it is estimated that there are more than one million killed and 50 million injured annually on the road network all over the world, [1]. In addition, 80 to 90% of noise results from roadway traffic (according to European Community). Among other factors, the accurate definition of the functional indicators related to texture can help reducing these statistics.

Factors such as tyre/pavement friction, [2], noise emission caused by tyre/road interaction, [3], driving comfort, [4], as well as rolling resistance, wear of tyres, [5], and other operating costs are influenced, to a great extent, by pavement irregularities and therefore by road texture and unevenness.

In order to assess, compare and improve the functional quality of roads, there has been an effort to standardize the measurement methods of texture at high speeds (travelling speeds), based on surface profiles. An exception is made for the case of the microtexture due to technical issues that are expected to be shortly overcome. Meanwhile research on predicting friction based on microtexture profiles is being carried out at present, [6].

This study is the second phase of a broader study that aimed at assessing the structural and the functional quality of a highly trafficked road in the north of Portugal.

This second phase aims at presenting a full assessment of the texture of a pavement from a network point of view by introducing indicators related to megatexture based on profiles acquired at high speeds.

Initially an overview of the concepts related to texture and to the effects of texture is portrayed, followed by the assessment of the functional quality of a road.

2. CONCEPTS RELATED TO TEXTURE

The profile of a surface may be described by two coordinates: the distance along a certain travel direction, the amplitude which is normal to the surface plane (Figure 1) and the texture wavelength defined as the (minimum) distance between periodically repeated parts of the curve.

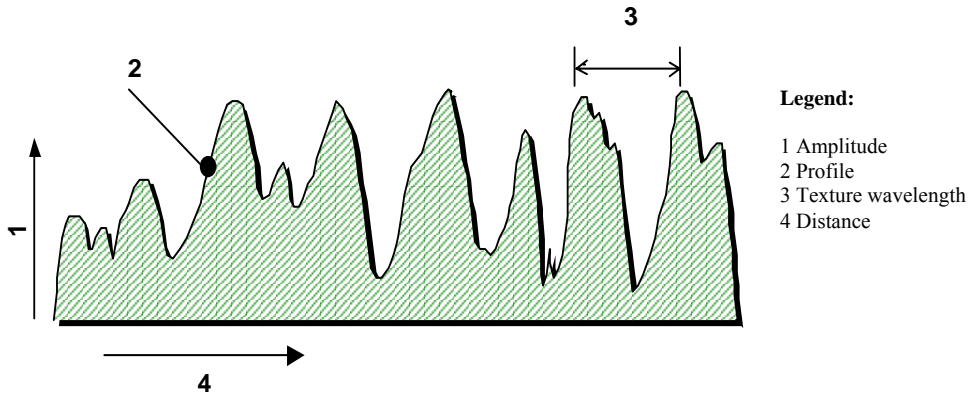


Figure 1. Example of a surface profile, [7]

Due to that possibility, the profile of a surface may be described as the sum of several sinusoids with a certain phase, wavelength or frequency and amplitude by means of mathematical Fourier techniques and therefore by its spectrum.

A texture spectrum is obtained when a profile curve has been analyzed by either mathematical Fourier techniques or by the corresponding filtering processes in order to determine the amplitude of its spectral components (wavelengths or spatial frequencies), [8].

In its turn, the pavement texture is the deviation of a pavement surface from a true planar surface within the wavelength range of the microtexture, the macrotexture, the megatexture and the unevenness, [8]. Although unevenness is described by the amplitude and the wavelength, some authors do not consider it as a texture descriptor.

According to ISO13473-1, the ranges of texture are defined as follows [8]:

- microtexture: the deviation of a pavement surface from a true planar surface with the characteristic dimensions along the surface of less than 0,5 mm; peak-to-peak amplitudes normally vary in the range of 0,001 mm to 0,5 mm;
 - macrotexture: the deviation of a pavement surface from a true planar surface with the characteristic dimensions along the surface of 0,5 mm to 50 mm; peak-to-peak amplitudes may normally vary in the range of 0,1 mm to 20 mm;
 - megatexture: the deviation of a pavement surface from a true planar surface with the characteristic dimensions along the surface of 50 mm to 500 mm; peak-to-peak amplitudes normally vary in the range of 0,1 mm to 50 mm;
- unevenness: the deviation of a pavement surface from a true planar surface with the characteristic dimensions along the surface of 0,5 m to 50 m.

3. INFLUENCE OF TEXTURE AND UNEVENNESS

The surface texture is mostly determined by the selection of the materials (especially aggregates), the mixture design, the finishing techniques and the behaviour of the mixture throughout time. In its turn, the surface texture determines the functional quality of the road for what respects to safety, [1], and driving comfort, [4], the structural quality due to dynamic loading, [9], and the environment quality relatively to vehicle emissions, wear, [5], and noise, [3]. Figure 2 shows the influence of texture ranges on pavement surface characteristics.

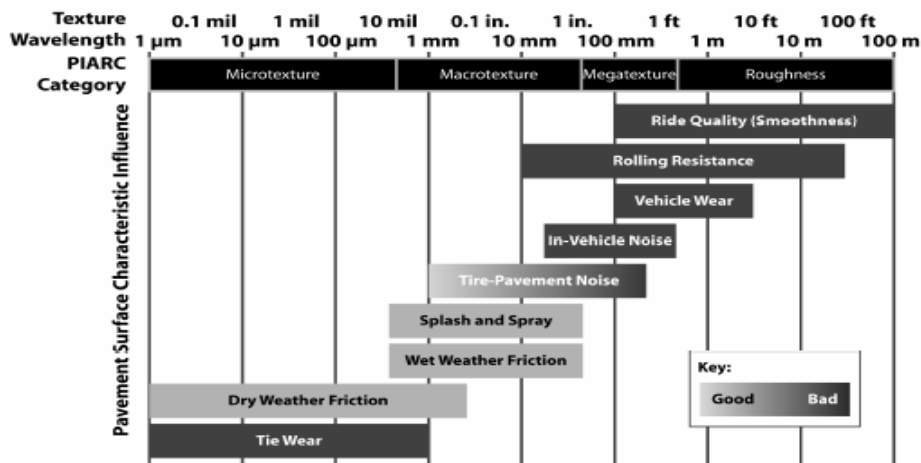


Figure 2. Influence of texture ranges on pavement surface characteristics, [10]

The microtexture is usually too small to be observed by the eye. It is obtained by the surface properties (sharpness and harshness) of the individual aggregates or other particles of the surface which are directly in contact with the tyres and therefore originating tyre-wearing. The microtexture provides adequate stopping on dry surfaces at typical vehicle operational speeds and on wet (not flooded) surfaces when vehicle speeds are inferior to 80 km.

The macrotecture is the texture which has wavelengths in the same order of size as tyre tread elements in the tyre/road interface. The macrotecture is obtained by a suitable proportion of the aggregate and mortar of the surface or by certain surface finishing techniques. Surfaces are normally designed with a certain macrotecture in order to obtain suitable water drainage in the tyre/road interface. The macrotecture provides adequate wet-pavement friction (in conjunction with the microtexture) and reduces splash and spray at high speeds. It greatly determines the tyre-pavement noise. High wavelengths (> 10 mm) also determine the noise inside the vehicles and the rolling resistance.

The megatexture is the texture of which wavelengths have the same order of size as a tyre/road interface. It results from inadequate compaction of the surface and from surface distresses such as potholes. High levels of megatexture increase the vehicle wear, the rolling resistance and have a negative impact on ride quality.

The unevenness includes longitudinal and transverse long waves. They result from a poor construction quality and from traffic loading. The longitudinal unevenness, through vibrations, affects the ride comfort (Figure 3 (a)), creates dynamic loadings and the road holding of vehicles and indirectly affects safety (Figure 3 (b)). The transverse unevenness, for instance due to rutting, affects safety through lateral instability and water accumulation. They also increase vehicle delay costs, fuel consumption and maintenance costs.

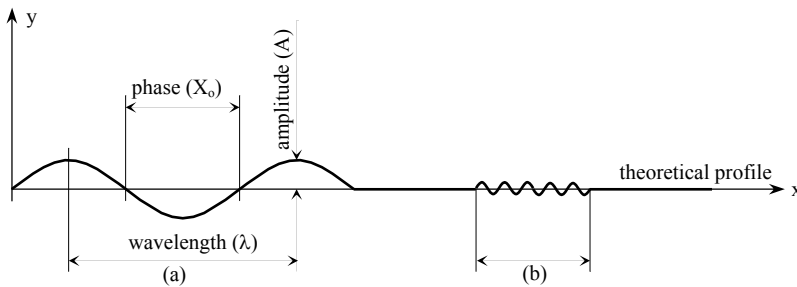


Figure 3. Characterization of the road profile: (a) long waves; (b) short waves, [11]

4. TEXTURE AND UNEVENNESS INDICATORS

There a number of texture and unevenness indicators. Some result from direct measurements of the surface profile by means of high speed profilometers, such as the texture profile level and the International Roughness Index, and others are indirect measures of the texture such as the friction coefficient or the Sand Patch used to assess microtexture and macrotexture. Nevertheless, whenever a surface profile is defined by its spectrum, the resulting amplitudes within a certain band may be transformed into a unique indicator defined as texture profile level (L). The texture profile level is a logarithmic transformation of an amplitude representation of a profile (Equation 1), [12].

Figure 4 shows an example of the use of this indicator to define several texture spectra for comparison purposes, which include all texture ranges. The texture level is usually between 20 dB and 80 dB, [13].

$$L_{tx \lambda} \text{ or } L_{TX \lambda} = 20 \lg \frac{a_{\lambda}}{a_{ref}} \tag{1}$$

were:

$L_{tx \lambda}$ = texture profile level in one-third-octave bands (re 10^{-6} m, in dB);

$L_{TX \lambda}$ = texture profile level in octave bands (re 10^{-6} m, in dB);

a_{λ} = root mean square value of the surface profile amplitude (in m);

a_{ref} = reference value = 10^{-6} m;

λ = subscript indicating a value obtained with a one-third-octave-band filter or octave band filter having centre wavelength λ

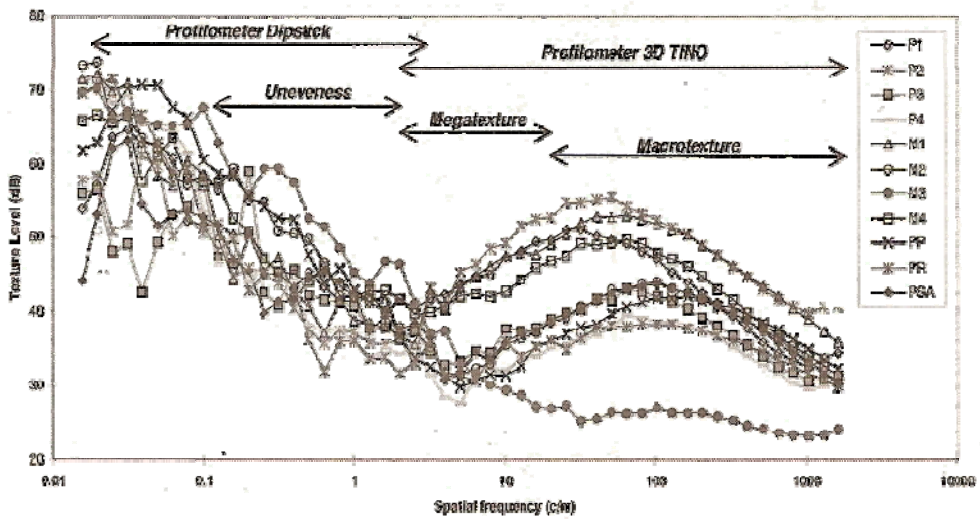


Figure 4. Examples of texture spectra for 1/3 octave bands, [15]

4.1 Microtexture

Due to the fine resolution necessary to acquire a profile on the microtexture range, no automated methods for measuring microtexture at highway speeds in situ exist. As a consequence, measuring the pavement surface microtexture is commonly carried out in laboratory, with laser profilers, or estimated in the field by using friction measurements. In the field either punctual measurements are effectuated by means of the British Pendulum, [14], or continuous measurements by means of high speed friction testers. In this case the higher the microtexture, the higher the friction coefficient.

4.2 Macrotexture

Two commonly used methods are the mean texture depth (MTD) and the mean profile depth (MPD). The MTD is determined by using the volumetric method (commonly referred to as the “sand patch test”, [16], whereas the MPD is determined using laser technology at highway speeds, [8].

The first method consists of spreading sand or glass spheres in a patch. The material is distributed with a rubber pad to form an approximately circular patch, whose average diameter is measured. The mean texture depth is obtained by dividing the volume of the material by the area covered.

The second method is calculated at a certain profile distance (base line) as indicated in Figure 5 (usually 10 cm). The MTD may be estimated through a conversion equation (presented in Figure 4). In this case the MTD is indicated as Estimated Texture Depth (ETD).

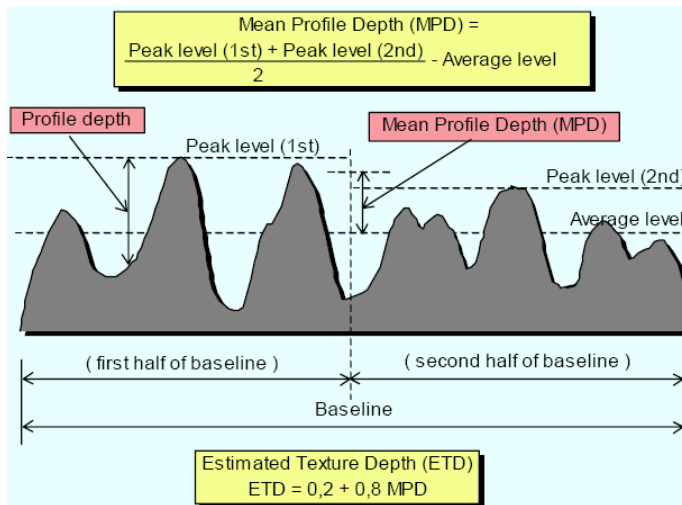


Figure 5. Illustration of the concepts of base line and profile depth and the texture indicators mean profile depth and estimated texture depth (in millimetres), [8]

4.3 Megatexture

Specifically for the analysis of the megatexture, which is probably the less studied range of the texture, the International Organization for Standardization (ISO) is preparing the ISO/CD 13473-5 “Characterization of pavement texture by use of surface profiles – Part 5: Measurement of megatexture”, [7], where the following texture profile level indicators (L) are proposed:

L_{Me} - an indicator representing an overall description of defects existing in the deviation between the pavement surface and a true planar surface, the characteristic dimensions of which range between 50 mm and 500 mm along the surface (this deviation corresponds to texture wavelengths analysed in one-third-octave bands, which include centre wavelengths from 63 mm to 500 mm);

L_{TX63} - it represents a description of the pavement defects having the shortest dimensions within the megatexture range (deviation between the real surface and a true planar surface corresponding to texture wavelengths analysed in one-third-octave bands which include centre wavelengths from 50 mm to 80 mm, being equivalent to an octave band with a centre wavelength of 63 mm);

L_{TX500} - it represents a description of the pavement defects having the longest dimensions within the megatexture range (deviation between the real surface and a true planar surface corresponding to texture wavelengths analysed in one-third-octave bands which include centre wavelengths from 400 mm to 630 mm, being equivalent to an octave band with a centre wavelength of 500 mm).

The L_{Me} is used when there is a requirement to characterise megatexture by a single measure. The L_{TX63} facilitates the characterisation of defects which correspond approximately to the length of a normal tyre/pavement contact patch and which, for this reason, play a direct role in the generation of tyre/road noise. The L_{TX500} indicator enables the characterisation of defects which can lead to tyres losing contact with the surface and therefore reduce safety (increase in stopping distances, loss of steering control in bends) and the comfort of the driver and passengers. This indicator is complementary to the information obtained by unevenness measurements at short unevenness wavelengths (0, 7 m to 1,3 m). An illustration of these indicators is presented in Figure 6.

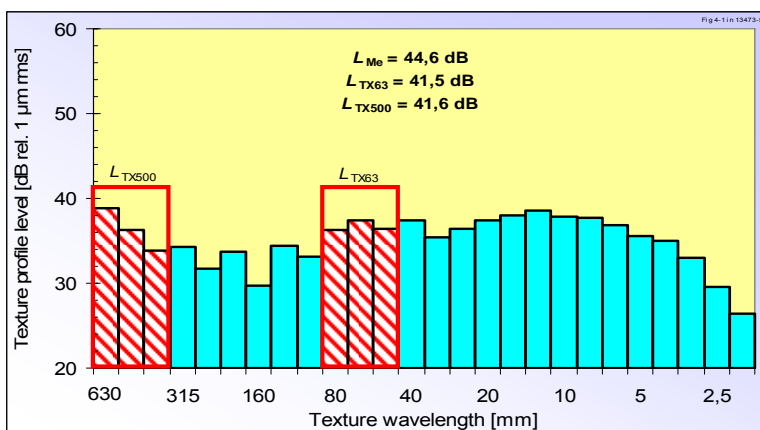


Figure 6. Example of one-third-octave band texture spectrum with indication of the texture levels of the octave bands L_{TX500} and L_{TX63} , [7]

4.4 Unevenness

The International Roughness Index is one of the most used indicators for the assessment of the unevenness of a road.

The IRI was developed by the World Bank in the 1980s. This index is used to assess the condition and the evolution of the longitudinal profile usually in the wheel track. The IRI constitutes a standardized roughness measurement and represents the average rectified slope of the profile, which is a filtered ratio of the accumulated suspension motion of a standard vehicle, [17], divided by the distance travelled by the vehicle during the measurement. The commonly recommended units of the IRI are meters per kilometre (m/km) or millimetres per meter (mm/m).

Other indicators based on the response of a users' panel have been developed, [18]. Since these indicators take into account the users' opinion on driving comfort, they are appropriate for defining functional maintenance strategies, [19].

5. CASE STUDY

5.1 Road location and geometry

The study of the texture was carried out on the EN 206 Variant, between Carreira and Guimarães (Portugal) as shown in Figure 7.



Figure 7. General view of the EN 206 Variant

This road is 2 km long and it is constituted by 2 lanes per direction (3,5 m each), a 3 m separation between carriageways, 2 service lanes (2,5 m each), and shoulders (1 m each). The current cross-section has a transversal slope of 2,5 % on both sides. The design structure of the pavement is constituted by 3 asphalt layers (wearing course – 6 cm; binder course – 6 cm; base layer – 12 cm) and an unbound sub base (graded aggregates – 20 cm).

5.2 Surface Condition

In a phase previous to this work that focused the structural condition of the road, [20], [21], the assessment of the surface condition was performed through visual inspection. The main distresses recorded were ravelling and cracking.

It was observed that, in general, the exterior lanes are more distressed than the interior ones. A different behaviour between driving directions was registered. In the direction from Guimarães to Carreira, the condition of the pavement is relatively homogenous and in a better condition if compared to the other direction. A small increase of the distress severity is recorded near the A7 roundabout, probably due to the high tangential forces as a result of braking.

On the Carreira–Guimarães direction, two homogenous stretches can be established regarding distress severity. The most distressed one is comprised along the first 700 m of the analyzed length and exhibits the highest distress severity and extent, if compared to the other stretches.

The raveling observed on the surface of the road exhibits different levels of severity. Some possible causes for the appearance of raveling are: loss of bond between the aggregate particles and the asphalt binder; aggregate segregation; inadequate compaction during construction; mechanical dislodging from certain types of traffic, such as vehicles with studded tires.

The cracking observed also exhibits different levels of severity which were originated at the top and progressed downwards. As a consequence, low MPD and high megatexture levels are expected.

5.3 Equipment and testing methodology

A high speed profilometer was used for data collection. It is equipped with 1 inertial motion sensor, 2 accelerometers and 5 lasers, 2 of which are prepared for measuring the macrotexture in both wheel paths (Figure 8).



Figure 8. University of Minho and Coimbra High Speed Profilometer

One pass-by was done on each lane and the following data were registered:

- Vehicle speed;
- Longitudinal profile - every 10 meters;
- Cross Profile Rutting: full rut, left and right wheel path - every 10 meters;
- Geometrical Data: crossfall, grade and radius of curve - every 10 meters;
- Roughness (IRI): every 10 meters;
- Macrotexture (MPD) - every meter.

6. ANALYSIS OF THE RESULTS

6.1 Longitudinal profile

The longitudinal profile of a road is defined after removing the grade and very long undulations. Figure 9 presents 12 profiles which correspond to 3 measurements per lane.

In each direction, the profiles are similar. This is an indication of small transverse variations along the road. On the traffic direction, the profile is variable. In this case, the range of deviations is -20 mm to 20 mm. Higher deviations may be also found, specifically near Carreira and at a distance of 800 m from there. For the latter, insufficient bearing capacity is a possible cause. For the former, there exists the possibility of settlement of the embankment that supports a bridge.

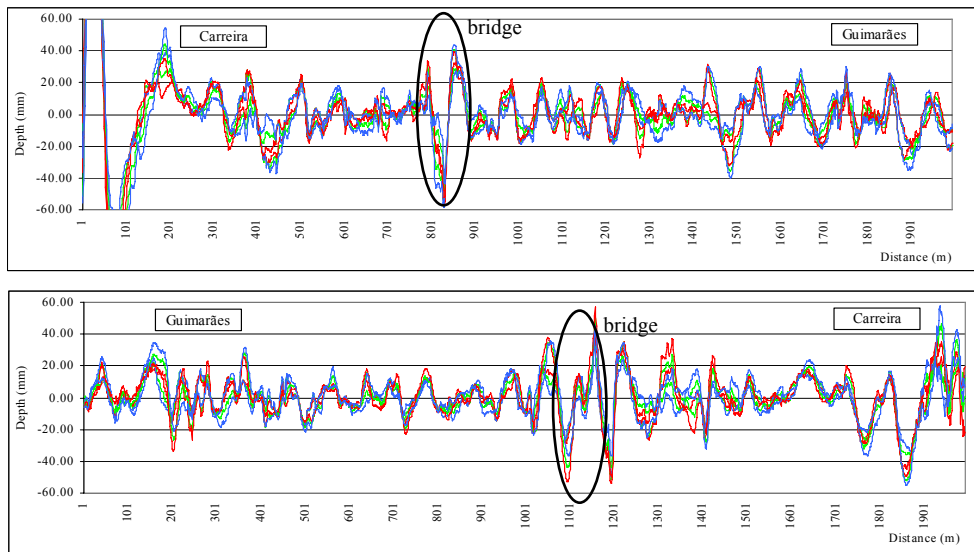


Figure 9. Profile depth

6.2 Unevenness

Figure 10 shows the IRI for the 12 profiles previously analyzed (3 in each lane).

Generally, the IRI is similar for the 3 profiles in each direction. In both directions, very high values may be found (more than 3 m/km). These high values correspond to the location of the bridge and to Carreira, as previously observed from the longitudinal profile. If these specific points are disregarded, a single homogeneous section can be considered in the direction from Carreira to Guimarães, while in the opposite direction two homogeneous sections may be identified. The first one from a distance 0 mm to 1200 m and the second one from 1200 m until the end of the road.

In this case the IRI evolution with distance does not match with the described surface condition. This fact may be an indication of the contribution of the subgrade condition on the evolution of IRI throughout time. In the future, the assessment of the surface condition and the IRI would confirm this hypothesis.

A general classification of the road unevenness is proposed by the Portuguese Road Administration, based on the percentage of road length of which the IRI obtained by 100 m overcomes a certain limit.

For the wearing course, the unevenness is classified with excellent if the following limits are simultaneously respected:

- IRI < 1,5 – 50% of the road length;
- IRI < 2,5 – 80% of the road length;
- IRI < 3,0 – 100% of the road length.

As can be verified in Figure 10, there are a few IRI values superior to 3 m/km which leads to less than 10% of the total distance out of compliance with the recommendations. For this situation, the road is classified with good. Thus, there are no major consequences in what respects the rolling resistance, riding quality and safety.

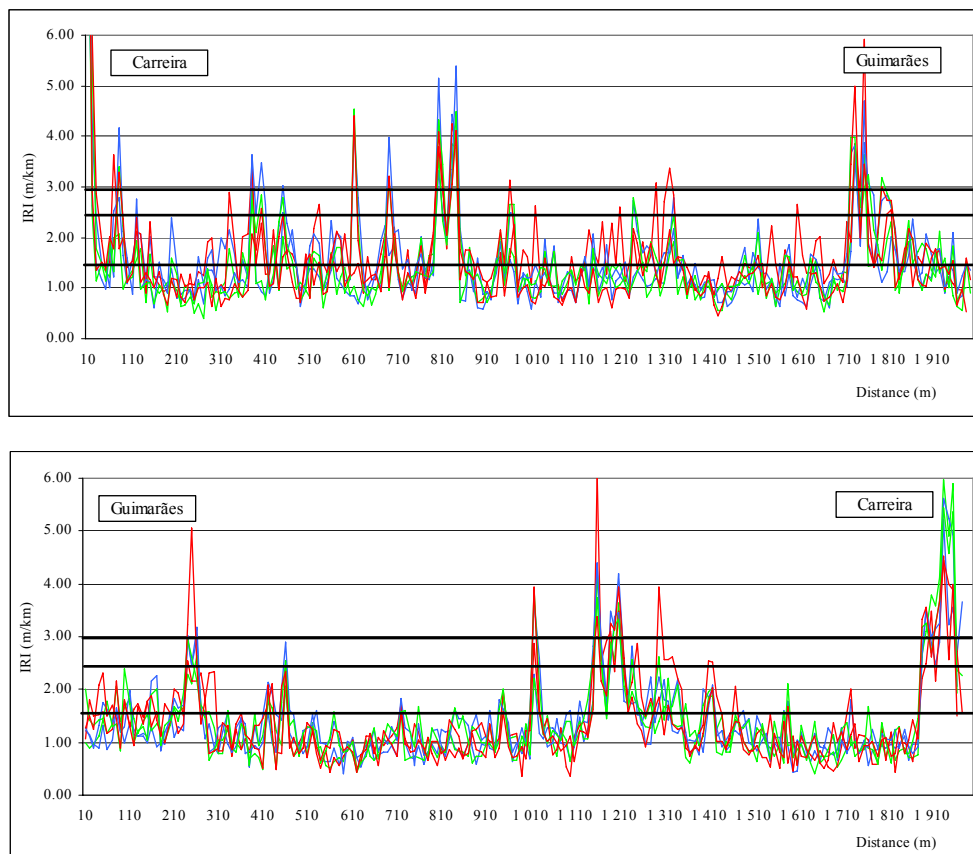


Figure 10. IRI for the right and the left lane in both directions

6.3 Rutting

Figure 11 shows the rutting measured in the 4 lanes for the right and left wheel paths.

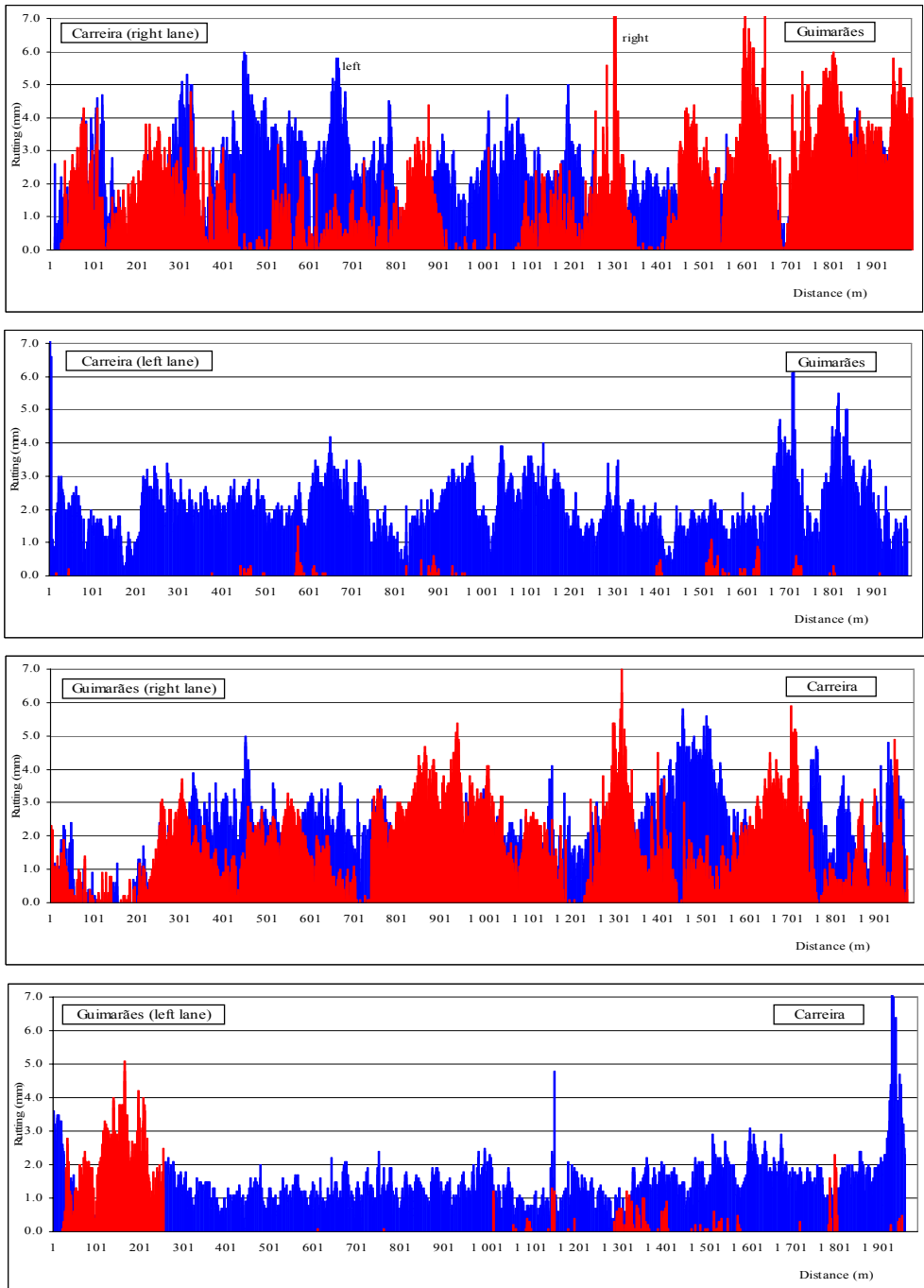


Figure 11. Rutting depth

In general the rut depth is lower than 3 mm. The right lane shows in both directions the highest variability and the highest values, although the threshold value considered for maintenance has never been reached. This threshold is 20 mm for the Portuguese conditions.

The best behaviour obtained for the Guimarães-Carreira direction is probably due to a better construction quality as supported by surface condition analysis.

For this road, safety is not compromised in what concerns water accumulation on the wheel paths.

6.4 Macrotexture

The indicator chosen for the analysis of the macrotexture was the Mean Profile Depth. Figure 12 shows the MPD for the right and left wheels path in both directions.

In view of the fact that about half of the design life of the pavement has passed by, a MPD near 0,6 mm would be expected, which is the threshold limit value. For both directions, the left lane, which is also the less trafficked, is quite homogeneous: Nevertheless, MPD of the right wheel path reaches values over 1,2 mm, which are characteristic of porous surfaces.

The MPD in the right lane is very heterogeneous, for both directions. In this case, the MPD is higher and may be related to the surface condition. In the direction of Carreira to Guimarães, at a distance of 1300 m, it is possible to notice a decrease of the MPD that corresponds to a change of the properties of the mixture that leads to less distress and thus a smaller MPD.

Based on these facts, it seems that the safety in what respects to friction in wet weather conditions is not affected. Nevertheless, environmental concerns must be taken into account as far as noise and rolling resistance are concerned. An important increase in noise levels has certainly occurred and it is predictable to continue increasing if no maintenance works are carried out in the near future.

6.5 Megatexture

For the analysis of the megatexture based on the indicators recommended in draft standard ISO 13473-5 a second pass-by on each lane is required. In this case the data required is as follows:

- Vehicle speed;
- Longitudinal profile - every 2,5 centimeters;
- Geometrical Data: crossfall, grade and radius of curve.

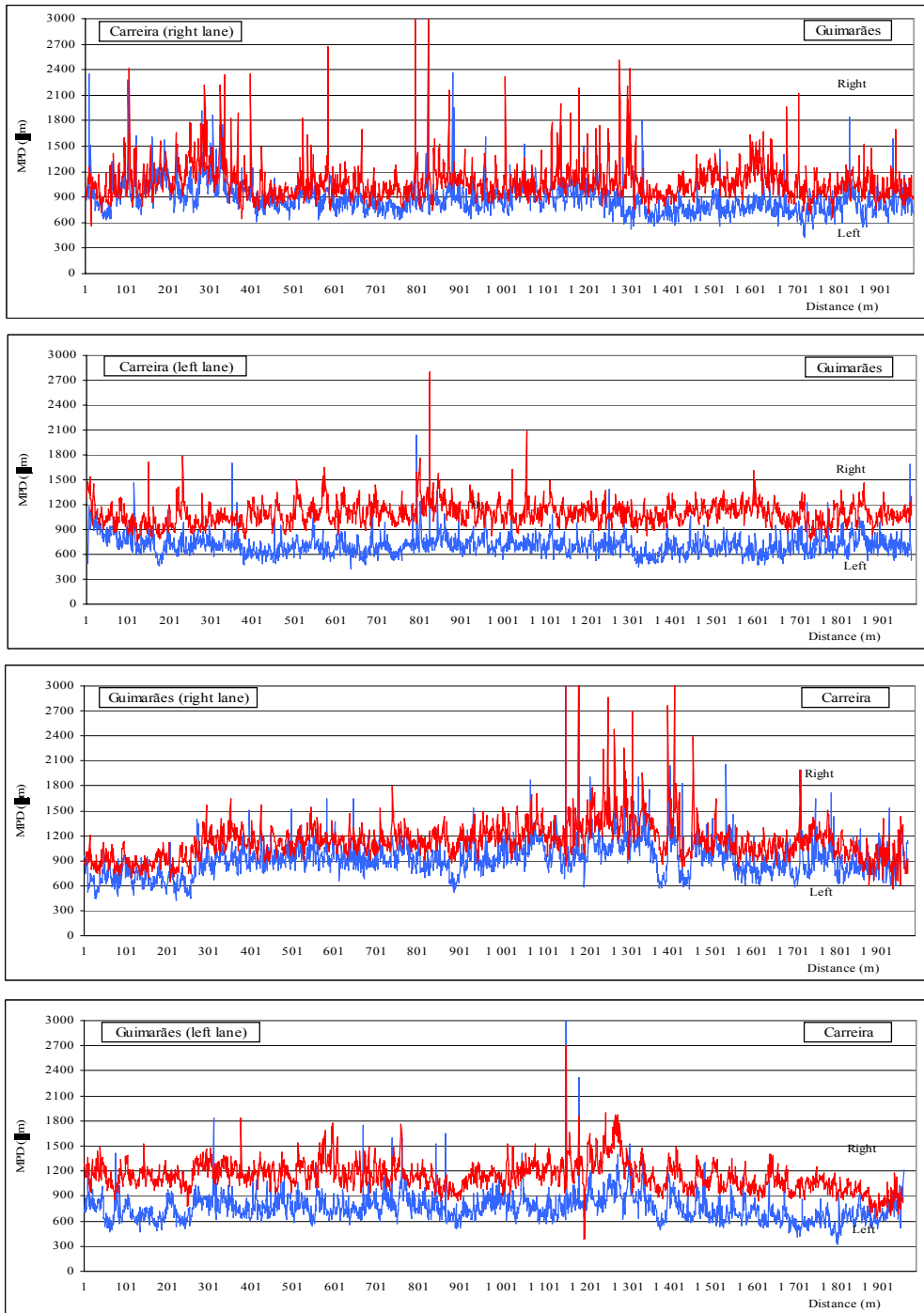


Figure 12. Mean profile depth

A computer software is being specifically developed for the analysis of the megatexture. This program is based on the power spectral density (PSD) of the measured profile. The PSD is a well-known method for the interpretation of complex signals containing a variety of wavelengths and amplitudes. The PSD analysis can be accomplished using the *pwelch* algorithm included in the Matlab® signal processing toolbox, [22]. Then the texture level and the texture level indicators are calculated from Equation 1.

7. CONCLUSIONS

Texture and unevenness highly influence safety, driving comfort and environment quality. Dealing with texture should be an easy assignment at a network level. For that reason, this paper dealt with both texture and unevenness. The concepts related to these surface characteristics were extensively presented. The ordinary texture indicators which regard microtexture, macrotexture and unevenness, such as the friction coefficient, the mean profile depth and the IRI were addressed. Indicators to assess megatexture at high speeds, relying on the concept of texture-profile level that can be used at a network level, were also included. The texture profile level is based on pavement profiles measured at high speeds. It represents a description of defects existing in the deviation between the pavement surface and a true planar surface within the megatexture wavelength ranges. Although it is recommended for the assessment of megatexture, it may be used for the assessment of texture in all ranges.

The second phase of a study regarding the condition of a roadway in Guimarães was also presented. The first phase was addressed to its structural condition. In this paper the aim of research was its functional condition. Important deviations of the longitudinal profile were measured, although, as far as unevenness is concerned, these deviations had led to a classification of good.

The macrotexture correlated well with the surface condition previously observed. The segregation and the raveling observed contributed to the high MPD. As a result, an increase of the noise level is expected.

Future work will include the assessment of the megatexture based on spectral analysis of the pavement profile obtained at high speed by means of the software under development.

References

1. Larson, R., Scofield, L., Sorenson, J, Pavement Functional Surface Characteristics, 5th Symposium on Pavement Surface Characteristics-Roads and Airports. World Road Association, Toronto, Canada, 2004.

2. NCHRP 291, Evaluation of Pavement Friction Characteristics, NCHRP Synthesis 291, Transportation Research Board, Washington DC, 2000.
3. SILVIA, “Guidance Manual for the Implementation of Low-Noise Road Surfaces”, FEHRL Report 2006/02, Forum of European National Highway Research Laboratories, Brussels, Belgium, 2006.
4. Delanne, Y., Daburon, P., Unevenness and Vibrational Comfort of light Cars, International Symposium of the Environmental Impact of Road Unevenness, Oporto, Portugal, 1999
5. Domenichini, L., Martinelli, F., Influence of the Road Characteristics on Tyre Wear, 5th Symposium on Pavement Surface Characteristics-Roads and Airports, World Road Association, Toronto, Canada, 2004.
6. Do M.-T., Marsac P., Delanne Y., Prediction of Tyre/wet Road Friction from Road Surface Microtexture and Tyre Rubber Properties, 5th Symposium on Pavement Surface Characteristics-Roads and Airports, World Road Association, Toronto, Canada, 2004.
7. ISO/CD 13473-5, Characterization of Pavement Texture by Use of Surface Profiles – Part 5: Measurement of megatexture, Draft standard ISO/CD 13473-5, International Organisation for Standardisation (ISO), Geneva, Switzerland.
8. ISO 13473-1:1997, Characterization of Pavement Texture by Use of Surface Profiles – Part 1: Determination of Mean Profile Depth, International Organisation for Standardisation (ISO), Geneva, Switzerland.
9. Dolcemascolo, V., Jacob, B., Influence of the Road Profile on Pavement Dynamic Loading. International Symposium of the Environmental Impact of Road Unevenness, Oporto, Portugal, 1999.
10. Snyder, M., Pavement Surface Characteristics: A Synthesis and Guide, American Concrete Pavement Association Publication EB235P, Skokie, IL, 2007.
11. Delanne, Y., Uni des Chaussées et Confort Vibratoire des Véhicules, Laboratoire Central des Ponts et Chaussées, Nantes, 1997.
12. ISO/CD 13473-4, Characterization of Pavement Texture by Use of Surface Profiles – Part 4: Spectral Analysis of Surface Profiles, Draft standard ISO/CD 13473-4, International Organisation for Standardisation (ISO), Geneva, Switzerland.
13. Sandberg, U., Ejsmont, J. Tyre / Road Noise Reference Book. Informex SE – 59040. Kisa. Sweden (www.informex.info), 2002.
14. ASTM E303-93: Standard Test Method for Measuring Surface Frictional Properties Using the British Pendulum Tester, Volume 04.03, Road and Paving Materials; Vehicle-Pavement Systems. American Society for Testing and Materials, 2003.
15. Domenichini, L., Fracassa, A., La Torre, F., Loprencipe, G., Ranzo, A., Scalamandrè, A., TINO Project: Relationship Between Road Surface Characteristics and Noise Emission, 1° International Colloquium on Vehicle Tyre Road Interaction “The Noise Emission”, Roma, Italy, 1999.
16. ASTM E965-96, Standard Test Method for Measuring Pavement Macrotexture Depth Using a Volumetric Technique, American Society for Testing and Materials, West Conshohocken, 2006.
17. Sayers, M., Karamihas, S., Little Book of Profiling, Basic information about measuring and interpreting road profiles, University of Michigan, 1998.
18. Delanne, Y., Pereira, P., Advantages and Limits of Different Road Roughness Profile Signal-Processing Procedures Applied in Europe, Transportation Research Record n° 1764, TRB, Washington, 2001.
19. Pereira, P., Delanne, Y., Freitas, E., “Etablissement des Classes d’Uni Pour la Gestion de l’Entretien des Routes”, International symposium on the environmental impact of road pavement unevenness, Oporto, Portugal, 22 e 23 de March 1999.
20. Ionescu, A.G., Freitas, E.F., “Modelling an Asphalt Pavement in Portugal”, Intersection/Intersectii, <http://www.ce.tuiasi.ro/intersections>, 2007.
21. Vrancianu, I.D., Freitas, E.F., “Definition of Homogenous Road Sectors According to COST 336”, Intersection/Intersectii, <http://www.ce.tuiasi.ro/intersections>, 2007.
22. MathWorks, Signal Processing Toolbox for Use with Matlab®, Users Guide, Version 6, 2006.

FRICION STIR WELDING – AN INNOVATIVE SOLUTION FOR CIVIL ENGINEERING

Ramona Gabor¹, Anca Gido² and Radu Bancila³

¹*Department of Steel Structures, Faculty of Constructions, Timisoara, 300224, Romania,
ramona.gabor@ct.upt.ro*

²*Department of Steel Structures, Faculty of Constructions, Timisoara, 300224, Romania,
anca.gido@ct.upt.ro*

³*Department of Steel Structures, Faculty of Constructions, Timisoara, 300224, Romania,
radu.bancila@ct.upt.ro*

Summary

Since his invention in 1991 at TWI Cambridge, Friction Stir Welding (FSW) has conquered the interest of the industrial companies because the good quality of the weld and because it possible to weld components with high requirements as regard compression strength and tightness.

The process is a solid – state one, being considered an ecological process. The applications to the industrial scale are known in aircraft industry, automotive industry and shipbuilding industry. Since the aluminum becomes more often used in civil engineering, FSW presents interest also in this domain.

Two of the big number of aluminum alloys that can be welded with FSW seems to be most indicated for superstructure of the bridges: AA 5083 and AA 6082. These two alloys have a very good behavior to corrosion – one of the biggest problems of steel bridges. This paper will present the future welds that can be used for bridge constructions.

KEYWORDS: Friction Stir Welding, Non-consumable tool, Aluminum bridges.

1. INTRODUCTION

Friction Stir Welding (FSW) is a solid-state welding process created and patented by The Welding Institute (TWI) in 1991. It is a relatively novel joining technology, which has caught the interest of many industrial sectors, including automotive, aeronautic and transportation due to its many advantages and clear industrial potential. The process adds new possibilities within component design and allows more economical and environmentally efficient use of materials [1].

Many light weight materials and in particular aluminum alloys may be joined by this technique, including the high strength aluminum alloys (2xxx and 7xxx series)

used in the automotive and aeronautic industries, which are very difficult to join by traditional welding techniques. The technique also brings about other advantages in terms of enabling joining of dissimilar alloys, different materials or even metal-based composites. Much work is also currently underway in order to make it possible industrially to join higher forging temperature and less ductile materials such as titanium, steel and stainless steel.

The main advantage of FSW over traditional welding technologies is that joining is achieved below the melting temperature avoiding deterioration of the material microstructure and joint mechanical properties often seen in traditional welding, and adding new dimensions to design and component optimization. Another important consequence is that the problems related to the working environment when using traditional arc welding processes, namely air pollution and ultraviolet light are absent with FSW.

2. THE FRICTION STIR WELDING (FSW) PROCESS

2.1. Description of the process

By a frictional heating and stirring technique materials are welded in the solid phase. A cylindrical shouldered tool with a profiled probe is rotated and traversed (forced) along the joint line, whereby the two materials are joined in what would resemble a continuous forging operation, see Figure 1. Due to the high frictional forces between the wear resistant tool and the parent material the workpiece temperature rises to a hot forging level (typically in the range of 70-85% of the melting temperature), where recrystallisation is balanced by plastic deformation allowing the material to flow under large plastic deformation leaving a solid phase bond between the two pieces [2].

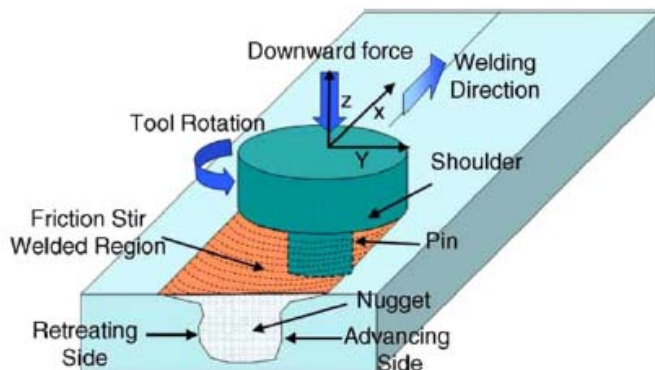


Figure 1. Presentation of the FSW process

The process can be divided in four steps like it is shown in Figure 2. Initially, the plates to be welded are clamped together and the tool is rotated (Figure 2a); the tool is plunged into the material (Figure 2b); the tool translates along the joint line, plasticized material is stirred and forged behind the trailing face of the pin (Figure 2c); finally the tool is removed consolidating the solid state weld (Figure 2d).

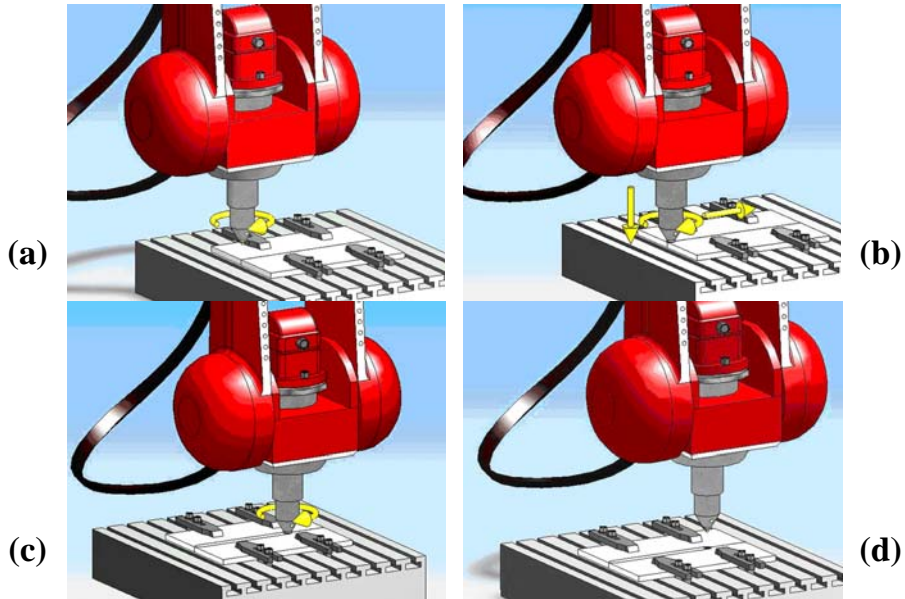


Figure 2. Schematic representation of the steps for FSW: (a) tool rotation, (b) tool plunge, (c) tool traverse, (d) tool exit.

The FSW **tools** (Figure 3) are manufactured from a wear resistant material with good static and dynamic properties at elevated temperature. They are made in a manner that permits up to 1 000 m of weld to be produced in 5 mm thick aluminum extrusions without changing the tool. The process has been used for the manufacture of butt and lap joints. For each of these joint geometries, specific tool designs are required which are being further developed and optimized [3].

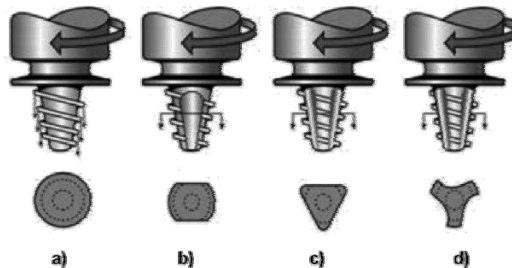


Figure 3. Some types of weld tools

The microstructure of the weld is presented in Figure 4.

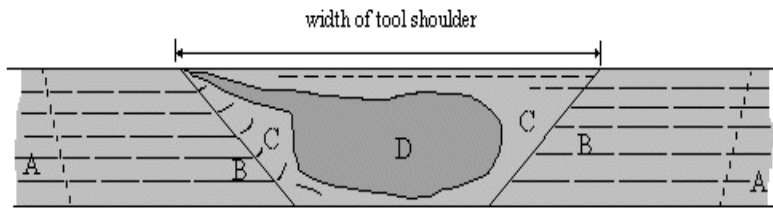


Figure 4. Weld zone

- A. Unaffected material
- B. Heat affected zone (HAZ)
- C. Thermo-mechanically affected zone (TMAZ)
- D. Weld nugget (Part of thermo-mechanically affected zone)

In the heat affected zone the material has experienced a thermal cycle that has modified the microstructure and/or the mechanical properties; however, there is no plastic deformation occurring in this area. The main microstructural changes due to the effect of temperature are precipitates dissolution and coarsening which may also affect the mechanical properties of the FSW joint.

In the TMAZ the material has been plastically deformed by the FSW tool, and the heat from the process will also have some influence on the material. In the case of aluminum, it is possible to have significant plastic strain without recrystallisation in this region, and there is generally a distinct boundary between the recrystallised zone (nugget) and the deformed zones of the TMAZ.

The weld nugget, or stir zone, is the region where the pin penetrates in the material, located in the centre of the weld. In this zone it is possible to notice the effect of severe plastic deformation and temperature on the microstructure. In the nugget is usually possible to see (looking at the macrograph of the transverse section of the weld) the presence of “onion rings”; swirl patterns in a plane 90° to the rotation plane of the tool. The material is characterised by a recrystallized microstructure with very fine grains, which can increase the hardness of some materials; however a reduction in some mechanical properties and eventual defects can also be found, such as lack of penetration, volumetric defects, among others. Another important characteristic of the nugget is the solubilization and re-precipitation of the original precipitates.

The shoulder contact zone is a wider zone of deformation that is limited to a shallow depth caused by the interaction between the rotating tool and the material surface [4]. It has been suggested that this area (which is clearly part of the TMAZ) should be given a separate category, as the grain structure is often different here; however it is treated as a sub-zone of the TMAZ. The microstructure here is determined by rubbing by the rear face of the shoulder.

With the almost unlimited design profile possibility of extruded aluminum parts, FSW offers a very interesting method to produce aluminum components. Based on the conventional butt and lap joints, other joint geometries can be achieved just varying and combining these joints. For all the joint configurations, complete penetration requirements must be taken into account when they are welded as well as the joint design practical aspects to avoid weld imperfections. Some joint geometry can be seen in the Figure 5.

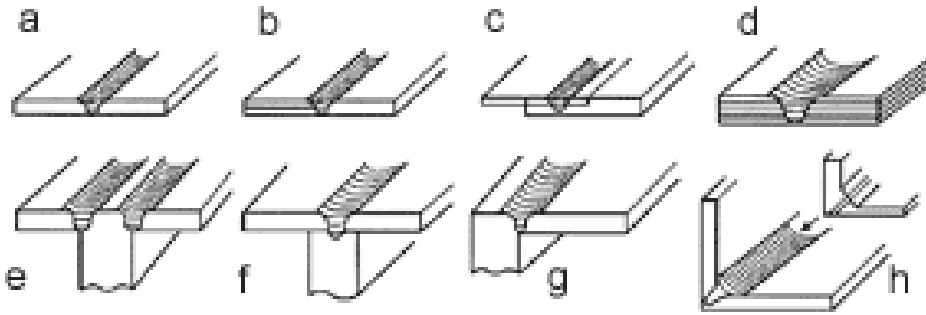


Figure 5. Joints geometry: *a.* Square butt and lap; *b.* Combined butt and lap; *c.* Single lap; *d.* Multiple lap; *e.* 3 piece T butt; *f.* 2 piece T butt; *g.* Edge butt; *h.* Possible corner fillet weld

2.2. The advantages of FSW

Environmentally Friendly

- Environmentally friendly process minimizes energy consumption and generates no smoke, gasses, or waste stream.

Product Improvement

- Join highly dissimilar metal combination to optimize your products, quality and properties.
- Joint strength equal to or greater than that of parent material.
- Low temperature solid state forging preserves microstructure and material properties (no melting)
- Full cross-sectional porosity-free bond.
- Very narrow heat-affected zone.
- Consistent & repeatable high quality welds through microprocessor-based automation.
- Unlimited part length.
- Only solid, internal materials exist across boundary- no third alloys.
- Allows flexibility to combine materials of different properties or prefab components made by different technologies

- Combining materials frees your design to combine properties like conductivity, reluctance, hardness, strength, weight, tubulars, non magnetic, etc.

Cost Savings

- Produce near net shape geometries not producible with forging, casting, or forming that reduce machining and waste.
- Create casting or forging-like blanks with minimal tooling costs and no minimum lot quantities.
- Save labor, material, and operations through near net size design.
- Simplification of component design.
- Ideal for small quantities/prototypes through high volume thanks to low initial costs.
- Low cycle times = High production rates and low costs.
- No joint preparation required - saw cuts are most commonly used.
- Join less costly, lighter, or tubular materials to expensive materials or prefabs to optimize designs.
- In-process flash removal – eliminates costly grinding.
- Standardization of components lets you reduce inventory.
- No fluxes, fillers, shield gasses or vacuum required.

But, like every thing that have advantages, FSW present also some disadvantages:

- Exit hole when tool is withdrawn.
- Large down force is required with heavy duty clamping necessary to hold the plates together.
- To some alloys the welding speed is lower than for another welding process and this is a disadvantage for the machine design.
- The welded components must be rigid fixed to avoid the movement of the pieces.
- The limited use of the portable welding machines.

2.3. Applications

Many industry fields that are using aluminum present interest for the new welding process. Since its invention, aerospace industry is one of the biggest appointee of FSW. At the very first begin FSW was used to weld window frames for airplanes. Nowadays the most part of the body of ECLIPSE 500 is realized with FSW. Also Airbus is very interested to help this new process to develop, because of the very good behavior of the aluminum (no corrosion) and because of the reduction of total airplane weight [4].

Shipbuilding industry is another field where FSW is often used. Applications of FSW can be found to [5]:

- Deck panels
- Deck and floor girders

- Boats structure (Figure 6)



Figure 6. Boat structure realized with FSW

Nowadays, the train building industry have more and more interest in using FSW to create train bodies that can improve the speed of the convoy. In Japan this already a technology very good implemented in industry. In figure 7 the body of an A-train is presented [6].

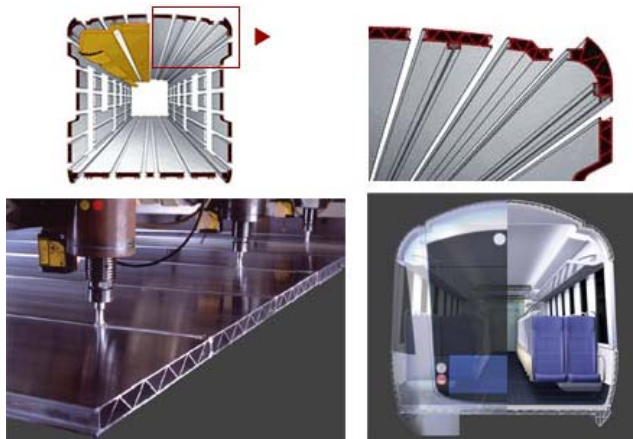


Figure 7. Elements from an A-train welded with FSW

The automotive industry has a big benefit using FSW. Big names in automotive industry like BMW, Mazda, Jaguar, Ford, and Mercedes are using FSW process to weld car engines, wheels, transmission case, spring-rigging, covers.

3. CIVIL ENGINEERING – NEW APPLICATION FIELD FOR FSW

3.1. Aluminum in civil engineering

In the last decade it can be observed an increasing of use of aluminum in civil engineering because of the good qualities in time, in contact with atmospheric actions and because of the aesthetical reasons. From the begin aluminum wasn't used as a structural material; it was used mostly for frontage of buildings, balustrades, windows frames.

Still, an embranchment of civil engineering presented interest for aluminum as a structural material. An important number of foot bridge decks were realized from aluminum or to replace the existing steel or wood deck with aluminum one. The first replace of a bridge deck with one of aluminum, was mentioned in 1933, in USA [7]. From that time, an important number of aluminum bridges or bridge decks were erected. But, because of the high price of aluminum and because the hardship to realize a good weld to aluminum, the interest for aluminum as a structural material was getting down.

Nowadays, with all this range of alloys with very good mechanical properties (some of these alloys have a very good resistance, comparable with steel) and cost savings for maintenances, the interest for aluminum increase dally.

3.2. Experimental program on AA 5083 and AA 6082 alloys

For civil engineering, as structural material, most indicate alloys are from the class 5xxx and 6xxx. Alloys of the class **6XXX**, with good formability and weldability at medium strengths, see wide use in conventional structural applications. The **5XXX** alloys provide good resistance to corrosion stress in marine atmospheres and good welding characteristics. This class of alloys has been widely used in low-temperature applications [8].

From these two alloys classes, the most suitable for civil engineering, especially for bridge constructions, are the AA 6082 and the AA 5083. Also, these two alloys present a very good weldability with FSW. An experimental program was realized at GKSS-Forschungszentrum, Germany for both alloys.

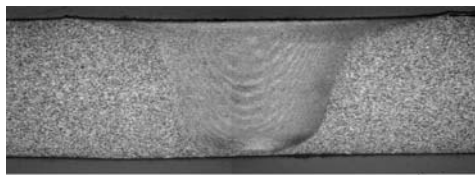


Figure 8. FS weld to 5 mm plates in AA 5083 alloy

The joint presented in Figure 8 was realized with a welding speed of 100 mm/min, a travel speed of 600 RPM, tool angle 2° and a downward force $F_z = 9000$ N. The bending tests (Figure 9) and the tensile tests (Figure 10) present very good results.



Figure 9. Bending Specimens Joint Surface (Up) and Joint Root (Down) with 5 mm Plate Thickness in Al 5083

In all bending tests for the joints in Al 5083 bending angles larger than 90° has been reached both in the surface and root area. For these good results in the root area a correct justage of the pin within a tolerance field. Too short a pin length and therefore too large the distance of the pin tip to the backing plate leads to bonding defects in the root area. Under tensile and bending load the root opens and in the worst case initiates the failure of the joint.



Figure 10. Top View Typical Tensile Specimens from Different Positions in Al 5083

The mechanical properties are mostly located marginally below the values for the base materials. The quality grades of the joints in Al 5083 H111 relating to R_m and $R_{p0.2}$ are located above 90 % of the base material values (Table 1).

Table 1. Mechanical properties of FS welded 5083

	R_m [MPa]	$R_{p0.2}$ [MPa]	A [%]
Base Material	326	190,2	22
FSW	298	150	16,4
Quality Grade	0,91	0,79	-

Average of minimum 3 Specimens

The hardness in the weld has no big variations in comparison with base material (Figure 11).

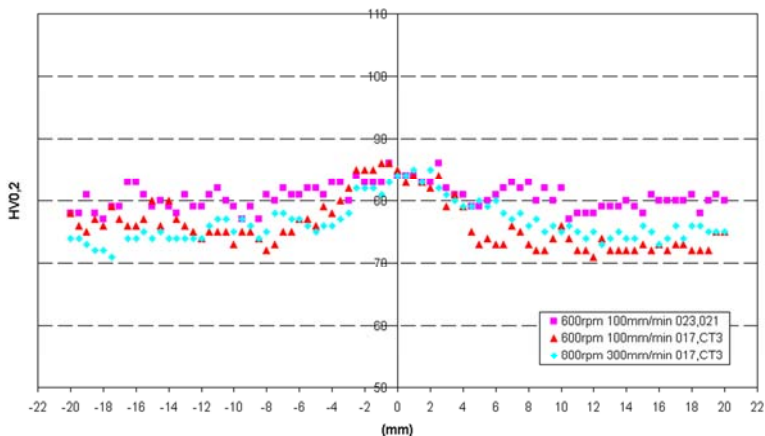


Figure 11. Microhardness of the welded AA 5083

Also weld to the AA 6082 alloy were realized. As welding parameters were used: welding speed of 400 mm/min, rotational speed 800 RPM, tool angle 1°, downward force $F_z = 8000$ N. The transversal macrostructure of the welding seam is presented in Figure 12.

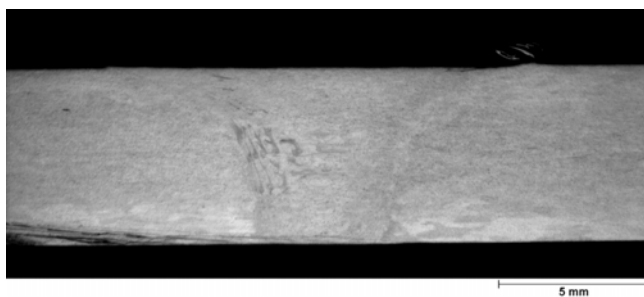


Figure 12. FS weld of 6082 alloy, 6 mm

The results of bending tests, tensile test and the microhardness present very good results in comparison with base material. The mechanical properties resulted from tensile tests are presented in Table 2.

Table 2. Mechanical properties of AA 6082 welded with FSW

	Rm [MPa]	Rp0.2 [MPa]	A [%]
Base Material	317	255	13,7
FSW	230	154	5,8
Quality Grade	0,72	0,61	-

Average of minimum 3 Specimens

3.3. Possible FS weld for civil engineering

For the erection of a bridge deck two possible geometries of welds are presented.

On the first hand longitudinal welding seams are proposed [9]. The welding seams are realized in T-overlap geometry. This welds will have the advantage of loads like bending moment and axial loads, without a shear load that can damage more the weld (the E – modulus for aluminum is 1/3 of that of steel).

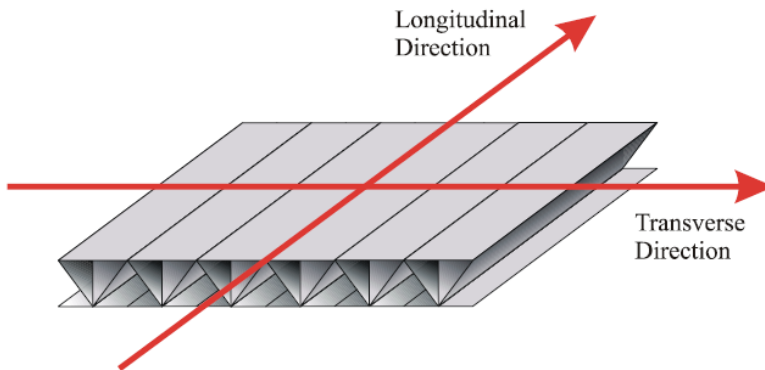


Figure 13. Longitudinal FS welds to a bridge deck

The disadvantage of this type of geometry is that of insufficient material intermixture in the bonding area (Figure 13). In this area at most a weak bonding exists.

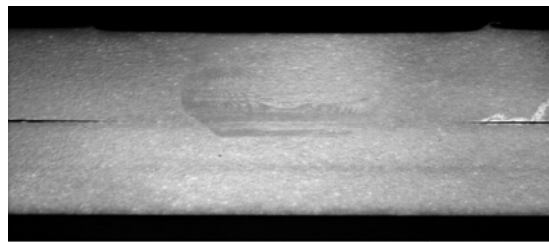


Figure 13. Macrostructure of an overlap joint

Another possible geometry is the simple butt joint. This may be realized in longitudinal or perpendicular on the traffic direction. As it was showed in the experimental part, this may be a good solution for using FSW process to realize an aluminum bridge deck.

Further experimental program will be taken, together with a finite element model to verify the tension distribution under the traffic loads.

4. CONCLUSIONS

The friction stir welding process has a large development and improvement potential in the area of lightweight construction. Further topics such as joining of modern materials and environmentally friendly production technology are for many of technologies of increasingly current significance. To achieve these goals, FSW will make an innovative contribution.

Acknowledgements

The authors would like to gratefully thank to the people from GKSS-Forschungszentrum, Geesthacht, Germany, for their support and helping to realize the welding. Special thanks to dr. J. dos Santos and dipl. Ing. R. Zettler.

References

1. www.twi.co.uk
2. Zettler, R., Konstruktion, Fertigung und Erprobung von innovative Leichtbau-Strukturen, *GKSS-Internband*, 2004.
3. von Strombeck, A., Schilling, C., dos Santos, J., Robotic Friction Stir Welding-Tool Technology and applications, *2ndFSW Symposium*, 26-28 June, 2000, Gothenburg, Sweden.
4. Lohnwasser, D., Application of Friction Stir Welding for Aircraft Industry, *2ndFSW Symposium*, 26-28 June, 2000, Gothenburg, Sweden.
5. Kallee, S., Application of Friction Stir Welding in Shipbuilding Industry, *Welding&Metal Fabrication*, November/December 2000.
6. <http://www.railway-technology.com/contractors/suburban/hitachi-ltd/>
7. Altenpohl, D., G., Aluminum: technology, applications and environment, Sixth edition. The Aluminum Association, Inc. 1998
8. Deimel, P., Sattler, E., Friction Stir Welding an den Aluminiumlegierungen EN AW-6082 und EN AW-5083. Materialprüfungsanstalt Universität Stuttgart.
9. Dobmeier J. M., Barton F.W., et co., analytical and experimental evaluation of an aluminum bridge deck panel, Part II: Failure Analysis, 1999

USING THE FINITE STRIP METHOD IN DETERMINING THE STATIC RESPONSE OF THE DECK BRIDGES

Ovidiu Gavris

Faculty of Construction, Tehnical University of Cluj Napoca

Abstract:

The article presents aspects related to using the Finite Strip Method in obtaining the static response (static displacement or static moments) of the road deck bridges, having various forms (rectangular, oblique or trapezoidal plates), a constant or variable thickness and various boundary conditions.

The method have a good apply to the deck bridges, modeled by orthotropic and isotropic plates and the results are very similar to the ones obtained through the analytical calculus.

KEYWORDS : Plate, Strip, Deck of bridge, Finite Strip Method , Matrix ,Static displacement, bending moment

1. INTRODUCTION

The calculus of the oblique and trapezoidal decks bridges has been a problem for engineers. In the current design practice, a simplified calculus is admitted in these situations. A detailed static response in different points of the deck bridge can be obtained by using the different calculus programs known. The existent programs generally use the Finite Element Method (FEM), although problems may appear while using these programs in the case of dividing into finite elements and establishing the boundary conditions.

By using the Finite Strip method for obtaining the static response of the decks bridges, we come across some advantages such as:

- a lower number of elements the plate is divided into;
- due to the lower number of elements, there are lower dimensions of the rigidity matrix, resulting in a shorter duration of the program execution;
- the numerical results obtained are very close to those obtained through the analytical study.

2. THE THEORETICAL PRESENTATION OF THE PROCEDURE

The plate is considered to be modeled as an assembly of narrow strips (assimilated to the bars) parallel to the y axis. These finite strips technique respect the boundary conditions of the plate in both directions.

If the plate does not have a regular form the strips models the plate only approximately . The accuracy of the results is conditioned by the greater number of strips. Plates of constant or variable thickness may be analyzed by means of this method on condition that the thickness of the strip is constant . The thickness may vary from a strip to another.

The length of the strips may be constant (rectangular or oblique plates – see Figure 1 and 2) or variable (for trapeze or triangular plates).

Based on the energy principles of structural mechanics , a conservative material system operated by a conservative system of forces is in equilibrium if the total potential energy is stationary for the boundary conditions of the system.

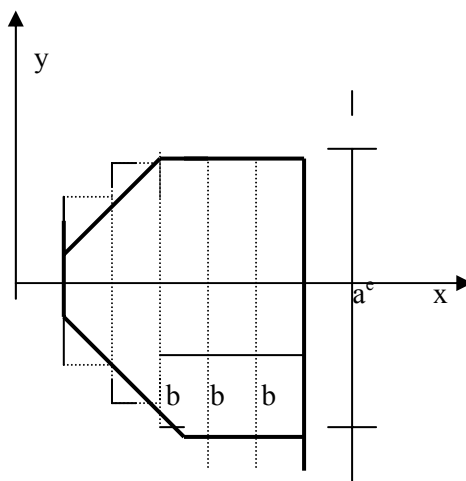


Figure 1 Mesh divisions of polygonal plates

$$\frac{\partial V}{\partial d} = 0$$

where

$$V = U - L \tag{1}$$

V – the total potential energy

U – the deformation energy of the plate

L – the work of external forces

d - generalized displacements

The deformation energy of a strip has the following form:

$$U^e = \frac{1}{2} \iint (\boldsymbol{\kappa}^e)^T \mathbf{D} (\boldsymbol{\kappa}^e) dx dy \quad (2)$$

$\boldsymbol{\kappa}^e$ – is the matrix of curvature and has the following shape:

$$\boldsymbol{\kappa} = \begin{vmatrix} -w_{,11} \\ -w_{,22} \\ 2w_{,12} \end{vmatrix}$$

\mathbf{D} - is the elasticity matrix and has the following shape:

$$\mathbf{D} = \begin{vmatrix} D_{11} & \nu D_{22} & 0 \\ \nu D_{22} & D_{22} & 0 \\ 0 & 0 & D_{12} \end{vmatrix} \quad (3)$$

$$\begin{aligned} D_{11} &= E_1 h^3 / 12 (1 - \nu_1 \nu_2) & D_{22} &= E_2 h^3 / 12 (1 - \nu_1 \nu_2) \\ D_{12} &= G h^3 / 12 (1 - \nu_1 \nu_2) \end{aligned} \quad (4)$$

For the isotropic plate $\nu_1 = \nu_2 = \nu$ and $D_{11} = D_{22} = D = E h^3 / 12 (1 - \nu^2)$
and $D_{12} = D (1 - \nu) / 2$

Applying Ritz's variation principle, the expression of the displacement is :

$$W^{(e)} = \sum_{i=1}^n \sum_{j=1}^m d_{ij}^e \cdot \Phi_i(x) \cdot F_j(y) \quad (5)$$

where :

$\Phi_i(x)$ – functions chosen to ensure the compatibility of linear displacements and rotations

across nodal lines;

$F_j(y)$ - functions chosen to ensure the edge conditions of the strip (Rayleigh functions)

d_{ij}^e - the generalized displacements of the e^{th} strip

The expression number (5) may be written in a matrix form as :

$$(6) \quad \mathbf{W}^{(e)} = \mathbf{C} \cdot \mathbf{d}^e = [\Phi_{F_1} \ \Phi_{F_2} \ \dots \ \Phi_{F_n}] \begin{vmatrix} \mathbf{d}_1^e \\ \mathbf{d}_2^e \\ \cdot \\ \cdot \\ \cdot \\ \mathbf{d}_n^e \end{vmatrix}$$

Where

$$(7) \quad \Phi = [\Phi_1 \ \Phi_2 \ \dots \ \Phi_n]$$

$$(8) \quad \mathbf{d}_{ji}^e = [d_{j1}^e \ d_{j2}^e \ d_{j3}^e \ \dots \ d_{jn/2}^e \ d_{jn/2+1}^e \ \dots \ d_{jn}^e]$$

the first n/2 elements are generalized displacements (rotations and displacements) associated with the border line on the left of the strip and the second n/2 are associated with the border line on the right of the strip .

By replacing the (6) and (5) relationships in (2) and observing that :

$$(9) \quad \mathbf{B}_j^e = \begin{vmatrix} -(\Phi_{F_j})_{,11} \\ -(\Phi_{F_j})_{,22} \\ 2(\Phi_{F_j})_{,12} \end{vmatrix}$$

The expression of the strip stiffness matrix can be written :

$$(10) \quad \mathbf{K}_{jk}^{(e)} = \iint (\mathbf{B}_j^e)^T \mathbf{D} (\mathbf{B}_k^e) dx dy$$

In an extended form, this expression may be written as :

$$(11) \quad \mathbf{K}^e = \begin{vmatrix} \mathbf{K}_{11}^e & \mathbf{K}_{12}^e & \dots & \mathbf{K}_{1n}^e \\ \mathbf{K}_{21}^e & \mathbf{K}_{22}^e & \dots & \mathbf{K}_{2n}^e \\ \dots & \dots & \dots & \dots \\ \mathbf{K}_{m1}^e & \mathbf{K}_{m2}^e & \dots & \mathbf{K}_{mm}^e \end{vmatrix}$$

The strip stiffness matrix is symmetric and has 4n order. The matrix (\mathbf{K}^e) can be partitioned in the following way :

$$\mathbf{K}^e = \begin{vmatrix} \mathbf{K}_{SS} & \mathbf{K}_{SD} \\ \mathbf{K}_{DS} & \mathbf{K}_{DD} \end{vmatrix}$$

Considering the stationary condition of the total potential energy, with respect the generalized displacements, the expression (17) takes the form of their following matriceal equation:

$$\mathbf{Kd} - (\mathbf{S}_p + \mathbf{S}_q) = 0 \tag{18}$$

and

$$\mathbf{d} = \mathbf{K}^{-1}(\mathbf{S}_p + \mathbf{S}_q)$$

The displacement of a point, is obtained from (5) by using generalized displacements and the functions F_j and Φ_i .

3. NUMERICAL RESULTS

A computer program has been elaborated in VISUAL BASIC, based on the theory presented above. This program computes the static displacements of the plates with several geometrical forms and several boundary conditions. The computed values are compared with those obtained by Timosenko [4]

The expressions of the approximating functions from the relation (5) and used in this computation are :

$$F_j(y) = \sin(j\pi y/a)$$

$$\Phi_1(x) = 1 - 3x^2/b^2 + 2x^3/b^3$$

$$\Phi_2(x) = x - 2x^2/b + x^3/b^2$$

$$\Phi_3(x) = 3x^2/b^2 - 2x^3/b^3$$

$$\Phi_4(x) = x^3/b^2 - x^2/b$$

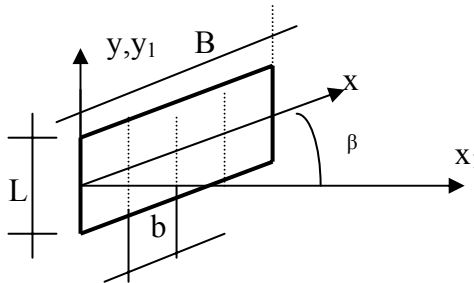


Figure 2 Finite strip mesh of the oblique plates

and

$$x = \frac{x_1}{\cos\beta}, \quad y = y_1 - x_1 \tan\beta$$

For isotropic plate, simple supported, and one force $P=1$ acting in middle of the plate, the parameters of the static displacements are presented in the following table:

Nr.punct	α cf [MFF]	α cf [4]	α cf [MFF]	α cf [4]
	(L/B=1.0)	(L/B = 1.0)	(L/B=0.5)	(L/B=0.5)
1	2 0.0113	3 0.0116	4 0.0163	5 0.0165

The static displacement is given by $w = \alpha PL^2/D$

3. CONCLUSIONS

The numerical method presented in the paper has the advantage of a low number of strips, which leads to a small number of equations and small width of the band. By using this method, the author elaborated program to compute the static displacements, vibration forms and the influence surfaces of the isotropic and orthotropic polygonal plates with different boundary conditions.

References:

1. BARSAN, G.M. – Vibratiile si stabilitatea placilor oblice si trapezoidale izotrope si ortotrope de grosime constanta si variabila – teza de doctorat 1971
2. GAVRIS, O - Modelarea placilor pentru analiza dinamica a acestora Metoda fasiilor finite – referat doctorat 1996
3. AVRAM, C s.a - Structuri din beton armat. Editura academiei 1984.
4. TIMOSHENKO s.a – Teoria plăcilor plane și curbe .Editura tehnică Bucuresti 1968

FATIGUE DESIGN CONSIDERATIONS OF THE STEEL PLATE GIRDERS

Ștefan I. Guțiu, Petru Moga and Cătălin Moga

*Faculty of Civil Engineering, Technical University of Cluj-Napoca, 400020, Romania,
Stefan.Gutiu@cfdp.utcluj.ro, Petru.Moga@cfdp.utcluj.ro, Catalin.Moga@bmt.utcluj.ro*

Summary

This paper presents the fatigue checking methodology of the steel bridge members according to Romanian norm SR 1911-98 and EC 3.

A comparative analysis regarding the fatigue checking of the main girders of a 30 m span steel railway bridge is made.

The concluding remarks and observations are useful in the design activity of this type of structures.

KEYWORDS: steel bridge; fatigue checking methodology; Eurocode 3; Romanian codes

1. INTRODUCTION

Composite steel-concrete bridge superstructures can be designed using allowable stress method (ASM) or ultimate limit states method (ULS).

In our country nowadays ASM is used because the composite structures are considered as being part of the steel bridges and the main elements are built-up of steel.

The European norms (EC 3; EC 4) are based on the ULS, these norms being in the process of implementation in our country.

This paper presents the fatigue verification methodology of the steel bridges according to Romanian norm SR 1911-98 and Eurocode 3.

A comparative analysis regarding the fatigue checking of the main girder of a 30 m span steel railway bridge is made here.

The concluding remarks and observations are useful in the safety and efficient design of this type of structures.

2. FATIGUE VERIFICATION OF THE RAILWAY STEEL BRIDGES

2.1. Fatigue verification according to Romanian norm SR 1911-98

The fatigue verification is made for the 1st Group of loads for rail traffic taking into account the dynamic factor.

The requirements of [11] regarding the fatigue phenomenon can be applied only for the design loading model T8.5. For other loading models the design procedures have been elaborated.

The fatigue verification of the members and joints is made in accordance with point 8.3.6. of [11] for every strength with the relations:

$$\Delta\sigma = \frac{1}{\Phi} (\psi \cdot \sigma_{\max, T8,5} - \psi \cdot \sigma_{\min, T8,5}) \leq \Delta\sigma_{Ra} ; \quad (1a)$$

$$\Delta\tau = \frac{1}{\Phi} (\psi \cdot \tau_{\max, T8,5} - \psi \cdot \tau_{\min, T8,5}) \leq \Delta\tau_{Ra} , \quad (1b)$$

in which:

$$\Phi = \Phi_{1,i} \cdot \Phi_2 \cdot \Phi_3 \quad (2)$$

The following influences are taken into account:

$\Phi_{1,i}$ - takes into account the characteristic member length "l", the static system and the detail category, Table 21, [11];

Φ_2 - takes into account the influence of the design loading meeting frequency on the structure with more than one track, Table 22, [11];

Φ_3 - takes into account the loading volume of the rail track, given by the total train load on year.

$\sigma_{\min, T8,5}$; $\sigma_{\max, T8,5}$; $\tau_{\min, T8,5}$; $\tau_{\max, T8,5}$ - are the maximum and minimum values of the normal strength and of the shear stress produced by the design load model T8,5;

$\Delta\sigma_{Ra}$, $\Delta\tau_{Ra}$ - are the allowable stress ranges for the fatigue verification given in [11] function of the asymmetry loading cycle factors given by:

$$R_{\sigma} = \frac{\sigma_g + \frac{1}{\phi} \cdot \Psi \cdot \sigma_{\min, T8,5}}{\sigma_g + \frac{1}{\phi} \cdot \Psi \cdot \sigma_{\max, T8,5}}; \quad R_{\tau} = \frac{\tau_g + \frac{1}{\phi} \cdot \Psi \cdot \tau_{\min, T8,5}}{\tau_g + \frac{1}{\phi} \cdot \Psi \cdot \tau_{\max, T8,5}} \quad (3a,b)$$

where σ_g and τ_g are the normal strength and shear stress produced by the permanent actions.

The fatigue verification is made for the most unfavorable combination of the normal stresses according to point 8.3.10. of [11], with the relation:

$$\left(\frac{\sigma_x}{\sigma_{xRa}} \right)^2 + \left(\frac{\sigma_y}{\sigma_{yRa}} \right)^2 - \frac{0,8 \cdot \sigma_x \cdot \sigma_y}{\sigma_{xRa} \cdot \sigma_{yRa}} + \left(\frac{\tau}{\tau_{Ra}} \right)^2 \leq 1 \quad (4)$$

where:

σ_x , σ_y are the normal stresses on x and respective y direction and τ is the shear stress in the point where the fatigue verification is made;

σ_{xRa} , σ_{yRa} and τ_{gRa} are the maximum allowable stresses, function of the detail category and asymmetry loading cycle factors, Tables 16, 17, 19 and 13 of [11].

2.2. Fatigue verification according to EC 3-1-9 and EC 3-2

Structural members shall be designed for fatigue such that there is an acceptable level of probability that their performance will be satisfactory throughout their design life.

For the fatigue verification of the railway bridges the characteristic values of the Load Model 71 (LM 71) are used [7], including the dynamic factor Φ_2 (relation 6.4. [7]) and according to the traffic data given by the competent authorities.

Fatigue verification procedure

According to [8] the following conditions shall be verified:

Stress ranges:

$$\Delta\sigma \leq 1.5 \cdot f_y \quad (5a)$$

$$\Delta\tau \leq 1.5 \cdot f_y / \sqrt{3} \quad (5b)$$

The conditions:

$$\gamma_{FF} \cdot \Delta\sigma_{E2} \leq \frac{\Delta\sigma_C}{\gamma_{Mf}} \quad \text{and} \quad \gamma_{FF} \cdot \Delta\tau_{E2} \leq \frac{\Delta\tau_C}{\gamma_{Mf}} \quad (6a,b)$$

The combined effect of the normal stress ranges and of the shear stress ranges:

$$\left[\frac{\gamma_{FF} \cdot \Delta\sigma_{E2}}{\Delta\sigma_C / \gamma_{Mf}} \right]^3 + \left[\frac{\gamma_{FF} \cdot \Delta\tau_{E2}}{\Delta\tau_C / \gamma_{Mf}} \right]^5 \leq 1 \quad (7)$$

In these relations:

$\Delta\sigma_C$, $\Delta\tau_C$ - the reference values of the fatigue strengths at 2 million cycles, for the relevant detail category, given in Tables 8.1...8.10, [8];

$\Delta\sigma_{E2}$ - equivalent constant amplitude stress range related to 2 million cycles:

$$\Delta\sigma_{E2} = \lambda \cdot \phi_2 \cdot \Delta\sigma_p \quad (8)$$

λ is damage equivalent factor. For railway bridges with a span up to 100 m, λ should be determined as follows:

$$\lambda = \lambda_1 \cdot \lambda_2 \cdot \lambda_3 \cdot \lambda_4 \quad \text{but} \quad \lambda \leq \lambda_{\max} \quad (9)$$

λ_1 is the factor for the damage effect of traffic and depends on the length of the influence line, Tables 9.3 and 9.4, [9];

λ_2 is the factor for the traffic volume, Table 9.5 [9];

λ_3 is the factor for the design life of the bridge, Table 9.6, [9];

λ_4 is the factor when the structural element is loaded by more than one track, Table 9.7 [9];

$\lambda_{\max} = 1.4$ (rel. 9.15, [9]);

$\Delta\sigma_p = |\sigma_{p,\max} - \sigma_{p,\min}|$ is the reference value of the stress range;

$\sigma_{p,\max}$ and $\sigma_{p,\min}$ are the maximum and minimum normal stresses calculated for the respective detail, using Load Model 71;

ϕ_2 is the dynamic factor, evaluated with relation 6.4, [7];

γ_{FF} is the partial factor for equivalent constant amplitude stress ranges;

γ_{Mf} is the partial factor for fatigue strength, Table 3.1, [8].

3. COMPARATIVE ANALYSIS: SR 1911-98 – EUROCODE 3

The analyzed structure – a steel railway bridge, have been designed in the book [3], using the allowable stress method in accordance with the Romanian norm SR 1911-98, for the design load train model T8.5.

The transversal section of the bridge and main girder are presented in Figure 1.

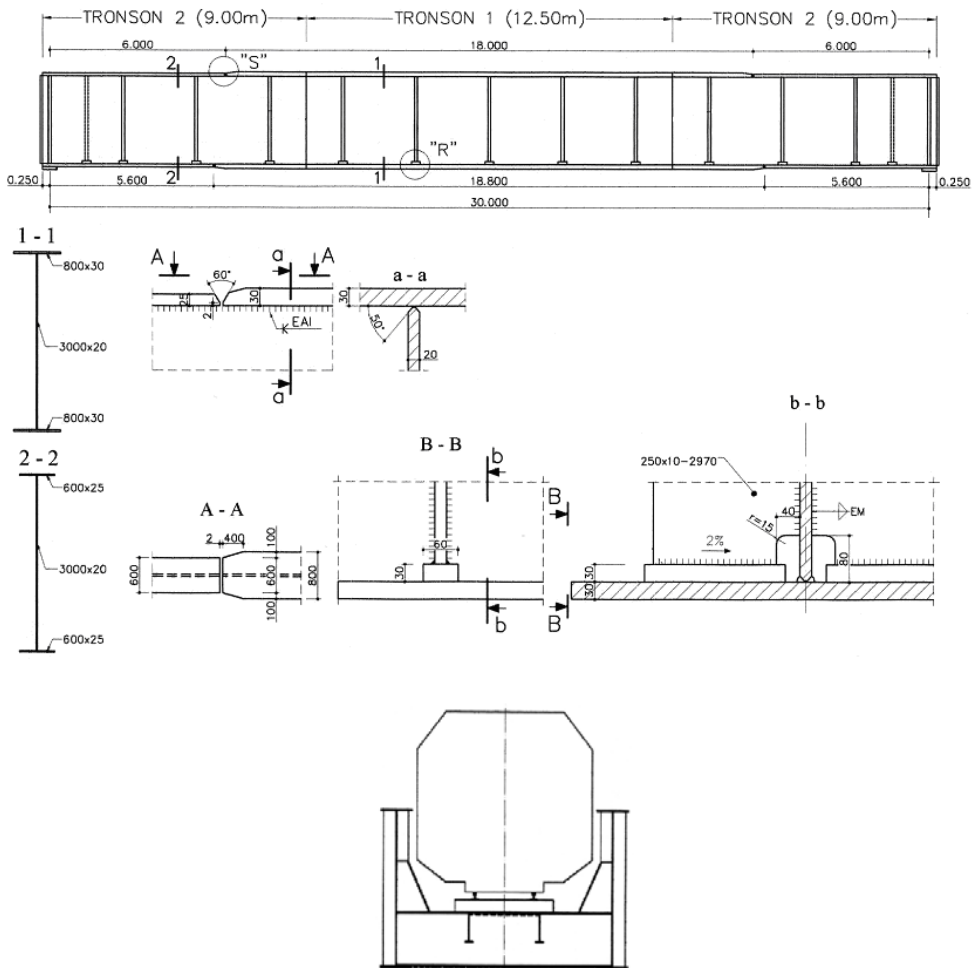


Figure 1. Transversal section of the bridge and main girder

Making the fatigue verification of the join weld between flange and web of the main girders, in accordance with Romanian norm SR 1911-98 and European norms EN 1993-1-9 and EN 1993-2, it can be concluded that the checking according to Romanian norm is more severe comparative with Eurocodes.

So according to [11] $\Delta\sigma$, is between 64% to 70% of $\Delta\sigma_{Ra}$ and according to [8] and [9], $\gamma_{FF} \cdot \Delta\sigma_{E2}$ is between 39% to 43% of $\Delta\sigma_C / \gamma_{Mf}$.

Also the influence of the normal stresses, evaluated using Romanian Load Model T8.5 and the European Load Model 71 as well as the influence of the dynamic factors and of the parameters λ and $1/\phi$ have been analyzed.

Figure 2 presents the bending moments on the simple supported main girder for different design load models.

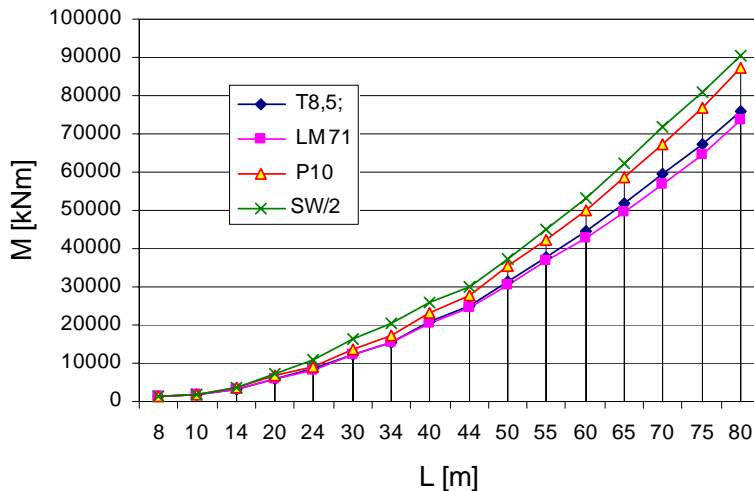


Figure 2. Bending moments on the simple supported main girder

Figure 3 presents the dynamic factors evaluated in accordance with Romanian norm –STAS 1489-78 and EC 1-2:

STAS 1489-78:

For $L > 10$ m

$$\psi = 1,05 + \frac{25}{40 + L} \geq 1,20 \text{ - unwelded rails} \quad (10a)$$

$$\psi = 1,10 + \frac{17}{35 + L} \geq 1,20 \text{ - welded rails} \quad (10b)$$

For $L \leq 10$ m

$$\psi = 1,55 + \frac{10 - L}{20} \tag{11}$$

EC I-2 (L_ϕ -determinant length, Table 6.2,[7]):

$$1 < \phi_2 = \frac{1,44}{\sqrt{L_\phi} - 0,2} + 0,82 < 1,67 \text{ - for carefully maintained track} \tag{12a}$$

$$1 < \phi_3 = \frac{2,16}{\sqrt{L_\phi} - 0,2} + 0,73 < 2 \text{ - for track with standard maintenance.} \tag{12b}$$

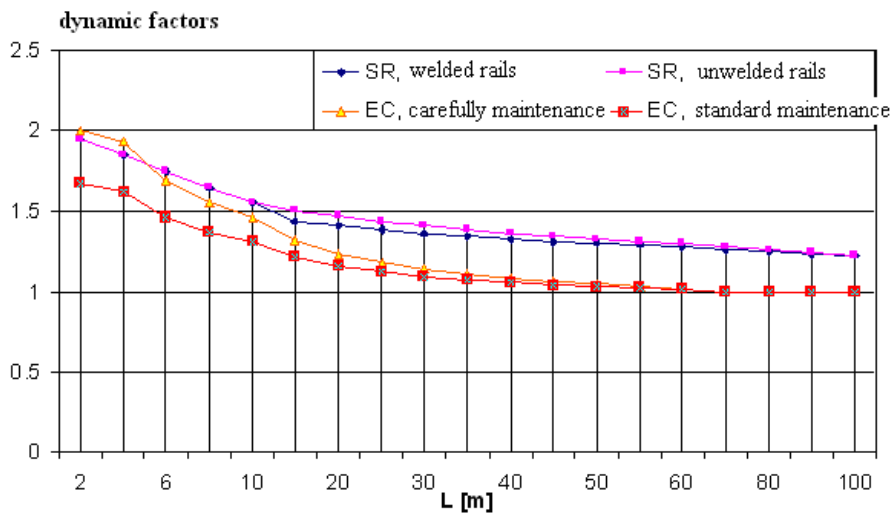


Figure 3. Dynamic factors

Beginning with a more than 25 m span, the value of the dynamic factor ϕ , represents about 80% of the ψ value, For determinant length more than 70 m, the values of the dynamic factors evaluated in accordance with EN 1991-2 are equal with 1.

Figure 4 presents the values of the bending moments, affected by the dynamic factor, evaluated according to Romanian norms and with Euronormes. It can be observed that $\phi_2 \cdot M_{LM71}$ represents about 80% of $\psi \cdot M_{T8.5}$ and implicitly $\phi_2 \cdot \Delta\sigma_p \cong 0.80 \cdot \psi \cdot \sigma_{\max.T8.5}$.

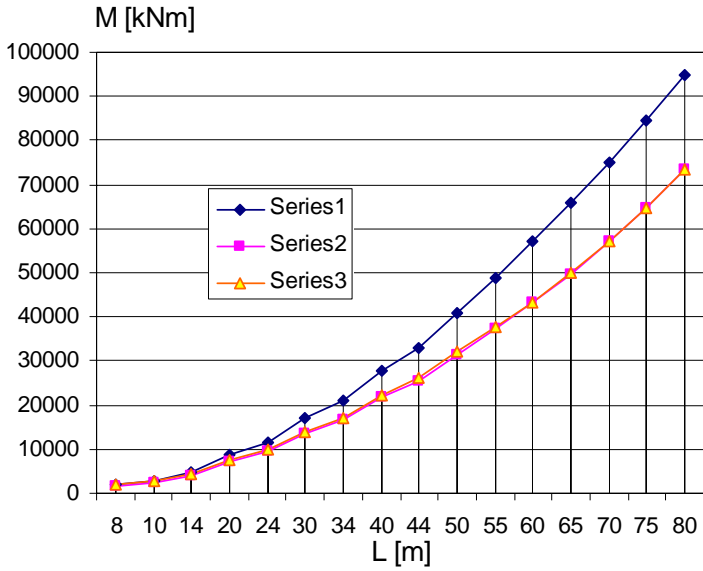


Figure 4. Bending moments, affected by the dynamic factor

Series 1: $\psi \cdot M_{T8,5}$; Series 2: $\phi_2 \cdot M_{LM71}$; Series 3: $\phi_3 \cdot M_{LM71}$

Figure 5 presents comparatively the values of λ_1 and $1/\phi_{1,i}$; can be observed that the values of λ_1 represents about 85% of $1/\phi_{1,i}$.

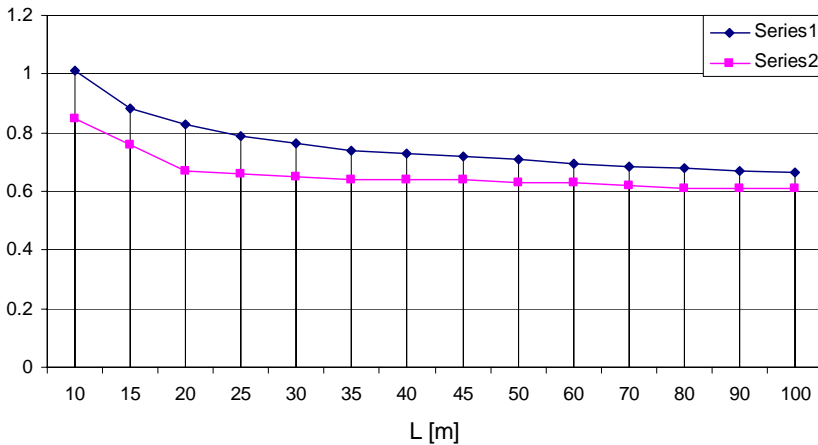


Figure 5. Series 1: $1/\phi_{1,i}$; Series 2: λ_1

3. CONCLUSIONS

By analyzing the obtained results it can be concluded that using Romanian norms, it results a super dimensioning of the bridge main girders resulted from the fatigue design, respectively:

$$\Delta\sigma_{E2} \cong (85\% \cdot 1/\phi) \cdot (80\% \cdot \psi \cdot \sigma_{\max,T8,5}) = 68\% \cdot \Delta\sigma$$

The required fatigue life should be achieved through design for fatigue and by serviceability checks.

References

1. Guțiu, I., Șt: Analiza capacității portante a grinzilor principale de poduri prin aplicarea normelor române și a normelor europene de proiectare. Teza de doctorat, UTCN 2007
2. Moga, P., Păcurar, V., Guțiu, I.- Șt., Moga, C : *Construcții și poduri metalice. Aplicare euronorme*. UTPRESS, 2007, ISBN 978-973-662-321-9
3. Moga, P., Păcurar, V., Guțiu, I.- Șt., Moga, C: *Poduri metalice. Suprastructură pod de cale ferată*. UT PRES, 2007, ISBN 978-973-662-268-7.
4. Moga, P., Păcurar, V., Guțiu, I.- Șt., Moga, C: *Calculul elementelor metalice. Norme române – Eurocode 3*, UTPRES, 2006, ISBN 973-662-205-3
5. Bolduș, D., Bolduș, B., Băncilă, R.: Analysis of Dynamic Behaviour under Traffic Loads of a Strengthened Old Steel Bridges, *5th International Conference of Bridges across the Danube 2004* “Bridges in Danube Basin”, Novi Sad, 2004
6. Băncilă, R., Petzek, E.: Rehabilitation of Steel Bridges in Romania. *Proceedings of the 6th Japanese German Bridge Symposium*, Munich 2005.
7. *** prEN1991-2. EUROCODE 1. *Actions on structures - Part 2: Traffic loads on bridges*, 2002
8. *** prEN1993-1-9. EUROCODE 3. *Design of steel structures. Part 1-9: Fatigue*. 2003
9. *** prEN1993-2. EUROCODE 3. *Design of steel structures. Part 2: Steel bridges*. 2005
10. *** STAS 3220-89. *Poduri de cale ferată. Convoaie tip*
11. *** SR 1911-98. *Poduri metalice de cale ferată. Prescripții de proiectare*
12. [12] *** NP 104-05: Normativ pentru proiectarea podurilor din beton și metal. Suprastructuri pentru poduri de șosea, cale ferată și pietonale, precomprimate exterior. *Buletinul construcțiilor*, vol. 10-13/2005
13. *** STAS 1489-78. *Poduri de cale ferată. Acțiuni*

Photogrammetric measurement of deformations during the load test of brick vault

Petr Kalvoda, Miroslava Suchá, Josef Podstavek and Jiří Vondrák¹

¹Department of Geodesy, University of Technology, Brno, 602 00, Czech Republic,
vondrak.j@fce.vutbr.cz

Summary

The area of constructional element strengthening and subsequently strengthening of construction has been researched many times. These techniques lead so far to dimensional redesigning of the construction. Usage of the new technological procedures and especially utilisation of new materials allows keeping existing dimensions of the construction. This project is part of research project focused on additional strengthening of engineering construction particularly on monolithic concrete and brick construction. Integral part of project is quantitative determine of deformation, which are observed during the load test of tested constructions. Few methods where used parallel together: tensiometric measurement, electronic tacheometry, very precise levelling and digital method of close range photogrammetry. The method of close range photogrammetry was used again as a complementary method just for data comparison and for photogrammetric technology improvement in application demanding high precision.

KEYWORDS: Photogrammetric measurement, deformations, load test.

1. INTRODUCTION

Whole experiment is part of research project, which is intent on additionally strengthening of building constructions. In our project, we deal with quantitative determining the deformations of testing constructions during the load test. For this purpose were currently used following methods: tensiometer wire with potentiometers, polar method, precise levelling and method of close range photogrammetry.



Figure 1. Brick vault

Measurement marks

Before the experiment has started, it was decided that processing would be run on two different photogrammetric software: Orpheus 3.2.1. and PhotoModeler 4.0. This decision has radical effect on selection of measurement marks. Software PhotoModeler provides automatic subpixel measurement, but software Orpheus not (at least not the version we have at our institute). For this reason, two types of measurement marks were used. The first type is suitable for subpixel measurement and second type is suitable for manual measurement (fig.2). For manual measurement were used black steel circular targets with diameter 28 mm with centric hole (diameter 2.5 mm). On both sides of vault (front – side „A“, back – „B“) was the same configuration of targets fig. 3.

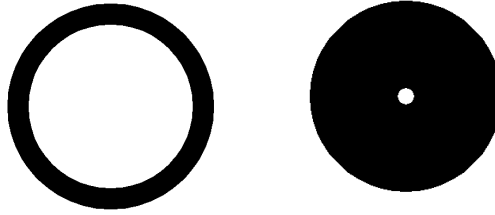


Figure 2. Types of measurement marks

2. OPTION AND MEASURING OF CONTROL POINTS, IMAGING OF THE VAULT CURVE

There were stabilized 23 control points on the vault. Due to use of two target types, there is a great number of control points. The control points were determined by polar method, for distance measurement was used reflecting foil, which was placed on targets. Images were taken by calibrated camera Nikon Coolpix 5000 with resolution 5 Mpix. Method of multi-image photogrammetry was used and images were taken from distance 3-4 m.

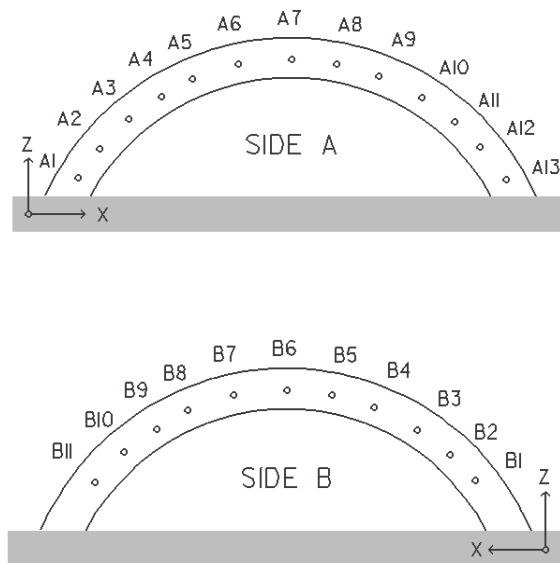


Figure 3. Orientation of line coordinate axis, placement and marking of points

3. TECHNIQUES OF THE PROCESSING

Local coordination system was designed for processing, axis X along console of the vault, axis Z vertically and axis Y perpendicular to X and Z. Deformations in direction of axis Y were not evaluated. Coordination system was designed, so that most of the errors affect coordinate Y, which was not the subject of the measurement.

Photogrammetrical measurement consists from comparing X and Z coordinates, which are computed in individual load states with basic zero state (without loading). Images were taken in all load states. For processing, images were chosen so that all points were at least on three images.

First processing phase consists of computation of spatial coordinates in all load states by means of software PhotoModeler 4.0. Precisions 0.6 mm, 1 mm, 0.5 mm were determined to individual coordinates X, Y, Z. The goal is to use strictly the automatic subpixel measurement, which PhotoModeler provides. For purpose of the polar method, three targets on both sides of the vault were exchanged by the other type of the targets. The new targets were improper for automatic subpixel measurement and they derogated the results. This operation was not consulted with group of photogrameters. During the second phase of processing we dealt with computing by means of the software Orpheus 3.2.1. Input precision of the control points was kept the same as precision in first phase. Spatial coordinates of the zero and tenth load states were computed in this software and only manual measurement was possible to use.

4. COMPARISON OF THE DETERMINATED DEFORMATIONS

Differences in X coordinate of individual points between shifts, which are determined by photogrammetry (with usage of software PhotoModeler) and polar method in all load states, are presented in table 1. Manual measurement was used for all of the points as it was explained above. Standard deviations of these points did not exceed value 1.5 mm.

Differences between shifts in Z coordinate, which was determined by photogrammetry (using PhotoModeler again) and precise leveling, are presented in table 2.

Table 1. Comparison of shifts, which are determined by photogrammetry and polar method

ΔX [mm]							
Method	Point	Shifts in the load states					Average deviation [mm]
		2	4	6	8	10	
Photogrammetry	A4	1.3	1.0	-0.1	-2.6	-8.8	
Polar method	A4	-0.3	-0.7	-2.0	-3.6	-6.6	1.7
Photogrammetry	A7		0.2	0.3	0.0	-1.2	
Polar method	A7	0.1	0.0	0.3	0.3	1.6	0.8
Photogrammetry	A10	1.1	1.0	2.8	6.0	8.1	
Polar method	A10	0.3	0.7	2.2	4.0	10.9	1.3
Photogrammetry	B3	0.4	-2.2	-1.4	-4.6	-9.4	
Polar method	B3	-0.3	-0.7	-2.2	-3.9	-7.3	1.2
Photogrammetry	B6	-0.3	-0.2	0.6	0.2	-1.0	
Polar method	B6	0.0	0.0	0.0	0.0	1.3	0.7
Photogrammetry	B9	-1.2	1.4	2.5	4.4	8.5	
Polar method	B9	0.2	0.7	2.4	4.2	11.1	1.0

Table 2. Comparison of shifts, which are determined by photogrammetry and precise levelling

ΔZ [mm]							
Method	Point	Shifts in the load states					Average deviation [mm]
		2	4	6	8	10	
Photogrammetry	A4	1.1	2.3	4.4	5.9	6.7	
Precise levelling	A4	0.1	0.4	2.3	4.5	8.9	1.7
Photogrammetry	A7		-2.9	-3.5	-5.2	-19.3	
Precise levelling	A7	-0.8	-1.9	-4.9	-8.1	-17.4	1.8
Photogrammetry	A10	1.6	2.7	4.7	7.3	14.3	
Precise levelling	A10	0.1	0.6	2.5	4.8	13.8	1.8
Photogrammetry	B3	1.1	3.1	3.5	5.5	6.7	
Precise levelling	B3	0.2	0.6	2.5	4.6	9.0	1.5
Photogrammetry	B6	-1.6	-2.3	-2.9	-5.3	-20.1	
Precise levelling	B6	-0.8	-1.8	-4.8	-7.9	-17.4	1.7
Photogrammetry	B9	0.6	2.9	3.3	5.0	9.8	
Precise levelling	B9	0.1	0.7	2.3	4.4	12.8	1.5

Comparison of the shifts, which were acquired by precise leveling (PL) and shifts acquired by photogrammetry, (processed in software PhotoModeler or

software Orpheus), are presented in table 3. It is evident, that by Orpheus were achieved results much closer to values achieved by precise levelling, than results achieved by the PhotoModeler. Standard deviation in the Z coordinate didn't exceed value 0.8 mm while using Orpheus.

Table 3. Differences between shifts from precise levelling, from PhotoModeler and form Orpheus in the Z coordinate.

ΔZ [mm]					
Point	PL	PhotoM	PL-PhotoM	Orpheus	PL-Orpheus
A4	8,9	6,7	2,2	7,5	1,4
A7	-17,4	-19,3	1,9	-18,9	1,5
A10	13,8	14,3	-0,5	12,7	1,1
B3	9,0	6,7	2,3	8,1	0,9
B6	-17,4	-20,1	2,7	-17,4	0,0
B9	12,8	9,8	3,0	14,4	-1,7
Average deviation [mm]		2,1		1,1	

The same comparison as in the table 3 is presented in the table 4, but for X coordinate. The standard deviation of the X coordinate, with usage Orpheus, did not exceed value 1.0 mm.

Table 4. Differences between shifts from polar method, from PhotoModeler and from Orpheus in the X coordinate.

ΔX [mm]					
Point	PM	PhotoM	PM-PhotoM	Orpheus	PM-Orpheus
A4	-6.6	-8.8	2,2	-5,2	-1,4
A7	1.6	-1.2	2,8	1,2	0,4
A10	10.9	8.1	2,8	9,7	1,2
B3	-7.3	-9.4	2,1	-7,7	0,4
B6	1.3	-1.0	2,3	0,5	0,8
B9	11.1	8.5	2,6	11,2	-0,1
Average deviation [mm]		2.5		0.7	

5. CONCLUSIONS

The goal of our experiment was to determine shifts of the individual points with standard deviation under 1 mm by software PhotoModeler and

Orpheus. We also compared results, gained from PhotoModeler and Orpheus, with results achieved from precise leveling and polar method. We expected that better results would be achieved by usage of automatic subpixel measurement in the PhotoModeler. In spite of that, we could not keep strict usage of automatic subpixel measurement and that is why the shift results are worse. The standard deviation of the points exceeded value 1 mm only when the manual measurement had to be use. The greatest difference between shifts from PhotoModeler and from precise leveling in the Z-coordinate is 3.0 mm. Amazingly, better results were achieved, while using Orpheus, which allows only manual measurement. The standard deviation didn't exceed value 1 mm for all the points. Final shifts in the Z-coordinate differed, from results achieved by precise leveling, not more than 1.7 mm. Significantly better results are given especially when one has the possibility to select individual parameters and characteristics of the precision. At present, only zero and tenth load state is processed by the software Orpheus, but the experiment is still running. It is evident, that using photogrammetry leads to less accurate results in comparison with results from precise leveling. On the other hand, only photogrammetry method gives information about process of deformation in the whole extend of the vaults curve.

References

1. PODSTAVEK, J. *Fotogrammetrické měření deformací panelů*, Aktuální problémy fotogrammetrie a DPZ, Praha 2003 (in Czech)
2. PODSTAVEK, J. SUCHA, M. KALVODA, P. *Fotogrammetrické sledování deformací při destruktivní zátěžové zkoušce cihelné klenby*, Aktuální problémy fotogrammetrie a DPZ, Praha 2004 (in Czech)
3. PODSTAVEK, J. MACHOTKA, R., VONDRÁK, J. *Integration of Orientation Systems and Cameras in Photogrammetry, tests and calibrations*, ISBN 86-85079-01-2, Republic Geodetic Authority, Republic of Serbia, Belgrade, Serbia, 2006
4. SUCHÁ M., KALVODA P., BRKL L., *Fotogrammetrické sledování deformací při zatěžovací zkoušce*, Sborník konference Juniorstav 2005, Brno 2005 (in Czech)

CONSIDERATIONS REGARDING THE REBUILDING OF A PRESTRESSED CONCRETE BRIDGE DAMAGED BY HIGH FLOODS

Eng. Iulian Mata

S.C. RUTIER-CONEX XXI BACAU, ROMANIA, rutierxxi@yahoo.com

1. INTRODUCTION

The year 2005 was certainly meteorologically different from the others in the last decades, for our country as well as for the entire European continent. The quantities of precipitations recorded have exceeded by far the average flow of the past years, leading to an increase in the water flows. This conclusion was reached at not only at the end of hydrological measurements but also by analysing the effects produced upon the communication ways and upon the human communities.

According to the report on the effects of floods worked out by the Minister of Environment and Water Administration, the water marks on the water courses were flooded during almost all the months of the year, the most significant floods being registered within the span of April-September 2005, when high floods took place on most of the rivers, some with historic water discharges that spread over extended areas and led to notable human losses of lives and material damages.

Although during the last 40-50 years there have been significant high floods in the majority of the hydrographic basins, never before, during the last 100 years, have the high floods spread over such an extended period of time (from February to September). Also, the previous high floods, the most significant of which being those from 1970 and 1975, have spread over more restricted areas than those that took place in 2005.

The impact on the substructure was serious, registering damages to 9860.63 km of county and district roads, 560.4 km of national roads, 2465.84 km locality streets, 2644.9 km forest roads, 9113 bridges and footbridges, 23.8 km railroad, water supply networks, electric and telephone wire networks.

The counties most affected, in 2005, by floods and dangerous meteorological phenomena were: Vrancea, Buzău, Timis, Caraş-Severin, Bacău, Teleorman, Mehedinţi, Olt, Galaţi, Botoşani, Dolj, Suceava, Satu Mare.

In Buzău, the county road DJ102B crosses over the Basca Chiojdului River by a prestressed concrete bridge situated 25+569 km, on the territory of Calvini rural district close to Băscenii de Sus village and constitutes the link between the localities Vălenii de Munte (Prahova county) – Băscenii de Sus – Brăieşti (Buzău

county), as well as the access to the county road DJ 120 L Cătina-Chiojdu-Lim (Buzău county) or the national road DN10, Buzău-Nehoiu-Braşov.

In the wake of significant precipitations during the formerly described time span, the construction suffered major damages that put it out of use. Due to ceasing traffic in this point of the road, circulation was deviated on a roundabout way about 30 km long.

2. A DESCRIPTION OF THE BRIDGE AND OF THE EVENTS THAT LED TO ITS DAMAGING

The existing bridge was built in 1972 with a total length between the ends of the wing walls $L=6 \times 21 \text{ m} + 2 \times 3.5 \text{ m} = 133.0 \text{ m}$, the superstructure of each opening being made of 4 precast, prestressed beams, with the height of 1.45 m, strengthened with boards and stiffened with reinforced concrete terminal and central cross-braces. The width of the carriage road is 7.80 m and the two pavements are 1.0 m wide each.

The substructures of the bridge were directly founded, the elevations of the piles being plate-like, widened out at the superior end and with a rule to prop up the superstructure.

After the high floods of the year 1975, the spans I and II (towards Vălenii de Munte) were destroyed, pier P1 being underwashed. Both spans and pier P1 were rebuilt the next year (1976) respecting the same constructive solution, but the bridging boards of the superstructure were prestressed.

During the earthquake on 4th March 1977 all bridge floors suffered an about 10cm displacement upstream. Both on the mobile and fix bearings the displacement resulted from the breaking of the cleats from the expansion bearings. The bridge floor of the opening II fell off the expansion bearings.

In August 1991 the flood damaged the Bascenii de Sus abutment on the left bank, which indicates the fact that the foundation solution as well as the foundation depth were inappropriate. This high flood destroyed both the Bascenii de Sus abutment and the superstructure of the opening adjacent to this one, as a consequence of damaging the pier P6 (fig.1).

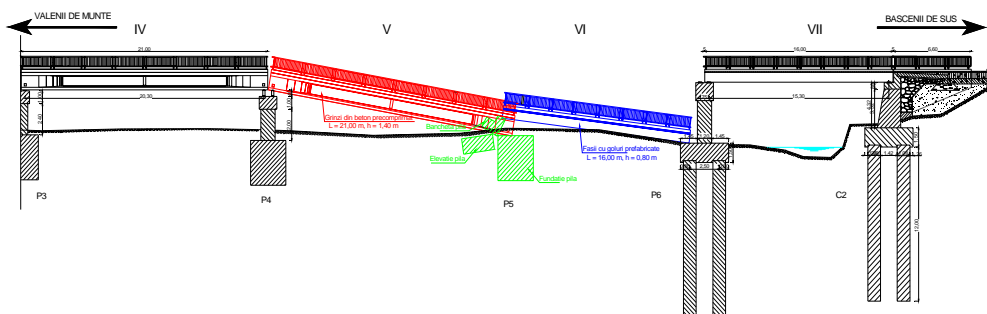


Fig.1

In 1992 the first consolidation consisted in the reconstruction of the Bascenii de Sus abutment, the pier P5 as well as the bridge floors on the last two openings in solution of prestressed concrete hollow beams, solidified with supra-concrete plate.

The foundations of the new substructures are made from piling piles with a big hole size (108 cm) and a foundation length of 12.00m. The elevations of the substructures are executed from reinforced concrete and are restrained in the floors at the top part of the piles.

In the 2005 spring the floods led to the complete erosion of the pier P5, and the opening V made from precast beams as well as the opening VI from hollow beams fell on the river bed.

At that time the substructures of the bridge consisted of:

2 huge abutments made from reinforced concrete, of which the one on the right bank is unconsolidated but has direct foundations, and the one on the left bank (new abutment, executed between 1992-1993) has pile foundation;

6 piers made from reinforced concrete, 5 of them have direct foundation and the other one (pier P6) executed between 1992-1993 has the foundation on pillars and the floor made from reinforced concrete.

All the plate-like pier elevations are completed at the top with a bridge seat made from reinforced concrete with two 1.25m overhangs. The elevations are designed with upstream cut-water and downstream pier nosing.

The bridge superstructure is realized on the first five openings from prestressed concrete beams (precast beams with a height of 1.45m and a length of 21.0m, with 4 beams with section view which are connected by means of 3 bridging boards – two of them on the bearings and the other one is central – and at the top part by means of the monolithic plate), and on the other two openings from prestressed concrete hollow beams (with a height of 80cm and a length of 16.0m, it has 9 foundation lengths with section view, over which a plate of overconcreting was executed). Thus, the length of the bridge was modified as follows: $L = 5 + 21, 0 + 2 \times 16.0 + 2 \times 3.5 = 144.0\text{m}$

The connection of the bridge with the embankments is fulfilled with quarters of cone. The bridge is straight, located in an alignment area, and in the longitudinal profile is on level.

On the right bank there is a protection made from gabions filled with stone of about 50.0m length upstream and of 15.0m downstream. On the left bank, the protections from gabions were destroyed by the latest flood to a great extent.

The bridge was designed under the category “E” of loading (special vehicle V80, convoy A30).

3. SOLUTIONS OF CONSOLIDATION

The existing condition of the bridge, the defects and degradations were subjected to expert's finding, resulting a technical condition index of 29 points, which causes the bridge to fall into the category V. Under these circumstances, the bridge hardly ensures the safety measures of traffic, being necessary both the rebuilding of the openings and the destroyed substructure, as well as the consolidation of the other substructures and the bridge rehabilitation on the whole, including the destroyed bank protections.

Taking into account the current technical condition of the bridge, its length as well as the importance and the volume of rehabilitation work, in order to ensure the minimum safety measures of traffic, to put an end to the degradation process and make the bridge work properly, it is required that a great deal of work should be done in clear stages:

the first stage includes the workload for re-establishing the traffic conditions on the bridge: the consolidation of the pier P4 and the reconstruction of the pier P5, of the superstructure on the openings 5 and 6, of the bank protections and correction of river.

The second stage – the consolidation of the abutment C1, of the piers P1, P2, P3, the reconstruction of the way on the openings I, II, II, VII, the connection with the embankments, the correction of river, and work on ramps.

2.2.1. Work on the bridge substructure

In order to re-establish the traffic conditions, it is necessary that the two collapsed openings V and VI should be rebuilt. Thus, the consolidation work of the pier P4 and the complete rebuilding of the pier P5 are essential.

The foundation solution chosen, both for the consolidation of the pier P4 and the rebuilding of the pier P5, is one of depth, with piling piles of 1,08m hole size and 12.0m length. The length was determined by means of calculations and recommended by the geotechnical study. The piers had direct foundations, blocks of 3.0x6.0x5.0m sizes, which resulted in the erosion and overturning of the pier P5.

The foundation of the piers P1, P2, P3 and P4 was similarly consolidated by executing 4 pillars of 1.08m hole size and 12.0m length, at the top part being restrained in a reinforced concrete floor of 1.80m height.

The floor was connected with the existing foundation block. The elevation of the pier as well as the bridge seat were plastered with reinforced concrete of 20cm thickness. The bridge seat was erected to the top part of the reinforced concrete mobile bearing.

In order to realize the connection between the existing structure and plastering, the deteriorated and separated areas of the concrete were repaired, the surface was roughened, cleaned and dried well, holes were executed to introduce the anchors of steel for reinforced concrete, then penetrated with plaster concrete reinforcement. In these holes there was introduced mortar based on epoxide pitches, which will fix the anchor in the concrete after stiffening.

Pier P5 had the same foundation system with 4 drilled piles with the diameter of 1.08 m, joined into a supra-concrete foundation plate 1.50 m high. The elevation of the pile has retained the same shape as the existing piles. The ruler has been adapted in order to support the two superstructures from spans V and VI, with different sections of the beams(fig.2.).

The bridge sets of the piers have been provided with antiseismic devices at the ends, which will prevent the superstructure from moving laterally during a possible earthquake.

Supporting mobile neoprene devices of the type 4M have been placed on pier P4.

For openings V and VI supporting fix devices of the type 3M have been placed on pier P5 and supporting mobile devices of the type 4M have been placed on pier P6.

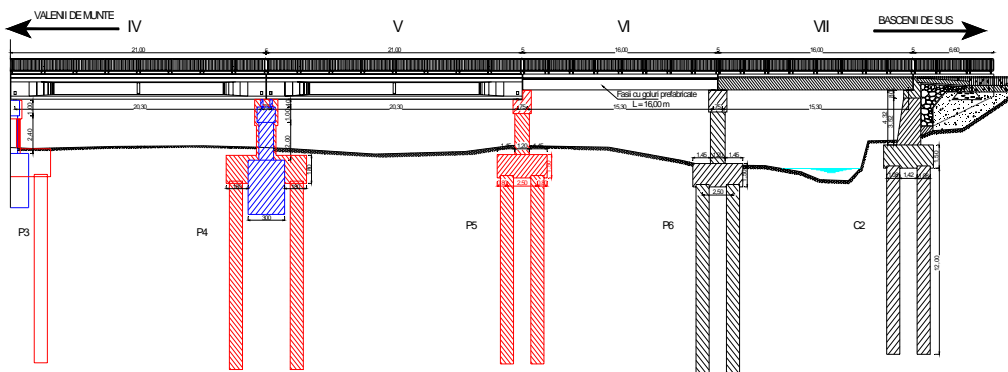


Fig. 2.

2.2.2. Workings on the superstructure of the bridge

The superstructure of opening V retained the same work solution, 4 “T” beams, 1.45 m high and 21.0 m long, with prestressed terminal and central bridging boards. Strengthening boards of 1.70x0.12 m were placed between the beams. Sloping 5-11 cm thick concrete layer was plastered over these beams.

The superstructure at span VI consists of 9 gaped strips 0.80 m high and 15.60 m long. These have been solidified with terminal bridging boards and supra-concrete boards.

Because the bridge is located inside a locality, it has been compulsorily provided with pavements 1.0 m wide on each side. The bridge way is framed with concrete kerbstones. When undoing the way, the existing beams have been examined to determine the degree of decay. The inferior part of the hollow beams has been provided with additional holes for ventilation and flowing away of infiltrated water. After placing the new beams in the section, these have been joined with the existing ones by a supra-concrete board at each span, and continued for the dilatation joints of the piles

. The board's minimal thickness is 10 cm and the maximum one, in the axle of the bridge, of 16 cm, with transversal slopes of 1.5%. Ferro-concrete connectors have been introduced between the existing strips so that the beams and supra-concrete board can blend together perfectly, and the new beams have been provided during production with "rods" at the superior end that have been placed near the bars from the supra-concrete.

For laying the layers of the way over the supra-concrete board, its surface was first of all homogenized by pouring sloping concrete of about 2 cm, over which the thermo-weldable hydroisolating membrane was thermo-applied, continuing all over the surface and rising to the parapet of the pedestal, under the pavement. This membrane is protected by a reinforced capping 4 cm thick, and then by two layers of thermo-cylindered asphalt concrete for bridges, 3.0 cm thick. The pavements are strengthened with embedded PVC pipes $d=125$ mm for eventual assembled networks. The covering of the pavement has been made with 2 cm thick asphalt. Romtix has been introduced in each joint between the concrete and the asphalt layers to ensure imperviousness.

The bridge being almost in landing position, 4 draining holes with draining pipes have been provided for each span. The dilatation joint between the superstructures has been realised in the modern fashion, replacing the classical solution of galvanized sheet iron in the form of pipes and mastic plugs with reduced viability.

2.2.3. Technological stages of consolidating the bridge

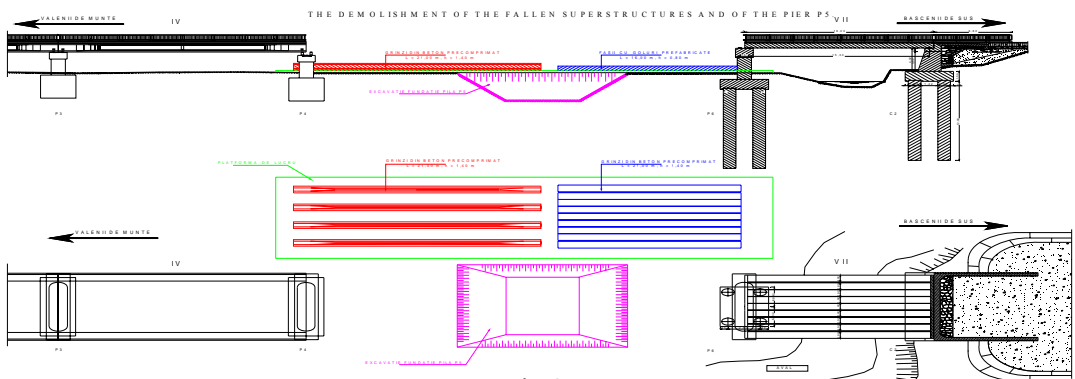
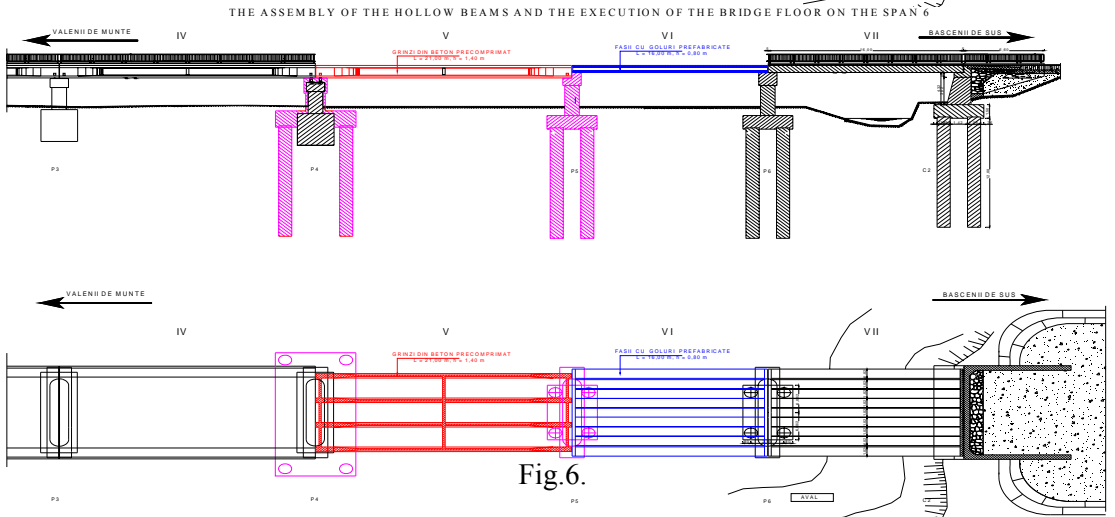
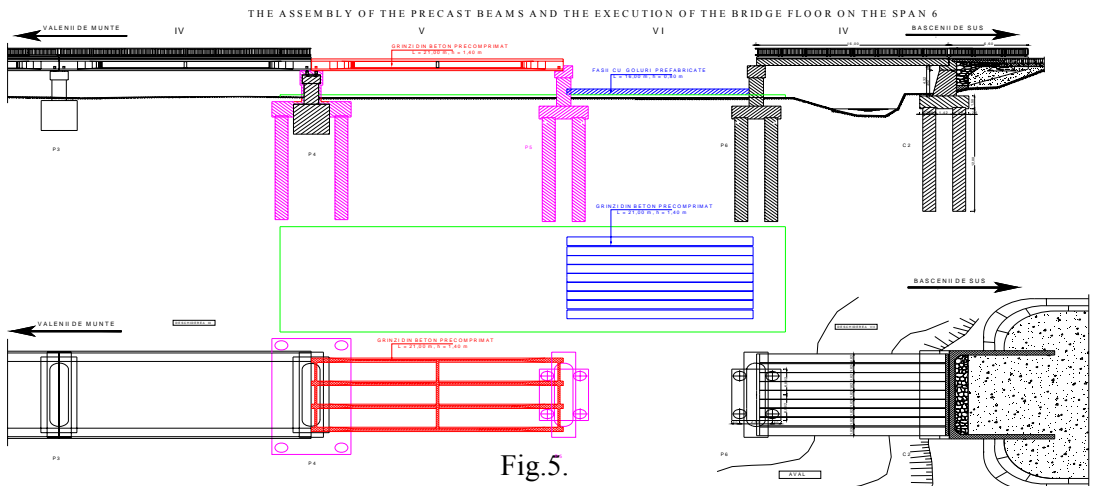
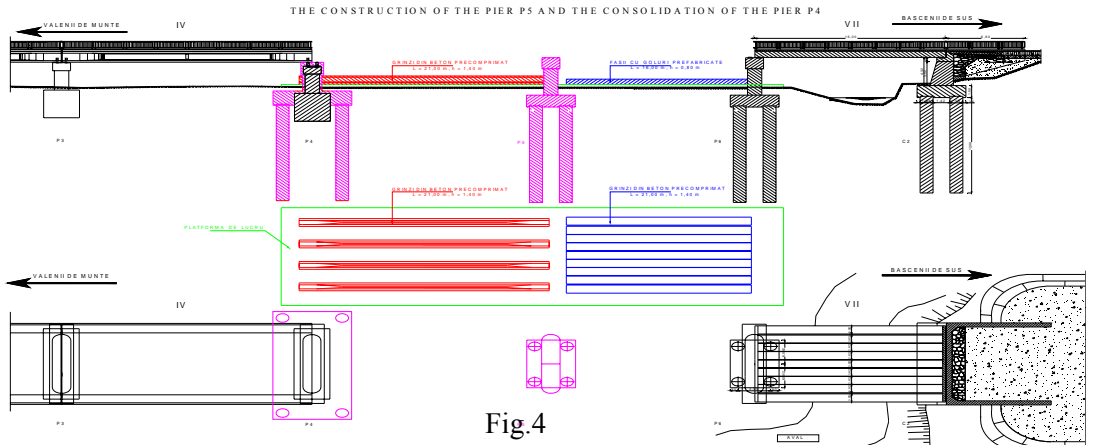


Fig.3



4. CONCLUSIONS

The above described situation is relevant to and coincides with many of the cases met during the period of February-September 2005, the lack of bank protection, the insufficient draining section or the insufficient foundations of the infrastructures contributing decidedly to bridge damaging.

To avoid such problems, starting with the designing phase, great attention should be paid to terrain expertise (topographic, hydrologic and geotechnical studies) with the help of which one can accurately determine:

- the water discharges with the measures of protection corresponding to the class of hydrotechnical importance, according to which the levels for estimation and checking are established;
- the length of the bridge, the number of spans and the elevation of infrastructures keeping a safety guard of free pass according to buoys;
- the correct building of bridges over the water courses;
- the best solution foundation taking into consideration the geological layers and the erosion depth;
- the correction of the riverbed and the execution of some transversal workings for decreasing the thalweg and of some proper bank protection systems to defend the access platforms of the bridge, etc.

Another factor is the lack of involvement from the part of administrators in actions of maintenance and periodical or capital repairing of bridges and bank protection devices, their accentuated decay eventually leading to the construction's lack of protection in front of high floods and finally ending in its collapse.

Another cause is represented by forest cutting and non-corresponding agrotechnical workings that facilitate the processes of corrosion which, in turn, lead to increasing the coefficient of water flowing down slopes carrying great amounts of alluvia and floating debris that affect the structure of the bridge and seriously erode the foundations or clog the span of the bridge.

5. REFERENCES

1. Report regarding the effects of the floods and dangerous meteorological phenomena in the year 2005, applied measures, measures for repairing the affected objectives and for diminishing or avoiding future damage – The Ministry of Environment and Water Administration.
2. Norms concerning the maintenance and repairing of public roads, ind AND 554-2002.
3. Technical instructions for determining the technical state of a bridge, ind AND 522-2002.
4. Instructions regarding the identification of flaws and damages of bridges, ind AND 534-2002.
5. Norms concerning the hydraulic designing of bridges and footbridges, ind. PD95-2002.

REPAIR OF SUB-BASE BY LARGE – SIZED GROUTING AND POTENTIAL USE OF RECYCLED RAW MATERIALS AS SUBSTITUTION OF BINDING COMPONENTS OF GROUTING MATERIALS

Pavla MATULOVA

*Institute of Technology of Building materials and component, Faculty of civil engineering, Brno
University of technology, 602 00, Czech republic, matulova.p@fce.vutbr.cz*

Summary

The cracks and caverns of different types belong to the most frequent failures within concrete, reinforced concrete and masonry structures. These can appear also in the bottom surface, in rocks and grounds under the structure. Very efficient method of these failures rehabilitation is the grouting with a medium which has better physical properties than the original structure.

The paper describes the possibilities of grouting strategy and especially the development of new progressive materials containing different by-product (fly ash, washing wastes, foundry sand, slag etc.) under respecting the increase of quality. Attention was paid especially to properties of the fresh mixture namely to the setting time of modified materials and to the fulfillment of demanded physic-mechanical parameters of the hardened mixture. Particular formulae were designed following optimization calculations for the broad utilization in practice.

KEYWORDS: Rehabilitation, foundation, grouting technology and materials, waste raw materials.

1. INTRODUCTION

Repeated problem in foundation of the pylon of bridge structure is the unstable subsoil with low bearing capacity. The stabilization of subsoil by grouting mixtures, in places where the original subsoil does not have the demanded bearing capacity is a technology known already for more decades. It concerns the pumping process of liquid with changeable viscosity into the soil, into disintegrated soil or concrete with the aim to decrease the permeability.

Clay-cement or purely cement suspensions were formerly used for this purpose. However this methods do not meet sufficiently the requirements of today is building industry. The endeavor or trend of the last years is the utilization of

economically not demanding waste materials. This is the advantageous utilization of these materials exactly into grouting mixtures for the stabilization of subsoil or for filling of bulk caverns. The basic condition to prepare grouting and filling materials of quality is the viscosity of this material. The viscous grouting and filling material should fill in or fill around the structure or element to establish a block against liquids or vapors. It is further of great importance to enable the escape of air and to prevent the formation of air pockets. The most suitable way of the solution of these problems with foundation of the pylon of bridge structure is technology of soil stabilization – grouting systems.

The grouting is the process of pumping the liquid with variable viscosity into the ground, into the fissured or loose ground, concrete or masonry in order to increase the density of these materials. The classical technology of grouting is well known for some centuries.

The principle of this technology is the filling of pores and cavities by the grouting mixture. The mixing of the grouting mixture with the original material forms a composite which has new physical properties. This is most frequently the way to improve the strength and the imperviousness of the material. The grouting can also secure the lasting position of unstable objects. Another typical application is the waterproofing of cracks and gaps (to secure the water tightness of cracks and gaps).

The problem of building structures subsoil hardening, of filling the cavities and the formed caverns became to be a very topical subject in the Czech Republic, especially after the year 2002, when the Czech Republic suffered under extensive floods, which caused the significant disturbance of foundation subsoil.

These problems can be successfully solved by the utilization of grouting technologies. This concerns the application of large scale grouting and possibilities are looked for to decrease the final price under keeping the demanded parameters for the grout mixtures. Considering the fact, that the floods came also in last year 2006, though they were not so great, the subject of large scale grouting is still very topical. The number of structures rehabilitated by grouting materials increases the demands on the research and development of new building materials.

Large-scale grouting in the ground work is connected with increasing demand to solve the question of large scale utilization of industrial wastes in the largest possible extent. The utilization of wastes would not only partially solve the problem with wastes disposal but the wastes application would have positive effect on the price of the work.

This paper represents the research and development of new grouting materials and strategies with the utilization of waste materials.

Special large scale grouting systems

- The problem of building structures subsoil hardening
- Cracks and caverns
- Filling the cavities
- Formed caverns under the structure

Objectives problems: building structures subsoil hardening, filling the cavities, caverns => successfully solved by the utilization of grouting technologies.

2 BASIC CHARACTERISTICS OF GROUTING

Basic characteristic of grouting are: good workability, volume stability, good penetration properties, good pump ability, great resistance against erosion, sufficient compression strength. And technological and technical variables are grouting material, curing time of the material, way of fastening, fastening of spacing distance, grouting pressure, grouting time for one connecting opening, grouted volume for one connecting opening and sequence of works.

The paper presents the proposal and the verification of methods for utilization of waste materials (power plant fly ash, foundry sand, wastes after washing and blast furnace slag) as the substitution of binder and subsequently also as filler in the grouting mixture.

The advantage of grouting mixtures filled by waste raw materials is the lower price and in the same time also the disposal of industrial waste. The processing of unutilized waste raw materials takes place in this way instead of depositing them in waste sites. The way of industrial wastes disposal by depositing them in waste sites is apart from the unfavorable effect to the environment demanding also economically.

Attention was paid especially to properties of the fresh mixture namely to the setting time of modified materials and to the fulfillment of demanded physic-mechanical parameters of the hardened mixture. Particular formulae were designed following optimization calculations for the broad utilization in practice.

3 DESCRIPTION OF APPLIED MATERIALS

For useful interpretation of the used materials were outlining the individual properties of these raw materials

Cement

Table 1. Main properties of applied cement

properties	unity	value
Specific surface	cm ² .g ⁻¹	375
Initial setting time	min.	160
Final setting time	min.	230
Compressive strength - 2 days	N/mm ²	15.4
Compressive strength - 28 days	N/mm ²	38.6

Bentonite

Content of montmorillonite 65-80 %

Table 2. Chemical analysis of bentonite

SiO ₂	Al ₂ O ₃	Fe ₂ O ₃	H ₂ O	TiO ₂	MgO	CaO	K ₂ O	FeO	Na ₂ O	MnO
50.0	15.7 -	8.8 -	5.3	3.8 -	3.8 -	1.7	0.3	0.1	0.1 -	0.1 -
-	17.3	17.0	-	6.3	6.3	-	-	-	1.0 %	0.3
57.0	%	%	6.3	%	%	3.1	1.2	1.0		%
%			%			%	%	%		

Quartz sand

Mass density: 2 500 kg/m³, apparent density: 1 650 kg/m³

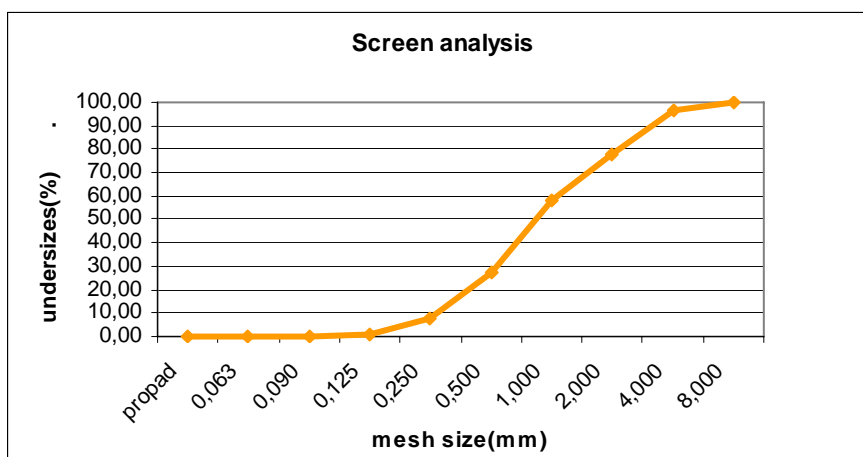


Fig. 1. quartz sand screen analysis

Fly ash (fossil- fuel power station Chvaletice Czech rep.)

Mass density: 2060 kg/m³, specific surface: 270 m²/kg

Table 3. Chemical analysis of fly ash

CaO	MnO	Al ₂ O ₃	Fe ₂ O ₃	sulfates	SiO ₂	Na ₂ O	MgO	K ₂ O	TiO ₂
[%]	[%]	[%]	[%]	[%]	[%]	[%]	[%]	[%]	[%]
1.79	0.03	28.93	6.08	0.2	56.82	0.32	1.31	1.79	2.02

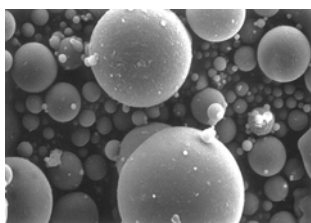


Fig. 2 Grain of fly ash enlarged 2500x

Granulated blast furnace slag (company Trinecke Zelezarny, Czech Republic)

Mass density 2850 kg/m³, specific surface 388, 7 m²/kg

Table 4. Chemical analysis of granulated blast furnace slag

SiO ₂	CaO	MgO	Al ₂ O ₃	Fe ₂ O ₃	SO
40.34	37.53	12.96	5.54	0.27	0.57

Wastes from crushed aggregates washing in quarry

Mass density 2 811 kg.m⁻³

Chemical analysis: CaCO₃ 1.79[%], MgCO₃ 0.03 [%], chlorides 28.93[%],element. sulfur 0.05[%].

Foundry sand:

Chemical analysis SiO₂ 91-98 %, bentonite 3-6 %, mass density 2 580 kg/m³

Bulk density 1 360 kg/m³

4 DESCRIPTION REALIZED WORKS

The research was focused on bonding material substitution in grouting systems.

Formulae were designed with the substitution of filler by 10 till 50% of waste materials. The reference mixture was the concentrate mixture (cement, bentonite, special admixtures) and quartz sand. We have performed the experimental verification of the partial substitution effect of filler by the grouting mixture. The filler (quartz sand) was substituted by waste materials (fly ash, foundry sand, wastes after washing and blast furnace slag). And in the second stage were

particular formulae designed following optimization calculations for selected mixture which has the best properties. And these mixtures were modified. The bonding material was substituted by fly ash. The fresh mixtures of all selected formulae were tested by following basic tests: consistency of the mixture, initial and final setting time, bending strength on test pieces, compression strength on test pieces, volume mass, shrinkage during hardening on test pieces (40/40/160 mm).

Substitution of bonding material by the grouting mixture

Particular formulae were designed following optimization calculations for selected mixture which had the best properties. And this mixture was modified. The bonding material was substituted by fly ash. There were designed two basic formulae with fly ash and slag filler substitution.

Modified Mixtures – bonding and filler material was substituted by fly ash

Table 5. Mixtures proportion – bonding and filler material was substituted by fly ash

sample	cement [kg]	additives [kg]	Fly ash (bending material) [kg]	quartz sand [kg]	Fly ash (filler)[kg]	water [kg]
ref.	533	40	–	1066	–	430
P80	426	40	–	729	253	381
P80-10	383	40	43	729	253	381
P80-20	341	40	85	729	253	381
P80-30	298	40	128	729	253	381
P80-40	256	40	170	729	253	381

P80- 80% of cement in ref. mixture

P80- 10 - 80% of cement in ref. mixture 10% substitution of cement by fly ash

P80- 20 - 80% of cement in ref. mixture 10% substitution of cement by fly ash

Table 6. Results of the tests after 7 and 28 days

sample	7 days			28 days		
	bulk density [kg/m ³]	bending strength [N/mm ²]	compression strength [N/mm ²]	bulk density [kg/m ³]	bending strength [N/mm ²]	compression strength [N/mm ²]
Sref.	1890	2.1	9.2	1820	5.2	14.7
P80	1755	2.9	9.3	1730	3.3	17.5
P80-10	1745	2.2	8.6	1735	3.2	15.9
P80-20	1715	2.1	8.1	1695	2.8	14.8
P80-30	1695	1.9	7.3	1670	2.7	10.1
P80-40	1675	1.8	4.6	1650	2.6	8.9

Table7. Initial and final setting time

Sample	Initial setting time [min]	Final setting time [min]
Sref.	50	120
P80	45	115
P80-10	50	115
P80-20	50	120
P80-30	55	130
P80-40	60	130

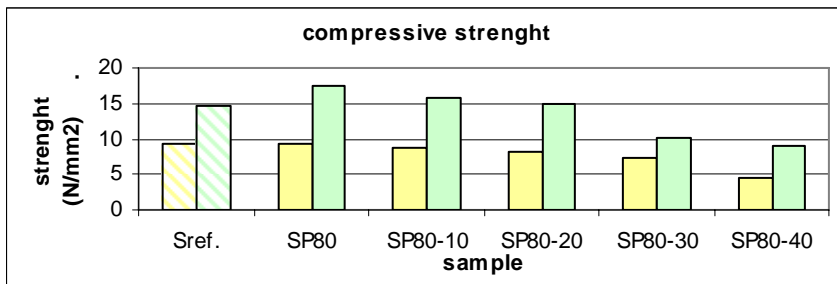


Fig.3 Compressive strength after 7 days and 28 days



Fig.4 Fresh mixture with utilization flay ash as a bonding material

5 CONCLUSION

It was determined, that the application of secondary raw materials caused the decrease of volume mass in the case of all mixtures. The water cement ratio of

modified mixtures must have been modified with the rising portion of fine particles (finely ground waste materials) in order to achieve the demanded workability. For this reason a significant increase of the w/c ratio was determined in the case of all mixtures with waste raw materials. It was first off all necessary to solve the question of filler substitution in grouting materials under maintaining the demanded physical-mechanical properties.

The grouting materials containing waste materials fulfill and in some properties significantly exceed the demanded values, expressed by the reference material. It was further proved that it is possible with the suitably selected substitution of the original filler by waste materials to manufacture grouting materials for utilization in practice which fulfill the given conditions. The greatest bending strength achieved the mixture with 20 % of blast furnace slag and the mixture with 40 % of fly ash. This is caused by the grain size composition of the filler (the nearer is this composition to the ideal grain size curve, the better strength values should show the formulae) and also by the perfect distribution of the grains (no sedimentation takes place). The formulae designed with the following filler proved to be most suitable: the substitution of 30 % of fly ash and 70 % of quartz sand and 20% of slag and 80% of quartz sand. The first stage shown very good results and in following research was provided that it is possible to substitute also bending material There were 40% of bonding material (cement) decreasing in the modified mixture. The research describes the possibilities of development of new rehabilitation grouting materials containing different wastes (fly ash, washing wastes, foundry sand etc.) under respecting the increase of quality. In praxis this research could case lower prices of large scale grouting works.

References

The given problems are solved in the framework of the Grant Project no. 103/05/H044 called: "Stimulation of Doctorands Scientific Development in the Branch of Building-Materials Engineering" and in the framework of the research project MSM 0021630511 called: "Progressive Building Materials with Utilization of Secondary Raw Materials and their Effect on Service Life of Structures" This support is gratefully appreciated.

References

1. *Emmons, P. H., Drochytka, R., Jeřábek Rehabilitation and Maintenance of Concrete in Pictures.* Brno CERM 1999, ISBN 0-87629-286-4 (in Czech).
2. *Jedlickova, J.R. Research and development of new progressive grouting system.* Dissertation, 2005 (in Czech)
3. *Drochytka, R., Dohnálek, J., Bydžovský, J., Pump Technical Conditions of the Concrete Structures Rehabilitation II* SSBK BEKROS Brno 2003, ISBN 80-239-0516-3
4. *Smykalová, R. Development of Grouting Materials with Utilization of Waste Raw Materials.* Dissertation, 2005 (in Czech).

RESEARCH UPON THE CRACKING INDUCED BY RESTRAINED CONTRACTION OF MASS CONCRETE ELEMENTS

Călin Mircea^{1,2}, M. Filip²

¹*Civil Engineering Faculty, Technical University of Cluj-Napoca, Cluj-Napoca, Romania,
calin.mircea@bmt.utcluj.ro*

²*National Building Research Institute [INCERC] Cluj-Napoca Branch, Cluj-Napoca, Romania,
calin.mircea@incerc-cluj.ro, mihai.filip@incerc-cluj.ro*

Summary

The paper presents aspects of an investigation made upon the cracking states induced by early age restrained shrinkage of concrete, at the piers and abutments of the bridges from the new Transylvania Motorway, Romania. The National Building Research Institute [INCERC] Cluj-Napoca Branch and Technical University of Cluj-Napoca performed the investigation at the request of the general contractor Bechtel International Inc.

At approximately one month age of concrete, crack widths range between 0.05-0.5 mm were observed. The paper emphasizes the analyses, interpretations and analytical predictions for the future progress of the cracking states, based on the data acquired from the technical documentation supplied by general contractor, and monitoring of the crack widths.

The good match of theoretical results with the real registered data led to the conclusion that cracking states are caused mainly by restrained volume contraction within the first week. Thus, repair measures could be done in time and the normal progress of the works continued.

KEYWORDS: cracking, base restraint, mass elements, reinforced concrete, shrinkage.

1. INTRODUCTION

Corrosion of reinforcement is a worldwide major cause for early damage of reinforced concrete motorway structures. Consequently, the huge costs related to replacement, rehabilitation, maintenance and indirect losses are a major concern for nowadays society. Until recently, structural design according to Limit States Theory was often reduced in current practice to Ultimate Limit States Analysis. Thus, serviceability conditions (i.e., controlled crack widths, deflections and vibrations) were considered satisfied by indirect design methods, which may result in lack of durability, early and uncontrolled failure.

Performance and durability based design is difficult to implement in current practice. Besides experience and time costly life cycles analyses, it also presumes monitoring of the works and adjustments made in relation with unpredictable local factors (e.g., weather conditions at a particular time, hidden defects of the soil etc.). Within this effort, an investigation was done upon the early cracking states that occurred at the abutments and piers of the bridges from the new Transylvanian Motorway, in Romania. The investigation was done by National Building Research Institute [INCERC] and Technical University from Cluj-Napoca, in cooperation with the general contractor Bechtel International Inc., by mutual consent that without a clear understanding of the cracking mechanism, a reasonable plan for future repair works cannot be considered, and, moreover, these might be ineffective.

As revealed by Figure 1, cracking control is a very important and complex issue. It requires the comprehension of several time dependent phenomena and their dependency, and involves the subjective human factor. Service load behavior depends primarily on the properties of concrete, which sometimes are not reliable predicted at the design stage.

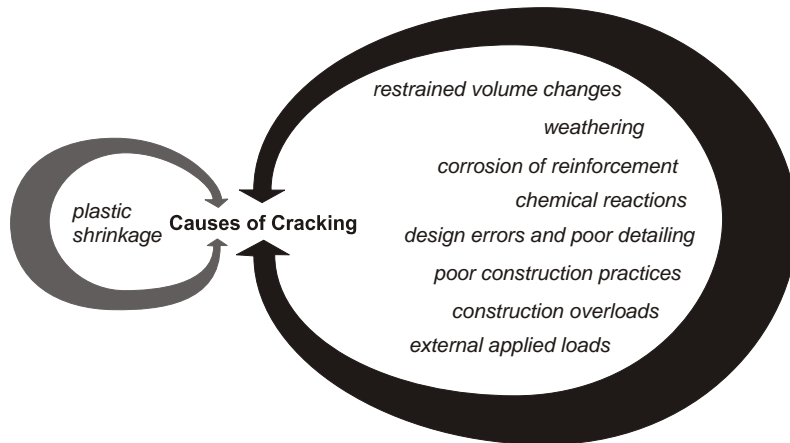


Figure 1. Causes of cracking in structural and mass concrete

Furthermore, concrete behaves inelastic and non-linear even under the service load, complicating serviceability predictions due to cracking, tension stiffening, creep, and shrinkage. Of these, shrinkage is the most problematic. Restraint to shrinkage causes time-dependent cracking and gradually reduces the positive effects of tension stiffening.

2. RESEARCH SIGNIFICANCE

An investigation was done in order to identify the causes of the early age cracking states installed at the massive concrete elements of the new Transylvanian Motorway. The aims were to recommend the appropriate repair methods and to provide guidance in avoiding such problems in the future. Inventory of the cracks and their monitoring, tests and time dependent computer analyses for the prediction and the evaluation of the cracking states within massive reinforced concrete elements, supplemented by engineering reasoning, led to the conclusion that restrained volume contraction due to initial temperature gradients are the cause of the early cracking, while drying shrinkage does not have a significant contribution to the medium and long term progress. Finally, the drawn conclusions allowed recommendations for repairs and future measures for the ongoing works, in accordance with the closing purpose of the investigation, to ensure the proper quality and durability of the structures.

3. OBJECT OF THE INVESTIGATION

Built in October and November 2006, the massive reinforced concrete members cracked almost instantly or within a few hours from formwork removal. The first step of the investigation, which began in December 2006, was the inventory of the cracks. Figure 2 shows typical cracking patterns registered at abutments, to which reference will be made next. At that time, cracks width range was between 0.05-0.5 mm. The largest crack widths were registered around the middle of the walls height, and these were well above the admissible crack width of 0.3 mm.

Cracks developed from the base of the walls. Considering the range of reasons (see Figure 1) justifying the cracking patterns and the magnitudes of the crack widths, restrained volume changes were considered as relevant both for the initial states at the time of investigation, and for the future progress of the cracking states respectively. External restraint to global volume change of concrete elements is provided by supports, while internal restraint is generated between parts of the same element that present different temperatures, moisture migration and embedded reinforcement.

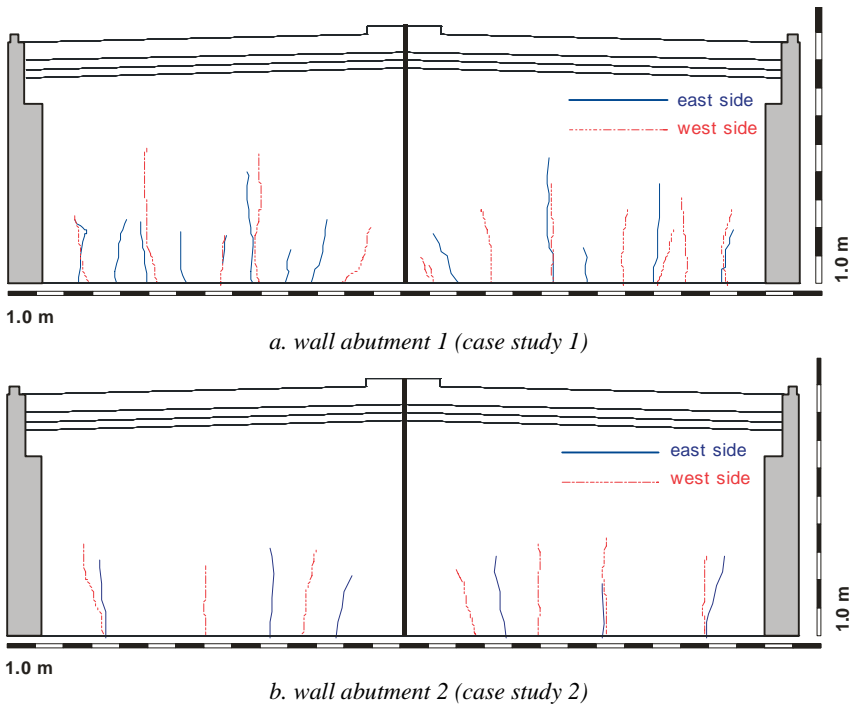


Figure 2. Typical cracking patterns at abutments

When the tensile stresses induced by the restraint to volume reduction exceed the tensile strength of concrete, the element cracks. Volume change of mass concrete elements is natural, the basic mechanisms being given below.

- Temperature gradients generated by the heat developed during hydration of cement lead to a general high temperature of the element. On cooling, the concrete element reduces its volume, while the supports provide an external restraint to it. Considering the large size of the members, temperature varies also within the depth of concrete and leads to an internal restraint, as shown in Figure 3. Similar inside temperature gradients also may arise when the temperature difference between the exposed surface of the mass concrete and the air is significant for long periods.

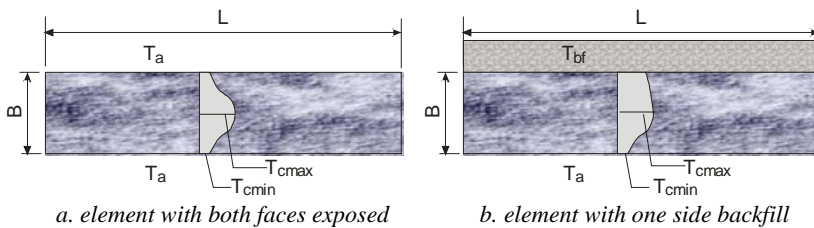


Figure 3. Temperature gradients inside mass concrete members

- Autogenous shrinkage is the consequence of the chemical reactions within concrete mass. It is associated with the loss of water from the capillary pores during hydration of cement, and initiates at the beginning of concrete setting. It lasts several years during hardening of concrete, but only the first month has practical significance.
- Drying shrinkage is the result of the loss of moisture from the cement paste constituent, which reduces its volume. The most important factors of influence are the w/c, the dosage and nature of aggregates. Other significant factors may be the admixtures that influence the water content of the fresh concrete mixture. The major progress of this type of shrinkage lasts about 3 years, but continues during the entire lifetime of the structure.

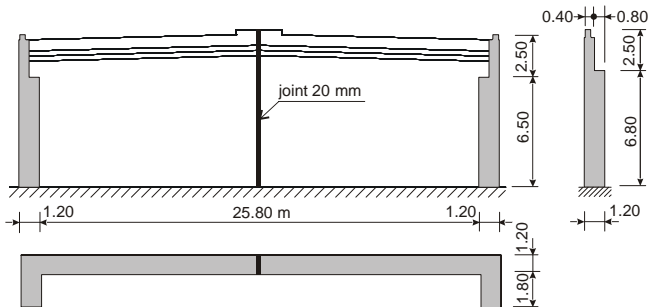
Summarizing, volume change of mass concrete elements has three major interdependent components. On cold weather, volume contraction due to initial heating caused by hydration of cement is amortized within approximately 1 week. While continuous base support and air temperatures balance the thermal gradient, the restraint contribution has a key relevance for the analyzed cases. However, concrete also suffers autogenous shrinkage that develops significant for about one month, and drying shrinkage that continues up to three, even for years. Because steel and concrete have similar values for the linear thermal coefficient, the reinforcement embedded within the mass element will generate internal restraint mainly against autogenous and drying shrinkage. On this restrained volume contraction background, tensile creep of concrete compensates partially the volume

reduction, and concrete continues to improve with different rates its strength properties. Thus, it is obvious that a complete evaluation must consider time as the fourth dimension and the weather parameters as variables.

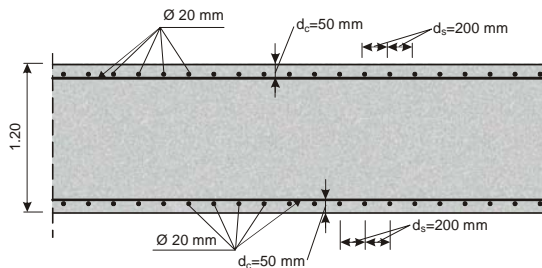
Review of the drawings revealed that abutments (Figure 4.a) were designed according to Eurocode 2 [1] for a concrete class C 25/30, with the characteristic cylinder compressive strength $F_{ck}=25.0 \text{ N/mm}^2$, mean cylinder compressive strength $F_{cm}=33.0 \text{ N/mm}^2$, and the secant Young modulus $E_{cm}=31,000 \text{ N/mm}^2$. Abutment walls were reinforced symmetrically (Figure 4.b) on both directions with 20 mm bars in diameter, disposed at $d_s=200 \text{ mm}$. The thickness of concrete cover to the center of the horizontal bars (i.e., the nearest to the face) is $d_c=50 \text{ mm}$. The properties of reinforcement are: characteristic yielding strength $F_{sy}=345 \text{ N/mm}^2$, ultimate strength $F_{su}=431 \text{ N/mm}^2$, elasticity Young modulus $E_s=210,000 \text{ N/mm}^2$, and ultimate elongation $\epsilon_{su}=20 \%$.

The reference mix used by the contractor is:

- Cement type and content: II 32.5 R;
- Cement content: 460 kg/m^3 ;
- Maximum aggregates size 31 mm;
- Gradation zone: II;
- Water content: $w/c=0.38$;
- Admixtures: air trainer 1.0 % and superplasticizer 0.5 %.



a. elevation and section of the abutment walls



b. horizontal section of the abutment walls

Figure 4. Geometry of the abutment walls

Testing reports exposed much more than needed compressive strengths. Based on the records available from the laboratory concerning the compression tests made on cube specimens at 2, 7 and 28 days, Table 1 shows the time evolution of the cylinder compressive strength and the tensile strength determined by Eurocode 2² relations.

Table 1. Strength characteristics of concrete at various ages

Age of concrete	Compression			Tension	
	$F_{c,cube}$ [N/mm ²]	F_{cm} [N/mm ²]	F_{ck} [N/mm ²]	F_{ctm} [N/mm ²]	F_{ctk} [N/mm ²]
2 days	-25.3	-21.2	-13.2	+1.67	+1.17
3 days	-	-25.1	-17.1	+1.99	+1.40
4 days	-	-27.8	-19.8	+2.20	+1.54
5 days	-	-29.9	-21.9	+2.34	+1.64
6 days	-	-31.4	-23.4	+2.46	+1.72
7 days	-43.0	-32.7	-24.7	+2.55	+1.78
28 days	-55.3	-42.0	-34.0	+3.15	+2.20
3 months	-	-46.9	-38.9	+3.44	+2.41
6 months	-	-48.9	-40.9	+3.56	+2.49
1 year	-	-50.3	-42.3	+3.64	+2.55
2 years	-	-51.4	-43.4	+3.70	+2.59
3 years	-	-51.8	-43.8	+3.73	+2.61
10 years	-	-52.8	-44.8	+3.78	+2.65

* Determined by standard compression tests

Besides monitoring the cracking states evolution and study of the documents, records and drawings, the investigation extended with theoretical analyses and tests performed in order to find out the mechanism of the cracking states, and to predict the future evolution of the cracks. These aspects will be presented forward, starting with the critical review of ACI 207.2R [2] (e.g., however the only comprehensive document on the phenomenon), recently emphasized by Mircea at all [3].

4. CRITICAL REVIEW OF ACI 207.2 REPORT

For a plane concrete massive element, Figure 5 presents the typical cracking pattern and sequence propagation that results from base restrained volume change, as described in ACI 207.2R [2]. The first crack (i.e., crack 1) initiates approximately at the middle of the restrained edge, and progresses up to the top. If $L/H > 2.0$ and the crack extends to about $0.20H - 0.30H$, the crack becomes unstable and will propagate on the entire height of the element. Due to the redistribution of the initial base restraint, the new pair of cracks (i.e., cracks 2) occurs at nearly half of the uncracked regions at the base, and progresses towards up in the same conditions like the first one if $L'/H > 1.0$, where $L' = L/2$. All successive cracking groups develop in a similar manner, until the sum of all cracks width compensates

the volume change. The maximum width for each crack is reached above the top of the previous initiated cracks. Unfortunately, the presence of steel reinforcement inside the concrete element cannot prevent cracking of concrete, but ensures the control by initiating more cracks with smaller widths. It also provides an additional internal restraint to autogenous and drying shrinkage.

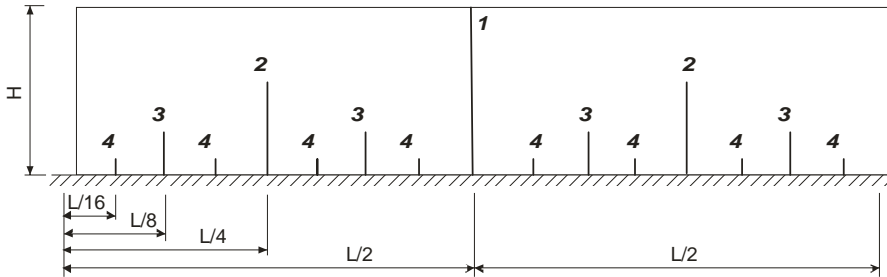


Figure 5. Cracking pattern and sequence propagation at mass plain concrete elements

ACI 207.2R [2] approach is based on the restraining factor (K_R) of the axial strain, starting from the tests performed by Carlson and Reading [4], [5] in 1937. Their work is synthesized by the graphs shown in Figure 6, which shows the variation of the axial strain restraining factor within the height of the wall. ACI 207.2R [2] considers the base restraining factor derived only from the axial force induced by restrained shrinkage, as shown in Figure 7.

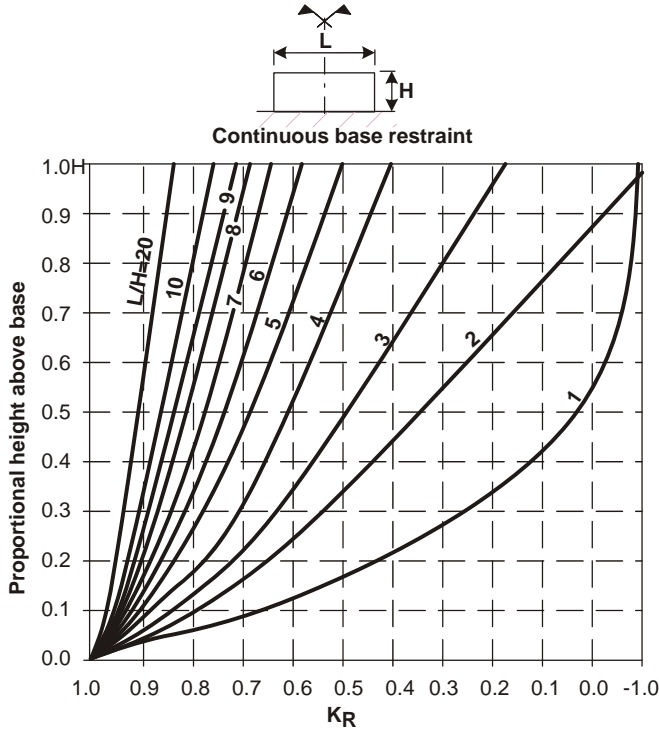


Figure 6. Restraining factor on the height of the wall, related to the length/height ratio

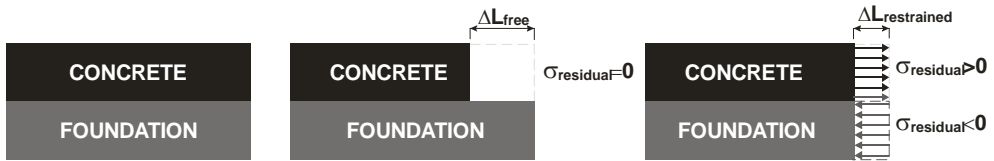


Figure 7. Simplified approach by relating the base restraint only to the axial stiffness

This approach leads to a base restraining factor given by:

$$K_{R0} = \frac{1}{1 + \frac{A_c E_c}{A_F E_F}} \tag{1}$$

where A_c is the gross area of concrete cross-section of the elevation, E_c is the sustained modulus of elasticity of concrete in elevation, A_F is the area of the cross-section of the foundation or other element restraining shortening, and E_F is the modulus of elasticity of the foundation or restraining element. The ACI 207.2R [2] gives satisfactory results in current design practice. However, it does not describe entirely the phenomenon, and is difficult to be applied when investigating a given

case. It does not explain the inclined path of the cracks at their root, and because leads to a constant base restrain factor (Figure 8), can be applied only on biographical procedures (Figure 9.a), where after each redistribution, the base restraining factors applies to smaller amounts of remained shrinkage strains.

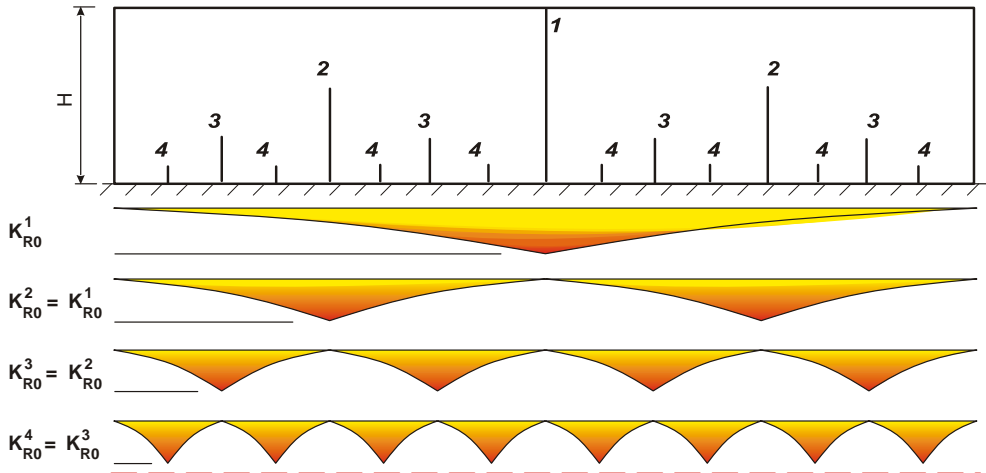


Figure 8. Incremental scheme for the base restraint redistribution

Instead of considering the axial stiffness based restraining factor at the base, Mircea at all [3] proposed a base restraining factor (see Figure 10) considering axial stiffness of the elevation and shear stiffness of the foundation at the contact surface. Introducing the transversal modulus of elasticity of concrete in foundation $G_F=0.4E_F$, relation (1) becomes:

$$K_{R0} = \frac{1}{1 + \frac{A_c E_c}{L' B E_F}} \tag{2}$$

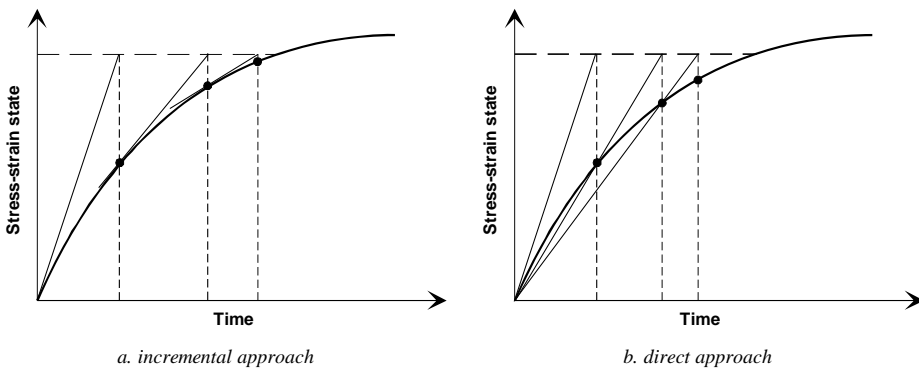


Figure 9. Basic schemes for time dependent analyses

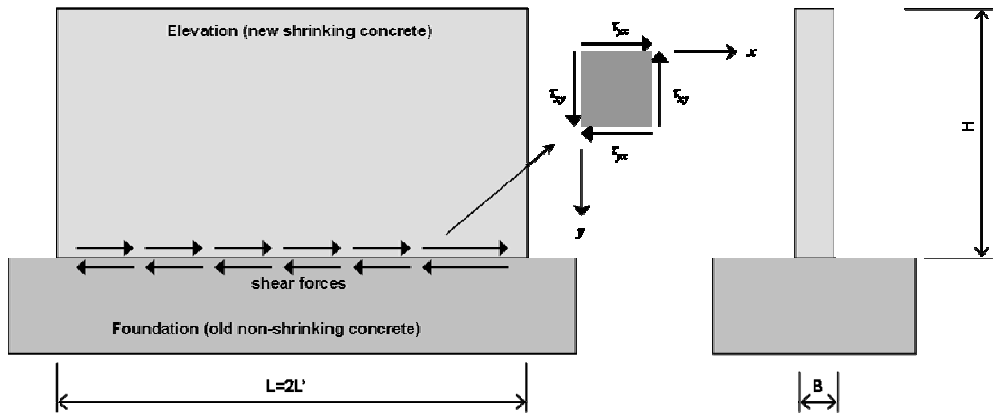


Figure 10. Simplified approach by considering pure shear at the contact surface

with $2L'$ the length of each uncracked panel, and B the width of the elevation. Thus, on a direct iterative approach, as shown in Figure 11, the value of the base restraining factor at each step decreases and convergence can be achieved when axial strains do not exceed the cracking limit.

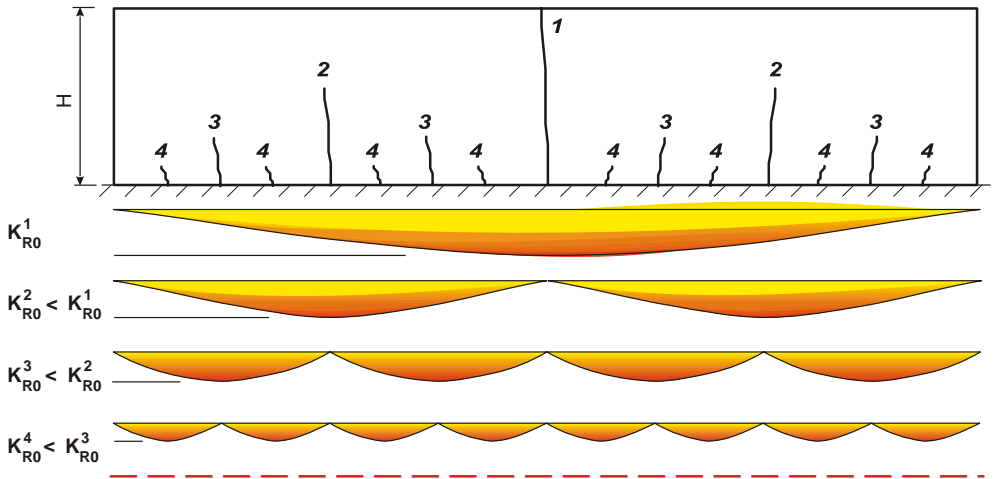


Figure 11. Base restraint redistribution based on the shear stiffness of the base support

The maximum shear force of the internal stress block corresponds to the crack initiation (i.e., stage 2), while the maximum base related moment of the internal stresses corresponds to the critical height of the crack (i.e., stage 4). Beyond this stage, as shown in Figure 12, reinforcement and concrete cannot sustain the maximum restraining moment at the base, and parasite stress concentrations at the crack ends will make the crack unstable and free to an uncontrolled propagation to the entire height of the element.

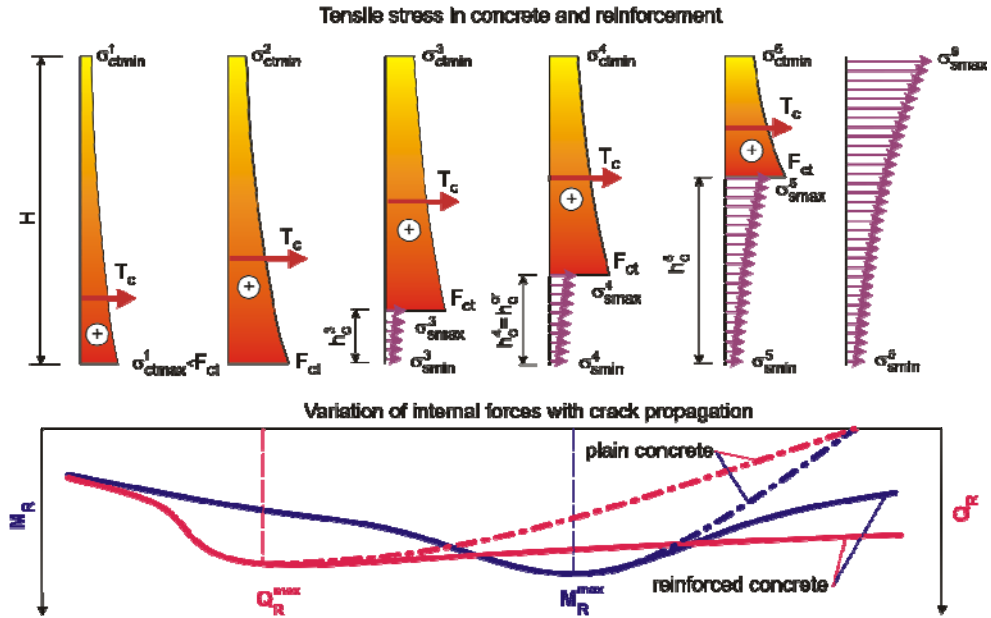


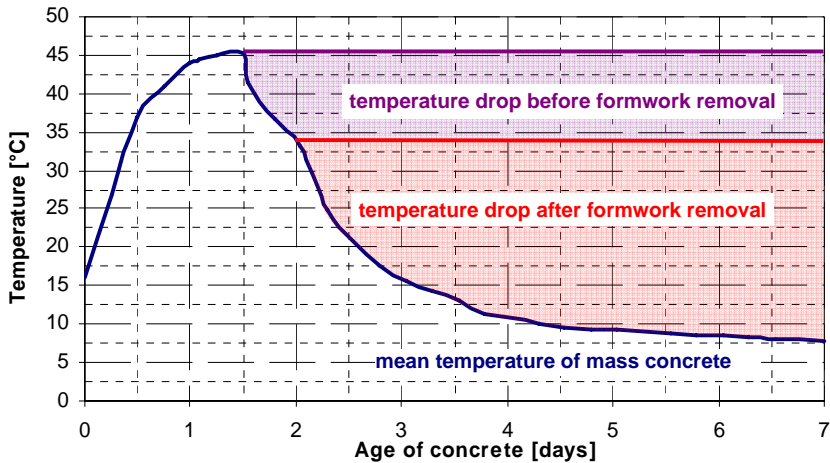
Figure 12. Crack initiation and propagation to the top of a wall with $L'/H \geq 1.0$

5. ANALYSIS OF THE ABUTMENT WALLS

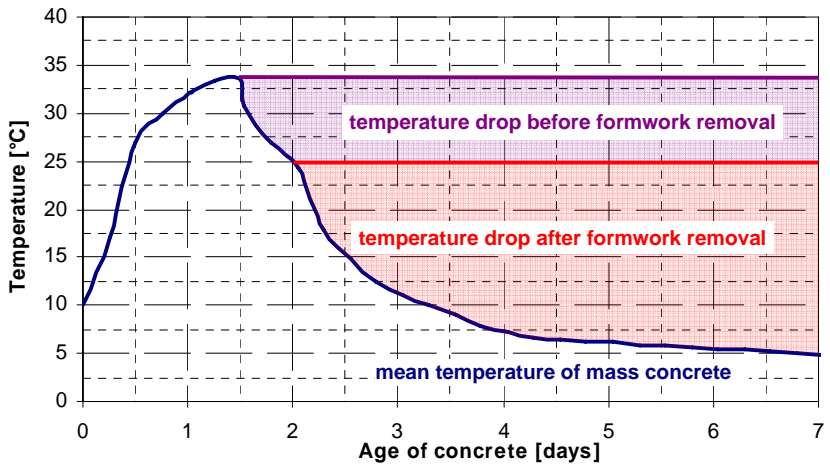
Considering an equivalent thickness of the wall equal with 1.59 m prior to formwork removal and the effective thickness of 1.20 m after that, Table 2 presents the characteristic temperatures calculated according to ACI 207.2R [2], and Figure 13 presents the evolution of the mean temperature in the mass concrete elements. Concrete reaches its peak temperature at 36 hours, while the formwork was removed after 2 days. The following notations are used in Table 2: T_{cp} - mean placing temperature of fresh concrete, T_a - mean air temperature at concrete placing, $T_{cp,eff}$ - effective placing temperature of concrete, T_{Am} - average air temperature over a week and T_{cpk} - temperature of concrete at the peak age.

Table 2. Characteristic temperatures of mass concrete elements

Sampling reports		ACI 207.2R ¹			
T_{cp}	T_a	Peak age	$T_{cp,eff}$	T_{Am}	T_{cpk}
[°C]	[°C]	[hr]	[°C]	[°C]	[°C]
<i>case 1</i>					
22	10	36	16	8	45
<i>case 2</i>					
21	-1	36	10	6	34



a. case 1



b. case 2

Figure 13. Evolution of the mean temperature in concrete

Unless more accurate information is available, Eurocode 2 [1] recommends a linear thermal coefficient for concrete of $C_T=10 \times 10^{-6} \text{ } ^\circ\text{C}^{-1}$. A simple calculation of the evolution of the tensile strains, based on the already calculated temperature gradients and the relations given by the European code, shows that the restraint to initial thermal contraction caused the cracking of the walls before formwork was removed. Figures 14 and 15 prove that after one week, concrete restrained tensile strains reach the upper limit. After 28 days, creep starts to compensate a significant part of these (i.e., approximately 20 % of total shrinkage in 3 years), and further drying shrinkage cannot reach the initial superior bound. Because internal restraint is not emphasized in this simple approach, time dependent structural analyses were performed to predict the long term behavior.

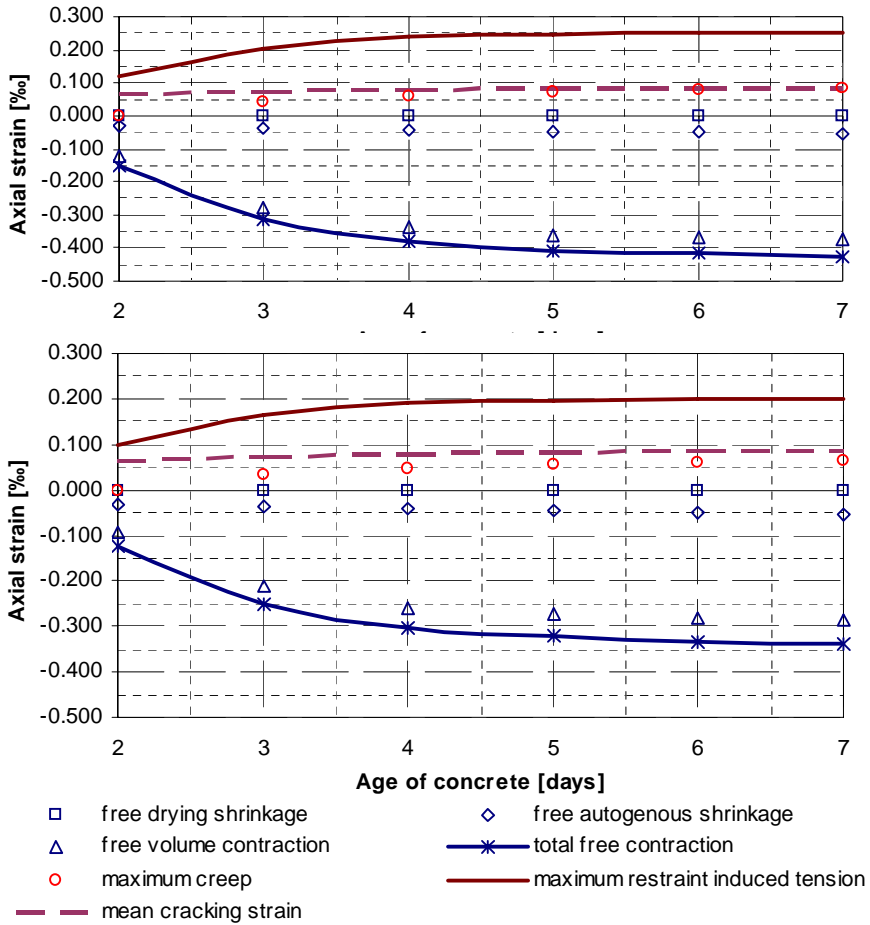


Figure 14. First weak evolution of the axial strain for mean relative humidity RH=60 %

Time dependent analysis was based on a direct iteration approach, which was considered much more effective than a gradual incremental procedure. Mean strength and deformational properties of concrete were time related according to Eurocode 2 [1] requirements. Based on the characteristic properties, for the steel reinforcement an idealized bilinear (with a second ascending branch) stress-strain diagram was adopted.

The initial external restraining factor at the base considers both time and cracks spacing as variables with the adapted relation (2), which becomes:

$$K_{R0}(L', t) = \frac{1}{1 + \frac{A_i(t)E_{c,eff}(t)}{L'BE_F}} \quad (3)$$

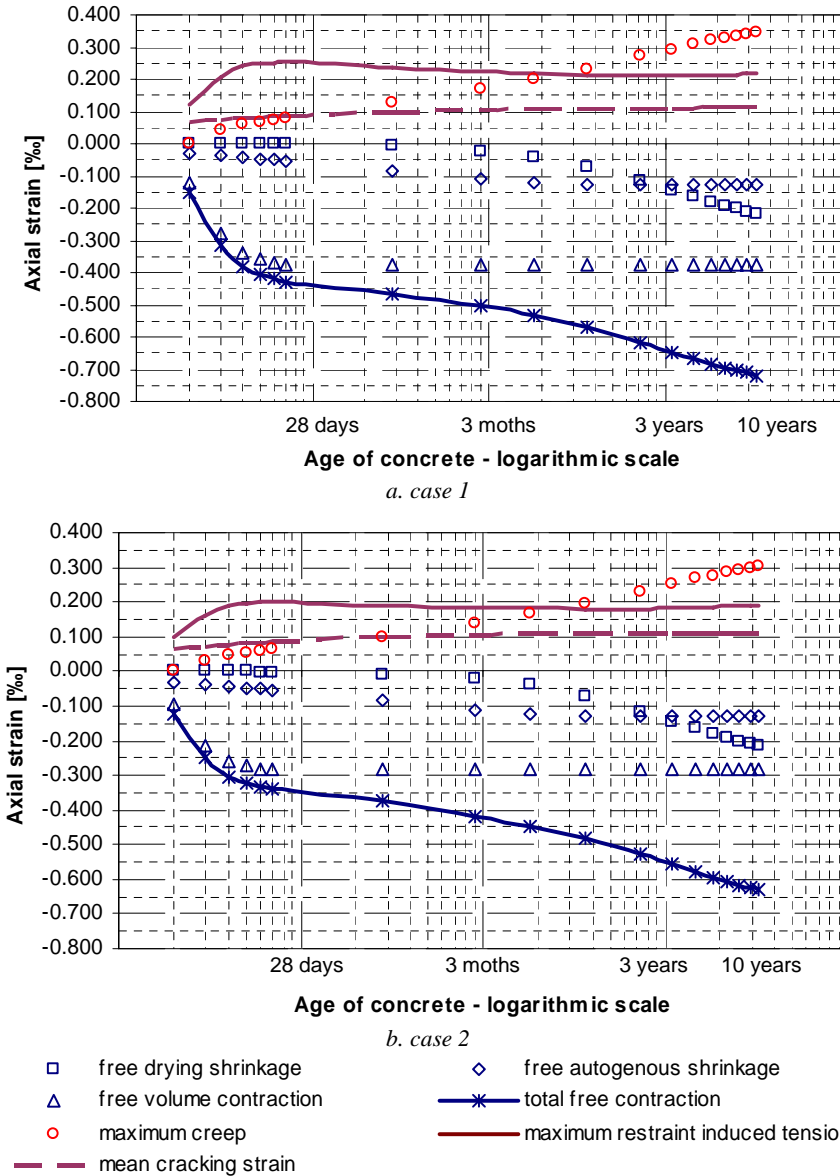


Figure 15. Ten years evolution of the axial strain for mean relative humidity RH=60 %

where $A_i(t)$ is the ideal area of the walls (i.e., gross area of concrete corrected by the reinforcing ratio), $B=1.20$ m is the thickness of the wall, $E_{c,eff}(t)$ is the effective Young modulus of concrete (i.e., including creep effects) in the walls, and E_F is the secant Young modulus of the concrete in foundation. Thus, through an iterative approach, the base restraining factor is redistributed after each cracking sequence to the uncracked regions, as shown in Figure 11.

Depending by the sizes of each uncracked region remained, the value of the external restraining factor at the current level h above base, is given by:

$$\begin{aligned} K_R(L', t) &= K_{R0}(L', t)(2L'/H - 2)(2L'/H + 1)^{h/H} \text{ if } 2L'/H \geq 2.5 \\ K_R(L', t) &= K_{R0}(L', t)(2L'/H - 1)(2L'/H + 10)^{h/H} \text{ if } 1.0 < 2L'/H < 2.5 \\ K_R(L', t) &= K_{R0}(L', t) \lim_{2L'/H \rightarrow 1} [(2L'/H - 1)(2L'/H + 10)^{h/H}] \text{ if } 2L'/H \leq 1.0 \end{aligned} \quad (4)$$

Internal restraint of reinforcement against autogenous and drying shrinkage results in a tensile stress in concrete given by:

$$\sigma_c(t) = \frac{[\varepsilon_{ca}(t) + \varepsilon_{cd}(t)]A_{s2}E_s}{d_s} \quad (5)$$

where $\varepsilon_{ca}(t)$ is the strain caused by autogenous shrinkage, $\varepsilon_{cd}(t)$ is the drying shrinkage strain, d_s is the vertical distance between bars, and A_{s2} is the area of the two bars disposed at the opposite faces.

Convergence is achieved when tensile strains in concrete do not exceed the tensile ultimate strain of concrete at a certain time. A mention should be made to the critical crack height. As the results presented in Tables 4 and 5 reveal, the stability of the cracks cannot be directly obtained in the model adopted, and were separately analyzed by iterative algorithms.

Tables 3-6 present the results of the analyses in the terms of crack widths and corresponding stress in reinforcement, calculated by the Gergely-Lutz [6] formula with $\beta=1.0$. Figure 16 shows the critical crack height at various ages of concrete, estimated by independent iterative analyses.

As emphasized in Table 3 and 4 (bold characters in the cracks height columns) for case 1, three cracks exceed the critical height. Because crack number 1 occurred first under an initial ratio $L'/H \geq 1.0$, seems that in time it might propagate to the top. However, the critical crack height was reached after the rest of the cracks had initiated. Due to redistribution of the stresses, appears much more possible that even unstable, it will propagate only on 80-90 % of the height of the wall, as cracks number 2.

In the same time, the three cracks that became unstable present (bold characters in the maximum crack width columns of Tables 3 and 4) widths higher than the admissible limit. In these, steel reinforcement reaches the yielding point (see bold characters in reinforcement maximum stress columns of Tables 3 and 4). A further estimation of the stress in reinforcement, considering the maximum internal moment (see Figures 12 and 17) as constant after the cracks became unstable, shows that the mean stress varies around 175 N/mm^2 , without important plastic strains. Therefore, figures written with bold-italic characters in Tables 3 and 4 might be acceptable for the steel stress.

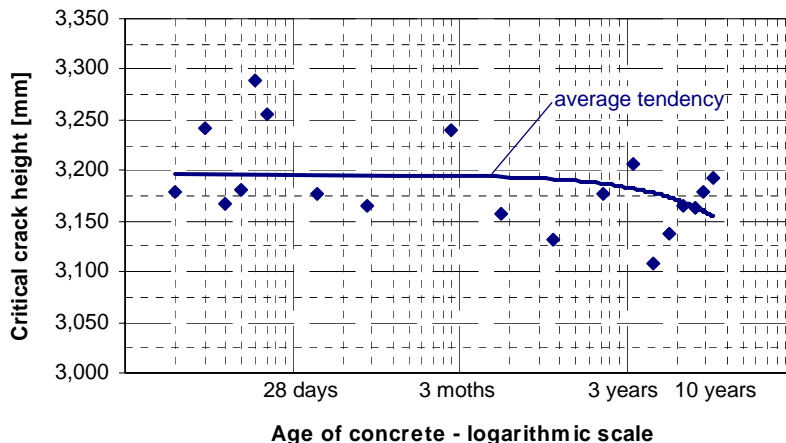


Figure 16. Variation with time of the critical crack height

Table 3. Theoretical short term cracks width and steel stresses (case 1)

Age of concrete	No. of cracks	h _c [mm]	w _{cr} [mm]		σ _s [N/mm ²]	
			max	min	max	min
2 days	7	143	0.069	0.062	70.1	62.4
	3	1,565	0.144	0.000	145.5	0.1
3 days	15	220	0.096	0.087	97.6	87.9
	7	697	0.186	0.145	188.2	146.9
	3	3,195	0.338	0.000	342.5	0.1
4 days	15	329	0.120	0.103	121.2	104.4
	7	805	0.221	0.175	223.5	176.8
	3	3,526	0.407	0.000	345.8	0.1
5 days	15	333	0.125	0.107	126.3	108.6
	7	808	0.230	0.182	232.5	184.0
	3	3,532	0.424	0.000	345.8	0.1
6 days	15	300	0.123	0.107	124.9	108.8
	7	775	0.230	0.181	233.0	183.7
	3	3,427	0.423	0.000	345.8	0.1
7 days	15	283	0.123	0.108	124.6	109.2
	7	756	0.231	0.182	233.9	184.1
	3	3,368	0.424	0.000	345.8	0.1
28 days	15	109	0.104	0.098	105.2	99.5
	7	570	0.210	0.162	213.0	164.0
	3	2,751	0.378	0.000	345.7	0.1
3 months	15	46	0.093	0.091	94.6	92.2
	7	486	0.195	0.149	197.4	150.7
	3	2,425	0.347	0.000	345.7	0.1
6 months	15	32	0.089	0.087	89.8	88.2
	7	455	0.187	0.142	188.9	144.1
	3	2,288	0.332	0.000	335.9	0.1

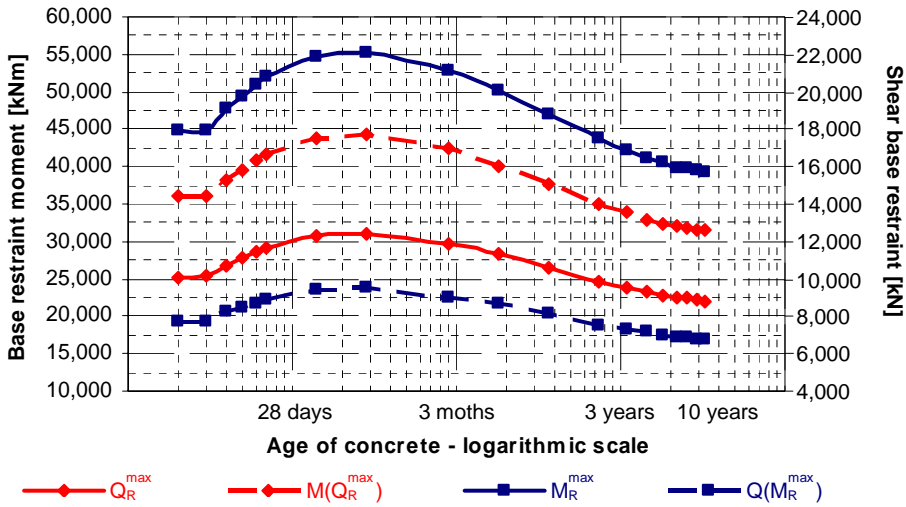


Figure 17. Variation in time of the maximum base related internal forces

Table 4. Theoretical medium and long term cracks width and steel stresses (case 1)

Age of concrete	No. of cracks	h_c [mm]	w_{cr} [mm]		σ_s [N/mm ²]	
			max	min	max	min
1 year	15	15	42	0.087	0.085	87.9
	7	7	446	0.181	0.139	183.6
	3	3	2,207	0.324	0.000	328.0
2 years	15	15	75	0.088	0.084	89.3
	7	7	463	0.181	0.140	182.8
	3	3	2,217	0.326	0.000	329.5
3 years	15	15	91	0.089	0.084	90.3
	7	7	470	0.181	0.140	183.0
	3	3	2,219	0.327	0.000	331.3
10 years	15	15	158	0.096	0.088	97.4
	7	7	521	0.188	0.148	190.1
	3	3	2,333	0.345	0.000	345.6

Medium and long term evolution (see Table 4) was estimated considering just one face exposed to drying (i.e., placing of the backfill was considered to be done at six months). As results from the comparative study of Tables 3 and 4, drying shrinkage will not bring a significant role to the progress of the cracking state. Thus, after six months from placing of concrete, the cracking state may be considered as stable.

For the second analyzed case, the data from Table 5 shows that in the short term, practically, the parameters of cracking state are within the admissible limits (i.e., no excessive cracks width and no yielding of the reinforcement). Some of the cracks even appear to close after the initial opening (i.e., cracks 8-15 that occurred at 4 days and closed until 28 days). In the medium and long term, Table 6 reveals

that the cracking state remains stable. Even if after 9 years cracks 8-15 may open due to drying shrinkage, the cracking state will not degenerate in an inadmissible one.

Table 5. Theoretical short term cracks width and steel stresses (case 2)

Age of concrete	No. of cracks	h _c [mm]	w _{cr} [mm]		σ _s [N/mm ²]	
			max	min	max	min
2 days	3	660	0.074	0.000	75.3	0.1
3 days	7	349	0.134	0.103	135.6	104.3
	3	1,933	0.240	0.000	243.2	0.1
4 days	15	44	0.080	0.077	80.5	78.3
	7	434	0.166	0.126	167.6	127.7
	3	2,192	0.294	0.000	297.7	0.1
5 days	15	41	0.082	0.080	82.9	80.8
	7	431	0.171	0.130	173.0	131.7
	3	2,180	0.303	0.000	307.0	0.1
6 days	15	23	0.082	0.081	82.8	81.6
	7	412	0.173	0.131	174.8	132.6
	3	2,122	0.305	0.000	309.2	0.1
7 days	15	11	0.081	0.081	82.4	81.8
	7	399	0.173	0.131	175.3	132.6
	3	2,079	0.305	0.000	309.2	0.1
28 days	7	262	0.143	0.114	144.4	115.5
	3	1,623	0.266	0.000	269.3	0.1
3 months	7	213	0.129	0.105	130.3	106.7
	3	1,419	0.246	0.000	248.6	0.1
6 months	7	198	0.123	0.101	124.4	102.4
	3	1,377	0.236	0.000	238.7	0.1

Table 6. Theoretical medium and long term cracks width and steel stresses (case 2)

Age of concrete	No. of cracks	h _c [mm]	w _{cr} [mm]		σ _s [N/mm ²]	
			max	min	max	min
1 year	7	206	0.123	0.101	125.0	101.8
	3	1,322	0.234	0.000	237.2	0.1
2 years	7	231	0.130	0.104	131.3	104.8
	3	1,366	0.241	0.000	244.2	0.1
3 years	7	246	0.134	0.106	135.8	107.1
	3	1,399	0.247	0.000	249.7	0.1
10 years	15	3	0.071	0.071	72.3	72.2
	7	330	0.153	0.116	154.5	117.8
	3	1,535	0.271	0.000	274.6	0.1

For both cases, Figure 18 presents the theoretical cracking patterns at various concrete ages obtained by analysis, over posed to the ones found on site at about one and five months. The observed patterns differ from the theoretical ones

because concrete cracking takes place following the weak zones created by the variable strength properties of concrete, different concrete ages, variable weather conditions etc. However, in terms of crack numbers, height and width, the theoretical results are quite satisfactory. Even if the inside temperature gradients were neglected because the walls were subjected to a relative fast cooling in the first week and thus were considered without major impact, on site measurements of the cracks width at the elements surface confirm the values of the calculated cracks width, and consequently the stress states in reinforcement and concrete.

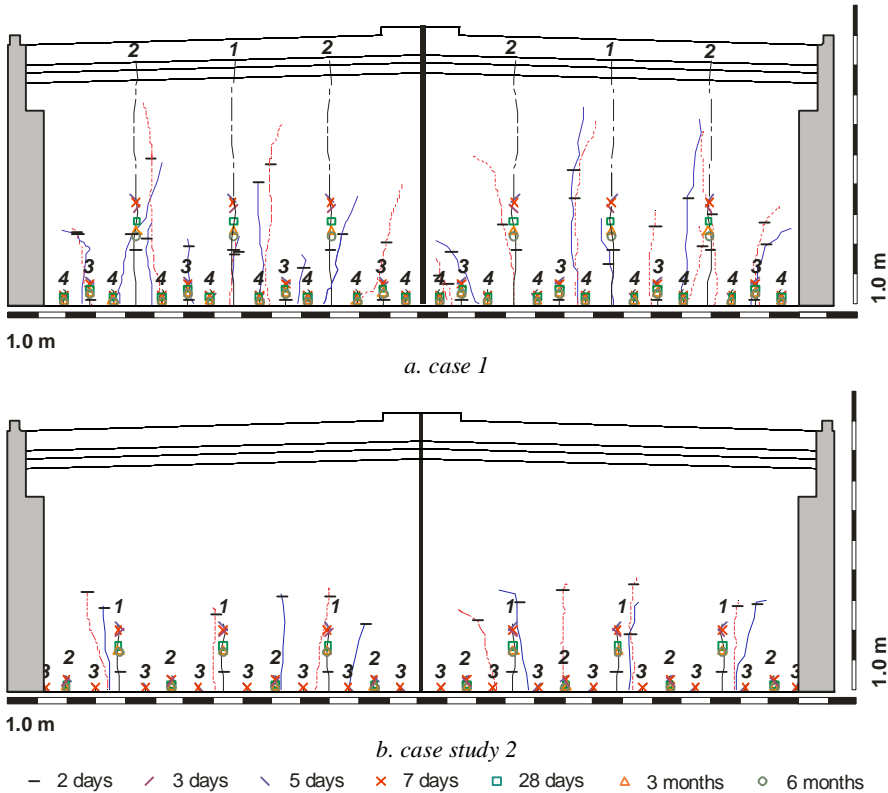


Figure 18. Cracking patterns and cracks propagation (theoretical and measured on site)

In the first case, the amount of reinforcement could not restrict the maximum cracks width to the allowable value (see Figure 19). For the temperature drop given in Figure 13.a, the necessary crack spacing L' is lower than the necessary one at approximately 2.5-3.5 m above base. For large temperature drops, the excessive crack widths are mainly the result of low reinforcing ratios in the base region of the wall, and not in the upper part. A higher base reinforcing ratio would increase the walls base stiffness and restrict the crack widths in this area, and consequently above it.

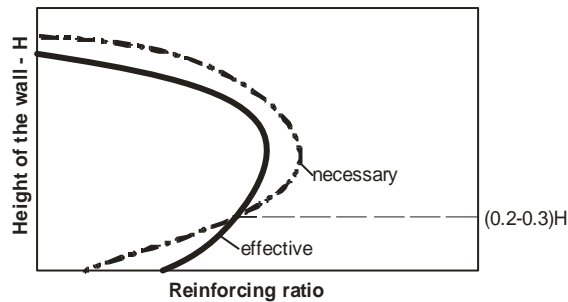


Figure 19. Variation of the reinforcing ratio in case 1

6. FINAL REMARKS

Shrinkage cracking is inevitable for many types of elements. The problem is to ensure their control. If in case 2, the initial design assured a cracking state within the allowable limits, in the case 1 it did not. Looking at the temperature values, the lower temperature at placing of concrete in the case 2 acted like a cooling treatment, resulting in a lower temperature drop. In the first case, the higher temperature drop of 38 °C requires a reinforcing ratio of about 0.0035 on 2.5 m above the base. Higher quality of concrete does not always result in a superior quality. In the case of mass elements, the high cement content easily results in uncontrolled cracking. For the analyzed cases, cracking states affect only the durability of the elements and not the integrity requirements. Therefore, the recommended repair measures were routing and sealing of the excessive cracks. For future works, the recommendation was to reconsider the mix design of concrete (lower cement content, other types of aggregates etc.).

References

1. EN 1992-1-1 Eurocode 2, *Design of Concrete Structures. General Rules and Rules for Buildings*, European Committee for Standardization, pp. 26-40, pp.207-209.
2. ACI Committee 207, 1995, *Effect of Restraint, Volume Change, and Reinforcement on Cracking of Mass Concrete* (ACI 207.2R-95), American Concrete Institute, Farmington Hills, MI, 26 pp.
3. Mircea, C., Filip, M., Ioani, A., *Investigation of Cracking of Mass Concrete Members Induced by Restrained Contraction*, American Concrete Institute Special Publication SP-246 *Structural Implications of Shrinkage and Creep of Concrete*, Fajardo, 2007, pp. 229-244.
4. Carlson, R. W., *Drying Shrinkage of Large Concrete Members*, ACI Journal, Proceedings V. 33, No. 3, Jan.-Feb. 1937, pp. 327-336.
5. Engineering Monograph No. 34, *Control of Cracking in Mass Concrete Structures*, U.S. Bureau of Reclamation, Denver, 1965.
6. Gergely, P., Lutz, L. A., *Maximum Crack Width in Reinforced Concrete Flexural Members, Causes*, American Concrete Institute Special Publication SP-20 *Mechanism, and Control of Cracking in Concrete*, Detroit, 1968, pp. 76-117.

SERVICE TESTS ON PC BEAMS

Călin Mircea^{1,2}, M. Filip²

¹Civil Engineering Faculty, Technical University of Cluj-Napoca, Cluj-Napoca, Romania,
calin.mircea@bmt.utcluj.ro

²National Building Research Institute [INCERC] Cluj-Napoca Branch, Cluj-Napoca, Romania,
calin.mircea@incerc-cluj.ro, mihai.filip@incerc-cluj.ro

Summary

The paper presents aspects from the testing of full scale PC prefabricated bridge girders, to be used at the new Transylvania Motorway. The tests were performed by INCERC Cluj-Napoca, at the order of Bechtel International Inc., general contractor and producer of the prefabricated units. The paper aims to offer to the specialists valuable experimental data, obtained through state of the art testing techniques.

After a brief introductory part, presenting the general frame and testing conditions, the paper continues with a comprehensive presentation of the tested PC girders, based on the design documentation, a non-linear evaluation and records of the producer.

After the description of the testing procedure and the equipment, results are emphasized in a synthetic manner, based on graphical figures resulted from digital processing, and commentaries.

The paper ends with the final remarks and the acknowledgement bring to the supporting colleagues from the general contractor.

KEYWORDS: prestressed concrete, beam, bridge, testing, analysis, serviceability.

1. INTRODUCTION

The paper deals with the service tests and their analyses performed on the 21.0 m span PC beams, to be used at the new Transylvania motorway. The beams were manufactured by Bechtel International Inc. Reno-Nevada, Cluj-Napoca Subsidiary, in accordance with the design completed by Iptana SA Bucharest, drawing references IP-OS-0-F-Z-0010-2112 and P-OS-0-F-Z-0010-2812.

Table 1 summarizes the relevant information about the age of the elements and weather conditions at testing. Tests (Figure 1) were carried out for service conditions on the stand from the Săvădisla plant, on the ground given by the designer’s procedure IPT-OS-0-F-Z-0010-0516 and STAS 12313-85 [1].

Table 1. Synthetic information of the testing conditions

Beam ID	Date of fabrication	Date of testing	Outside temperature	Average relative humidity
T 48/34	11.10.2006	20.11.2006	8-16 °C	60 %
T 48/27	05.10.2006	22.11.2006	12-19 °C	60 %
T 48/07	12.09.2006	23.11.2006	11-16 °C	60 %
T 18/10	30.06.2007	18.09.2007	18-21 °C	58 %

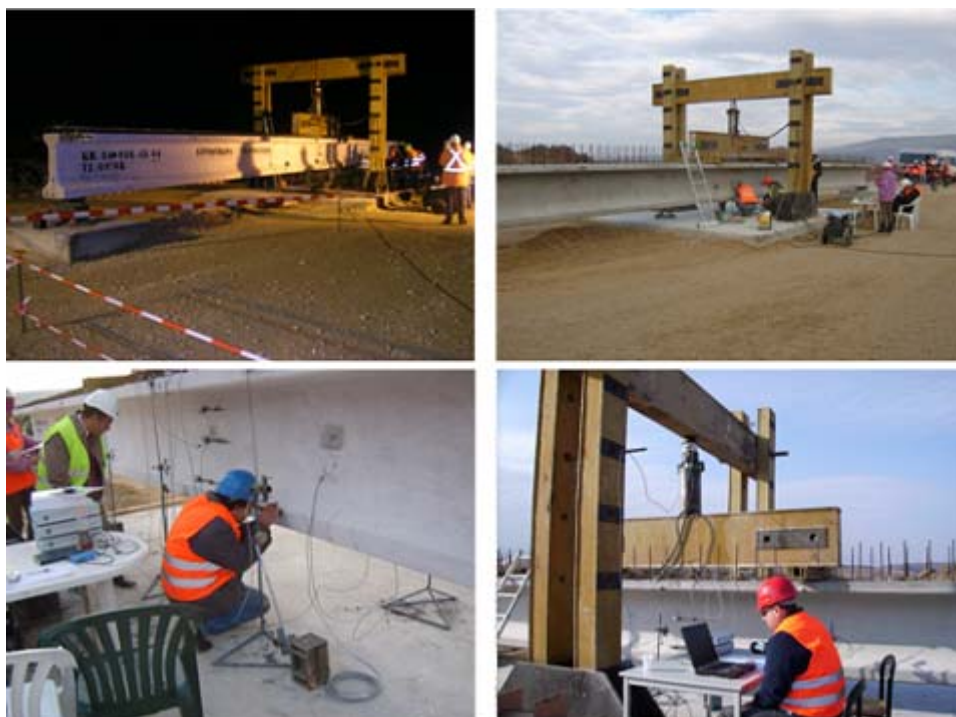


Figure 1. Sequences from the tests

2. CHARACTERISTICS OF THE PC MEMBERS

The self-weight of the PC members is 17.30 tons. Elements were designed with a concrete class C 35/45, with the mix characteristics given below:

- Cement type and content: I 42.5 R, 600 kg/m³ for T 48/34, 48/27 and 48/07, 450 kg/m³ for T 18/10 respectively;
- Water/cement ratio: w/c=0.4;
- Maximum aggregate size: 16 mm;
- Granularity zone: II;
- Slump class: T5.

Table 2 presents the effective concrete compressive strength determined by standard compression tests, in comparison with the design characteristics. Prestressed tendons consist in 38 strands TBP 12, 36 in the area of the bottom flange, and 2 in the superior flange, as shown in Figure 2. Passive reinforcement is made of steel PC 52 and OB 37.

Table 2. Concrete compressive strength at 28 days age of concrete

Beam ID	Effective cubic compressive strength at age of 28 days $F_{c,cube}$ [N/mm ²]	Design compressive strength [N/mm ²]		
		$F_{ck,cube}$	F_{ck}	F_{cm}
T 48/34	66.1	45.0	35.0	43.0
T 48/27	69.3			
T 48/07	65.7			
T 18/10	54.8			

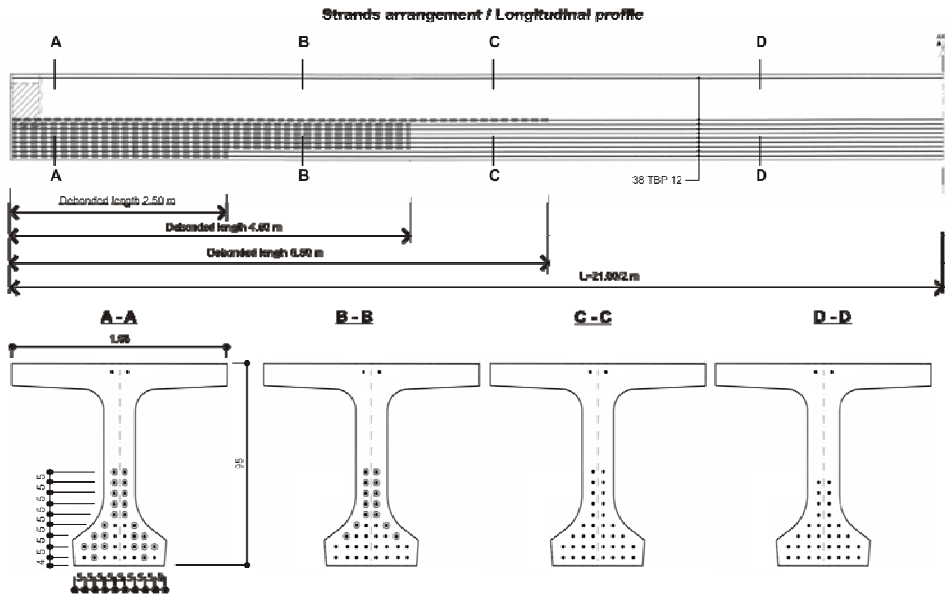


Figure 2. Active tendons layout, longitudinal and transversal profiles

No dimensional deviations were observed at the formwork removals. Until testing, the beams were kept into the open deposit of the manufacturer, near the technological platform. Transportation to the stand and handling was ensured by a mobile crane.

Prior testing, a non-linear analysis was performed in order to get a more accurate evaluation of the PC beams under consideration. Numerical algorithms developed by Mircea and Petrovay [2], [3] were assembled in a classical Newton-Raphson incremental scheme, implementing the CEB-FIB [4] constitutive model for concrete (the mean design cylinder compressive strength was considered as peak stress), bilinear with consolidation stress-strain diagrams for the active and passive reinforcement (resulted from the characteristic strengths and strains), and 12 % stress losses in the tendons. Figure 3 shows the results of the analysis at the mid span cross-section in the terms of moment – curvature relation.

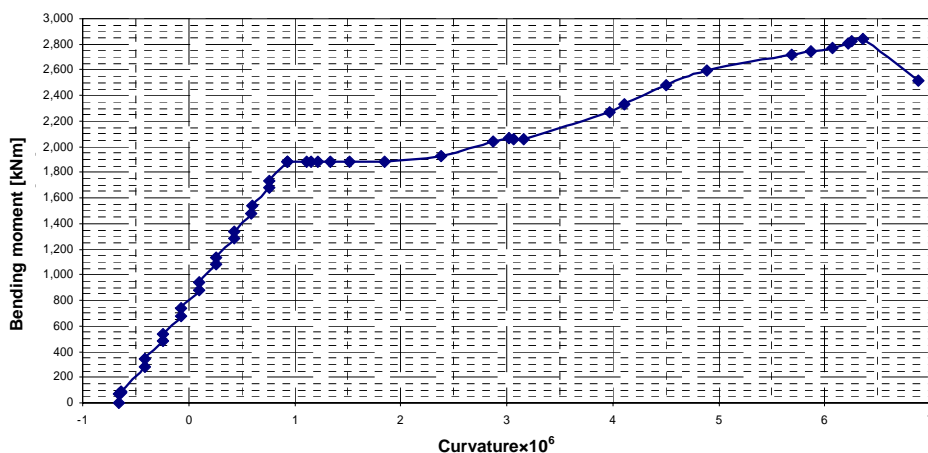


Figure 3. Moment-curvature relation in the mid span cross-section

Table 3 presents the deflections due to the negative camber of the PC specimens at transfer and before testing, in comparison with the calculated values.

Table 3. Relevant deflections due to negative camber after prestressing

Beam ID	Deflection due to negative camber [mm]			
	effective after transfer	before testing	design	numerical analysis
T 48/34	67	79	63	65
T 48/27	59	73		
T 48/07	61	76		
T 18/10	54	71		

The stress states of the mid span cross-section resulted from design and non-linear analysis are shown in Figure 4.

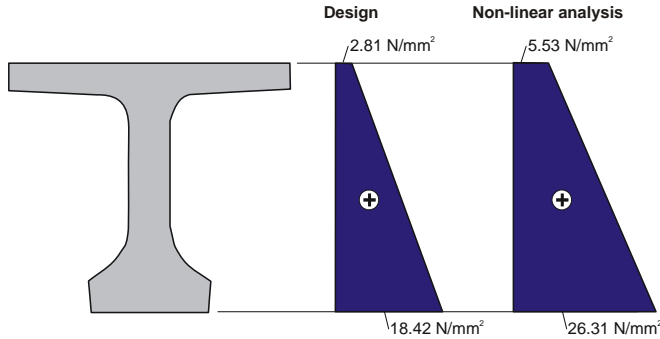


Figure 4. Theoretical compressive stress states in the mid span cross-section

3. TESTING PROCEDURE AND EQUIPMENT

The beams were subjected to statically bending tests through the non-destructive method, at loading levels corresponding to the Serviceability Limit States. The supporting and loading scheme is shown in Figure 5. Loads were applied in three cycles (see loading program in Figure 6), as follows:

At the cycles C_1 and C_2 , force P was increased in successive steps up to the values of 40 kN, 70 kN, 100 kN, 130 kN and 152 kN (i.e., load corresponding to the decompression moment). Unloading after each cycle was done considering half of the loading steps, the force P decreasing to 100 kN, 40 kN and 7.5 kN (i.e., level of the loading device weight);

In the third cycle C_3 , the force increased similarly up to 40 kN, 70 kN, 100 kN, 130 kN, 152 kN, 160 kN and 164 kN (i.e., load corresponding to the cracking moment). After the theoretical cracking load, because no cracking occurred, the force P was increased in small steps until cracking was initiated.

Readings were registered after the displacements and strains became stable, but not less than 15 min at the extreme steps, and 5 minutes at the intermediary steps.

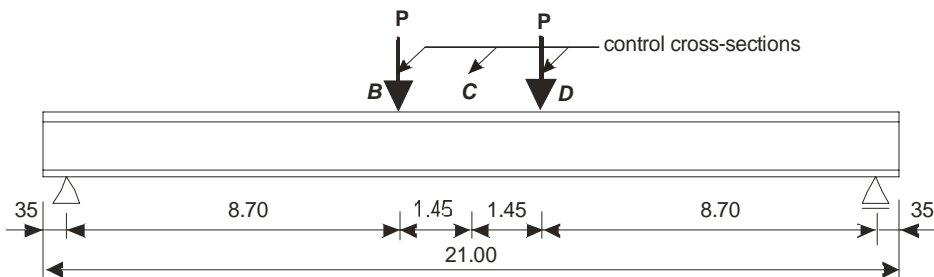


Figure 5. Loading and supporting scheme

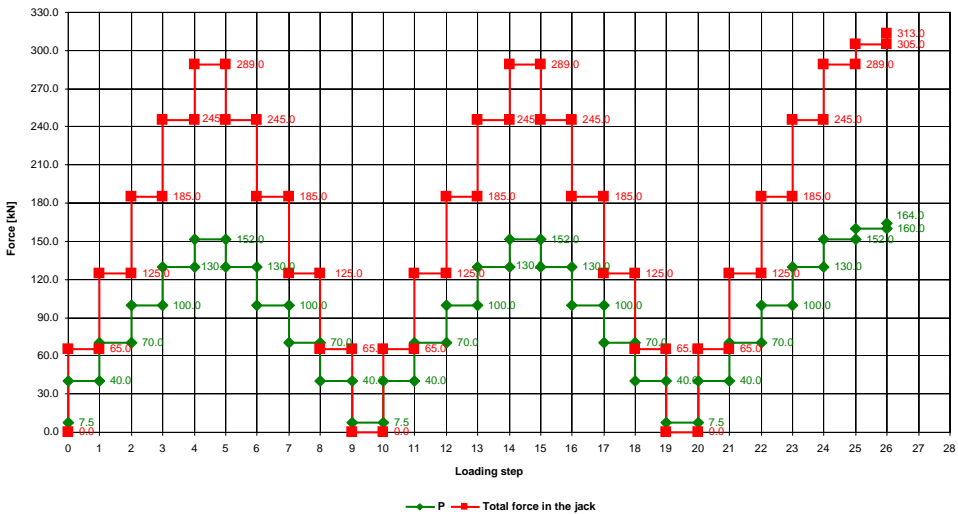


Figure 6. Loading program

Forces P were induced through a hydraulic jack of 1200 kN placed between a steel beam and the superior beam of the bearing frame (see Figure 1). Real time monitoring of the tests was ensured by the following equipment:

- One force transducer C6A/2000 kN placed between the hydraulic jack and the beam of the bearing frame;
- Displacement transducers HBM-WA/300 mm (10 devices) positioned on both sides of the elements, as shown in Figure 7;
- For the compilation of data and storage, a 12-channel measuring amplifier (Spider 8 - Hottinger) connected to a mobile PC station. Settings, data acquisition and processing were performed with the Catman Easy software.

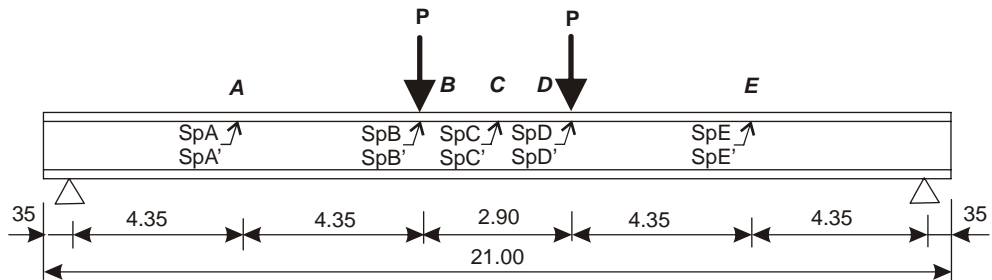


Figure 7. Loading program

Axial strains in the mid span cross-section (section C) were measured with one quarter bridge and for half bridge strain mechanical gauges with rod (precision class 10^{-2} mm), placed as shown in Figure 8. Figure 9 illustrates data registered by the real time monitoring system.

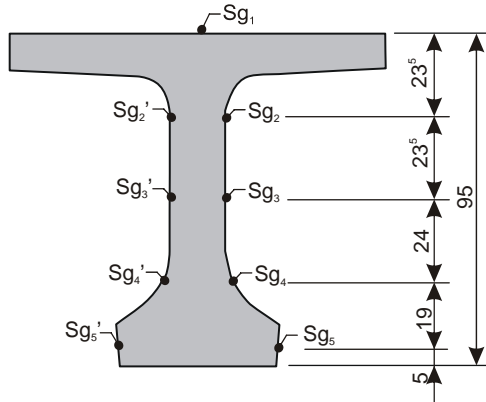
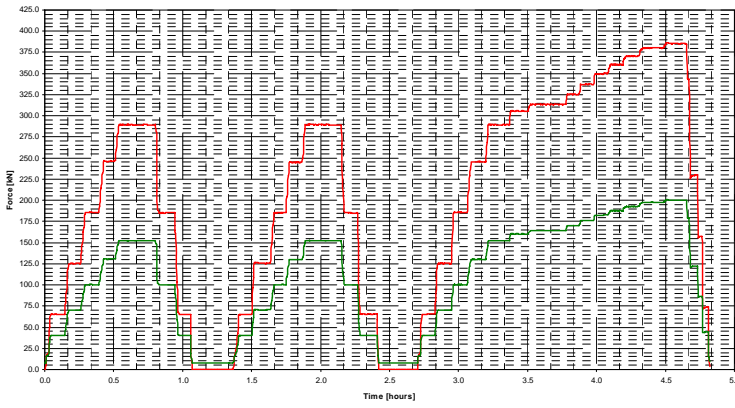
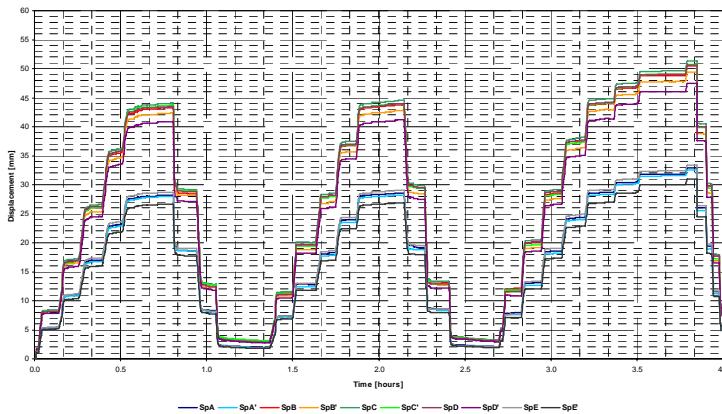


Figure 8. Position of the strain gauges at mid span cross-section



a. force variation at the first test



b. displacements evolution at the last test

Figure 9. Real time records for force and displacements

Supplementary and complementary to the digital monitoring devices of the displacements, mechanical deflection gauges were used to measure at the relevant stages the deflections in the control cross-sections (i.e., B, C and D) and at the ends of the elements

4. RESULTS AND COMMENTS

Figure 10 presents in a synthetic graphic manner the relevant data digitally recorded in the control cross-sections, both for loading and unloading parts of the three applied cycles (mean values of the displacement related to the total applied force). Figure 11 shows the experimental mid span deflections compared to the ones derived from numerical analysis and design.

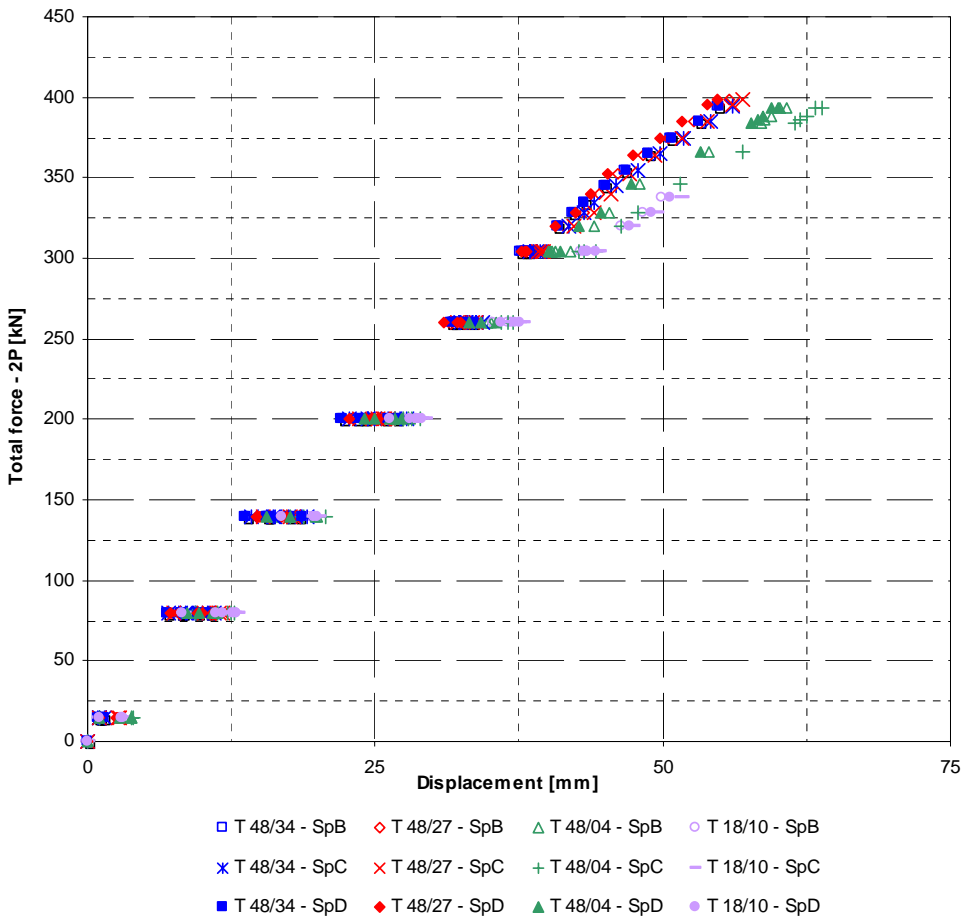
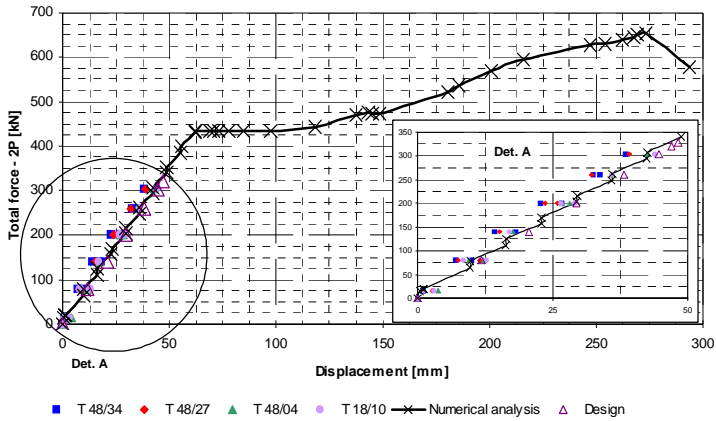
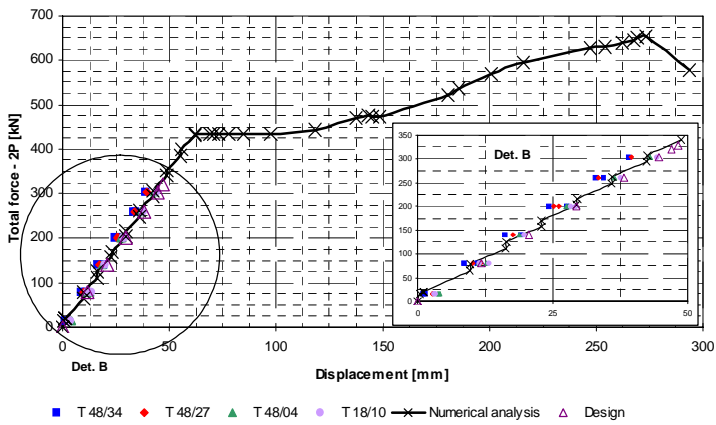


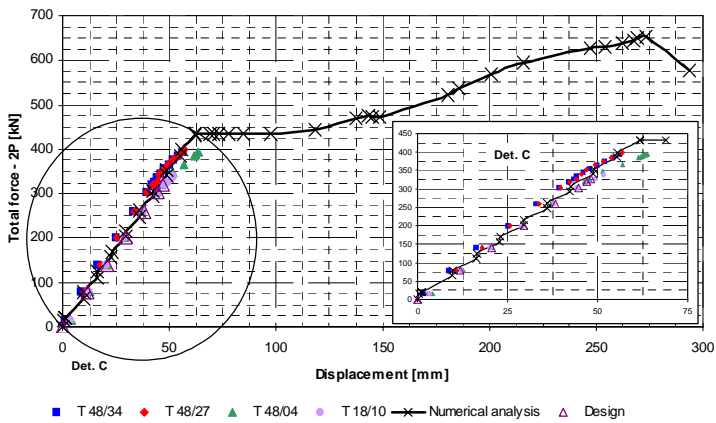
Figure 10. Significant force-displacement records in the control cross-sections



a. cycle C_1



b. cycle C_2



c. cycle C_3

Figure 11. Comparison of the theoretical and experimental mid span deflections

In the terms of displacements, maximum differences are 10 % between tests and design values, and 7.5 % between tests and numerical analysis values. These differences were registered at the first cycle (C_1), being reduced at the following cycles.

As Figure 11 shows, differences that are more significant appeared in respect with the cracking load. Table 4 presents the experimental and theoretical values of the cracking moment. In comparison with the design data, experimental values are conservative even at the last tested beam (T18/10), where due to a lower content of cement, recommended by the authors after a few tests, the effective compressive strength was much closer to the one asked by the design. In relation with the numerical analysis, effective cracking moments are lower up to 9 % for beams T 48 series, and up to 22 % for the beam T 18/10. This differences may be explained by the gross estimation of the stress losses, the age of the element at testing, and by the consideration in analysis of the constitutive model derived from the design mean cylinder compressive strength. However, all elements comply with the design criterion. As Figure 12 shows, at the decompression load (i.e. $P=152$ kN) that is equal with the characteristic load, all elements were under compressive stresses.

Table 4. Cracking moments and differences

Beam ID	Cracking moments [kNm]				
	test M_{ft}	design M_{fd}	numerical analysis M_{fna}	M_{ft}/M_{fd}	M_{ft}/M_{fna}
T 48/34	1,718	1,427	1,883	1.20	0.91
T 48/27	1,736			1.22	0.92
T 48/07	1,712			1.20	0.91
T 18/10	1,470			1.03	0.78

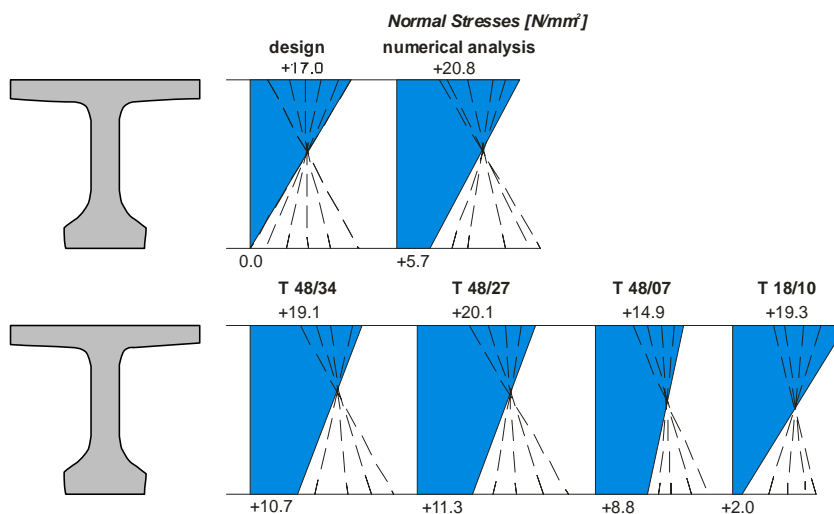


Figure 12. Normal stress in the mid span cross-sections - cycle C_1 (based on axial strains)

The same condition was met even at the third cycle (C_3). Figure 13 presents the experimental deflections diagram for the beams. Such as Figure 14 confirms, the beams satisfy the conditions with regard to deflections.

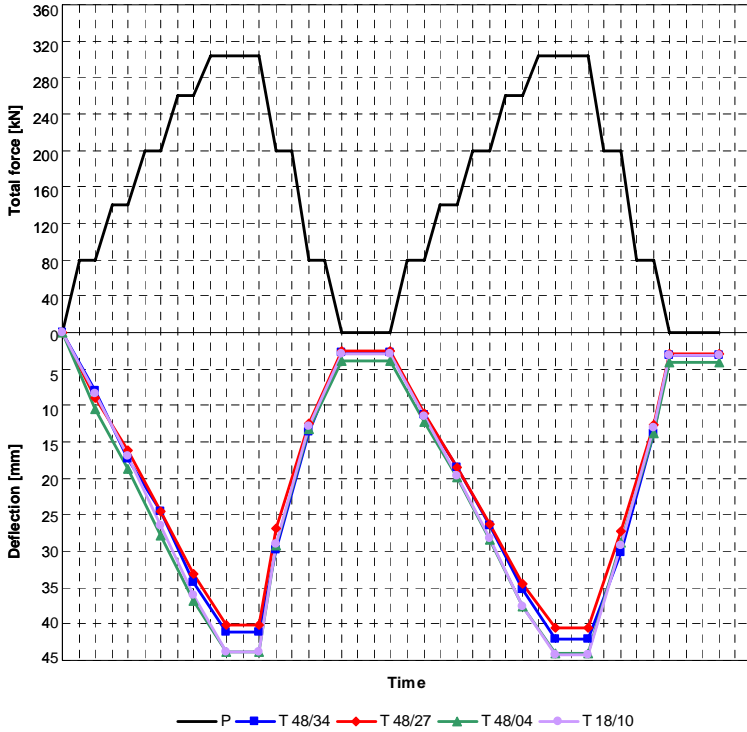


Figure 13. Deflections diagram at cycles C_1 and C_2

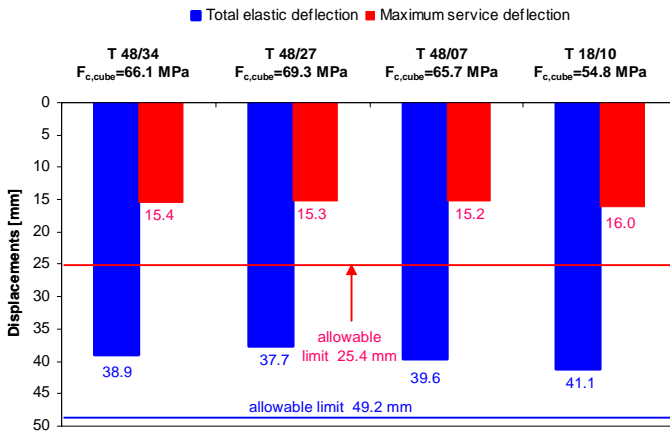


Figure 14. Mid span deflections at cycle C_2 and admissibility criteria

5. FINAL REMARKS

Besides compliance with the design and standard exigencies of the tested PC beams, tests also revealed a significant elastic capacity of deformation for all specimens. Plastic deformation coefficients were all well beyond 0.01, a very important characteristic for the future service. This feature was also noticed at the beams with spans of 15 m and 18 m.

All beams proved a predictable behavior, result of the adequate quality of the work made on the plant. Based on the experimental data, review of the mix content was also possible, resulting in a significant reduction of the cement consume. Future tests will be performed on 36.1 m span PC beams, with hollow cross-section.

ACKNOWLEDGEMENT

Tests were carried out with the support of the Structural Division from the Romanian branch of Bechtel International Inc. The authors wish to express appreciation to Ayhan Yeltik, Head of Division, Murat Olcer, Head of the Prefabrication Plant and Dragoş Munteanu, Manager of Spectromas Ltd. (official representative of HBM Hottinger Baldwin Messtechnik GmbH) for their support regarding this work.

References

1. STAS 12313-85 *Poduri de cale ferată și șosea: Încercarea pe stand a elementelor prefabricate din beton, beton armat și beton precomprimat.*
2. Mircea, C., Petrovay, G., Virtual Bitmaps Application in Sectional Analysis of Composite Members, *Proceedings of IASS International Symposium 2004*, Montpellier, France, September 2004, p. 272-273 (abstract) and 8 pp. in electronic CD-ROM format.
3. Mircea, C., Petrovay, G., New Approach in Non-Linear Sectional Analysis of RC and PC Members, *Proceedings of FIB International Symposium “Keep Concrete Attractive”*, Budapest – Hungary, 23-25 of May 2005, vol. II, p. 736-741.
4. EN 1992-1-1 Eurocode 2, *Design of Concrete Structures. General Rules and Rules for Buildings*, European Committee for Standardization, pp. 26-40.

GEODETIC MEASUREMENT OF LINE CONSTRUCTIONS FOR CONTROL AND SECURITY OF CONSTRUCTION RELIABILITY

Jana Neumanová

*Department of Special Geodesy, Czech Technical University in Prague, Prague, 166 29, Czech
Republic, jana.neumanova@fsv.cvut.cz*

Summary

The report appropriates to theoretic problems (correct terminology) in the area of geometric accuracy that affecting resulting quality the constructions. Further it is aimed to the applications of empirically intended tolerant intervals, especially to the non - parametric methods that it is possible bring to bear into verification of geometric accuracy of the roads and highways. These method have more general usage, the calculation is simpler and their characteristics are independent on the distribution of basic set.

In the next parts is described graphic model of geometric parameters like possibility to visualization results of geodetic control measuring of geometric accuracy. The graphic model is given from difference measured and project highs of line constructions by the help of izogram for individual constructional section.

KEYWORDS: Geometric accuracy, tolerance interval, non-parametric methods.

1. INTRODUCTION

The principal criterion influencing the final quality of the construction is the accuracy of geometrical parameters. The knowledge of geometrical parameters ensures the functionality, durability and reliability of constructions.

The methods of statistical checking represent an effective tool for check-up of geometrical accuracy. They bring reduction of geodetic fieldwork and cut in control measurement. They make possible objective decision making about the quality of checked data and at the same time they guarantee with a prescribed probability that only the statistical files will be accepted meeting the predefined requirements between the provider and customer. The utilization of statistical methods is the basic requirement for quality control application in accordance with ISO standards row 9000.

2. STANDARDS FROM THE AREA OF GEOMETRICAL ACCURACY OF CONSTRUCTIONS AND THE AREA OF APPLIED STATISTICS

The important standards are quoted directly in the text, further standards and sources are listed in the References.

2.1 Terminological standards

ČSN ISO 3534-1:1994 Statistics – Vocabulary and symbols Part 1: Probability and general statistical terms.

ČSN ISO 3534-2:1994 Statistics – Vocabulary and symbols Part 2: Statistical quality control.

2.2 Standards from the area of applied statistics and statistical data interpretation

ČSN O1 0250:1973 1973 Statistical methods in industrial practice – General principles, comments inclusive.

ČSN O1 0253:1976 1973 Statistical methods in industrial practice III - Basic distribution - free methods, comments inclusive.

ČSN ISO 16269-6:2007 2007 Statistical interpretation of data - Part 6: Determination of statistical tolerance intervals.

This standard describes procedures for determination of tolerance intervals that comprise at least a specified portion of the population with a fixed confidence level. Both one-sided as well as two-sided statistical tolerance intervals are offered where one-sided intervals possess either the upper or the lower limit and two-sided intervals are with both limits. Two methods are introduced: a parametrical one for the case when the studied characteristic has normal distribution and a distribution independent method for the case when no information about the distribution is available, but the fact it is continuous.

ČSN ISO 16269-8:2005 Statistical interpretation of data - Part 8: Determination of prediction intervals.

In this standard, prediction intervals are described that are applicable in practice whenever it is required to predict the results of a subsequent retrieval of a given number of discrete units on the basis of results of the previous selection of units produced under the same conditions. The intention of this standard is to clarify the differences between prediction intervals, confidence intervals and statistical

tolerance intervals and to provide procedures for some of the types of prediction intervals for which large newly calculated tables exist.

ČSN ISO/TR 10017:2004 Guidance on statistical techniques for ISO 9001:2000.

This technical report is a guide for selection of suitable statistical methods that may be appropriate for development, introduction, maintenance and improvement of quality management systems.

2.3 Standards from the area of statistical control

ČSN ISO 7870:1995 Control Charts – General guide and introduction.

ČSN ISO 8258:1994 Shewhart Control Charts.

The standard represents a guide of utilizing and understanding of the relation of control charts to methods for statistical control of production processes. This international standard is restricted to procedures for applying methods of statistical control via Shewhart Control Charts only.

2.4 Standards from the field of statistical acceptance

ČSN 01 0254:1976 Sampling inspection by attributes, comments inclusive.

ČSN ISO 2859-0:1997 Sampling procedures for inspection by attributes – Part 0: Introduction to the standard ISO row 2859 attribute sampling system.

ČSN ISO 2859-10:2007 Sampling procedures for inspection by attributes – Part 10 Introduction into standards ISO row 2859 for acceptance test by comparison.

This standard describes parts of ISO standards row 2589:

- ČSN ISO 2859-1:2000 Sampling procedures for inspection by attributes - Part 1: Sampling schemes indexed by acceptance quality limit (AQL) for lot-by-lot inspection, containing sampling systems for inspection of each lot from a continuous series of lots coming from one process and one provider.
- ČSN ISO 2859-2: 1992 Statistic acceptance by comparison - Part 2: Sampling procedures for inspection by attributes. Part 2: Sampling plans indexed by limited quality (LQ) for isolated lot inspection specifying sampling plans for situations where quality of individual or isolated lots is to be verified
- ČSN ISO 2859-3: 2006 Sampling procedures for inspection by attributes - Part 3: Skip-lot sampling procedures. It makes possible implementation of occasional acceptance for lots creating a continuous series and yielding higher quality levels than the AQL values contracted between the parties
- ČSN ISO 2859-4:2003 Sampling procedures for inspection by attributes - Part 4: Procedures for assessment of declared quality levels prepared for need of acceptance procedures that are suitable for systematic checkups such as screening

and auditing where the quality levels declared for a certain entity is to be verified - ČSN ISO 2859-5:2007 Sampling procedures for inspection by attributes - Part 5: System of sequential sampling plans indexed by acceptance quality limit (AQL) for lot-by-lot inspection. It is concentrated on plans by sequential sampling inspection and with escalated efficiency that corresponds to the efficiency used in ČSN ISO 2859-1 standard.

ČSN ISO 21247:2007 Systems of statistic acceptance with acceptance number zero and procedures of statistical control interconnected for product inspection.

It provides an interconnected system of acceptance plans and a system for statistical regulation of a process, that is worked out for acceptance plans with acceptance number zero together with statistical regulation of a process. It is applicable in all types of processes where acceptance by comparison or by variables is used and where the process has nature of a batch production. This system provides information about efficiency of the inspection system for each of the above mentioned variants. The information is supplied in the form of numerical values of operational characteristics both for acceptance probabilities at given quality levels as well as for quality levels in the process for given three levels (0,95; 0,50 a 0,10) of acceptance probabilities [1].

3. METHODS OF STATISTIC INSPECTION

Among the methods of statistic inspection it is necessary to mention sample inspection embracing statistic acceptance by comparison, by variable and statistic regulation.

For acceptance testing by comparison where no assumption about normal distribution is postulated, the procedure is the following one: When checking geometrical accuracy of constructions, factual deviations are sorted as conforming or nonconforming ones with respect to limit deviation given in the standard, project documentation, in testing and checking plans, in technological standards or in constructional technological procedures.

For acceptance testing by variables, the geometrical parameter is measured and its accuracy characteristics are stated.

In general, statistical regulation is intended for running processes.

When the construction technology is good and all the prescribed principles for measuring are met, but the tolerance interval according to standards, technical specifications etc. is too narrow, it means that the standard cannot be used without modification. In such a case, one should take account of specific properties of the construction process and to use **statistic tolerance limits** established in empirical

way according to hitherto behaviour of the construction process. Then, the limit deviations of geometrical parameters should result from those tolerance limits.

Statistic tolerance limits can be according to [2] either parametrical ones, when normal distribution is supposed, or non parametrical ones when no such supposition is made.

A reverse case may arise when the production process is not well fitted to limit deviations given in the standard etc. and therefore, it does not fulfil them. **To assess suitability of such a production process** is possible on the basis of statistical analysis and statistical regulation.

3.1 Suitability assessment of a production process

3.1.1 One-dimensional statistical analysis of process capability

Accuracy verification according to [3] is complemented by capability index of the control measurement in accordance with [4].

The capability index is calculated:

$$C_p = \frac{T}{2 \cdot u \cdot s} \quad (1)$$

Where T is (construction) tolerance,

u is standardized random variable (u is selected to be 2),

s is standard deviation of a sample.

If $C_p \geq 1$ then the process of control measurement is considered as suitable, for $C_p < 1$ the process is not suitable and it is necessary to proceed to its analysis via control charts [5].

3.1.2 Multi-dimensional analysis

In the real world, one encounters multi-dimensional analysis more frequently than one-dimensional data. E.g. when classifying geometrical parameters of line constructions, then there is, for each point, more than one value (X,Y,Z) measured. It is possible to separate the values and to analyze each of them separately by the methods of one-dimensional analysis, but, in such a way, not all the information available in the data is utilised.

When applying multi-dimensional analysis, it is necessary to consider the values as a random sample from a given distribution. The density of the standardized two-

dimensional distribution with components x_1, x_2 , zero expectations $\mu_1 = 0, \mu_2 = 0$ and unit variance $\sigma_1^2, \sigma_2^2 = 1$ is of the form

$$f(x_1, x_2) = \frac{1}{2\pi\sqrt{1-\rho^2}} \cdot \exp\left[-\frac{x_1^2 - 2\rho x_1 x_2 + x_2^2}{2(1-\rho^2)}\right] \quad (2)$$

where ρ is correlation coefficient . In case of more variables, matrix notation is used to put down density of m-dimensional normal distribution [6]:

$$f(x) = (2\pi)^{-\frac{1}{2}m} \sum^{-\frac{1}{2}} \cdot \exp\left(-\frac{1}{2}(x-\mu)^T \sum^{-1}(x-\mu)\right) \quad (3)$$

3.1.3 Statistic control

There exist one-dimensional charts (e.g. Shewhart control charts) as well as multidimensional control charts

One considers the stability of expectation μ , respectively of variance σ^2 with Shewhart control charts.

The analysis of geometrical accuracy via control chart, constructed according to [7] proceeds in such a way that upper control limit S_H is calculated according to:

$$s_H = \frac{T}{5.u} \sqrt{\frac{\chi_\alpha^2(n-1)}{(n-1)}} \quad (4)$$

Where T is (construction) tolerance and T/5 is limit error of the check survey,

u is the value of normalised random quantity (u = 2 if probability that the check survey process error is within limits p = 0,95),

$\chi_\alpha^2(n-1)$ is: α – critical value of χ^2 division, $\alpha = 0,05$ with (n – 1) degrees of freedom,

n is the number of checked points in one section.

Control charts make possible to analyze stability and grounds for a construction process not to be suitable due to the accuracy deterioration in one individual section or globally [4, 5, 8].

Let us mention, among the multi-dimensional control charts, the Hotelling control chart based on the Mahalanobis distance, the robust Hotelling control chart or PCA – control chart [6].

3.2 Statistical empirical tolerance limits

The boundary values of a statistical tolerance interval are tolerance limits. For an interval, there exists a fixed probability, so-called confidence level $(1 - \alpha)$, that the interval will cover at least a proportion p of the population from which the sample was chosen. The risk that this interval will cover less than portion p of the population is α (error of the first kind).

In inspection of geometrical accuracy of constructions, this method can be applied only when the units were chosen randomly from the population and are independent. Statistical tolerance interval can be one-sided or two-sided.

3.2.1 Parametrical tolerance interval

Parametrical tolerance limits suppose that the distribution of real deviations of a geometrical parameter is the normal one.

The standard [9] sets down a calculation procedure for two-sided as well as one-sided tolerance interval when the distribution of the observed characteristic is the normal one. Two alternatives are considered here. Namely, the first alternative supposes that standard deviation σ of the population is known and that the mean of the population is unknown. The second alternative supposes that both mean and standard deviation are unknown.

When know just sample characteristics \bar{x} a s^2 of the random sample of size n , it is not possible to set the limits covering the proportion p of the population with certainty. However, in such a case, it is possible to determine at least the limits that will cover the proportion p of the population with a given probability $1 - \alpha$. The ignorance of standard deviation σ of the population has to be paid for by certain "taxation" i.e. by extension of the tolerance interval.

Two-sided tolerance limits are of the form:

$$\bar{x} \pm ks \tag{5}$$

where \bar{x} is sample mean and s is standard deviation of a sample of a random sample of size n .

The constant value k is dependent on n, p a $(1 - \alpha)$ [10]. The most usual values of confidence level are 0,95 and 0,99 ($\alpha = 0,05$ a 0,01).

As majority of populations of geometrical parameters does not have the normal distribution, it is necessary to utilize non-parametrical methods for their inspection.

3.2.2 Non-parametrical tolerance interval

The properties of non-parametrical tolerance interval are independent of the population’s distribution.

In [9] supplement A, the determination of statistical tolerance interval is described for arbitrary distribution. The method mentioned makes use of extreme values in the sample.

For one-sided limited dispersions, the following formula, between sample size n , confidence level $(1 - \alpha)$ and proportion p of the population over x_m (the least value in the sample) or under x_M (the greatest value in the sample), is valid:

$$p^n = \alpha \tag{6}$$

If the values of p a $(1 - \alpha)$ are fixed, it is possible to determine the minimal sample size n for which one can claim with probability equal at least to $(1 - \alpha)$, that over x_m (the least value) or under x_M (the greatest value) in the sample the proportion of the population will equal at least p .

For two-sides limited dispersions, the following formula, between sample size n , proportion p of the population that lies between x_M (the greatest value in the sample) and x_m (the least value in the sample) and confidence level $(1 - \alpha)$, is valid:

$$np^{n-1} - (n - 1)p^n = \alpha \tag{7}$$

If the values p a $(1 - \alpha)$ are fixed, it is possible to determine the minimal sample size n for which one can claim with probability equal at least to $(1 - \alpha)$, that the portion of population laying between the least and the greatest value in the sample will equal at least p .

The sizes n are tabulated as functions of p and $(1 - \alpha)$, see tab.1 [10].

Tab. 1 Sample sizes n for proportion p at confidence level (1-α)

p \ 1 - α	0,90	0,95	0,99
0,90	38	77	388
0,95	46	93	473
0,99	64	130	662

4. GRAPHICAL DEVIATION MODEL

In this part, the graphical deviation model of geometrical parameters is drawn attention to as a possibility for visualisation of results of geodetic measurements of geometrical parameters coming from the differences of measured and project heights with the help of isolines for separate construction levels.

Basically DMT are used for analysis and visualisation of measurement results for geometrical parameters of line constructions. To build the model, software system Atlas DMT KresCom is used.

In the first case, the digital model of the project and of the actual state is created from the project coordinates and heights whereas in the second case, measured coordinates and heights of points for separate construction levels are used.

Further, the deviation model of the project and actual state can be created. The building of the model is more intricate since it is necessary to recalculate all the heights of the project points (as project points coordinates are not identical with coordinates of the points really measured).

The differences between the heights measured and modified in the project form and the original project heights are calculated. Then finally, the deviation model for separate construction layers is built [11].

7. CONCLUSION

The contribution is devoted to the theoretical problems in the area of geometrical accuracy that influences the final quality of constructions. Further, assessment of suitability of a production process (both one-dimensional and two-dimensional), application of empirically found tolerance intervals and especially, non-parametrical methods are discussed. These methods can be used for check-up of geometrical accuracy of line constructions. Their calculation is simpler and their properties are independent of the distribution of the population.

Next, graphical deviation model of geometrical parameters is described as a possibility for visualisation of geodetic inspection results for geometrical accuracy.

Acknowledgements

This research has been supported by internal grant CTU0703811 Non-parametrical methods and their usage and application in engineering geodesy.

References

1. Horálek, V.: *Standards ČSN a ČSN ISO from the area of applied statistics*, Workshop The new and under preparation standards ISO from the area of applied statistics, [Proceedings of the workshop], ČSĽ, Praha, 2007.
2. ČSN 01 0253:1972 *Statistical methods in industrial practice III. Basic distribution-free methods* (010253).
3. ČSN 73 0212-4:1994 *Geometrical accuracy in building industry. Accuracy checking. Part 4: Line structures.* (730212).
4. ČSN ISO 8258:1994 *Shewart control charts.* (010271).
5. Neumanová, J., Vorel, V.: *Suitability analysis of the process of check survey of roads*, Workshop 2007, Prague CTU, 2007, Part B, p.646-647.
6. Kupka, K.: *Multi-dimensional analysis and prediction methods*, [Firm material], TriloByte, Pardubice, 2007.
7. ČSN ISO 7870:1995 *Control Charts – General guide and introduction.* (010272).
8. Matějka, Z.: *Geometrical accuracy of constructions*, 1.imp., Montanex Ostrava, 1999, 119 s.
9. ČSN ISO 3207:1993 *Statistical interpretation of data. Determination of statistical tolerance interval.* (010232).
10. ČSN 01 0250:1972 *Statistical methods in industrial practice. General principles.* (010250).

Considerations Regarding the Quality Costs in the Process of Total Creation of a Bridge

Nicuță Alina Mihaela¹, Ionescu Constantin²

¹Faculty of Civil Engineering and Building Services, Iași, Romania alinush1905@yahoo.com

²Faculty of Civil Engineering and Building Services, Iași, Romania, cionescu@ce.tuiasi.ro

Summary

The necessary costs for a high quality must be evaluated in order to be able to predict and control the total cost for quality.

Quality costs have the purpose to assure a good quality on a long period of time. The idea is to consider the principle of the work "well done from the first time".

In order for a construction to fulfill the principles of quality system is necessary to create equilibrium between quality and costs. The decrease in quality determines an increase of the costs. Quality costs are the costs due to the NON creation of a quality product or service.

The quality system has two types of costs: quality costs and non-quality costs. First of them include prevention costs and evaluation costs. The other ones include the costs of internal faults and costs of external faults. The paper will present some examples of detailed activities that determine these costs. Each and every cost is influenced by its own specific activities.

The quality costs implied by a bridge construction are of different types. Some of them are rarely taken into consideration in the bridge construction phases. Other are known but formulated differently or too small to be expressed in a project and so are included in other costs as a percent value. Can be mentioned here the direct, indirect costs, opportunity costs or costs in control or out of hand, fixed or variable costs.

Currently there isn't a unified or strict determination of the costs components for the area of bridges. Researchers have transferred some of the general cost components to the construction area.

In order to create a unified quality cost system for the area of bridge engineering is necessary to take into consideration the phases of the bridge construction which means design, execution, exploitation and post-utilization with the included proper costs.

The paper wishes to be an introduction to this unification and determination process of the quality costs.

KEYWORDS: quality costs, bridge, users, efficiency.

1. INTRODUCTION

The quality costs problem must be treated in concordance with user's exigency but in the same time must be considered the financial resources available for the needs fulfillment.

A construction work quality is a balance between user's needs and the capabilities to satisfy them.

The quality cost can be considered a very complex and sometimes wrong understood. He isn't the price of creating a quality product or service. It is the cost of NON creation of a good product or service. The quality cost components have a traditional approach. The standard approach contains the costs for prevention, valuation and deficiency. This last one contains the internal and external failures. The objective in the determination of these costs is diminishing the total cost for quality.

Considering these general considerations this paper presents a new approach of quality costs specialized for the bridge area. This approach takes into consideration the steps in a bridge life time.

There are several obstacles in order to create a financial evaluation of this type due to the complexity of the necessary information but also to the difficulty of gathering the data.

2. THE IMPORTANCE OF SATISFYING THE USERS EXIGENCIES

In order to satisfy the user's needs first is necessary to know them. For this it is necessary a strict monitoring and measurement of the user satisfaction.

There are more information sources in order to collect, analyze and use these information in view of improving the performance of the organization.

The transport agency must establish and use the information in order to satisfy the needs and anticipate the next ones.

An organization must plan and establish the processes in order to follow the “user voice”. Planning these processes should define and implement the data collecting methods, collecting frequency and data analysis.

Examples of information sources referring to the user satisfaction contain:

- User petition,
- Direct communication with users,
- Questionnaire,
- Subcontracting of data collecting and analysis,
- Focus group¹,
- User's organizations reports,
- Reports from mass media,
- Fields and industrial researches etc.

The transport agency is integrated in a input – output process where considering the information the agency take decisions and implements them.

The interested parts are:

- Final users,
- Transportation agency personnel,
- Owners – investors,
- Partners and providers,
- The agency itself,
- The society, more exactly the community and public affected by the construction work etc.

Seen as a degree of need satisfaction, the quality has a great subjectivism. It is influenced by the user social level, education, temperament, artistic sense, requested and expected satisfaction etc.

The quality can be considered as a correspondence between technical, economical and social characteristics of a construction work.

The quality for a bridge construction work is influenced by technical, economical and social elements.

In order for a system to fulfill the optimal state is necessary to consider parameters as the system efficiency, value, utility. This gets to a combined analysis between efficiency and cost.

The bridge efficiency is the measure in which this performs to the established parameters or fulfills the determined objectives.

¹ Focus Group is a qualitative method of market search by which a group is being selected by sampling.

3. QUALITY EVALUATION

A bridge construction quality can be considered from the economical point of view as a synthesis of programming, organization, ways of communication and other elements in the technical – material base.

The notion of quality has a complex content, “a product quality is a notion too general, too vast and too complex in order to have a brief definition”².

The quality has these main characteristics:

- Perfection,
- Consistence,
- Speed of execution,
- Concordance with norms and standards,
- Good performance from the beginning,
- Users need satisfaction.

The central element of the quality is the consumer/user (for transportation) with its needs and expectations.

4. QUALITY COSTS IN STANDARD AND NEW APPROACH

The quality costs can appear in every step of the bridge life cycle but also in all the operational levels of the transport agency. The quality cost is a very often used term and many times misunderstood.

Each and every time a work needs to be redone, the quality cost grows. Every unexpected cost contributes to the quality cost.

The standard approach of the quality costs considers:

- Prevention costs: costs of the projected activities for the prevention of bad quality of the construction work,
- Evaluation costs: costs associated with measuring, evaluation or audit in order to assure the conformity with the quality standards and performance,
- Failure costs: costs resulted from the construction works which aren't in conformity with the user's or agency's needs. Failure costs are of two types: internal and external costs.

² Definition gave by a group of French researchers from the French association of Quality Industrial Control

- Internal failure costs: costs of the failures which appear before the exploitation of the bridge.
- External failure costs: costs that appear after the bridge exploitation,

There isn't a general model in order to determine these costs same as it doesn't exist a general classification of the quality costs components.

A new approach of the quality costs which is specialized for bridge construction works has as starting point some ideas in the "Transports Quality" of Toader Gherasim.

This new approach take into consideration in particular for the bridge construction works complementary cost elements, which hadn't been considered before. I am talking about some small particular cost components which are included in the four big components from the standard approach.

Figures 1 and 2 consider the "Identification of quality costs in bridge engineering area" and the "Interactions regarding the quality in the constructions from the point of view of the concept of quality technical expertise for a bridge".

The first figure considers the steps in a total creation of a bridge: design – execution – exploitation – post-utilization with the components in the process and which impose the determination of several quality elements with its costs.

The second figure refers to the interactions regarding the quality in constructions from the point of view of technical expertise for a bridge quality.

The new approach takes into consideration as costs components:

1. Deficiency prevention costs:
 - Costs at minister and department level: costs for the creation of norms and standards for quality.
 - Costs for the control of bridge construction development or control organisms: documentation for the construction quality, work security, personnel instruction.
2. Quality determination costs
 - Quality control cost: intermediary and final control,
 - Costs for the data processing and analysis from the quality control area.
3. Deficiency removal costs
4. Quality improvement costs
5. Controllable and uncontrollable costs
6. Direct, indirect and opportunity costs
7. Stable and variable costs

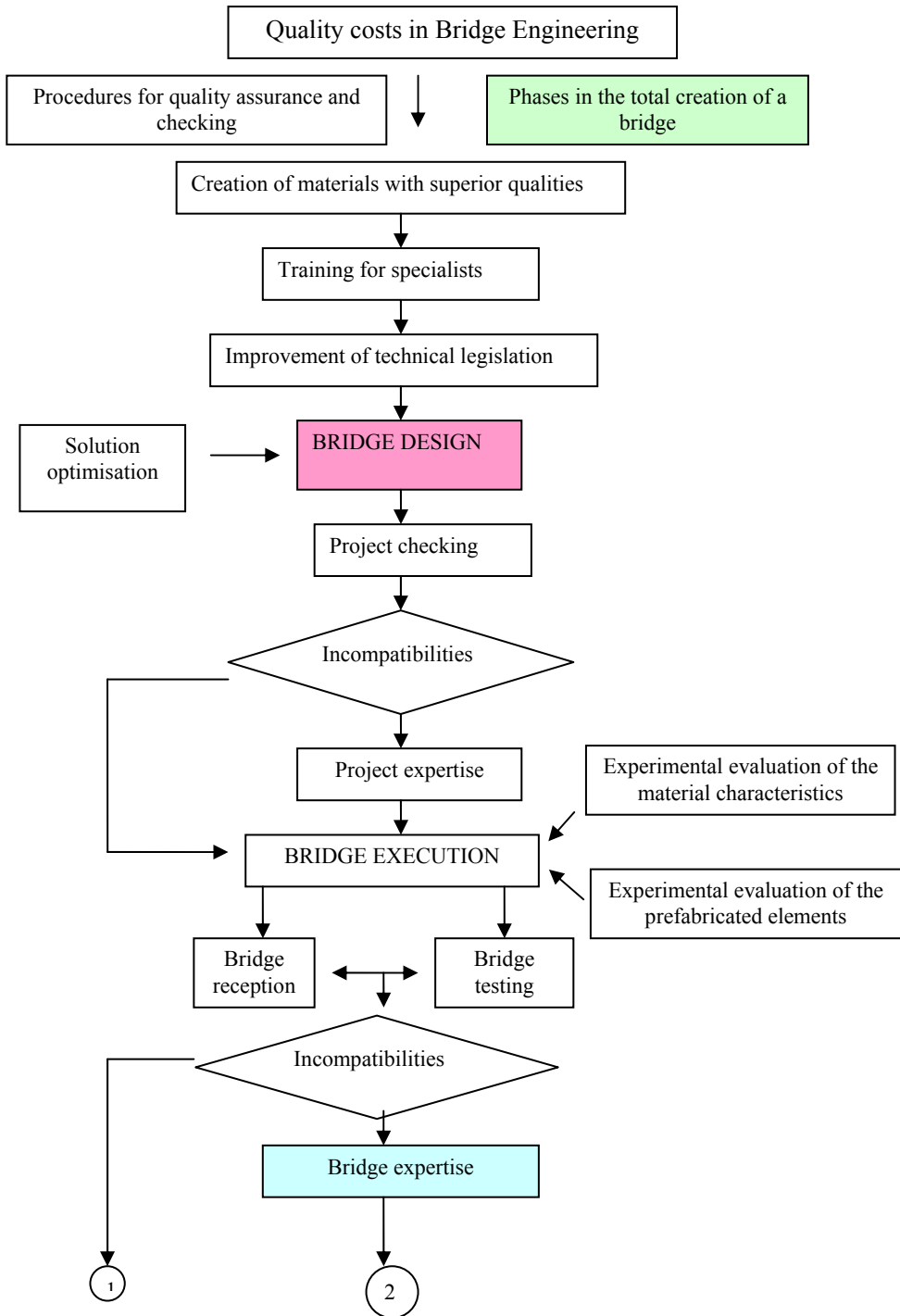


Fig. 1 Quality Costs Identification in Bridge Engineering

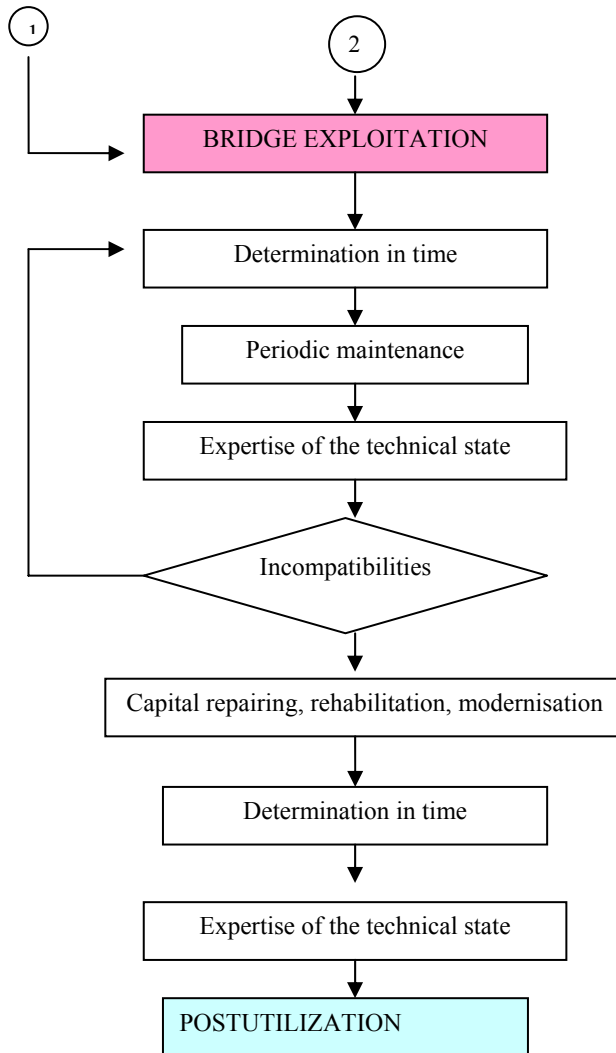


Fig. 1 Quality Costs Identification in Bridge Engineering (continuation)

Interactions regarding the quality in constructions from the point of view of the technical expertise concept of a bridge quality

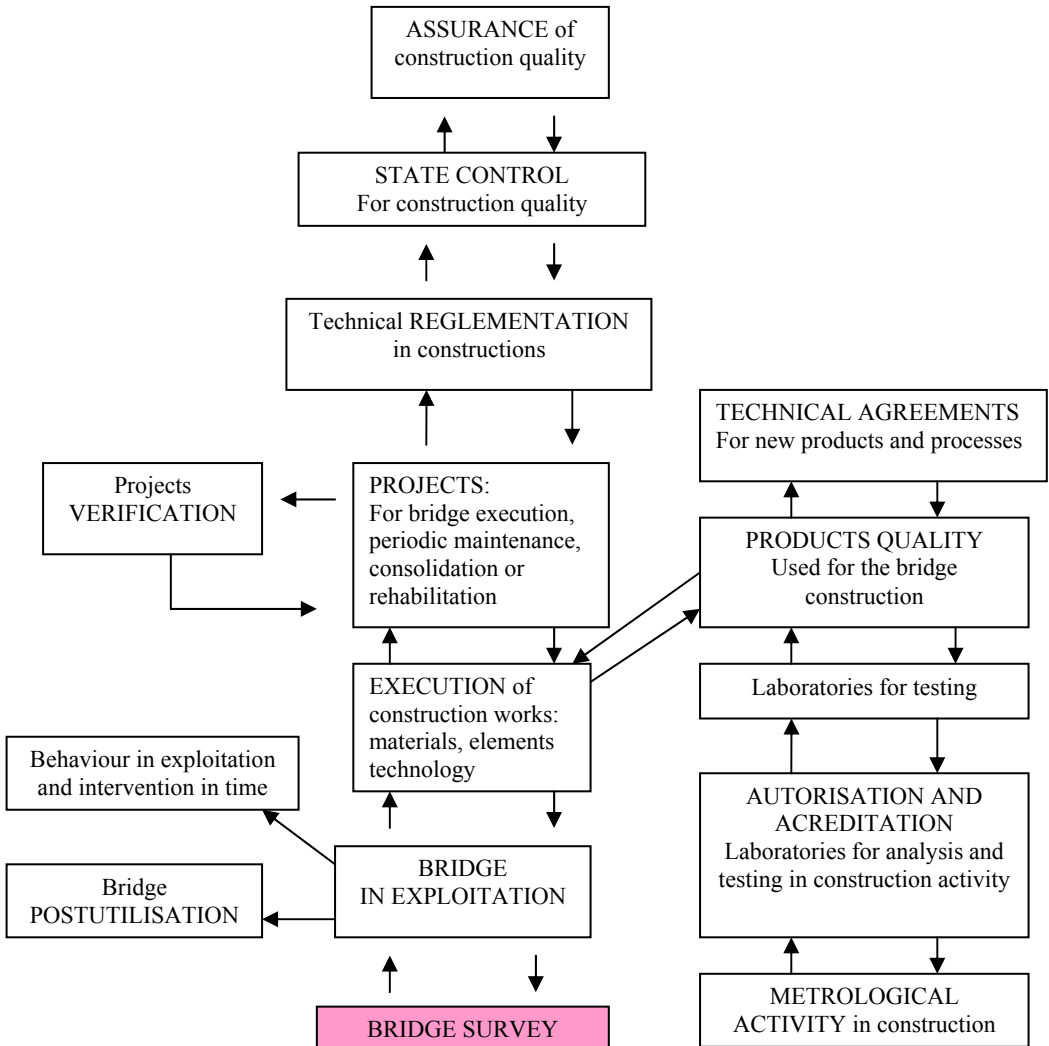


Fig. 2 Interactions on Quality from the Point of View of Quality Technical Expertise of a Bridge

There is a lack of unity between the components of the Total Cost for Bridge Quality and also some of them have a casual use.

The new approach of the quality costs proposes a model which takes into consideration all these costs with a proportional value in the total cost of the quality. Figure 1 and 2 are necessary in order to establish connection between the phase of the bridge engineering and the costs associated with the phase.

5. CONCLUSIONS

The various aspects of the quality must be considered in connection from the point of view of the user, available financial resources, information components and the society. In order to support the idea of “work done perfect from the first time” is necessary to change the working concepts.

The complexity of the quality analysis system, the diversity of approaches regarding the quality costs leads towards a unified costs system for bridge engineering.

The area of total quality costs and its long term applications is a very critic and various one. The challenge is to use fewer resources, to do rare interventions and to have a better quality. So that can be obtained is necessary a better administration of the quality costs components, their uniformity and an extent of cost components towards more detailed elements.

References:

1. Agnone A.M. (1989), Quality cost measurement and control, in Grimm A.F. (Ed. Eds), Quality Costs: Ideas and Applications. A collection of Papers, Quality Press, Milwaukee vol I p 77-89.
2. Beard C (1993) ISO 9000 in the building and construction industry, Kuala Lumpur, seminar on Quality in the Building and Construction through ISO 9000,
3. CIDB (1989), Managing construction quality, A CIDB Manual on Quality Management Systems fro Construction Operations, Construction industry Development Board, Singapore,
4. Gherasim T., Calitatea transporturilor, Ed. Univ. Al.I.Cuza, Iasi, 1997.
5. Niculita L., Managementul si ingineria calitatii, 2005,
6. Olaru M, Costurile referitoare la calitate, în Managementul calității, ediția a IIa,

Pavement Recycling: an environmentally sustainable rehabilitation alternative

Joel Oliveira¹, Hugo Silva² and Paulo Pereira³

¹Department of Civil Engineering, University of Minho, Guimarães, 4800-058, Portugal,
joliveira@civil.uminho.pt

² Department of Civil Engineering, University of Minho, Guimarães, 4800-058, Portugal,
hugo@civil.uminho.pt

³ Department of Civil Engineering, University of Minho, Guimarães, 4800-058, Portugal,
ppereira@civil.uminho.pt

Summary

The preservation of environment by reducing the use of material and natural resources together with important economic savings have led pavement recycling to be a prime solution for pavement maintenance/rehabilitation. It is based on sustainable development, by reusing materials reclaimed from the pavements and reducing the disposal of asphalt materials.

The present paper focuses on the analysis of a heavily trafficked urban road rehabilitation project. The original pavement design did not take into account the current traffic levels which are considerably above the initial values. The pavement was reaching failure in several areas and needed urgent measures to avoid complete failure. The pavement condition was a result of lack of structural strength and a deficient drainage.

A semi-rigid pavement structure was proposed in order to improve the bearing capacity of the pavement and minimize the maintenance operations in the future. The operations involved cold "in situ" recycling of part of the existing bituminous layers and the top part of the granular layers with the addition of cement, and the overlay with new bituminous mixtures incorporating a significant percentage of materials reclaimed from the surface course of the same pavement. This solution allowed the maintenance of the pavement level (without the need for footpath reconstruction) and minimized the use of new materials, contributing towards a sustainable development.

KEYWORDS: pavement rehabilitation; cold "in situ" recycling; hot in plant recycling; cement.

1. INTRODUCTION

Nowadays, local and international authorities and organisations are seriously concerned about the disposal of waste materials and its impact in environment. Therefore, its elimination (and any by-products) passes through the optimization of their use in the industrial processes. Existing deteriorated material can be reused; its characteristics can be rehabilitated, recycled and improved. The old material can be successfully reused for what it was initially intended, or as part of a new material [1]. If the recycling process is carried out in plant, only temporary deposits to store the old material will be needed before it is mixed with the new material. If the process is undertaken “in situ” no storage will be needed.

From a study about recycled material applied on surface courses [2], it was proved that the most conditioning factor in the production of recycled mixtures with at least 50% reclaimed material is the maximum temperature at which new aggregates are heated in plant. Besides, researchers did not verify any undesirable effect on the properties of the mixtures with a high percentage of recycled material.

Potter and Mercer [3] carried out a study including several trials on public roads and on full-scale accelerated load testing facilities. They evaluated the performance of recycled materials used in the construction of sections of these trials. One of the main conclusions of the study was that the performance of the recycled materials was as good as that of equivalent conventional materials.

Another research carried out by Servas et al. [4] included the assessment of the mechanical properties of hot bituminous mixtures after the incorporation of reclaimed material in different percentages (0, 30, 50 and 70%). In that study, no clear correlation was found between the percentages of recycled material and the properties of the resulting mixture. Therefore, given an adequate mix design, the amount of recycled material to be included depends upon other factors related to the material itself, the type of plant used and even economic and ecological policies.

The rate of reclaimed material to be used can be limited by several factors, which include [5]:

- Grading;
- Aggregate properties;
- Binder properties;
- Heating, drying and plant capacity;
- Moisture of the reclaimed material and new aggregates;
- Temperature at which new aggregates need to be heated;
- Ambient temperature of the recycling material and new aggregates;
- Other factors.

A research study carried out by Oliveira et al. [6], to assess the benefits of including recycled materials in pavement design, has shown that the costs of applying a recycled mixture (with up to 50% reclaimed material) as a base or binder course were reduced by more than half, when compared with the costs of applying a new bituminous mixture, for the same expected life. The authors emphasized that a high amount of reclaimed material was used to produce the recycled mixture. This is practicable only if the right batch plant is available. Nevertheless, the study showed that it is worth to invest in the right technology.

This paper presents a case study, which comprises a heavily trafficked urban road (approximately 3 km long) linking the city of Braga with the Portuguese highway network. The traffic assessed during this study showed an Average Annual Daily Traffic (AADT) value of about 50000 vehicles, 2000 of which were classified as heavy vehicles. The road cross-section comprises a dual carriageway, each with three traffic lanes, along 1 km, and two traffic lanes along the other 2 km.

Although the pavement has been in service for less than 15 years, several maintenance operations have already been carried out, including overlays and surface course replacements in some areas. Nonetheless, the pavement is reaching failure in a major part of the length. Visual observation of the pavement condition showed a high level of degradation for several distress types, namely rutting and alligator cracking.

The best solution to repair cracking is by eliminating it. A plausible and highly recommendable solution may consist of milling the cracked layers. The milled material could be reused in plant or recycled “in situ”. Control and elimination of cracking is one of the advantages of pavement recycling if compared with structural overlaying.

2. TYPES OF RECYCLING TECHNIQUES

Producing bituminous mixtures by using reclaimed materials may be carried out using hot or cold production methods. Both alternatives may be undertaken in plant or “in situ”.

In hot recycling processes, in general, the recycling ratio may vary between 10% and 40% depending on the type of procedure and on the type of plant used. These values are generally lower than those observed in cold recycling, which reaches nearly 100% in most cases.

The differences among the various in plant recycling processes reside in the type of plant used, fixed or portable, continuous or batch production, and in the production processes which may be diverse. On the other hand, “in situ” recycling techniques differ from each other essentially on the type of binder used. For instance, the same

equipment can be used for cold “in situ” recycling using bituminous emulsion, foamed bitumen or cement as binder.

In general terms, hot in plant recycling involves the following stages:

- storage and preparation of the reclaimed asphalt pavement material (RAP), whose size needs to be reduced through fragmentation, and make it more homogeneous;
- study the mix design of the final mixture (including the reclaimed material);
- production of new bituminous mixtures using old and new materials ;
- application of the resulting bituminous mixture by using traditional methods and equipments.

Cold recycling is a rehabilitation technique generally used to solve structural problems in flexible pavements. Thus, it may be used for rehabilitating either one or more bituminous layers in poor condition or even including part of the granular layers underneath. This type of operation is usually finished by overlaying the recycled layer by one or more traditional bituminous mixtures.

Lately, “in situ” cold recycling with cement has been widely used in Europe, especially in Germany, France and Spain, where it has been applied successfully. This development owes its success to three main factors:

- a better knowledge of the mechanical characteristics of the material modified with cement;
- the development of a more powerful equipment that provides more efficiency and working depth;
- an ecological aware attitude which promoted this technique in view of the benefits for the environment.

The cement used in pavement recycling develops the bearing capacity of the layer more rapidly and allows pavement recycling of deeper layers in contrast with recycling with bituminous emulsion. Thus, it is an adequate way for situations in which a considerable increase in the pavement bearing capacity is intended by using the less number of new layers. The cohesion and resistance of cement-recycled layers increase throughout time, what means a higher stability and bearing capacity under variable moisture conditions, allowing the use of materials with lower quality. On the other hand, recycling with cement does not require a so long curing time as emulsion recycling mixtures do. Therefore the surface course may be applied more rapidly. The main inconvenient of recycling with cement is the natural appearance of surface cracking, due to shrinkage of the recycled layer (transversal cracks spaced from 5 to 30 m).

The cement may be mixed through different processes: i) spread as powder over the pavement before the action of the recycling equipment, which will mix it with the milled material and will add the necessary hydrating moisture; (ii) spread as powder by the recycling equipment, just before the milling/mixing chamber; (iii)

placed directly in the milling/mixing chamber as a cement slurry through the spraying nozzles (Figure 1).

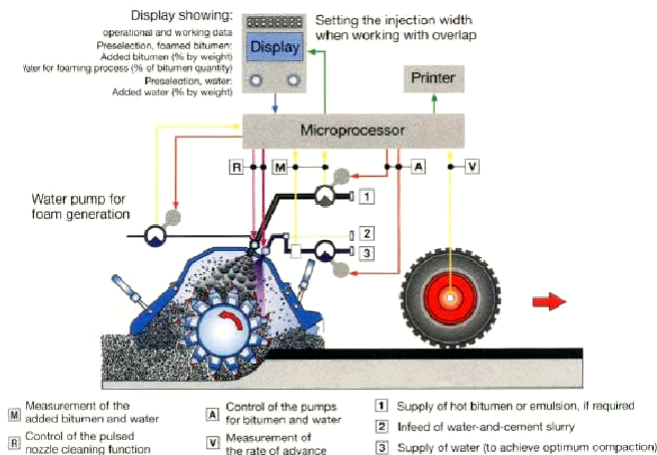


Figure 1. System for the injection of the binder and water in the milling/mixing chamber of the recycling equipment [7]

Compaction should immediately follow the mixing process. It is carried out by several passes of a roller compactor with vibration over the new layer and/or a pneumatic cylinder. After the first passes of the roller compactor, the surface level shall be corrected by means of a grader over the compacted layer and then further passes of the compacting equipment shall be made, [8]. The entire process needs to be carried out immediately after recycling because of the limited manoeuvring time, before the cement starts to set, which should not exceed 2 to 3 hours under good conditions. Under high ambient temperatures, a water tank should be available “in situ” to moisten the surface of the recycled material in case of excessive evaporation. In order to prevent the evaporation, a layer of tack coat should be sprayed over the surface. This allows the hydration of the cement and an adequate curing of the recycled material.

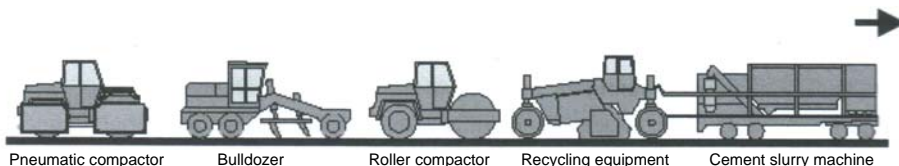


Figure 2. Equipment used in the recycling operation [8]

Amongst other reasons, the success of recycling with cement depends on the mechanical characteristics of the reclaimed materials and on a correct mix design study of the layer that is to be recycled.

3. MIX DESIGN STUDY OF RECYCLED MATERIALS

In order to obtain good results with recycling processes, it is essential to carry out a prior study to assess the thickness and the characteristics of the existing materials, in order to determine the type and quantities of new materials that should be added to the final mixture. When recycled “in situ”, the pavement may present a variable behaviour depending on the constitution of the original pavement (thicknesses of each layer and variability of the material within each layer), emphasizing the need for an adequate mix design study. Furthermore, that study will lead to establishing homogeneous sections which will conduct to eventual modifications of the mixture for certain sections of the pavement. The mix design will necessarily be different if recycling involves only bituminous layers or if it also involves part of the granular layers. The mix design study should be carried out by using materials preferably milled by the equipment that will be used in the recycling works. This will avoid obtaining a different aggregate grading, what would compromise the design study.

Independently from the mix design method used for hot recycled mixtures (Hveem, Marshall or Superpave), special attention needs to be paid to the heterogeneity of the material. Some segregation or contamination may appear when materials are stockpiled. Therefore, it is recommendable not to collect all the material from the same pile so that the sample of reclaimed material can be representative.

In order to predict the behaviour of the final recycled mixture, it is essential to study the characteristics of the reclaimed material. These characteristics can be obtained by extracting and recovering the existing bitumen, separating it from the aggregates and testing both. Thus, it is possible to know the quantity and characteristics of each constituent and decide which materials should be added to make the final mixture.

One of the issues that needs further study when investigating recycled mixtures is related to the possible mix between the old binder of the reclaimed material and the new binder which is to be added. McDaniel & Anderson (1997) (cited in [9]) carried out some tests in material reclaimed from three different sources. They used two types of new bitumen and two different recycling ratios (10 and 40%), so that they could study the mix between the old and the new bitumen. They concluded that the reclaimed material is not a simple “aggregate”. According to the same researchers, it is not reasonable to consider that the mixture between old and new bitumen is complete but partially achieved.

Another factor to consider in the mix design study is moisture in the recycling material. A high percentage of moisture may oblige to devote a higher quantity of time and energy while heating. It also may originate an incorrect value regarding the amount of material weighted (it will include water).

In hot recycled mixtures, the bitumen content is one of the most important parameter that needs to be controlled. Pereira et al. [10] studied some of the fundamental properties (stiffness, fatigue and permanent deformation) of bituminous mixtures produced with 50% reclaimed material at a range of bitumen contents. A conventional mixture of identical gradation and material composition, made of 100% virgin aggregates, was also studied to be compared with the behaviour of recycled mixtures. In that study, the authors concluded that an increase in the binder content does not necessarily means an improvement on the fatigue life of the recycled mixtures, since there is an optimum value above which the properties of the mixture do not improve any longer. It was also concluded that the recycled mixtures present a better performance to permanent deformation and a worse performance to fatigue than the conventional mixture (produced with 100% new materials).

4. CASE STUDY: THE REHABILITATION OF A HEAVILY TRAFFICKED URBAN ROAD

4.1. Project

The rehabilitation project of this case study resulted from a previous study carried out by Oliveira et al. [11] on a heavily trafficked urban road. The original pavement design did not take into account the current traffic levels which are well above the initial values. The pavement is reaching failure in several areas and needs urgent measures to avoid complete failure. The pavement condition is also a result of lack of structural strength and a deficient drainage. Different pavement rehabilitation alternatives were assessed in order to choose the best solution, which should improve the bearing capacity of the pavement, through the rehabilitation of the existing layers and the improvement of the drainage systems, in order to minimize the maintenance operations in the future. The rehabilitation alternatives were also analysed in terms of the impact of the maintenance operations in the environment.

The rehabilitation project comprised the recycling of part of the existing materials, in order to improve the bearing capacity of the pavement without significantly increasing the need for new materials and the disposal of construction waste. In order to reduce the influence of the structure variability throughout the road length, this project included the milling of the surface course material (30% of which should be included in the production of the bituminous mixture for the new binder course) and the recycling of the remaining bituminous material with part of the granular layers (in a thickness of about 200 mm) with the addition of cement. This should be the main structural layer and the pavement will become semi-rigid. The

thickness of the new binder and surface courses were designed in accordance with the expected future traffic. The project also included the construction of a subsurface drainage system. This should increase the stiffness of the subgrade and granular layers and reduce the thickness of the new bituminous bound layers. A Stress Absorbing Membrane Interlayer (SAMI) was also considered in the project, to be applied between the cement recycled layer and the new bituminous layers, in order to reduce the crack propagation phenomenon, which is usually observed in pavements with cementitious base courses due to shrinkage of the base.

According to the results presented in this paper, the main conclusions to be drawn are as follows:

- Significant savings can be obtained by choosing rehabilitation strategies that include recycled materials in the new layers (overall cost savings of up to 24% in the present project);
- Significant environmental cost savings can be obtained when using recycled materials, (reductions of more than 55% in the consumption of new resources and of more than 45% in the disposal of construction by-products were calculated for the present project);
- CO₂ emissions can be greatly reduced by using rehabilitation strategies comprising “in situ” recycled materials.

4.2. Mix Design Studies

4.2.1. Cold “in situ” recycling with cement

The mix design of this type of mixtures consists essentially on the assessment of the optimum water content for several cement ratios. In order to characterise the final mixture and to assess if it would meet the specifications, in terms of compressive strength and indirect tensile strength, several samples of material were collected after the top bituminous layers were milled off and several specimens were produced on the laboratory. According to the Portuguese specifications for hydraulically bound mixtures applied on base and or sub-base layers, the minimum requirements for this type of mixtures are those presented in Table 1.

Table 1. Minimum requirements for hydraulically bound materials

Curing Time	Indirect Tensile Strength (MPa)
7 days	0.2
28 days	1.0

4.2.2. Hot in plant recycling

At the present stage of the mix design study, the batch mixing plant that will be used for the production of the hot recycled mixture is being adapted for allowing the incorporation of reclaimed material into new bituminous mixtures. Meanwhile, the final composition of the mixture is being studied at the laboratory, in order to meet the specifications and to determine the optimum binder content. As stated above, the first step in the mix design study of hot recycled mixtures is to assess the characteristics of the reclaimed material.

In order to characterise the components of the recycled mixture it is necessary to separate the aggregates from the bitumen of the reclaimed material. This can be achieved by using a solvent that will reduce the bitumen viscosity until it becomes liquid, allowing its separation from solid elements (aggregates and filler). This process is known as bitumen recovery and it is carried out in two phases: (i) bitumen-aggregate separation by means of a solvent, in a conventional centrifuge for coarse aggregates (Figure 3-a) and in a high rotation centrifuge for the finer elements that can not be separated in the first equipment (Figure 3-b); (ii) bitumen-solvent separation through a rotary evaporator (Figure 4).

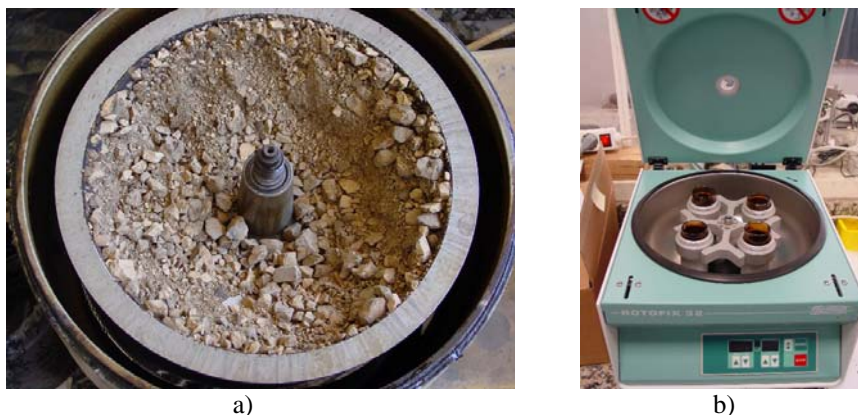


Figure 3. Centrifuges (University of Minho) used to separate the aggregates from the bitumen-solvent solution: a) for coarse aggregates; b) for fine aggregates and filler

Bitumen recovery is carried out following the European Standard EN 12697-3 [12]. This procedure can also be used to verify if the properties of the bitumen present on the final mixture meet the requirements set for the mix design. If the bitumen presents a very low penetration value, becoming too hard, it may be necessary to change the penetration grade of the new binder added to the mixture in order to make the final blended bitumen more flexible and, therefore, more resistant to fatigue.



Figure 4. Rotary Evaporator (University of Minho) used to recover the bitumen

Although this process is still being carried out and no results are available regarding the properties of the binder, it was already possible to study the grading of the aggregate that was separated from the bitumen. As can be observed in Figure 5, the grading of the reclaimed material did not meet the specification limits in some parts of the curve. This was corrected by manipulating the grading of the new aggregate added to the recycled mixture as shown in Figure 5.

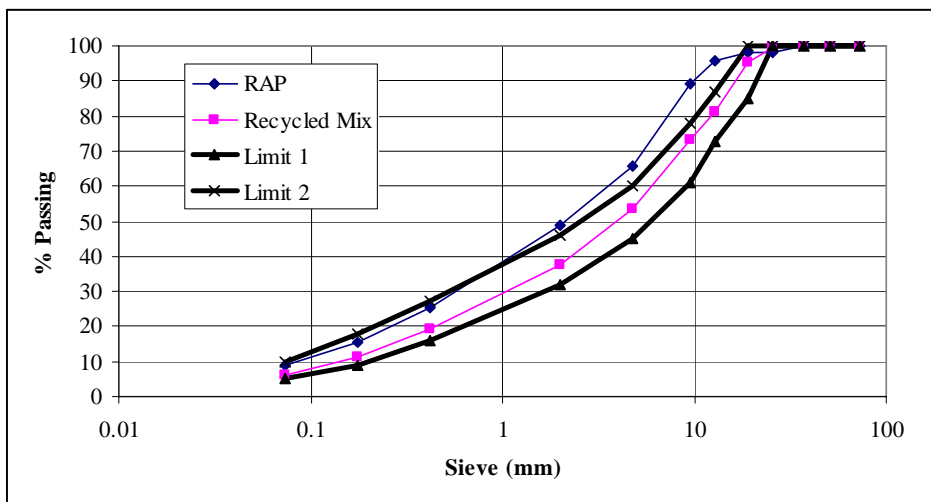


Figure 5. Grading of reclaimed material, recycled mixture and specification limits

The tests carried out during the mix design study for both types of mixture produced some results that are presented in the following section.

4.2.3. Laboratory Results

The first recycling operation that would take place in the rehabilitation of the pavement is the cold “in situ” recycling. Therefore, in the mix design study of that mixture the optimum cement ratio was determined by the results of indirect tensile strength tests carried out over laboratory prepared cylindrical specimens with different percentages of cement. The study started with 3% cement (by mass of mixture) and stopped after the results obtained fulfilled the minimum requirements of the specification. The results of this study are presented in Table 2.

Table 2. Results of the mix design study for the mixture recycled with cement

Cement ratio (%)	Indirect Tensile Strength at 7 days (MPa) (average of 3 specimens)
3	0.13
4	0.26

According to the results obtained it was decided to carry out the recycling operation with 4 % cement.

For the hot recycled mixture, the specifications were more restrict since the properties of the final mixture are more susceptible to variations in its composition. Therefore, after the collection of a representative sample from the stockpile and prior to the evaluation of the final mixture properties, the binder content of reclaimed material was determined by the ignition method (ASTM Standard D6307 – 98) [13] and was estimated to be of 4.99% (by mass of mixture). Therefore, the amount of new binder, to be added to the recycled mixture to obtain the optimum binder content, must be calculated taking into account that about 30% of the material already has 5% bitumen.

In the present project, the mix design procedure should not only consist on the verification of the optimum binder content (using the Marshall mix design method), but also on the study of the stiffness moduli and fatigue resistance of three mixtures (one with the optimum binder content and the other two with a binder content of, respectively, 0.5% above and below the optimum). This process is still being done and the results obtained so far are relative to the optimum binder content and to a traditional bituminous mixture applied on binder courses (produced with 100% virgin materials).

The stiffness moduli obtained for the recycled mixture and for the traditional bituminous mixture are presented in Table 3. Figure 6 shows the results of fatigue tests carried out on a 4-point bending test equipment, at the University of Minho, for the studied mixtures.

Table 3. Stiffness moduli of the studied hot bituminous mixtures, at 20 °C and 10Hz

Specimen	Stiffness Moduli (MPa)	
	Recycled mixture	Traditional mixture
A	5327	5703
B	5339	5594
C	5440	5072
D	5406	5775
E	5371	5412
F	5367	4961
G	5623	5348
H	5784	5349
I	5741	5466
Average	5489	5409

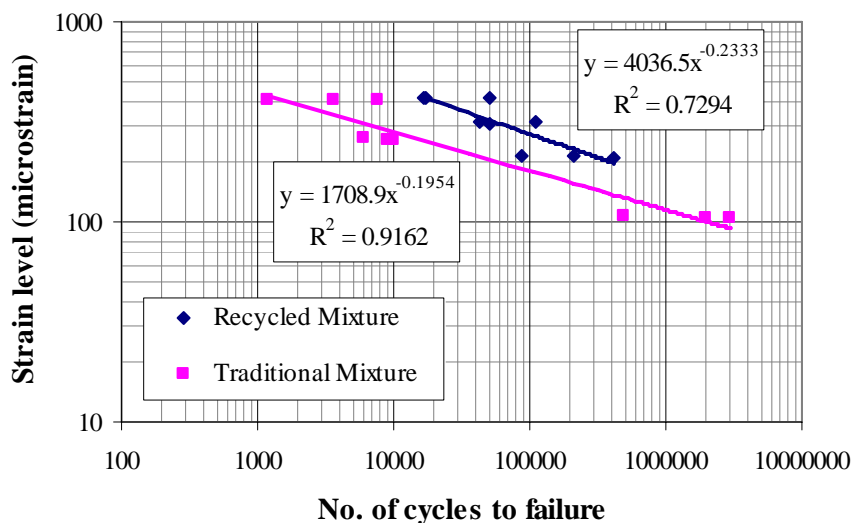


Figure 6. Fatigue life of the studied bituminous mixtures, at 20 °C and 10Hz

As it can be observed from Table 3 and Figure 6, the recycled mixture shows results that point towards a better performance than that of the traditional mixture. Nevertheless, the stiffness moduli of both mixtures are slightly below the value of 6000 MPa expected on the pavement design stage. Therefore, the next step is to verify if, by reducing the binder content of the recycled mixture, the behaviour of the mixture will not be compromised in terms of fatigue and the stiffness modulus will increase to the expected value.

4.3. Trial Section and Pavement Rehabilitation Operations

Due to limitations in the closure of the road to perform the rehabilitation works, the layer recycled with cement will have to withstand the traffic passing on this busy urban road. Therefore, to assess the influence of the traffic on the properties of the recycled layer a trial section was defined. In this trial, all the procedures were verified and the equipment calibrated for a correct performance on the reminder of the rehabilitation works (Figure 7).



Figure 7. “In situ” recycling with cement on the trial section

After 7 days of curing, the trial section was opened to traffic in order to verify if it would damage the recycled material. The bearing capacity of the pavement was periodically measured by Falling Weight Deflectometer (FWD) tests. The results of these tests can be observed in Figure 8.

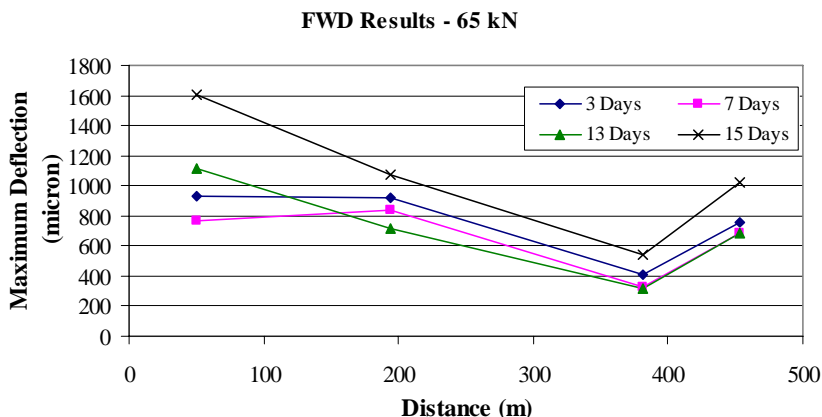


Figure 8 – FWD results obtained over the recycled material in the trial section for a standard load of 65 kN

The results presented in Figure 8 clearly show that severe damage was imposed in the recycled material by the traffic loads. Initially, the bearing capacity was increasing, as it can be interpreted from the reduction in the maximum deflection measured for a load of 65 kN, verified in all points up to 7 days, after which the trial was opened to traffic. However, one week after the opening, not only the positive evolution of the bearing capacity had stopped, but also some damage was imposed to the material. The results presented in the previous figure are complemented with visible damage of the material (disintegration of the top part of the layer) as can be observed in Figure 9.

Besides studying the effects of opening to traffic after 7 days of curing, the trial section was used to extract some cores of the recycled material and to compare the results of indirect tensile strength tests carried out on them with those obtained during the mix design study. Due to unexpected circumstances, the cores were only tested after 10 days of curing time and the average strength obtained was 0.38 MPa, which is perfectly in line with the results obtained in the mix design study for 7 days of curing.



Figure 9 – Visible damage in the recycled material 8 days after opening to traffic

5. CONCLUSIONS

Based on literature review and on the authors' previous experience in this subject, it can be stated that recycling of pavements is highly recommendable, not only in

terms of improvement of pavement characteristics, but also for the purpose of saving scarce resources and reducing construction waste.

Before proceeding to any rehabilitation operation, a prior study needs to be carried out to apply the most adequate technique. In that prior study it is essential to define homogeneous sections, not only as for degradation, but also in relation to the geometric characteristics of the pavement and of existing materials. Thus, when using recycling techniques, it is possible to carry out a more adequate mix design study of the new recycled layer and of the final pavement design, namely recycling depth and number of new layers to be applied.

While works are being undergone, it might be necessary to revise the recycling process if significant variations occur in the materials or in external conditions, such as water in the recycling material when dealing with cold recycling. This factor demands a more rigorous control and supervision of works to obtain satisfactory results.

When using milled materials that have been stored for the manufacturing of new bituminous hot mixtures, special attention must be paid to their characteristics, i.e., binder variability, grading or moisture. All these factors need proper consideration in the mix design study in order to obtain a mixture with similar characteristics to those of a conventional bituminous mixture.

In the case study presented in this paper, the main conclusions and recommendations that could be drawn are the following:

- the results obtained in the mix design study for the cold “in situ” recycling with cement pointed towards a minimum of 4% cement ratio (by mass of mixture);
- the curing time of the cement recycled material before opening to traffic (7 days), was clearly insufficient, as it can be observed by the damage obtained in the trial section;
- cold “in situ” recycling with cement should not be used in situations where it is predicted that traffic will be passing over the material before the application of at least one bituminous overlay (which should only be applied after a curing period of the hydraulic bound layer of at least 7 days);
- the results obtained for the hot recycled mixture showed that it is possible to obtain mixtures whose fatigue performance is as good as traditional bituminous mixtures, using less virgin materials;
- the behaviour of the whole pavement will be continuously monitored in the near future and further publications shall be made about this rehabilitation project.

References

1. Fernández del Campo, J. A., Recycling in Road Pavements, *MAIREPAV03 - Third International Symposium on Maintenance and Rehabilitation of Pavements and Technological Control*, University of Minho, Guimarães, 2003.
2. Woodside, A., Phillips, P., Mills, A., Maximisation of Recycled Asphalt Use in Cold Mix and Hot Mix Environment, *Proceedings of the 3rd European Symposium on Performance and Durability of Bituminous Materials and Hydraulic Stabilised Composites*, pp 401-412, Leeds, 1999.
3. Potter, J. F., Mercer, J., Full-scale Performance Trials and Accelerated Testing of Hot-Mix Recycling in the UK, *8th International Conference on Asphalt Pavements*, Seattle, 1997.
4. Servas, V. P., Ferreira, M. A., Curtayne, P. C., Fundamental Properties of Recycled Asphalt Mixes, *Proceedings of the Sixth International Conference on Structural Design of Asphalt Pavements*, Vol. 1, pp 455-465, Ann Arbor, Michigan, 1987.
5. McDaniel, R. S., Anderson, R. M., *Recommended use of Reclaimed Asphalt Pavement in the Superpave Mix Design Method: Technician's Manual*, NCHRP Report 452, Transportation Research Board, National Research Council, Washington, D.C., 2001.
6. Oliveira, J., Pereira, P., Pais, J., Picado-Santos, L., Benefits of Including Hot Mix Recycled Materials in Pavement Design, *International Symposium on Pavement Recycling*, São Paulo, Brazil, 2005.
7. Kavussi, A., Atabaki, M. A., Subgrade Stabilization with Lime and Base Strengthening with Cement-Foam Bitumen, a Case Study in Assalouyeh Airport in Iran, *Proceedings of First International Symposium on Subgrade Stabilization and In Situ Pavement Recycling Using Cement*, pp 479-492, Salamanca, 2001.
8. Wirtgen, *Wirtgen cold recycling manual – 2nd revised issue*. Wirtgen (ISBN 3-936215-00-6), Windhagen, 2001.
9. McDaniel, R. S., Soleymani, H., Anderson, R. M., Turner, P., Peterson, R., *Recommended use of Reclaimed Asphalt Pavement in the Superpave Mix Design Method*, Report prepared for: NCHRP, Transportation Research Board, National Research Council, Washington, D.C., 2000.
10. Pereira, P. A. A., Oliveira, J. R. M., Picado-Santos, L. G., Mechanical Characterization of Hot Mix Recycled Materials, *The International Journal of Pavement Engineering*, Vol. 5 (4), pp. 211-220, 2004.
11. Oliveira, J.R.M., Pereira, P.A.A., Picado-Santos, L.G., Rehabilitation Study of a Heavily Trafficked Urban Road, *Mairepav5 – 5th International Conference on Maintenance and Rehabilitation of Pavements and Technological Control*, Park City, Utah, 2007.
12. CEN, Comité Européen de Normalisation, European Standard 12697-3: *Bituminous mixtures – Test methods for hot mix asphalt – Part 3: Bitumen recovery: Rotary evaporator*, Brussels, 2000.
13. ASTM, American Society for Testing and Materials, Standard D6307 – 98: *Standard Test Method for Asphalt Content of Hot-Mix Asphalt by Ignition Method*, West Conshohocken, PA, USA, 1998.

The Improvement of Pavement Performance Using Asphalt Rubber Hot Mixes

Jorge C. Pais¹ and Paulo A. A. Pereira²

¹ Assistant Professor; E-mail: jpais@civil.uminho.pt

² Professor; E-mail: ppereira@civil.uminho.pt

Abstract

The need of a better pavement performance has led researchers to develop new road materials, mainly for the asphalt layers, where the modification of the asphalt is the main example. This modification usually forces the use of polymers and fibers and, more recently, the use of crumb rubber from ground tires, where the modified asphalt is known as asphalt rubber. This asphalt rubber used in asphalt mixtures produces a superior performance if compared to the asphalt mixtures with conventional asphalt. The crumb rubber modification of the asphalts also presents a higher resistance to climatic effects, compared to the other binders. Based on these assumptions, this paper presents the results of the evaluation of mechanical properties, related to the pavement performance, of asphalt rubber mixtures when compared to conventional mixtures. Two types of aggregate were used (pebble and diorites) and two binders utilized (asphalt rubber and conventional asphalt). The aging effect due to the asphalt mixture production and compaction was taken into account. The materials performance was evaluated through stiffness, fatigue and permanent deformation tests. Reflective cracking performance was also predicted using a mechanistic-empirical method.

1. INTRODUCTION

1.1. Aggregate gradation

The aggregate gradation of a conventional mixture is defined according to the maximum aggregate size and the main applications for the material. The typical thickness of the layer where the mixture will be applied on is considered in the selection of the aggregate gradation. Some recommendations for the aggregate gradation, mainly due the permanent deformation, were drawn during the SHRP program, which led to the definition of the restricted zone. The restricted zone, around the maximum density line, is defined by some control points to avoid the lack of stability of the asphalt mixture.

For asphalt rubber mixtures, some recommendations should be defined once the binder used in these mixtures presents more viscosity and the content normally doubles that of traditional mixtures. Asphalt rubber mixtures have more than 7.5% of binder content, but this value can reach 9.5% for certain applications. The inclusion of such amount of binder in asphalt mixtures is obtained by acting in the aggregate gradation. In this case two types of aggregate gradations were used for asphalt rubber mixtures: the gap-graded and the open-graded gradation. The gap-graded gradation produces a rough asphalt rubber mixture and the open-graded gradation produces a draining mixture. These two aggregate gradations allow using a high content of binder in the mixtures and a highly viscous binder.

The typical aggregate gradations (gap-graded and open-graded) used in asphalt rubber mixtures are presented in Table 1 and represented in Figure 1.

Table 1 – Aggregate gradations (% passing) used for asphalt rubber mixtures

Sieve Size	Gap-graded		Open-graded	
	Upper Limit	Lower Limit	Upper Limit	Lower Limit
19.0 mm (3/4 in.)	100	100	100	100
12.5 mm (1/2 in.)	85	100	100	100
9.5 mm (3/8 in.)	70	85	90	100
4.75 mm (No. 4)	28	40	35	50
2.00 mm (No. 10)	12	20	6	10
0.425 mm (No. 40)	6	12	3	7
0.075 mm (No. 200)	2	5	2	3

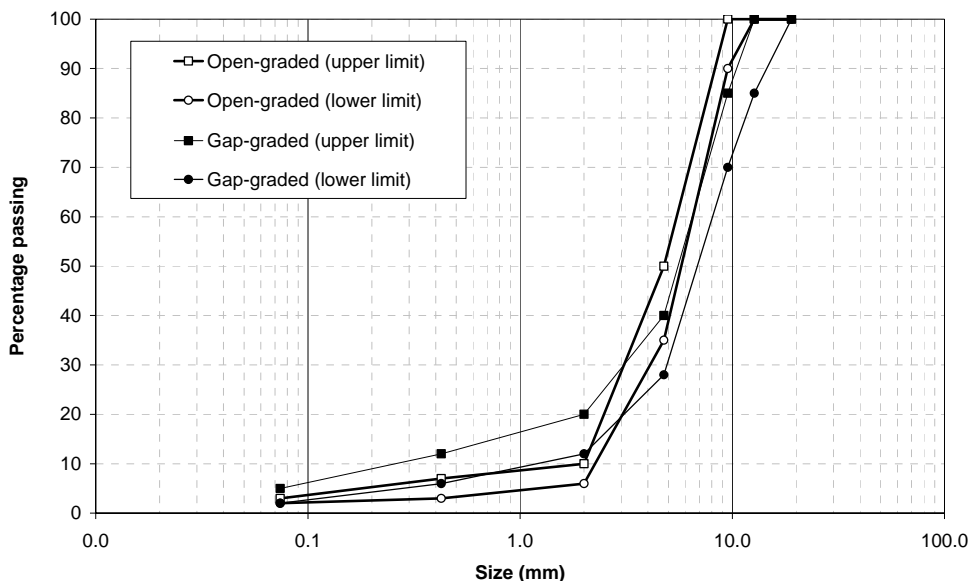


Figure 1 – Aggregate gradation curves used for asphalt rubber mixtures

The analysis of Figure 1 allows concluding that both aggregate gradation curves are very similar. In the fine part of the aggregate gradation (up to 2 mm), open-graded mixtures present less fine particles than gap-graded mixtures. In the coarse part of the aggregate gradation the gap-graded has also fewer particles than the gap-graded mixture.

Despite these differences, the most important aspect of these aggregate gradation curves is the fact that, for open-graded mixtures, the upper and lower limits are very closed thus requiring a suitable quality control to ensure the quality of the material.

1.2. Crumb rubber

The modification of asphalt to obtain asphalt rubber is made by the digestion of crumb rubber into asphalt. The crumb rubber is obtained through grinding of the tires using two different techniques: ambient grinding and cryogenic process.

Ambient grinding can be accomplished in two ways: granulation and crackermills. Ambient describes the temperature of the rubber or tire as it is being size reduced. Typically, the material enters in the crackermill or granulator at ambient or room temperature. The temperature of the rubber will rise significantly during the process due to the friction generated, as the material is being torn apart. Through granulation the rubber size is reduced by means of cutting and shearing actions. The rubber particles produced in the granulation process generally have angular surface shape, rough in texture, with similar dimensions on the cut edges.

Cryogenic processing uses liquid nitrogen or other materials/methods to freeze (-87 °C to -162 °C) tire chips or rubber particles prior to size reduction. The surface is glasslike, and thus has a much lower surface area than ambient ground crumb rubber of similar gradation. Cryogenic grinding is a cleaner, slightly faster operation resulting in the production of fine mesh sizes. The main disadvantage is the slightly higher production cost due to the added cost of liquid nitrogen (Baker et al., 2003).

These two types of crumb rubber produce rubber with different particle shapes. Crumb rubber particles produced through the ambient process generally have a porous or fluffy appearance (Amirkhanian and Shen, 2005). On the other hand, in the cryogenic process, the surface of the crumb rubber is glasslike, and thus has a rather lower surface area than ambient ground crumb rubber with similar gradation (Baker et al., 2003). These conclusions can be observed in Figure 2 obtained from Scanning Electron Microscopy.

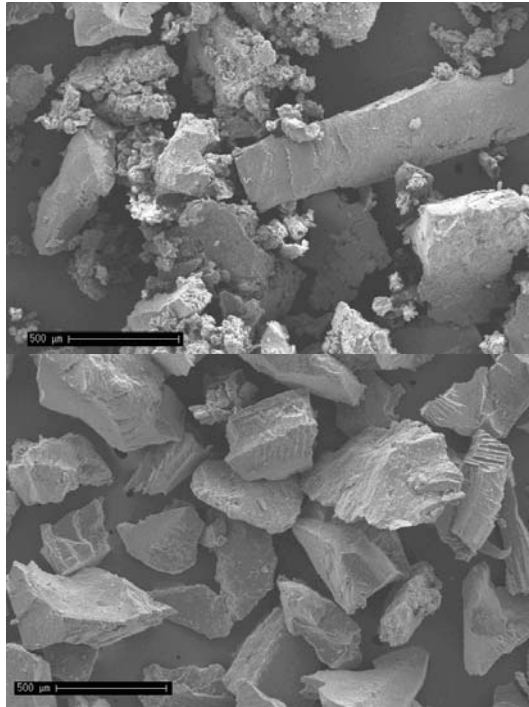


Figure 2 – Ambient crumb rubber (left) cryogenic crumb rubber (right)

Typically, the crumb rubber gradation, resulting from ambient grinding and from cryogenic process, to be used in the production of the asphalt rubber, is presented in Figure 3, where the main differences appears in the fine part of the gradation.

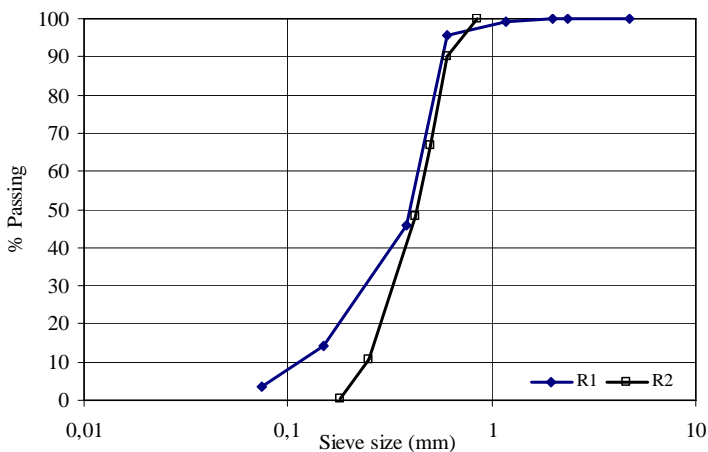


Figure 3 – Grain size distributions for rubber types (R1 – ambient grinding; R2 – cryogenic process)

1.3. Asphalt rubber

The production of the asphalt rubber is a process characterized by the incorporation of crumb rubber into asphalt. It is not a simple addition of crumb rubber into asphalt. The modification of the asphalt is obtained through the digestion of the crumb rubber by the asphalt during a certain period of time.

The compatibility of the asphalt/rubber system guarantees the achievement of asphalt rubber with its common properties. Compatibility can be characterized not only in terms of the achievement of a particular morphology, i.e. the structural arrangement of the polymer particles, chains or groups within the asphalt matrix, but also in terms of thermodynamic stability, i.e. if the conformation of the polymer particles or chains that may be in a low energy state. It may also be characterized in terms of practical storage stability. Finally, it may be based on the fact that a given property or set of properties are achieved and can be maintained for a suitable period of time (Holleran and Reed, 2000).

The interaction between rubber particles and asphalt is characterized by the fact that the asphaltenes and light fractions of the conventional asphalt binder and the rubber particles interact to form a gel coated particle (Figure 4). Rubber particles swell in a process similar to what occurs in polymer asphalt systems. The large increase in viscosity along the early times of digestion is due to the continuation of this solvation process. However, this system is not thermodynamically stable and leads to significant change of properties throughout time (Neto et al., 2006).

The design of asphalt rubber requires the definition of some variables which include the amount of crumb rubber, digestion time and temperature, based on the base asphalt properties. Hard asphalts can only interact with low crumb rubber content while soft asphalts interact with high crumb rubber content.

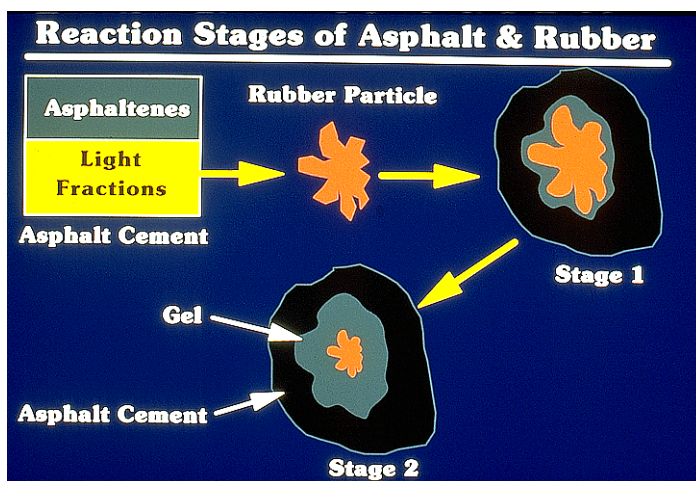
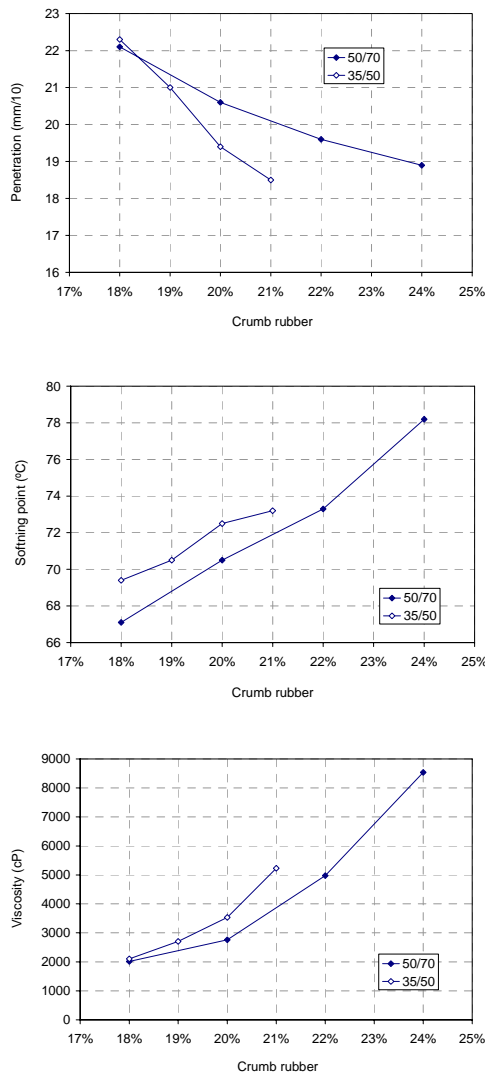


Figure 4 – Interaction between asphalt rubber and asphalt (Holleran and Reed, 2000)

The criteria to establish the proper rubber content and the digestion time and temperature are usually based on physical tests carried out in the asphalt rubber, i.e. penetration, softening point, resilience and, most important, viscosity. The addition of crumb rubber to the base asphalt increases viscosity significantly due to the gel and swelling.

In Figure 5 the influence of crumb rubber content on the asphalt rubber characteristics for two base asphalts (35/50 pen and 50/70 pen asphalt) is illustrated. These results were obtained for a digestion time of 45 minutes and a temperature of 175 °C.



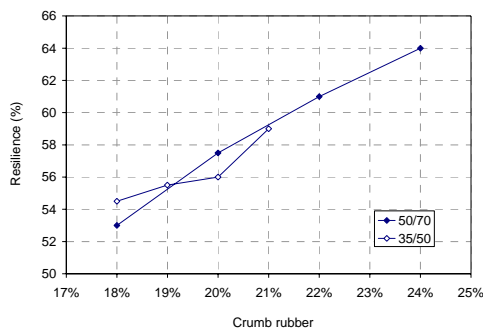


Figure 5 – Influence of crumb rubber content on the asphalt rubber characteristics

The results of the design of the asphalt rubber allow observing that the increase of crumb rubber reduces penetration: the more content of crumb rubber, the harder asphalt rubber becomes. The same conclusion may be drawn for viscosity and softening points. In terms of resilience, the increase in crumb rubber produces a more elastic asphalt rubber.

As expected, these two types of asphalts that are used to produce asphalt rubber produce different final products. The main difference is that the 50/70 pen asphalt allows adding about 1% more crumb rubber than the 35/50 pen asphalt.

The design of asphalt rubber is intended to define the crumb rubber content necessary to produce asphalt rubber. The main reason for choosing the crumb rubber content has to do with the asphalt rubber viscosity, as it is important in order to ensure a correct mixing of the binder with the aggregates and a correct compaction of the final mix.

The production of asphalt rubber mixes is mainly made by using the continuous blend process in which asphalt rubber is produced near the asphalt mix plant with the help of specific equipment, and supplied to the asphalt mix plant in accordance with needs. To reach the asphalt mix plant, asphalt rubber needs to have a specific viscosity to be pumped appropriately. Nowadays equipments can supply asphalt rubber with a viscosity inferior to 5000 cP.

Based on the presented results, a content of 22% crumb rubber may be used to produce asphalt rubber with the 50/70 pen asphalt. For the 35/50 pen asphalt, only 20% crumb rubber can be used.

1.4. Asphalt rubber hot mixture

There are two methods through which asphalt-rubber mixtures are produced: wet process and dry process. In the wet process, the conventional binder is heated up at temperatures around 180°C in a super-heating tank in hermetic conditions and

immediately transported to an adapted mixture tank. In the mixture tank, crumb rubber is added to the preheated conventional binder.

In the dry process, dry particles of crumb rubber are added to the preheated aggregate before adding a conventional binder (Visser and Verhaeghe, 2000).

The aggregate is heated at temperatures of approximately 200°C. Then the crumb rubber is added and the mixing continues for approximately 15 seconds or until the formation of a homogeneous composition of aggregate-crumb rubber. After that, a conventional binder is added to the mixture aggregate-crumb rubber following conventional methods in a mixing plant.

The structural performance of the asphalt rubber hot mixtures is directly related to the mechanical properties of the asphalt rubber binder used. In this type of mixtures, the binder content is around 7.5% to 9.5%, what has an important effect on the material performance mainly in terms of fatigue response where it is expected to have at least 10 times more fatigue life than a conventional asphalt mixture where the binder content is about 5% (Minhoto et al., 2005). This behavior is attributed to the larger flexibility of the mixtures provided by the incorporation of crumb rubber into the conventional binder.

In terms of permanent deformation, several studies indicate a satisfactory performance of asphalt rubber hot mixes in relation to those produced with conventional binders, mainly due to the aggregate gradation used to produce the mixture and due the thickness of the layers where the mixture is placed (Antunes et al., 2000).

Asphalt rubber mixtures have their principal application in the field of pavement rehabilitation, where reflective cracking resistance is the main property required from mixtures. An experience of more than 30 years of application of these mixtures in very cracked pavements shows their capacity for retarding crack propagation from the old pavement to the surface (Way, 2006).

2. OBJECTIVE

The research presented in this paper reports some of the results of a project undertaken by the University of Minho in the study of the modification of the asphalt using crumb rubber and the evaluation of the performance of asphalt rubber mixtures used in pavement rehabilitation.

For this work some asphalt mixtures with different compositions were studied aiming at pavement rehabilitation. Two types of aggregate, pebbles and diorites, mixed with two binders, namely 35/50 pen asphalt and 35/50 pen asphalt modified by crumb rubber were used.

The material performance was evaluated through stiffness and fatigue tests carried out in a four point bending device and the permanent deformation tests were carried out in the wheel tracking device. The aging effect due the production and compaction of the mixture was also regarded. The reflective cracking was assessed through the application of an empirical-mechanistic approach which uses fatigue test results to evaluate the cracking reflection resistance.

3. MATERIAL USED IN THIS WORK

The asphalt mixtures studied present a composition defined in Table 2, where it can be observed the existence of two mixtures with diorite aggregate and three mixtures with pebble aggregate. The binder was asphalt rubber produced with conventional 35/50 pen asphalt modified by 19% of crumb rubber and conventional 35/50 pen asphalt without any modification. The aging effect was applied to both mixtures to simulate the production and compaction of the asphalt mixtures. This aging was induced by placing the asphalt mixture in an oven at 85°C during 5 days as proposed by the SHRP program.

Table 2 also presents the physical characterization of the materials tested in this project expressed in terms of air void and binder content. The asphalt rubber mixtures with a gap-graded aggregate gradation had, on average, 8.3% binder content. For the conventional mixtures the binder content was about 5.3%, which represents a typical value for wearing course mixtures. In terms of air void content, the asphalt mixtures presented values of about 5%, whereas for the conventional mixtures the air void content was about 3.5%.

Table 2 – Asphalt mixtures description

Asphalt mixture	Aggregate	Binder	Aging effect	Air void content (%)	Binder content (%)
D-AR-N	Diorite	Asphalt rubber	No	4.7	8.0
P-C-N	Pebble	Conventional 35/50 pen asphalt	No	3.3	5.6
P-AR-N	Pebble	Asphalt rubber	No	2.6	8.5
P-C-Y	Pebble	Conventional 35/50 pen asphalt	Yes	3.8	5.1
D-AR-Y	Diorite	Asphalt rubber	Yes	5.7	8.4

4. STIFFNESS AND FATIGUE RESISTANCE

The test procedures to characterize the stiffness and fatigue resistance of all the studied mixtures included two tests: (i) frequency sweep tests; (ii) fatigue tests. Prior to the tests, the specimens were placed in an environmental chamber for nearly 2 hours in order to reach the test temperature.

The configuration used in this study was based on the four-point bending test in controlled strain, what means that the strain is kept constant and that the stress decreases during the test. In general, controlled strain testing has been associated with thin pavements. The test configuration is represented in Figure 6. The bending device and the servo-hydraulic testing machine are shown in Figure 7.

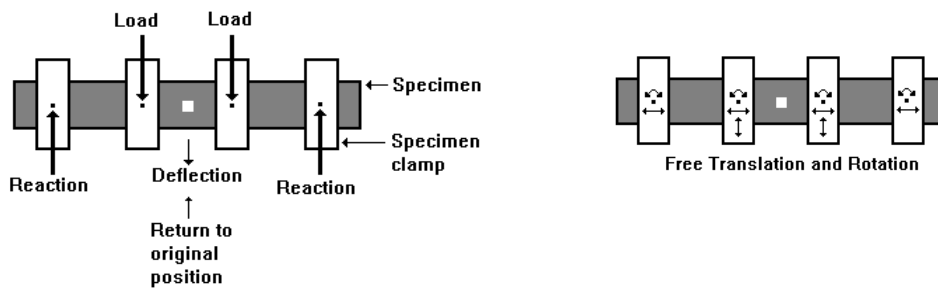


Figure 6 – Schematic representation of the four point test setup

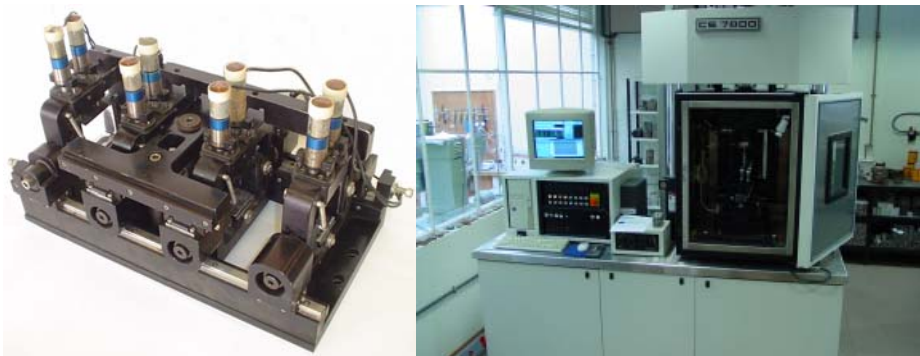


Figure 7 – Four point bending device and servo-hydraulic testing machine

Flexural fatigue tests were conducted according to the AASHTO TP 8-94 (Standard Test Method for Determining the Fatigue Life of Compacted HMA Subjected to Repeated Flexural Bending). All tests were carried out at 20 °C and at 10 Hz. The flexural beam device allows testing beam specimens up to 50 mm x 63

mm x 380 mm. Fatigue failure was assumed to occur when the flexure stiffness is reduced to 50 percent of the initial value, as shown in Figure 8. Before the fatigue test, the frequency sweep test was conducted in the same testing equipment, using the same specimen.

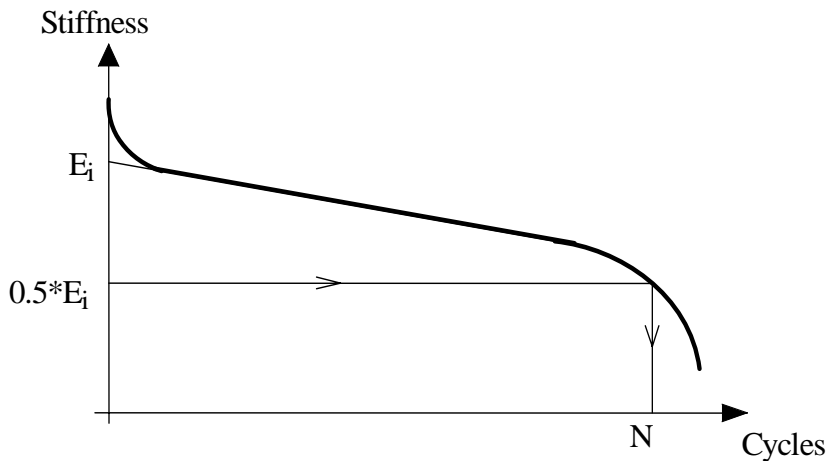


Figure 8 – Stiffness evolution during fatigue tests and definition of test failure

The frequency sweep test measures the stiffness and the phase angle of mixtures when subjected to different loading frequencies. In this study, seven frequencies were tested (10; 5; 2; 1; 0,5; 0,2; 0,1 Hz) in 100 cycles to avoid damage in the specimen. The stiffness and phase angle of the studied mixtures, conducted at 20 °C, are shown in Figures 9 and 10, respectively.

The analysis of the obtained results allows concluding that the asphalt rubber mixtures exhibit lower stiffness than the conventional mixtures. At 10 Hz, the asphalt rubber mixtures present stiffness moduli that range between 1900 MPa up to 3200 MPa, depending on the aggregate type, gradation and air void content. On the other hand, conventional mixtures present stiffness values higher than 6000 MPa.

In terms of phase angle, asphalt rubber mixtures present values that are in the same range as conventional mixtures. This allows concluding that the expected permanent deformation resistance is probably in the same range of conventional mixtures.

The aging applied to the specimen prior the test had a reduced influence in both mixtures. In conventional mixtures the aging effect was only visible at low test frequencies. In asphalt rubber mixtures the aging effect increased the stiffness modulus of 1000 MPa.

The stiffness modulus and phase angle at 10 Hz for all mixtures can be observed in Table 3.

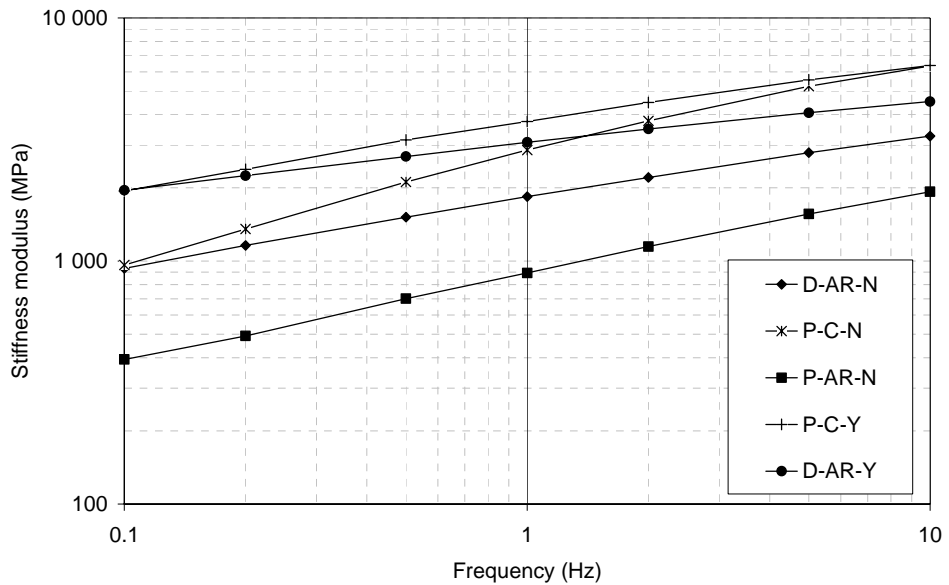


Figure 9 – Stiffness modulus of the studied mixtures

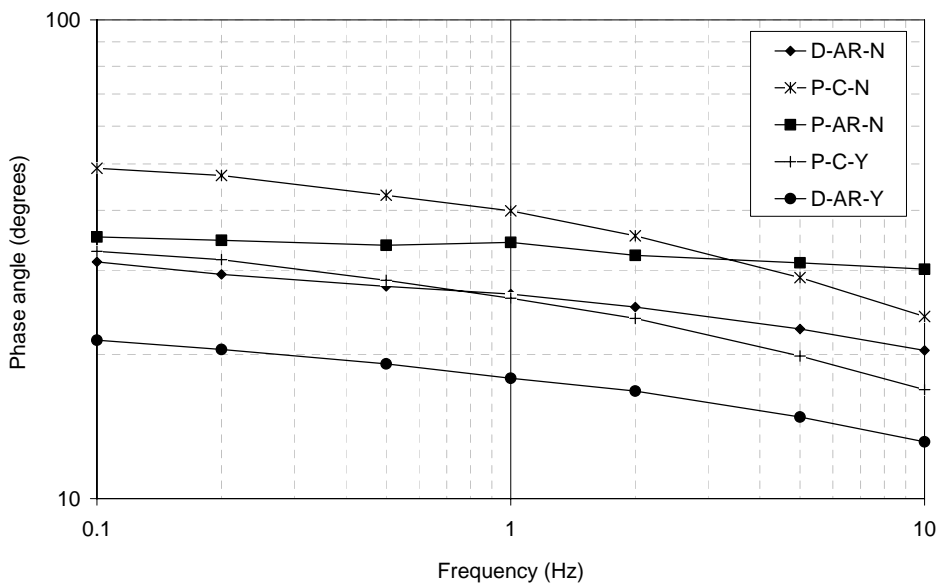


Figure 10 – Phase angle of the studied mixtures

Table 3 – Stiffness and phase angle at 10 Hz

Asphalt mixture	Stiffness modulus (MPa)	Phase angle (degree)
D-AR-N	3266	20.4
P-C-N	6350	24.0
P-AR-N	1929	30.1
P-C-Y	6378	16.9
D-AR-Y	4529	13.1

The fatigue tests carried out on the studied mixtures were performed according to the AASHTO TP 8-94 at 20 °C and 10 Hz. For each mixture, six specimens were tested at two different strain levels and the results were fitted in fatigue laws represented in Figure 11.

The analysis of these results allows concluding that mixtures with asphalt rubber have an important increase in terms of fatigue life if compared to the mixtures with conventional binder. This difference is about 10 times superior as it can be observed from the comparison between mixture P-AR-N and mixture P-C-N. The aging in asphalt rubber mixtures is not significant, as it was observed in mixtures (D-AR-N and D-AR-Y) unlike to what happens in mixtures with conventional binder (P-C-N and P-C-Y). The use of different aggregate types can also lead to different fatigue responses, as observed in mixtures P-AR-N and D-AR-N, where the difference in terms of fatigue life is about 5 times superior.

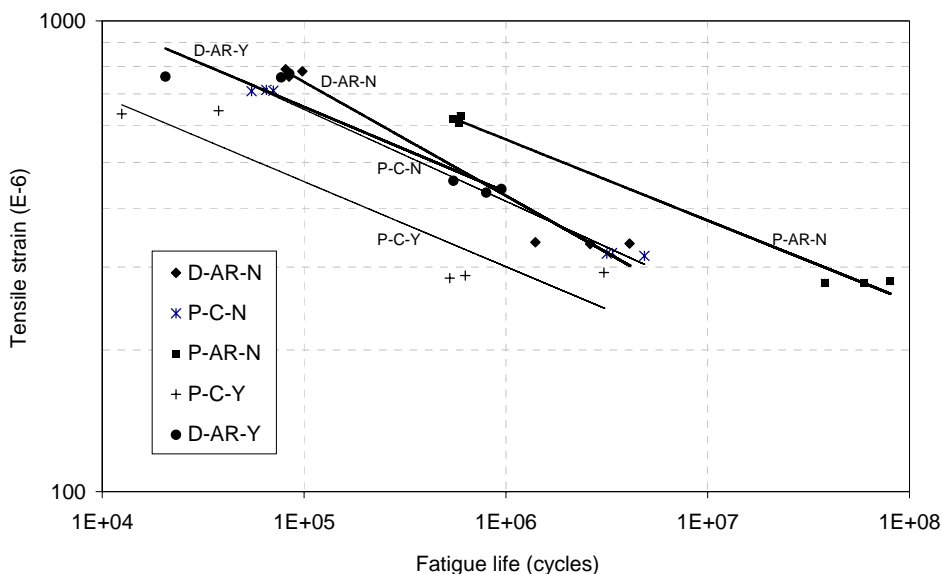


Figure 11 – Fatigue curves of the studied mixtures

5. PERMANENT DEFORMATION RESISTANCE

Rutting in asphalt concrete layers develops gradually from the number of load applications, and it usually appears as longitudinal depressions on the wheel paths accompanied by small upheavals on the sides. It is caused by a combination of densification (a decrease of volume and hence, an increase of density) and shear deformation (Sousa et al., 1994).

To complement the comparison study between mixtures with and without asphalt rubber, and once the mixtures with pebble aggregate showed excellent fatigue behaviour, permanent deformation tests on this mixture were carried out to verify the resistance of these mixtures.

The permanent deformation resistance tests were performed on P-C-N and D-AR-N mixtures, following the NLT 173-94 standard and using a wheel tracking testing device. The tests were carried out at 60 °C test temperature. A contact tension of 700 KPa was applied, as recommended in the BS 598-110:1998 standard.

The results expressed in terms of vertical deformation throughout time are presented in Figure 12, where it can be observed that the asphalt rubber mixture

(D-AR-N) presents the highest permanent deformation resistance if compared to the conventional mixture (P-C-N).

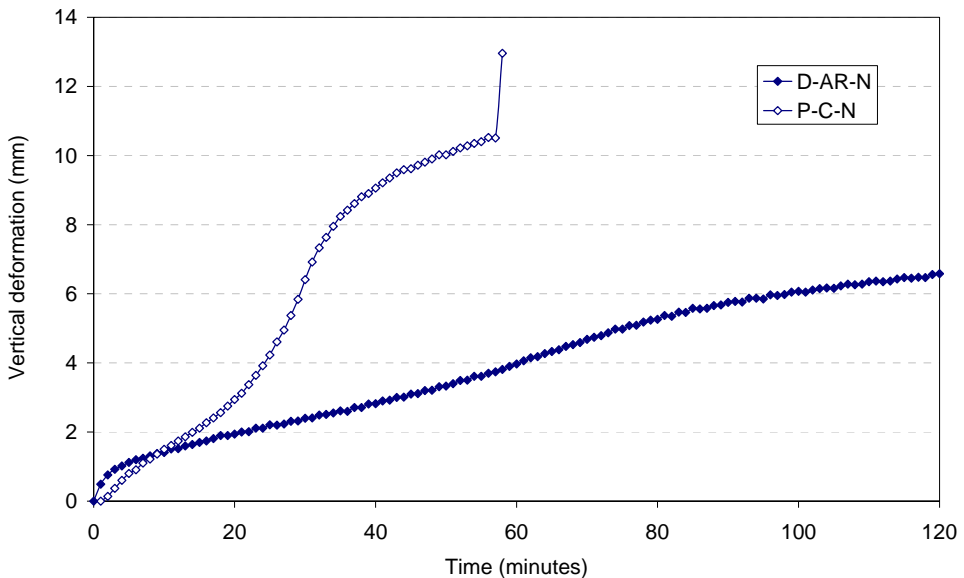


Figure 12 – Permanent deformation resistance

6. REFLECTIVE CRACKING RESISTANCE

When a mixture is applied on a pavement overlay it is subjected to cracking propagation, directly above the cracks of the existing pavement due to static and repetitive loading during the first few years of service. This type of distress is traditionally known as "reflective cracking" and it is a major problem for highway agencies throughout the world. Thus, road administrations are concerned about the prevention of cracking occurrence, in order to provide a good functional and structural performance for their pavements.

The temperature variations, daily and seasonal, and associated thermal stresses could be some of the causes for premature overlay cracking, affecting the overlay life of asphalt pavements. In regions that experience large daily temperature variations or extremely low temperatures, thermal conditions play a major role in the reflective cracking response of a pavement. On the one hand, binder properties, such as stiffness, ageing or penetration among others, are sensitive to temperature variations. On the other hand, the combination of two of the most important effects - wheel loads passing on or near the cracks and the increasing tension in the

material above the crack (i.e. in the overlay) due to a rapid decrease of temperature - have been identified as the most probable causes of high states of stress and strain above the crack and responsible by the reflective cracking phenomena.

The evaluation of the reflective cracking resistance for the studied mixtures was carried out through the mechanistic-empirical method developed by Sousa et al. (2002), which uses fatigue resistance and stiffness to predict the overlay life.

The mechanistic-empirical methodology is capable of assembling simultaneously Modes I and II crack opening. The influence of pavement characteristics on the state of stress and strain was considered by defining a deviator strain such as the Von Mises stress. This mechanistic-empirical methodology is based on the results of flexural fatigue tests, in controlled strain, based on the Von Mises deviator strain as the “controller” parameter of the phenomenon. For beam fatigue test conditions subjected to four-point bending the tensile strain can be correlated to the Von mises strain.

The application of this method required a pavement to be rehabilitated. The one considered had a subgrade of 110 MPa, a granular layer of 25 cm with 250 MPa and 17 cm of existing asphalt layer with 2250 MPa. The results of the method application led to the overlay thickness defined in Figure 13.

As it can be observed in that figure, for the same overlay life, the asphalt rubber mixture requires half of the overlay thickness of the conventional mixture.

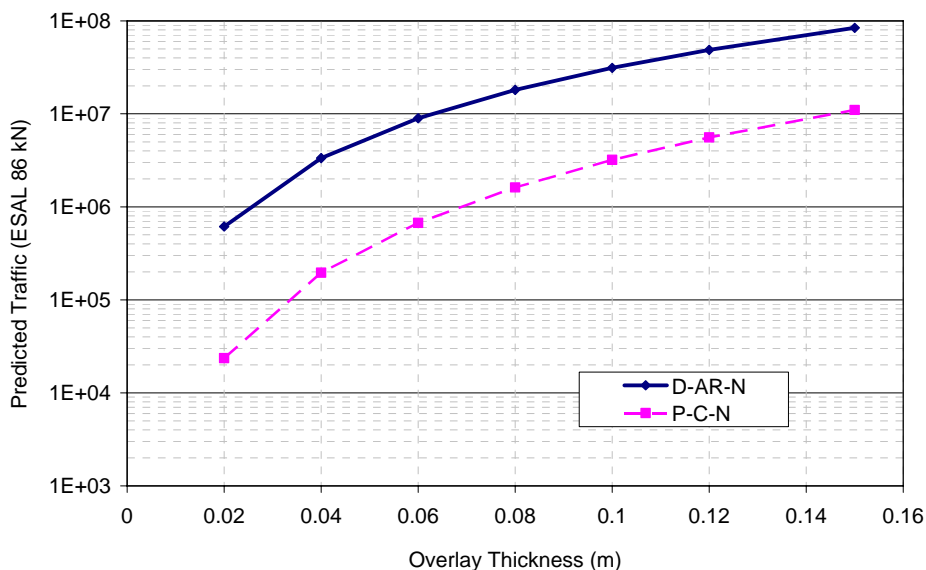


Figure 13 – Estimation of overlay life

7. CONCLUSIONS

The study undergone in this project and presented in this paper reports the evaluation of pavement performance based on the asphalt material properties herewith studied and the contribution of asphalt rubber mixtures to the improvement of pavement performance.

The study was carried out by considering mixtures with two different type of aggregates (pebble and diorite), and two types of asphalt binder (asphalt rubber and conventional asphalt). The aging induced by the asphalt mix production and compaction was also considered.

The asphalt mixture performance was assessed by stiffness, fatigue and permanent deformation tests and reflective cracking performance.

The results allowed to conclude that the stiffness of asphalt rubber mixtures is inferior to the one obtained from conventional mixtures. In terms of fatigue response, asphalt rubber mixtures exhibit about 10 times more fatigue resistance than conventional mixtures. The aggregate type has a significant influence on the fatigue response. Asphalt mixtures with pebble aggregate presented a longer fatigue life than those produced with diorite aggregate.

The permanent deformation study showed that the mixture with diorite aggregates and asphalt rubber had more permanent deformation resistance than the conventional mixture with diorite aggregates.

The application of the reflective cracking prediction model to the same mixtures here evaluated through the permanent deformation study confirmed the superior behaviour of asphalt rubber mixtures.

References

1. Amirkhanian, S., Shen, J. “The Influence of Crumb Rubber Modifier (CRM) Microstructures on the High Temperature Properties of CRM Binders”. *The International Journal of Pavement Engineering*, Vol. 6, 2005.
2. Antunes, M.L, Baptista, F., Eusébio, M.I., Costa, M.S., Miranda, C.V., “Characterization of Asphalt Rubber Mixtures for Pavement Rehabilitation Projects in Portugal”, *Asphalt Rubber 2000 – Proceedings*, Portugal, 2000, p.285-307.
3. Baker, T. E., Allen, T.M., Jenkins, D.V., Mooney, T., Pierce, L.M., Christie, R.A., Weston, J.T., “Evaluation of the Use of Scrap Tires in Transportation Related Applications in the State of Washington”, *Washington State Department of Transportation*, Washington, D.C., 2003.
4. Holleran, G., Reed, J.R., “Emulsification of asphalt rubber blends”, *Asphalt Rubber 2000 – Proceedings*, Portugal, 2000, p. 383-409
5. Minhoto, Manuel J.C., Pais, Jorge C., Pereira, Paulo A.A.,Picado-Santos, Luís G., “Predicting Asphalt Pavement Temperature with a Three-Dimensional Finite Element Method”, *Journal of the Transportation Research Board*, nº 1919, 2005, pp. 96-110.

6. Neto, S.A.D., Farias, M.M., Pais, J.C.,Pereira, P.A.A., “Influence of Crumb Rubber and Digestion Time on the Asphalt Rubber Binders”, Road Materials and Pavement Design, vol 7, n° 2, 2006, p. 131-148.
7. Sousa, J.B.; Craus, J., Monismith, C.L. Summary Report on Permanent Deformation in Asphalt Concrete. Strategic Highway Research Program. National Research Council, Washington, DC, 1994.
8. Sousa, J.B., Pais, J.C., Saim, R., Way, G.B., Stubstad, R,N, “Development of a Mechanistic Overlay Design Method Based on Reflective Cracking Concepts”, Transportation Research Board, 80th Annual Meeting, Washington D.C., January , 2002.
9. Visser, A.T.,Verhaeghe, B. “Bitumen-rubber: Lessons learnt in South Africa”. Proceedings of the Asphalt Rubber 2000 Conference. Vilamoura. Portugal. 2000.
10. Way, G.B. “OGFC meets CRM: Where the rubber meets the rubber: 15 years of durable success”. Proceedings of the Asphalt Rubber 2006 Conference. Palm Springs, USA. 2006.

Surface application of polymer coating for concrete curing

Vít Petránek¹

¹ Institute of Technology of Building Materials and Components, Faculty of Civil Engineering, Brno University of Technology, Czech Republic, petranek.v@fce.vutbr.cz

Summary

One of the most important factors for final surface quality in concreting of large dimension slabs is to secure minimum vaporization of water and limit the undesirable tensile and compressive stresses in concrete structure which can be formed by quick drying of the concrete surface.. Only purpose of ordinary type of treatment for fresh concrete is to secure sufficient amount of water during hydration. These materials have to be removed or left on place to be worn off. New material based on polymer resin has been developed to keep necessary amount of water to secure proper hydration process in concrete. The intended use of the newly developed product is mainly for horizontal concrete slabs, floors. Polymer is applied onto fresh concrete before or during final surface treatment. Main aim of the research described in the proposed paper is to evaluate effect of polymer on vaporization and with consequences on hydration process. Different amount of dosage of treated and not treated concrete were compared. Paper also describes three different testing methods of evaluation. Main advantage of this product is that this product can be also used as final treatment of concrete with good quality and appearance but also as bonding agent for following polymer layers.

KEYWORDS: fresh concrete, polymer coating

1. INTRODUCTION

One of the main factors for a final surface quality, at the process of concreting large slabs, is a guarantee of minimum evaporation of water necessary for hydration. Therefore a new material based on polymer resin was developed for protection of hydrating concrete. The goal of this work is a comparison of resistance of treated and untreated concrete and evaluation of applicability of specific tested materials including a determination of testing methodology. During a proper treatment of concrete it is necessary to provide enough of water for hydration and reduce undesirable tensile and compressive stress in concrete structure, which can be caused by rapid drying of concrete surface.

2. SURFACE PROTECTION OF CONCRETE

In the long term the concrete is deteriorated by physical (abrasion, frost in connection with moisture) and chemical (aggressive liquids and gasses) effects of environment.

In most cases an active protection, i.e. composition and processing of concrete, is not sufficient to prevent an intensive effect of aggressive media and it is necessary to use a passive protection based on a surface treatment.

As a protection against corrosion, the concrete surface is impregnated with penetration agents. Impregnation reduces water absorption through capillaries, the concrete surface is hydrophobed but diffusion of water vapor is not limited. Hardening stops penetration of water and water vapor into the porous structure of concrete and then there are applied paintings or coatings on the concrete surface. Refinishing methods of surface treatment of monolithic concrete as well as reinforced concrete elements, where not only durability but also esthetic appearance is required, can be also classified as a passive protection. [2] On one hand a surface protection of concrete increases its resistance, but on the other hand some defects can occur which can be caused by a number of influences.

2.1. Mechanisms of defects

Defects of impermeable layers, with long-term moisture effect, can have chemical or physical nature. Their most often manifestation is the following:

- softening of flooring (in larger extent at parts with bigger porosity or smaller diffusion resistance).

- development of cracks (the most often at surface and final layers), see fig. 1; separation of flooring from the base and creation of bulges (bubbles) filled with liquid and their perforation.

All these defects worsen or eliminate original advantages of flooring (protection layer), speed up destruction of flooring during its mechanical loading, decrease its esthetic appearance and damage its hygiene and biological quality.



Figure 1: Separation of flooring from the base and creation of bulges

3. EPOXY RESIN TREATMENT OF CONCRETE

Impregnation agent for treatment of concrete based on epoxy resin is two component low viscous material, water soluble. It is specially formulated hardening system with additives controlling hardening according to temperature of the surroundings.

3.1. Procedure for application of coating material

After concreting, laying and leveling, the concrete is let to mature and when it achieves such tensile strength that adult can carefully walk over it without any deformation, machine or manual processing must be immediately started. In the first phase, unification of surface with drawing of cement grout to surface and creation of homogenous even layer of cement paste is carried out. An even layer of

polymer epoxy coating is then applied without any delay by pouring and spreading on surface of the paste.

4. RESULTS OF EXPERIMENT MEASUREMENT

So far there were no effects, of treatment by above mentioned polymer agent, determined and/or documented, therefore the experimental part is focused on determination of surface moisture for specially treated concrete and implementation of testing which can characterized properties of treated material.

4.1. Monitoring of moisture under the surface coating by resistance method

The hydrometer GANN H-85 was used for measuring. Moisture was measured through the resistance by two stabilized probes embedded into the sample. The calibration curve of the instrument was applied and according to it, a new regression curve considering measured values was subsequently created, see fig. 1. Percentage moisture is then solution of given function.

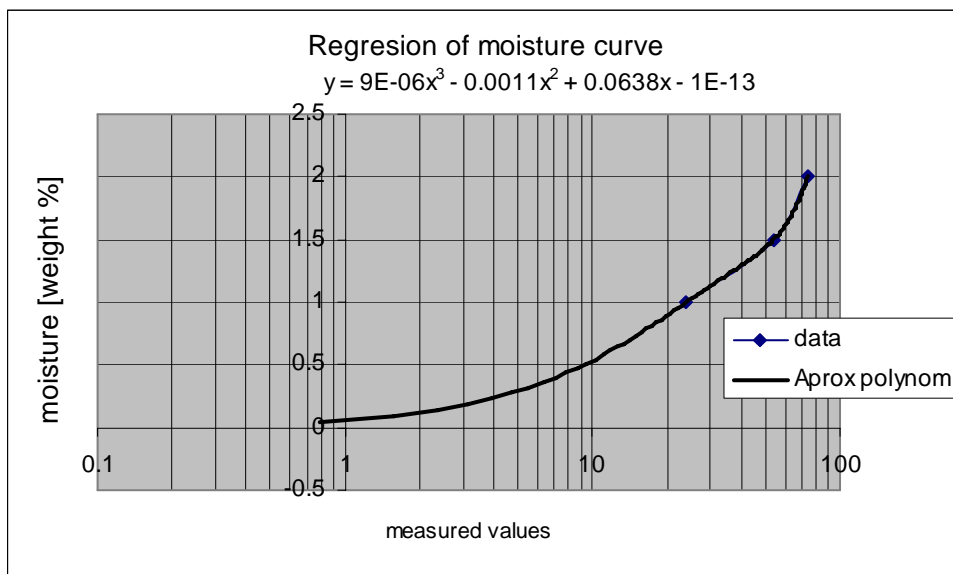


Figure 2: Regression curve showing relation between measured values of instrument and moisture of samples, which was created according to calibration curve of the instrument

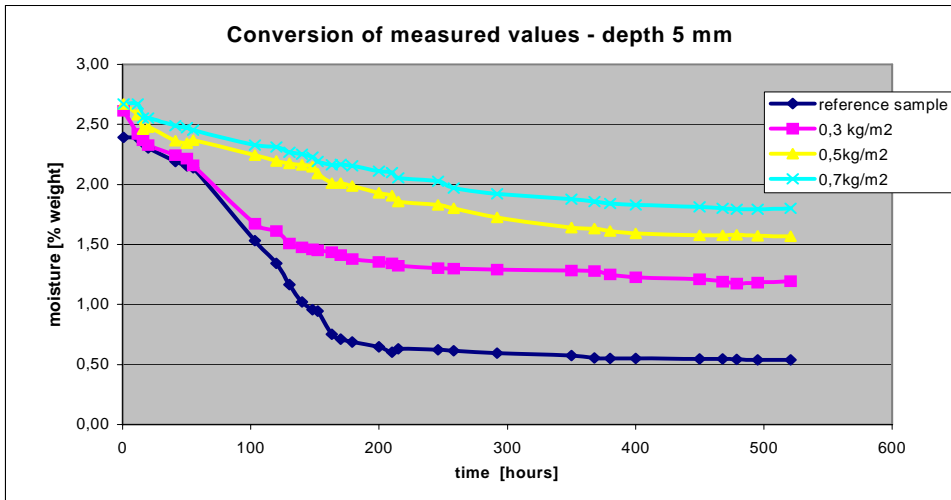


Figure 3: Moisture-time relationship; moisture was measured by two probes (embedded 50 mm deep in the sample underneath a surface polymer layer) in time intervals. Moisture is given in weight percentage

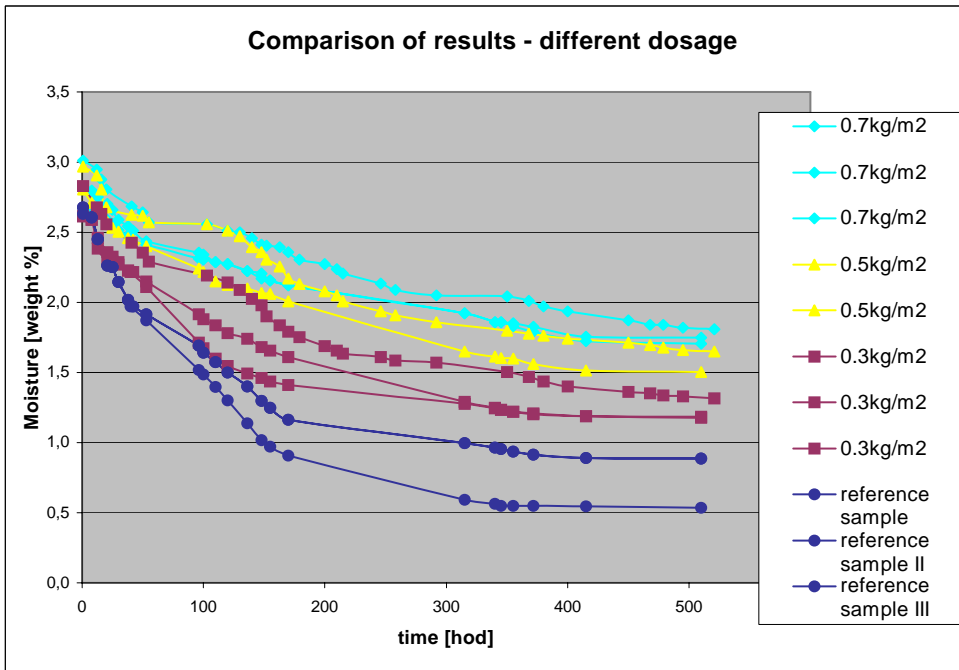


Figure 4: Demonstration of comparison of results for individual material layers during repeated moisture measurement by two embedded probes which scanned electric current running between them in time intervals

4.2. Gravimetric method – weighing of silicagel weight increase

An apparatus consisting of glass container, size 0.7 x 0.4 x 0.6 m, electric scale, thermometer, hygrometer, dish with annealed silicagel, PVC pad and sample of concrete was assembled at the laboratory.

The joint between the pad and glass container was filled with silicone in order to achieve, inside of container, constant conditions unvarying in time and particularly to avoid any penetration of environmental moisture to weighed silicagel. The sample with polymer surface coating was installed into one set and sample without polymer surface coating into the other.

Measured weight increase of silicagel was then directly proportional to absorbed moisture which evaporated from the sample. Measurement of silicagel weight increase was carried out in period of 360 hours until weight increases were stabilized.

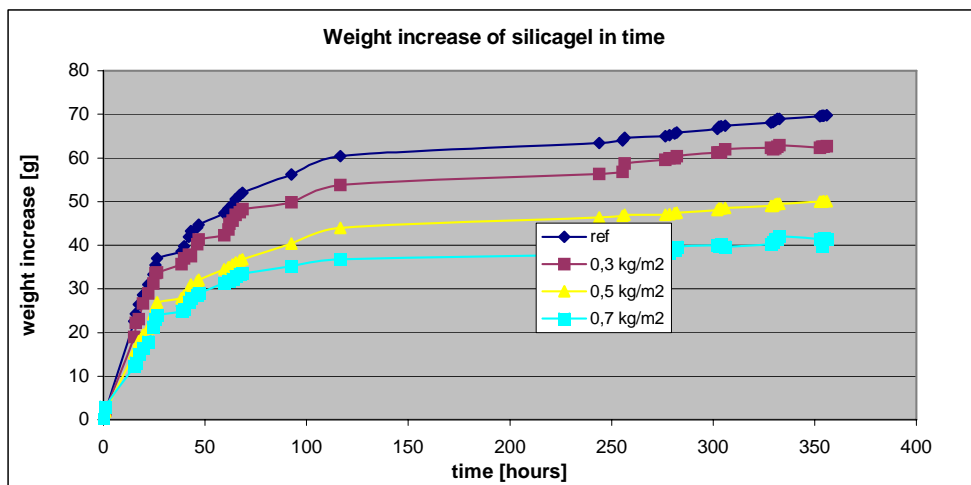


Figure 5: Weight increase of silicagel in time. Weight increase of silicagel was directly proportional to moisture evaporated from the sample and absorbed by silicagel

4.3. Gravimetric method – weighing of weight decrease of sample

Four samples with polymer surface coating of 0.3 kg/m²; 0.5 kg/m²; 0.7 kg/m² and reference sample were prepared.

These samples were weighted in regular time intervals on electric scale with an accuracy of two decimal places. Weight decrease of sample detects an evaporation of water from sample. Temperature in laboratory was 20°C and relative humidity 40%.

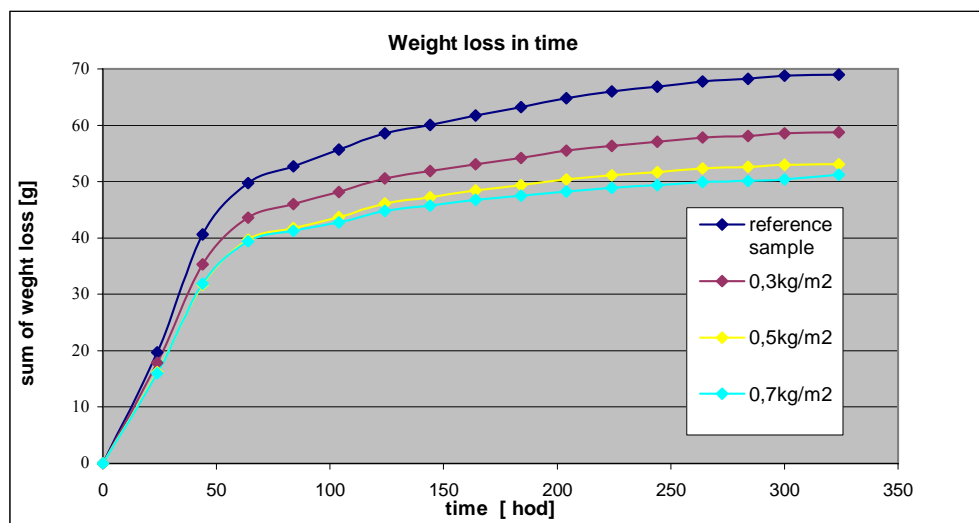


Figure 6: Sum of weight decreases of samples in time. Weight of samples was measured in regular intervals; weight decrease demonstrates evaporation of water from sample

4.4. Additional tests characterizing properties of concrete treated with impregnation

Determination of abrasivity resistance:

This test was implemented according to standard EN 67 3073 and EN 73 1324

Determination of permeability for water vapor:

Test of material permeability for water vapor was carried out according to EN ISO 7783-2. This test is proving ability or disability to create barriers for moisture transport through materials. The foundation of the method is a determination of weight increase of reacted absorber – silicagel diffused by water vapor through tested material placed in a measuring unit closed by tested sample with given area.

Test for surface finish adhesion of building structures to the base:

Test was carried out according to ČSN 73 2577. The foundation of this test is a measurement of force needed for separation of surface layer with a specific area by perpendicular traction. Testing steel plates with diameter of 50 mm are glued to surface coating. Plates are glued to surface with appropriate adhesive and afterwards the surface layer is cut with cutter. The depth of cut is such as cut does not reach the base but goes through the whole surface coating layer. The testing device DYNA was used for separation.

Adhesiveness was also determined on samples which were exposed to 10-month impact of petroleum products.

4.5. Results of additional tests

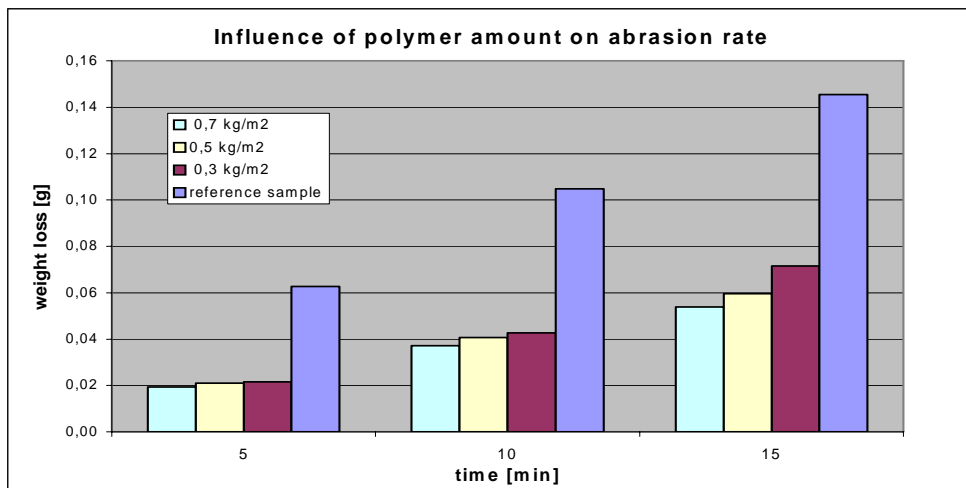


Figure 7: Effect of amount of polymer surface layer on abrasivity. There was measured a weight decrease of samples with application of polymer surface coating due to abrasive impact on sample

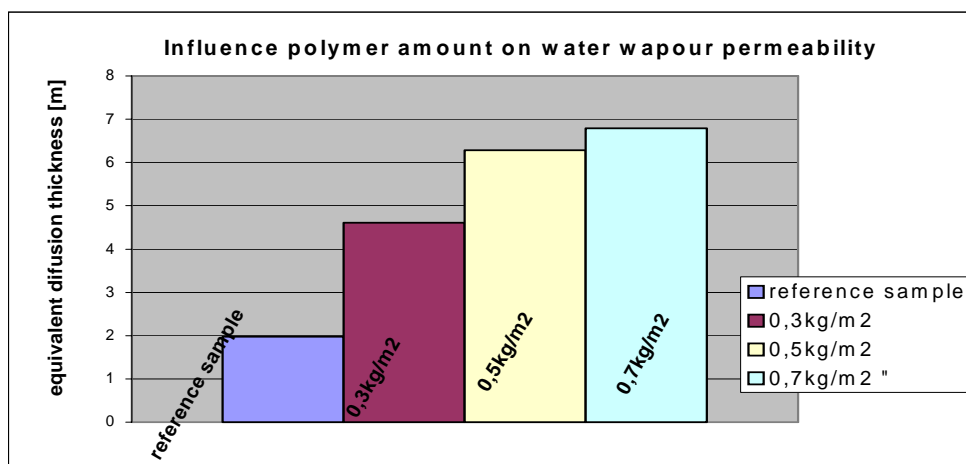


Figure 8: Effect of amount of polymer surface layer on permeability for water vapor. Graph is showing increasing equivalent diffusion thickness with higher dosage.

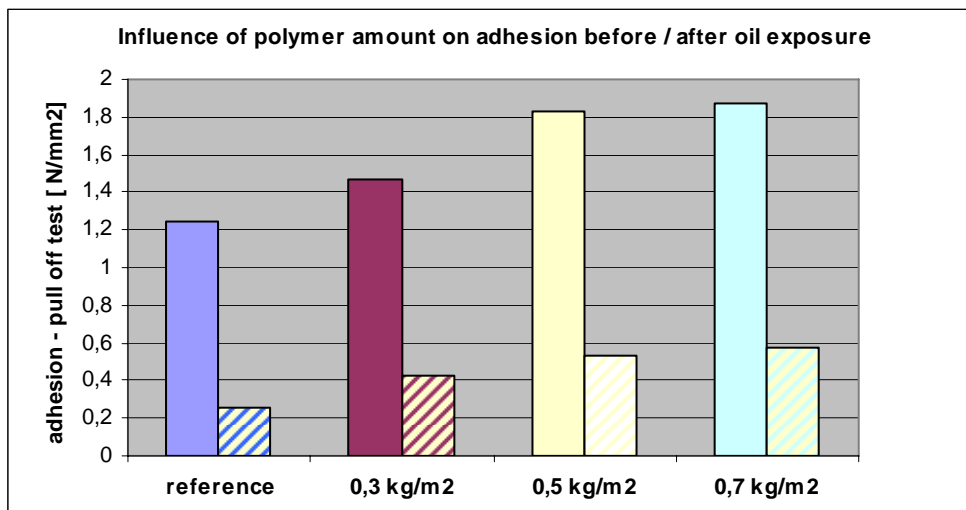


Figure 9: Effect of amount of polymer surface layer on adhesiveness of surface layer. Adhesiveness was measured on samples treated by polymer surface coating and compared with untreated samples; hereafter they were compared with samples exposed to 10-month impact of petroleum products

5. CONCLUSIONS

Based on all results obtained by measurement of moisture under impregnation agent, type: water-based epoxy resin, it can be stated that the biggest moisture decrease occurred during first 250 hours and moisture curve became stabile after 25 days. At measured polymer surface layer, i.e. treated samples, moisture release was slower than at untreated sample. A number of micro-cracks (noticeable through magnifying glass with 15-times optic enlargement) occurred on surface of untreated samples. Cracks were caused by fast water evaporation from sample due to hydration heat.

Coming out of evaluation of individual methods from the viewpoint of their implementation, the gravimetric method - weighing of weight decrease of sample – can be determined as the easiest for execution. For the resistance method with stabilized probes embedded into the sample and hydrometer GANN H-85, it is necessary to maintain a stable position of probes and prevent any power failure. It is also necessary to create relatively complicated regressive curve according to curve of instrument and recalculate a given function, which prolongs time needed for this method. Very varying data with no value were obtained after three-day measurement. This was due to large transitional resistances at individual metal probes.

Generally it can be said that with an increasing amount of polymer concrete coating, the permeability for water vapor decreases. This is due to epoxy resins, which have excellent resistance against penetration of water vapor. In the case of adhesiveness test of surface layer, samples treated by polymer surface coating demonstrated higher adhesiveness of surface layer than untreated samples. Further there was evident relationship between measured value of adhesiveness and amount of applied polymer layer. Adhesiveness of surface layer was increasing with increasing amount of applied polymer.

From presented results it is obvious that polymer surface coating significantly decreases water evaporation from concrete and improves its physical mechanical properties as well as increases a resistance of concrete against various corrosion effects. For example, from the progress of measurement of samples, which were exposed to 10-month impact of petroleum products, it was evident that degradation of treated samples was lower than for reference samples.

Acknowledgements

This paper was prepared with financial support from grant of the Czech Grant Agency 103/05/P262, entitled: "Thin layer protection systems for concrete exposed to special environment" and from the research project CEZ - MSM 0021630511, entitled: "Progressive Building Materials with Utilization of Secondary Raw Materials and their Impact on Structures Durability".

References

1. Drochytka, R., *Plastické látky ve stavebnictví (Plastic Materials in Building Industry)*, CERM, Brno, 1998.
2. Pytlík, P., *Technologie betonu. (Technology of Concrete)*, VUTIUM, Brno, 2000.
3. Bodnářová, L., *Teoretické základy kompozitních materiálů. (Theoretical Foundations of Composition Materials)*, CERM, Brno, 2003.

Slip-resistant Surface Treatments on Bridge Construction Walking Areas – the First Stage

Vít Petránek¹, Tomáš Melichar²

¹ Faculty of Civil Engineering, Institute of Technology of Building Materials and Components, Brno University of Technology, Brno, 602 00, Czech Republic, petranek.v@fce.vutbr.cz

² Faculty of Civil Engineering, Institute of Technology of Building Materials and Components, Brno University of Technology, Brno, 602 00, Czech Republic, melichar.t@fce.vutbr.cz

Summary

Fact that nowadays bridges and highways are inherent part of wide road-traffic infrastructure of each mature state or city there's no need to stress. Design of bridge in itself includes wide conception starting with geophysical exploration of subsoil, over design and construction reliability examination after as much as finishing work.

Problem of the article is aimed at the construction completing period of bridge structure, whereas research of suitable slip-resistant surface treatment for bridge sections, where it is demanded or appropriate. Contribution of the research performed within the paper is secondary raw material (SR) utilization on the surface treatment preparation.

Primarily optimal SR was selected, which was then applied in suitable specific proportion and grain size to prepared matrix (epoxy resin). In the next phase of the research, basic properties determination of the prepared mixtures was carried out, i. e. tensile strength by rip off test by another name standstill to bedding. During the last one stage some tests, which are characterizing durability of investigated surface treatment, will be performed, concretely abrasive and frost resistance.

KEYWORDS: surface treatment, slip-resistant, epoxy resin, secondary raw material, tensile strength, durability.

This paper was published with the financial contribution of research project CEZ - MSM 0021630511, “Progressive Building Materials with Utilization of Secondary Raw Materials and their Impact on Structures Durability and also of research grant GAČR 103/05/P262, “Thin layer surface protection systems for concrete structures exposed to special conditions”.

1. INTRODUCTION

The ecological aspects lead us to look for alternative material sources. A problem of mankind approach to waste or secondary raw materials utilization in assorted industries has been becoming still more topical. That is not else even in civil engineering, whether in case of bulk cargo bridge elements production or minim final works. With regard to fact, that building materials industry is one of the largest excrements producers and one of the hugest energy consumers, tendency of secondary raw materials utilization and together with it a depression of current technologies energy intensity is rising. Obviously, at the same time these facts has to be necessarily showed in economical point of the problem, which acts very important part too.

In principle, the paper is aimed to finding optimal slip-resistant surface treatments on bridge construction walking areas. This is forms significant part of bridges on the part of requirement for usage construction safeness.

2. THEORETICAL SECONDARY RAW MATERIALS ANALYSIS

At first a materials from which the surface treatments consist are need to be considered. Final composition of these mass is composite character. Composite is a material system, which is compound from two or more phases. The scale shows properties, which were not possible to attain by simple summation of single constituents. One of the simplest composite types is a binary system compound from matrix and filling agent. The system does not contain poruses (so-called third phase).

In our case the macromolecular-based matrix was used, concretely epoxy resin. With regard to its excellent parameters and output product required final properties the phase was not modified.

Attention was focused on only modifying the filling agent. It was necessary to find such secondary raw material, which occurs in suitable quantity and has not another significant usage in other industries. Important criterions at evaluation were composition and microstructure of the material. By virtue of situation survey in Czech Republic (CR) followed on several SR namely, fly ash, slag and recycled glass (RG). For purposes the research RG (which was from CRT – Cathode Ray Tube screen) was used. Nowadays it is recycled in CR, but not used for reverse utilization in some industries. With regard to CRTs chemical composition, strictly speaking contain of some lead, thermal behaviour and so on, it is not possible to utilize in the field of container glass production.

2. EXPERIMENTAL WORK

2.1. CRT Glass preparing

For purposes of the paper, CRTs glass was used. This forms as a waste material (fallout) at sintered glassilicate products manufacture (i.e. it is not suitable in light of fraction size). For reasons given passes, that energy intensity for the SR preparation is inconsiderable (hardly naught) within the scope of the research. Substitution of required fractions was modified only by sieve analysis. In term of slip-resistance and good material workability two kinds of fractions were chosen, 0,25 – 1 mm a 1 – 2 mm. These were used in part as filling agent as well as fill, whereas their combinations were seemly applied too.

2.2. Samples preparing

As mentioned earlier, research work has to do with two-part composite system, whose matrix is formed by epoxy resin. Two-part epoxy resin – Lena P102 was used for the experimental work. In advance prepared glass was applied to epoxy matrix partly as filling agent and partly as spreading. Thereby procedure an emphasis was posed first to slip-resistance, physical, mechanical and chemical (durability) of final substance. View of constitutors’ percentage substitution of particular specimens is stated in Table 1.

Table 1. Percentage substitution of particular constitutors in each batch (in percents)

Ground	Batch	Epoxy resin Lena P102 - component		Glass inside matrix – fraction		Glass fill – fraction	
		A	B	0,25 - 1 mm	1 – 2 mm	0,25 - 1 mm	1 – 2 mm
Concrete pavement	1	22,2	11,1	66,7	-	-	-
	2	18,2	9,1	27,3	-	-	45,5
	3	33,3	16,7	-	50,0	-	-
	4	33,3	16,7	50,0	-	-	-
	5	18,2	9,1	-	18,2	54,5	-
Ceramic tile	6	23,5	11,8	-	23,5	41,2	-
	7	21,5	10,8	-	21,5	46,2	-

Ad interim only two types of base course mechanical properties were investigated, namely concrete pavement and ceramic tile. In to the future among others a steel ground is considered. Immediately after the preparing test specimens the tensile strength determination by pull-out test according to appropriate standards was carried out. Steel discs of 50 mm in diameter were used for the determination. Test apparatus Dyna matches standard demands, i.e. makes possible to set up tensile

strength (adhesion) with an accuracy of two decimal places, without any computation necessity.

2.3. Samples testing

At rip off test (tensile adhesion determination) is proceeded so that disc dislocation is considered at first, their fastening on investigated surface treatment (by two-part special adhesive) is following. After the adhesive curing the discs are trimmed on eight sides (octagonal shape). In the next stage the tensile strength determination is carried out by means of afore mentioned apparatus.

Principle of tensile strength testing is showed in the Figure 1 (test specimen 3C). Place of failure registration is very important at testing. This puts us valuable information about the surface treatment physico-mechanical parameters. It is not suitable, if a failure on ground and surface treatment interface occurs abreast with low strength value (i.e. less than $1,5 \text{ N} \times \text{mm}^{-2}$). This verity is already predicating about insufficient adherence of the material on ground.



Figure 1. Principle of testing tensile strength by pull-out (rip-off) method

Achieved strength values view including place of failure is state in the Table 2. At cells marked with dash was not possible to determine strength value for some reason.

Table 2. Strength values of single treatment sample (batch)

Ground	Batch	Place of testing	Adhesive strength [$N \times mm^{-2}$]		
			max.	\emptyset	Place of failure
Concrete pavement	1	A	5,78	4,36	concrete
		B	6,64		concrete
		C	4,92		concrete
		D	-		-
	2	A	2,66	4,43	concrete
		B	4,76		ER upper-class
		C	5,73		concrete
		D	4,55		ER upper-class
	3	A	6,22	6,30	ER upper-class
		B	6,48		ER upper-class
		C	5,68		ER upper-class
		D	6,82		ER upper-class
	4	A	3,99	4,35	concrete
		B	4,19		concrete
		C	4,41		concrete
		D	4,81		concrete
	5	A	0,82	1,07	interface
		B	0,86		interface
		C	1,61		interface
		D	0,98		interface
Ceramic tile	6	A	0,73	0,67	interface
		B	0,73		interface
		C	0,57		interface
		D	0,64		interface
	7	A	0,64	0,73	interface
		B	0,81		interface
		C	0,75		interface
		D	-		interface

Figures of some specimens after the testing are showed on the next pages, where the places of failure and slip-resistance of surfaces are possible to clearly see. In case of ceramic tile ground, failure of the ground occurred.

Graphic evaluation of average strength values was performed for easier orientation and result comparing. This is showed on Figure 6.



Figure 2. Typical place of failure (sample 4A) in concrete ground (marked in Table 2 - concrete)



Figure 3. Typical place of failure (sample 3C) in surface treatment (marked in Table 2 - ER upper-class)



Figure 4. Typical place of failure (sample 5D) in interface of concrete ground and surface treatment (marked in Table 2 - interface)



Figure 5. Typical place of failure (sample 7C) in interface of concrete ground and surface treatment (marked in Table 2 - interface) – failure of ground

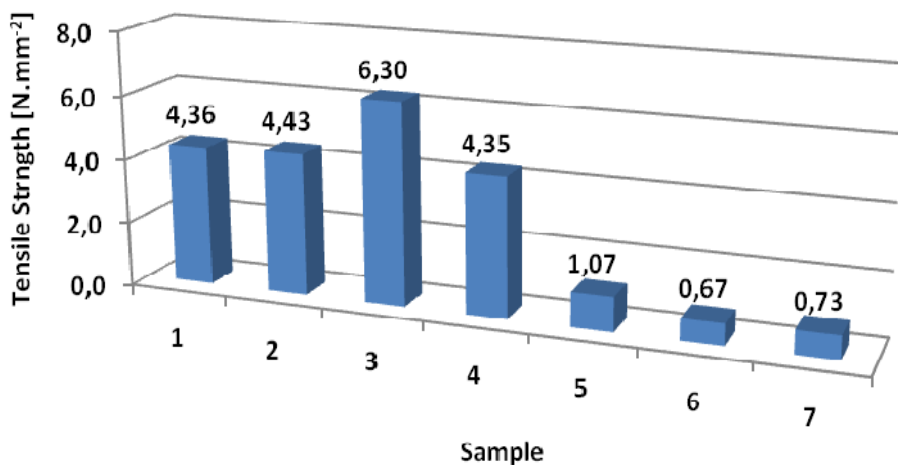


Figure 6. Average values of examined samples' tensile (adhesive) strength

3. CONCLUSIONS

Within the scope of the research a zero (preliminary) and the first stage were finished. These were concerned with development of optimal composite material, which is applicable as a slip-resistant surface treatment on bridge construction walking areas. The material under examination is macromolecular (matrix) and silicate-based (filling agent). Optimization was carried out by filling agent substitution with secondary raw material (SR). CRT recycled glass of two fractions was used, which is nonutilisable by-product at modified sintered glassilicate tiles manufacture. Contemporary filling agents of slip-resistant surface treatments are for example various sorts of fine sand, metal particles and other resistant materials.

A certain relation between tensile strength (adhesion) and some several factors passes out of accomplished physico-mechanical determinations. At first is clear, that strength values are considerably depending on used ground. As a quite unsuitable type of ground can be regarded ceramic tile. Next application criterion of the modified surface treatment is a filling agent bulk and fraction size. An important role plays method of filling agent (slip-resistant) application, i.e. whether bring glass inside to matrix or lay on surface by strewing. With aforementioned criterions nearly cohering bulk of the matrix, which approves oneself together with the filling agent application way to economical problem.

In term of usability for another research are showing as suitable batch 1 – 4. The maximum strength was attained in case of batch 3, which is with regard to application simplicity optimal. The filling agent is directly in matrix and only one fraction is there. On other hand this batch is not solving utilization of all SR fractions. In consequence a batch 2 is more suitable, which strength values are not reaching as high as batch 3, but the all SR fraction utilization is solved here. With regard to bulk of used epoxy resin batch 2 is the most economical.

In fine can be stated, that on the basis of slip-resistant surface treatments on bridge construction walking areas adhesion determination carried out is the most suitable the batch 3. With respect to fact, that the surface treatment essential criterion is slip-resistance, abrasive and frost resistance. These are subjects of the research next stages with batches 1-4. Then a steel ground influence is going to be investigated. Into the future, the slip-resistant surface treatments substituted with filling agent of SR character are real and suitable. However it is important to consider heavy metals influence (contain of lead 0-3 %) in CRT glass. This concerned with environment, i.e. their leach hazard.

Acknowledgements

This paper was published with the financial contribution of research project CEZ - MSM 0021630511, “Progressive Building Materials with Utilization of Secondary Raw Materials and their Impact on Structures Durability and also of research grant GAČR 103/05/P262, “Thin layer surface protection systems for concrete structures exposed to special conditions”.

References

1. Melichar, T., Petránek, V., *Využití druhotných surovin na silikátové bázi ve stavebním průmyslu*, Silichem 2007, Vysoké učení technické v Brně, Fakulta stavební, Brno, 2007. ISBN 978-80-214-3475-2

Seismic isolation of the Italian bridge: a case study

Mario Paolo Petrangeli¹, Luigi Fieno², Ciprian Dan Loata³

¹ *Bridges Design and Construction, “La Sapienza” University of Rome, 00184, Italy,
mario.petrangeli@mpaing.it*

² *Associate of Mario Petrangeli & Associati s.r.l., Rome, 00184, Italy, luigi.fieno@mpaing.it*

³ *Employee of Mario Petrangeli & Associati s.r.l., Rome, 00184, Italy, ciprian.loata@mpaing.it*

INTRODUCTION

The transversal communication between the Tirreno and the Adricatico coasts of the Italian peninsula, hindered by the presence of the Appennini mountain range, has been tackled quite late compared to the rest of the motorway network, in spite of its fundamental relevance for the socio-cultural development of the country. The designing and building processes of the connection between Abruzzo and Lazio regions began only in the early 70's, with the realization of A24 “Roma-L'Aquila-Teramo” and A25 “Teramo-Pescara” motorways.

Due to the complex orography of the terrain in question, the construction of several motorway bridges, artificial galleries and other structural works was necessary, bearing heavily on the costs and leading to the subdivision in multiple lots and a noticeable delay in the finishing of the works.

So much so that its completion is currently still in the construction phase, with the doubling of carriageways in the last single-carriageway tract going from Villa Vomano to Teramo. Its executive design has been prepared by Mario Petrangeli & Associates s.r.l. for Strada dei Parchi s.p.a. who currently manages the interested motorways in association with ANAS (a public limited company managing the majority of the Italian road and motorway network). Works, carried out by contractor TOTO s.p.a., amount to slightly more than 100 million Euros and comprise a natural gallery, about 800m long, and two viaducts for a total length of 3500m, as well as several minor works and landfills.

1. SEISMICITY OF THE ITALIAN TERRITORY

The Italian peninsula is subject to relevant seismic phenomena due to its location where the African, Euro-Asian and Adriatic tectonic plates meet, with their border developing exactly along the Appennini mountain range. The epicenter of the most significant seismic events of the 20th century is in fact in this area and they have been in 1908 – earthquake with epicenter in Messina, 83000 casualties; in 1915 –

Abruzzo, 30000 casualties; in 1976 – Friuli, 6,4° Richter scale earthquake, 982 casualties; in 1980 – Campania and Basilicata, 10° Mercalli scale, 3000 casualties.

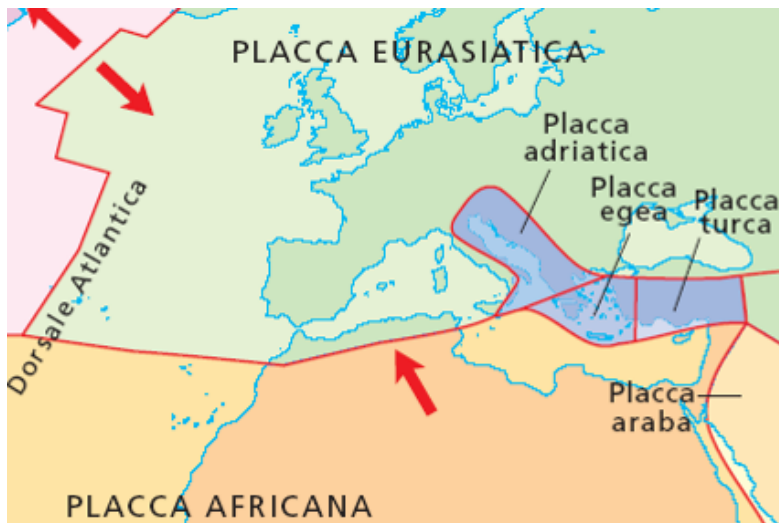


Figure 1. Tectonic plates

The evolution of the Italian seismic classification may be synthesized as shown in the following figure.

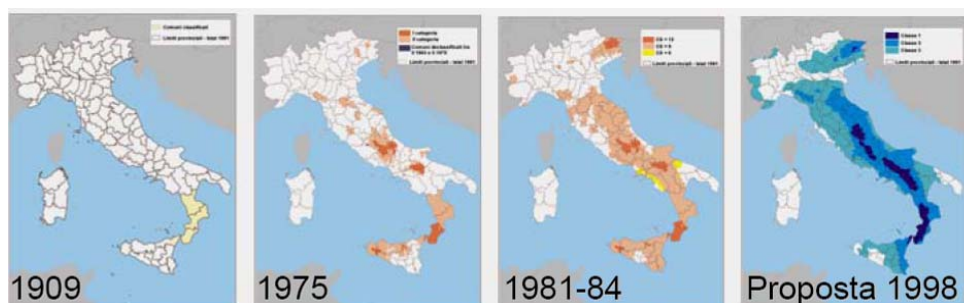


Figure 2. Evolution of the Italian seismic classification from 1909 (DPC-SSN)

Examining what happened during last century, it can be noticed that until 1980 classification followed the events, instead of foreseeing them. Only at the end of the 70’s, with the Geodynamic Finalized Project by CNR, which followed Friuli region earthquake of 1976, giving impulse to specific studies, danger level maps were created with proper scientific data and procedures. With these maps, between 1981 and 1984, a conspicuous portion of the territory previously considered non-seismic has been re-classified, extending from 25% to about 45% the portion of Italian territory classified in one of the three available categories.

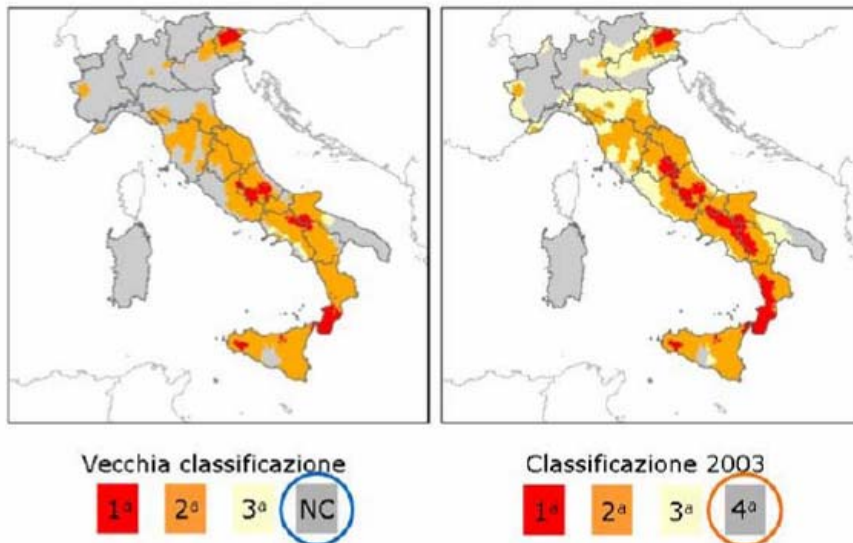


Figure 3. Comparison between old and new classification (DPC-SSN)

The new ordinance 3274 of 2003, brings to 67% the territory subject to seismic events and prescribes a minimum of one design seismic action for each new construction in non-seismic areas.

2. DESIGN CONSTRAINTS AND CHOICES

The design theme was atypical, as it concerned the doubling of existing roading. There had been two main critical aspects governing the design choices:

- constraints on the additional carriageways layout, which necessarily had to follow the existing one;
- the integration with the environmental context, with the necessity of keeping the structure coherent with what had been built previously in the area.

The Client input has obviously been to maintain span lengths, pier dimensions, general conformation and used materials of the existing viaducts. The roadbed of the new carriageway has been enlarged compared to the existing one and comprises of two 3,5m wide carriageways plus one 3,0m wide emergency lane, for a total width of 13m.

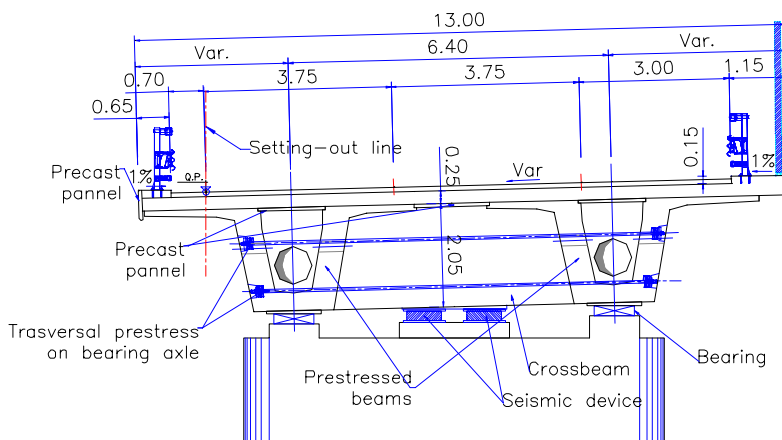


Figure 4. Transversal section

The choice made has been to maintain double box-girders in prestressed-concrete, similar in conformation and height to the nearby viaduct. The spans lengths have also been kept as similar as possible to the existing ones and such to guarantee the minimum axial difference between piers in order to avoid a visually unpleasant “wall effect” and in accordance with the horizontal alignment of the layout. Moreover, constructive requirements connected to beams prefabrication and more in general to construction cost-containment, as well as several interferences experienced at the piers basements, lead to the individuation of three classes of spans of 35,4m, 35m and 28m.

The design process has been long and complex and was concluded with the approval of the DEFINITIVE DESIGN after the completion of the Procedure of Evaluation of Environmental Impact (*design analysis from the environmental integration point of view carried out by Ministry of the Environment together with Territorial Superintendence for Artistic and Archeological Heritage, Local Authorities, etc*), and after CONFERENCE ON SERVICES (*a procedure during which the design has been introduced to local Authorities and all other public and private Administrations interested by the construction, under the mediation of Public Works Authority*),

The chosen solutions have not been dictated solely by the integration with what had been previously built, but also by matters of a more specifically structural nature. First of all, the presence of landslides for long portions of the layout, an issue tackled with solutions similar to those used by the existing viaducts: foundations on caissons 10 to 30m deep and 7 to 10m wide, variable according to the thickness landslide soil layers, with obvious negative effect on costs.



Figure 5. Caissons

Solving the issues linked to the site seismicity has been lot more complex.

The area where the viaducts are erected is classified as part of zone II of seismic risk according to the latest zoning of the Italian territory, which confirmed the classification given by the previous normative. The Client insisted for the structure to be classified as strategic (infrastructure that must maintain its functionality even after a disastrous seismic event to guarantee continuity for emergency relief and communications) and as such to be dimensioned with an increasing coefficient for seismic actions of 30%.

In the following paragraphs the variation in the normative approach will be treated in greater detail, what is brought to attention at this stage thought is how the increased cost of the seismic actions to be considered according to the new normative, the peculiar orography of the territory with consequent alternation between short and stout piers and tall and slender ones, the limitations in the piers and foundations dimensions, all concurred in the necessity of reducing as much as possible the seismic phase actions, with the choice of the most efficient seismic decoupling devices available.

Another decisive design choice has been the reduction of expansion joints between spans. This is in accord with the present trend shared by the totality of infrastructures managements, which aims for the reduction of maintenance costs and is also corroborated by the experience accumulated over the years on bridges and motorway viaducts erected mostly according to the simply supported beam scheme that has expansion joints on every pier and abutments.

The length of the treated viaducts lead nevertheless to the necessity of introducing a number of intermediate joints due to two main reasons: (i) the limitation of excursion of the joints and the support devices, having a direct influence on the piers longitudinal dimensions; this aspect brought to a maximum limit of excursion

in seismic phase of 250mm; (ii) and the necessity of limiting the longitudinal actions in seismic phase on the slab, which are obviously proportional to the mass connected to it and consequently to the number of connected spans.

On the basis of such considerations, the Sant’Antonio viaduct is divided into 5 minor viaducts with a maximum of 20 spans with continuous slabs, and each of these viaducts is linked in the longitudinal direction with 5 piers placed in their mid-spans.

3. BRIEF DESCRIPTION OF THE STRUCTURES

In this example are described the 777m long Vomano viaduct and the 2504m long Sant’Antonio viaduct which, together with Carestia Gallery represent the main structures for the completion of the doubling of Teramo – L’Aquila motorway in the Appennini tract, as shown in the layout plan below.

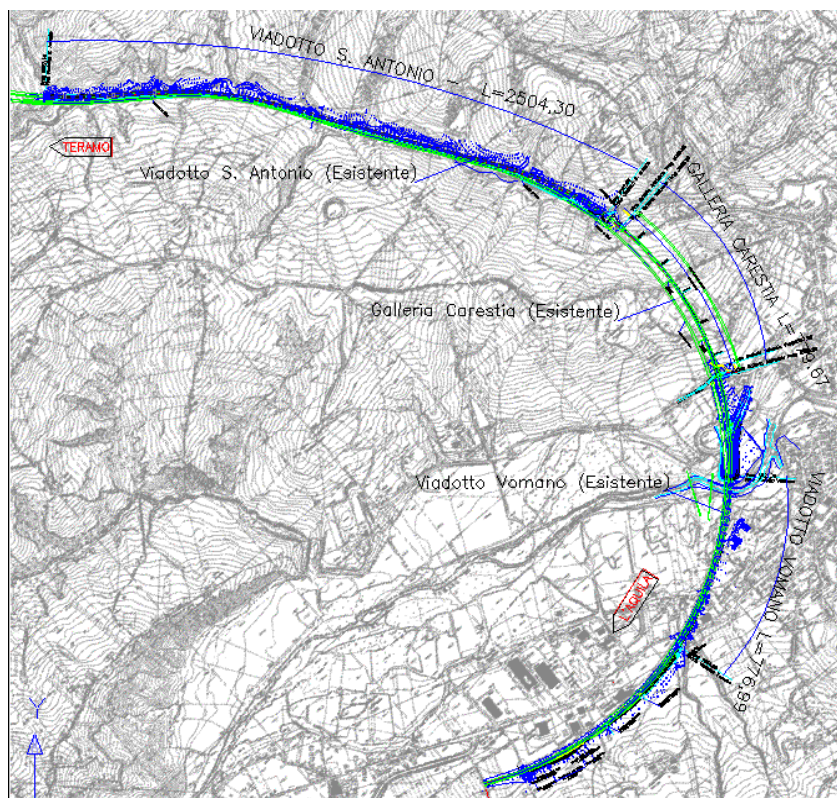


Figure 6. Appennine tract of A24 layout plan

The Vomano viaduct is composed by eighteen 35,4m long and two 28m long simply supported prestressed concrete spans, with continuous slab and no expansion joints, whereas Sant'Antonio viaduct is composed by seventy-two 35,4m or 35m long spans with three expansion joints. Decks are identical for both viaducts and are made of two box-girders 2,05m high, pre-fabricated in situ and prestressed with pre-tensioned strands, and cast in place of two cross-beams at support axis and of the 0,25m thick slab. (see figure 4)

The terrain morphology lead to a great variability of piers heights (4m to 18m), which have a 8,40x3,60m pseudo-rectangular hollow section, with 60cm thick walls.

The choice of viaduct foundation typology was influenced by the presence of landslide soil layers, so that it was necessary to use foundations on caissons of variable diameter and depth as already done with the twin viaduct; such caissons are butted 3m deep into the marlstone substrata.

In other places instead it was opted for more economical foundations on large diameter piles.

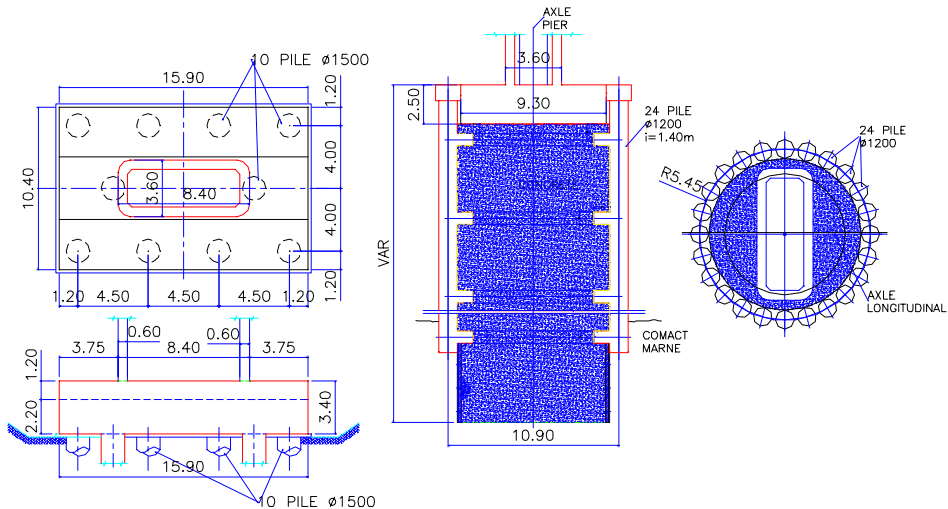


Figure 7. Foundations on plinth and Caisson

The supports scheme of a typical viaduct is shown in the following figures.

- For the longitudinal direction, each sub-viaduct is connected to 5 piers placed near the mid-span of the viaduct itself by means of double-effect, elastic behavior isolating devices; on other piers and on the abutments there are instead mobile supports with maximum excursions of $\pm 260\text{mm}$;

- for the transversal direction, an elastic bonding device of variable rigidity according to pier height is placed on each pier; fixed bonds are instead placed on abutments and expansion joints piers.

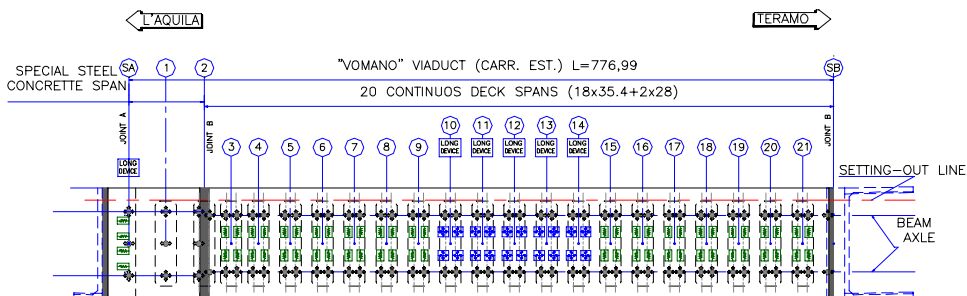


Figure 8. Supports scheme

Table 1. Characteristics of the seismic devices used

SEISMIC DEVICE					
	ELASTOMETRIC UNIDIRECTIONAL DEVICE				
	N°	WORK DIR.	H. Max(kN)	K. (kN/m)	δ (mm)
ABUTMENT A	4	LONG	800	3200	±260
P3,4,5,6	4X4	TRASV	1200	20000	±260
P7	4	TRASV	1200	16000	±260
P8,9,15...21	4X9	TRASV	1200	10000	±260
	ELASTOMETRIC BIIDIRECTIONAL DEVICE				
	N° PEZZI	Hlmax(kN)	Htmax(kN)	Kl(kN/m)	Kt(kN/m)
P10 ...14	4x5	2000	1200	10000	10000
JOINT					
JOINT TYPE A		Escursione max ± 150mm			
JOINT TYPE B		Escursione max ± 200mm			

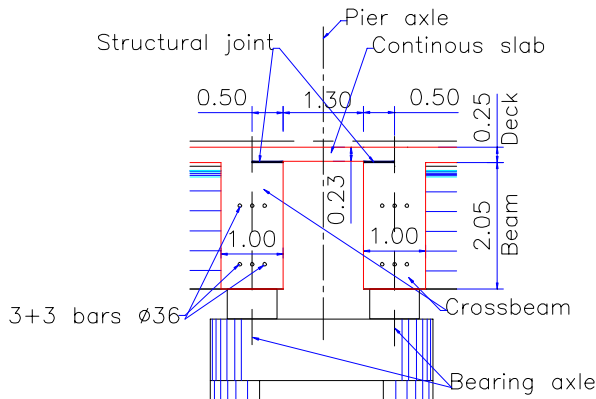


Figure 9. Continuity slab

The longitudinal expansion joints are dimensioned to guarantee creep due to normal service and frequent seism, implicitly accepting the cost of substitution in case of an exceptional seismic event which might break them.

4. SEISMIC ISOLATION

As it's widely known, the seismic isolation of a structure represents a very efficient technique to guarantee security against collapses and damages to persons and/or other structures in case of a catastrophic seismic event, and it is therefore expressively suggested by normative, especially in sites of medium to high seismicity. In the case of bridges and viaducts such technique finds its natural implementation due to their “mono-dimensional” conformation and their structural response. The new Italian seismic legislation, adhering to international regulations and specifically to the Eurocodes approach, proposes two main methodological approaches for the dimensioning of bridges under seismic actions: “elastic” or “ductile”.

The “ductile” approach has never managed to be properly implemented due to its lesser cost-effectiveness particularly for the dimensioning of foundations works. The ductile approach consists in dimensioning the works with a “design” spectrum reduced, in comparison to the elastic one predicted for the site, by a structural coefficient “ $q > 1$ ”; the reduction varies according to several characteristics such as the capacity of the sub-structures to guarantee a pronounced ductile behavior. Such attitude for a structure consists in its ability to guarantee great deformation in post-

elastic phase before reaching the breaking threshold and is exemplified by the formation of plastic hinges where the beneficial effect of energy dissipation is concentrated. About this, together with dispositions and constructive details widely codified by normative for different structures, the conformation and dimensioning of the sub-structures is of paramount importance. Viaducts with tall and slender piers (high H/b ratio), can be dimensioned with high structural coefficients (4,5); whereas with short and stout piers or, as the case in exam, with alternation or great irregularity of height and distribution of rigidity, lower structural coefficients are applied (1,5-2).

In the case of the viaducts in exam, the peculiar orographic conformation of the site has required short and stout piers alternated to much more slender ones and, more in general, a not-homogeneous distribution of rigidity, which impaired the regularity criteria determining reduced structural coefficients, which in turn readdressed the calculation to an “elastic” approach. The following picture shows the comparison between the two spectra.

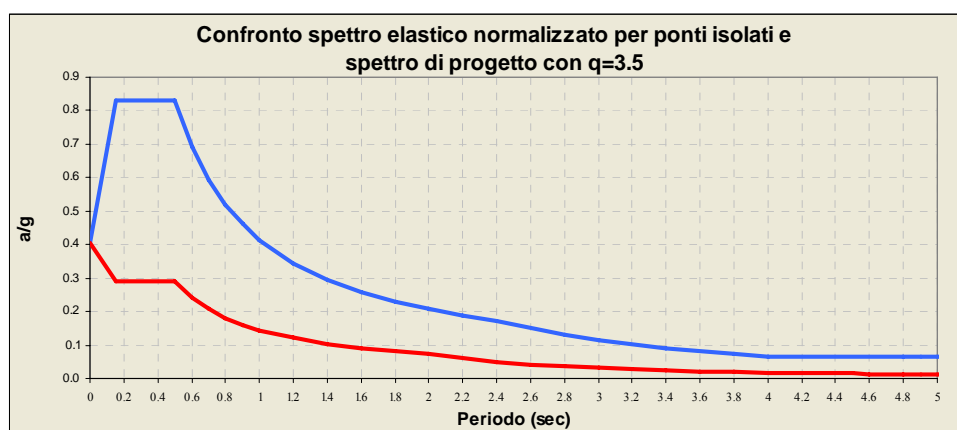


Figure 10. Comparison between “ductile” and “elastic” approaches

It is evident how the “elastic” approach is more demanding; in some cases it might then be more cost-efficient the use of passive control techniques of structural response such to reduce the seismic effects. There are several solutions that have been developed over the years and in this field the Italian experience is at the forefront with many companies manufacturing advanced systems.

In the case in exam the isolation technique has been applied which consists in the use, between two structural portions, of decoupling devices able to modify the response of the structure subject to seismic action. The isolated structure must remain in an essentially elastic phase and, because of this, structural coefficients of $q > 1,5$ are not allowed, so that their structural behavior during seismic event can be univocally determined.

The nature of such devices can vary (elastic, elastic-plastic, elastic-viscous), depending on the required effect. For the viaducts in exam simple elastic devices in vulcanized rubber with shear behavior were used, and they isolate the macro-viaducts in both longitudinal and transversal directions.

The usage of elastic-plastic devices would have allowed for example the introduction of a threshold to the forces transmitted by the device itself and thus to limit the stresses to the substructures with a general increase of the allowed displacements on the joints, as well as the costs and maintenance expenses.

In the following notes, a brief comparison between the various approaches mentioned above is given, showing the cost-effectiveness of seismic isolation in situations analogous to those of the viaducts in exam, re-enacting the logic progression of the chosen solutions.

INPUT DATA

- Infrastructure typology: roadway viaduct on 35,4m long spans, with 11,20m wide roadbed comprising two 3,5m carriageways plus 3,0m emergency lane;
- Structural typology: p.c. viaduct with prefabricated beams and cast in place continuous slab; total length of macro-viaduct: 660m; weight: 155000kN;
- Seismic zoning: site in zone II ($a_g=0,25$), terrain type E ($S=1,25$), strategic work ($I=1,3$).

DESIGN CONSTRAINTS

- Landslide surface soil; necessity of limiting foundations stresses;
- Limiting of deck-pier relative displacements ($\delta_{max} = 25\text{cm}$);
- Span lengths fixed to follow the existing twin viaduct.

DESIGN APPROACHES

- A. Isolated structure: intervention aimed at modifying the structural response → isolated structure → long. isolation or transv. isolation or long.+transv. isolation
- B. Non-isolated structure: determination of fixed elements on which “release” the horizontal actions;
 - B1. slender piers (design spectrum approach → constructive details to guarantee sufficient ductility → structural factor $q>1$ → criteria of resistance hierarchy check;
 - B2. stout piers or abutments → structure must remain in elastic phase → $q=1-1,5$.

Case A1 – ELASTIC ISOLATORS

N° FIXED PIERS= 5 piers= 17,7m

Devices= elastic devices with double rigidity effect= 40000kN/m/pier

Total rigidity k_{Tot} = 200000kN/m

Elementary oscillator vibration period $T_0 = 2 \pi \sqrt{m/k_{Tot}} = 1,77 \text{ sec}$

Seismic analysis → elastic spectrum for isolated bridges:

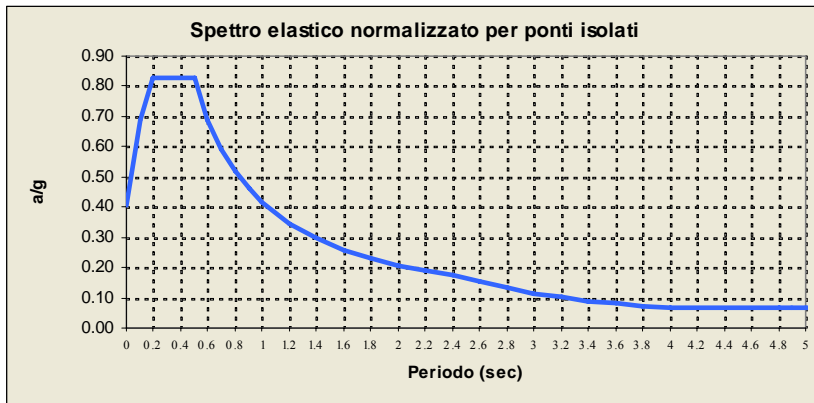


Figure 11. Elastic spectrum for isolated bridges

$a/g=0,25$, $S=1,25$, $\gamma I=1,3$, $\mu=10\%$

Corresponding spectral ordinate → $S(T_0) = 0,2343$ → $H = 1550000 \times 0,2343 \approx 36200 \text{ kN}$

For each pier $H = 36200/5 \times 1,15$ (coefficiente di sovra-resistenza) = 8326 kN

Maximum seismic displacement $\delta l = 208 \text{ mm}$

Case A2 – ELASTIC-PLASTIC ISOLATORS

It is possible to identify two variants:

- to connect the same 5 piers as in the previous example;
- to create a seismic retaining device on one of the abutments.

In the first case the same condition as in case A1 is obtained, but with slightly more expensive supplying costs and higher maintenance costs, with the end result of a reduction in actions transmitted to the sub-structures, but with larger displacements.

The second case would be of difficult application in the situation in exam due to the viaduct length and the displacements geometric limit.

Pros: limitation of design actions on substructures and foundations, lesser cost and complexity of piers ordinary reinforcement.

Cons: large displacements, greater cost for expansion joints.

Case B1 – NON-ISOLATED STRUCTURE IN DUCTILE APPROACH: $q > 1$

N# FIXED PIERS= $5/h = 17,5\text{m}$

Joint devices: fixed joint on central pier and impulsive type couplers on the two couple of adjacent piers.

Pier stem rigidity: $J_{\text{pier}} = 23,4\text{m}^4$; $k = 3EJ/h^3 = 4,4E + 0,5\text{kN/m}$

Total rigidity $k_{\text{Tot}} = 2,2E + 0,6\text{kN/m}$

Elementary oscillator vibration period $T_0 = 2\pi \sqrt{m/k_{\text{Tot}}} = 0,53\text{sec}$

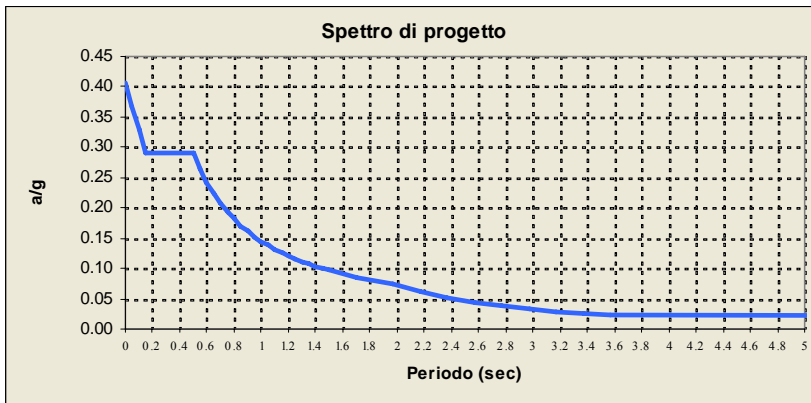


Figure 12. Design spectrum

Seismic action → Design spectrum with $q = 3,5$: $a/g = 0,25$, $S = 1,25$, $\gamma I = 1,3$, $\mu = 5\%$,

Corresponding spectrum ordinate → $S(T_0) = 0,273$ → $H = 1550000 \times 0,273 \approx 42315\text{kN}$

For each pier $H = 42315 / 5 = 8463\text{kN}$

Pros: limitation on displacements and reduction of actions for checks of piers sections;

Cons: coupling devices cost, greater cost of piers ordinary reinforcement to guarantee sufficient ductility, greater actions on foundations with consequent cost increase.

Case B2 – NON-ISOLATED STRUCTURE WITH STOUT SUBSTRUCTURES (piers or abutments)

Horizontal actions too great → modification of structural scheme and/or lighter deck.

5. CONSTRUCTION METHODS

The erection of the structure in exam imposed a careful study of the building site activities, especially in the case of Sant’Antonio viaduct. This was due to the presence of an existing viaduct in service and a torrential river which, in several occasions, interfered with the foundations of the new viaduct.

To complicate the situation further, was the presence of large portions of landslide soil layers that, as well as influencing the choice of foundations as mentioned above, required expensive and difficult site protection works ($\Phi 1000$ pile bulkheads).

Two building sites were appointed: the main one placed in correspondence with Vomano viaduct was used as prefabrication and stocking site for the prestressed beams; these were later launched by means of a metallic launching equipment.



Figure 13. Caisson foundation



Figure 14. Beams prefabrication site



Figure 15. Launching of a beam



Figure 16. Launching of a beam

6. CONCLUSIONS

What explained above, even with such ordinary structural typology, could be an example of correct design approach, which is to aim toward the right mediation between structural and security requirements, as well as limiting construction and maintenance costs of the structure to be erected. Concerning this, the introduction of new legislation brought on a real revolution in design approach that involved non only new works, but also those already erected which now have to be conformed to new dispositions.

Seismic isolation finds wide application in this area. There are several examples of this kind of interventions on existing motorway viaducts, some of them designed by the author, that making use of seismic isolation allowed the structure adjustment to the new legislation and further development of the motorway networks, while sensibly limiting costs. In some cases for example it was possible to maintain foundations and substructures, limiting interventions to decks by modifying or changing them with lighter ones (steel – concrete).



Figure 17. Application example of seismic isolation of existing viaducts by decks substitution and deployment of elastic-plastic dissipators on abutments

Generally speaking, it is possible to synthesize the Italian experience in bridge seismic isolation by defining it a relatively less expensive technique which, in association with a correct design approach as well as a correct construction procedure, allows to effectively and elegantly solve the issue of conformation to seismic regulation even for large structures.

The Influence of Size of Asphalt Mixture Samples Compacted with Gyrotory Compactor on Volumetric Properties

Carmen Răcănel¹, Adrian Burlacu²

¹Department of Roads and Railways, T. U. C. E., Bucharest, Romania, carmen@cfdp.utcb.ro

²Department of Roads and Railways, T. U. C. E., Bucharest, Romania, aburlacu@cfdp.utcb.ro

Summar

The actual European norms stipulate the volumetric mix design. This can be made by using the gyrotory compactor.

This paper has the propose to study the influence of size of asphalt mixture samples by means of mix quantity on volumetric properties of asphalt mixture: air voids, voids in mineral aggregates and voids filled with asphalt.

The results are obtained on a classical asphalt mixture, BA16 and an asphalt mixture with fiber, MASF16 and are presented in suggestive graphs.

KEYWORDS: asphalt mixture, gyrotory compaction, volumetric properties

1. INTRODUCTION

When it is considered the behavior of an asphalt mixture, it must take into account the volumetric properties of aggregates and asphalt mix. The volumetric properties of a compacted asphalt mixture are: air voids in mix, voids in mineral aggregates and voids filled with asphalt (bitumen). All these provide some indications on asphalt mixture performance during service life.

The gyrotory compactor is used in order to have samples with density close to field density, that will be tested in a specific laboratory equipment to obtain finely some information concerning to the mix behavior to the main distresses: fatigue and permanent deformation.

It is known that the asphalt mix design consists in selecting a proper mix between aggregates and asphalt so that the resulted asphalt mixture will be as durable as possible. A very important factor is the air voids. An asphalt mixture with a lower air voids that come from a high asphalt (bitumen) percent will lead to rutting and exudation. A high air voids that come from a low asphalt (bitumen) percent cause a sub-compacted asphalt mixture and will lead to deterioration of asphalt wearing course.

The goal of compaction is to transform the loose mix into a bound mix that can be able to support the traffic loads. Another goal of compaction is to make a tight and waterproof structure. An increase of mix density will lead to a strong mix but not necessarily to a strong pavement. It must be correlated the optimum density of asphalt mixture with the best combination between durability and stability.

The mix density depends on traffic and temperature (climate). The laboratory simulation of traffic is achieved by imposing a specific number of gyrations in gyratory compactor machine. Taking into account many weights of asphalt mixture and doing the samples compaction to the same number of gyrations it can be obtained specimens with different high and different density (so, different air voids) and it can be concluded what is the influence of samples size on volumetric properties.

2. THE USED MATERIALS AND RECIPES

This study was carried out in Roads Laboratory of Faculty of Railways, Roads and Bridges (Technical University of Civil Engineering of Bucharest) on two types of asphalt mixtures: a classical asphalt mixture BA16 type and an asphalt mixture with fiber MASF16 type.

The aggregates used to preparing the asphalt mixture were of Turcoaia and the filler, of Basarabi. It was used a bitumen of Romania, Arpechim D 60/80. The fiber from MASF16 mixture was Topcel.

The grading curves and grading zones for the studied asphalt mixtures are shown in figure 1 and 2 and the asphalt mixtures recipes are presented in table 1.

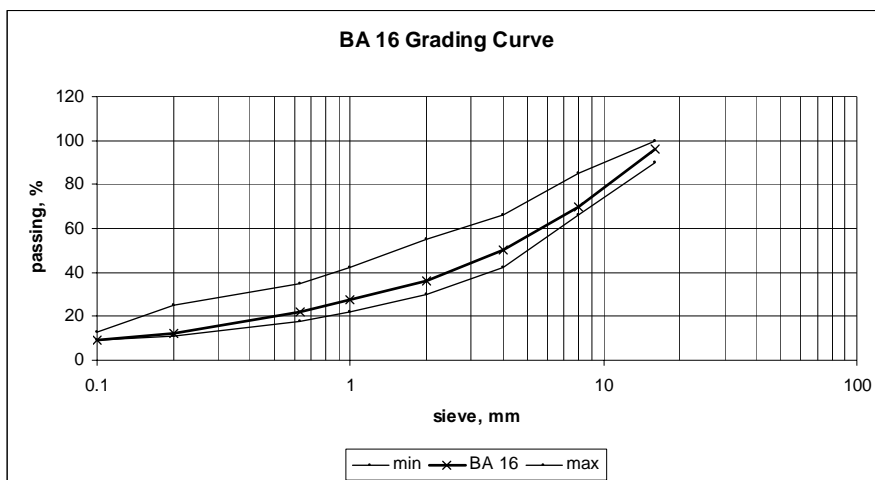


Figure 1. Grading curve and grading zone for BA16 asphalt mixture

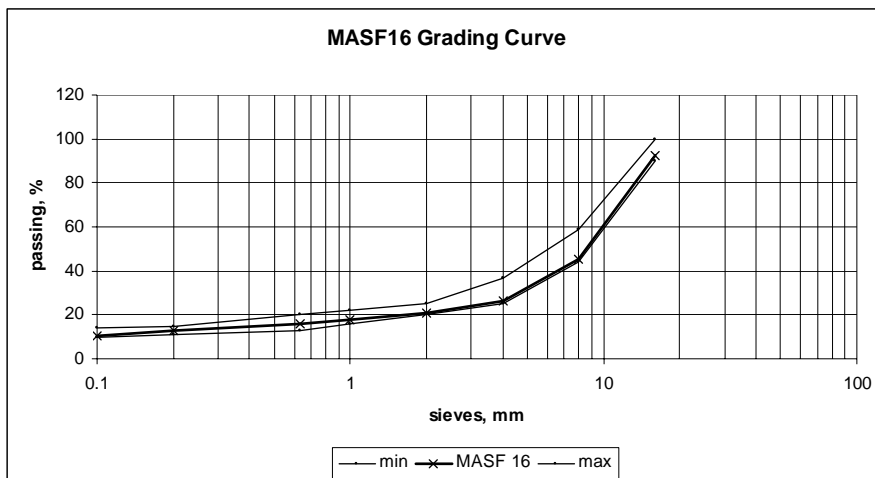


Figure 2. Grading curve and grading zone for MASF16 asphalt mixture

Table 1. The recipes of the used asphalt mixtures

Mixture	% Crashed rock			% Filler	% Fiber by mixture	% Bitumen by mixture
	8/16	4/8	0/4			
BA16	28	23	38	11	-	5.75
MASF16	53	22	12	13	0.6	6.50

3. THE RESEARCH METHODOLOGY

From the two mix types were prepared cylindrical samples with TROXOLER 4140 Gyratory Compactor (figure 3). The diameter of all samples was 100 mm. The compaction was performed in accordance with European norms.

To gauge the influence of sample size on volumetric properties of the mixes, seven sample sizes were used for MASF16 mix.



Figure 3. TROXOLER 4140 Gyratory Compactor

The sample sizes will result in sample heights ranging from 51 to 111 mm for BA16 asphalt mixture and from 63 to 71 mm for MASF16 asphalt mixture. The samples have 100 mm in diameter.

The samples heights were continuously recorded during compaction (figure 4 and 5). All mix were subjected to 288 gyrations which is the maximum recommended number of gyrations for the most severe conditions of traffic and environment in accordance with Strategic Highway Research Program.

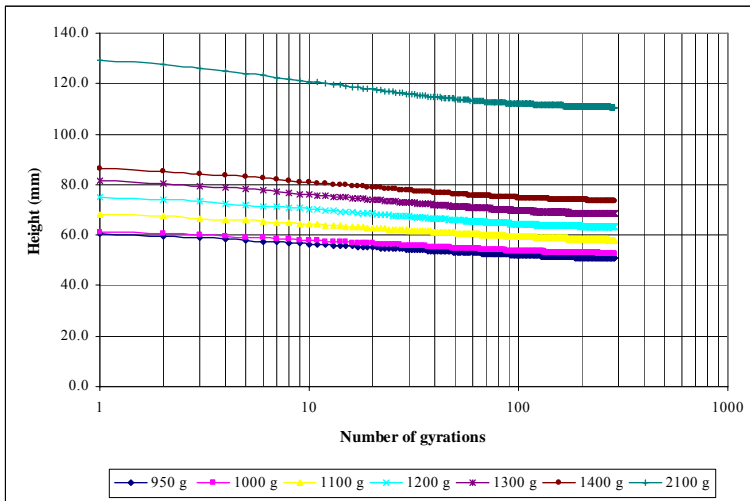


Figure 4. The samples heights versus number of gyrations, BA16 asphalt mixture

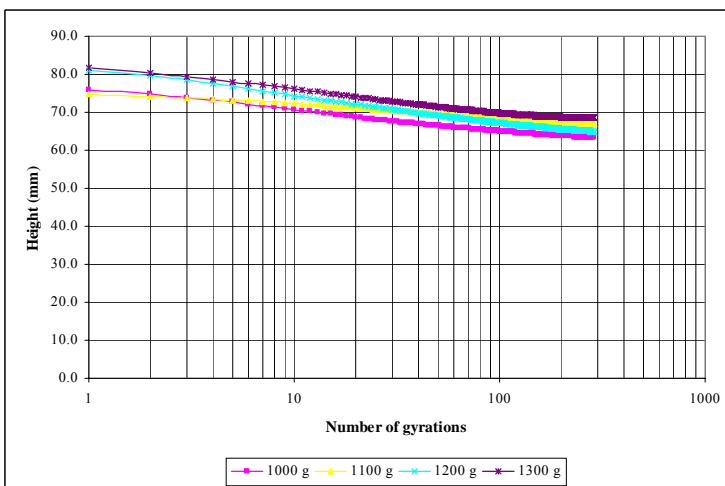


Figure 5. The samples heights versus number of gyrations, MASF16 asphalt mixture

4. RESULTS

First, based on compacted samples sizes and compacted samples weights were obtained the bulk specific gravity and the maximum theoretical specific gravity at 288 gyrations (table 2 and 3).

Table 2. Bulk specific gravity and maximum specific gravity at 288 gyrations, BA16

BA16 asphalt mixture	Sample	h, cm	G_{mb}, g/cm³	G_{sb}, g/cm³	G_{se}, g/cm³	G_{mm}, g/cm³
950	1	5.2	2.396	2.833	2.259	2.570
	2	5.1	2.419	2.833	2.280	2.570
1000	1	5.3	2.424	2.833	2.284	2.570
	2	5.3	2.416	2.833	2.277	2.570
1100	1	5.8	2.416	2.833	2.277	2.570
	2	5.8	2.418	2.833	2.279	2.570
1200	1	6.45	2.383	2.833	2.246	2.570
	2	6.3	2.420	2.833	2.280	2.570
	3	6.4	2.419	2.833	2.280	2.570
1300	1	6.9	2.412	2.833	2.274	2.570
	2	6.9	2.416	2.833	2.278	2.570
1400	1	7.4	2.414	2.833	2.275	2.570
	2	7.4	2.426	2.833	2.287	2.570
2100	1	11	2.423	2.833	2.284	2.570
	2	11.1	2.412	2.833	2.273	2.570

Table 3. Bulk specific gravity and maximum specific gravity at 288 gyrations, MASF16

MASF16 asphalt mixture	Sample	h, cm	G_{mb}, g/cm³	G_{sb}, g/cm³	G_{se}, g/cm³	G_{mm}, g/cm³
1000	1	6.3	2.277	2.830	2.129	2.537
	2	6.4	2.285	2.830	2.137	2.537
1100	1	6.7	2.303	2.830	2.154	2.537
	2	6.7	2.283	2.830	2.135	2.537
1200	1	6.5	2.421	2.830	2.264	2.537
	2	6.5	2.417	2.830	2.260	2.537
1300	1	7	2.421	2.830	2.263	2.537
	2	7.1	2.413	2.830	2.256	2.537

Where: h is height;

G_{mb} - bulk specific gravity of mixture;

G_{sb} - bulk specific gravity of total aggregate

G_{se} - effective specific gravity of total aggregate

G_{mm} - maximum theoretical specific gravity

Following the performing of gyratory compacted samples, using Gyratory Compactor Software, were obtained the results of maximum theoretical specific gravity (figure 6 and 7), air voids in compacted mix (figure 8 and 9), voids in mineral aggregate (figure 10 and 11) and voids filled with asphalt (figure 12 and 13) for a specific number of gyrations.

In figure 14, 15, 16 it is shown the influence of sample size represented by the weight of specimens on samples height, air voids, voids in mineral aggregate and voids filled with asphalt at 288 gyrations.



Figure 6. Maximum theoretical specific gravity versus number of gyrations, BA16 asphalt mixture

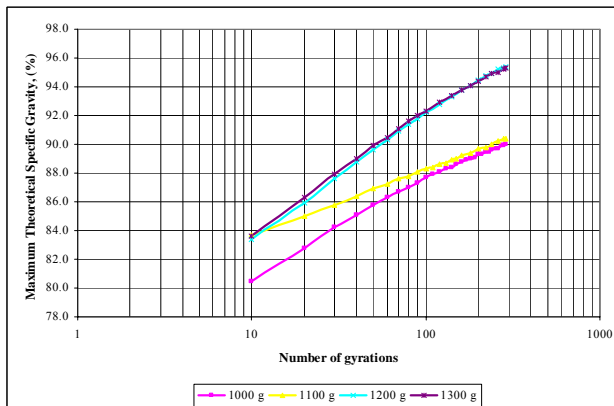


Figure 7. Maximum theoretical specific gravity versus number of gyrations, MASF16 asphalt mixture

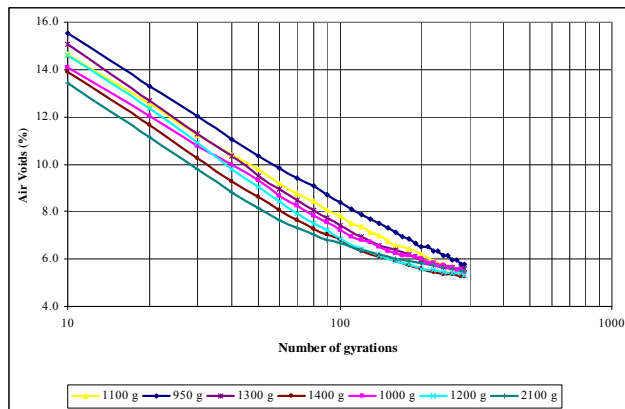


Figure 8. Air voids versus number of gyrations, BA16 asphalt mixture

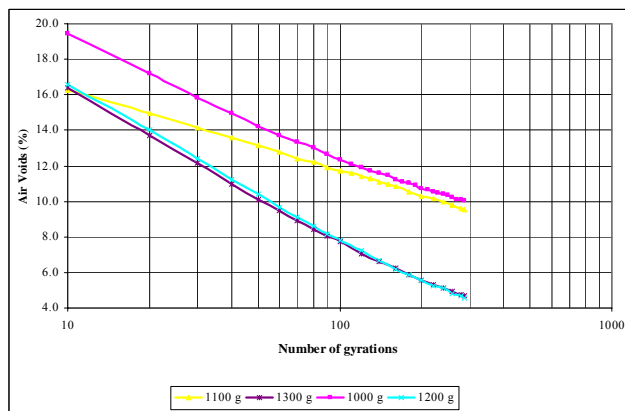


Figure 9. Air voids versus number of gyrations, MASF16 asphalt mixture

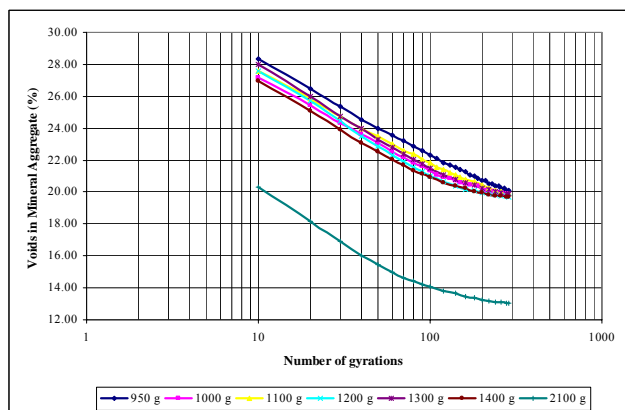


Figure 10. Voids in mineral aggregate versus number of gyrations, BA16 asphalt mixture

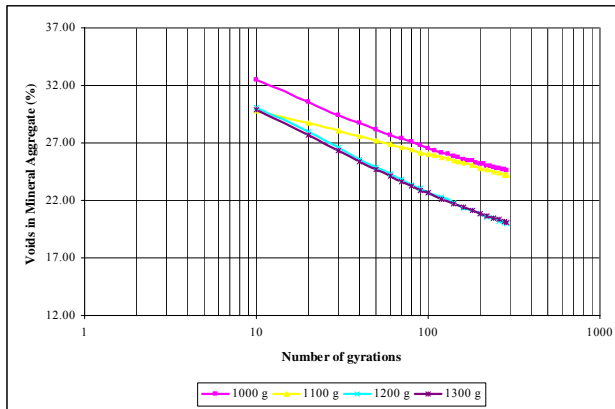


Figure 11. Voids in mineral aggregate versus number of gyrations, MASF16

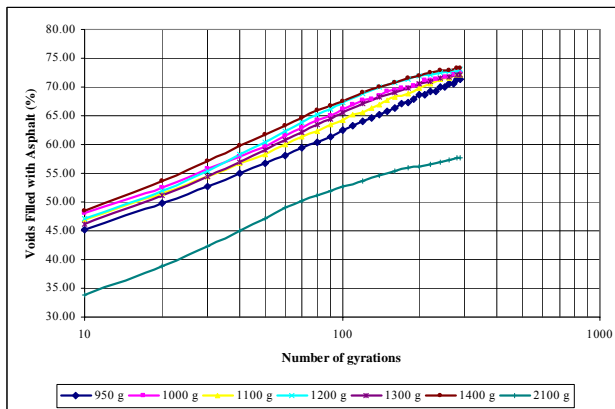


Figure 12. Voids filled with asphalt versus number of gyrations, BA16

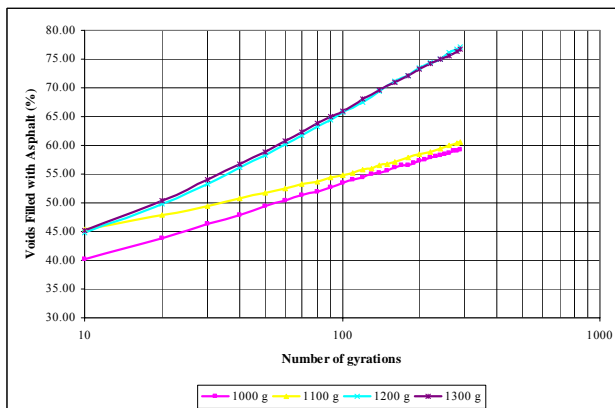


Figure 13. Voids filled with asphalt versus number of gyrations, MASF16

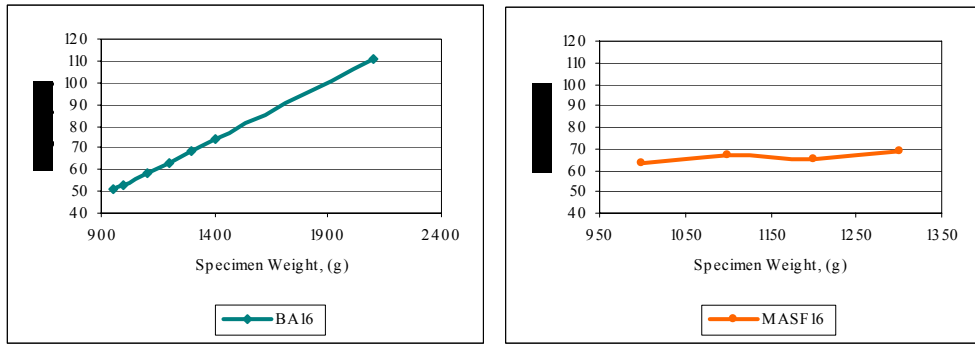


Figure 14. Weight of specimens versus samples height at 288 number of gyrations

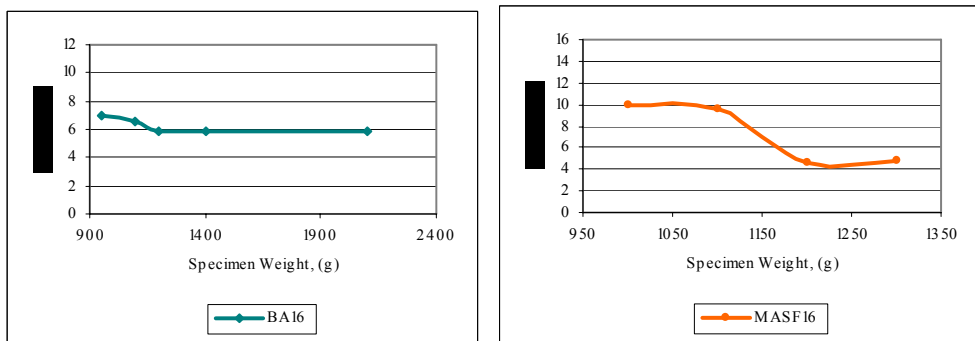


Figure 15. Weight of specimens versus air voids at 288 number of gyrations

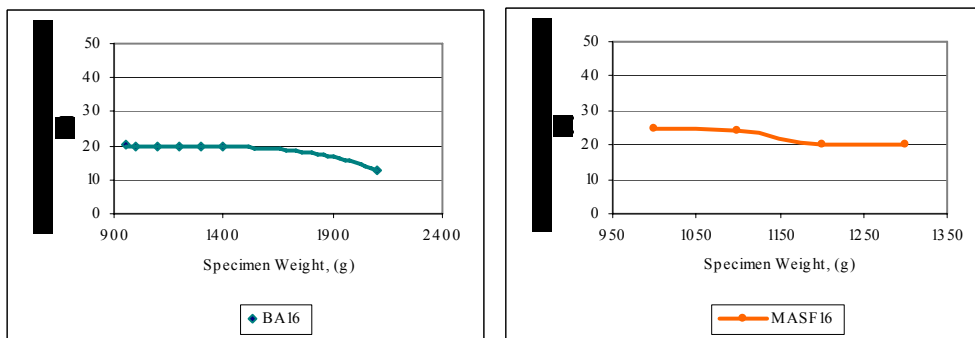


Figure 16. Weight of specimens versus voids in mineral aggregate at 288 number of gyrations

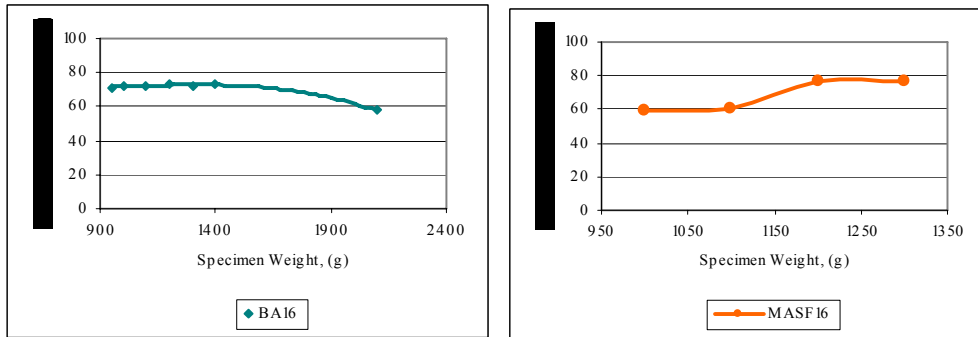


Figure 17. Weight of specimens versus voids filled with asphalt at 288 number of gyrations

5. CONCLUSIONS

As it is known, the gyratory compaction is essential to volumetric mix design and sample fabrication.

The sample size has the potential to affect the behavior of the asphalt mixture in the gyratory compactor.

From this experimental study, with respect to sample size, the following conclusions can be drawn:

1. The air voids and the voids in mineral aggregate decrease with the number of gyrations, irrespective of the type of asphalt mixture;
2. The voids filled with asphalt and the maximum theoretical specific gravity increase with the number of gyrations, irrespective of the type of asphalt mixture.
3. The same value of the air voids it is reached for a different number of gyrations depending on sample weight, irrespective of the type of asphalt mixture.
4. For BA16 asphalt mixture, number of gyrations smaller than 100, for air voids, bigger the weight of samples smaller the number of gyrations, in the case of 950 g, 1400 g and 2100 g weight. But in the case of 1000 g, 1100 g, 1200 g, 1300 g weight, the air voids curves are very close each other.
5. For BA16 asphalt mixture, number of gyrations greater than 100, for air voids, there are not differences between the air voids curves, irrespective of the sample size.
6. For MASF16 asphalt mixture, for air voids, bigger the weight of samples smaller the number of gyrations.
7. The same conclusions it was drawn for the voids in mineral aggregate curves.

8. For BA16 asphalt mixture, 47 % increase of sample weight lead to 17% decrease of air voids, 2% decrease of voids in mineral aggregate and 2% decrease of voids filled with asphalt.

9. For MASF16 asphalt mixture, 30 % increase of sample weight lead to 53% decrease of air voids, 18% decrease of voids in mineral aggregate and 30% increase of voids filled with asphalt.

It is important to specify that the gradations and the bitumen percent for the mixes used in this study is base on Marshall method.

The research should be continued in order to compare compaction and volumetric properties of laboratory samples representing various sample sizes to field samples representing various thickness.

References

1. Răcănel, C. *Proiectarea moderna a retetei mixturii asfaltice*, Editura MatrixRom, București 2004. (in Romanian)
2. Transportation Research Record No 1545, *Asphalt Pavement Surfaces and Asphalt Mixtures*, National Academy Press Washington, D.C., 1996.
3. SR 174-1/2002, *Îmbrăcămiși bituminoase cilindrate executate la cald.*
4. SR EN 12697-31/2006, *Bituminous mixtures. Test methods for hot mix asphalt. Part 31: Specimen preparation by gyratory compactor.*

The evaluation of dynamic effect of vehicles on bridges using the finite element method

Ionuț Radu Răcănel

Department of Bridges, T. U. C. E., Bucharest, Romania, ionut@cfdp.utcb.ro

Summary

The knowledge of the dynamic effects of vehicles on road and railway bridges is of major importance for establishing the response of those structures under these external loads. For design and verification purposes, the maximum values of stresses on the structural element cross section should be established by accounting the dynamic effect of moving loads.

Generally, the dynamic effect of vehicles is accounted for in calculations by considering some coefficients, which are specified in the national standards. The values of these coefficients take into account the vehicle type, the static scheme of the bridge, the position of vehicles on the bridge deck in transverse and longitudinal direction, the number of vehicles, the type of the way and also the type of the material in the structural elements.

The multiplication of the stresses, obtained from a static analysis, by the value of the dynamic coefficient, can lead to unrealistic results, because the direct superposition of the stresses to obtaining the maximum values for design and verification assumes that all stresses have the same distribution law with respect to time. In reality, the maximum values of the stresses following a dynamic analysis depend on time and therefore, the peaks are produced at different time steps. Considering the maximum values of the stresses at the same time step is conservative, but for slender structures, sensible to dynamic actions, can lead to unrealistic results, to over sizing of the cross section dimensions and by this to considering expansive construction details.

For this reason, this paper presents a methodology for the evaluation of the response of a bridge structure on the dynamic action of vehicles, which cross the bridge at different several speeds. Then, considering the variation in time of the stresses on elements cross section, a method is proposed for the stresses superposition, in order to obtain the values for design and verification.

KEYWORDS: bridge deck, moving loads, dynamic effect, time step, cross section

1. INTRODUCTION

The dynamic effect of vehicles crossing the bridges should be taken into account for design and verification, especially for slender structures as those having tall and slender piers and abutments. Generally, in calculations, the consideration of the dynamic effect is made by multiplying the values of stresses resulted from static analyses by a dynamic coefficient, which is given in national codes and standards.

The values of the dynamic coefficient given in standards were established both using theoretical and testing methods. The first category uses the integration of differential equations given by the structural dynamics. The second category uses the results of stresses and displacements measurements performed on a large number of bridges. The value of the dynamic coefficient is finally established as the ratio between the value of the stress (or displacement), measured when a vehicle crosses the bridge at a particular speed and the value of the same parameter when the vehicle stands still on the bridge.

The use of the dynamic coefficients given in norms in the calculation of old bridges shows, for some structures and structural elements, major over passing of allowable limits of stresses for some verification criteria. In the same time, the inspection of these bridges has shown that are no reason for worry, because no severe damages are present. This lead to the conclusion that the values of the dynamic coefficient specified in norms can be larger than in the reality.

In this paper are presented the results of a dynamic analysis performed on a concrete bridge structure, which was analyzed considering a 3D finite element model. The bridge has tall piers, and following the analysis, the evolution of stresses with time on the piers cross section, during the vehicle action, was established.

2. DESCRIPTION OF THE ANALYZED STRUCTURE

The bridge structure presented in this paper is in fact a viaduct on the future motorway “Transilvania”, on the road section between Târgu Mureş and Cluj-Napoca, km 18+502.42 and km 18+659.72. The bridge (Fig.1) is placed in a curve with a radius of 1600 m, has a longitudinal slope of about 5% and was designed in the solution with four spans: the two end spans have 38.55 m and the other two current spans have 40.00 m.

The bridge substructure consists in two wall abutments (A1 and A2) and three piers (P1, P2 and P3) having a box cross section made in reinforced concrete class C25/30 (Fig.2) and variable heights between 22.00 and 40.00 m. The superstructure for a roadway consists in four juxtaposed prefabricated U beams

made in reinforced and prestressed concrete (Fig.2) covered by a concrete slab having a thickness of 25 cm. The height of the girders is 2.20 m and there are made in concrete of class C35/45. The width of the carriage way on the bridge is 12.00 m. The bearing of the superstructure on the substructure is made through neoprene bearing devices type XII, these having a depth of 63 mm.

All substructure elements (abutments and piers) have shallow foundations. The foundation mat is in plane a rectangle with the following dimensions: 8.00m in bridge longitudinal direction, 10.00 m in transverse direction and a thickness of 2.00 m.

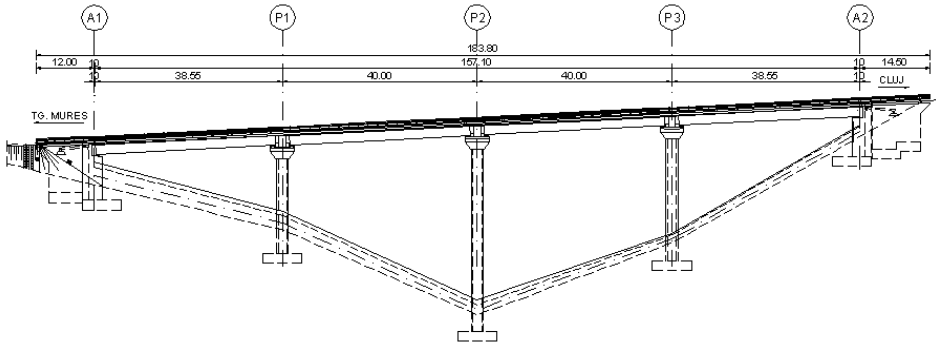


Figure 1. Elevation of the bridge

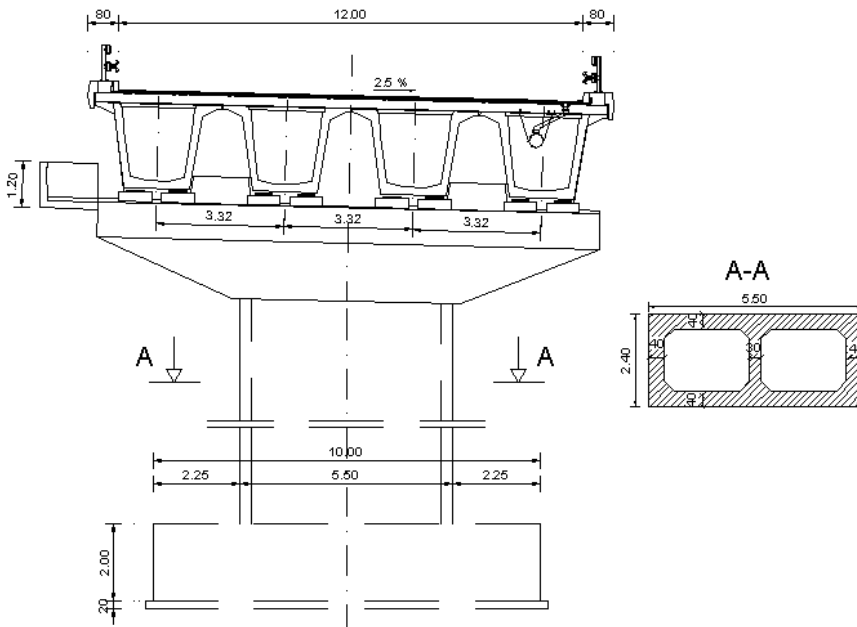


Figure 2. Transversal view of the bridge and pier cross section

3. FINITE ELEMENT MODELS

Because of the special geometry of the bridge, caused both by the presence of the longitudinal slope, but also by the pier height, the analyses were performed using the finite element method.

Two types of discrete models, according to the type and way of action of external loads were considered: one model which corresponds to actions which are varying slow with time (their variation in time is similar to the those of the concrete shrinkage and creep) and another model which consider that all external loads are applied quick (they act on the structure in very short time period, with respect to the duration of shrinkage and creep phenomena).

The 3D finite element model of the bridge (Fig.3) was realized so that it respects the static scheme of the structure, taking into account the fact that, in the construction stage of girders they act as simply supported beams and after pouring the concrete slab, they form a continuous girder with four spans.

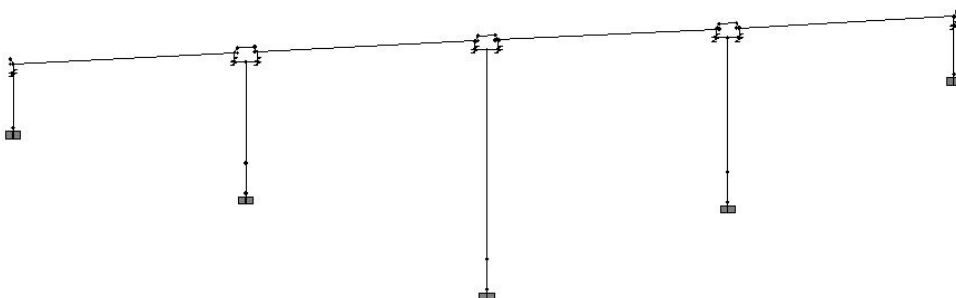


Figure 3. 3D finite element model of the bridge

The bridge deck was modeled with two nodes straight frame elements having activated all six degrees of freedom (three translations and three rotations). These finite elements were disposed in the centroid of the whole superstructure and they include the geometrical characteristics of all four U beams together with the concrete slab. Above the piers, the frames, which model the deck, were interrupted and in order to create the effect produced by the presence of the continuous concrete slab, a system consisting in orthogonal beams was created. Through this system, the connection between superstructure and substructure (piers and abutments) is made and between the beams, which model the deck in the span, and the beam, which represents above each pier the concrete slab (Fig.4). The finite elements, which model the concrete slab, are similar to those which model the deck, but placed with an eccentricity according to the neutral axis of the superstructure in the span. The eccentricity was assumed as the vertical distance

between the centroid of the slab and the centroid of the superstructure in the span. This distance represents also the length of the connection beams. The pier caps, where the bearing of the superstructure is made, were modeled also using two nodes straight frame elements. In the common joint placed in the pier axis the connection between the pier cap and the pier elevation is made. Between the bridge superstructure and the pier cap, dummy finite elements were introduced, their length being equal with the vertical distance measured between the neutral axis of the superstructure and the bearing surface on the pier cap.

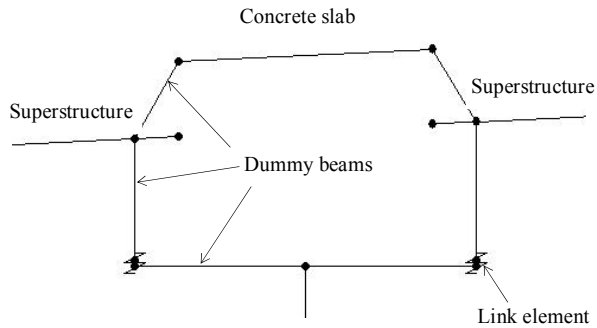


Figure 4. Detail regarding the modeling of the concrete slab and of the bearing devices on the pier cap

The connection beams between those which model the superstructure in the span and those which model the continuous concrete slab above the piers, between the superstructure and the substructure and also those which model the pier cap, were considered with very high values of axial, shear, bending and torsion stiffness. The stiffness of the beam, which models the concrete slab, corresponds to its real width and thickness.

The substructure elements (abutments and piers) were also modelled using two nodes straight frame elements, their geometrical characteristics corresponding to the real dimensions of their cross section.

The neoprene bearing devices were modelled using two nodes “link” elements. (Fig.4), for which the axial, shear, bending and torsion stiffness were computed according to the material characteristics (longitudinal and shear modulus of elasticity). The shear stiffness was considered according to the way of actions of the loads on the structure, assuming two different values for the shear modulus: one for slow actions and other for quick actions. The behaviour of link elements was assumed as linear elastic and the length of the links corresponds to the real depth of the bearing devices.

Because of the presence of the shallow foundations for abutments and piers, for the performed analyses, the bridge structure was fully fixed at the ground by restraining, for all the joints, all degrees of freedom.

The dynamic response of the bridge under the action of live loads was established through dynamic linear time history analyses, using a direct integration method for the equations of motions, on a specified time domain. The linear character of the response was assumed because, for usual values of the speed of vehicles, the structure not exhibit large displacements and the behavior of the material still remain in linear elastic domain.

In the following, some theoretical aspects regarding the methods used in the performed analyses will be summarized.

4. METHODS USED IN THE PERFORMED DYNAMIC ANALYSES

For establishing the response of the structure under the dynamic loads produced by the action of vehicles crossing the bridge, the finite element software SAP2000 together with a direct integration method of the dynamic equilibrium equations were used.

In literature [1], [2], [3], [4] many methods for the direct integration of the dynamic equilibrium equations are presented: Newmark's method, Wilson's- θ method, Hilber-Hughes-Taylor- α method, the average acceleration method and others. Generally, the use of these methods requires the division of a certain time domain τ , accepted for the structural response, in many small time steps Δt . In each time step it can be accepted, that the stiffness and damping of the structure have no significant variations, so that the approximation in solving the equations of motions is small enough. The displacements, velocities and accelerations of each point of the structure should be computed in each time step, through the integration of dynamic equilibrium equations. Once these elements established, the final values for stresses and strains can be also determined.

The major advantage of the use of the methods based on the direct integration algorithms with respect to the modal analyses, is that they do not require the previously establishing of the eigenvalues and eigenforms of the structure, which lead to a significant reduction of the time spent for the numerical calculations.

For the use of a method based on the direct integration, it is necessary to assume a variation law for the acceleration of each point, in each considered time step. Commonly, a linear variation for the acceleration is adopted and thus, the variation of velocities and displacements can be also established. The values for acceleration, velocity and displacement computed at the end of each time step will be used as initial parameters for the next time step of the analysis.

The dynamic equilibrium equations for a static system can be expressed as following:

$$[M]\{\ddot{\delta}\} + [C]\{\dot{\delta}\} + [K]\{\delta\} = \{P(t)\} \quad (1)$$

where $[M]$, $[C]$, $[K]$ are the mass, damping and stiffness matrices of the structural system and $\{\ddot{\delta}\}$, $\{\dot{\delta}\}$, $\{\delta\}$ are the acceleration, the velocity and the displacement.

Assuming a linear variation for acceleration in the time step Δt (Fig.5a), the variations for the velocity and displacement looks like in figure 5b and 5c respectively.

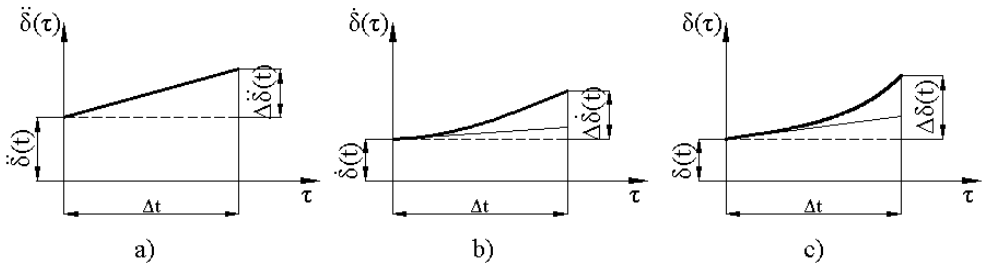


Figure 5. Variations laws for acceleration, velocity and displacement

The relations describing the mathematical connection between the parameters $\{\ddot{\delta}\}$, $\{\dot{\delta}\}$, $\{\delta\}$ over a time domain (assumed here as τ) are:

$$\{\ddot{\delta}\}_{\tau} = \{\ddot{\delta}\}_t + \{\Delta\ddot{\delta}\}_t \frac{\tau}{\Delta t} \quad (2)$$

$$\{\dot{\delta}\}_{\tau} = \{\dot{\delta}\}_t + \{\ddot{\delta}\}_t \tau + \{\Delta\ddot{\delta}\}_t \frac{\tau^2}{2\Delta t} \quad (3)$$

$$\{\delta\}_{\tau} = \{\delta\}_t + \{\dot{\delta}\}_t \tau + \{\ddot{\delta}\}_t \frac{\tau^2}{2} + \{\Delta\ddot{\delta}\}_t \frac{\tau^3}{6\Delta t} \quad (4)$$

where t represents the start of the time step.

The dynamic equilibrium equations at the end of the time step $t + \Delta t$ can be obtained from (1) as following:

$$[M]\left\{\ddot{\delta}\right\}_{t+\Delta t} + [C]\left\{\dot{\delta}\right\}_{t+\Delta t} + [K]\{\delta\}_{t+\Delta t} = \{P\}_{t+\Delta t} \quad (5)$$

In order to obtain the values for velocity and displacement with respect to the response of the system at the start of the time step, the equation (3) can be rewritten as following:

$$\left\{\dot{\delta}\right\}_{t+\Delta t} = \left\{\dot{\delta}\right\}_t + \left\{\ddot{\delta}\right\}_t \Delta t + \left(\left\{\ddot{\delta}\right\}_{t+\Delta t} - \left\{\ddot{\delta}\right\}_t\right) \frac{\Delta t}{2} \quad (6)$$

or

$$\left\{\dot{\delta}\right\}_{t+\Delta t} = \left\{\dot{\delta}\right\}_t + \left\{\ddot{\delta}\right\}_t \frac{\Delta t}{2} + \left\{\ddot{\delta}\right\}_{t+\Delta t} \frac{\Delta t}{2} \quad (7)$$

In a similar manner using equation (4) it results:

$$\begin{aligned} \{\delta\}_{t+\Delta t} &= \{\delta\}_t + \left\{\dot{\delta}\right\}_t \Delta t + \left\{\ddot{\delta}\right\}_t \frac{\Delta t^2}{2} + \left(\left\{\ddot{\delta}\right\}_{t+\Delta t} - \left\{\ddot{\delta}\right\}_t\right) \frac{\Delta t^2}{6} = \\ &= \{\delta\}_t + \left\{\dot{\delta}\right\}_t \Delta t - \left\{\ddot{\delta}\right\}_t \frac{\Delta t^2}{3} + \left\{\ddot{\delta}\right\}_{t+\Delta t} \frac{\Delta t^2}{6} \end{aligned} \quad (8)$$

Equations (7) and (8) are expressed in the literature [...], [...] under the form:

$$\left\{\dot{\delta}\right\}_{t+\Delta t} = \left\{\dot{\delta}\right\}_t + (1-\gamma)\left\{\ddot{\delta}\right\}_t \Delta t + \gamma\left\{\ddot{\delta}\right\}_{t+\Delta t} \Delta t \quad (10)$$

$$\{\delta\}_{t+\Delta t} = \{\delta\}_t + \left\{\dot{\delta}\right\}_t \Delta t + \left(\frac{1}{2}-\beta\right)\left\{\ddot{\delta}\right\}_t \frac{\Delta t^2}{2} + \beta\left\{\ddot{\delta}\right\}_{t+\Delta t} \Delta t^2 \quad (11)$$

with β and γ called integration parameters. For Newmark’s method, in order to obtain an unconditionally stable solution, the values for these two constants are: $\beta=1/6$ and $\gamma=1/2$.

By introducing the relations (7) and (8) in (5) it will be obtained a general equations system:

$$[M^*]\left\{\ddot{\delta}\right\}_{t+\Delta t} = \{P^*\} \quad (12)$$

where $[M^*]$ and $\{P^*\}$ are the effective mass matrix and effective load vector respectively, having the following expressions:

$$[M^*] = [M] + [C] \frac{\Delta t}{2} + [K] \frac{\Delta t^2}{6} \quad (13)$$

$$\{P^* = \{P\}\}_{t+\Delta t} - \left(\left\{ \dot{\delta} \right\}_t + \left\{ \ddot{\delta} \right\}_t \frac{\Delta t}{2} \right) [C] - \left(\left\{ \delta \right\}_t + \left\{ \dot{\delta} \right\}_t \Delta t + \left\{ \ddot{\delta} \right\}_t \frac{\Delta t^2}{3} \right) [K] \quad (14)$$

The equations system (2) can be solved using all known methods and thus, the accelerations values at the end of the time step are obtained. Having the accelerations, further the velocities and displacements values can also be obtained.

It is possible to transform the system of equations defined by (1) in order to obtain the known form of the static equilibrium equations. Therefore, at the start of time step we will have:

$$[M] \left\{ \ddot{\delta} \right\}_t + [C] \left\{ \dot{\delta} \right\}_t + [K] \left\{ \delta \right\}_t = \{P\}_t \quad (15)$$

in addition, subtracting the above equation from (5) we obtain:

$$[M] \left\{ \Delta \ddot{\delta} \right\} + [C] \left\{ \Delta \dot{\delta} \right\} + [K] \left\{ \Delta \delta \right\} = \{ \Delta P \} \quad (16)$$

The variations of the velocity and displacement into the time step can be expressed as following:

$$\left\{ \Delta \dot{\delta} \right\} = \left\{ \dot{\delta} \right\}_t \Delta t + \left\{ \Delta \ddot{\delta} \right\} \frac{\Delta t}{2} \quad (17)$$

$$\left\{ \Delta \delta \right\} = \left\{ \delta \right\}_t \Delta t + \left\{ \dot{\delta} \right\}_t \frac{\Delta t^2}{2} + \left\{ \Delta \ddot{\delta} \right\} \frac{\Delta t^2}{6} \quad (18)$$

From equations (17) and (18) we can write the variations of accelerations and velocities with respect to the displacements. Thus, it will be obtained:

$$\left\{ \Delta \ddot{\delta} \right\} = \frac{6}{\Delta t^2} \left\{ \Delta \delta \right\} - \frac{6}{\Delta t} \left\{ \dot{\delta} \right\}_t - 3 \left\{ \ddot{\delta} \right\}_t \quad (19)$$

$$\left\{ \Delta \dot{\delta} \right\} = \frac{3}{\Delta t} \left\{ \Delta \delta \right\} - 3 \left\{ \dot{\delta} \right\}_t - \frac{\Delta t}{2} \left\{ \ddot{\delta} \right\}_t \quad (20)$$

Now, by introducing the relations (19) and (20) in equation (16) it results the following equations system:

$$[K^*]\{\Delta\delta\} = \{\Delta P^*\} \tag{21}$$

with $[K^*]$ being the effective stiffness matrix and $\{\Delta P^*\}$ the vector containing the effective variations of the loads. They have the expressions below:

$$[K^*] = \frac{6}{\Delta t^2} [M] + \frac{3}{\Delta t} [C] + [K] \tag{22}$$

$$\{\Delta P^*\} = \{\Delta P\} + \left(\frac{6}{\Delta t} \left\{ \dot{\delta} \right\}_t + 3\{\delta\}_t \right) [M] + \left(3\left\{ \dot{\delta} \right\}_t + \frac{\Delta t}{2} \left\{ \ddot{\delta} \right\}_t \right) [C] \tag{23}$$

Solving the pseudo-static equations system (21) it results the variations of the displacement during the time step Δt and using these variations, the complete response in displacements, velocities and accelerations of the structure at the end of the time step is obtained. The final values for these parameters are computed using the relations below:

$$\{\delta\}_{t+\Delta t} = \{\delta\}_t + \{\Delta\delta\} \tag{24}$$

$$\left\{ \dot{\delta} \right\}_{t+\Delta t} = \left\{ \dot{\delta} \right\}_t + \left\{ \Delta \dot{\delta} \right\} \tag{25}$$

$$\left\{ \ddot{\delta} \right\}_{t+\Delta t} = \left\{ \ddot{\delta} \right\}_t + \left\{ \Delta \ddot{\delta} \right\} \tag{26}$$

In all numerical analyses performed for this bridge structure, the Hilber-Hughes-Taylor- α (HHT- α) method was used. The equations system (5) describing the motion of the structure it's modified as following:

$$[M] \left\{ \ddot{\delta} \right\}_{t+\Delta t} + (1 + \alpha)[C] \left\{ \dot{\delta} \right\}_{t+\Delta t} + (1 + \alpha)[K] \{\delta\}_{t+\Delta t} = (1 + \alpha)\{P\}_{t+\Delta t} - \alpha\{P\}_{t+\Delta t} + \alpha[C] \left\{ \dot{\delta} \right\}_t + \alpha[K] \{\delta\}_t \tag{27}$$

Denoting with a , v , d the acceleration, the velocity and the displacement respectively, the implicit integration scheme for HHT- α method assume that for each time step $n = 1, \dots, N - 1$ the following equation is solved:

$$[M]\{a\}_{n+1} + (1 + \alpha)[C]\{v\}_{n+1} - \alpha[C]\{v\}_n + (1 + \alpha)[K]\{d\}_{n+1} - \alpha[K]\{d\}_n = (1 + \alpha)\{P\}_{n+1} - \alpha\{P\}_n \tag{28}$$

with

$$\{d\}_{n+1} = \{d\}_n + \Delta t \{v\}_n + \frac{\Delta t^2}{2} [(1 - 2\beta)\{a\}_n + 2\beta \cdot \{a\}_{n+1}] \quad (29)$$

$$\{v\}_{n+1} = \{v\}_n + \Delta t [(1 - \gamma)\{a\}_n + \gamma \cdot \{a\}_{n+1}] \quad (30)$$

5. ANALYSES RESULTS AND CONCLUSIONS

In order to establish the dynamic effect of the vehicles action on the analyzed bridge structure, three different speeds have been taken into account: 8.33 m/s (corresponding to 30 km/h), 22.22 m/s (corresponding to 80 km/h) and 33.33 m/s (corresponding to 120 km/h).

Figures 6, 7 and 8 show the three different deformed shapes of the structure, each form corresponding to a particular value for the speed of the vehicle.



Figure 6. Deformed shape of the structure for a vehicle speed of 30 km/h



Figure 7. Deformed shape of the structure for a vehicle speed of 80 km/h



Figure 8. Deformed shape of the structure for a vehicle speed of 120 km/h

In figure 9 and 10 can be observed the evolution with time of longitudinal (U_x) and transverse (U_y) displacement of the point in the top of the highest pier (P2 in figure 1).

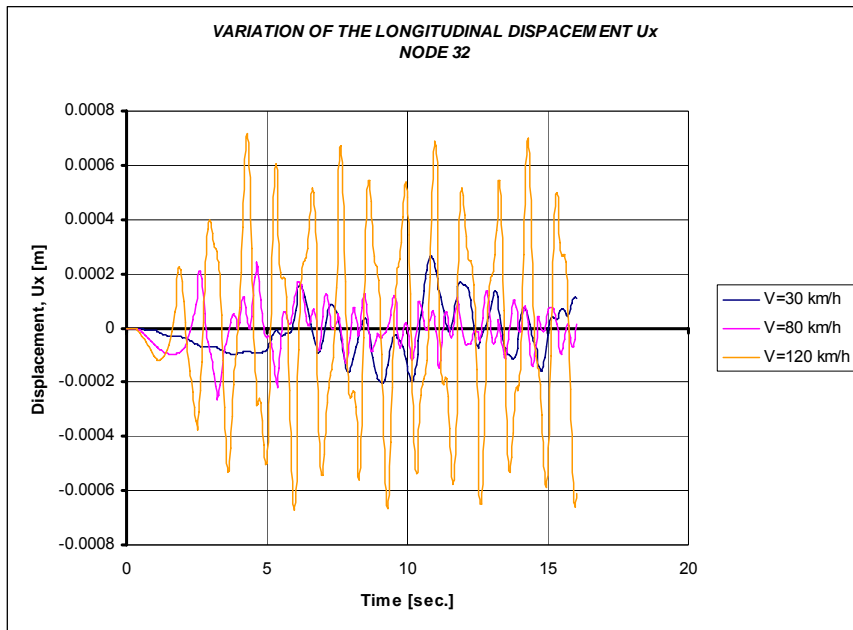


Figure 9. Time-history of the longitudinal displacement

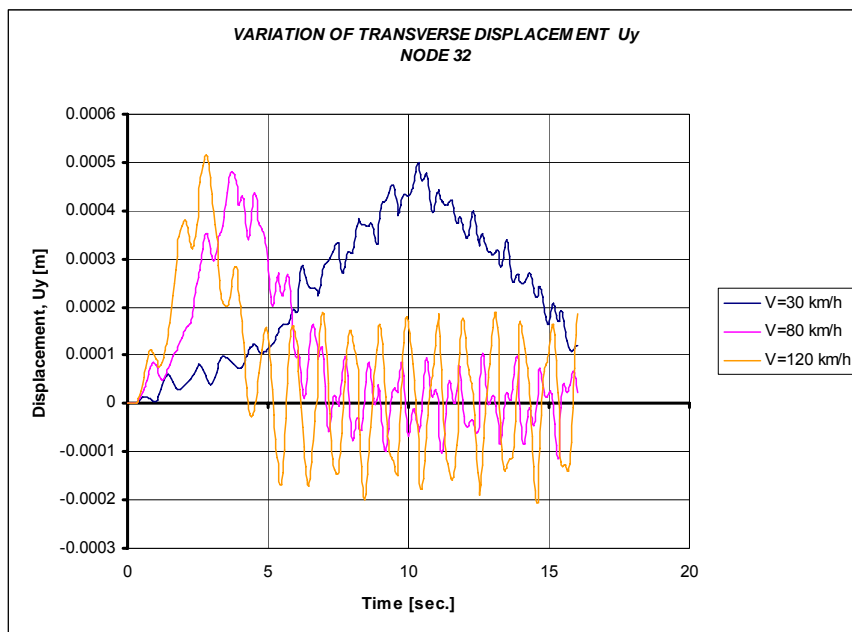


Figure 10. Time-history of the transverse displacement

The deformed shape of the structure corresponding to the first eigenmode is a displacement in longitudinal direction. It can be clearly seen in figure 9, that the biggest peak value for the longitudinal displacement is obtained, as expected, for the situation when the vehicle crosses the bridge at a speed of 120 km/h. This happens because the vehicle causes a significant excitation of the first eigenmode of the structure. In figure 10 it can be observed that the peak values of the transverse displacements are almost the same for all three considered cases.

In order to estimate the influence of the dynamic vehicle action, at different speeds, on the stresses on the cross section of structural elements, the evolution with time of axial stress and the transverse bending moment for pier P2 was established. From figures 11 and 12 it can be concluded that the maximum peak values of the stresses (axial and transverse bending moment) are obtained for the situation when the vehicle crosses the bridge at 80 km/h and not for the maximum speed. This seems to be abnormal, but for this structure with four spans, the displacement amplitude and through this, the stresses values, are strong influenced by the behavior of the neoprene bearing devices.

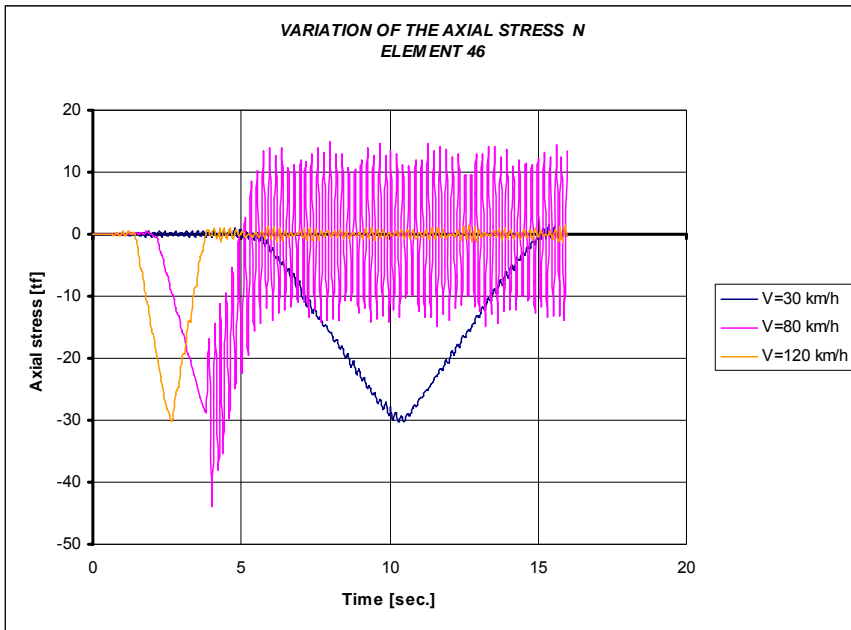


Figure 11. Time-history of the axial stress

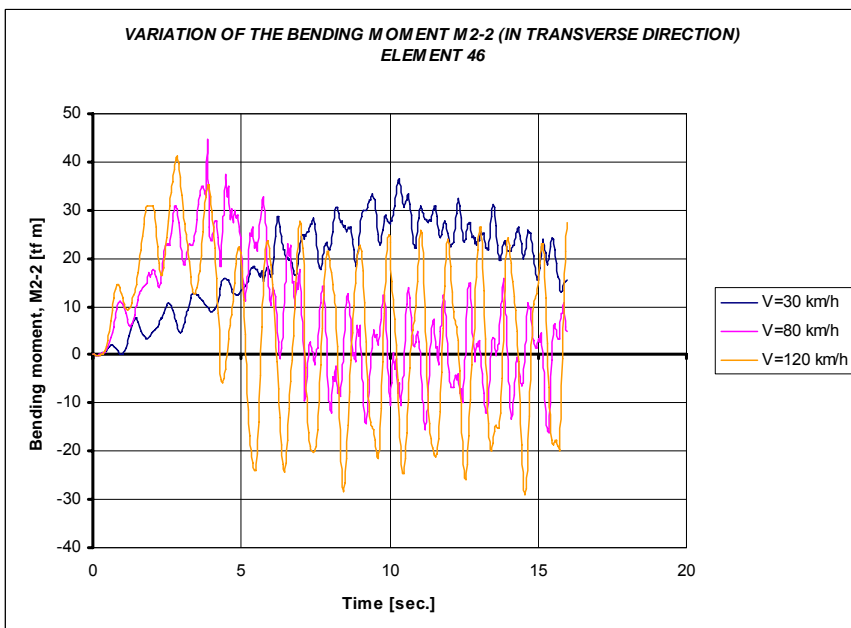


Figure 12. Time-history of the bending moment

The maximum peak value for the axial force into the pier is reached for the first case ($V=30$ km/h) when the vehicle is near to the half of the bridge and for the third case ($V=120$ km/h), when the vehicle is near to the middle of the second span. For the second case ($V=80$ km/h), it can be observed, that strong oscillations of the stress with respect to the horizontal axis exist and these are caused by the excitation and superposition of the higher eigenmodes of the structure.

The analysis of the structure using time-history and direct integration allow to identify the real maximum values for the displacements and stresses, which appear at different time steps, so at different time moments (Fig. 13). In this situation, the superposition of the stresses for design and verification purposes can be made in the right way, which is not the case in a modal analysis, where after the modal and directional combination, all the resulted stresses have maximum values.

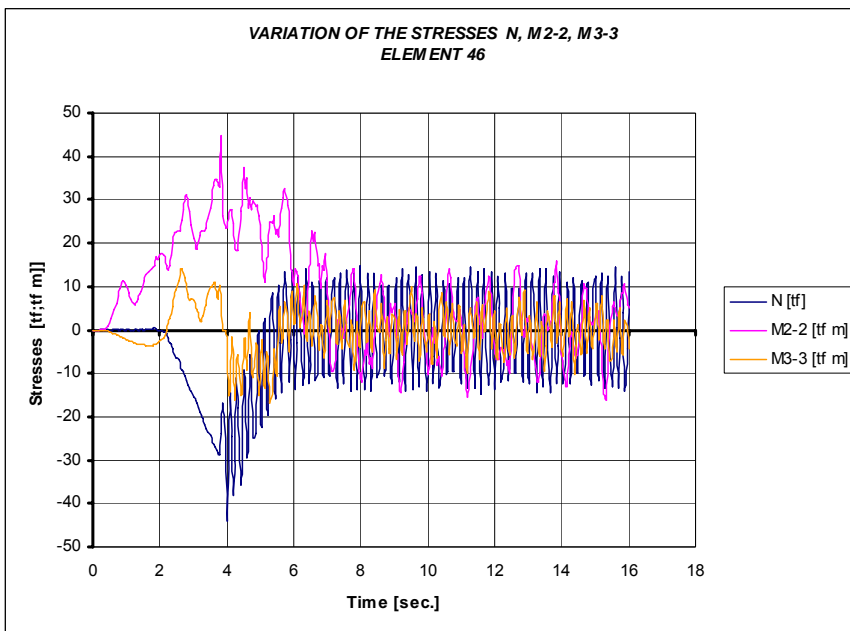


Figure 13. Time-history of the axial force bending moments M2-2 and M3-3

In order to consider the damping, for practical calculations, the damping matrix is formed as a combination of mass and stiffness matrices using the relation:

$$[C] = \alpha[M] + \beta[K] \quad (31)$$

where $[M]$, $[C]$, $[K]$ are the mass, damping and stiffness matrices of the structural system and α and β and coefficients.

Note: Here β has other meaning as for the Newmark method.

In figure 14 is presented the evolution with time of the axial stress on the pier P2 cross section for three different values of α and β . It can be seen in the figure that after a certain time, for α and β greater than zero, the amplitude of the stress is decreasing until it reaches the zero value.

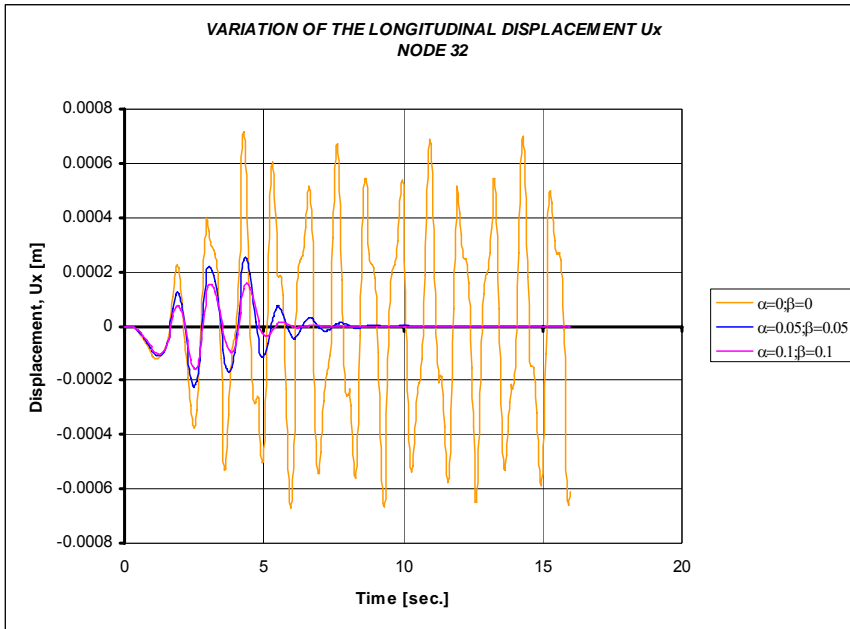


Figure 14. Time-history of the longitudinal displacement considering different values for the damping of the system

From all performed analyses it can be concluded the fact, that a dynamic time-history procedure offers much more accurate results with respect to modal analyses, allowing to establish the evolution with time of all parameters of the structure: displacements, velocities, accelerations, stresses. Supplementary, much more accurate values for the maximum stresses, resulted as combination between different dynamic load cases can be obtained.

References

1. Fierbințeanu, V., *Calculul automat al structurilor*, Atelierele de reprografie I.C.B., 1984 (in Romanian)
2. Ifrim, M., *Dinamica structurilor și inginerie seismică*, Editura Didactică și Pedagogică, București, 1984 (in Romanian)
3. Wilson, E.L. *Three-Dimensional Static and Dynamic Analysis of Structures*, Computers and Structures Inc., Berkeley, California, 2002
4. ***, *CSI Analysis Reference Manual for SAP2000, Etabs and Safe*, Computers and Structures Inc., Berkeley, California, 2007

Applicability conditions of various methods for mitigation of the scour phenomena to road bridges infrastructures

Claudiu Romanescu¹, Cristina Romanescu² and Rodian Scînteie³

¹Road Bridges Department, CESTRIN, Bucharest, 061101, Romania, cromanescu@gmail.com

²Road Bridges Department, CESTRIN, Bucharest, 061101, Romania, bridge@cestrin.ro

³CERT-CESTRIN, Bucharest, 061101, Romania, rodian.scinteie@gmail.com

Abstract

The recent history of Romania, and not only, brought to the public attention problems of a great importance regarding the safety of road users related to the road bridges stability. Important degradations occurred to the road bridges infrastructures, caused on their great majority by the processes of lowering of the riverbed and foundations scour as a result of the floods that took place on the traversed rivers. This led to total destruction or heavily affected of several road bridges imposing enormous expenses for rebuilding these structures.

The actual solutions to mitigate these phenomena are various and are chosen depending mainly on the local situation. One may therefore find hydraulic, structural and biological (for the riverbanks stability) solutions and also anti-scour designing solutions. Monitoring means and riverbed evolution techniques can give important information to help decide the best countermeasures that must be put in place to ensure the safety of the road bridges.

This paper presents a method to choose the optimal solution between various methods function of the type of the scour, the environment, riverbanks type, etc. to put in the hands of the road manager a decision helping instrument.

KEYWORDS: stability, scour, riverbed protection methods.

1. INTRODUCTION

During the lifetime of a road bridge, the most unpleasant moments are when, due to various causes, degradations of some construction parts occurs leading to traffic restrictions, or, in extreme situations to temporary or permanent disruption of the road. The engineers struggled for a long time to find the best solutions for these kinds of problems and came up with a series of constructions types meant to stop the deteriorations of the riverbanks and lowering of the riverbed. The choice between various solutions may be sometimes difficult to be done.

2. THE ACTUAL SITUATION IN ROMANIA

The stability of the riverbanks and the riverbed is one of the main issues that must be solved by road administrators. Bridges in a good structural condition may be destroyed by the lowering of the terrain around its foundations, as a result of scour, embankments failure, falling riverbanks and so on. Several examples can be found below.



County Road 675C, km 0+650 at Targu Logresti, Gorj County, Romania. Here, the failure of the upstream embankment led to dangers for the foundations of the structure.



County Road 607C, km 1+708, at Varciorova, Mehedinti County, Romania. The deviation of the river course led to increased transport around the second infrastructure and lowered the riverbed.



National Road 2F, km 3+412, at Holt, Bacau County, Romania. The destruction of the bridge's quarter cone due to strong floods in the summer of 2005 led to the scour of the infrastructure and closing of one lane.

3. DESCRIPTION OF THE METHODS

This paper proposes a simple but efficient method to choose the type of protection to be used depending on the environment and the type of construction.

Countermeasures have been organized into groups based on their functionality with respect to scour and stream instability. The three main groups of countermeasures are: hydraulic countermeasures, structural countermeasures and monitoring.

3.1. Hydraulic countermeasures

Hydraulic countermeasures are those which are primarily designed either to modify the flow or resist erosive forces caused by the flow. These methods are divided into two groups: river training structures and armoring countermeasures. The performance of hydraulic countermeasures is depending on the design considerations such as filter requirements (granular or geosynthetic) and edge treatment (the head, toe, and flanks).

River training structures are designed to modify the flow. These structures are distinctive because they alter hydraulics to mitigate undesirable erosional and/or depositional conditions at a particular location or in a river reach. River training structures can be constructed of various material types and are not distinguished by their construction material, but rather, by their orientation to flow. River training structures are described as transverse, longitudinal or areal depending on their orientation to the stream flow.

Transverse river training structures are countermeasures which project into the flow field at an angle or perpendicular to the direction of flow.

Longitudinal river training structures are countermeasures which are oriented parallel to the flow field or along a bankline.

Areal river training structures are countermeasures which cannot be described as transverse or longitudinal when acting as a system. This group also includes countermeasure “treatments” which have areal characteristics such as channelization, flow relief and sediment detention.

Armoring countermeasures are distinctive because they resist the erosive forces caused by a hydraulic condition. These methods do not necessarily alter the hydraulics of a reach, but act as a resistant layer to hydraulic shear stresses providing protection to the more erodible materials underneath. Armoring countermeasures generally do not vary by function, but vary more in material type. Armoring countermeasures are classified by two functional groups: revetments and bed armoring or local armoring.

Revetments and bed armoring are used to protect the channel bank and/or bed from erosive/hydraulic forces. They are usually applied in a blanket type for areal coverage. These methods may be classified as either rigid or flexible/articulating. Rigid revetments and bed armoring are typically impermeable and do not have the ability to conform to changes in the supporting surface. These countermeasures often fail due to undermining. Flexible/ articulating revetments and bed armoring can conform to changes in the supporting surface and adjust to settlement. These countermeasures often fail by removal and displacement of the armor material.

Local scour armoring is used specifically to protect individual substructure elements of a bridge from local scour. Generally, the same material used or revetments and bed armoring is used for local armoring, but these countermeasures are designed and placed to resist local vortices created by obstructions to the flow.

3.2. Structural countermeasures

Structural countermeasures involve modification of the bridge structure (foundation) to prevent failure from scour. Typically, the substructure is modified to increase bridge stability after scour has occurred or when a bridge is assessed as scour critical. These modifications are classified as either foundation strengthening or pier geometry modifications.

Foundation strengthening includes additions to the original structure which will reinforce and/or extend the foundations of the bridge. These countermeasures are designed to prevent failure when the channel bed is lowered to an expected scour elevation, or to restore structural integrity after scour has occurred. Design and construction of bridges with continuous spans provides redundancy against catastrophic failure due to substructure displacement as a result of scour. Retrofitting a simple span bridge with continuous spans could also serve as a countermeasure after scour has occurred or when a bridge is assessed as scour critical.

Pier geometry modifications are used to either reduce local scour at bridge piers or to transfer scour to another location. These modifications are used primarily to minimize local scour.

A countermeasure group not included in the matrix is *biological countermeasures* such as biotechnical/bioengineering stabilization. This group was not listed because it is not as well accepted as the classical engineering approaches to bridge stability. Bioengineering is a relatively new field with respect to scour and stream instability at road bridges. There is research being conducted in this field, but bioengineering techniques have generally not been tested specifically as a countermeasure to protect bridges in the riverine environment. These kind of non-conventional methods are specifically designed for the protection of the riverbanks.

3.3 Monitoring

Monitoring describes activities used to facilitate early identification of potential scour problems. Monitoring could also serve as a continuous survey of the scour progress around the bridge foundations. Monitoring allows for action to be taken before the safety of the public is threatened by the potential failure of a bridge. Monitoring can be accomplished with instrumentation or visual inspection. A well designed monitoring program can be a very cost effective countermeasure. Two types of instrumentation are used to monitor bridge scour: fixed instruments and portable instruments. Fixed instrumentation describes monitoring devices which are attached to the bridge structure to detect scour at a particular location. Typically, fixed monitors are located at piers and abutments. The number and location of piers to be instrumented should be defined, as it may be impractical to place a fixed instrument at every pier and abutment on a bridge. Instruments such as sonar monitors can be used to provide a timeline of scour, whereas instruments such as magnetic sliding collars can only be used to monitor the maximum scour depth. Data from fixed instruments can be downloaded manually at the site or it can be telemetered to another location.

The use of these various methods has to be ruled using the table above. It doesn't have a compulsory characteristic, but is highly recommendable.

The author takes no liability regarding the misuse of these recommendations and is not legally responsible for the unwanted results.

References

1. Lagasse, P.F., Zevenbergen, L.W., Schall, J.D., Clopper, P.E., "Bridge Scour And Stream Instability Countermeasures", Fort Collins, Colorado
2. Brown, S.A., 1985, "Design of Spur-type Streambank Stabilization Structures," FHWA/RD-84/101, FHWA, Washington, D.C.
3. Brown, S.A., 1985, "Streambank Stabilization Measures for Highway Engineers," FHWA/RD-84/100, FHWA, Washington, D.C.
4. Brown,S.A., E.S. Clyde, 1989, "Design of Riprap Revetment," Hydraulic Engineering Circular No. 11, FHWA-IP-016, prepared for FHWA, Washington, D.C.
5. Richardson, E.V., D.B. Simons, P.F. Lagasse, 2001, "Highways in the River Environment," HDS-6, FHWA, Washington D.C.
6. Bradley, J.N. 1978, "Hydraulics of Bridge Waterways," Hydraulic Design Series No.1, U.S. Department of Transportation, FHWA.
7. Clopper, P.E., 1989, "Hydraulic Stability of Articulated Concrete Block Revetment Systems During Overtopping Flow," FHWA-RD-89-199, Office of Engineering and Highway Operations R&D, McLean VA.
8. McCorquodale, J. A., 1991, "Guide for the Design and Placement of Cable Concrete Mats," Report Prepared for the Manufacturers of Cable Concrete.
9. McCorquodale, J. A., 1993, "Cable-tied Concrete Block Erosion Protection," Hydraulic Engineering 93, San Francisco, CA., Proceedings (1993), pp. 1367-1372
10. Brice, J.C, Blodgett, J.C., 1978 "Countermeasure for Hydraulic Problems at Bridges, Volumes 1 and 2," FHWA-RD-78-162 and 163, USGS, Menlo Park, CA.

11. Odgaard, A.J. and Wang, Y., "Sediment Management with Submerged Vanes, I and II," Journal of Hydraulic Engineering, ASCE Voi. 117, 3 (1991a and b) pp. 267-283 and 284-302.
12. Karim, M., 1975, "Concrete Fabric Mat" Highway Focus, Vol. 7, pp. 16-23.
13. Lagasse, P.F., Richardson, E.V., Schall, J.D., Price, G.R., 1997, "Instrumentation for Measuring Scour at Bridge Piers and Abutments," NCHRP Project 21-3, Transportation Research Board, February.
14. Clopper, P.E., 1992, "Protecting Embankment Dams with Concrete Block Systems," Hydro Review, Voi. X, No. 2, April.
15. Simons, D.B., Chen Y.H., et al., 1984, "Hydraulic Tests to Develop Design Criteria for the Use of Reno Mattresses." Civil Engineering Department - Engineering Research Center, CSU, Fort Collins, Co, Report.
16. Fotherby, L.M., Ruff, J.F., 1995, "Bridge Scour Protection System Using Toskanes - Phase 1," Pennsylvania Department of Transportation, Report 91-02.
17. Paice, C., Hey, R., 1993, "The Control and Monitoring of Local Scour at Bridge Piers," Hydraulic Engineering 93, San Francisco, CA., Proceedings (1993), pp. 1061-1066
18. Bertoldi, D.A., Jones, J.S., Stein, S.M., Kilgore, R.T, Atayee, A.T., 1996, "An Experimental Study of Scour Protection Alternatives at Bridge Piers" FHWA-RD-95-187, Office of Engineering and Highway Operations, McLean VA.
19. Chang, F. and M. Karim, 1972, "An Experimental Study of Reducing Scour Around Bridge Piers Using Piles," South Dakota Department of Highways, Report.

Countermeasure Group	Countermeasure Characteristics																Estimated Allocation of Resources
	FUNCTIONAL APPLICATIONS				SUITABLE RIVER ENVIRONMENT								MAINTENANCE				
	Local Secur	Construction Siting	Stability	River Type	Stream Size	Bank Factor	Velocity	Bed Material	Top/bottom	Bank Condition	Flow	Flow	Flow	Flow	Flow	Flow	
	Abutment	Flow/Channel	Vertical/Leak	Bed/Channel	Wide/Med	Low/Med	Med/High	Coarse/Fine	High/Med	Good/Poor	High/Med	High/Med	High/Med	High/Med	High/Med	High/Med	
STRUCTURAL COUNTERMEASURES																	
MONITORING																	
FOUNDATION STRENGTHENING																	
Catch basin underpinning	Yes	Yes	Yes	Y	Y	Y	Y	Y	Y	Y	Y	Y	Y	Y	Y	Y	L
Case babbler	Yes	Yes	No	Y	Y	Y	Y	Y	Y	Y	Y	Y	Y	Y	Y	Y	L
Continuous beam	Yes	Yes	Yes	Y	Y	Y	Y	Y	Y	Y	Y	Y	Y	Y	Y	Y	L
Pier and abutment under footing	Yes	Yes	Yes	Y	Y	Y	Y	Y	Y	Y	Y	Y	Y	Y	Y	Y	M
Group foundation	Yes	Yes	Yes	Y	Y	Y	Y	Y	Y	Y	Y	Y	Y	Y	Y	Y	L
PIER GEOMETRY MODIFICATION																	
Expanded footings	N/A	N/A	N/A	Y	Y	Y	Y	Y	Y	Y	Y	Y	Y	Y	Y	Y	L
Pier shape modification	N/A	N/A	N/A	Y	Y	Y	Y	Y	Y	Y	Y	Y	Y	Y	Y	Y	M
Deck or diaphragm	N/A	N/A	N/A	Y	Y	Y	Y	Y	Y	Y	Y	Y	Y	Y	Y	Y	R-M
Vertical pile foundation	N/A	N/A	N/A	Y	Y	Y	Y	Y	Y	Y	Y	Y	Y	Y	Y	Y	R-M
FIXED INSTRUMENTATION																	
Scour probe markers	Y	Yes	Yes	Y	Y	Y	Y	Y	Y	Y	Y	Y	Y	Y	Y	Y	M
Automatic leveling collar	Yes	Yes	Yes	Y	Y	Y	Y	Y	Y	Y	Y	Y	Y	Y	Y	Y	M
Fixed sonar station	Yes	Yes	Yes	Y	Y	Y	Y	Y	Y	Y	Y	Y	Y	Y	Y	Y	L
Removable scale	Y	Yes	Yes	Y	Y	Y	Y	Y	Y	Y	Y	Y	Y	Y	Y	Y	R
PORABLE INSTRUMENTATION																	
Parished probes	Yes	Yes	Yes	Y	Y	Y	Y	Y	Y	Y	Y	Y	Y	Y	Y	Y	L
Flow probe	Yes	Yes	Yes	Y	Y	Y	Y	Y	Y	Y	Y	Y	Y	Y	Y	Y	L
VISUAL MONITORING																	
Periodic inspection	Yes	Yes	Yes	Y	Y	Y	Y	Y	Y	Y	Y	Y	Y	Y	Y	Y	R
Point watch	Yes	Yes	Yes	Y	Y	Y	Y	Y	Y	Y	Y	Y	Y	Y	Y	Y	R

N/A = not applicable
 No = unsuitable/rarely used
 ? = possible application/secondary use
 Yes = well suited/primary use
 Y = suitable for the full rang

Condition assessment of reinforced concrete bridges using nondestructive testing techniques

Cristina Romanescu¹, Claudiu Romanescu² and Rodian Scînteie³

¹Road Bridges Department, CESTRIN, Bucharest, 061101, România, bridge@cestrin.ro

²Road Bridges Department, CESTRIN, Bucharest, 061101, România, cromanescu@gmail.com

³CERT-CESTRIN, Bucharest, 061101, România, rodian.scinteie@gmail.com

Summary

The transportation infrastructure in the Romania is deteriorating and will require significant improvements. A major component of maintenance is the ability to accurately assess the condition of the transportation infrastructure.

A realistic and reliable assessment of a damaged bridge structure must comprise the evaluation of bridge condition, load bearing capacity, remaining service life and functionality.

It is essential for a reliable condition assessment to have records indicating the initiation of defects and deterioration processes and of their propagation from the beginning of bridge service life. As such records seldom exist for older existing structures and it is imperative to supplant them by other information using NDT techniques. Nondestructive testing methods help quickly diagnose hidden problems and assess bridge condition.

This paper present defects, the factors having strong impact on the deterioration and different nondestructive testing techniques used in the assessment of concrete bridge structure and promote the ability of these methods to detect defects with varying precision.

Defects evaluation should be done for individual structural materials with respect to the damage type, its intensity and extent and to the affected structural element.

Bridge engineers involved in the routine or extraordinary inspection of bridges have to take correct and reliable decision about the defect type, the associated deterioration process, the relevant cause and possible propagation of the damage in the future. This evaluation should be not based only on the expertise, engineering judgment and experience of the inspector.

KEYWORDS: defects, NDT techniques, assessment, deterioration processes and mechanisms.

1. INTRODUCTION

A defect means the absence of something necessary for completeness or perfection, a deficiency and an opposed to superfluity, a physical or moral imperfection. Also, a defect is a specific inadequacy in the structure or its components that materially affect its ability to perform some aspect of its intended current or future function.

Related terms are deficiency, damage, degradation, deterioration and disintegration. [2]

A deficiency is a lack of something essential for the ability of the structure to perform its intended function, as a result of an error in design, construction or maintenance. Damage is a physical disruption or change in the condition of a structure or its components, brought about external actions, such that some aspect of the current function of the structure or its components is impaired. The worst damage is disintegration which means a severe physical damage of a structure or its components which results in its break-up into fragments, with the possibility of gross impairment of functional capability.

A worsening of condition with time may result in two ways: usually in damage and this is called degradation and in a progressive reduction in the ability of the structure or its components to perform some aspect of their intended function and this is called deterioration.

Nondestructive testing (NDT) has been defined as comprising those test methods used to examine an object, material or system without impairing its future usefulness. Ultrasound, X-rays and endoscopes are used for these kinds of testing. Nondestructive testing is used to investigate the material integrity of the test object. Often, in NDT and Quality control defect, flaw, imperfection, non-conformance are the terms used when the material tested deviates from ideality. Though all of them look similar, there exists a vast difference in their meaning and interpretation. The term ‘flaw’ means a detectable lack of continuity or a detectable imperfection in a physical or dimensional attribute of a part. The term ‘nonconforming’ means only that a part is deficient in one or more specified characteristics.

2. ASSESSMENT OF A DAMAGED BRIDGE STRUCTURE

Assessment of the condition of a bridge structure starts with the identification of the damages relevant for the evaluation of the bridge condition, its bearing capacity, remaining service life and functionality. For every detected defect or damage the inspector has to identify the type of damage, the severity or degree of damage and its extent.

Causes for the majority of deterioration processes and associated damages on concrete bridges are generally known.

Many types of defects have characteristic visual signs on the surface. During visual inspection of structures such signs can give valuable information about defects themselves, their nature and cause. The time when signs become visible can vary from a few hours up to many years after the construction. [2]

Deteriorations lead to many problems such as functional, load carrying and long-term durability. The factors having strong impact on the deterioration of concrete bridge structure are:

- design;
- materials used for construction;
- construction methods;
- applied loads;
- environmental actions;
- maintenance of the structure in service.

The impact of every one of the influencing factors on the occurrence of defects and damages is included in table 1.

Table 1: Influencing factors and causes for occurrence of defects and damages

No.	Influencing factors	Causes for occurrence of defects and damages
1	Design stage	Standards and design norms used at the time of construction could be out of present interest
		Degradation of concrete due the inadequate detailing of specific parts of the structure
		Suffering unexpected severe damages because not taking into account the micro-climate conditions near or around the bridge
2	Materials used for construction	Serious durability or load bearing problems because the components of concrete and/or the reinforcement do not meet the design requirements
3	Construction stage	Inconsistent quality control during construction process may lead to severe durability and load carrying problems like excessive cracks and deflections, or even collapse
4	Applied loads	Excessive deflections of bridge than calculated because of excessive loads of passing vehicles
		Displacements of the infrastructures because of greater earth-pressure or global instability of the foundation
		Severe mechanical defects can be brought by collision with different objects
		Defects that remain visible for many years because of loading due to natural disasters
5	Maintenance of the structure in service	Deterioration of an existing structure is due the delayed or inadequate rehabilitation methods applied

The types of defects that may be assessed using NDT methods can be classified into three major groups:

- inherent defects - introduced during the initial production of the base or raw material.
- processing defects - introduced during processing of the material or part.
- service defects - introduced during the operating cycle of the material or part.

Some kind of defects which may exist in these three groups are:

- cracks on surface and subsurface, arising from a large number of cases;
- porosity;
- breakings;
- laminations;
- lack of bond;
- inclusions;
- segregation;
- fatigue defects etc.

The origin of defects in a material can take place during manufacturing stage, during installation or during in service. In the first two cases quality can be achieved essentially by good engineering practice.

However, the occurrence of some form of imperfections during manufacture is inevitable and there will be a typical distribution of imperfection sizes associated with a particular manufacturing process and quality. The ideal situation is where the inherent distribution of initial imperfection sizes is well separated from the distribution of critical defect sizes which may cause failure. Hence, the role of NDT is not only to detect the defects but also to give information about the distribution.

There are little benefits derived out of repairing the parts/components with defects for their delivery to the customer. Here, the industry should aim at produce parts / components without defects. In the subsequent section, it is shown how to achieve this objective.

On the other hand, in the in-service scenario, defects will be generated due to deterioration of the component/structure as a result of one or combination of the operating conditions like elevated temperature, pressure, stress, hostile chemical environment and irradiation leading to creep, fatigue, stress corrosion, embattlement, residual stresses, microstructural degradation etc. which, in turn, result in deterioration of mechanical properties, crack initiation and propagation, leaks in pressurized components and catastrophic failures.

NDT techniques are increasingly applied to components/systems for the detection and characterization of defects, stresses and microstructural degradation to ensure the continued safety and performance reliability of components in industry. NDT techniques improve the performance reliability of components through periodic in-service inspections, by way of preventing premature and catastrophic failures.

NDT also provide valuable inputs to plant specification and design i.e. to determine which components are the most likely to fail and then to ensure that those have easy maintenance access for repair or replacement. In in-service scenario, it is rather difficult to stop the formation of defects and the growth of defects already formed. [4]

NDT in the assessment flowchart is shown in Appendix 1.

There are three types of assessments, depending on the considered safety criteria for the existing road bridges: one exceptional heavy load (one time), bridge capacity is affected by on-going deterioration and new loads (heavier axle loads or higher speeds). The levels of detail may be element assessment (part of a bridge), bridge assessment (one bridge) and line assessment (number of bridges).

Typical assessment criteria for the three states are:

- ultimate limit - safety of persons an/or the bridge
- serviceability limit state - functioning under normal use, comfort of passengers and appearance
- fatigue limit state - relationship between safety and normal use
- durability limit state - environmental actions that causes degradation with time.

From the complexity point of view of procedures there are initial, intermediate and advanced assessments.

Initial assessment supposes site visit, study of documents and simple calculations (e.g. comparison between design load and required load, simple hand calculations, moment, shear force).

Intermediate assessment consists on further inspections (visual inspection, delamination check, crack measurements), simple tests (material properties like yield strength, concrete compression strength, simple load measurements) and detailed calculations (linear finite element analysis, plastic analysis)

Advanced assessment means laboratory investigation, load models, reliability-based, monitoring, refined calculations and decision analysis [3].

Deterioration may be categorized as early age deterioration (such as shrinkage cracking and settlement cracking over rebar), long-term deterioration (including pattern cracking due to alkali-silica reactions, and delamination from rebar corrosion), and in-service deterioration (such as midspan spalling due to overloading, and cracking and corrosion from defective expansion joints).

The nondestructive evaluation methods includes GPR and infrared thermography for locating delaminations and voids, impact echo techniques for determining the extent and depth of voids and locating embedded metallic materials, and radiography for locating voids and major corrosion of reinforcing steel.

2. DEFECTS WITHIN THE ROMANIAN BMS DATABASE THAT CAN BE ASSESSED USING NDT METHODS

An analysis of the Romanian Bridge Management System database pointed that the national roads and motorways network comprising 3171 road bridges are suffering of various damages induced mainly by the severe lack of maintenance and by the environment. The large majority of structures are affected by infiltrations and efflorescence, cracks, reinforcement corrosion, segregation and carbonation of the concrete.

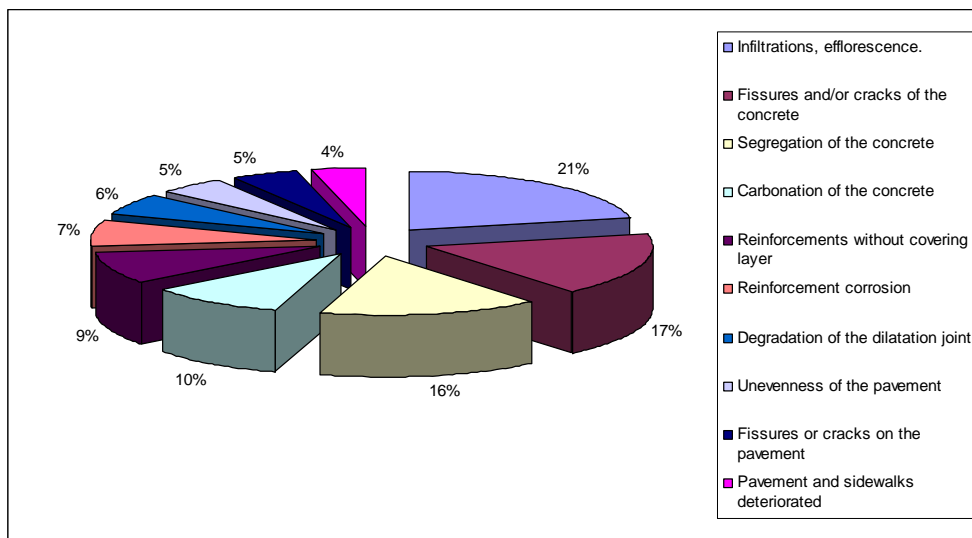


Figure 1. Diagram of the most common defects of the Romanian national roads and motorway bridges

As may be observed on the figure above, the main three degradations that have been seen on visual inspections for entire Romanian national network are: infiltrations and/or efflorescence, fissures and/or cracks of the concrete and segregation of the concrete. The causes for these degradations are mainly the same, the systematic lack of maintenance due to insufficient funds and the poor quality of concrete.

Diagrams for each of the seven regions within the Romanian National Roads and Motorway National Company are shown in Appendix 2.

One may observe that all these defects can be assessed using NDT methods. A preventive evaluation may lead to the mitigation of the effects of these devastating degradations for the Romanian bridges. Infiltrations, carbonation of the concrete and the reinforcement corrosion occur simultaneously, within the same degradation

process. Therefore it is considered very important to study the deterioration mechanism that stands as the base of phenomena, meaning the chloride ingress.

3. MODELS FOR DETERIORATION MECHANISMS

By using models of the most frequently occurring deterioration mechanisms the anticipated or remaining service life of concrete structures can be predicted with good probability.

Failures in the structures do occur as a result of premature reinforcement corrosion. Chloride ingress is a common cause of deterioration of reinforced concrete structures. Concrete may be exposed to chloride by sea water or deicing salts. The chloride initiates corrosion of the reinforcement which through expansion disrupts the concrete. Modelling the chloride ingress is an important basis for designing the durability of concrete structures. There are several mathematical models available which predict chloride ingress into concrete.

The most widely adopted technique for modelling chloride ingress in concrete is Fick's 2nd Law. If diffusion is assumed to be one-dimensional then the relevant equation is

$$\frac{\partial C}{\partial t} = D \frac{\partial^2 C}{\partial x^2} \tag{1}$$

where C = chloride concentration at a distance x from the surface after time t

D = diffusion coefficient

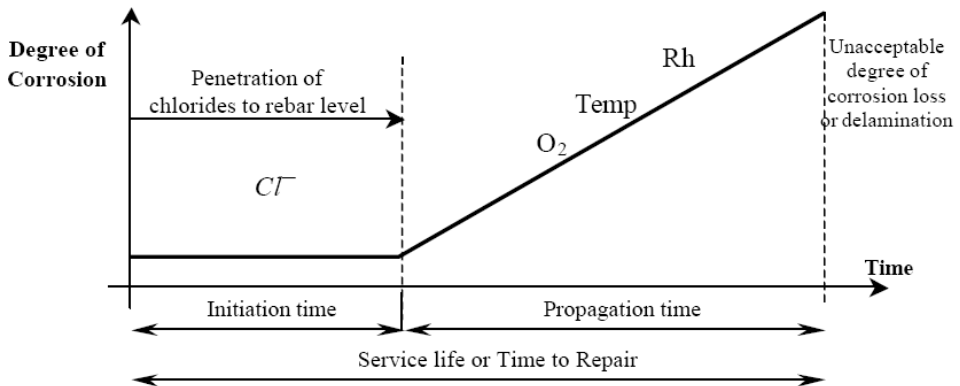


Figure 2. Schematic diagram of the corrosion process of steel in concrete

Assuming constant chloride concentration at the surface of the concrete, the commonly used solution to the above equation is

$$C(x,t) = C_s \left[1 - \operatorname{erf} \left(\frac{x}{2\sqrt{Dt}} \right) \right] \quad (2)$$

where $C(x,t)$ = chloride concentration at depth x after time t

erf = the error function

C_s = chloride surface concentration (assumed constant)

It is possible to evaluate effective diffusivity values, D , and the time for chloride initiated corrosion to begin by setting $C(x,t)$ equal to a critical chloride corrosion threshold C_{th} . The assumptions made are that:

- one dimensional diffusion in a semi-infinite homogeneous body is representative of the chloride ingress process in concrete structures
- chloride surface concentration, C_s , is constant through time
- the diffusion coefficient, D , is spatially and temporally constant

The first assumption neglects the effect of other processes which are important especially if chloride exposure is intermittent and the structure undergoes a number of wet-dry cycles. Structures are intermittently exposed to chloride attack, it well known that de-icing salts are applied only during part of the year, and that this process is repeated annually. Under these conditions, an alternative solution to Fick's 2nd Law has been used given by

$$C(x,t) = \frac{M}{\sqrt{\pi Dt}} \exp \left(\frac{-x^2}{4Dt} \right) \quad (3)$$

where M = quantity of accumulated chloride on concrete surface per unit time in $\text{kg/m}^2/\text{year}$.

The third assumption concerns time and space variations of the diffusion coefficient. Temporal variations have been neglected because they are no so noticeable. Space variations are intricately linked with dependencies on temperature, water/cement ratio, cement type, humidity and workmanship and are known to be important.

That improves the understanding of transport mechanisms and deterioration processes in concrete structures. Permanent monitoring of the new and existing structures will increase our confidence in specifying probabilistic parameters for key deterioration variables, and in quantifying their systematic and random variability as a function of measuring and environmental influences.[1]

3. CONCLUSIONS

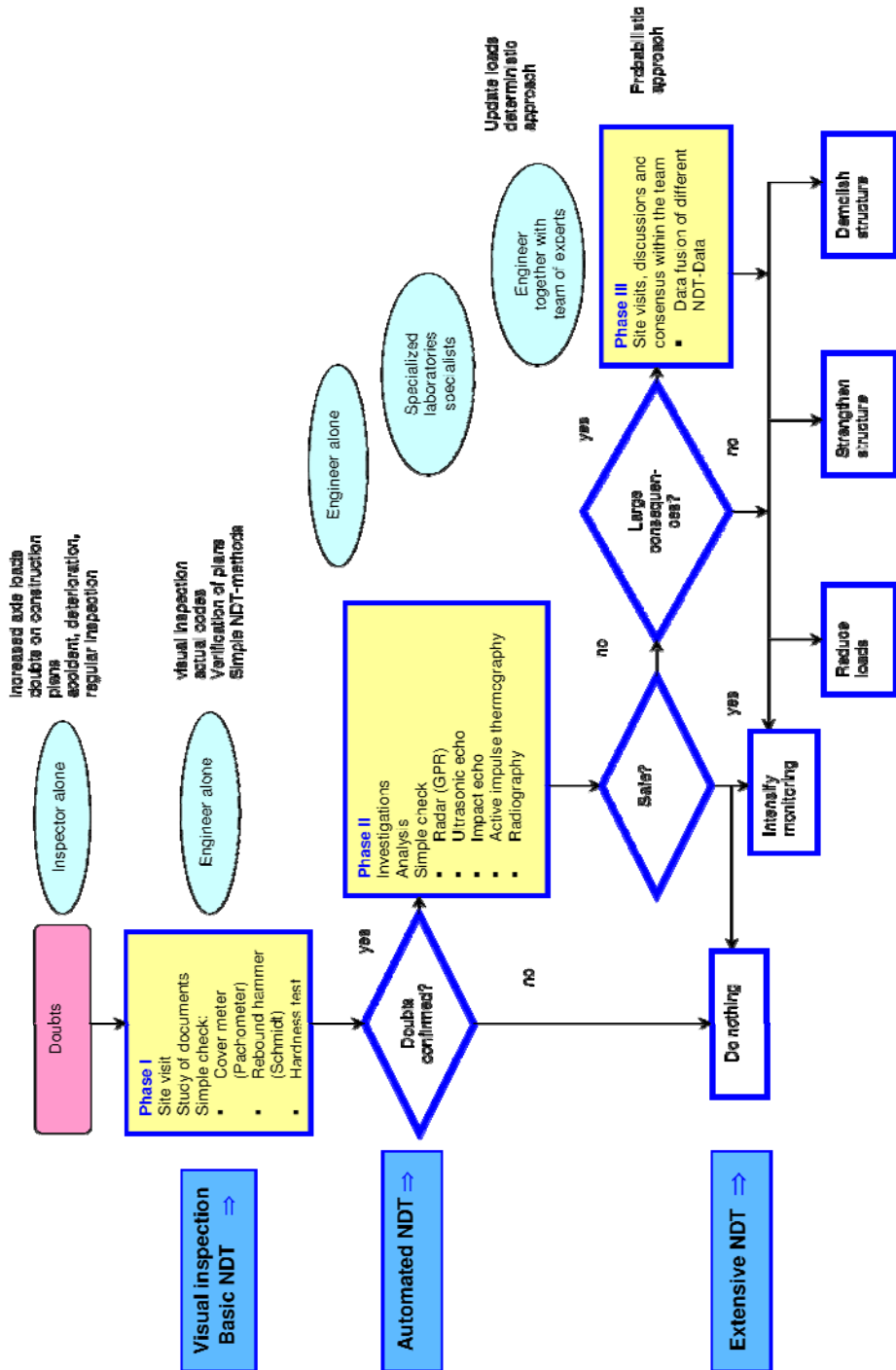
NDT methods should to be integrated into the condition assessment procedures and applied by the administrator of the road.

It is essential to improve the integration of deterioration modelling with reliability assessment through pragmatic and balanced approaches, in order to support technical and financial decisions that need to be taken.

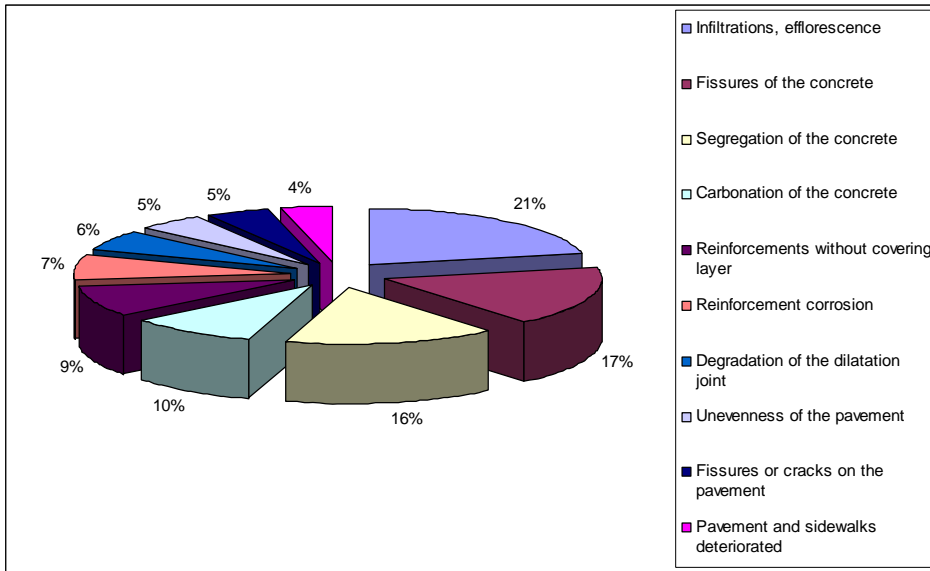
References

1. Marios Chryssanthopoulos and Garry Sterritt, *Integration of deterioration modelling and reliability assessment for reinforced concrete bridge structures*, 2002
2. Aleš Znidaric, *Handbook of damages*,2005
3. Rosemarie Helmerich, *NDT in Inspection and Condition Assessment*, 2006
4. B. Purna Chandra Rao, *Introduction to Non-Destructive Testing (NDT)*, 2007
5. *** *Instruction for technical condition assessment of a bridge*, 2006
6. *** *Manual for defects identification occurred on road bridges and remedial measures*, 1998

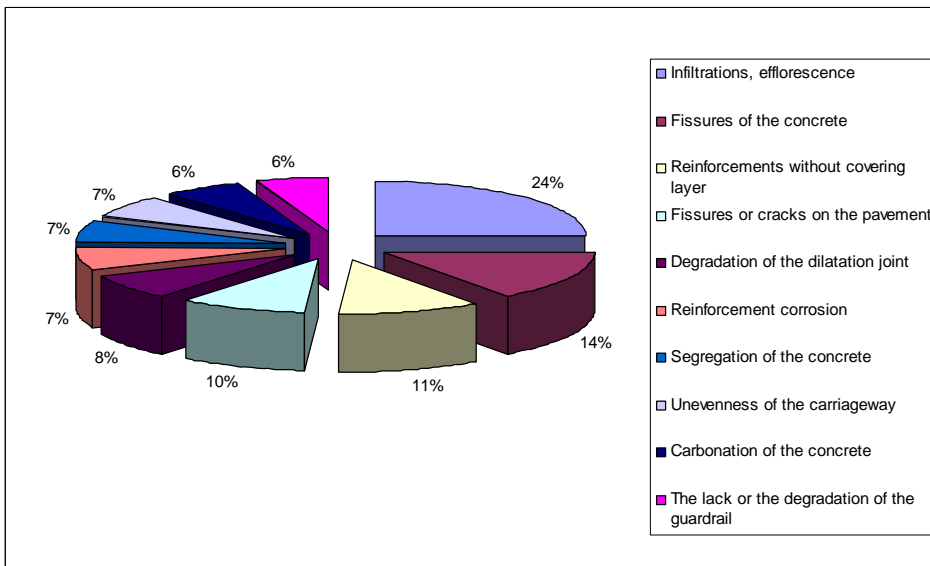
Appendix 1. NDT assessment flowchart



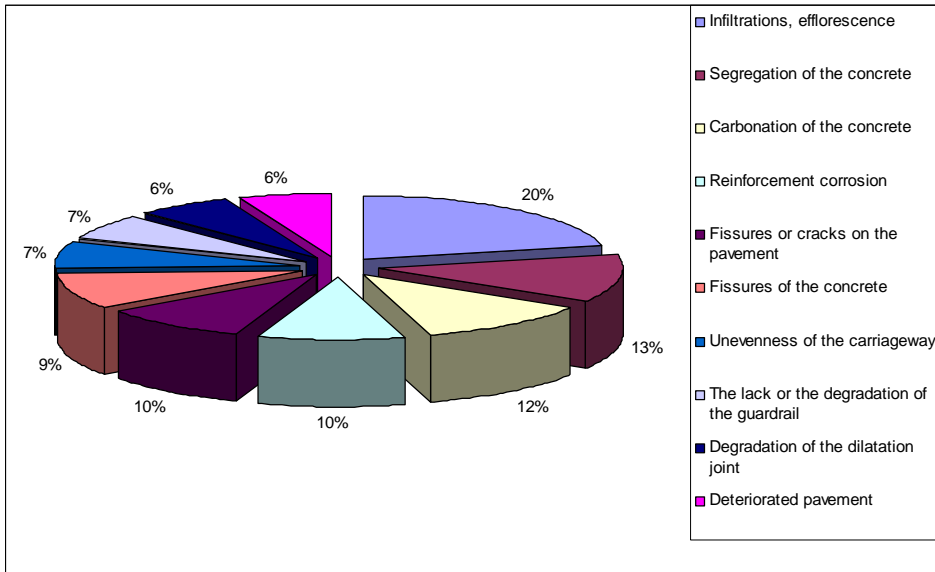
Appendix 2. Diagrams of the most frequently defects within the Romanian BMS database for every seven Regions



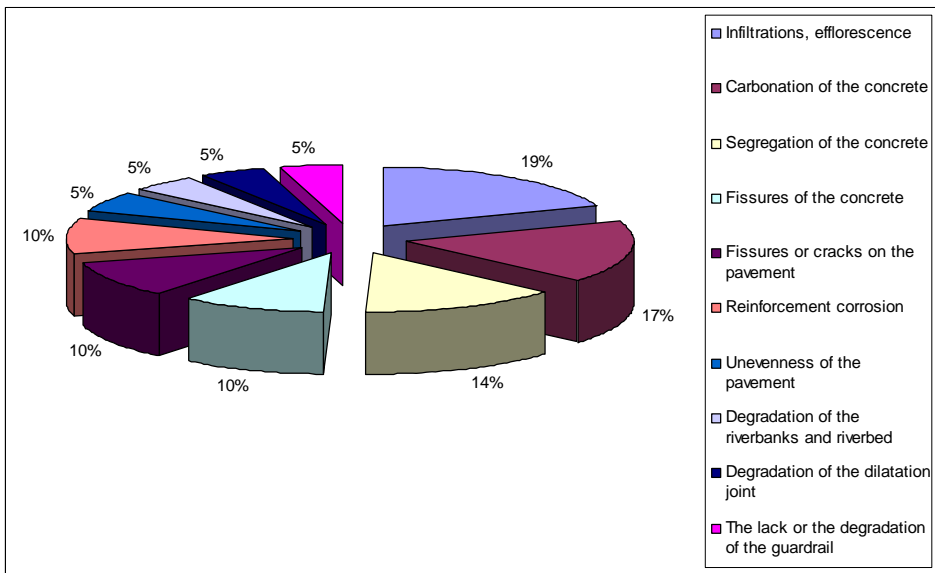
Bucharest Region



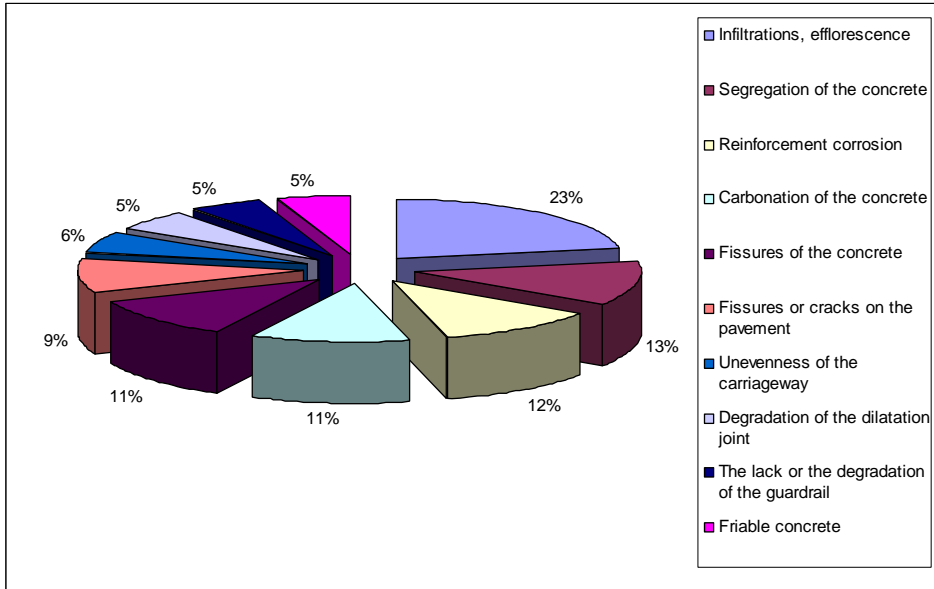
Craiova Region



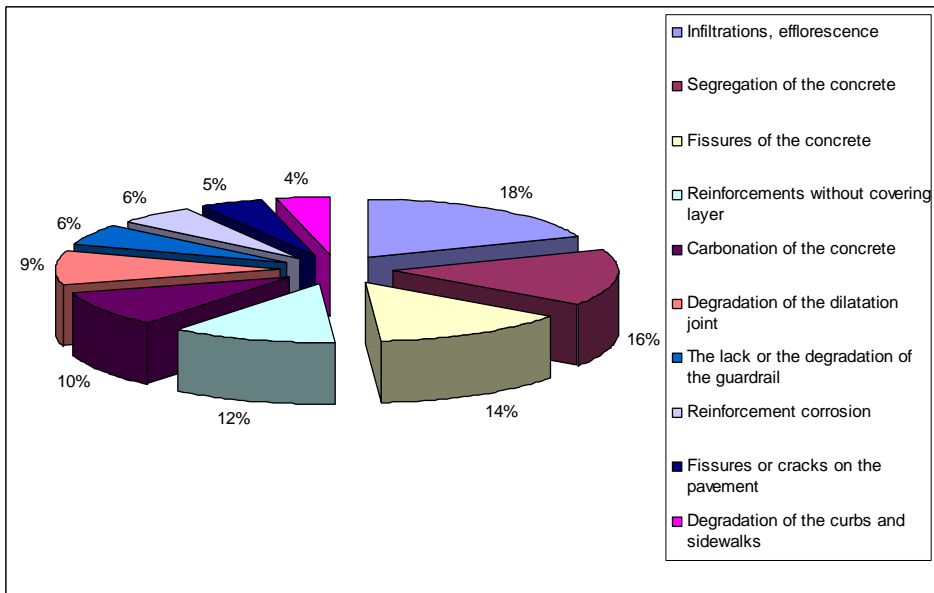
Timisoara Region



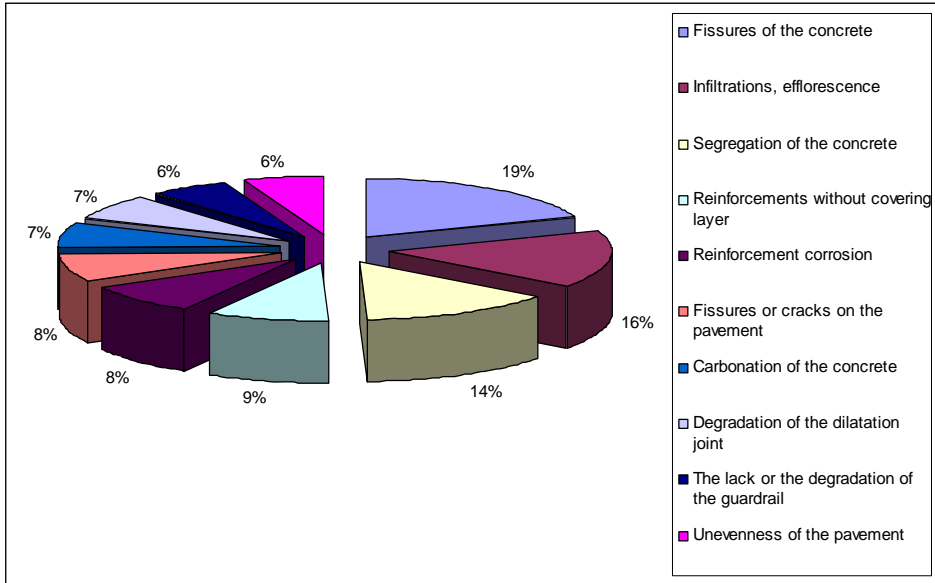
Cluj Region



Brasov Region



Iasi Region



Constanta Region

Present Trends in Improving Quality of Pavement Bitumen

Liliana Stelea¹

PhD Student, School of Construction, Technical University Timișoara, Romania

SUMMARY:

The article presents the experience with modified bitumen in Romania, especially on national roads. More experimental sectors were set and evolution of the condition is observed. Laboratory tests results are presented for different sources of bitumen and different additives.

Tests were performed according to SHRP methods which are based on performance. Considering SHRP algorithm for temperature and traffic prediction may generate effective asphalt mixtures.

KEY WORDS: modified bitumen, roads materials, roads design.

1. INTRODUCTION

Studies on bitumen binder were a permanent concern for materials specialists from road area. In Romania, as in many other countries bitumen is the main road binding material. Asphalt pavements represent 98% from network while the rest of 2% are mainly concrete cement. Present trend is to use it for the entire country. Therefore, an increase of the performance is required. To achieve this, the quality of all components of the asphalt mix must be improved: bitumen, natural aggregates, additives, fibres etc. so the durability to be increased. Bitumen binders used for road works include the bitumen itself and derived products: emulsions, cutback bitumen, and fluxed bitumen.

Main components of the bitumen are oils, resins, asphaltenes, asphaltogen acids and their anhydrides.

Based on the origin, there are two types: the petrol bitumen resulted after processing crude oil in refineries; and natural bitumen obtained directly from natural sediments.

The petrol bitumen used in Romania for road works the composition of fractions corresponds as following:

- Oils 40...60%;
- Resins 18...48%;
- Asphaltenee 15...35%.

Natural bitumen extracted from Derna-Tatarus presents a higher content of oils and a lower percentage of asphaltens:

- Oils 67...72%;
- Resins 21...22%;
- Asphaltenes 1...11%.

The behaviour, composition and characteristics of the bitumen, are influenced by external factors (light, temperature, level of oxygen in air, etc.) which act continuously after laying in place. Due to these factors the bitumen suffers a generally irreversible ageing process characterized by the oxidation and polymerization of the oils which transform partly into resins and resins further into asphaltenes.

Increase of the asphaltene percentage over a certain limit produces a fragile and brittle binder, therefore unfit for roads, generating cracks.

Considering the paraffin content two types are considered:

- non-paraffin bitumen (<2% paraffin),
- paraffin bitumen (between 2% and 4% paraffin).

Bitumen is used for pavements in three forms:

- pure bitumen,
- bitumen with additives,
- modified bitumen.

Current laboratory tests on bitumen are:

- tests related to the consistency (penetration; and viscosity);
- tests concerning the plasticity (softening point; Ubbelohde; Fraass; and ductility)
- adherence test;
- bitumen ageing resistance in preparation of the asphalt mix and in operation:
 - o mass loss through warming (standardized method);
 - o stability in thin layer of the bitumen through TFOT and RTFOT (according to Romanian AND instructions)
 - o accelerated ageing – PAV method (according to Romanian AND instructions)
- chemical composition (according to Romanian technical instructions 52R/1996)

Beside these specific tests the following standardized measurements are performed:

- density;
- solubility in carbon disulphide or carbon tetrachloride;
- flammability point;
- content of paraffin.

Based on the composition, softening point IB and penetration at 25°C other structural characteristics are calculated:

- colloidal instability index, IC
- aromaticity index, IA
- penetration index, IP.

2. USE OF MODIFIED BITUMEN FOR ASPHALT MIX

Improving the characteristics of asphalt mixtures to resist longer periods under traffic actions and severe meteorological conditions is a permanent concern for engineers. New polymeric additives, both reactive and non-reactive, are promoted for the road bitumen to obtain a elasto-visco-plastic material, where the elasticity component to be significant.

2.1. Polymer modified bitumen

Polymer modified bitumen is a binder with specific physical and chemical characteristics. It is obtained in special installations by processing pure bitumen with certain types of polymers, at 160-180°C.

The advantages of polymer modified bitumen, comparing with pure bitumen are:

- increase in resistance to permanent deformations at high temperatures;
- increase of resistance to cracking at low temperatures and to fatigue;
- decrease of ageing susceptibility both in preparation of the mix and in operation;
- improved cohesion and adherence to natural aggregates.

2.2. Types of polymers

The polymers used for preparation of modified bitumen are grouped in two main categories:

- elastomers: products consisting in styrene co-polymers, the most important being: SBS – styrene-butadiene-styrene; SIS – styrene-isopropene-styrene;
- plastomers: products based generally on ethylene co-polymers, like: EVA – ethylene-vinyl-acetate; EMA – ethylene-methyl-acryl.

Both elastomeric and plastomeric form similar networks while incorporate in bitumen, a continuous one with flexible strings connected by thermo-reversible links.

Main factors which influence the existence of these networks and improvement of the performances of the bitumen are:

- chemical composition of the bitumen, especially the asphaltene contents;
- polymer's structure
- the compatibility between bitumen (i.e. oils and resins) and the flexible network of the polymer;
- polymer's dosage.

Mainly, the elastomeric polymers (i.e. SBS) are compatible with aromatic bitumen, while the plastomeric polymers (i.e. EVA) are compatible with paraffin and less aromatic bitumen.

2.3. Studies and test performed on polymer modified bitumen

Between 1996 and 2007 studies were carried to CESTRIN Bucharest and DRDP Timisoara for different dosages of SBS polymer modified bitumen (trade marks Carom, Cariflex and CAPS) and reactive polymer (trade mark Elvaloy).

2.3.1 Bitumurile Petrolsub D 60/80 si Arpechim D 60/80 modificate cu Carom si Cariflex

For usual characterization of the modified bitumen the influence of the polymer on penetration, softening point, and Fraass were observed.

After modification of two types of Romanian bitumen, the following observations were made: penetration decreases remarkable, softening point increases, and Fraass improves. Also, from elastic behaviour at 13°C test, it was observed that Carom and Cariflex polymers induce elasticity in bitumen, more than 70% (minimal condition is 60%).

Bitumen ageing through RTFOT produces the same changes in original and modified bitumen, with the remark that they are smaller in modified bitumen, which reflects a better resistance to ageing justified by the higher level of elastic behaviour.

Concerning the rheological characteristics tested according SHRP methodology on Petrolsub and Arpechim bitumen, the modification with polymer increases the viscosity no matter the penetration class of the original bitumen.

DSR (Dynamic Shear Rheometer) test indicates that the modifier improves the superior temperature to which the bitumen resists (increasing for Petrolsub bitumen from 64°C to 76° for Carom modifier, and to 70°C for Cariflex; for Arpechim bitumen the increase is from 58°C to 70°C for Carom modifier).

When using BBR test, no change of the resistance to low temperature is detected, but modified bitumen is less rigid and therefore able to relax after thermal efforts accumulated at low temperature.

In tables 1 and 2 characteristics of D60/80 Petrosub P1 and Arpechim A1 bitumen both original and modified with SBS.

Table 1. Physical-mechanical characteristics of the bitumen (i.e. D 60/80 Petrosub P1 and Arpechim A1; original and modified with SBS)

Characteristic	Petrosub D60/80 bitumen				Arpechim D60/80 bitumen			Norm. 549/1999
	original	+4% Carom	+5% Carom	+4% Cariflex	Original	+4% Carom	+4% Cariflex	
Penetration (1/10mm)	70.2	38	33	35	61	45.6	44.3	55...70
Softening point (°C)	46	58.5	64.4	58.6	44.7	50	52.2	min.55
Ductility @25°C (cm)	150	55	49	30	130	94	114	min.100
Ductility @13°C (cm)	-	32	31	31.5	-	45	55	min.40
Elastic behaviour @13°C (%)	-	74	78	80	-	70	71.5	min.60
Fraass (°C)	-23	-24	-24	-24	-15	-18	-18	max.-20
RTFOT ageing								
Mass loss (%)	0.513	0.310	0.282	0.406	-0.05	-0.08	-0.105	max.0.8
Ductility @25°C (cm)	120	26.3	43.3	30	100	75	90	
Ductility @13°C (cm)	-	24	22.5	23	-	28.2	36	min.40
Elastic behaviour @13°C (%)	-	72	75	70	-	63.5	66	min.60
Increase in softening point (°C)	7	4	1.7	5.1	3.3	8	4.8	max.9
Residual penetration (%)	50	76.3	77	74.3	50	78	55	min.50

Table 2. Rheological properties according to SHRP methodology: simple and SBS polymer modified D60/80 bitumen

Test	SHRP - Rheological properties						
	Petrosub P1				Arpechim A1		
	simple	+4% Carom	+5% Carom	+4% Cariflex	simple	+4% Carom	+4% Cariflex
Brookfield Viscosity	@135°C, max. 3.0 Pa.s						
	0.285	1.020	1.250	1.100	0.300	0.970	0.975
DSR on original bitumen	$G^*/\sin \delta$ (SHRP condition: min.1.0 KPa)						
T=64°C	1.01	6.01	5.8	4.0	0.86	5.2	3.5
T=70°C	0.51	2.90	2.90	1.8	0.50	2.01	0.94
T=76°C	-	1.47	1.50	0.93	0.30	0.92	-
T=82°C	-	0.82	0.86	-	-	-	-
DSR on residual bitumen RTFOT	$G^*/\sin \delta$ (SHRP condition: min.2,2 KPa)						
T=64°C	3.51	10.7	11.9	12.6	2.28	8.7	10
T=70°C	1.60	5.1	6.3	6.7	1.5	4.3	5.2
T=76°C	-	2.8	3.4	3.9	0.8	2.0	3.
DSR on residual bitumen PAV	$G^*\sin \delta$ (SHRP condition max..5000 KPa)						
T=22°C	1555	1463	1276	1289	3834	3620	3500

Test	SHRP - Rheological properties									
	Petrolsub P1				Arpechim A1					
	simple	+4% Carom	+5%Carom	+4%Cariflex	simple	+4%Carom	+4%Cariflex			
T=19°C	2190	2049	1758	1784	5028	4800	4600			
T=16°C	2975	2769	2151	2446	8555	8020	7890			
T=13°C	4067	3769	2843	3301	-	-	-			
BBR	SHRP Condition S = max.300Mpa m= min.0.3									
	S	m	S	m	S	m	S	m		
T=-12°C	-	-	-	-	174	0.378	169	0.345	175	0.330
T=-18°C	-	-	-	-	317	0.340	280	0.320	309	0.312
T=-24°C	181	0.372	178	0.367	121	0.364	175	0.354	-	-
T=-30°C	378	0.336	343	0.340	323	0.332	316	0.320		
Class of performance	64-34		76-34		76-34		70-34		58-22	
									70-28	
									64-22	

2.3.2 ESSO D 50/70 bitumen: simple and modified with Elvaloy

After ESSO D50/70 bitumen is modified with reactive polymer Elvaloy the following changes are observed:

- increase in softening point from 44.3°C to 49.9°C;
- decrease of the penetration from 77.1 to 75.7 1/10mm;
- improving the Fraass from -10.1 to -17.3.

Ageing with TFOT/RTFOT is manifesting with small mass variations and with the decrease of ductility which implies the lack of elasticity of the material. This happens because of the presence of highly volatile compounds.

SHRP tests indicate the followings:

- the modifier enhances the superior temperature to which the road bitumen resists: increasing from 58°C for the original bitumen to 64°C for the modified bitumen;
- the modifier improves the fatigue resistance of the bitumen (i.e. 4546.9 kPa @19°C for modified bitumen comparing to 4423.1 kPa for original bitumen).
- for ESSO D50/70,

Table 3 presents, in detail, the characteristics of ESSO D50/70 bitumen simple and modified with Elvaloy.

Table 3. ESSO D50/70 bitumen: simple and modified with Elvaloy

	Characteristic	U.M.	Results			
			ESSO 50/70 (1 st load)	+ 1.5% ELVALOY (1 st load)	ESSO 50/70 (2 nd load)	+ 1.5% ELVALOY (2 nd load)
1.	Softening point	°C	44.3	49.4	43.2	49.5
2.	Penetration @25°C	1/10 mm	77.1	75.7	72.7	70.2

3.	Ductility @25°C	cm	150	150	150	150
4.	Ductility @13°C	cm	-	-	-	-
5.	Elastic behaviour @13°C	%	-	52.5	-	55.0
6.	Fraass	°C	-10.1	-17.3	-13.2	-10.2
7.	Penetration @0°C	1/10 mm	4.8	5.5	4.9	7.4
8.	Penetration index	-	-1.75	-0.3	-2.24	-0.5
RTFOT						
9.	Mass loss	%	+0.105	+ 0.112	+0.039	+0.099
10.	Increase in softening point	°C	3.7	3.7	5	2.3
11.	Residual penetration @25°C	%	56.5	67.4	57.6	66.7
12.	Ductility @25°C	cm	150	98.1	150	112.3
13.	Ductility @13°C	cm	-	-	-	18.5
14.	Penetration @0°C	1/10 mm	3.3	5.2	4.0	4.9
15.	Penetration index	-	-2.0	- 0.4	-2.0	-0.9
TFOT						
16.	Mass loss	%	+0.087	+0.089	+0.045	+0.101
17.	Increase in softening point	°C	3.7	2.8	4.6	2.0
18.	Residual penetration @25°C	%	56.5	66.0	59.3	68.7
19.	Ductility @25°C	cm	150	106.0	150	105
20.	Ductility @13°C	cm	-	25.0	-	19.7
21.	Elastic behavior @13°C	%	-	-	-	-
22.	Penetration @0°C	1/10 mm	4.3	-	3.8	3.6
23.	Penetration index	-	-2.0	- 0.7	-2.1	-0.9

Test	Results			
	ESSO 50/70 1 st load	ESSO 50/70+1.5% Elvaloy 1 st load	ESSO 50/70 2 nd load	ESSO 50/70+1.5% Elvaloy 2 nd load
Brookfield viscosity	La T = 135 ⁰ C, max. 3.0 Pa*s			
	0.316	0.710	0.361	0.760
DSR on original bitumen	G*/sinδ (SHRP condition min. 1.0 kPa)			
T= 58°C	1.929	2.362		2.634
T= 64°C	0.942	1.228		1.375
T= 70°C		0.659		0.747
DSR on RTFOT residual bitumen	G*/sinδ (SHRP condition min. 2.2 kPa)			
T= 58°C	3.650	4.626		4.423
T= 64°C	1.636	2.417		2.224
DSR on PAV residual bitumen	G*/sinδ (SHRP condition max.5000 kPa)			
T= 16°C		5468.3		
T= 19°C	5372.5	4546.9		6813
T= 22°C	4423.1	3070.4	2986.4	4339.7

BBR	SHRP condition; s=max.300MPa; m=min.0.3							
	S	m	S	m	S	m	S	m
T= -12°C	287.81	0.307	316.29	0.304	277.69	0.302		
T= -18°C	533.6	0.251	580.6	0.235	540.3	0.243		
	PG=58-22		PG=64-22				PG=64-22	

2.4. Assessing colloidal instability index IC

Bitumen used for modification were Petrolsub and ESSO from import. The modifier was Elvaloy AM (1%; 1.5%; 1.75%). Glycidyl-methacrylate (GMA) and asphaltenes is followed by measuring the viscosity.

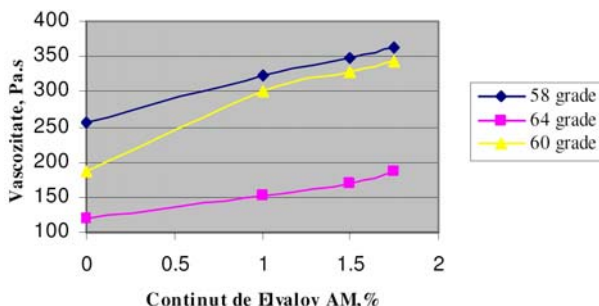


Fig. 1: Viscosity evolution for different temperatures

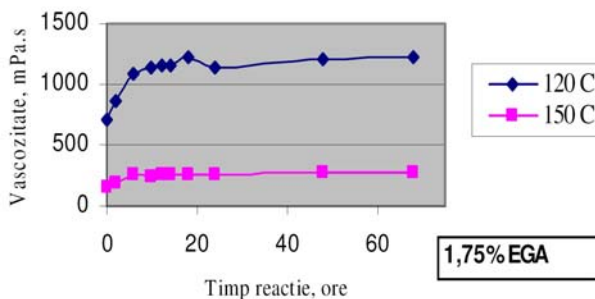


Fig. 2: Viscosity evolution for different temperatures

EGA modified bitumen:

- eliminates the inconvenience of phase separation;
- used in reduced quantities (1...2%)
- improved characteristics using 1.5% of reactive polymer
- improved behaviour at high temperatures (superior CP)
- at low temperature, similar behaviour as the original bitumen.

SBS modified bitumen:

- enhance resistance to permanent deformations;
- improved resistance to low temperatures for the original bitumen with weak properties;
- improved behaviour to high temperatures (superior CP)
- improved properties to fatigue.

2.5. Classical characterization of modified bitumen

SBS Polymers:

- decrease penetration;
- increase softening point;
- improve Fraass;
- improve elasticity.

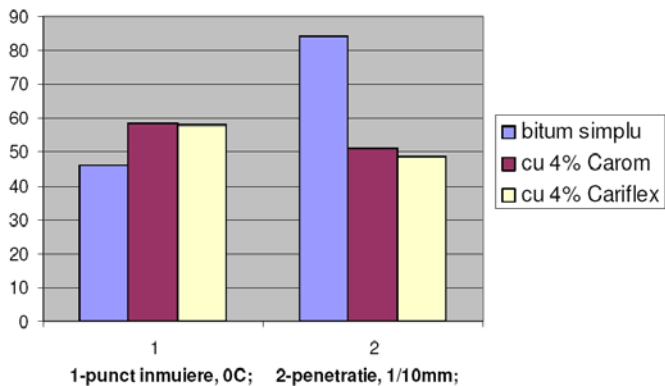


Fig. 3. (1. softening point; 2. penetration)

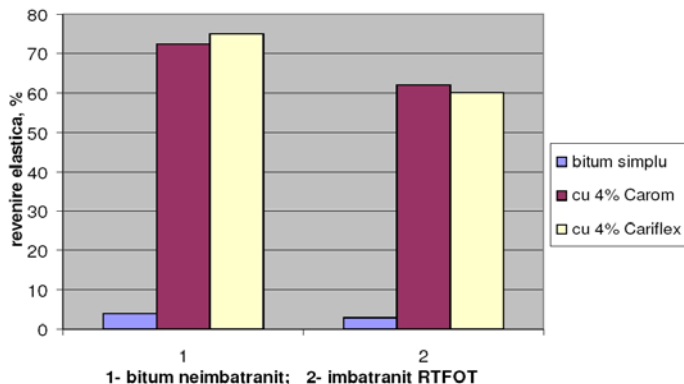


Fig. 4. Elastic behaviour (1. new bitumen; 2. aged bitumen)

5. CONCLUSIONS

1. Using SHRP methods (based on performance criteria; using 7 consecutive days maximal temperature according to SHRP algorithm) for testing highway bitumen results in high performance asphalt mix design.
2. Early initiation of degradations, with unpleasant effects for traffic, is a consequence of the use of inappropriate bitumen.
3. Implementing SHRP methodology, that allows characterization of the bitumen on classes of performances through use of effective equipment, may bring supplemental indications concerning the behaviour of the bitumen at low and high temperatures, based on its viscosity and chemical composition.
4. Although the laboratory tests indicated several degrees difference in Fraass point and the temperature obtained through BBR (Bending Beam Rheometer) it is necessary to adapt “technical conditions” to the specific climate from Romania when European Norms are adopted.
5. Use of polymer modified bitumen might be a proper solution to this issue.
6. Separation of phases (stability to storing) must be avoided and a uniform dispersion of the polymer in bitumen (homogeneity with fluorescent microscope) must be ensured.
7. To obtain effective asphalt mixes, it is recommended that design to be performed after a complete laboratory study, implying testing the aggregates, bitumen (including optimal dosage), binder, additives, fibres etc.
8. Performances of asphalt mixes depend firstly on the quality of materials, imposing to the material producers to observe and maintain a high and constant quality for the products according to technical parameters imposed by technical specifications.

BIBLIOGRAPHY:

1. Nicoara L. Indrumator pentru laboratoarele de drumuri, UT Timișoara 1998.
2. *** - “Utilizarea biturilor modificate si executarea sectoarelor experimentale”; Proceduri de Lucru, Laborator DRDP Timisoara,
3. Romanescu C; Racanel C. – Reologia liantilor bituminoși și a mixturilor asfaltice, ISBN:973-685-566-X, MatrixRom, Bucuresti; 2003
4. Beica V. “Imbatranirea calitatii bitumului rutier prin modificarea cu polimer”. (in Romanian) PhD Thesis, 2005.

Comparison between the parabolic counter deflection and the one made up of the average deflections in the case of a high speed railway bridge

Mircea Suciu¹

¹*Civil engineering, Tehnical University, Cluj, 400027, Romania, Mircea.Suciu@cfdp.utcluj.ro,*

Summary

Objectives:

The paper analyses two shapes of counter deflection from the point of view of the vertical deformations of a high speed railway bridge. The bridge has a 50m span and is made of steel-concrete without ballast bed.

Work method:

The running track of the bridge has a special structure: the rails are continuously fixed into the concrete slab using the Edilon material, without ballast bed.

In order to determine the impact of the increased speed upon the vibrations and deflections of a mixed section railway bridge superstructure, this superstructure has been carried into the SAP2000 finite element calculation programme.

Two shapes of counter deflection have been analysed, a parabolic one and one where the counter deflection has been made based on the average of the deflections obtained in the bridge that had a straight running track.

Twelve non-linear dynamic analyses have been performed for each counter deflection shape, with the Thalys train that covers the analysed models with speeds: 1, 10, 20...110m/s (3.6...396km/h).

The maximal value of the parabolic counter deflection is 14mm (25% of the maximal static deflection obtained in the superstructure from the Eurocode LM71 train) and the one based on the average of the deflections is 10.32mm.

Conclusions:

The paper presents comparatively the deformations and vibrations obtained under the action of the Thalys train running with the above-mentioned speeds for the superstructure with two different counter deflection shapes.

The superstructure with counter deflection made up of the average deflections has a better behaviour (lower vibrations), for speeds higher than 90m/s.

KEYWORDS: railway superstructure, counter deflection, high speed train, Thalys.

1. INTRODUCTION

The counter deflections of the bridges are discontinuities which appear in the path of the axles of high speed trains. The suspension and damping systems are meant to absorb these shocks so that the comfort of the passengers is not significantly reduced at the passage over bridges. The capacity of shock absorption is limited and the admitted vertical accelerations should not exceed 2m/s^2 inside the coach during travel (the recommended value is 1m/s^2).

The reduction of the deflections and of the vibrations under the action of high speed trains begins in the stage of conception of the structure through a correct choice of a counter deflection shape. Certain shapes of counter deflection have a good behavior for certain speed ranges whereas for other speeds they can generate the amplification of the vibrations.

A counter deflection shape which can be suggested is the parabolic one, having the maximal value in mid-span equal to 0.25 of ΔLM71 , where ΔLM71 is the maximal static deflection obtained in the superstructure from the Eurocode LM71 train.

The second suggested shape can be the one that has the counter deflection of a section equal to the average of the deflections obtained under the calculation train in the superstructure with a straight running track. In order to determine this shape of counter deflection we need to go through the following steps. A dynamic analysis will be performed for the structure which has a straight running track, using a calculation software. For a desired speed, all the deflections under the action of the real train in all the sections of the superstructure will be recorded. If, for that particular superstructure the counter deflection in a section will be the average of the deflections recorded in that section under the train running on the horizontal track bridge, there is a possibility that the vibrations of the counter deflection bridge be close to a horizontal line. In case the vibrations will take place around a horizontal line, the comfort of the passengers will grow because only the deviations from the straight line which unites the bridge expansion joints are felt by the passengers and the rolling stock.

2. OBJECTIVES

The determination of the deflections for two superstructures which have the same rigidity but different shapes of counter deflection. The first shape of counter deflection analysed will be the parabolic one, with the maximal value in mid-span equal to a quarter of the maximal deflection obtained in the superstructure under the static load of the LM71 train. The second shape to be analysed will be the one

having the counter deflection of a section equal to the average of the deflections recorded in the straight running track superstructure.

Non-linear dynamic analyses will be performed using the Thalys train with speeds between 1...110m/s (3.6...396km/h) and the SAP2000 programme.

The values of the deformations obtained with the two shapes of suggested counter deflections will be compared and the critical speed where the phenomenon of amplification of the vibrations appears will be determined.

3. WORK METHOD

The superstructure of a mixed section railway bridge without ballast bed, with a 50m span and the cross section as shown in Figure 1, has been carried into the SAP2000 finite element calculation programme.

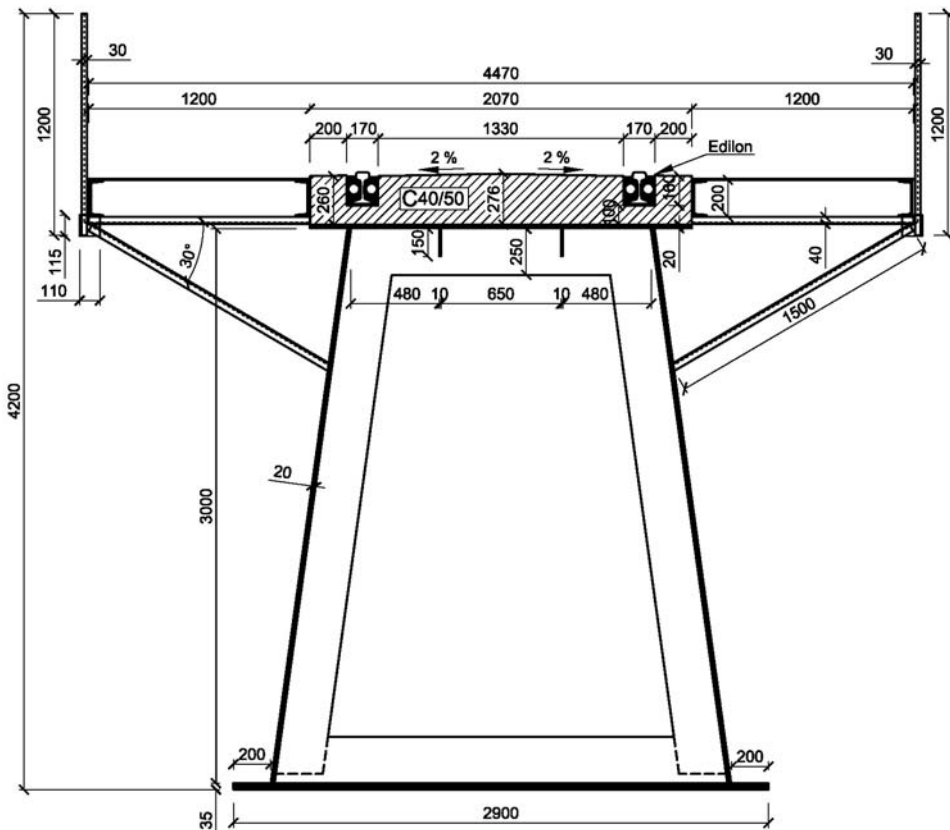


Figure 1. Cross section of the superstructure

The superstructure has been divided and carried into the SAP2000 finite element calculation programme taking into consideration 0.5-meters-long elements along the bridge. 103 characteristic sections have thus been obtained.

The plates of the box section and of the sidewalks are considered as “shell” plane elements, the rails and the linear elements of the sidewalks have been inserted as “frame” type elements, the concrete slab the rails are fixed into has been inserted as “solid” type elements. As a result, the model the analyses will be performed upon has been obtained (Figure 2).

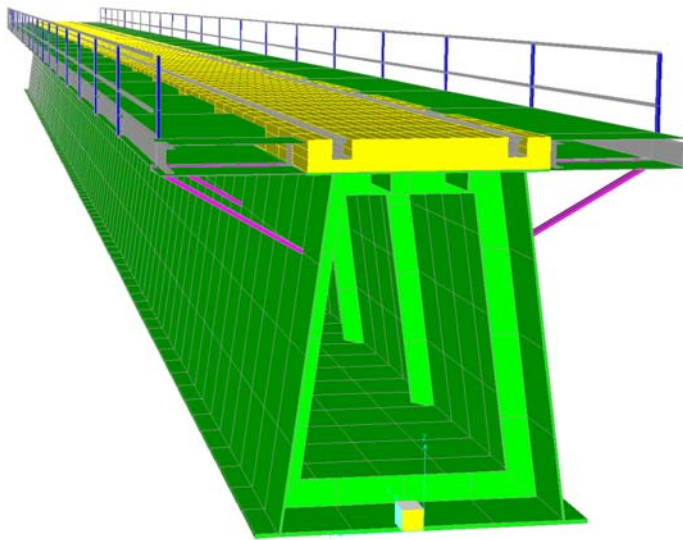


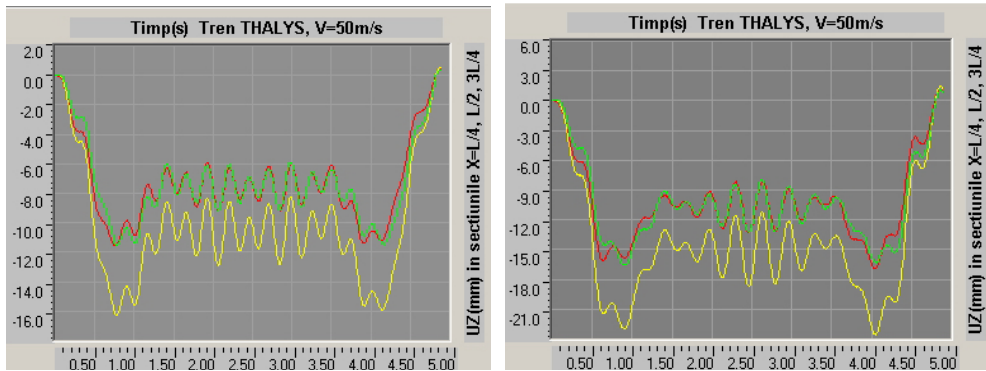
Figure 2. The structure analysed with the SAP2000 programme

The first shape of counter deflection has been obtained through the following steps. The straight running track bridge has been statically loaded with the Eurocode LM71 train. The value of the maximal deflection obtained as a result was 54mm. The sections of the superstructure have been shifted upwards with the value resulted from the equation of the second degree parabolic which passes through the joints and has the value 14mm (a quarter from 54mm) in mid-span.

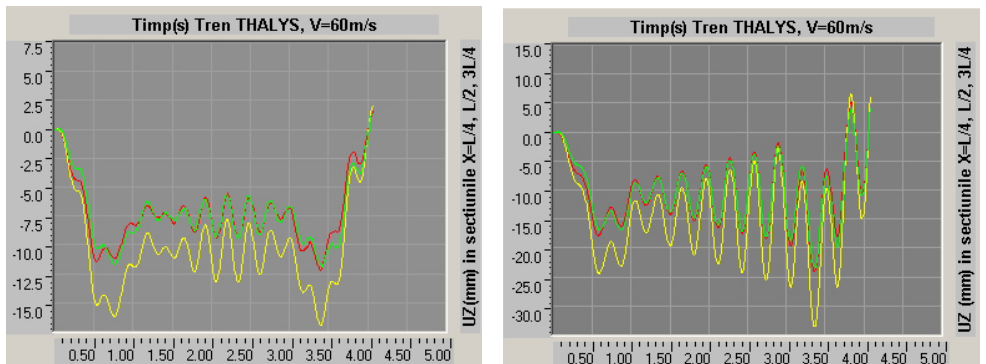
The second shape of counter deflection analysed has been obtained through the following steps. Thalys is a high speed train made up of 2 engines and 8 intermediary cars, with axle loads between 7.25 and 8.5 tons, the distance between the car bogies of 18.7m. The total length of the train is $L_{conv}=193.14m$. The superstructure with a straight running track has been loaded with the Thalys train running with the speed of 60m/s. In each of the 103 characteristic sections of the superstructure, the deflections have been recorded for all the 490 loading steps, until the last axle of the train left the bridge.

For each section of the superstructure, the average of the 490 loading steps has been made and 103 average values have been obtained. All the 103 sections of the superstructure have been shifted upwards with the average value of the deflection recorded in that particular section; thus, the second shape of counter deflection analysed in this paper has eventually been obtained. For the second shape, the maximal value of the mid-span counter deflection is 10.323mm. The dynamic analyses are non-linear and they have been made using the direct integration method, with a 5% damping coefficient ($c=0.05$ directly proportional with the weight).

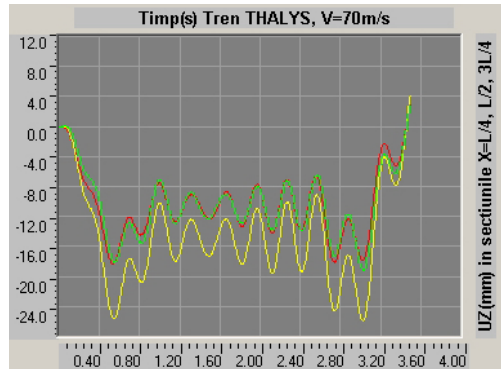
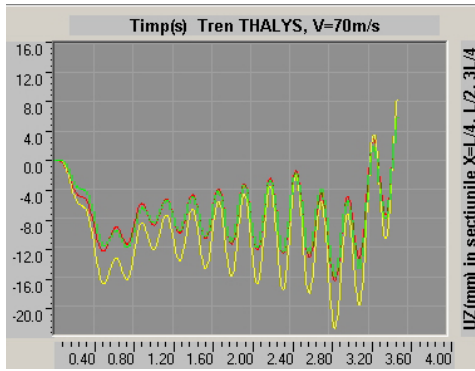
The deflections obtained in 3 of the 103 characteristic sections, namely the ones situated at $L/4$ (red), $L/2$ (yellow), and $3L/4$ (green), are represented in the graphics below, Figures 3, 4, 5, 6, 7, 8. The displacements of the superstructure with parabolic counter deflection and the ones of the superstructure which has a counter deflection obtained as an average of the deflections appear on the left and on the right, respectively, in the following figures.



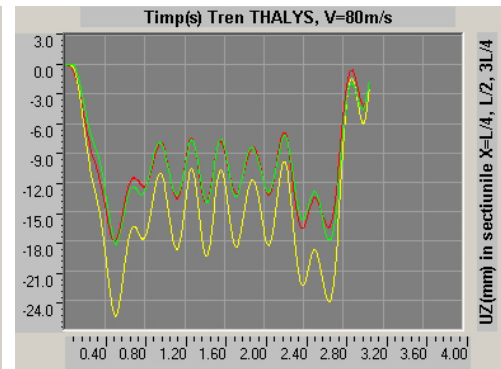
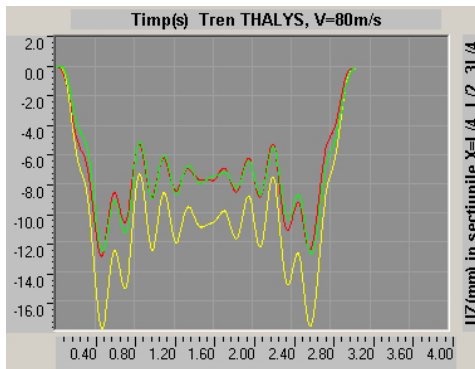
-16.24mm for parabolic counter deflection, -23.55mm for counter deflection based on av.
Figure 3. Vertical displacements UZ (mm), Thalys, V=50m/s (180km/h)



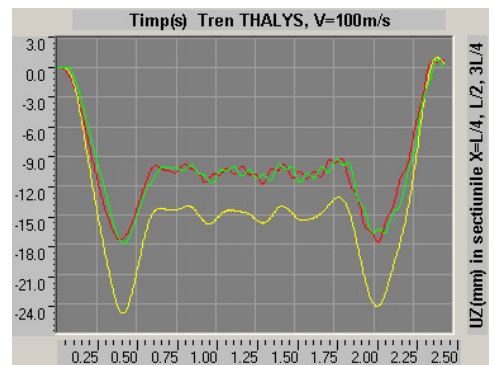
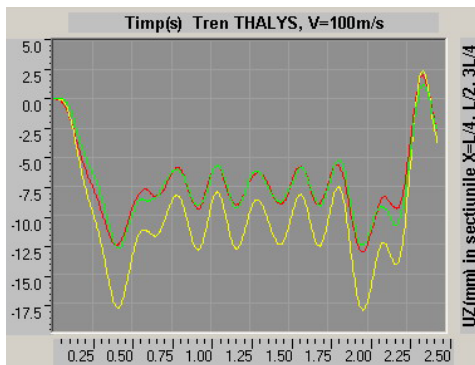
-16.99mm for parabolic counter deflection, -33.59mm for counter deflection based on av.
Figure 4. Vertical displacements UZ (mm), Thalys, V=60m/s (216km/h)



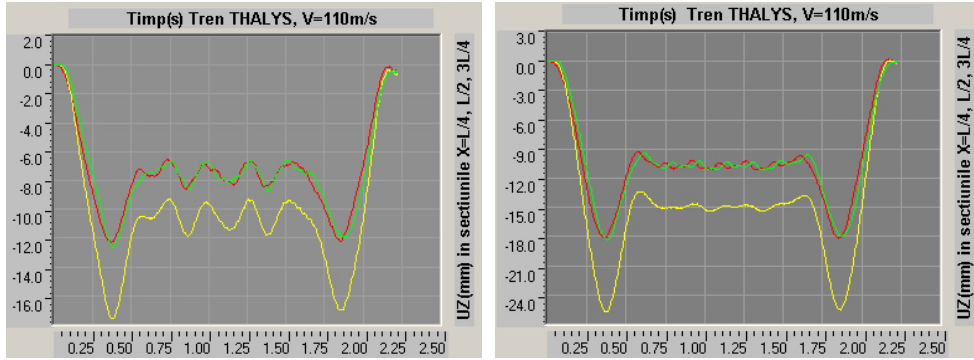
- 23.11mm for parabolic counter deflection, -25.89 mm for counter deflection based on av.
Figure 5. Vertical displacements UZ (mm), Thalys, V=70m/s (252km/h)



- 17.94mm for parabolic counter deflection, -25.74mm for counter deflection based on av.
Figure 6. Vertical displacements UZ (mm), Thalys, V=80m/s (288km/h)



- 18.14 mm for parabolic counter deflection, -24.99 mm for counter deflection based on av.
Figure 7. Vertical displacements UZ (mm), Thalys, V=100m/s (396km/h)



- 17.60 mm for parabolic counter deflection, -25.74 mm for counter deflection based on av.
 Figure 8. Vertical displacements UZ (mm), Thalys, V=110m/s (396km/h)

The amplification of the vibrations is obtained at the speed of 70m/s (252km/h) for the parabolic counter deflection bridge and of 60m/s (216km/h) in the case of the bridge which has a counter deflection based on the average deflections.

Table 1 comprises the centralization of the results that have been obtained by the 24 dynamic analysis of the 51-meters-long superstructure with the Thalys train.

Table 1. Vertical displacements of the superstructure loaded with the Thalys train.

THALYS train speed	Maximal and average deflections UZ (mm) measured at mid-span throughout the time when axles of the train cross the section							
	Bridge with parabolic counter deflection, Cs(max.)=14mm				Bridge with counter deflections obtained from the average of the deflections, Cs(max.)=10.323mm			
	Related to the horizontal line		Related to the non-deformed structure		Related to the non-deformed structure		Related to the horizontal line	
V m/s (v km/h)	UZ max (1)	UZ avg (2)	UZ max (3)	UZ avg (4)	UZ max (5)	UZ avg (6)	UZ max (7)	UZ avg (8)
(0)								
1m/s(3.6)	-15.36	-11.71	-1.36	2.29	-21.93	-16.63	-11.61	-6.31
10 (36)	-15.74	-11.71	-1.74	2.29	-22.47	-16.63	-12.15	-6.31
20 (72)	-15.40	-11.71	-1.40	2.29	-22.25	-16.63	-11.93	-6.31
30 (108)	-15.98	-11.71	-1.98	2.29	-24.78	-16.67	-14.46	-6.35
40 (144)	-15.81	-11.72	-1.81	2.28	-24.59	-16.65	-14.27	-6.33
50 (180)	-16.24	-11.73	-2.24	2.27	-23.55	-16.74	-13.23	-6.42
60 (216)	-16.99	-11.77	-2.99	2.23	-33.59	-16.69	-23.27	-6.37
70 (252)	-23.11	-11.83	-9.11	2.17	-25.89	-16.82	-15.57	-6.50
80 (288)	-17.94	-11.77	-3.94	2.23	-25.74	-16.83	-15.42	-6.51
90 (324)	-18.21	-11.74	-4.21	2.26	-25.24	-16.76	-14.92	-6.44
100 (360)	-18.14	-11.77	-4.14	2.23	-24.99	-16.82	-14.67	-6.50
110 (396)	-17.60	-11.82	-3.60	2.18	-25.74	-16.94	-15.42	-6.62

For speeds lower than 90m/s the parabolic shape counter deflection has a better behaviour (lower amplitudes of the vibrations and lower deflections).

For speeds higher than 90m/s the counter deflection made up based on the average of the deflections has a better behaviour. For the speed of 110m/s (396km/h) the vibrations are significantly reduced (at the passage of the cars the superstructure practically does not vibrate at all).

The significance of the values in the table:

- for a certain running speed, the SAP2000 programme records in all the 103 characteristic sections of the superstructure all the deflections that occur in the 490 loading steps with the Thalys train;
- out of the 490 values recorded in the mid-span section we have selected only the maximal deflections, inserted in columns (1), and (5) in the table;
- we have made the arithmetical average of the 490 values of the deflections recorded in the mid-span section (all throughout the time when axles of the train are present on the superstructure) and we have inserted them in the table in columns (2), and (6);
- if the value of the counter deflection in a certain section is subtracted from the maximal values related to the non-deformed structure, columns (1) and (5), the maximal deflections of the track related to the horizontal line are obtained; they appear in columns (3) and (7);
- if the value of the counter deflection in a certain section is subtracted from the average values of the deflections recorded in the presence of the train, the average value of the recorded deflections related to the horizontal line which unites the level of the track in the joints is obtained; these values appear in columns (4), (8);
- the sign (-) or (+) in the table means that the deflections or the deflection averages in that column are below (or above, respectively) the horizontal line which unites the end joints of the superstructure;

3. CONCLUSIONS

From the point of view of the maximal deflections (columns 1 and 5 compared), they are larger at the bridge with the counter deflection made up of the deflections average (33.59mm for the speed of 216km/h) than at the parabolic counter deflection bridge (23.11mm for the speed of 252km/h);

From the point of view of the average values around which the vibrations of the two analysed structures occur, the one with the parabolic counter deflection has a

better behaviour (2.25mm above the horizontal line, as compared to 6.41 below the horizontal line; columns 4 and 8 compared);

If the analyses are made from the point of view of the comfort of the passengers (who feel the frequency and amplitude of the vibrations), we notice that the superstructure with counter deflection made up of the average deflections has a better behaviour, for speeds higher than 90m/s (the vibrations from the graphics in Figure 8 compared);

The introduction of a counter deflection made up of the average of the deflections recorded under the train in the horizontal running track bridge leads to the increase of the strain and deformations in the superstructure (the maximal deflection is 10.48mm larger than the one obtained with the parabolic counter deflection).

The graphical representation of the counter deflection shapes analysed in this paper are presented below, in Figure 9.

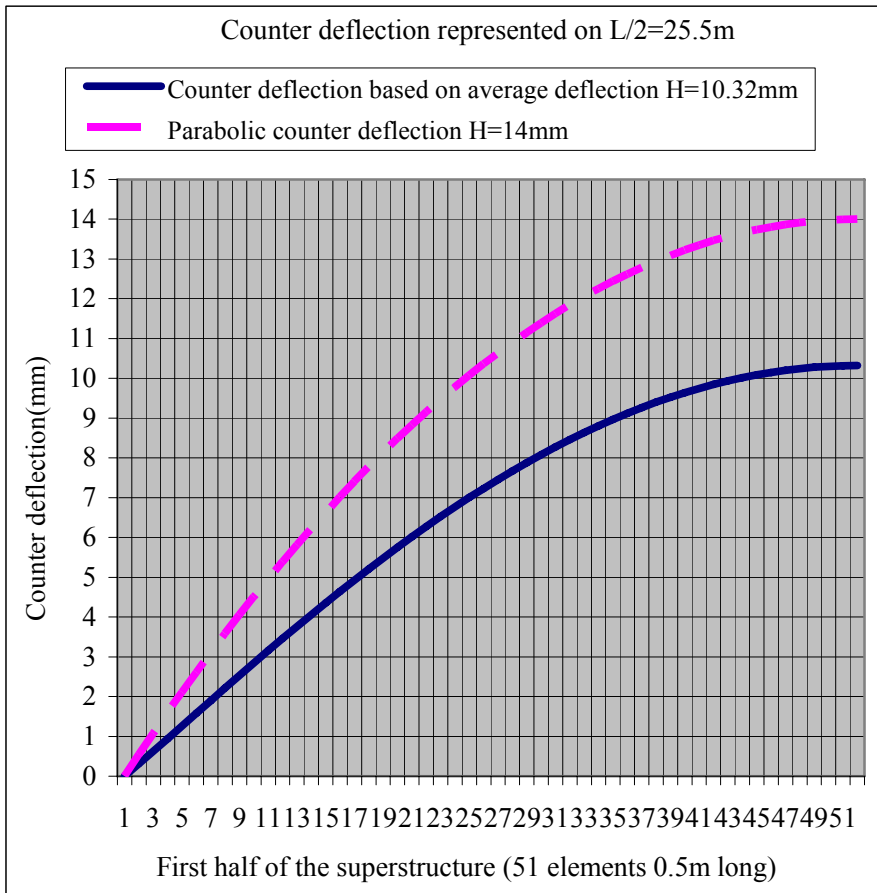


Figure 9. Graphical representation of analysed counter deflection shapes

References

1. Bârsan, G.M.: *Dinamica și stabilitatea construcțiilor*, Editura didactică și pedagogică București 1979. (in Romanian)
2. Esveld, C.: *Modern Railway Track*, MRT-Productions, ISBN 0-800324-1-7, 1989
3. Esveld, C. and Kok, A. W. M.: *Dynamic Behavior of Railway Track*, Railway Engineering Course TU Delft, Department of Civil Engineering, November 1996
4. Esveld, C.: *Modern Railway Track*, Second Edition, Delft University of Technology 2001.
5. Goicolea, J.M., Domínguez, J., Navarro, J.A., Gabaldón, F.: *New dynamic analysis methods for railway bridges in codes IAPF and Eurocode 1*, RAILWAY BRIDGES Design, Construction and Maintenance, Spanish group of IABSE, Madrid, 12–14 June 2002
6. Jantea, C., Varlam, F.: *Poduri metalice. Alcătuire și calcul. (Metallic bridges. Elements and calculation)* Casa editorială “Demiurg”. Iași. 1996. (in Romanian)
7. Kollo, G., Moga, P., Guțiu, I.-Șt., Moga, C.: *Bending resistance of composite steel-concrete beams in accordance with Eurocode 4*, 10th International conference of civil engineering and architecture, EPKO 2006, Sumuleu Ciuc, 14-16 June. (in Romanian)

Advantages and disadvantages of the counter deflection based on the average of the deflections recorded in the sections of the superstructure of a railway bridge

Mircea Suciu¹, Gavril Kollo²

¹Civil engineering, Technical University, Cluj, 400027, Romania, Mircea.Suciu@cfdp.utcluj.ro,

²Civil engineering, Technical University, Cluj, 400027, Romania, gavril.kallo@cfdp.utcluj.ro,

Summary

Objectives:

The paper analyses the vertical displacements of a railway bridge with a special shape of counter deflection, steel-concrete composition, 50m span, under the action of a high speed train.

Work method:

The running track of the bridge has a special structure, without ballast bed, with rails continuously fixed into the concrete slab using the Edilon material.

In order to determine the impact of the increased speed upon the vibrations and deflections of a mixed section railway bridge superstructure, this superstructure has been carried into the SAP2000 finite element calculation programme.

Two variants of superstructure have been analysed, one without counter deflection and one with counter deflection, based on the average of the deflections obtained in the bridge that had a straight running track.

Twelve non-linear dynamic analyses have been performed for each model, with the Thalys train that covers the analyzed models with speeds: 1, 10, 20...110m/s (3.6...396km/h). The maximal value of the counter deflection is 10.323mm.

Conclusions:

The paper presents comparatively the deformations and vibrations obtained under the action of the Thalys train running with the above-mentioned speeds for two analyzed superstructures.

The superstructure with counter deflection made up of the average deflections has a better behaviour (lower vibrations), for speeds higher than 90m/s.

KEYWORDS: high speed train, Thalys, railway superstructure, counter deflection.

1. INTRODUCTION

The increase of the running speed on the railway determines the apparition of deformations and vibrations in the superstructures of the bridges, which can be amplified under certain conditions. The limitation of the deformations and vibrations can be made from the very stage of conception of the structure, by choosing and appropriate shape of the counter deflection.

In the case of high speed trains, the choice of the counter deflection is even more important because the superstructure is crossed over a shorter period of time than in the case of regular speeds. If the value of the counter deflection is too high or the shape that has been chosen is wrong, the shock created can be too difficult to be taken over by the damping systems of the rolling stock.

Based on the following observations, a shape of counter deflection can be suggested. For the crossing of a superstructure that has a horizontal running track, the vibrations and deformations around an average value will be recorded in each section of the superstructure. If, for that particular superstructure, the counter deflection of a section is the average of the deflections recorded in that section under the train running on that bridge with a horizontal running track, there is a possibility that the vibrations be brought close to a horizontal line.

In case the vibrations are close to a horizontal line the comfort of the passengers will grow because only the deviations from the straight line that unites the joints are felt by the passengers and the running stock.

2. OBJECTIVES

The determination of the vertical displacements for a superstructure that has the counter deflection of a section equal to an average of the deflections recorded in the superstructure with a straight running track.

Non-linear dynamic analyses will be performed using the Thalys train with speeds between 1...110m/s (3.6...396km/h) and the SAP2000 programme.

The values of the deformations obtained for the bridge with counter deflection will be compared to the ones resulted from the dynamic analyses performed for the bridge that has a horizontal running track.

The critical speed where the phenomenon of amplification of the vibrations and increase of the value of the vertical deformations appears will be determined.

3. WORK METHOD

The superstructure of a steel-concrete section railway bridge without ballast bed, with a 50m span has been carried into the SAP2000 finite element calculation programme. The 51-meters-long superstructure presented in Figure 1 has been divided taking into consideration 0.5-meters-long elements along the bridge, thus 103 characteristic sections have been obtained.

The box-section and sidewalks plates are considered as “shell” plane elements, the rails and the linear elements of the sidewalks have been inserted as “frame” elements, the concrete slab has been inserted as “solid” type elements. The analyzed model is presented in Figure 2.

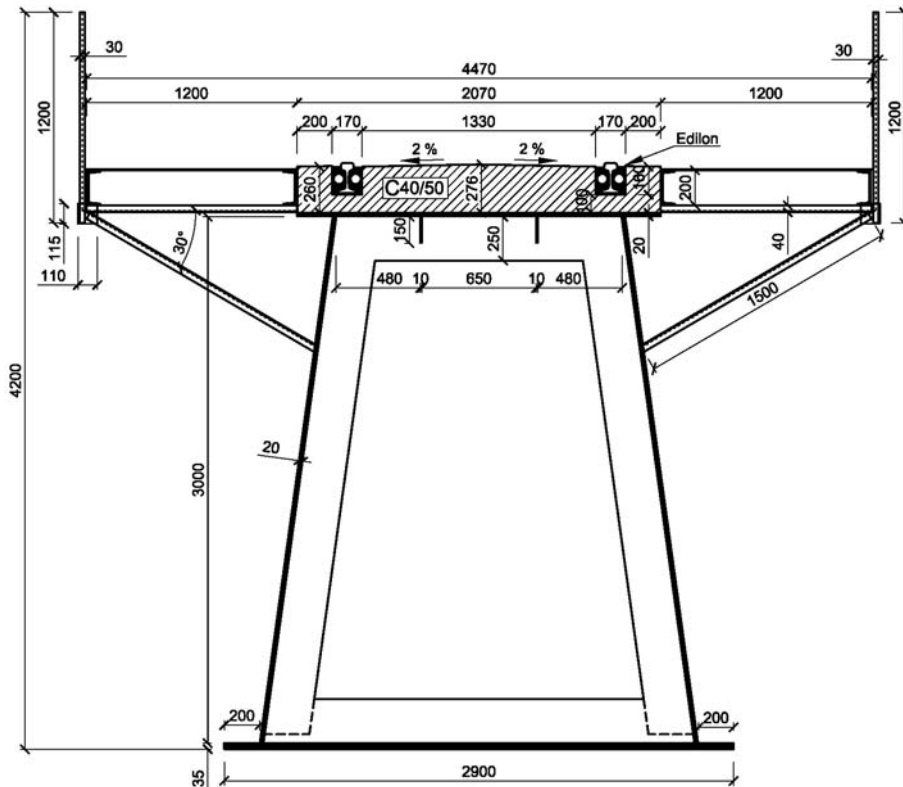


Figure 1. Cross section of the superstructure

Thalys is a high speed train made up of 2 engines and 8 intermediary cars, with axle loads between 7.25 and 8.5 tons, the distance between the car bogies of 18.7m. The total length of the train is $L_{train}=193.14m$.

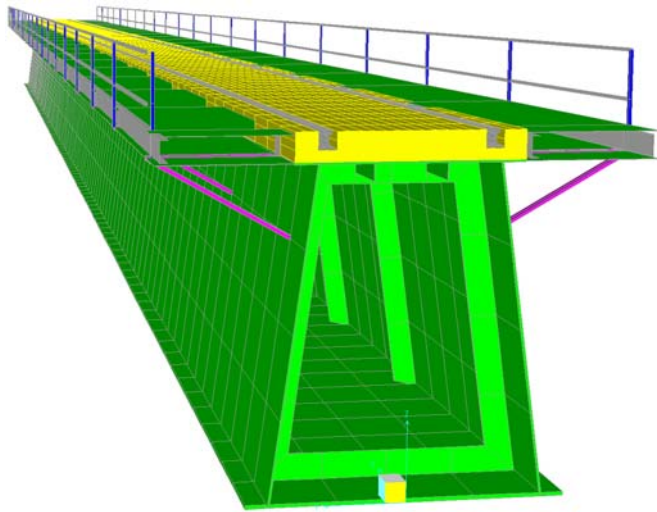
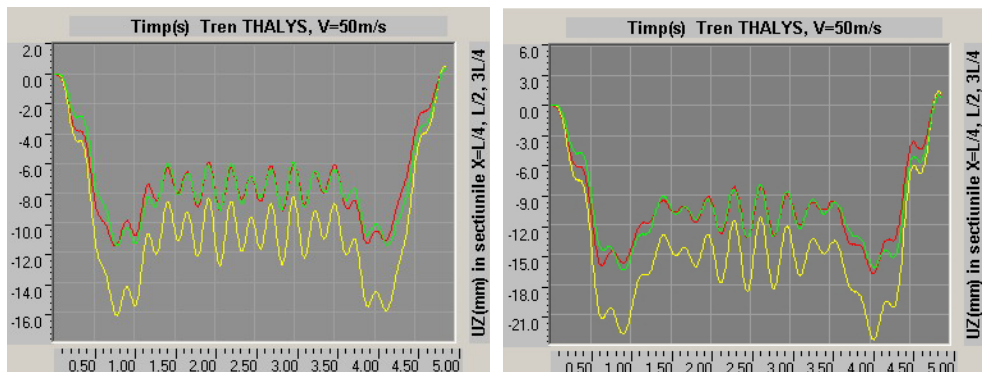


Figure 2. The structure analysed with the SAP2000 programme

From the moment the first axle enters the superstructure until the last axle leaves the superstructure, the train covers 102 elements 0.5m-long and has 490 successive loading steps. The vertical displacements of the superstructure have been recorded at the level of the rails, for all the 490 loading steps. The dynamic analyses are non-linear and they have been made using the direct integration method, with a 5% damping coefficient, directly proportional with the weight.

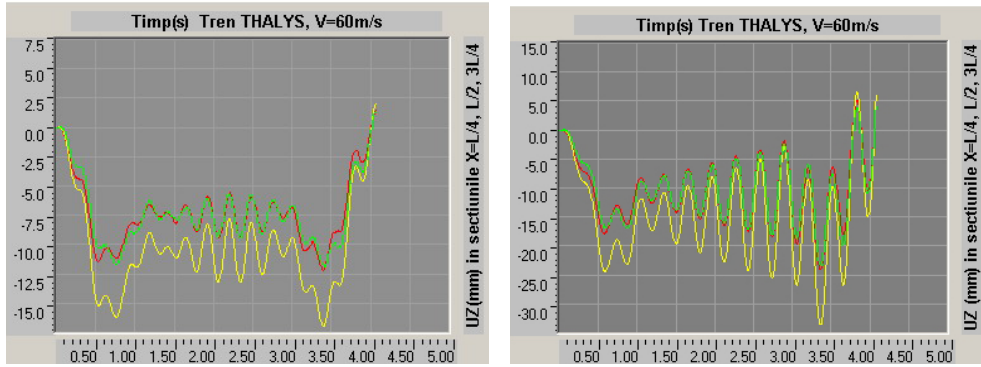
The vertical displacements obtained in 3 of the 103 characteristic sections, namely the ones situated at $L/4$ (red), $L/2$ (yellow), and $3L/4$ (green), are represented in the graphics below (Figures 3, 4, 5, 6, 7). The deflections of the superstructure with a horizontal track appear on the left and the ones of the bridge with counter deflection appear on the right side of the figures.



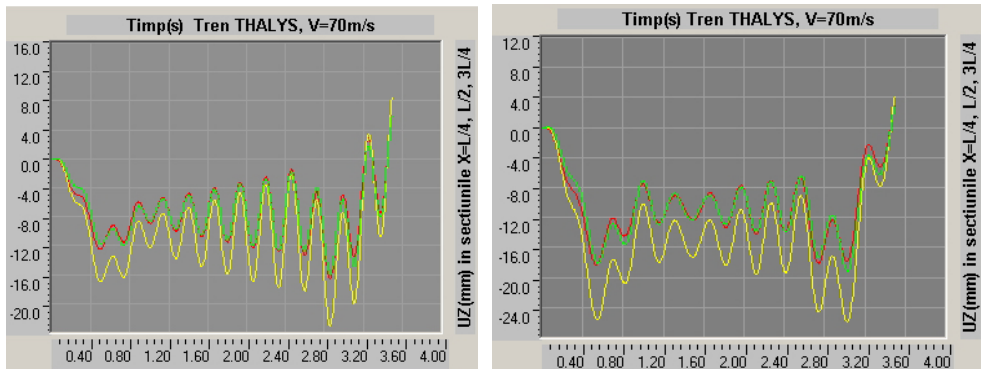
-16.24mm for the straight track

-23.55mm for the counter deflection track

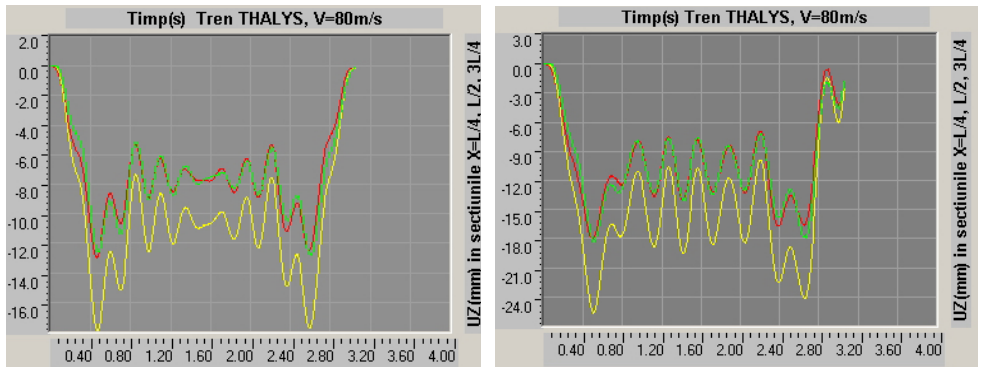
Figure 3. Vertical displacements UZ (mm), Thalys, V=50m/s (180km/h)



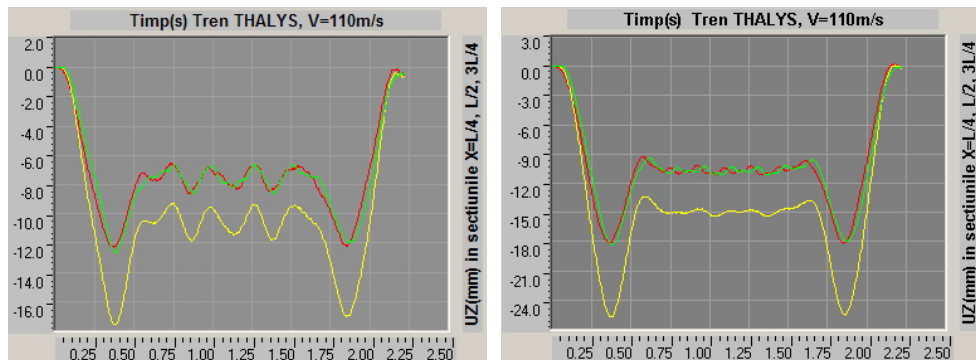
- 16.99mm for the straight track
-33.59mm for the counter deflection track
Figure 4. Vertical displacements UZ (mm), Thalys, V=60m/s (216km/h)



- 23.10mm for the straight track
-25.89mm for the counter deflection track
Figure 5. Vertical displacements UZ (mm), Thalys, V=70m/s (252km/h)



- 17.94mm for the straight track
-25.74mm for the counter deflection track
Figure 6. Vertical displacements UZ (mm), Thalys, V=80m/s (288km/h)



- 17.61 mm for the straight track
 -25.74mm for the counter deflection track
 Figure 7. Vertical displacements UZ (mm), Thalys, V=110m/s (396km/h)

Table 1 comprises the centralization of the results that have been obtained by the 24 dynamic analysis of the 51-meters-long superstructure with the Thalys train.

Table 1. Vertical displacements of the superstructure loaded with the Thalys train.

THALYS train speed	Maximal and average deflections UZ (mm) measured at mid-span					
	Horizontal bridge		Bridge with counter deflection 10.323mm			
	Related to the horizontal line		Related to the non-deformed structure		Related to the horizontal line	
V m/s (v km/h) (0)	UZ(-) max (1)	UZ(-) avg (2)	UZ(-) max (3)	UZ(-) avg (4)	UZ(-) max (5)	UZ(-) avg (6)
1m/s(3.6)	15.36	10.12	21.93	16.63	11.61	6.31
10 (36)	15.74	10.12	22.47	16.63	12.15	6.31
20 (72)	15.40	10.12	22.25	16.63	11.93	6.31
30 (108)	15.98	10.09	24.78	16.67	14.46	6.35
40 (144)	15.81	10.12	24.59	16.65	14.27	6.33
50 (180)	16.24	10.11	23.55	16.74	13.23	6.42
60 (216)	16.99	10.11	33.59	16.69	23.27	6.37
70 (252)	23.10	10.16	25.89	16.82	15.57	6.50
80 (288)	17.94	10.12	25.74	16.83	15.42	6.51
90 (324)	18.21	10.12	25.24	16.76	14.92	6.44
100 (360)	18.13	10.09	24.99	16.82	14.67	6.50
110 (396)	17.61	10.13	25.74	16.94	15.42	6.62

The significance of the values in the table:

- for a certain running speed, the SAP2000 programme records in all the 103 characteristic sections of the superstructure all the vertical deformations that occur in the 490 loading steps with the Thalys train;

- out of the 490 values recorded in the L/2 section we have selected only the maximal deformations, inserted in columns (1), and (3) in the table;
- we have made the arithmetical average of the 490 values of the deformations recorded in the 490 loading steps (all throughout the time when axles of the train are present on the superstructure) and we have inserted them in the table in columns (2), and (4);
- if the value of the counter deflection in a certain section is subtracted from the values related to the non-deformed structure, columns (3) and (4), the vertical deformations of the track related to the horizontal line are obtained; they appear in columns (5) and (6);
- the sign (-) that appears near Uz means that all the deflections in that column are below the horizontal line of the track in the absence of the train;

3. OBSERVATIONS AND CONCLUSIONS.

- The phenomenon of amplification of the vibrations is obtained at the speed of 70m/s (252km/h) for the straight superstructure and 60m/s (216km/h) for the counter deflection bridge.
- At the speed of 110m/s (396km/h) the vibrations decrease, the superstructure with counter deflection having the best behaviour (the superstructure practically does not vibrate at the passage of the cars).
- From the point of view of the maximal deformations, they are bigger at the counter deflection bridge than at the straight running track bridge (columns 1 and 3 compared);
- If the analyses are made from the point of view of the comfort of the passengers (who feel only the deviations from the straight line that unites the joints), we notice that the superstructure with counter deflection has a better behaviour, except for the speed of 60m/s (columns 1 and 5 compared);
- For the superstructure with a straight running track the most unfavourable speed is that of 70m/s (252km/h) with a maximal deflection of 23.10mm at L/2;
- For the counter deflection superstructure the most unfavourable speed is that of 60m/s (216km/h) with a maximal deformation of 33.59mm at L/2;
- For speeds higher than 90m/s (324km/h) the vibrations decrease significantly at the counter deflection bridge as compared to the ones recorded at the bridge without counter deflection (Figure 7);

Flaws of the analysed counter deflection shape:

The introduction of a counter deflection made up of the average of the deflections recorded under the train in the horizontal running track bridge leads to an increase

of the strain and of the deformations in the superstructure (33.59mm as compared to 23.10mm in the bridge without counter deflection).

Advantages of the analysed counter deflection shape:

The vibrations are around an average value which is closer to the straight line (6.41mm instead of 10.12mm) which has as an effect the decrease of the strain in the rolling stock. The comfort will increase because the passengers will feel only the deviations from the straight line.

For speeds higher than 90m/s (324km/h), both the maximal value of the deviations from the horizontal line decreases and the amplitude of the vibrations of the counter deflection bridge decreases significantly. At these speeds, the behaviour of the counter deflection superstructure is much superior to the straight running track superstructure.

References

1. Bârsan, G.M.: *Dinamica și stabilitatea construcțiilor*, Editura didactică și pedagogică București 1979. (in Romanian)
2. Esveld, C.: *Modern Railway Track*, MRT-Productions, ISBN 0-800324-1-7,1989
3. Esveld, C. and Kok, A. W. M.: *Dynamic Behavior of Railway Track*, Railway Engineering Course TU Delft, Department of Civil Engineering, November 1996
4. Esveld, C.: *Modern Railway Track*, Second Edition, Delft University of Technology 2001.
5. Goicolea, J.M., Domínguez, J., Navarro, J.A., Gabaldón, F.: *New dynamic analysis methods for railway bridges in codes IAPF and Eurocode 1*, RAILWAY BRIDGES Design, Construction and Maintenance, Spanish group of IABSE, Madrid, 12–14 June 2002
6. Jantea, C., Varlam, F.: *Poduri metalice. Alcătuire și calcul. (Metallic bridges. Elements and calculation)* Casa editorială “Demiurg”. Iași. 1996. (in Romanian)
7. Kollo, G., Moga, P., Guțiu, I.- Șt., Moga, C.: *Bending resistance of composite steel-concrete beams in accordance with Eurocode 4*, 10 th International conference of civil engineering and architecture, EPKO 2006, Sumuleu Ciuc, 14-16 June. (in Romanian)

Experimental testing and assessment of stiffness modulus and fatigue of various cold recycling mixes

Jan Valentin¹, Michal Grochal² and Tomáš Prudký³

¹Road Construction Department, Faculty of Civil Engineering, Czech Technical University, Prague, 166 29, Czech Republic, jan.valentin@fsv.cvut.cz

²Geotechnical and Transport Construction Department, Technical University Košice, Košice, 040 00, Slovakia, michal.grochal@tuke.sk

³ Faculty of Civil Engineering, Czech Technical University, Prague, 166 29, Czech Republic, tomas.prudky@fsv.cvut.cz

Summary

Cold recycling in pavement rehabilitation and new construction records growing utilization and forms a part of sustainability strategies in road engineering. Usually reclaimed asphalt pavement (RAP) is used for mixes where bitumen emulsion or bitumen foam is used together with suitable hydraulic binders. Besides RAP there are possibilities of part substitution by secondary or waste materials from quarries.

From the technical point of view, these mixes have to be tested by traditional and more advanced testing methods explaining performance behavior of these mixes. The performance and related characteristics can be in best manner described and assessed by rheologic properties. During the experimental work the focus concentrated especially on measurement of stiffness modules at different temperatures (5°C, 15°C, 27°C) representing different pavement conditions during the year and fatigue tests for different stress conditions. Results and their comparison for different mixes are be presented and discussed in the paper.

KEYWORDS: cold asphalt recycling, bitumen emulsion, stiffness modulus, fatigue, Nottingham Asphalt Tester.

1. INTRODUCTION

In a number of contributions and specialist articles, it is possible to notice the attention paid by the road construction community to the implementation and further optimization of recycling technology. Primarily, cold technologies have experienced relatively great development in the Czech Republic and Slovakia since, besides the benefits of waste and recyclable material processing, other advantages are said to be the lower energy demands and protection against

excessive greenhouse gas emissions. This trend, championed also by e.g. the EAPA (European Asphalt Pavement Association), is undoubtedly desirable since it activates a certain degree of road construction self-sufficiency as well as an ability to implement the principles of sustainable and ecologically acceptable construction. On the other hand, the trend has its pitfalls, which primarily include the still limited knowledge of the functional behavior of such mixes and the subsequent degree of uncertainty as to whether such cold mixes are utilized as efficiently as they could be in construction and whether the design and useful behavior of the entire road structure is optimized.

The key parameters in this context and the assumed contributors towards the utilization of such mixes in road structures can certainly be identified as stiffness (expressed by the relevant stiffness modulus) and fatigue characteristics, each of which should assist in predicting the durability of such structures. Due to the considerable heterogeneity of such mixes, even though the reclaimed material is sorted, it is impossible to ensure a homogenous quality when milling multiple surface layers, therefore determining the parameters is not the easiest of tasks. It is further complicated by the availability of several methods that can be utilized, particularly in the event of monitoring fatigue characteristics. This contribution is an attempt to depict the rheological behavior of cold mixes, into which emulsified asphalt and cement have been applied.

2. TEST MIX PREPARATION

The selection of mix composition and the method of preparing test samples, including their subsequent curing, have an undisputable effect on the results in the characteristics examined. This fact is even more significant in the case of rheological qualities where a certain characteristic is always examined in relation to another variable.

Two sets of lab-designed mixes have been selected for this contribution while, in the case of fatigue characteristics, comprehensive results could only be compiled for the first set. The test mix set was produced at the Geotechnical and Transport Construction Department at the Technical University in Košice. Out of the total number of 8 mixes, two mixes were selected for the experiments as described below. The mixes were characterized by differing proportions of reclaimed material and ground aggregate as well as by the quantity of emulsified asphalt and cement added. The composition of the mixes is specified in Table 1a, b, where the mixes are designated as AE1 and AE2.

The mixes were designed to conform with the Slovak technical standard STN 73 6121 in accordance with their expected use in the base layer. Cationic Emultech P bitumen emulsion and blast furnace Portland cement II/B-S 32.5 R were used in

their production. The basic components involved were sorted reclaimed material 0-16 and grading 0-2 limestone. To increase the proportion of fine particles, rock (limestone) powder was added to one of the mixes. To determine the stiffness modulus and fatigue characteristics, test slabs were made using static pressure of 75 kN. Marshall specimens were prepared at the same time.

The other group of mixes, for which only stiffness modulus values have so far been determined, has been produced by the Road Construction Department laboratory at the Czech Technical University in Prague. Seven mixes were designed; recyclable material of grade 0-11 was used to produce mixes EC1-EC 5 while mixes EC8 and EC9 contained sorted recyclable material of grading 0-22. In the case of selected mixes, a proportion of fine aggregate 0-2 was designed, which is classified by the producer as a material difficult to utilize (melaphyre, Košťálov quarry). To produce laboratory mixes EC8 and EC9, similarly to the Košice mixes, cationic bitumen emulsion, Emultech P, was used; bitumen emulsion Vialit RE60 was applied to the remaining mixes. Blast furnace Portland cement 32.5 R was used as the hydraulic binder for all mixes. In the case of two mixes, a part of the cement component was replaced by residual filler from aggregate production, which represents another recycled material that is currently verified as a potential component for cold recycling mixes.

Table 1a: Cold recycling mix composition with reclaimed asphalt material (RAP) and bitumen emulsion.

Mix		EC1	EC2	EC3	EC4	EC5
Binder		bitumen emulsion + cement				
RAP : additional aggregate ratio		100:0	80:20	70:30	100:0	100:0
Bitumen emulsion content	: %-b.m.	2.5	2.5	2.5	2.5	2.5
H2O content	: %-b.m.	5.1	5.1	5.1	5.1	5.1
Cement kontent	: %-b.m.	3.0	3.0	3.0	2.75	1.5
Residua filler	: %-b.m.	-	-	-	0.75	1.5

Table 1b: Cold recycling mix composition with reclaimed asphalt material (RAP) and bitumen emulsion.

Mix		AE1	AE2	EC8	EC9
Binder		bitumen emulsion + cement			
RAP : additional aggregate ratio		75:25	60:40	100:0	100:0
Bitumen emulsion content	: %-hm.	3.5	3.0	2.2	3.5
H2O content	: %-hm.	n.a.	n.a.	3.4	2.5
Cement kontent	: %-hm.	1.5	3.0	2.0	2.0
Residua filler	: %-hm.	6.0	-	-	-

Test samples of mixes produced at CTU in Prague were prepared using the Marshall test compaction, applying 2x50 blows despite the fact that, in accordance with the applicable Czech technical conditions (TP112, TP126 or TP162), the preferred treatment tends to use the static pressure method. As additional information, we can state that last year basic measurements were carried out on samples made on a Superpave Gyratory Compactor while the objective for the near future is to compare all methods.

Subsequently, test samples of both sets were cured for 28 days under laboratory conditions followed by stiffness modulus determination and fatigue testing. In the case of several mixes, the measurements were performed 9 months after the test samples were made; at this time a minimum increase of strength characteristics due to cement hydration and curing of the specimens can be expected.

3. DETERMINATION OF STIFFNESS MODULUS AND FATIGUE CHARACTERISTICS

2.1. General

The stiffness modulus was determined using the Nottingham Asphalt Tester (NAT) developed at the end of 1980's at Nottingham University (Cooper & Brown) with the objective of facilitating routine testing for rheological characteristics of asphalt mixes. This type of test device is primarily utilized in cases where standard methods such as the Marshall test have provided insufficient qualitative evidence and cannot deliver a qualified assessment of the relevant asphalt mix. As has been previously stated (e.g. [1]), the NAT allows monitoring of the following rheological characteristics of the material in a broad range of temperatures (-10 °C to +40 °C):

- stiffness modulus determined by means of repetitive transverse tension test,
- resistance against permanent deformation by means of repetitive axial load test,
- resistance against permanent deformation by means of dynamic asphalt mix curing test,
- resistance against permanent deformation by means of static asphalt mix curing test,
- resistance against repetitive load (fatigue) by means of a transverse tension test.

An advantage of the device is the possibility of using common test specimens as well as road samples, both of which are adapted to a 100 mm diameter. The tester consists of a testing frame, pneumatic unit (units with an hydraulic mechanism are an alternative option), control unit, temperature chamber and a PC with the evaluation software.

2.2. Stiffness Modulus

The asphalt mix stiffness modulus is an important deformation characteristic that, along with the Poisson number, is used in road structure design. The stiffness modulus is defined as the ratio of tension and relative deformation under a certain temperature that has a specific Poisson number value, and characterizes the material in its ability to resist the effects of load. The ability to transfer higher load effects increases with increasing stiffness modulus values.

Stiffness modulus values are determined based on the repetitive transverse tension test, which is usually carried out on Marshall specimens. Direct pressure load transferred in the vertical section plane of the sample results in transverse tension perpendicular to the load direction. During the test, LVDT sensors measure horizontal deformation. Stiffness modulus measurements are usually taken at temperatures of 15°C to 40°C. In the case of cold recycling mixes, temperatures of 5°C, 15°C and 27°C were selected. The load affecting the specimen cannot be influenced directly and, therefore, only the values of the assumed resulting horizontal deformation changes can reduce or increase the value of the load in action. The maximum required horizontal deformation is usually selected from the interval of 5-10 microns. The test yields the asphalt mix stiffness modulus calculated from the average of five measurements taken.

2.3. Fatigue

Fatigue tests are generally divided into several groups:

- performed on test specimens in the shape of a truncated wedge (trapezoid) under constant tension or with a permanent deformation,
- performed by means of the NAT device through a test of repetitive transverse tension loads on Marshall specimens,
- performed using the four-point beam method.

The NAT device allows the performance of the fatigue test using the dynamic transverse tension test when a repetitive constant tension is applied. This method of fatigue testing utilizes a permanent pressure force that affects the test specimen and generates tension, which is criticized by a number of experts; therefore, this method is being replaced in the harmonized European standard by the four-point beam method. However, it has been proven in practice that, even in the case of fatigue testing by transverse tension under repetitive tension, if the fatigue testing method is consistent for all samples, the results for tested materials end up in a sequence identical to that evidenced by, often, more difficult methods of fatigue testing.

Based on the fatigue test results the resistance of the mix tested against the effects of repetitive tension is formulated. The test simulates tension generated in the road

structure layers by a dynamic load. The basic principle of the test is the generation of a repetitive movement of pressure load in the vertical section plane of the sample, which generates repetitive tension load in the transverse direction perpendicular to the direction of the load effect (Fig. 1).

This test measures the vertical deformation of the sample up to the breaking (cracking) point. Rupture is manifested by the occurrence of cracks in the vertical direction of the specimen section, which can lead to the breaking of the specimens made with brittle materials. The vertical deformation of the specimen is measured by LVDT sensors with a linear range of up to 10 mm.

The result of the fatigue test is the development of vertical deformation of the specimen until the breaking point, depending on the number of load cycles. The values obtained are evaluated in the Wöhler diagram, which depicts the dependence of the load effects upon life of the material. This dependency usually represents a straight line in a logarithmic scale and it is assumed that its incline is a good expression of the fatigue life of asphalt mixes. The vertical axis of the diagram covers the maximum value of the relevant load in the logarithmic scale while the horizontal axis covers the number of load cycles necessary to rupture the test specimen. To generate a Wöhler diagram, it is necessary to perform the test under at least three different tension levels.

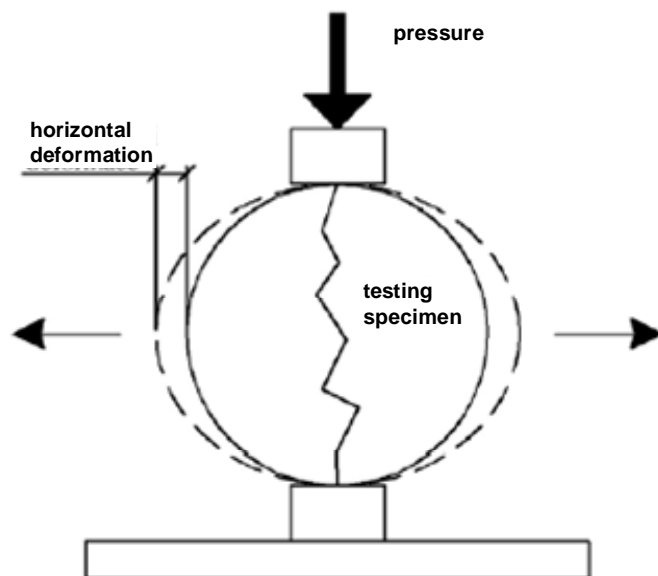


Figure 1: Description of the fatigue test method with repetitive transverse tension loads.

When using the NAT device, fatigue testing is usually carried out under temperatures of 15°C to 40°C which does not fully cover the admissible conditions

as stipulated in the present EN, which requires fatigue characteristics assessment under lower temperatures as well. With respect to the fact that the testing procedure of determining fatigue characteristics for cold recycling mixes has not been used in the Czech Republic, this partial disagreement can be considered insignificant. Moreover, with better quality mixes the device, installed in the Civil Engineering Faculty of the CTU, only facilitated testing under lower temperatures with difficulties. The power source of the NAT device is weak and does not always allow proper deterioration of the asphalt mix at the required level of tension (or the resulting deformation). Due to these reasons, a comparative measurement has been taken in the past, which proved the relatively negligible effect of temperature in the Wöhler diagram evaluation ($\log \varepsilon$ versus $\log N$). The conclusions were obtained by measurements performed with truncated wedge specimens in the sense of Czech technical standard ČSN 73 6160. The comparative measurement was performed for the ABS I mix. Five specimens were tested under 40°C, three specimens under 15°C.

The result of the fatigue test acquired by use of the NAT, which represents input for the determination of standard fatigue parameter values, is depicted in Fig. 2. The figure describes the logarithmic dependence between the vertical deformation level ε and the number of load repetitions until rupture, N .

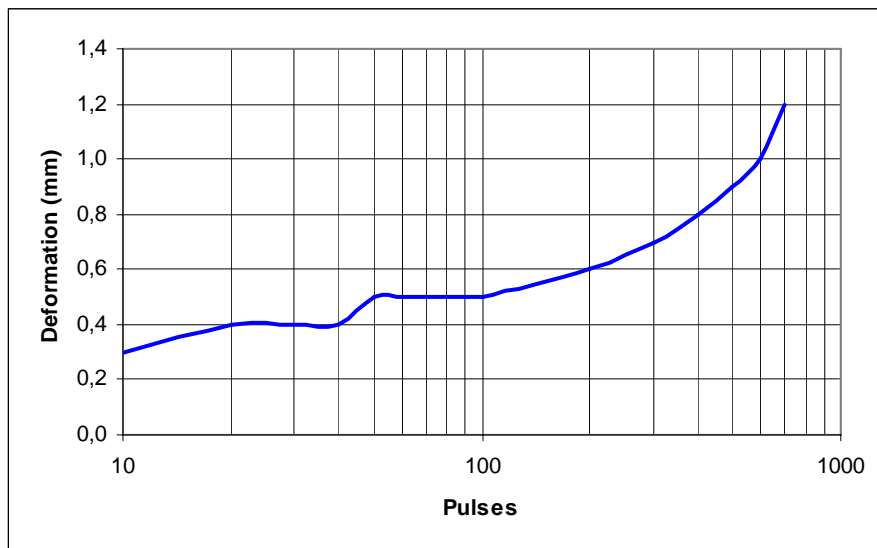


Figure 2: Result of fatigue test on NAT apparatus.

The evaluation determines the fatigue characteristics based on the Wöhler diagram and on the following equations in which N stands for the number of load cycles until rupture of the specimen and $\varepsilon_{0,j}$ represents the maximum amplitude of the relative deformation under test conditions (j) at the beginning of the measurement,

while ε_0 is the average deformation size derived from the fatigue curve with 10^6 load cycles, expressed in 10^{-6} $\mu\text{m}/\text{m}$.

$$\log \varepsilon_{0j} = \log \alpha - 3 + \beta \log N \quad (1)$$

which corresponds with

$$\varepsilon 10^3 = \alpha N^\beta \quad (2)$$

The fatigue relation according to the applicable methodology is expressed as

$$\log \varepsilon = -a - B^{-1} \log N \quad (3)$$

and, therefore, the fatigue parameters of laboratory tests α and β are related to the design method fatigue parameters by relations, [5]:

$$\log \alpha + a = 3 \quad \text{and} \quad B = -1/\beta \quad (4)$$

which means that

$$\log \varepsilon_{0j} = a_j + B \cdot \log N \quad \text{or} \quad \varepsilon 10^{-3} = A \cdot N^{-B} \quad (5).$$

3. RESULTS, DISCUSSION AND SUMMARY

The results of stiffness modulus determination for temperatures of 5°C, 15°C and 27°C with the corresponding Poisson numbers (0.25; 0.33 and 0.39) are listed in the following figures, 3-5. The test was performed on at least three test specimens for each temperature. Mixes EC1, EC3 and EC4 were subject to non-destructive repetitive transverse tension load test after 28 days of curing and the results led to the following conclusions:

- the positive impact of the proportion of fine aggregate (which is obvious also in the case of the fatigue test, according to the partial results so far),
- the negative impact of substituting a part of the cement component with residual filler.

The first conclusion may be explained by the increased proportion of finer particles, despite the fact that sorted reclaimed material of 0-11 grade was used for those mixes. The other finding should not be to the detriment of using residual filler. On the contrary, mixes where a part of the reclaimed material is substituted by residual dust and the proportion of cement has remained constant should be the subject of further examination, along with the behavior of mixes in cases when the proportion of cement is slightly decreased and the proportion of residual filler exceeds at least 5%-by mass of the mix. The considerably broad range of stiffness modulus values (e.g. for 15°C it amounts to 1,800-6,000 MPa) is rather surprising.

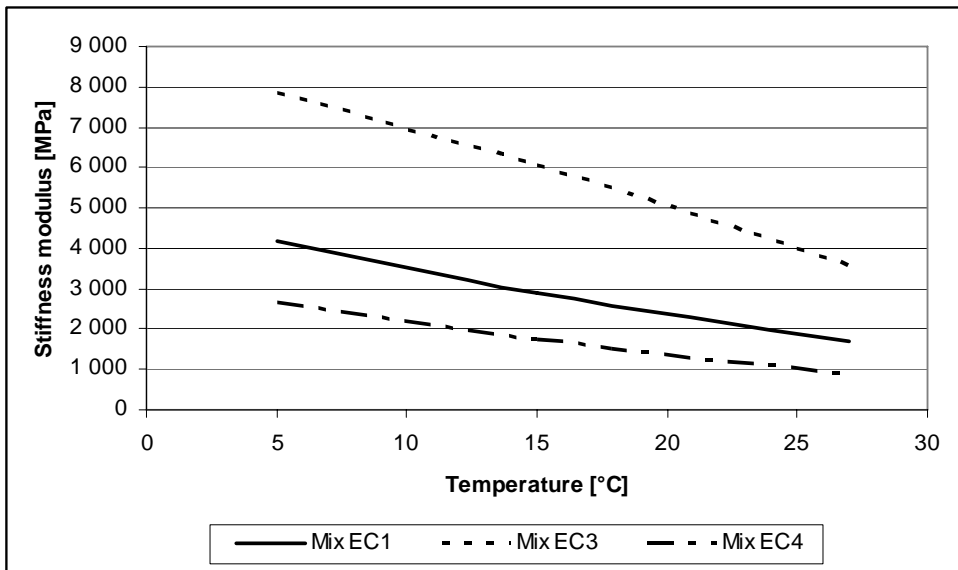


Figure 3: Stiffness modulus of mixes EC1, EC3 and EC4 at 5°C, 15°C and 27°C.

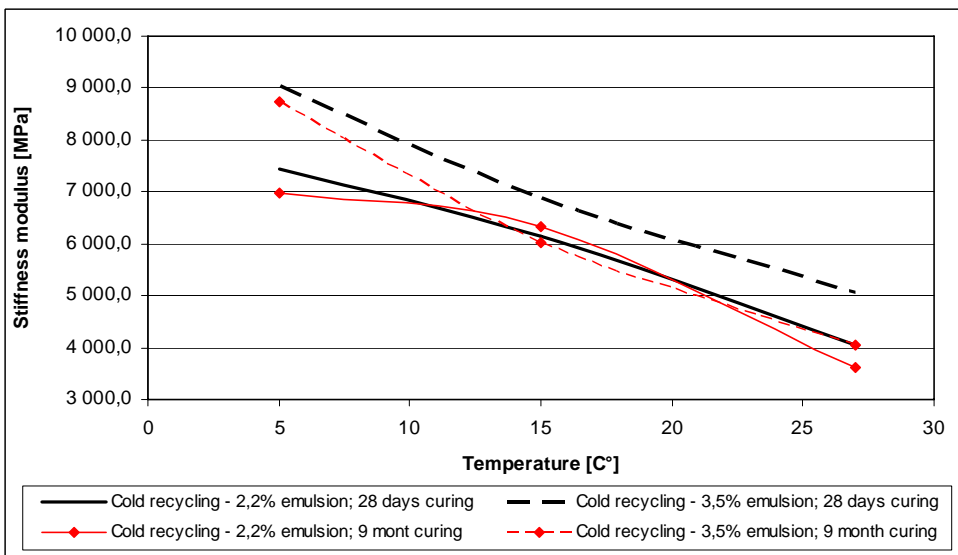


Figure 4: Stiffness modulus of mixes EC8 and EC9 at 5°C, 15°C and 27°C.

Two effects were examined in the determination of stiffness modulus of mixes EC8 and EC9, as depicted in Fig. 4 – the effect of varying the bitumen emulsion

proportion and the effect of varying the curing time. In the first case, the expected positive impact of the bitumen emulsion (with an unmodified proportion of cement) on the stiffness modulus value was proven; with regards the curing time the results are not absolutely unambiguous. In the case of the mix containing 3.5%-by mass of bitumen emulsion, the stiffness modulus value decreased on average by about 12%; the mix containing 2.2% of bitumen emulsion the values after 28 days and 9 months of curing are almost identical (in the case of 15°C the stiffness modulus value even slightly increased; however, this has not been reconfirmed by another test and may be caused by the heterogeneous nature of the material).

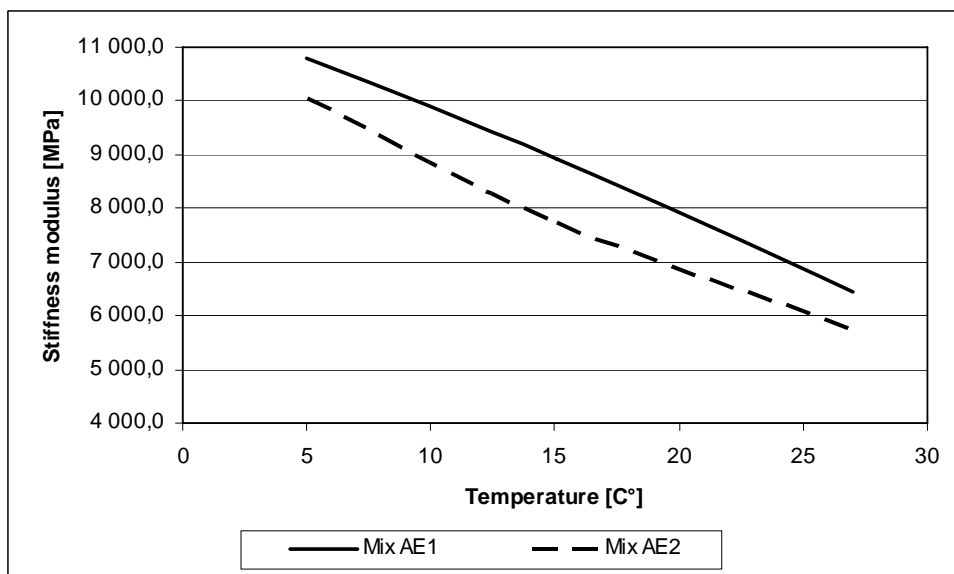


Figure 5: Stiffness modules of mixes AE1 and AE2 at 5°C, 15°C and 27°C.

With mixes AE1 and AE2, the stiffness modules were determined after 9 months of curing. In comparison to mixes EC1-EC5, these also confirm the assumingly positive impact of the added aggregate. The difference between values of mixes AE1 and AE2 is probably due to the higher proportion of bitumen emulsion in the first mix. At the same time it is possible to believe that in increasing the proportion of finely ground aggregate, this increase from a certain level starts having a negative effect, which might be another cause of the lower stiffness modulus values of mix AE2. Values for 27°C were used for the subsequent determination of fatigue characteristics.

In the evaluation of fatigue tests we assume that the material tested is homogenous and isotropic and that its deformation is governed by the linear visco-elastic – Boltzmann – material. The way asphalt mix samples rupture depends primarily on the temperature under which the fatigue testing is carried out and on the magnitude of the tension or deformation. Ruptures can be classified as brittle, which means

the material is separated by a fracture; plastic, which means shearing along sliding areas and pliable, in which case the material divides along the edges of grains. Asphalt mixes undergo combinations of such ruptures. Under low temperatures, the brittle character prevails while at temperatures above 20°C the ruptures more closely resemble the pliable type. In the case of cold recycling mixes, based on the results listed below, it is possible to discover brittle rupture types with a distinct fracture. In the case of this type of mix, the effects of deformation due to the weight of the test specimen itself, which has a negative impact on maintaining the shape of the test specimens and is characteristic for certain asphalt mixes under test temperature of 40°C, were not examined.

The results of the fatigue test achieved are summarised in Table 2 and in figures 6 and 7, while the determination of fatigue characteristics as such was carried out according to the previous procedure applied in Czech technical standard ČSN 73 6160, which also corresponds with the figures and, is in accordance with the procedure as stipulated in EN 12697-24, where the horizontal axis covers the relative deformation and the vertical axis the number of load cycles. When comparing both approaches it is obvious that results according to EN yield slightly higher values.

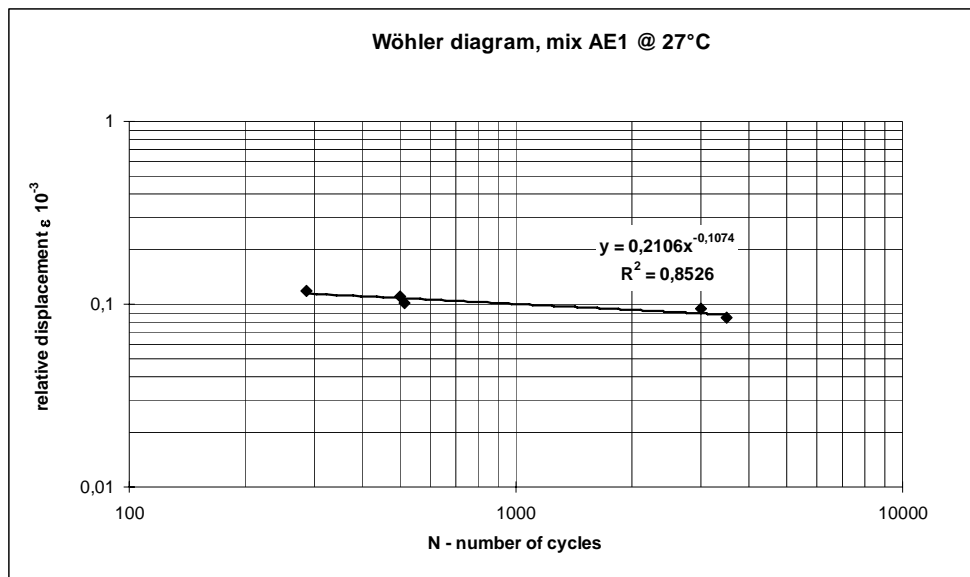


Figure 6: Result of fatigue test of mix AE1.

The interpretation of the results of fatigue behavior of the cold recycling mixes tested is not absolutely unambiguous and reflects the problem of homogeneity of the reclaimed material used. From the perspective of parameter “a”, mix AE2

shows a better fatigue behavior; on the other hand, parameters “B” and “ ϵ_6 ” prove a better fatigue behavior of mix AE1. This, moreover, is in line with the conclusions of the fatigue tests with the trapezoid samples, [3]. When comparing the mixes analyzed with a selected representative of bitumen coated aggregate mixes, the cold recycling mixes show mediocre fatigue behavior and, therefore, a shorter life.

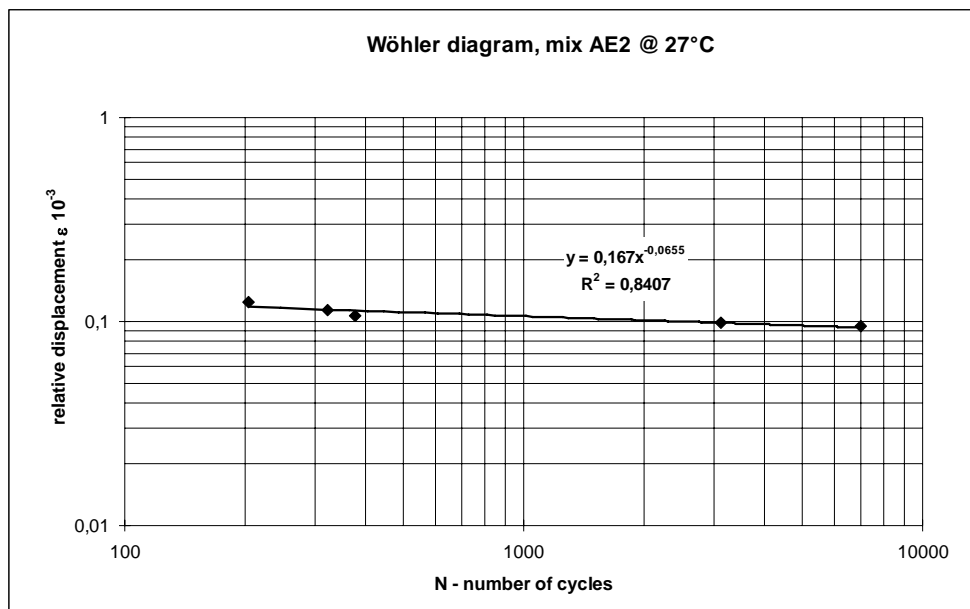


Figure 7: Result of fatigue test of mix AE2.

Table 3: Summarization of fatigue characteristics.

Mix	Fatigue characteristics according ČSN 73 6160 calculation			Fatigue characteristics according EN 12697-24 calculation		
	α	β	$\epsilon_6 (x10^3)$	α	β	$\epsilon_6 (x10^3)$
AE1	0.2106	-0.1074	0.04776	0.2346	-0.1259	0.04119
AE2	0.1763	-0.0655	0.07132	0.1810	-0.0779	0.06166
OKH I	1.8063	-0.2900	0.03287	1.9685	-0.3023	0.03022

From the point of view of the homogeneity of reclaimed material, which enters the cold recycling mixes as a significant factor, we consider the knowledge of its material composition including the quantity of binder and basic characteristics of such binder one of the key determining facts. In the effort of aiming to use reclaimed material to the optimum level, this fact should result in consistent sorting as well as in a need to mill the individual layers of the pavement structure separately to prevent heterogeneities of the milled material that might lead to

negative effects on the resulting recycling mix characteristics that might be difficult to forecast.

Acknowledgements

This result was achieved within the framework of grant GAČR 103/05/2055.

References

1. Tesař, Z., *Vliv nízkoteplotních pojiv na vybrané mechanicko-fyzikální a reologické vlastnosti asfaltových směsí*, Master theses, Faculty of Civil Engineering, CTU Prague, 2005. (in Czech)
2. Valentin, J., Mondschein, P., Pešková, Š., *Assessment of Stiffness Modulus of Cold Recycling Mixes as a Basis for their further Optimization*, ISAP 2008, Zürich. (not published yet)
3. Gillinger, J., *Reologické vlastnosti za studena recyklovaných zmesí. Acta Montanistica Slovaca, vol. 12(2007), No. 1, pp. 53-61.*, 2007. (in Slovak).
4. Valentin, J., Mondschein, P., *Porovnání vybraných vlastností směsí studené recyklace s asfaltovou emulzí a asfaltovou pěnou*, VIII. Vedecká konferenci s medzinárodnou účasťou, Košice, 2007. (in Czech)
5. Ministry of Transport of Czech Republic, *TP170 – Designing of road pavements*, Prague, 2004.

Preliminary results obtained with various structural design methods, considered for validation of Long Lasting Rigid Pavements (LLRP) concept using Accelerated Testing (ALT) Facility

Irinel – Diana Vrancianu

Department of Roads and Foundations, Technical University "Gh. Asachi", Iasi,, 700050, Romania,
vrancianu_diana@yahoo.com

Summary

One of the aims in developing new pavement design methods and using new pavement materials is to obtain longer service life, at lower initial and maintenance costs. Long Lasting Rigid Pavements (LLRP) is the concept answering these goals.

In the frame of Ecolanes Project – an international endeavor with participants from 7 European countries, at which the Technical University "Gh. Asachi" is partner – steel fibers recovered from used tires are to be incorporated in rigid pavement structure, in order to reduce the thickness of the pavement layers. The use of this type of steel fibers would answer the need to develop new recycled products and applications. Also, rolled compacted concrete (RCC), with or without steel fibers, is to be used as base of the proposed pavement structures.

The validation of the new pavement structure performance is to be obtained by numerical analysis, testing on the Accelerated Load Testing (ALT-LYRA) circular track at the Technical University "Gh. Asachi" Iasi and demonstration road sectors on the National Road 17 (NR 17).

For the initial thickness design study with these solutions, three design methods are envisaged to be used, namely: the Romanian NP 081-2002 method [4], the U.K. Highway Agency Method [5] and the Mechanistic – Empirical Pavement Design Guide (M-E PDG) developed by AASHTO in USA. This paper presents the early results of this study, using the first two methods.

KEYWORDS: rigid pavement, structural design methods, steel fibers reinforced concrete (SFRC), rolled compacted concrete (RCC), ALT

1. INTRODUCTION

In the frame of EcoLanes Project, it was proposed the accelerated testing on the circular track of the Technical University “Gh. Asachi” Iasi, of four different structural solutions, on 6 sectors of various lengths. The aim is to be able to compare the performance of various slabs, having the same thickness, but constructed with different materials, namely:

- unreinforced cement concrete (UPC) slab
- steel fiber reinforced concrete (SFRC) slab
- unreinforced RCC
- steel fibers reinforced RCC.

For RCC slab, a hot mix asphalt (HMA) coating has been provided, for surface texture and protection reasons, which was not considered in the design. Also, the sectors constructed with SFRC have various lengths, in order to assess the behavior of this material at different joints' spacing. Figure 1 presents the circular sectors on the ALT-LYRA test facility.

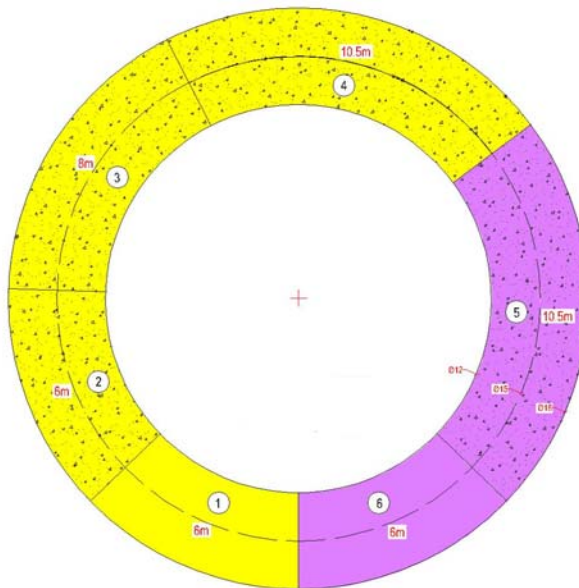


Figure 1. Proposed experimental sectors on the ALT circular track facility

Key:

- 1 – Unreinforced Cement Concrete; length – 6m;
- 2, 3, 4 – Steel Fibers Reinforced Concrete (SFRC); length – 6m, 8m and 10.5m respectively;
- 5 – Steel Fibers Reinforced Rolled Compacted Concrete (SFRCC); length – 10.5m;
- 6 – Rolled Compacted Concrete (RCC); length – 6m.

These circular sectors and their respective pavement structures have been proposed by the working group from our University, involved with ALT testing [1], [2], approved, in principle, during the last EcoLanes meeting, held in Antalia [3] and their structures are presented in Figure 2 and Figure 3. Our studies have been conducted on these pavement structures.

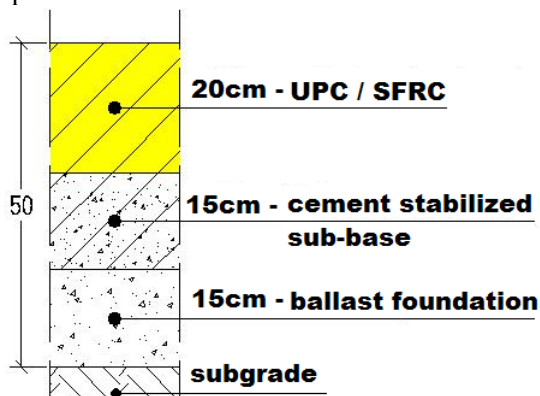


Figure 2. Pavement structure for sectors 1,2,3 and 4, on the ALT circular track facility

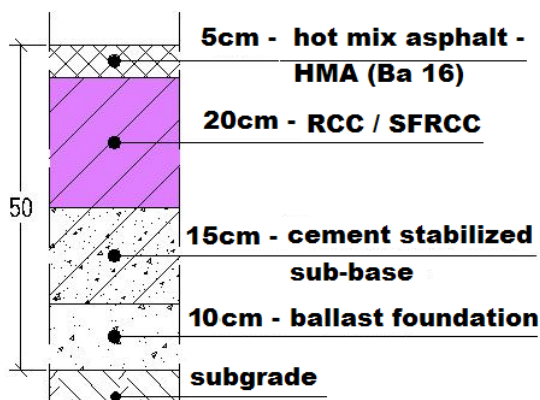


Figure 3. Pavement structure for sectors 5 and 6, on the ALT circular track facility

2. RIGID PAVEMENTS DESIGN ACCORDING TO ROMANIAN STANDARD NP 081 – 2002

The thickness design of the rigid pavements according to [4] is based on the allowable strength criterion, considering the tensile strength from bending in the cement concrete, σ_{tadm} . The computation model is a finite element one, using a multi-layer structure, made-up from the Portland cement concrete layer and an

equivalent layer of the under-lying real layers (base course, subbase course, foundation).

Preliminary studies are necessary, in order to obtain data concerning the composition, intensity and evolution of traffic, the geotechnical characteristics of the foundation soil, the hydrologic regime on the site. The design traffic for the design period, N_c is expressed in millions of standard axles, and it is established based on the average annual daily traffic. For this design purpose, the computed design traffic was of 19.495 millions standard axles (m.s.a.), for a design life of 30 years.

The support of the rigid pavement structure is made up by the foundation soil, and, optionally, the subbase course. The deformability characteristic characterizing the bearing capacity of the rigid pavement structure, for its design, is the coefficient of sub-grade reaction, K_0 (MN/m³). Its value is determined using plate load test “in situ” or correlation to other tests’ results: the dynamic soil modulus E_p (MPa) and the California bearing ratio (CBR) (%). [4] gives the approximate values of the sub-grade reaction, function of the climate and hydrologic regime, and type of soil, which were used in the design.

The bearing capacity at the level of the base course is expressed by the coefficient of reaction at the surface of the base course, K , determined function of the coefficient of sub-grade reaction K_0 and the equivalent thickness of the base/sub-base courses, H_{ech} .

The design criterion is expressed as follows:

$$\sigma \leq \sigma_{t,adm} \quad (1)$$

where σ is the tensile stress from bending in the concrete plate, determined in various design hypothesis and $\sigma_{t,adm}$ is the allowable tensile stress from bending.

The allowable tensile stress from bending for the Portland cement concrete ($\sigma_{t,adm}$) is determined using the relationship:

$$\sigma_{t,adm} = R_{inc}^k \times \alpha \times (0.70 - \gamma \times \log N_c) \quad (MPa) \quad (2)$$

where R_{kinc} is the bending characteristic strength of the concrete at 28 days, α is the concrete strength increasing coefficient in the interval 28-90 days, equal to 1.1, N_c is the traffic for the design period, γ is a coefficient equal to 0.05 and the expression in-between the brackets is the fatigue law.

The design hypotheses are:

a) for technical class I and II roads;

$$\sigma = \sigma_t + 0.8 \times \sigma_{t\Delta t} \leq \sigma_{t,adm} \quad (3)$$

b) for technical class III and IV roads:

$$\sigma = \sigma_t + 0.8 \times 0.65 \times \sigma_{t\Delta t} \leq \sigma_{t,adm} \tag{4}$$

c) for technical class V roads:

$$\sigma = \sigma_t \leq \sigma_{t,adm} \tag{5}$$

The concrete slab dimensioning is performed by using the design charts, or by using design equations, with coefficients interpolated from tables.

The design algorithm and the results for the proposed pavement structures are presented in Figures 4 to 6.

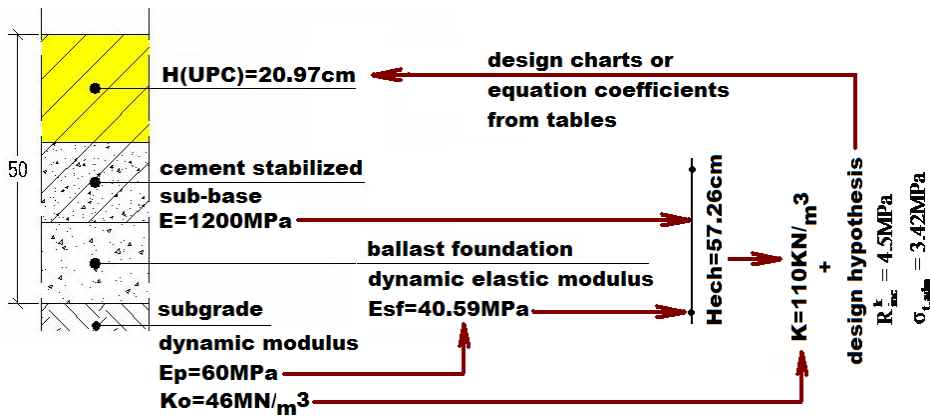


Figure 4. Thickness design according to Romanian Standard NP 081 – 2002, for Sector 1

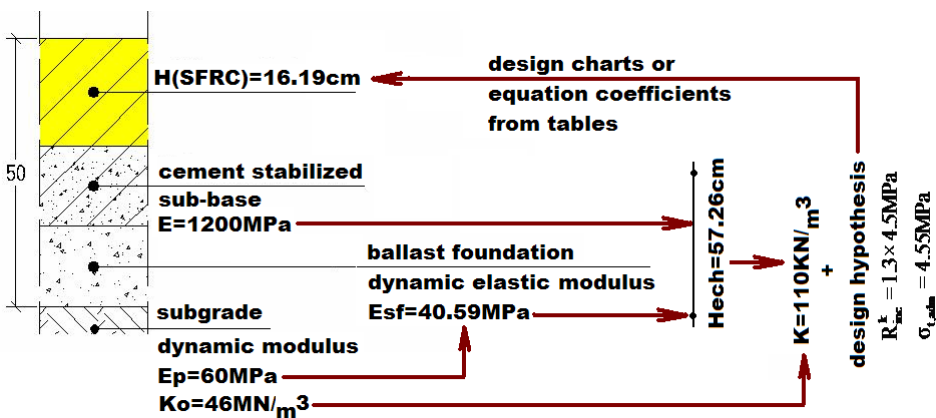


Figure 5. Thickness design according to Romanian Standard NP 081 – 2002, for Sectors 2, 3 & 4

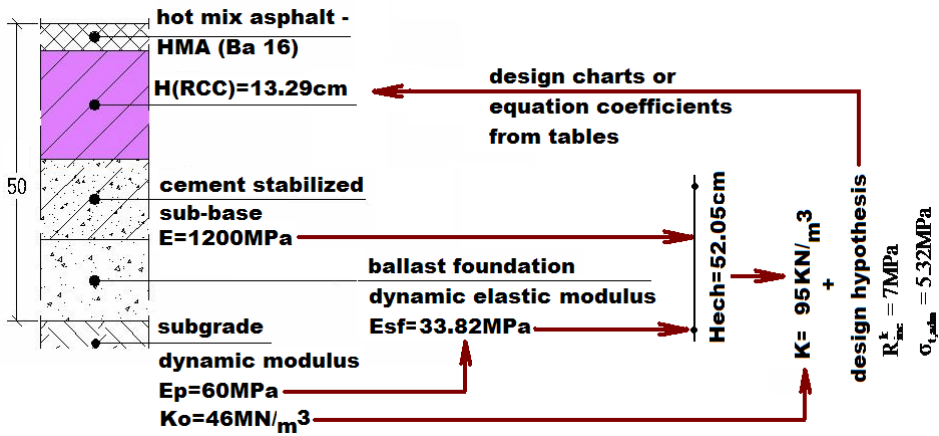


Figure 6. Thickness design according to Romanian Standard NP 081 – 2002, for Sector 6

3. THICKNESS DESIGN ACCORDING TO U.K. HIGHWAY AGENCY METHOD

The U.K. Highway Design Method is described in detail by the TRRL Research Report 87 [5]. This report presents design curves, based on observations made on experimental roads (29 unreinforced and 42 reinforced forms of construction). The structural performance was assessed and pavement life equations were derived by multiple regression analysis. The established equations are relating the pavement life, in terms of equivalent standard 80 kN axles, to the major pavement variables: the concrete slab thickness, concrete strength and foundation support.

The support offered by the foundation to the concrete slabs is evaluated in terms of Young's modulus of an equivalent uniform elastic foundation of infinite depth. According to [5], for 15 cm lean concrete upper layer and 15 cm capping layer, with the sub-grade having CBR=5, the equivalent foundation modulus is approximately 350 MPa.

The traffic load is expressed in terms of equivalent standard 80 kN axles. For our design, the traffic of 1.5 millions 115 kN standard axles was converted to 80kN standard axles, using equivalence coefficients [6]. It resulted that the traffic load for the experimental sectors on the ALT circular track is of 19.35 millions standard 80 kN axles.

The failure criteria devised to define the pavement life are associated to actual structural condition and linked to identifiable defects. For unreinforced concrete pavement, the bays were judged to have failed if any of the following defects were present:

- a crack of width equal to or greater than 0.5 mm crossing the bay longitudinally or transversally;
- a longitudinal and transverse crack intersecting, both starting from an edge and greater than 0.5 mm wide, and each longer than 200mm;
- corner cracking wider than 1.3 mm and more than 200 mm radius;
- a replaced or structurally repaired bay.

Multiple regression of the experimental data gave the regression estimate of cumulative traffic, in m.s.a., that can be carried before failure as:

$$\ln(L) = 5.094 \ln(H) + 3.466 \ln(S) + 0.4836 \ln(M) + 0.08718 \ln(F) - 40.78 \quad (6)$$

where:

- L is the estimate of the cumulative traffic, in msa;
- H is the thickness, in mm, of the plain concrete slab;
- S is the 28-day mean compression strength, in MPa, of cubes made from the pavement concrete;
- M is the equivalent modulus, in MPa, of a uniform foundation, giving the same support as the actual foundation;
- F is the percentage of failed bays (10%...50%).

For the UPC surface slab structure (sector 1), considering S=45MPa, M=350MPa and F=15, the design curve is presented in Figure 7. For the given design traffic, the thickness of the UPC surface layer is 220.202mm.

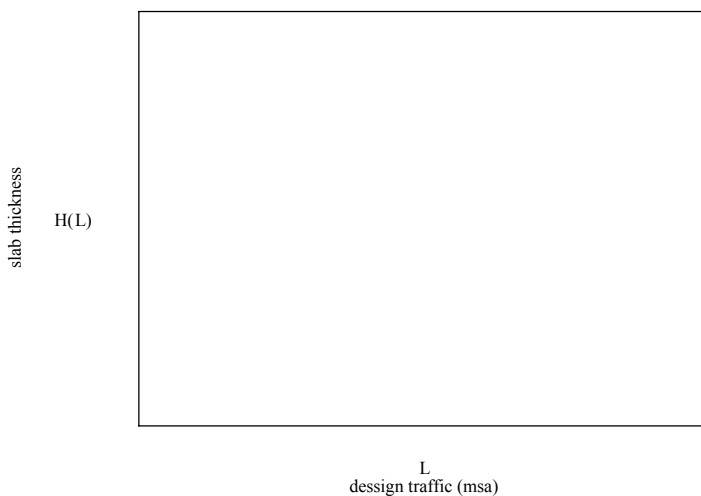


Figure 7. Thickness design according to TRRL Research Report 87, for Sector 1

For the SFRC surface slab structure (sectors 2 to 4), considering S=50MPa, M=350MPa and F=15, the design curve is presented in Figure 8. For the given design traffic, the thickness of the SFRC surface layer is 204.969mm.

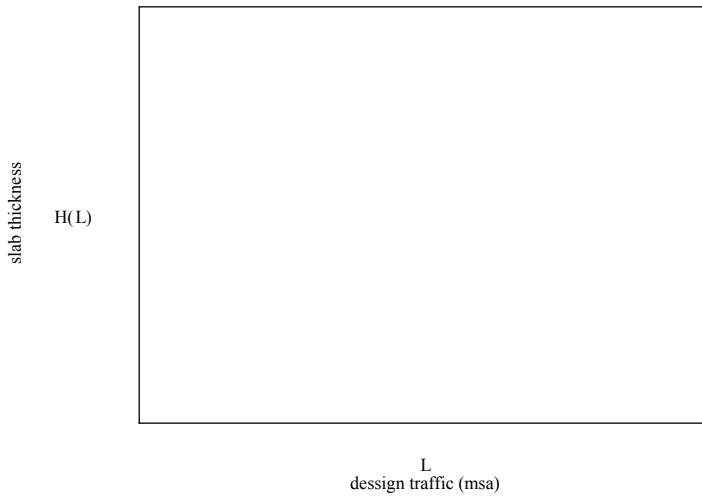


Figure 8. Thickness design according to TRRL Research Report 87, for Sectors 2 to 4

For the RCC surface slab structure (sector 6), considering $S=80\text{MPa}$, $M=350\text{MPa}$ and $F=15$, the design curve is presented in Figure 9. For the given design traffic, the thickness of the RCC surface layer is 148.868mm.

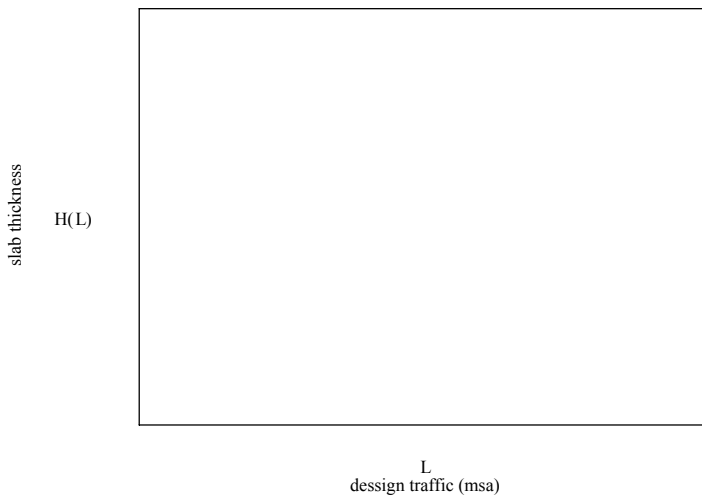


Figure 9. Thickness design according to TRRL Research Report 87, for Sector 6

For sector 5, the design was not performed, due to lack of data, at this stage, concerning the mechanical characteristics of steel fibre reinforced RCC.

4. CONCLUSIONS AND RECOMMENDATIONS

Table 1 presents the design results for the surface layer, using both methods considered.

Table 1. Thickness Design Results

	Sector 1	Sectors 2-4	Sector 6
	UPC	SFRC	RCC
NP 081-2002	20.97cm	16.19cm	13.29cm
TRRL	22.02cm	20.5cm	14.89cm

This incipient comparative design study has been undertaken by using Romanian and UK methods of design. Both design methods used in the investigation produced thickness of SFRC slab lower than that obtained for unreinforced concrete slab, and significantly reduced in case of the Romanian method. The reason for this may consist in the difference in philosophy of design and criteria (flexural concrete strength/RO vs. compressive strength/UK).

The study is under way and it will be extended to the AASHTO Mechanistic – Empirical Pavement Design Guide (M-E PDG) and other methods.

References

1. Incipient Deliverable 3.2 Report: Laboratory Accelerated Load Testing & Further Developments on Deliverable 3.1, EcoLanes Internal Report, 2007
2. N. Taranu, EcoLanes WP 3 Monthly Progress Report, Antalia, 2007
3. <http://ecolanes.shef.ac.uk>
4. NP 081 – 2002, Normativ pentru dimensionarea sistemelor rutiere rigide (in Romanian)
5. TRRL Research Report 87, Thickness Design of Concrete Roads
6. N. J. Garber, Lester A. Hoel, Traffic and Highway Engineering, PWS Publishing, 1999

Calculation of the Equivalent Traffic Based on Structural Design Criteria of Flexible and Semirigid Pavements

Horia Gh. Zarojanu¹, Radu Andrei²

¹Department of Roads and Foundations, Technical University "Gh. Asachi", Iasi., 700050, Romania,
zarojan@ce.tuiasi.ro

²Department of Roads and Foundations, Technical University "Gh. Asachi", Iasi., 700050, Romania,
randreir@ce.tuiasi.ro

Summary

The paper presents a methodology for calculation of the equivalent traffic, intended to be applied in the frame of an analytical structural design method for flexible and semirigid pavements. This methodology eliminates conventional or empirical equivalence, by using the structural design criteria expressed in terms of allowable deformation/stresses. Finally, for a representative construction case for a European/National Road, a comparison between the proposed method and the actual one, used in the frame of structural design of pavements in Romania, is given.

KEYWORDS: flexible/semi-rigid pavement design, equivalent traffic, standard vehicles, physical vehicles, equivalence coefficients

1. INTRODUCTION

The maximum allowable axle loads permitted for various categories of vehicles and the relatively frequent trend to overpass them in order to reduce the costs of road transport justify the importance of traffic parameters in the structural design of pavements.

In accordance to the actual analytical method of structural design [1] of flexible/semirigid pavements, the criterion for the equivalence of physical vehicles in standard vehicles (standard axle load 115 kN) does not take into consideration the design criteria, which are the following:

- the allowable horizontal tensile strain (ϵ_r) at the subgrade level;
- the allowable longitudinal tensile stress (σ_r) at the bottom of cementitious/puzzolanic binder stabilized aggregates base course layers;
- the allowable compressive vertical strain (ϵ_z) at the subgrade level.

The fatigue laws adopted for the design [1], assume the logarithmic relation between the total estimated number of standard axle loads for the envisaged service

life – N, and the ϵ_r , σ_r and ϵ_z parameters which are defining the design criteria. The method proposed for the equivalence of physical vehicles in standard vehicles (115 kN), by taking into consideration the design criteria described previously eliminates the disadvantage of the existing conventional or empirical methods.

2. THE CALCULATION OF THE COEFFICIENTS FOR THE EQUIVALENCE OF THE PHYSICAL VEHICLES IN STANDARD AXLE LOADS (ESAL) OF 115KN

The method for calculation is based on multilayer Burmister model, where the total bonding between the main layers is considered in accordance with the analytical method [1], and with the loss of bonding for the foundation layers, occurring during the service of the pavement. The pavement structure considered for the calculation of coefficient of equivalence of physical vehicles is detailed in Table 1.

Table 1: Description of the typical pavement structure considered for calculation

Type of layer	Materials used	Layer thickness (cm)	Main characteristics of materials				Bonding at the layers interface		
			Climatic type						
			I + II		III		I	II	III
			E(MPa)	v	E(MPa)	v			
wearing course	asphalt mix *) (HMA) SR 174/1	4	3600	0.35	4200	0.35	A	A	A
binding course	asphalt mix *) (HMA) SR 174/1	5	3000	0.35	3600	0.35	A	A	A
base course	asphalt mix *) (HMA) SR 174/1	8	5000	0.35	5600	0.35	A	A	a
foundation superior layer	cement stabilized natural aggregates	23	1200	0.25	1200	0.25	A	a	a
foundation bottom layer	ballast	25	250**)	0.27	225**)	0.27	A	a	a
improved subgrade	ballast	15	135**)	0.27	95**)	0.27	A	a	a
subbase	soil category P4 [1]	-	70	0.35	50	0.35	A	a	a

*) Asphalt mixes (HMA) prepared with bitumen D80/100

***) Values calculated with the relation Claessen/Shell

A- with bonding;

a- loss of bonding.

The categories of vehicles observed during the last traffic census (undertaken during 2005 year) have been considered in this approach, the representative vehicles established in accordance with the 96/53/EC Directive and with the Romanian norms [2] are presented in Table 2.

Table 2: The main characteristics of the representative vehicles, according to 96/53/EC Directive and the Romanian norms

Crt. No.	The group of representative vehicles	Specific loads on axles (kN)			Total load (kN)	Position in OMT 43/97
		Simple	Tandem	Tridem		
1	Trucks and similar vehicles with two axles	80;80	-	-	160	2.3.1; 3.4.2
2	Trucks and similar vehicles with 3&4 axles	70;70	2x90	-	320	2.3.3; 3.2.3
3	Articulated vehicles type (TIR) with more than four axles	60	2x70	3x80	440	2.2.2(c); 3.4.1
4	Busses	80;100	-	-	180	
5	Trucks with 2, 3 or 4 axles and trailers (road-trains)	60;80;80	2x90	-	400	2.2.1(b); 3.4.1

The calculation of the ϵ_r , σ_r and ϵ_z parameters defining the design criteria is done for the physical (standard) semi-axle loads transmitted to the pavement surface by circular prints, whose characteristics are shown in Table 3.

The standard semi-axle load has the following characteristics:

- the total load on the twin wheels: 57,5 kN;
- the contact pressure: 0,625 MPa;
- the radius of the surface of the equivalent print: 0.1711 m.

The calculation is conducted for all types of semi-axes, by considering each category of vehicles and the semi-axle type that has the maximum influence on loading.

For these three interface bonding hypothesis, the values of the equivalence coefficients, calculated using the following ratios:

$$\frac{\epsilon_r}{\epsilon_r(\text{ESAL115kN})}; \frac{\sigma_r}{\sigma_r(\text{ESAL115kN})}; \frac{\epsilon_z}{\epsilon_z(\text{ESAL115kN})} \quad (1)$$

are given in Table 4 (ϵ_r - microdeformations; σ_r MPa)

Table 3: The main characteristics of the circular type prints of physical vehicles

Type of axle	Axle load (kN)	Semi-axle load (kN)	Radius of print (m)	The tyre pressure on the print (MPa)	Distance between axles (m)
Simple	60	30	0.1261	0.600	
	70	35	0.1363	0.600	
	80	40	0.1428	0.625	
	100	50	0.1565	0.650	
Tandem	2x70	2x35	2x0.1363	0.600	1.3
	2x90	2x45	2x0.1485	0.650	1.3
Tridem	3x80	3x40	3x0.1428	0.625	1.4

Table 4. The equivalence coefficients values calculated for each type of semi-axle load

Semi-axle load (kN)	Climatic type	The design criterion								
		ϵ_r			σ_r			ϵ_z		
		$\epsilon_{r(ESAL115kN)}$			$\sigma_{r(ESAL115kN)}$			$\epsilon_{z(ESAL115kN)}$		
		Bonding interface hypothesis								
		I	II	III	I	II	III	I	II	III
30	I+II	0.74	0.71	0.65	0.56	0.55	0.56	0.53	0.53	0.53
	III	0.73	0.70	0.64	0.56	0.55	0.56	0.53	0.53	0.53
35	I+II	0.80	0.78	0.72	0.64	0.64	0.65	0.62	0.62	0.62
	III	0.79	0.76	0.71	0.64	0.64	0.64	0.62	0.62	0.62
40	I+II	0.87	0.85	0.80	0.73	0.72	0.74	0.70	0.70	0.71
	III	0.86	0.84	0.79	0.72	0.72	0.73	0.70	0.70	0.71
50	I+II	0.98	0.96	0.93	0.89	0.89	0.89	0.87	0.88	0.88
	III	0.97	0.96	0.93	0.89	0.89	0.89	0.88	0.88	0.88
2x35	I+II	0.80	0.80	0.76	0.70	0.70	0.68	0.72	0.72	0.66
	III	0.79	0.80	0.76	0.70	0.72	0.68	0.75	0.75	0.68
2x45	I+II	0.93	0.95	0.92	0.88	0.89	0.85	0.93	0.93	0.85
	III	0.93	0.95	0.93	0.90	0.91	0.86	0.96	0.96	0.88
3x40	I+II	0.86	0.90	0.87	0.83	0.84	0.78	0.91	0.91	0.78
	III	0.86	0.91	0.88	0.86	0.88	0.80	0.96	0.97	0.82

Finally, the average values calculated by considering the three interface bonding hypothesis are adopted, as shown in Table 5. The design criterion which is significant for the calculation of equivalence coefficients is ϵ_r (see Table 4).

Table 5. The values of equivalence coefficients proposed for the various groups of representative vehicles^{*)}

The group of representative vehicles	Equivalence coefficients for various axles			Total / vehicle	The new proposed coefficients	The actual used coefficients (RO Norms)
	Simple	Tandem	Tridem			
1	0.83	-	-	1.66	0.80	0.40
2	0.76	0.93	-	2.45	0.90	0.60
3	0.69	0.78	0.88	2.35	0.90	0.80
4	0.95	-	-	1.78	0.95	0.60
5	0.83	0.93	-	3.28	0.95	0.80

^{*)} Average values calculated according to the three interface bonding hypothesis

3. THE CASE STUDY

The case study was conducted on some sectors of European road (see Table 6) and of National (principal) road (see Table 7) and considering a service life of 15 years. The difference between the equivalent traffic, expressed in Average Daily Traffic – ADT 2020, calculated according to the actual norms [1], and that calculated according to the proposed methodology described in this paper, is of 47.7%, higher for the European road, and of 46.4%, higher for the National (principal) road, respectively.

Table 6. Calculation of the equivalent traffic for an European road

Vehicles group	ADT 2005	Correlation coefficients 2005 - 2020	ADT 2020	Equivalence coefficients		ADT 2020 Standard vehicles	
				^{*)}	^{**)}	^{*)}	^{**)}
1	469	1.99	933	0.40	0.80	373	746
2	253	1.55	392	0.60	0.90	235	353
3	557	1.47	819	0.80	0.90	655	737
4	465	1.96	911	0.60	0.95	546	865
5	93	1.35	126	0.80	0.95	101	120
TOTAL			3181			1910	2821 (147.7%)

^{*)} According to actual Romanian norms

^{**)} According to the proposed method

Table 7. Calculation of the equivalent traffic for a National (principal) road

Vehicles group	ADT 2005	Correlation coefficients 2005 - 2020	ADT 2020	Equivalence coefficients		ADT 2020 Standard vehicles	
				*	**	*	**
1	365	1.65	602	0.40	0.80	241	482
2	264	1.63	430	0.60	0.90	258	387
3	283	1.50	425	0.80	0.90	340	383
4	282	1.40	395	0.60	0.95	237	375
5	155	1.50	233	0.80	0.95	186	221
TOTAL			2085			1262	1848 (146.4%)

*) According to actual Romanian norms

***) According to the proposed method

4. CONCLUSIONS

The most significant design criterion for calculation of the equivalence coefficients of physical vehicles in standard axle (ESAL 115kN) vehicles is the allowable horizontal tensile strain, ϵ_r , at the bottom of the asphalt layers.

The equivalence of the physical vehicles in standard axles (ESAL 115kN), based on the design criteria of flexible/semi-rigid pavements, leads to the conclusion that the equivalent traffic calculated in accordance with the analytical design method [1] used now in Romania is under-evaluated.

References

1. *Normativ pentru dimensionarea sistemelor rutiere suple si semirigide (metoda analitica) PD 177 – 2001* (in Romanian)
2. *Anexa 2 (OTA 26/2003). Ordonanta nr. 43/1997 (republicata/actualizata) – 2006* (in Romanian)
3. *Recensamantul general al circulatiei 2005. Coeficientii de echivalare ai vehiculelor fizice in vehicule etalon* (in Romanian)

Highway and Bridge Engineering 2007 in images



Photo 1. Opening session – Neculai Tautu, PE, President APDP-Moldova Branch



Photo 2. Prof. Neculai Taranu – Dean of School of Constructions Iasi



Photo 3. Prof. N. Taranu awarding Diploma of Excellence of Technical University “Gh.Asachi” Iasi to prof. Paulo Pereira from University of Monho, Portugal



Photo 4. Prof. Paulo Pereira



Photo 5. A presentation



Photo 6. Prof. N. Botu presenting an article



Photo 7. dr. Laurențiu Stelea – points of view



Photo 8. dr. Victor Popa



Photo 9. Image from the audience



Photo 10. Image from the audience



Photo 11. Image from the audience



Photo 13. Image from the audience



Photo 14. Image from the audience



Photo 16. Images from the audience



Photo 17. Imagine din sala de conferință



Photo 18. Imagine din sala de conferință

COLECȚIA
MANIFESTĂRI ȘTIINȚIFICE



ISBN 978-973-8955-29-5